

Methods in
Molecular Biology 2326

Springer Protocols

Xiaoping Pan
Baohong Zhang *Editors* → ↘ ↑



Environmental Toxicology and Toxicogenomics

Principles, Methods,
and Applications

 Humana Press

METHODS IN MOLECULAR BIOLOGY

Series Editor

John M. Walker

School of Life and Medical Sciences

University of Hertfordshire

Hatfield, Hertfordshire, UK

For further volumes:
<http://www.springer.com/series/7651>

For over 35 years, biological scientists have come to rely on the research protocols and methodologies in the critically acclaimed *Methods in Molecular Biology* series. The series was the first to introduce the step-by-step protocols approach that has become the standard in all biomedical protocol publishing. Each protocol is provided in readily-reproducible step-by-step fashion, opening with an introductory overview, a list of the materials and reagents needed to complete the experiment, and followed by a detailed procedure that is supported with a helpful notes section offering tips and tricks of the trade as well as troubleshooting advice. These hallmark features were introduced by series editor Dr. John Walker and constitute the key ingredient in each and every volume of the *Methods in Molecular Biology* series. Tested and trusted, comprehensive and reliable, all protocols from the series are indexed in PubMed.

Environmental Toxicology and Toxicogenomics

Principles, Methods, and Applications

Edited by

Xiaoping Pan and Baohong Zhang

Department of Biology, East Carolina University, Greenville, NC, USA

Editors

Xiaoping Pan
Department of Biology
East Carolina University
Greenville, NC, USA

Baohong Zhang
Department of Biology
East Carolina University
Greenville, NC, USA

ISSN 1064-3745
Methods in Molecular Biology
ISBN 978-1-0716-1513-3
<https://doi.org/10.1007/978-1-0716-1514-0>

ISSN 1940-6029 (electronic)
ISBN 978-1-0716-1514-0 (eBook)

© Springer Science+Business Media, LLC, part of Springer Nature 2021
This work is subject to copyright. All rights are reserved by the Publisher, whether the whole or part of the material is concerned, specifically the rights of translation, reprinting, reuse of illustrations, recitation, broadcasting, reproduction on microfilms or in any other physical way, and transmission or information storage and retrieval, electronic adaptation, computer software, or by similar or dissimilar methodology now known or hereafter developed.

The use of general descriptive names, registered names, trademarks, service marks, etc. in this publication does not imply, even in the absence of a specific statement, that such names are exempt from the relevant protective laws and regulations and therefore free for general use.

The publisher, the authors, and the editors are safe to assume that the advice and information in this book are believed to be true and accurate at the date of publication. Neither the publisher nor the authors or the editors give a warranty, expressed or implied, with respect to the material contained herein or for any errors or omissions that may have been made. The publisher remains neutral with regard to jurisdictional claims in published maps and institutional affiliations.

Cover Illustration Caption: Crude oil-dispersant mixture affected reproduction by enhancing germ cell apoptosis in *Caenorhabditis elegans*; arrows point to apoptotic cells in the gonad of *C. elegans* exposed to 500X dilution of crude oil/dispersant.

This Humana imprint is published by the registered company Springer Science+Business Media, LLC, part of Springer Nature.

The registered company address is: 1 New York Plaza, New York, NY 10004, U.S.A.

Preface

With rapid advancements of industrialization, agricultural productions, and urbanization, environmental pollutions have been becoming one major issue faced by humans and the ecosystem. Many toxic chemicals including emerging industrial by-products have been detected in environmental compartments including air, soil, and water. Studying the detection, toxicity, and related mechanisms of environmental pollutants will provide knowledge necessary to develop strategies to prevent and manage their negative effects. Environmental toxicology has become a popular major nowadays; more and more research has investigated the impacts of environmental pollution at the population (ecology and biodiversity), individual (lethal and sublethal), developmental, physiological, cellular, and molecular levels. To enhance the development of this research field, it is necessary and important to highlight the current methodology for studying environmental pollutions.

The goal of this book is to provide an accessible compendium of up-to-date methods in the fields of environmental toxicology, molecular toxicology, and toxicogenomics. Rapid development of these fields generated an extensive body of methodology, making it difficult for researchers to follow. Furthermore, given the journal requirements, many papers do not focus on presenting methodology in the great detail necessary for other laboratories who would potentially apply similar methods. Collecting reliable methods from world-renowned laboratories will provide an important resource and significantly reduce the time and efforts required for seeking these methods from the scientific community. To achieve this goal, we invited environmental scientists around the world to contribute to this methodology book based on their expertise.

This book is organized into four major parts. The first part includes fourteen chapters presenting methods mainly utilizing model animal species, such as nematode, fruit fly, mice, chicken, and amphibians. The second part includes five chapters mainly using plants to study chemical toxicity. The third part includes one chapter presenting the Ames assay for chemical mutagenicity study. The last part of this book collects five method chapters for environmental chemical analysis. Although this book was divided into four parts, all the methods can be used across species.

We greatly appreciate all the authors who made excellent contributions to this book. Their wonderful research and significant efforts provide detailed protocols and strategies for studying environmental toxicology at different levels and also make this book a very valuable resource for the scientific community, particularly for young scientists and graduate and undergraduate students, inspiring more research in the field of environmental toxicity, molecular toxicology, and toxicogenomics. We would also like to express our sincere appreciation to Professor John M. Walker, the *Methods in Molecular Biology* Series Editor, and Mr. David C. Casey and Ms. Anna Rakovsky from Springer Protocols for their invitation, support, and commitment during this book's preparation.

Greenville, NC, USA

*Xiaoping Pan
Baohong Zhang*

Contents

Preface	v
Contributors	ix

PART I ANIMAL TOXICITY

1 Detection of <i>Caenorhabditis elegans</i> Germ Cell Apoptosis Following Exposure to Environmental Contaminant Mixtures: A Crude Oil-Dispersant Mixture Example.....	3
<i>Joseph Ryan Polli, Mary Farwell, and Xiaoping Pan</i>	
2 High-Throughput Measurement for Toxic Effects of Metal Mixtures in <i>Caenorhabditis elegans</i>	19
<i>Kathy S. Xue and Lili Tang</i>	
3 Evaluations of Environmental Pollutant-Induced Mitochondrial Toxicity Using <i>Caenorhabditis elegans</i> as a Model System	33
<i>Fuli Zheng, Michael Aschner, and Huangyuan Li</i>	
4 Methods to Assay the Behavior of <i>Drosophila melanogaster</i> for Toxicity Study	47
<i>Guiran Xiao</i>	
5 Investigating the Joint Effects of Pesticides and Ultraviolet B Radiation in <i>Xenopus laevis</i> and Other Amphibians.....	55
<i>Shuangying Yu and Mike Wages</i>	
6 Identification of Stable Reference Genes for Toxicogenomic and Gene Expression Analysis	67
<i>Xiaoping Pan and Baohong Zhang</i>	
7 Semi-Quantitative RT-PCR: An Effective Method to Explore the Regulation of Gene Transcription Level Affected by Environmental Pollutants	95
<i>Fan Wang</i>	
8 Employing Multiple New Neurobiological Methods to Investigate Environmental Neurotoxicology in Mice.....	105
<i>Ping Cai and Huangyuan Li</i>	
9 Analyses of Epigenetic Modification in Environmental Pollutants-Induced Neurotoxicity	123
<i>Guangxia Yu, Zhenkun Guo, and Huangyuan Li</i>	
10 The Application of Omics Technologies in the Research of Neurotoxicology	143
<i>Wenya Shao and Huangyuan Li</i>	

11	Flow Cytofluorometric Analysis of Molecular Mechanisms of Premature Red Blood Cell Death..... <i>Mohammad A. Alfhili and Myon Hee Lee</i>	155
12	Practical Methods and Technologies in Environmental Epidemiology <i>Chuancheng Wu, Donghong Wei, Huangyuan Li, and Siying Wu</i>	167
13	In Ovo Early-in-Life Inhalation Exposure to Gas/Aerosol with a Chicken Embryo Model <i>Qixiao Jiang, Xiaohui Xu, Hao Ni, Yajie Guo, Junhua Yuan, and Yuxin Zheng</i>	197
14	DNA Damage in Liver Cells of the Tilapia Fish <i>Oreochromis mossambicus</i> Larva Induced by the Insecticide Cyantraniliprole at Sublethal Doses During Chronic Exposure <i>Tongmei Fan, Chengbin Xu, and Weiguo Miao</i>	203

PART II PLANT TOXICITY

15	Impact of Nanoparticles on Plant Growth, Development, and Biomass..... <i>Ilya N. Boykov and Baohong Zhang</i>	217
16	Biochemical and Physiological Toxicity of Nanoparticles in Plant <i>Zhiyong Zhang and Baohong Zhang</i>	225
17	Determination of Oxidative Stress and Antioxidant Enzyme Activity for Physiological Phenotyping During Heavy Metal Exposure <i>Samrana Zahir, Fan Zhang, Jinhong Chen, and Shuijin Zhu</i>	241
18	Comprehensive Phytotoxicity Assessment Protocol for Engineered Nanomaterials <i>Lok R. Pokhrel, Chukwudi S. Ubah, and Sina Fallah</i>	251
19	Detection of Cadmium Toxicity in Plant..... <i>Xiaoxiao Liu, Lina Yin, Shiwen Wang, and Zhiyong Zhang</i>	267

PART III MICROBE TOXICITY

20	Mutagenicity Evaluation of Nanoparticles by the Ames Assay <i>Xiaoping Pan</i>	275
----	---	-----

PART IV EXTRACTION AND DETECTION ANALYTICAL METHODS

21	Dispersive Solid-Phase Extraction of Multiresidue Pesticides in Food and Water Samples <i>Hongxia Guan</i>	289
22	Quantitative Analysis of Multiresidue Pesticides Using Gas Chromatography–Mass Spectrometry <i>Qingsong Cai and Hongxia Guan</i>	301
23	Determination of the N-Nitroso Compounds in Mouse Following RDX Exposure <i>Xiaoping Pan</i>	315

24	Determination of Metal Content in <i>Drosophila melanogaster</i> During Metal Exposure..... <i>Guiran Xiao</i>	327
25	Microplastics: A Review of Methodology for Sampling and Characterizing Environmental and Biological Samples..... <i>Christiana H. Shoopman and Xiaoping Pan</i>	339
	<i>Index</i>	361

Contributors

- MOHAMMAD A. ALFHILI • *Chair of Medical and Molecular Genetics Research, Department of Clinical Laboratory Sciences, College of Applied Medical Sciences, King Saud University, Riyadh, Saudi Arabia*
- MICHAEL ASCHNER • *Department of Molecular Pharmacology, Albert Einstein College of Medicine, Bronx, NY, USA*
- ILYA N. BOYKOV • *Department of Biology, East Carolina University, Greenville, NC, USA*
- PING CAI • *The Key Laboratory of Environment and Health, School of Public Health, Fujian Medical University, Fuzhou, China*
- QINGSONG CAI • *The Complex Carbohydrate Research Center, University of Georgia, Athens, GA, USA*
- JINHONG CHEN • *College of Agriculture and Biotechnology, Zhejiang University, Hangzhou, Zhejiang, China*
- SINA FALLAH • *Department of Agronomy, Faculty of Agriculture, Shahrekord University, Shahrekord, Iran*
- YONGMEI FAN • *Key Laboratory of Green Prevention and Control of Tropical Plant Disease and Pests, Ministry of Education, College of Plant Protection, Hainan University, Haikou, China*
- MARY FARWELL • *Department of Biology, East Carolina University, Greenville, NC, USA*
- HONGXIA GUAN • *School of Science and Technology, Georgia Gwinnett College, Lawrenceville, GA, USA*
- YAJIE GUO • *School of Public Health, Qingdao University, Qingdao, Shandong, China*
- ZHENKUN GUO • *The Key Laboratory of Environment and Health, School of Public Health, Fujian Medical University, Fuzhou, China; Department of Preventive Medicine, School of Public Health, Fujian Medical University, Fuzhou, China*
- QIXIAO JIANG • *School of Public Health, Qingdao University, Qingdao, Shandong, China*
- MYON HEE LEE • *Division of Hematology/Oncology, Department of Internal Medicine, Brody School of Medicine, East Carolina University, Greenville, NC, USA*
- HUANGYUAN LI • *The Key Laboratory of Environment and Health, School of Public Health, Fujian Medical University, Fuzhou, China; Department of Preventive Medicine, School of Public Health, Fujian Medical University, Fuzhou, China*
- XIAOXIAO LIU • *State Key Laboratory of Soil Erosion and Dryland Farming on the Loess Plateau, Institute of Soil and Water Conservation, Chinese Academy of Sciences and Ministry of Water Resources, Yangling, Shanxi, China; University of the Chinese Academy of Sciences, Beijing, China; Institute of Soil and Water Conservation, Northwest A&F University, Yangling, Shanxi, China*
- WEIGUO MIAO • *Key Laboratory of Green Prevention and Control of Tropical Plant Disease and Pests, Ministry of Education, College of Plant Protection, Hainan University, Haikou, China*
- HAO NI • *School of Public Health, Qingdao University, Qingdao, Shandong, China*
- XIAOPING PAN • *Department of Biology, East Carolina University, Greenville, NC, USA*
- LOK R. POKHREL • *Department of Public Health, The Brody School of Medicine, East Carolina University, Greenville, NC, USA; Department of Health Education and*

Promotion, College of Health and Human Performance, East Carolina University, Greenville, NC, USA

JOSEPH RYAN POLLIS • Department of Biology, East Carolina University, Greenville, NC, USA

WENYA SHAO • The Key Laboratory of Environment and Health, School of Public Health, Fujian Medical University, Fuzhou, China; Department of Preventive Medicine, School of Public Health, Fujian Medical University, Fuzhou, China

CHRISTIANA H. SHOOPMAN • Department of Biology, East Carolina University, Greenville, NC, USA

LILI TANG • Department of Environmental Health Science, College of Public Health, University of Georgia, Athens, GA, USA

CHUKWUDI S. UBAH • Department of Public Health, The Brody School of Medicine, East Carolina University, Greenville, NC, USA

MIKE WAGES • The Department of Environmental Toxicology, Texas Tech University, Lubbock, TX, USA

FAN WANG • School of Biological Science, Luoyang Normal University, Luoyang, China

SHIWEN WANG • State Key Laboratory of Soil Erosion and Dryland Farming on the Loess Plateau, Institute of Soil and Water Conservation, Chinese Academy of Sciences and Ministry of Water Resources, Yangling, Shanxi, China; University of the Chinese Academy of Sciences, Beijing, China; Institute of Soil and Water Conservation, Northwest A&F University, Yangling, Shanxi, China

DONGHONG WEI • The Key Laboratory of Environment and Health, School of Public Health, Fujian Medical University, Fuzhou, China; Department of Epidemiology and Statistics, School of Public Health, Fujian Medical University, Fuzhou, China

CHUANCHENG WU • The Key Laboratory of Environment and Health, School of Public Health, Fujian Medical University, Fuzhou, China; Department of Preventive Medicine, School of Public Health, Fujian Medical University, Fuzhou, China

SIYING WU • The Key Laboratory of Environment and Health, School of Public Health, Fujian Medical University, Fuzhou, China; Department of Epidemiology and Statistics, School of Public Health, Fujian Medical University, Fuzhou, China

GUIRAN XIAO • School of Food and Biological Engineering, Hefei University of Technology, Hefei, Anhui, China

CHENGBIN XU • Key Laboratory of Green Prevention and Control of Tropical Plant Disease and Pests, Ministry of Education, College of Plant Protection, Hainan University, Haikou, China

XIAOHUI XU • School of Public Health, Qingdao University, Qingdao, Shandong, China

KATHY S. XUE • Department of Environmental Health Science, College of Public Health, University of Georgia, Athens, GA, USA

LINA YIN • State Key Laboratory of Soil Erosion and Dryland Farming on the Loess Plateau, Institute of Soil and Water Conservation, Chinese Academy of Sciences and Ministry of Water Resources, Yangling, Shanxi, China; University of the Chinese Academy of Sciences, Beijing, China; Institute of Soil and Water Conservation, Northwest A&F University, Yangling, Shanxi, China

GUANGXIA YU • The Key Laboratory of Environment and Health, School of Public Health, Fujian Medical University, Fuzhou, China; Department of Preventive Medicine, School of Public Health, Fujian Medical University, Fuzhou, China

SHUANGYING YU • Sciences Division, Central Piedmont Community College, Charlotte, NC, USA

JUNHUA YUAN • School of Basic Medicine, Qingdao University, Qingdao, Shandong, China

- SAMRANA ZAHIR • *College of Agriculture and Biotechnology, Zhejiang University, Hangzhou, Zhejiang, China*
- BAOHONG ZHANG • *Department of Biology, East Carolina University, Greenville, NC, USA*
- FAN ZHANG • *College of Agriculture and Biotechnology, Zhejiang University, Hangzhou, Zhejiang, China*
- ZHIYONG ZHANG • *Henan Collaborative Innovation Center of Modern Biological Breeding and Henan Key Laboratory for Molecular Ecology and Germplasm Innovation of Cotton and Wheat, Henan Institute of Science and Technology, Xinxiang, Henan, China*
- FULI ZHENG • *The Key Laboratory of Environment and Health, School of Public Health, Fujian Medical University, Fuzhou, China; Department of Preventive Medicine, School of Public Health, Fujian Medical University, Fuzhou, China*
- YUXIN ZHENG • *School of Public Health, Qingdao University, Qingdao, Shandong, China*
- SHUIJIN ZHU • *College of Agriculture and Biotechnology, Zhejiang University, Hangzhou, Zhejiang, China*

Part I

Animal Toxicity



Chapter 1

Detection of *Caenorhabditis elegans* Germ Cell Apoptosis Following Exposure to Environmental Contaminant Mixtures: A Crude Oil-Dispersant Mixture Example

Joseph Ryan Polli, Mary Farwell, and Xiaoping Pan

Abstract

Crude oil disasters, such as the Deepwater Horizon accident, have caused severe environmental contamination and damage, affecting the health of marine and terrestrial organisms. Some previous studies have demonstrated cleanup efforts using chemical dispersant induced more potent toxicities than oil alone due to an increase in bioavailability of crude oil components, such as PAHs. However, there still lacks a systematic procedure that provides methods to determine genotypic and phenotypic changes following exposure to environmental toxicants or toxicant mixture, such as dispersed crude oil. Here, we describe methods for identifying a mechanism of dispersed crude oil-induced reproductive toxicity in the model organisms, *Caenorhabditis elegans* (*C. elegans*). Due to the genetic malleability of *C. elegans*, two mutant strains outlined in this chapter were used to identify a pathway responsible for inducing apoptosis: MD701 bcIs39 [lin-7p::ced-1::GFP + lin-15(+)], a mutant strain that allows visualization of apoptotic bodies via a green fluorescent protein fused to CED-1; and TJ1 (cep-1(gk138) I.), a p53/CEP-1 defective strain that is unable to activate apoptosis via the p53/CEP-1 pathway. In addition, qRT-PCR was utilized to demonstrate the aberrant expression of apoptosis (*ced-13*, *ced-3*, *ced-4*, *ced-9*, *cep-1*, *dpl-1*, *efl-1*, *efl-2*, *egl-1*, *egl-38*, *lin-35*, *pax-2*, and *sir-2.1*) and cytochrome P450 (*cyp14a3*, *cyp35a1*, *cyp35a2*, *cyp35a5*, and *cyp35c1*) protein-coding genes following exposure to dispersed crude oil. The procedure outlined here can be applicable to determine whether environmental contaminants, most of time contaminant mixture, cause reproductive toxicity by activation of the proapoptotic, p53/CEP-1 pathway.

Key words Environmental contaminants, Mixture toxicity, Oil spill, Apoptosis, *C. elegans*, Genotoxicity, PCR, GFP

1 Introduction

Crude oil spill disasters, such as the one from the Deepwater Horizon platform, cause serious environmental issues for terrestrial and marine life in the affected areas. Crude oil is a mixture entity composed of numerous organic toxicants, such as polycyclic aromatic hydrocarbons (PAHs), which are known genotoxic, carcinogenic, and teratogenic agents [1–5]. Due to crude oil and PAHs

being insoluble in water, chemical dispersants are widely used to reduce viscosity and increase solubility of surface oil. Chemical dispersant, Corexit 9500, was used in response to the DWH accident [6]. Although dispersion of crude oil enhances microbial degradation [7], the formed micelles also enhance the bioavailability of crude oil in higher order marine and terrestrial species, such as *Caenorhabditis elegans* (*C. elegans*), increasing the risk of intoxication by PAHs [8]. Absorbed PAH molecules are metabolized by cytochrome P450 (CYP450) enzymes to become reactive species that can actively bind DNA, forming DNA adducts, which subsequently interfere with polymerases during DNA replication, repair, and transcription [9–14]. In addition to converting PAHs to their DNA-reactive species, PAHs can also induce expression of CYP450 protein-coding genes through activation of the AhR pathway [15–17]. These compounding mechanisms following PAH exposure may result in various organ-specific toxicities, with reproductive toxicity among the most notable [5].

C. elegans are a versatile biological model, which enable various techniques and methods to evaluate genotypic and phenotypic alterations following exposure to individual toxicant or environmental contaminant mixtures (e.g., crude oil and PAHs), including reproduction and programmed cell death during oogenesis. The reproductive system in *C. elegans* is unique as these organisms are hermaphrodites that produce both oocytes and sperms. One can identify easily the female ovaries as two U-shaped gonadal arms through the transparent cuticle of *C. elegans*, allowing for visualization of gametogenesis and morphological alterations following exposure to environmental toxicants [18, 19]. Apoptosis is a natural process of elimination of unstable cells within the gonadal loop of *C. elegans*. At any point in time under normal environmental conditions, usually 2–3 cell corpses may be observed for several days following maturation into an adult worm [19]. However, environmental stressors or toxicant exposures that cause DNA damage can increase the number of apoptotic cell bodies due to activation of the CEP-1 (p53) pathway [20]. CEP-1 activation by toxicant-induced DNA damage signals then begins a cascade of responses. Firstly, beginning with transcription of *egl-1* and *ced-13*, which encode proapoptotic BH3-only proteins [21–23]. In turn, EGL-1 and CED-13 antagonize CED-9/CED-4 complexes, *C. elegans* homologs for anti-apoptotic Bcl-2 protein and Apaf-1 in mammalian cells, dissociating CED-4, facilitating CED-4 association to CED-3 proenzymes [24–26]. The association of CED-4 and CED-3 initiates release of caspase that ultimately prosecutes the cell into an apoptotic state [27–29]. A number of other proapoptotic components have been identified within *C. elegans* that share homology with vertebrate organisms, such as LIN-35 (Retinoblastoma (pRb) protein), DPL-1 (E2F heterodimeric subunit),

and EFL-1/-2 (E2F proteins which interact with DPL-1) [21, 30–32]. The genetic malleability of *C. elegans* has allowed development of various tester strains that provide unique ways to observe and evaluate the impacts of environmental contaminants on germ line apoptosis and its pathways listed above. For example, a strain known as MD701 (bcIs39 [lim-7p::ced-1::GFP + lin-15(+)]) was generated to aid in visualization of apoptotic cell bodies through use of a green fluorescent protein fused to CED-1, a protein expressed on phagocytic cells that recognizes cell corpses [33]. Another strain known as TJ1 is a CEP-1 defective, where activation of apoptosis by CEP-1 no longer occurs following exposure of a DNA damage inducing toxicants, such as PAHs. Experiments using both of these strains can provide insight into the mechanism of reproductive toxicity caused by environmental toxicants.

In this chapter, several methods are outlined to evaluate germ cell apoptosis in *C. elegans* from a genotypic and phenotypic perspective following exposure to the environmental contaminant mixture, the dispersed crude oil. This includes the utilization of *C. elegans* tester strains to visualize apoptotic bodies within the germ line and quantitative real-time PCR (qRT-PCR) technique to test gene expressions related to apoptosis pathways for toxicity mechanism study [20].

2 Materials

All solutions listed below should be prepared using ultrapure water or distilled water, preferably from a water purification system that can reach a resistivity of 18 MΩ·cm, and analytical grade reagents.

2.1 Buffers

1. Calcium chloride solution (1 M CaCl₂): Weigh and dissolve 147 g of CaCl₂·2H₂O with water and bring total volume to 1 L. Sterilize by autoclaving. Store at room temperature and only use in a sterile working environment.
2. K-medium solution: Weigh and dissolve 2.39 g KCl and 2.98 g NaCl with water and bring total volume to 1 L. Sterilize by autoclaving. Store at room temperature and only use in a sterile working environment.
3. M9 Buffer: Weigh and dissolve 6.0 g of sodium phosphate dibasic, 3 g potassium phosphate monobasic, 5 g sodium chloride, 0.25 g of magnesium sulfate heptahydrate with water and bring total volume to 1 L. Sterilize by autoclaving. Store at room temperature and only use in a sterile working environment.

4. Magnesium sulfate solution (1 M MgSO₄): Weigh and dissolve 246 g of MgSO₄·7H₂O with water and bring total volume to 1 L. Sterilize by autoclaving. Store at room temperature and only use in a sterile working environment.
5. Potassium phosphate buffer (1 M potassium phosphate, pH 6.0): First, to obtain a 1 M solution of potassium phosphate monobasic, weigh and dissolve 136 g with water and bring total volume to 1 L. Second, to obtain a 1 M solution of potassium phosphate dibasic, weigh and dissolve 174 g water and bring total volume to 1 L. To obtain potassium phosphate buffer with pH = 6.0, mix 869 mL of 1 M potassium phosphate monobasic with 132 mL of potassium phosphate dibasic. Following sterilization by autoclaving, check pH using a pH meter. Adjust pH using HCl or NaOH as needed. Store at room temperature.
6. Sodium hydroxide solution (10 M NaOH): Weight and dissolve 100 g NaOH in 250 mL water. Store at room temperature.
7. *C. elegans* synchronization solution: For a 5 mL solution, mix 1 mL of household bleach (NaOCl 5–6%), 0.25 mL of 10 M NaOH, and 3.75 mL of sterilized water.
8. Tween-20.

2.2 Growth Media for *C. elegans*

1. Cholesterol solution (5 mg/mL): Weigh and dissolve 50 mg of cholesterol in 10 mL of 200 proof ethanol. Do not autoclave.
2. Luria broth: Weigh and dissolve 10 g tryptone, 5 g yeast extract, and 5 g of NaCl with water to bring total volume to 1 L. Sterilize by autoclaving, cooldown to 55 °C and add 200 mg streptomycin. Store refrigerated and only use in a sterile working environment.
3. LB medium: Weigh and dissolve 10 g tryptone, 5 g yeast extract, 10 g NaCl, and 10 g agar with water and bring total volume to 1 L. Sterilize by autoclaving. Store refrigerated and only use in a sterile working environment.
4. Nematode growth medium (NGM): Weigh and dissolve 17 g agar, 3 g NaCl, and 2.5 g peptone and 975 mL water. Autoclave. Cool to 55°C and add 1 mL cholesterol solution, 1 mL 1 M CaCl₂, 1 mL 1 M MgSO₄, 25 mL potassium phosphate buffer (pH 6.0), and 0.2 g of streptomycin.
5. Glycerol 50%: Obtain analytical grade glycerol from Sigma-Aldrich. Mix 10 mL of ultrapure water and 10 mL of glycerol to a 20 mL tube. Vortex to ensure solution is homogenous. Store at room temperature.
6. *Escherichia coli* (*E. coli*) OP50 (Caenorhabditis Genetics Center (CGC) of University of Minnesota).

2.3 C. elegans Strains

Obtain *C. elegans* strains from *Caenorhabditis* Genetics Center (CGC) of University of Minnesota.

1. MD701 (bcIs39 [(lim-7)ced-1p::GFP + lin-15]).
2. TJ1 (cep-1(gk138) I.).
3. N2 (wild-type isolate).

2.4 C. elegans Germ Line Apoptosis Assay

1. Agar (2%): Weigh and dissolve 2 g of agar in 98 mL of water in a 250 mL Erlenmeyer flask. Microwave until dissolved completely.
2. Pasteur Pipettes.
3. Clear nail polish.
4. Levamisole 10 mM: Weigh and dissolve 24.1 mg levamisole hydrochloride in 10 mL of water.
5. SYTO™ 12 Green Fluorescent Nucleic Acid Stain (Thermo Fisher Scientific, Grand Island, NY).
6. Microscope slides and covers (Fisher Scientific, Waltham, MA, USA).
7. Deepwater Horizon Oil (BP Company).
8. Corexit 9500 chemical dispersant (NALCO Co, Naperville, IL).
9. Shaker or rotation device.

2.5 Apoptosis Gene Expression Assay

1. mirVana™ miRNA Isolation Kit obtained (Life Technologies, Carlsbad, CA).
2. NanoDrop ND-1000 (Nanodrop Technologies, Wilmington, DE, USA).
3. Acid-phenol:chloroform, pH 4.5 (Thermo Fisher Scientific, Grand Island, NY).
4. Primers (MilliporeSigma, Burlington, MA) (Table 1).
5. Reverse Primer PolyT (MilliporeSigma, Burlington, MA).
6. Eppendorf microcentrifuge tubes (250 μ L).
7. DNase/RNase-free water (Thermo Fisher Scientific, Grand Island, NY).
8. RNase Inhibitor (20 U/ μ L) (Thermo Fisher Scientific, Grand Island, NY).
9. dNTPs (100 mM) (Thermo Fisher Scientific, Grand Island, NY).
10. RT Buffer 10 \times (Thermo Fisher Scientific, Grand Island, NY).
11. MultiScribe™ Reverse Transcriptase (50 U/ μ L) (Thermo Fisher Scientific, Grand Island, NY).
12. Eppendorf Mastercycler® Pro PCR machine.

Table 1
Primer information for genes in germ line apoptosis pathway

Gene	Forward primer	Reverse primer
<i>Germ line apoptosis pathway</i>		
<i>ced-3</i>	AACAGTGCTCGTGGATCATG	TGACTTCAGTCAGCAGCTAAC
<i>ced-4</i>	TGCTGATGCTAAAAAGCGAAGACGA	TGGACGATCAATGAGTGCCTTGCA
<i>ced-9</i>	TGCACAGACAGATCAATGTCC	TTGTGTTCCCTCCAGTTGTTGC
<i>ced-13</i>	ATGCTTGCAACTCAAACACC	ACGTCTTGAATCCTGAGCCTAG
<i>cep-1</i>	AGGGCACGATTCACTGTTG	TTCATCGCTTCCTGGATGC
<i>dpl-1</i>	TACTCTACTGTACCTCCAGATCG	TCTCTGTTGCACTTGATGTGG
<i>ebl-1</i>	AGCAAGTCGAGATAACACG	TCATCTGGAGCATCAGCGTC
<i>ebl-2</i>	AGCACCAAGTGGCTCACAC	TCACATCGTCCTCGTCCTC
<i>egl-1</i>	TCTCAGGACTTCTCCTCGTG	GTCCAGAAAGACGATGGAAGA
<i>egl-38</i>	TCCTCTTGCTGACACAGTCG	TACACCTGGTCTGACAGATC
<i>lin-35</i>	TGATGATCTACGAGACGAAC	AGATCTTGAAGTCGACGAGC
<i>pax-2</i>	TTCCAGGAACGACACATTC	TGACCATTGGAGTTCTCATTGC
<i>sir-2.1</i>	TACTGAGATGCTCCATGAC	AGCAAGACGAACCACACGAAC

13. SYBR green PCR Master Mix.
14. PCR Plate, 384-wells (Thermo Fisher Scientific, Grand Island, NY).
15. MicroAmp™ Optical Adhesive Film and Applicator.
16. Liquid nitrogen.

3 Methods

3.1 NGM Agar Plates for *C. elegans* Maintenance and Synchronization

1. Prepare fresh NGM agar (*see* Subheading 2.2, item 4). Pour approximately 20 mL of cooled agar into 10 cm petri dishes, respectively. Place lids on covering 90% of the media to allow evaporation and let cool to room temperature under a sterile environment, and then fully cover the plate with lid.
2. Seal plates with parafilm tape and store in 4 °C.

3.2 *E. coli* OP50 Stocks and Seeding of NGM Agar

1. Prepare fresh Luria broth (*see* Subheading 2.2, item 2). Add ampicillin to a concentration of 1 mM. Make five aliquots of 3 mL each for stock bacteria.
2. Upon arrival of *E. coli* OP50 from CGC, isolate a single colony and inoculate a 3 mL aliquot. Repeat for other aliquots. Incubate at 37 °C overnight.

3. On the next day, take three of the four OP50 samples and dilute 1:1 with 50% glycerol. Aliquot all samples into 1.5 mL centrifuge tubes and store at -80 °C. These will serve as *E. coli* OP50 stocks to begin new cultures.
4. Aliquot 80–100 μ L (20–25 μ L) of bacteria from the fourth sample onto 10 cm NGM agar plates. Create a lawn of bacteria covering 50% of the agar using a sterile plastic spreader. Incubate at room temperature overnight.

3.3 Maintenance and Synchronization of C. elegans

1. Upon arrival of *C. elegans* (i.e., MD701, N2, and TJ1) from CGC, cut out several small pieces of agar containing worms and transfer with a flame-sterilized spatula to individual *E. coli* OP50 seeded NGM plates (50 mm). Place plates in an incubator set to 20°C.
2. Within each piece of transferred agar, there will be both worms and eggs. Hatching of eggs takes 10–12 h at 20°C [34]. Incubate plates until approximately 75% confluent with worms (i.e., 3–5 days). Worms will lay eggs during this period.
3. Isolate eggs using synchronization solution. Carefully pipette the egg/worm solution into a 15 mL falcon tube. Pellet worms by centrifuging for 2 min at 1200 $\times \text{g}$. Wash worms with M9 twice.
4. Let isolated eggs hatch and mature to larval stage 1 (L1) without food in M9 buffer. Transfer food-starved L1 worms to an NGM agar plate seeded with *E. coli* OP50 until L4 (~ 30 h from L1 stage at room temperature).
5. Repeat steps 1–4 to maintain the strain during experiment.

3.4 Preparation and Treatment of C. elegans

1. Prepare a 20:1 (v:v) stock solution of DWH oil and Corexit 9500 chemical dispersant (oil-dis) and then dilute ten times with K-media. Vortex vigorously to ensure a well-mixed solution.
2. Synchronize fresh worms (e.g., N2, MD701, or MD701) from five 10 cm agar plates using Subheadings 3.1–3.5. Hatch eggs and mature to L4. Harvest worms by washing plates five times with M9 buffer and pipetting into 50 mL conical tubes. Centrifuge worms at 1200 $\times \text{g}$ for 2 min. Carefully, aspirate media and discard. Repeat twice more with M9 buffer and once with K-media.
3. For oil-dis treatment solutions, add 100 μ L of *E. coli* OP50, 100 μ L worm solution, and 4 mL of K-media. Make three serial dilutions of oil-dis mixture stock: 10 \times , 40 \times , and 100 \times . Aliquot 100 μ L into treatment tubes which correspond to treatments of 500 \times , 2000 \times , and 5000 \times oil-dis mixture. Bring total volume up to 5 mL with K-media.

4. Incubate treatment solutions at 25 °C on a rotating shaker (60 RPMs) for 24 h. Proceed to Subheading 3.5 for expression of genes associated with germ line apoptosis, Subheading 3.6 for assessment of apoptotic cells within gonad arms of MD701 worms, or Subheading 3.7 for assessment of apoptotic cells within gonad arms of TJ1 worms.

3.5 Expression of Apoptosis-Associated Genes and Cytochrome P450 Genes

All tips and tubes used for the following procedure must be autoclaved and stored in a sterile environment to prevent contamination during PCR.

1. Following treatment of N2 adult worms, centrifuge and rinse with 10 mL of K-medium five times to remove residual oil-dis mixture and bacteria. Transfer the worm pellet to a 1.5 mL microcentrifuge tube and remove excess supernatant. Immediately flash-freeze the samples in liquid nitrogen and store at –80°C until RNA extraction.
2. Total RNA will be extracted using *mirVana™* miRNA Isolation Kit (Life Technologies). Remove frozen N2 worms from freezer and aliquot 400µL of lysis/binding solution and sonicate for 15–30 s to aid in digestion of the worm cuticle.
3. Add 40µL of miRNA homogenate additive to the worm lysate and mix well by vortexing and inverting the tube for many times. Incubate on ice for 10 min.
4. After the 10 min incubation, add 400µL of Acid-phenol: chloroform (*see Note 1*). Vortex vigorously for 30–60 s. Centrifuge at 10,000 × *g* for 5 min at room temperature.
5. Following centrifugation, the mixture will have two distinct phases. Carefully aspirate the aqueous layer (upper phase) and aliquot into a fresh 1.5 mL centrifuge tube.
6. Add 500µL of 100% ethanol to the RNA aqueous phase and mix thoroughly by vortexing.
7. For each sample, place a filter cartridge in collection tubes provided by the *mirVana™* miRNA Isolation Kit. Pipette sample lysate–ethanol mixture into the filter cartridge. Centrifuge the samples at 10,000 × *g* for 10 s at room temperature (*see Note 2*).
8. Discard the flow-through, as RNA will be bound to the filter cartridge resin. Rinse the filter once more with 500µL of 100% ethanol to remove any residual contaminants. Centrifuge and discard the flow-through as described in step 7.
9. Add 700µL *miRNA Wash Solution 1* from the *mirVana™* miRNA Isolation Kit to each sample filter cartridge and centrifuge at 10,000 × *g* for 10 s at room temperature. Discard the flow-through.

10. Add 500µL *miRNA Wash Solution 2/3* to each sample filter cartridge and centrifuge at 10,000 × φ for 10 s at room temperature. Discard the flow-through and repeat for a third wash with *Wash Solution 2/3*. Discard the flow-through.
11. Transfer sample filter cartridges to fresh collection tubes and apply 50µL of preheated 95 °C, nuclease-free H₂O to the center of the filter resin. Centrifuge the tube at 10,000 × φ for 30 s at room temperature (*see Note 3*).
12. Evaluate the quality and purity of total RNA by using a Nano-Drop ND-1000 (Nanodrop Technologies, Wilmington, DE, USA). Good-quality RNA for RT-PCR should have A_{260}/A_{280} of 1.8–2.2 and A_{260}/A_{230} ratios of >1.75. This is a stopping point in the procedure where samples can be stored at –20 °C until RT-PCR.
13. RT-PCR will be conducted using the *TaqMan® MicroRNA Reverse Transcription Kit* from Thermo Fisher. Thaw PCR reagents on ice and mix carefully prior to use. Make RT-PCR 15µL as described in Table 2 using 250µL microcentrifuge tubes.
14. Close tube caps tightly and place samples into an Eppendorf Mastercycler® Pro PCR machine with the temperature program: (1) initial stage of 16 °C for 30 min, (2) followed by 42 °C for 30 min, and (3) a final stage of 85°C for 5 min followed by a holding period at 4 °C until samples could be stored at –20 °C.
15. Thirteen protein-coding genes (*ced-13*, *ced-3*, *ced-4*, *ced-9*, *cep-1*, *dpl-1*, *efl-1*, *efl-2*, *egl-1*, *egl-38*, *lin-35*, *pax-2*, and *sir-2.1*) in the germ line apoptosis pathway and five cytochrome P450 (CYP450) genes (*cyp14a3*, *cyp35a1*, *cyp35a2*, *cyp35a5*, and *cyp35c1*) encoding enzymes responsible for metabolizing

Table 2
Reverse transcription (RT) PCR solution

Component	Volume
Nuclease-free H ₂ O	Vol. dependent on RNA concentration
RNase inhibitor, 20 U/µL	0.19
100 mM dNTPs (with dTTP)	0.15
10× reverse Transcription buffer	1.5
Poly(T) Primer mix (1:10 dilution in nuclease-free H ₂ O)	2.00
MultiScribe™ reverse transcriptase, 50 U/µL	1.00
RNA Sample (1000 ng)	Vol. dependent on RNA concentration
Total	15

Table 3
Quantitative real-time PCR (qRT-PCR) solution

Component	Volume
Nuclease-free H ₂ O	5.5
SYBR Green PCR master mix	7.5
cDNA (diluted 1:1 in nuclease-free H ₂ O)	1
Primer	1
Total	15

PAH compounds were tested following exposure of oil-dis and PAH compounds to *C. elegans*. Y45F10D.4, a gene that codes for an iron–sulfur binding protein required for embryonic viability, will be used as a reference gene for normalization of data using the $\Delta\Delta C_t$ method [6, 35].

16. Thaw cDNA and reagents on ice and mix thoroughly. Prepare reactions in triplicate based on Table 3. Keep samples and qRT-PCR sample plate on ice during the loading process. Use a 12-channel pipette to carefully load samples into the wells of a 384-well plate (see Note 4).
17. Seal the qRT-PCR plate with clear MicroAmp™ Optical Adhesive Film using the MicroAmp™ Adhesive Film Applicator. Briefly, centrifuge plates to ensure reaction solutions reach the bottom of the wells and to remove any bubbles formed during the loading process.
18. Place the plate into the sample tray of a ViiA™ 7 Real-Time PCR System. Program the following temperature settings: an initial enzyme activation step of 95 °C for 10 min, followed by denaturation for 15 s at 95 °C, and lastly, an annealing/extension step for 60 s at 60 °C. Repeat the final two steps, denaturing and annealing/extension, for 40 cycles. Export data following completion of the 40th cycle and analyze data using the $\Delta\Delta C_t$ method [35] (Fig. 1).

3.6 Assessment of Apoptotic Germ Cells in MD701 Worms

1. Following a 24 h exposure period, pellet worms by centrifuging at 1200 × g for 2 min and thoroughly wash worms with 10 mL of K-media.
2. Transfer worms to an NGM agar seeded with *E. coli* OP50 during the observation process.
3. Place a small dot of fresh 2% liquid agar in the middle of a microscope slide using a Pasteur pipette and apply another microscope slide (the second slide) on top of the dot at 90° angle with the first slide to press the agar dot into a thin layer.

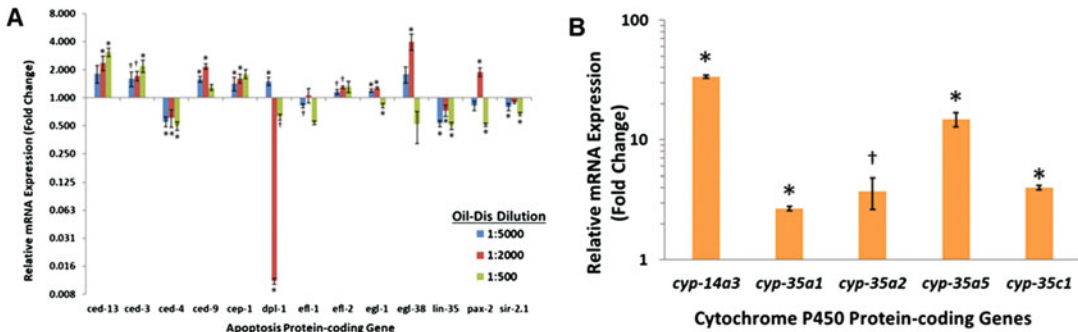


Fig. 1 (a) mRNA expression of apoptosis following exposure to various solutions of dispersed crude oil (oil-dis mixture), normalized to reference gene Y45F10D.4 using the $\Delta\Delta CT$ method [20]. (b) CYP450 protein-coding genes following exposure to 1:5000 dispersed oil [5]. Values greater than one are classified as upregulation; values less than one are classified as downregulation of the gene. The function of these genes can be further studied using the advanced technologies, including transgenic, RNAi and CRISPR/Cas genome editing [36]. Notations above the expression bars indicate statistical significance at either $p < 0.05$ (†) or $p < 0.01$ (*).

After the agar layer is solidified, remove the second slide. This should result in a thin layer of agar to allow observation of *C. elegans* under a fluorescence microscope.

- Using a compound light microscope, transfer 1–5 worms onto a 2% agar microscope slide. Carefully add 2 μ L of 10 mM levamisole to paralyze worms, preventing worm movement during analysis. Let the slide rest for 2–3 min. Place a clear microscope coverslip over the worms and seal with a thin layer of clear nail polish (*see Note 5*).
- Prepare the Zeiss Axio Observer Z1 microscope by first turning on the microscope and power source. Let warmup for 15 min prior to analysis.
- Place the agar slide onto the stage upside down. Isolate a single worm under transmitted light. Add a small drop of oil prior to slide contact and switch to a 64 \times oil-immersion objective. Once the worm gonad arm is within view, switch to the GFP cube of the microscope. Adjust the fine focus until the loop area of the worm gonad comes into view. Apoptotic cells are bright green fluorescent circles in the loop area of the gonad arm (Fig. 2). Count and record apoptotic cells in both gonad loop arms (Fig. 3).

3.7 Assessment of Apoptotic Germ Cells in TJ1 Worms

As TJ1 does not contain a GFP to visualize apoptotic bodies, the cells must first be stained prior to observation. The following protocol for SYTO 12 staining was adapted from Gumienny et al. [19]. Since SYTO 12 stains nucleic acids and apoptotic cells have condensed chromosome arrangement, the apoptotic germ cells can be identified as solid GFP dots.

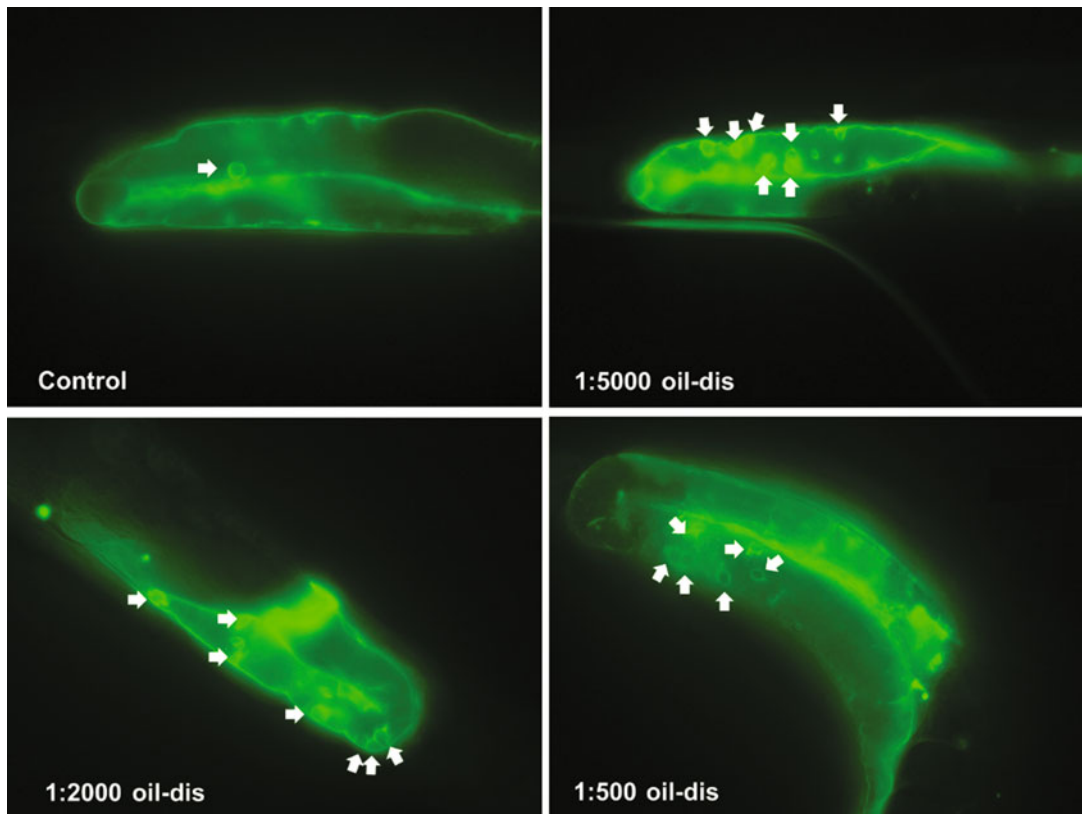


Fig. 2 Germ cell apoptosis located in the gonad arm loop identifiable as green fluorescent circles in the MD701 (bcls39 [(lim-7)ced-1p::GFP + lin-15(+)]) strain worms [20]. As shown with the images, worms treated with oil-dis mixtures demonstrated a greater number of apoptotic cell bodies

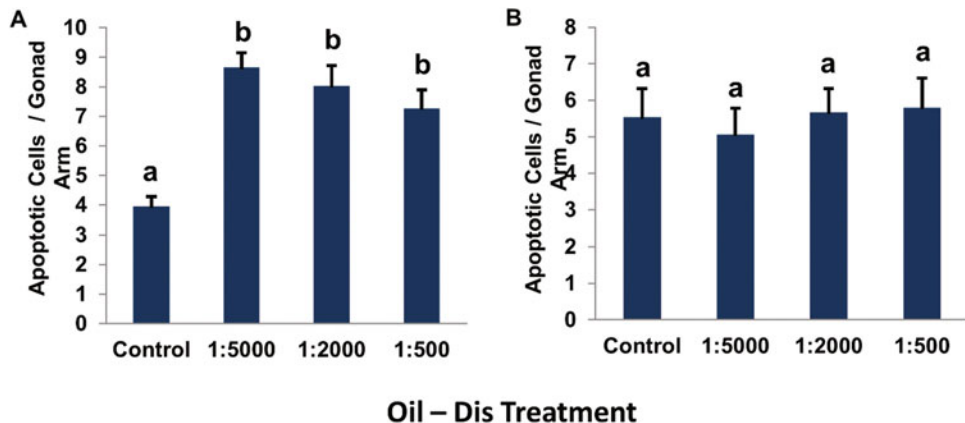


Fig. 3 Apoptotic cell counts per gonad arm of (a) MD701 and (b) TJ1 worms treated with various dilutions of the oil-dis mixture [20]. Statistical significance was determined by one-way ANOVA with a p -value < 0.05 . Different letters above the standard error of the mean bars determine statistically significant groups. There are no significant differences among control and different treatments

1. Thaw SYTO 12 stain on ice while covered or wrapped in aluminum foil to protect from direct light.
2. Following a 24 h exposure period, pellet worms by centrifuging at $1200 \times g$ for 2 min and thoroughly wash worms with 10 mL of K-media.
3. Dilute worms to approximately 50 worms/100 μ L in M9. Aliquot 100 μ L into a 250 μ L centrifuge tube and add 0.75 μ L of SYTO 12 stain; wrap in aluminum foil. Incubate with slow inversion to ensure efficient mixing for 1–2 h.
4. After incubation, pellet worms by centrifugation at $1200 \times g$ for 2 min. Discard supernatant and add 200 μ L of M9/0.1% Tween-20. Centrifuge, discard supernatant, and repeat for three washes.
5. Transfer worms to an NGM agar plate seeded with *E. coli* OP50. Allow worms to rest for 1 h at 25 °C.
6. Prepare a thin layer of agar pad as described in Subheading 3.6, step 3 for microscope observation.
7. Using a compound light microscope, transfer 1–5 worms onto a 2% agar microscope slide. Carefully add 2 μ L of 10 mM levamisole to paralyze worms, preventing worm movement during analysis. Let the slide rest for 2–3 min. Place a clear microscope coverslip over the worms and seal with a thin layer of clear nail polish.
8. Prepare the Zeiss Axio Observer Z1 microscope by first turning on the microscope and power source. Let warmup for 15 min prior to analysis.

Place the agar slide onto the stage upside down. Isolate a single worm under transmitted light. Add a small drop of oil prior to slide contact and switch to a 64 \times oil-immersion objective. Once the worm gonad arm is within view, switch to the GFP cube of the microscope. Adjust the fine focus until the loop area of the worm gonad comes into view. Apoptotic cells

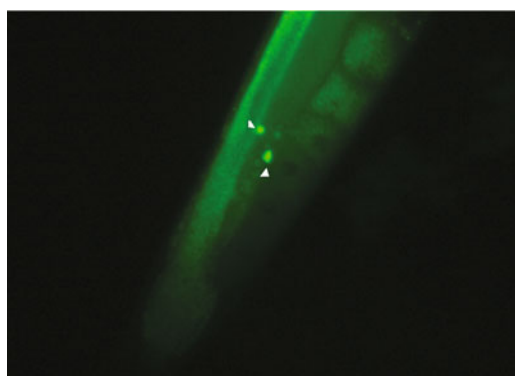


Fig. 4 A demonstration of SYTO 12 staining/apoptotic cells appear as solid bright green fluorescent dots in the gonad arm

are solid bright green fluorescent dots in the loop area of the gonad arm (Fig. 4). Count and record apoptotic cells in both gonad loop arms.

4 Notes

1. Acid-phenol:chloroform solution has two phases, an aqueous (upper) and an organic (lower) phase. RNA extraction using this reagent requires the organic phase (lower). Collect the organic (lower) phase by making sure the pipette is fully plunged of air prior to entering the aqueous (upper) phase. This will limit the amount of aqueous solution used during RNA extraction.
2. Take caution when centrifuging the filter cartridges as it is possible for them to shift up, causing the filter not to lie flat on the surface of the cartridge. To prevent this from happening, reduce spinning force and the length of time for operation.
3. Begin heating nuclease-free H₂O prior to extraction of RNA. Carefully apply the water to the middle of the filter resin. Spin through and collect the flow-through. To help with recovery, it is possible to reapply the flow-through to the resin.
4. Loading of the 384-well PCR plate can be challenging, as 15µL is difficult to see in the small wells. To help with visualizing sample loading, place the pipette tips at a 45° angle and insert into well, without touching the sides. Load the sample onto the well plate walls. A small droplet of liquid should be easily visible, confirming proper loading of the sample. The PCR droplet will be pulled down to the bottom of the well during centrifugation.
5. If the agar layer is too thick, the coverslip will not seal the agar to the slide possibly making observation of worms more challenging under oil-immersion objectives. To fix this problem, draw a 2 cm diameter circle using clear nail polish on a slide and let air-dry for a few minutes. Drop fresh, warm 2% agar in the middle, and spread by applying another slide on the top of the first the microscope slide in 90° angle with the agar pad in the intersection. Let dry and continue with Subheading 3.5, step 4.

References

1. Almeda R, Wambaugh Z, Wang Z, Hyatt C, Liu Z, Buskey EJ (2013) Interactions between zooplankton and crude oil: toxic effects and bioaccumulation of polycyclic aromatic hydrocarbons. PLoS One 8
2. De Flora S, Bagnasco M, Zanacchi P (1991) Genotoxic, carcinogenic, and teratogenic hazards in the marine environment, with special reference to the Mediterranean Sea. Mutat Res 258:285–320

3. Finch BE, Wooten KJ, Faust DR, Smith PN (2012) Embryotoxicity of mixtures of weathered crude oil collected from the Gulf of Mexico and Corexit 9500 in mallard ducks (*Anas platyrhynchos*). *Sci Total Environ* 426:155–159
4. Speight JG (1999) The chemistry and technology of petroleum, 3rd edn. Marcel Dekker, New York
5. Polli JR, Rushing BR, Lish L, Lewis L, Selim MI, Pan X (2020) Quantitative analysis of PAH compounds in DWH crude oil and their effects on *Caenorhabditis elegans* germ cell apoptosis, associated with CYP450s upregulation. *Sci Total Environ* 745:140639
6. Zhang YQ, Chen DL, Ennis AC, Polli JR, Xiao P, Zhang BH, Stellwag EJ, Overton A, Pan XP (2013) Chemical dispersant potentiates crude oil impacts on growth, reproduction, and gene expression in *Caenorhabditis elegans*. *Arch Toxicol* 87:371–382
7. Techtmann SM, Zhuang M, Campo P, Holder E, Elk M, Hazen TC, Conmy R, Santo Domingo JW (2017) Corexit 9500 enhances oil biodegradation and changes active bacterial community structure of oil-enriched microcosms. *Appl Environ Microbiol* 83: e03462-16
8. Mu J, Jin F, Ma X, Lin Z, Wang J (2014) Comparative effects of biological and chemical dispersants on the bioavailability and toxicity of crude oil to early life stages of marine medaka (*Oryzias melastigma*). *Environ Toxicol Chem* 33:2576–2583
9. Kim JH, Stansbury KH, Walker NJ, Trush MA, Strickland PT, Sutter TR (1998) Metabolism of benzo[a]pyrene and benzo[a]pyrene-7,8-diol by human cytochrome P450 1B1. *Carcinogenesis* 19:1847–1853
10. Shimada T, Fujii-Kuriyama Y (2004) Metabolic activation of polycyclic aromatic hydrocarbons to carcinogens by cytochromes P450 1A1 and 1B1. *Cancer Sci* 95:1–6
11. Thakker DR, Yagi H, Sayer JM, Kapur U, Levin W, Chang RL, Wood AW, Conney AH, Jerina DM (1984) Effects of a 6-fluoro substituent on the metabolism of benzo(a)pyrene 7,8-dihydrodiol to bay-region diol epoxides by rat liver enzymes. *J Biol Chem* 259:11249–11256
12. Thakker DR, Yagi H, Akagi H, Koreeda M, Lu AH, Levin W, Wood AW, Conney AH, Jerina DM (1977) Metabolism of benzo[a]pyrene. VI. Stereoselective metabolism of benzo[a]pyrene and benzo[a]pyrene 7,8-dihydrodiol to diol epoxides. *Chem Biol Interact* 16:281–300
13. Dinu D, Chu C, Veith A, Lingappan K, Couroucli X, Jefcoate CR, Sheibani N, Moorthy B (2016) Mechanistic role of cytochrome P450 (CYP)1B1 in oxygen-mediated toxicity in pulmonary cells: a novel target for prevention of hyperoxic lung injury. *Biochem Biophys Res Commun* 476:346–351
14. Choi DJ, Marino-Alessandri DJ, Geacintov NE, Scicchitano DA (1994) Site-specific benzo[a]pyrene diol epoxide-DNA adducts inhibit transcription elongation by bacteriophage T7 RNA polymerase. *Biochemistry* 33:780–787
15. Shiizaki K, Kawanishi M, Yagi T (2017) Modulation of benzo[a]pyrene-DNA adduct formation by CYP1 inducer and inhibitor. *Genes Environ* 39:14
16. Shimizu Y, Nakatsuru Y, Ichinose M, Takahashi Y, Kume H, Mimura J, Fujii-Kuriyama Y, Ishikawa T (2000) Benzo[a]pyrene carcinogenicity is lost in mice lacking the aryl hydrocarbon receptor. *Proc Natl Acad Sci U S A* 97:779–782
17. Spink DC, Wu SJ, Spink BC, Hussain MM, Vakharia DD, Pentecost BT, Kaminsky LS (2008) Induction of CYP1A1 and CYP1B1 by benzo(k)fluoranthene and benzo(a)pyrene in T-47D human breast cancer cells: roles of PAH interactions and PAH metabolites. *Toxicol Appl Pharmacol* 226:213–224
18. L'Hernault SW (2009) The genetics and cell biology of spermatogenesis in the nematode *C. elegans*. *Mol Cell Endocrinol* 306:59–65
19. Gumienny TL, Lambie E, Hartwig E, Horvitz HR, Hengartner MO (1999) Genetic control of programmed cell death in the *Caenorhabditis elegans* hermaphrodite germline. *Development* 126:1011–1022
20. Polli JR, Zhang Y, Pan X (2014) Dispersed crude oil amplifies germ cell apoptosis in *Caenorhabditis elegans*, followed a CEP-1-dependent pathway. *Arch Toxicol* 88:543–551
21. Gartner A, Boag PR, Blackwell TK (2008) Germline survival and apoptosis. *WormBook : the online review of C elegans biology*:1–20
22. Conradt B, Horvitz HR (1998) The C-elegans protein EGL-1 is required for programmed cell death and interacts with the Bcl-2-like protein CED-9. *Cell* 93:519–529
23. Schumacher B, Schertel C, Wittenburg N, Tuck S, Mitani S, Gartner A, Conradt B, Shaham S (2005) C-elegans ced-13 can promote apoptosis and is induced in response to DNA damage. *Cell Death Differ* 12:153–161
24. Shaham S, Horvitz HR (1996) An alternatively spliced C-elegans ced-4 RNA encodes a novel cell death inhibitor. *Cell* 86:201–208

25. Bossy-Wetzel E, Newmeyer DD, Green DR (1998) Mitochondrial cytochrome c release in apoptosis occurs upstream of DEVD-specific caspase activation and independently of mitochondrial transmembrane depolarization. *EMBO J* 17:37–49
26. Lord CE, Gunawardena AH (2012) Programmed cell death in *C. elegans*, mammals and plants. *Eur J Cell Biol* 91:603–613
27. Xue D, Shaham S, Horvitz HR (1996) The *Caenorhabditis elegans* cell-death protein CED-3 is a cysteine protease with substrate specificities similar to those of the human CPP32 protease. *Genes Dev* 10:1073–1083
28. Shaham S, Reddien PW, Davies B, Horvitz HR (1999) Mutational analysis of the *Caenorhabditis elegans* cell-death gene ced-3. *Genetics* 153:1655–1671
29. Chen F, Hersh BM, Conradt B, Zhou Z, Riemer D, Gruenbaum Y, Horvitz HR (2000) Translocation of *C. elegans* CED-4 to nuclear membranes during programmed cell death. *Science* 287:1485–1489
30. Chi W, Reinke V (2009) DPL-1 (DP) acts in the germ line to coordinate ovulation and fertilization in *C. elegans*. *Mech Dev* 126:406–416
31. Ceol CJ, Horvitz HR (2001) Dpl-1 DP and efl-1 E2F act with lin-35 Rb to antagonize Ras signaling in *C. elegans* vulval development. *Mol Cell* 7:461–473
32. Boxem M, van den Heuvel S (2002) *C. elegans* class B synthetic multivulva genes act in G (1) regulation. *Current Biol* 12:906–911
33. Zhou Z, Hartwig E, Horvitz HR (2001) CED-1 is a transmembrane receptor that mediates cell corpse engulfment in *C. elegans*. *Cell* 104:43–56
34. Sulston JE, Schierenberg E, White JG, Thomson JN (1983) The embryonic cell lineage of the nematode *Caenorhabditis elegans*. *Dev Biol* 100:64–119
35. Livak KJ, Schmittgen TD (2001) Analysis of relative gene expression data using real-time quantitative PCR and the 2(-Delta Delta C (T)) method. *Methods* 25:402–408
36. Li C, Brant E, Budak H, Zhang BH (2021) CRISPR/Cas: a Nobel Prize award-winning precise genome editing technology for gene therapy and crop improvement. *Journal of Zhejiang University SCIENCE B*, 22 (4):253–284. <https://doi.org/10.1631/jzus.B2100009>.



Chapter 2

High-Throughput Measurement for Toxic Effects of Metal Mixtures in *Caenorhabditis elegans*

Kathy S. Xue and Lili Tang

Abstract

The contamination of heavy metals, a class of naturally occurring and persistent toxicants, has become a major public health concern due to increasing industrial and anthropogenic activities. The use of COPAS Biosort, a flow cytometer capable of measuring thousands of nematodes in minutes via high-throughput assays, has been widely applied in *C. elegans* studies for assessing toxicity of individual metals; however, such application yet to be seen for metals or other chemical mixtures. In the present protocol, we investigated toxic effects of individual metals, Cd, Pb, and Mn, as well as their binary and ternary mixtures, using nematode *C. elegans*. The toxic outcomes, including effects on growth, reproduction, and feeding behavior, were measured using high-throughput platform analysis (COAPS Biosort).

Key words *Caenorhabditis elegans*, Cadmium, Manganese, Lead, Metal mixtures, COPAS Biosort, Growth, Brood size, Feeding

1 Introduction

It is well known that exposure to heavy metals can cause serious health problems, such as bone damage, kidney disease, renal tubular dysfunction, cancer, and even death [1–5]. Furthermore, metals can induce neurotoxicity, which includes altered neuronal excitability and impaired chemosensation, processes that were prominently involved in neurodegenerative diseases [6]. In natural environments, these metals are typically found as mixtures, which organisms that inhabit these environments are likely exposed to [7, 8]. Although the individual concentrations of these metals in the environment may be low, the combined concentrations could result in significantly greater toxicity via possible interactions [9]; therefore, further understanding of the combined toxic effects of metal mixtures, such as additive, synergistic, or antagonistic effect, are needed. With the broad usage of chemicals, as well as increasing number of new chemicals introduced into the environment over

time, strategies for rapid toxicological assessment, in a manner predictive of the chemicals' effects on human health, are in high demand.

C. elegans is a genetically and molecularly tractable model organism that provides many advantages for the assessment of environmental toxicants [10–13]. High-throughput toxicity screens using *C. elegans* can be carried out via robotic liquid-handling workstations, the most popular being COPAS Biosort (Biosort, Union Biometrica, Inc., Holliston MA), a flow cytometer capable of measuring thousands of nematodes in minutes [14]. This instrument also has the capacity for simultaneous analyses of multiple parameters, including length, motion, and fluorescence, of worms deposited in 96-well plate experiments, thus allowing for a quick and inexpensive method for toxicity testing [15–17]. While high-throughput assays using COPAS Biosort has been widely applied in *C. elegans* studies assessing toxicity of single metals, such application has yet to be seen in studies involving metal mixtures.

In this chapter, we investigated toxic effects of metals, Cd, Pb, and Mn, in their binary and ternary mixtures, using nematode *C. elegans*. The toxic outcomes, including effects on growth, reproduction, and feeding behavior, were measured using high-throughput platform analysis (COAPS Biosort). For the purpose of identifying and quantifying the interactions between the three metals, results were then analyzed using the combination index (CI) method [18], which has previously been applied to pollutant interactions [19, 20].

2 Materials

2.1 *C. elegans Strains*

The wild-type N2 strain of *C. elegans* was obtained from the *Cae-norhabditis* Genetics Center (Minneapolis, MN). Following the standard procedures, the worms were grown and maintained on nematode growth medium (NGM) plates seeded with *E. coli* strain OP50.

2.2 *Solutions Preparation*

All solutions were prepared with ddH₂O, and stored at room temperature, unless otherwise indicated.

1. OP50 broth (*E. coli* stock solution): Dissolve 0.25 g NaCl and 0.5 g Bacto-peptone in 50 mL ddH₂O and autoclave (see Note 1). A loop of starter culture is then inoculated and grown for 24 h in 37 °C water bath with aeration. Stored broth at 4 °C. Make 50 mL broth.
2. LB broth: Weigh out 3.00 g beef extract, 5.00 g Bacto-peptone, and 5.00 g lactose, then dissolve contents in 1 L of ddH₂O in flask. Autoclave the contents (see Note 1). Inoculate

the LB broth with approximately 1 mL of OP 50 stock broth, then incubate overnight at 37 °C with aeration. Store broth at 4 °C which may be used for up to 1 month.

3. K-medium: Dissolve 2.36 g KCl and 3 g NaCl in 1 L ddH₂O, then autoclave. Makes 1 L solution.
4. 1 M CaCl₂: Dissolve chemical in ddH₂O, then autoclave.
5. MgCl₂: Dissolve chemical in ddH₂O to a final 1 M concentration, then autoclave.
6. M9 buffer: Dissolve 3 g KH₂PO₄, 6 g Na₂HPO₄, 5 g NaCl, and 1 mL 1 M MgSO₄ in 1 L ddH₂O, then autoclave. Makes 1 L solution.
7. Bleaching solution: Dissolve 1 g NaOH in 80 mL ddH₂O mixed with 20 mL 5.25% NaClO (Clorox). No autoclave required. Makes 100 mL solution. Prepare fresh prior to use.
8. Cholesterol: Dissolve 0.5 g cholesterol in 100 mL ethanol, with slow heating to facilitate dissolution if necessary. Makes 100 mL of 5 mg/mL cholesterol stock solution. Store at 4 °C and do not autoclave.
9. Red fluorescent microsphere beads: Dilute the fluorescent microsphere beads solution (Polysciences, Inc.) to 1:20 in K-medium.
10. Stock chemical solutions for dosing: Dissolve analytical grade metal salts, cadmium chloride (CdCl₂), lead chloride (PbCl₂), or manganese chloride (MnCl₂), in K-medium to make 1 M stock solutions. Serial-dilute the stock solutions using K-medium [21] to make work concentrations, with OP50 (1 mg/mL) [22] as food source, unless required for specific test conditions (*see Note 2*).
11. Nematode growth medium (NGM) plates: Dissolve 2.36 g KCl, 3 g NaCl, 2.5 g Bacto-peptone, and 17 g Bacto-agar in 1 L ddH₂O in flask, then add a magnetic stir bar into the flask and autoclave with flask opening covered with double tin foil. When cooled to approximately 55 °C (close to cool-to-touch), add 1 mL 1 M CaCl₂, 1 mL 1 M MgSO₄, and 1 mL cholesterol (5 mg/mL) to agar, and mix well. Using sterile procedure, dispense 25 mL aliquots of agar into standard size (100 mm) petri plates (for alternative sizes, *see Note 3*). Allow agar to solidify at room temperature with UV treatment for at least 2 h, up to overnight. One liter of agar should yield ~40 standard size plates.
12. Nematode growth medium (NGM) + OP50: Seed ~100 µL of OP50 broth onto each NGM plate (this is for standard 100 mm size; for alternative sizes, *see Note 3*). Spread the liquid droplets evenly onto the plate with a sterile glass spreader. The spreader may be sterilized for repeated use, by

first dipping it into distilled deionized water, then in ethanol, and then burn the ethanol off in flame. Allow the liquid to dry, then stack the plates within their original plastic packaging bags and incubate at 37 °C for least 24 h to establish a bacterial lawn with sufficient OP50 count. Store the seeded plates at 4 °C in fridge.

2.3 Preparation of Reagents for COPAS Biosort

Reagents listed here are required for a typical run with COPAS Biosort regardless of experimental design. For detailed usages, see Note 4.

1. 10% sodium hypochlorite (Clorox): Dilute 200 mL in milli-Q water, bring to 2 L. Filter with 1 L Stericup (Millipore) to sterilize and remove all particulate matter.
2. Sterile H₂O: Autoclave 4 L milli-Q water.
3. Sheath fluid: Prepare 3 L PBS and add Triton X-100 to final concentration of 0.01%. Filter to sterilize.

1. COPAST™ Biosort (Union Biometrica).
2. 96-well plates.
3. Plate shaker.
4. Dissecting microscope.
5. 20 °C incubator, 4 °C fridge, water bath capable of temperature adjustment.

3 Methods

3.1 Preparation of Age-Synchronized L1 Growth-Arrested Larvae

1. Rinse gravid three-day-old adult nematodes and embryos off NGM plates with K-medium, and transfer to 15-mL centrifuge tubes.
2. Centrifuge the worms at $450 \times g$ for 7 min, then carefully aspirate the supernatant.
3. Resuspend the pellet with 10 mL of bleaching solution, gently agitate the contents to break up clumps of pellet with a glass dropper for approximately 4 min. Then centrifuge the tube at $450 \times g$ for 7 min. Immediately aspirate the supernatant after centrifugation, as prolonged exposure to concentrated bleaching solution may reduce egg quality.
4. Resuspend the pellet once more with approximately 10 mL K-medium. Agitate gently via shaking, then pellet the contents via centrifugation at $700 \times g$ for 7 min. Carefully aspirate the supernatant to approximately 0.5 mL of volume. Repeat this process twice to further dilute the remaining bleaching solution.

5. Gently resuspend the embryos with a sterile glass pipet and transfer all contents to a sterile, large well culture plate (with lid), containing K-medium approximately 5 mm in height from the bottom of the wells.
6. Incubate the embryos in 20 °C with cover and allow them to hatch in the absence of food overnight, to yield a synchronized L1 population.

3.2 Preparing Food Source for Liquid-Based Test

Food source was prepared from L-broth, which was pelleted via centrifugation, washed with K-medium, and finally combined with the rest of the contents of the work solution. The work solution concentrations should be prepared in advance by direct measurement or by dilution. Here the chemicals tested are water-soluble salt and thus diluted via K-medium and added directly to food source (for alternatives, *see Note 2*). Typical 48-h test requires approximately 1 mg/mL OP50, though for longer durations or larger populations, the OP50 concentration may be increased to 2 mg/mL, i.e., using twice the amount of L-broth.

1. Determine total amount L-broth needed. For the 1 mg/mL concentration used in typical 48-h test, the amount of L-broth needed is usually equivalent to total work solution volume, though may multiply by 1.5 to be safe. Zero the weighing scale with a centrifuge tube of appropriate size, then pour L-broth into the said tube. Heat the foil and neck of flask with the flame before replacing foil onto flask.
2. Centrifuge the L-broth at $1000 \times g$ for 6 min to pellet the OP50. Rinse the contents twice with K-medium (resuspend with same volume, centrifuge at $1000 \times g$ for 6 min, then aspirate supernatant). Weigh the final pellet in the tube on the zeroed scale.
3. Resuspend the contents in K-medium to a final OP50 concentration of 1 mg/mL for typical 48-h test, vortex to mix.
4. Determine the total amount of work solution required for control and test concentrations (total required \times 1.5) and dispense the resuspended OP-50 of the same volume to each designated tube. Pellet each tube once more via centrifugation ($1000 \times g$, 6 min) and remove the supernatant.
5. Add the required volumes of work solution to each tube (onto the pellets).
6. Vortex to resuspend pellet. Each tube should now have the desired concentrations of the test solution, in media, with food source present. These can then be dispensed into the well trays for each test.

3.3 General Experimental Design

1. Solutions of Cd, Pb, Mn, and their binary and tertiary combinations were prepared as described in previous section.
2. The concentration ranges were determined by $4\times$, $2\times$, $1\times$, $0.5\times$, and $0.25\times$ of EC₅₀ of individual metals, which were generated in exposure experiments with individual metal, plus a zero concentration as uninhibited control (Table 1).
3. *C. elegans* was treated with serial dilutions of individual metal, as well binary and tertiary combinations at a fixed constant ratio of 1:1 or 1:1:1 in terms of EC₅₀ values of individual metals.
4. All treatment groups, including control groups, were tested in three independent experiments with replicates.

Table 1
Concentration design template for metal mixtures of Cd, Mn, and Pb

Cd	Mn	Pb
4× EC ₅₀	4× EC ₅₀	—
2× EC ₅₀	2× EC ₅₀	—
EC ₅₀	EC ₅₀	—
0.5× EC ₅₀	0.5× EC ₅₀	—
0.25× EC ₅₀	0.25× EC ₅₀	—
—	4× EC ₅₀	4× EC ₅₀
—	2× EC ₅₀	2× EC ₅₀
—	EC ₅₀	EC ₅₀
—	0.5× EC ₅₀	0.5× EC ₅₀
—	0.25× EC ₅₀	0.25× EC ₅₀
4× EC ₅₀	—	4× EC ₅₀
2× EC ₅₀	—	2× EC ₅₀
EC ₅₀	—	EC ₅₀
0.5× EC ₅₀	—	0.5× EC ₅₀
0.25× EC ₅₀	—	0.25× EC ₅₀
4× EC ₅₀	4× EC ₅₀	4× EC ₅₀
2× EC ₅₀	2× EC ₅₀	2× EC ₅₀
EC ₅₀	EC ₅₀	EC ₅₀
0.5× EC ₅₀	0.5× EC ₅₀	0.5× EC ₅₀
0.25× EC ₅₀	0.25× EC ₅₀	0.25× EC ₅₀

3.4 Prepare Worms for Sorting Using COPAS Biosort

1. Wash worms off the plates with K-medium, if grown on NGM. Transfer the media containing worms to a 15 mL centrifuge tube.
2. Wash worms: Allow worms to settle via gravity (for L4 stage or adult worms) or centrifugation at $120 \times g$ for 1 min (for L1 stage worms). Remove supernatant until approximately 0.5 mm liquid remains above pellet. Resuspend the pellet with 10 mL K-medium and repeat the wash twice.
3. Resuspend the content to approximately 100 animals/mL in K-medium. Check for any particulate matter under dissecting microscope and remove any visible debris with a micropipette.

3.5 Optimizing COPAS Biosort for Worm Sorting and Dispensing

1. Prime COPAS Biosort (*see Note 4*).
2. Place worms into the sample cup and fasten the lid to ensure system pressure is maintained. Acquire data on 500 animals to collect the population distribution data. Adjust the sample pressure to obtain stable flow of the objects (optimally 15–50 events per second). Edit GATE and SORT regions to select the desired population. For defining GATE and SORT region, it is recommended to use age-synchronized worms as required by the experiment.
3. Click Fill button to dispense five worms to five wells. Confirm sorting of correct number and size of worms under a microscope. If the number of dispensed worms is not accurate, adjust the Width and Delay values in COPAS software. Then repeat the confirmation steps until obtaining an accurate number of dispensed worms.
4. Once the sorting parameters have been optimized, worms are ready to be dispensed.
5. Click “Plate Formats” on the top panel of the COPAS software, select the plate format to obtain a blank SORT GRID. Input the plate design in the grid.
6. Place the ideal plate on the stage and click Fill on the main screen to start dispensing worms.
7. Clean up after use/each strain to minimize cross contamination (*see Note 4*).

3.6 High-Throughput Assays for Growth, Brood Size, and Feeding

High-throughput assays were performed using COPAS Biosort methods as previously described by Boyd et al. [15, 16] with slight modifications. Experiments were performed in triplicates for each strain-treatment combination. After adding the test solutions containing K-medium, bacterial food, and chemicals, age-synchronized worms were dispensed to designated wells using COPAS Biosort and then incubated at required time and temperature with plate shaking. Prior to measurement, 10 μ L formalin (10%) were added to the wells, to kill and straighten the

animals for proper measurement. The contents in each well were aspirated using the ReFLx module of the BISORT (*see Notes 5 and 6*) and analyzed for five parameters: extinction (EXT), time of flight (TOF), as well as green, yellow, and red fluorescence. Data was read, processed, and plotted using the R software.

3.6.1 Growth

1. Prepare age-synchronized L1 culture as described in Subheading 3.1.
2. Prepare exposure work solution with food source as described in Subheading 3.2.
3. Dispense 50 L1 nematodes (~10 µL; *see Note 7*) into designated wells on 96-well plate using COPAS Biosort, then add 90 µL exposure work solution to each well.
4. Cover the plate and seal with parafilm, then incubate for 48 h at 20 °C.
5. Observe nematodes using a dissecting microscope to qualitatively check the health of the negative controls, level of contamination, and concentration response to the test chemical.
6. Use COPAS Biosort to aspirate and measure the TOF and EXT as size parameters for individual *C. elegans*.

3.6.2 Brood Size

1. Transfer age-synchronized L1-stage worms to NGM and allow to grow to L4 stage (*see Note 8*).
2. Prepare exposure work solution with food source as described in Subheading 3.2.
3. Wash L4 stage worms off the NGM plates with K-medium. Dispense five worms into each designated well on a 96-well plate using COPAS Biosort (~5 µL; *see Note 7*).
4. Check each well under dissection microscope to verify whether it contains the correct number of worms. If not, keep a note for final adjustment.
5. Add 95 µL of exposure solution or LB into each designated well, mix well, and incubate on plate shaker in 20 °C for 48 h.
6. Use COPAS Biosort to aspirate and measure the total event counts per Well ID as brood size per replicate. The number of larvae produced during this period is an indication of the effect of the metals on nematode fecundity.
7. Adjust final count according to initially recorded worm count in step 4.

3.6.3 Feeding

1. Prepare age-synchronized L1 culture as described in Subheading 3.1.
2. Dispense 25 age-synchronized L1 stage worms (~10 µL; *see Note 7*) into each designated well on 96-well plate, then add 90 µL exposure work solution to each well.

3. Cover the plate and seal with parafilm, then incubate for 24 h at 20 °C.
4. Add 5 µL red fluorescent microsphere beads solution into each well and allow accumulation in worms for 15 min.
5. Use COPAS Biosort to aspirate and measure red fluorescence signal as indication of ingestion of the beads for individual *C. elegans*. Nematode sizes (TOF and EXT) are also recorded.
6. Calculate the parameter for feeding behavior, which was expressed as size-corrected red fluorescence for cohorts of nematodes, $\log(\text{red fluorescence})/\log(\text{TOF})$.

3.7 Chou-Talalay Combination Index (CI) Method for Assessing the Toxicity of Metal Mixtures

The combined toxicity of metal mixtures was assessed using Chou-Talalay CI method for chemical combination [23]. This method is based on the median-effect equation, which provides the theoretical basis for the combination index (CI)-isobologram equation that allows quantitative determination of chemical interactions.

This method plots the dose–effect curves for each chemical and their combinations in multiple diluted concentrations by using the median-effect equation:

$$\frac{f_a}{f_u} = \left(\frac{D}{D_m} \right)^m \quad (1)$$

where D indicates the concentration of metal, f_a and f_u are the fractions of the organism system affected and unaffected ($f_a + f_u = 1$), D_m is the EC₅₀, m is a Hill-type coefficient indicating the shape of the dose–effect curve, and $m < 1$, $m = 1$, and $m > 1$ signify negative (flat) sigmoidal, hyperbolic, and sigmoidal dose–effect curves, respectively. In addition, the linear correlation coefficient (r) of the median-effect plot can manifest the conformity of the data to the median-effect plot, and $r = 1$ displays excellent conformity.

These parameters were then used to calculate dose of the metals and their combinations required to produce various effect levels according to Eq. (1); for each effect level, combination index (CI) values were then calculated according to the general combination index equation for n chemical combination at $x\%$ inhibition [18]:

$$\begin{aligned} {}^n(\text{CI})_x &= \sum_{j=1}^n \frac{(D)_j}{(Dx)_j} \\ &= \sum_{j=1}^n \frac{(Dx)_{1-n} \left\{ [D]_j / \sum_1^n [D] \right\}}{(D_m)_j \left\{ (fax)_j / \left[1 - (fax)_j \right] \right\}^{1/m_j}} \end{aligned} \quad (2)$$

where ${}^n(\text{CI})_x$ is the combination index for n chemicals at $x\%$ inhibition; $(Dx)_{1-n}$ is the sum of the dose of n chemicals that exerts $x\%$ inhibition in combination; $\frac{[D]_j}{\sum_1^n [D]}$ is the proportionality of the dose

Table 2
Description and symbols of the degree of combined toxicity grading in isobolograms method

Combination index	Description	Grading symbols
<0.1	Very strong synergism	+++++
0.1–0.3	Strong synergism	++++
0.3–0.7	Common synergism	+++
0.7–0.85	Moderate synergism	++
0.85–0.90	Slight synergism	+
0.90–1.10	Nearly synergism	±
1.10–1.20	Slight antagonism	—
1.20–1.45	Moderate antagonism	--
1.45–3.3	Common antagonism	---
3.3–10	Strong antagonism	----
>10	Very strong antagonism	-----

of each of n chemicals that exerts $x\%$ inhibition in combination; and $(D_m)_j \left\{ (fax)_j / \left[1 - (fax)_j \right] \right\}^{1/m_j}$ is the dose of each chemical alone that exerts $x\%$ inhibition. CI values, $CI < 1$, $= 1$, and > 1 , indicate synergism, additive effect, and antagonism, respectively (Table 2).

The JavaScript software, CompuSyn (CompuSyn Inc., USA), may be used to facilitate the calculation of combination index. It is available for download at <http://www.combosyn.com/>.

1. Convert data points into effect fractions when compared to control. For example, a growth inhibitory effect of 20% should be converted to 0.2.
2. Input the data into CompuSyn software for single chemical and combo, with dose, effect, and combination ratio should it be applicable, and press Enter to confirm each input. Note the software only takes in values between 0 and 1 (does not include 0 and 1), thus any effect of ≥ 1 should be imputed as 0.9999, while those ≤ 0 should be imputed as 0.0001. As the software has no limit on the number of significant digits for the inputted effects value, it is possible to simply copy the raw converted result into the effect slot of the form. Other input parameters, such as unit and chemical name, are arbitrary and do not affect calculations, but may be useful for keeping track of data.
3. To calculate f_a based on known concentration of chemicals, concentration of chemicals and chemical combo ratios from a known f_a , as well as CI for combination and DRI of individual

chemicals, click on the button “Calculate Parameters,” and input the known values. Press Enter to obtain the results of the unknown values, as well as CI and DRI of individual chemicals based on the current f_a . The calculations are based on currently inputted data.

4. Click on “Generate Report” to obtain a comprehensive analysis of interactions.

4 Notes

1. For growing L-broth or OP50 cultures overnight, prior to autoclaving, the flask should be plugged with a chunk of glass wool or cotton large enough to fit snugly into the flask, half way into the flask, with a 1 mL glass graduated pipette pushed through the plug with tapered end facing the liquid. The pipette may be replaced with trimmed glass dropper should the flask be too small. The flask opening is then wrapped with double-layer tin foil and secured with autoclave tape. An additional piece of double-layer tin foil is used to cover up the top opening of the glass pipette/dropper during autoclave. After inoculation, the plug is fit back into the flask with wrapped tin foil, and the glass pipette/dropper is pushed downward to reach the liquid while allowing at least one inch above the plug to allow connection to an air pump via rubber tubing for overnight aeration.
2. Compounds are typically diluted in K-medium or 1% DMSO, depending on aqueous solubility. For chemicals from DMSO stock, the work solutions should be prepared at 100× higher concentration to then allow for 1% DMSO in the final work solution. As a small volume of chemical in DMSO will be added to work solution, after OP50 is rinsed (three times instead of two), the final volume of 1 mg/mL OP50 will be distributed to each tube. DMSO stock solutions is then added on top of it to reach the desired final concentration; for example, to make 10 mL work solution + OP50, add 101 μ L of 100× stock chemical solution in DMSO to 10 mL of 1 mg/mL OP50. For chemicals that alter the pH of the exposure solution, an alternative buffer should be used in place of K-medium. For chemicals that increase the pH above 8.5, M9 buffer is substituted for K-medium. In cases for which the pH decreases below 4.5, K-medium should be buffered with 1 N KOH up to a pH of 5.5.
3. Petri plates of various sizes may be used with adjusted volumes: for 60 mm plates, pour 10 mL agar and inoculate with ~60 μ L OP50. For 150 mm plates, pour 50–55 mL agar and inoculate with ~150 μ L OP50.

4. Optimal operation of COPAS Biosort requires priming upon start-up, cleanup after runs, and weekly calibration using control particles. Detailed protocols for each can be found in operating manual for the instrument. In general, start-up priming requires initial warming-up of the laser and sorter system for at least 1 min, equilibrating system pressure, and removal of bubbles and debris from tubing. For a typical run using COPAS Biosort, sheath fluid should stay within a specific level such that air pressure would stay relatively constant, allowing for constant flow rate. Should the sheath level fall too low, fill in with sheath fluid, or buffer used for experiment, to an appropriate level. Cleaning up of the instrument system follows the order of sterilized H₂O → 10% Clorox → COPAS cleaning solution (Union Biometrica) → rinse with sterilized H₂O and store. For flow cell, first rinse the sampling cup thoroughly, then perform each step three times, via adding 40 mL of the required solvents to the sampling cup, and allow to flow-through the system. If the ReFLx module is used, cleaning up for the module follows the same four steps, each via aspirating corresponding solvents from six wells in a 96-well plate.
5. COPAS Biosort ReFlx module is liable to carryover contamination, in which nematodes aspirated from previously sampled wells may not be completely flushed out of flow cell, and consequently may be counted toward subsequent wells. The content and viscosity of the experiment media may affect the likelihood of worms getting trapped in flow cell. Other structural components within the system positioned before flow cell, including filter, bubble traps, tubings, may also be liable to having worms trapped. It is therefore recommended to sequence one blank well containing only sheath solvent, K-medium, or whichever buffer media used, in between the sampling of each experiment wells, especially those of different treatment groups, to allow the system to rinse out the trapped worms.
6. When running the ReFLx module, ensure that all the exposure media from the sample wells are aspirated and that there is no of air bubbles aspirated, and look out for other potential sampling errors. A number of conditions may affect COPAS Biosort sampling efficiency or data quality, including clogging of the flow cell, sample tubing, or aspirating tool; leaking of the waste tubing; disrupted flow due to pressure changes; and excessive sampling due to air bubbles, waste, or chemical precipitates. If the Biosort is observed to be clogging or leaking, the run should be aborted, and the machine cleaned and primed. If clogging or noise is not observed until after sampling is complete, in some cases, the data may be “cleaned” using mathematical modeling. A certain level of noise is normal

in COPAS Biosort data. This routine noise may include dead bacteria, shed cuticles from molting (especially if development is delayed due to chemical exposure), dead nematodes, and air bubbles in the system. Routine noise may be modeled and removed automatically by setting a sort region with respect to parameters of interest within the COPAS Biosort software, or manually via sort function in Microsoft Excel.

7. Drop size for COPAS Biosort dispenser is not set in actual volume. Instead, it is set as an arbitrary size parameter-per-worm in the parameters of Width and Delay. It is possible to set the parameter and then test a few drops to ensure the droplet is not too large. The size of droplets may be estimated quantitatively via micropipetting, or qualitatively via size comparison to a droplet of medium with known volume. Typically, the droplet should be less than 10% of final volume, but not too small as to cause fluctuations in the number of worms.
8. Development of *C. elegans* from L1 to L4 larvae takes approximately 48 h at 20 °C [24]. This time range was chosen for growth assays to allow for maximum development, while avoiding the production of offspring at later times.

References

1. Byber K, Lison D, Verougstraete V, Dressel H, Hotz P (2016) Cadmium or cadmium compounds and chronic kidney disease in workers and the general population: a systematic review. Crit Rev Toxicol 46(3):191–240. <https://doi.org/10.3109/10408444.2015.1076375>
2. Cinnirella S, Hedgecock IM, Sprovieri F (2014) Heavy metals in the environment: sources, interactions and human health. Environ Sci Pollut Res Int 21(6):3997–3998. <https://doi.org/10.1007/s11356-013-2486-z>
3. Jomova K, Valko M (2011) Advances in metal-induced oxidative stress and human disease. Toxicology 283(2–3):65–87. <https://doi.org/10.1016/j.tox.2011.03.001>
4. Lim JT, Tan YQ, Valeri L, Lee J, Geok PP, Chia SE, Ong CN, Seow WJ (2019) Association between serum heavy metals and prostate cancer risk—a multiple metal analysis. Environ Int 132:105109. <https://doi.org/10.1016/j.envint.2019.105109>
5. Rehman K, Fatima F, Waheed I, Akash MSH (2018) Prevalence of exposure of heavy metals and their impact on health consequences. J Cell Biochem 119(1):157–184. <https://doi.org/10.1002/jcb.26234>
6. Caito S, Aschner M (2015) Neurotoxicity of metals. Handb Clin Neurol 131:169–189. <https://doi.org/10.1016/b978-0-444-62627-1.00011-1>
7. Balistrieri LS, Mebane CA (2014) Predicting the toxicity of metal mixtures. Sci Total Environ 466–467:788–799. <https://doi.org/10.1016/j.scitotenv.2013.07.034>
8. Adebambo OA, Ray PD, Shea D, Fry RC (2015) Toxicological responses of environmental mixtures: environmental metal mixtures display synergistic induction of metal-responsive and oxidative stress genes in placental cells. Toxicol Appl Pharmacol 289 (3):534–541. <https://doi.org/10.1016/j.taap.2015.10.005>
9. Cobbina SJ, Chen Y, Zhou Z, Wu X, Feng W, Wang W, Mao G, Xu H, Zhang Z, Wu X, Yang L (2015) Low concentration toxic metal mixture interactions: effects on essential and non-essential metals in brain, liver, and kidneys of mice on sub-chronic exposure. Chemosphere 132:79–86. <https://doi.org/10.1016/j.chemosphere.2015.03.013>
10. Leung MC, Williams PL, Benedetto A, Au C, Helmcke KJ, Aschner M, Meyer JN (2008) *Caenorhabditis elegans*: an emerging model in biomedical and environmental toxicology. Toxicol Sci 106(1):5–28. <https://doi.org/10.1093/toxsci/kfn121>

11. Meyer D, Williams PL (2014) Toxicity testing of neurotoxic pesticides in *Caenorhabditis elegans*. J Toxicol Environ Health B Crit Rev 17 (5):284–306. <https://doi.org/10.1080/10937404.2014.933722>
12. Hunt PR (2017) The *C. elegans* model in toxicity testing. J Appl Toxicol 37(1):50–59. <https://doi.org/10.1002/jat.3357>
13. Queiros L, Pereira JL, Goncalves FJM, Pacheco M, Aschner M, Pereira P (2019) *Caenorhabditis elegans* as a tool for environmental risk assessment: emerging and promising applications for a “nobelized worm”. Crit Rev Toxicol 49(5):411–429. <https://doi.org/10.1080/10408444.2019.1626801>
14. Pulak R (2006) Techniques for analysis, sorting, and dispensing of *C. elegans* on the COPAS flow-sorting system. Methods Mol Biol 351:275–286. <https://doi.org/10.1385/1-59745-151-7:275>
15. Boyd WA, Smith MV, Kissling GE, Freedman JH (2010) Medium- and high-throughput screening of neurotoxicants using *C. elegans*. Neurotoxicol Teratol 32(1):68–73. <https://doi.org/10.1016/j.ntt.2008.12.004>
16. Boyd WA, McBride SJ, Rice JR, Snyder DW, Freedman JH (2010) A high-throughput method for assessing chemical toxicity using a *Caenorhabditis elegans* reproduction assay. Toxicol Appl Pharmacol 245(2):153–159. <https://doi.org/10.1016/j.taap.2010.02.014>
17. Boyd WA, Smith MV, Freedman JH (2012) *Caenorhabditis elegans* as a model in developmental toxicology. Methods Mol Biol 889:15–24. https://doi.org/10.1007/978-1-61779-867-2_3
18. Chou TC (2006) Theoretical basis, experimental design, and computerized simulation of synergism and antagonism in drug combination studies. Pharmacol Rev 58(3):621–681. <https://doi.org/10.1124/pr.58.3.10>
19. Wang Y, Chen C, Qian Y, Zhao X, Wang Q, Kong X (2015) Toxicity of mixtures of lambda-cyhalothrin, imidacloprid and cadmium on the earthworm Eisenia fetida by combination index (CI)-isobogram method. Ecotoxicol Environ Saf 111:242–247. <https://doi.org/10.1016/j.ecoenv.2014.10.015>
20. Rodea-Palomares I, Petre AL, Boltes K, Leganes F, Perdigon-Melon JA, Rosal R, Fernandez-Pinas F (2010) Application of the combination index (CI)-isobogram equation to study the toxicological interactions of lipid regulators in two aquatic bioluminescent organisms. Water Res 44(2):427–438. <https://doi.org/10.1016/j.watres.2009.07.026>
21. Williams PL, Dusenberry DB (1990) Aquatic toxicity testing using the nematode, *Caenorhabditis elegans*. Environ Toxicol Chem 9 (10):1285–1290
22. Brenner S (1974) The genetics of *Caenorhabditis elegans*. Genetics 77(1):71–94
23. Chou TC, Talalay P (1984) Quantitative analysis of dose-effect relationships: the combined effects of multiple drugs or enzyme inhibitors. Adv Enzym Regul 22:27–55
24. Boyd WA, Smith MV, Kissling GE, Rice JR, Snyder DW, Portier CJ, Freedman JH (2009) Application of a mathematical model to describe the effects of chlorpyrifos on *Caenorhabditis elegans* development. PLoS One 4(9): e7024



Chapter 3

Evaluations of Environmental Pollutant-Induced Mitochondrial Toxicity Using *Caenorhabditis elegans* as a Model System

Fuli Zheng, Michael Aschner, and Huangyuan Li

Abstract

Environmental pollutants inevitably exert adverse effects on humans and other species. Quick identification and in-depth characterization of the pollutants are requisite objectives for clinicians and environmental health scientists. The nematode *Caenorhabditis elegans* has been utilized as a model organism for toxicity evaluation of environmental pollutants, due to its transparency, short lifespan, entire genome sequencing, and economical characteristics. However, few researchers have systematically addressed mitochondrial toxicity in response to toxicants, despite the critical role mitochondria play in energy production and respiration, as well as the generation of reactive oxygen species. Mitochondria are vulnerable to environmental pollutants, and their dysfunction contributes to cellular damage and toxicity in plethora of diseases. Here, we describe methods in step-by-step for mitochondrial toxicity evaluation in response to pollutants, including exposure of *C. elegans* to toxicants, mitochondrial ROS detection, mitochondrial morphology analysis, mitochondrial function analysis, such as ATP production and oxygen consumption, and gene expression studies, with the application of corresponding genetically modified strains.

Key words *Caenorhabditis elegans*, Environmental pollutants, Mitochondrial toxicity, Mitochondrial morphology, ATP production, Oxygen consumption, *drp-1*

1 Introduction

Living organisms are surrounded with environmental pollutants. A strong link between environmental pollutants and human health has been validated by extensive studies. Redox toxicity is proposed as one of the main mechanisms of chemical-induced pathology in humans [1]. Mitochondrion is one of the main targets of cellular toxicity owing to not only its critical function in energy production and respiration but also its rapid generation of reactive oxygen species (ROS) [2]. Thus, mitochondrion can be both the most

vulnerable organelle upon environmental pollutant exposure and also the causative agent for cellular damages and toxicity. The tubular, elongated, interconnected mitochondrial networks are generated by fusion, while fission leads to the generation of discrete fragmented mitochondria [2]. The balance between mitochondrial fission and fusion is of great importance for optimal energy generation and supply, and thus cell viability, while damaged mitochondria are separated by fission, then proceed through mitophagy [3]. On the other hand, disruption of normal mitochondrial fission and fusion can also generate ROS, thus leading to oxidative stress [4].

Caenorhabditis elegans is a powerful *in vivo* model to study environmental pollutant-induced toxicity, both for mechanistic studies and for high-throughput screening purposes, with comparative results found with rat studies [5–7]. *C. elegans* started to be used as an important experimental model only since 1974 [8]. More than 30,000 studies indexed in PubMed and three Nobel prizes have confirmed its success and popularity as a model animal. Its small size, transparency, ease of maintenance, short lifespan, completed sequenced genome, and highly conserved genes and their functions make it attractive to the fields of biological, medical, toxicological, and environmental sciences [9, 10]. *C. elegans* is a valuable tool to investigate mitochondrial gene–environment interactions, since mitochondrial functions along with many pathways are well conserved with those in humans [11–13]. Moreover, a large number of the regulating signals arise from diverse tissues and cell types, which are lost when studying in *in vitro* models, emphasizing the importance of *in vivo* study of mitochondrial structure and function [14]. However, few studies have systematically summarized the mitochondrial toxicity evaluation of the toxicants. Thus, it could be helpful to logically sort out the workflow of mitochondrial toxicity evaluation using *C. elegans*.

In this chapter, several methods are described in details to evaluate mitochondrial toxicity upon pollutant exposure, including exposure of *C. elegans*, mitochondrial ROS detection, mitochondrial morphology analysis, mitochondrial ATP production, and oxygen consumption, with the application of corresponding genetic-modified strains.

2 Materials

Prepare all solutions using ultrapure water (prepared by purifying deionized water to attain a resistivity of 18 MΩ cm at 25 °C) and analytical grade reagents. Prepare and store all reagents at room temperature (unless indicated otherwise). Diligently follow all waste disposal regulations when disposing of waste materials.

2.1 Strains

C. elegans strains, Bristol N2, SD1347 (ccIs4251 I. [Pmyo-3p::GFP + Pmyo-3p::mitochondrial GFP]), CU6372 [*drp-1*(tm1108)], and *Escherichia coli* OP50, grown on nematode growth medium (NGM, *see* Subheading 2.3, item 2 for preparation details) and cultured at 20 °C [8].

2.2 Equipment and Instruments

1. Dissection microscope/stereomicroscope.
2. Leica SP8 confocal microscope with a 63× oil lens with excitation/emission wavelengths at 488/520 nm for GFP and 510/580 nm for RFP.
3. Nikon ECLIPSE 80i fluorescence microscope with a 60× oil lens with excitation/emission wavelengths at 488/520 nm for GFP.
4. Platinum picker.
5. 20 °C incubator.
6. Rotator.
7. Tabletop centrifuge.

2.3 Chemicals

1. Exposure stock solution: Dissolve the toxicant with ddH₂O. Then use M9 buffer (or 85 mM NaCl, *see* Note 1) to make 20× exposure stock solutions (*see* Note 2).
2. 35 mm NGM plates: Weigh 3 g NaCl, 17 g agar, and 2.5 g peptone, and dissolve with approx. 975 mL ddH₂O. Autoclave. Once the mixture is cooled to 50 °C, add 1 mL 5 mg/mL cholesterol, 1 mL CaCl₂, 1 mL 1 M MgSO₄, 25 mL 1 M KPO₄ (pH 6), 1.25 mL nystatin, and 0.5 mL 100 mg/mL streptomycin, separately. Swirl to mix thoroughly after each addition. After finishing all the additions, take 4 mL NGM media and add into one 35 mm plate.
3. M9 buffer: Mix 6 g KH₂PO₄ with 12 g Na₂HPO₄ and 10 g NaCl in a beaker with 2 L ddH₂O. Autoclave the mixture. Once the mixture is cooled to 50 °C, add 2 mL of 1 M MgSO₄ and mix.
4. 85 mM NaCl: Weigh 10 g NaCl and dissolve in 2 L ddH₂O. Autoclave.
5. 1 M CaCl₂: Weigh 73.5 g CaCl₂·2H₂O and dissolve in 500 mL ddH₂O. Autoclave.
6. 1 M MgSO₄: Weigh 123.24 g MgSO₄·7H₂O and dissolve in 500 mL ddH₂O. Autoclave.
7. 5 mg/mL cholesterol: Prepare one 500 mL autoclaved empty bottle. Weigh 2 g cholesterol and dissolve in 400 mL 95% ethanol. Mix well. Filter the mixture into a new 1 L autoclaved bottle using a sterile filter.
8. Nystatin. Store at -20 °C.

9. 100 mg/mL streptomycin sulfate: Weigh 1 g streptomycin sulfate and dissolve in 10 mL ddH₂O. Mix well. Aliquot 1 mL to each 1.5 mL tubes. Store at -20 °C.
10. 1 M KPO₄: Mix 108.3 g KH₂PO₄ with 35.6 g K₂HPO₄, and dissolve in 990 mL ddH₂O. Calibrate pH to 6.0. Filter the mixture into a new 2 L autoclaved bottle using a sterile filter.

2.4 Mitochondrial Staining and Microscopy

1. MitoSOX Red.
2. Coverslips.
3. Microscope slides containing a 4% agarose pad: Mix 4 g agarose with 100 mL ddH₂O. Heat to 70 °C for complete dissolve of the agarose powder. Use a plastic pipette to move a droplet of 4% agarose onto one slide, and quickly cover with another microscope slide on top of the droplet. Carefully remove one slide to obtain a slide containing 4% agarose pad. The pads should be prepared fresh to avoid evaporation of the liquids.
4. 1 mM levamisole: Weigh 2.41 g of levamisole and dissolve in ddH₂O to make 10 mL solution. Aliquot to 500 µL per tube.
5. MitoTracker red CMXRos.

2.5 ATP Production Assessment

1. ATP Bioluminescence Assay Kit CLS II.
2. Pierce BCA Protein Assay Kit.
3. Luminometer.
4. MYOB dry mix: Weigh 27.5 g Tris-HCl, 12 g Tris-base, 230 g Bacto-tryptone, 100 g NaCl, and 0.4 g cholesterol (95%). Mix to make 370 g MYOB dry mix.
5. MYOB: Weigh 7.4 g MYOB dry mix and dissolve with 1 L ddH₂O. Autoclave and cool.
6. ATP standard solution: Dissolve lyophilized ATP by adding the appropriate volume of distilled water to get final concentration of 10 mg/mL or 16.5 mM. Store ATP standard solution at -20 °C. ATP standard solutions are stable for at least 1 week.
7. Opaques 96-well plates.

2.6 Oxygen Consumption Measurement

1. Seahorse XF96 Flux Analyzer (Seahorse Bioscience, USA).
2. XF96 extracellular flux assay kits (Seahorse Bioscience, USA).
3. XF96 cell culture microplates.
4. 10 mM FCCP stock solution: Mix 2.54 mg of carbonyl cyanide 4-(trifluoromethoxy) phenylhydrazone (FCCP) in 1 mL of DMSO and make 25 µL aliquots. Store at -20 °C for up to 4 months (*see Note 3*).

5. 100 µM FCCP: Dilute 25 µL 10 mM FCCP stock solution in 2.475 mL M9 buffer. Prepare freshly (less than 24 h before use).
6. 400 mM sodium azide stock solution: Mix 78 mg of sodium azide in 3 mL of ddH₂O. Prepare freshly (less than 24 h before use) (*see Note 4*).
7. 1× PBS + 0.05% (vol/vol) Triton X-100: To make PBS, add 8 g of NaCl, 0.2 g of KCl, 1.44 g of Na₂HPO₄, and 0.24 g of KH₂PO₄ (pH 7.4) to 1 L ddH₂O. Add 0.5 mL of Triton X-100 to 1 L of PBS (0.05%). The mixture can be stored at 4 °C for up to 1 month.
8. Calibration solvent, pH 7.4 (Seahorse Bioscience, USA).

2.7 Mitochondrial Gene Expression and Modifications Assessment

1. Liquid nitrogen.
2. TRIzol.
3. NanoDrop 2000 spectrophotometer.
4. High Capacity cDNA Reverse Transcription kit.
5. Taqman gene-expression assay probes (Thermo Fisher Scientific). Commonly used probes are Ce02412618_gH (*tba-1*); Ce02407440_g1 (*drp-1*); Ce02433121_g1 (*fzo-1*); Ce02463146_g1 (*miro-1*); Ce02484980_g1 (*egl-1*); Ce02452076_g1 (*ced-9*); Ce02446175_g1 (*ced-4*); Ce02466776_m1 (*ced-3*); Ce02463990_m1 (*bec-1*); Ce02433594_g1 (*lgy-1*).
6. Thermal cycler.
7. Real-time system.

3 Methods

3.1 Exposure and Survival Assay

1. Expose 2500 synchronized L4 nematodes (*see Note 5*) with 25 µL liquid exposure solutions, respectively, in 500 µL reaction system for 2 h at 20 °C (*see Note 6*).
2. Remove toxicants with two washes using 85 mM NaCl (*see Note 7*).
3. Transfer approx. 30–40 nematodes to 35 mm NGM plates freshly seeded with OP50 in triplicates.
4. Score the nematodes with a stereomicroscope as alive or dead. In some cases, dead nematodes are confirmed by touching the head region with the point of a picker.
5. Analyze survival rates and select appropriate dosage for further studies.

3.2 Mitochondrial ROS Detection

1. Grow synchronous L4 nematodes on NGM plates spread with OP50 and 10 µM MitoSOX Red for 24 h (*see Note 8*).
2. Collect the young adult nematodes (after 24 h from the above step, the nematodes turn into young adults) and expose with the environmental pollutant of interest (*see Subheading 3.1, steps 1 and 2* for details).
3. Recover the exposed nematodes on NGM plates containing OP50 for 1 h (*see Note 9*).
4. Pick the nematodes to a droplet of 1 mM levamisole on the coverslip (*see Note 10*).
5. Mount the coverslip onto a microscope slide containing a 4% agarose pad.
6. Label strains and conditions of the experiments.
7. Examine fluorescent intensity in the posterior pharyngeal bulb of the nematodes with 510 and 580 nm (excitation/emission) wavelengths.
8. Quantify fluorescent intensity using Fiji software to unveil the effect of environmental toxicants on mitochondrial ROS (*see Note 11*).

3.3 Mitochondrial Morphology Analysis

1. Grow synchronous L4 nematodes on fresh NGM plates spread with OP50 mixed with 5 µM MitoTracker red CMXRos for 24 h (*see Note 12*).
2. Expose nematodes with environmental toxicants and prepare slides for fluorescent microscopy (*see Subheading 3.2, steps 2–6* for details).
3. Capture mitochondria using fluorescent microscope with a 60× oil lens with excitation/emission wavelengths at 488/520 nm for GFP.
4. Blindly score mitochondrial morphology in at least 30 nematodes analyzed for each condition. The morphological categories of mitochondria were defined as follows: (1) tubular: a majority of mitochondria were interconnected and elongated like tube shape; (2) intermediate: a combination of interconnected and fragmented mitochondria; (3) fragmented: a majority of round or short mitochondria in the image taken [15, 16] (Fig. 1).
5. Analyze and quantify the proportions of each categories upon each exposure to determine potential mitochondrial morphology changes induced by environmental pollutants (*see Note 13*).
6. Alternatively, nematodes with mitochondria-tagged GFP in body wall muscle, strain SD1347 (*ccIs4251 I.*), can be used to assess alterations in mitochondrial morphology upon toxicant exposure (Fig. 2).

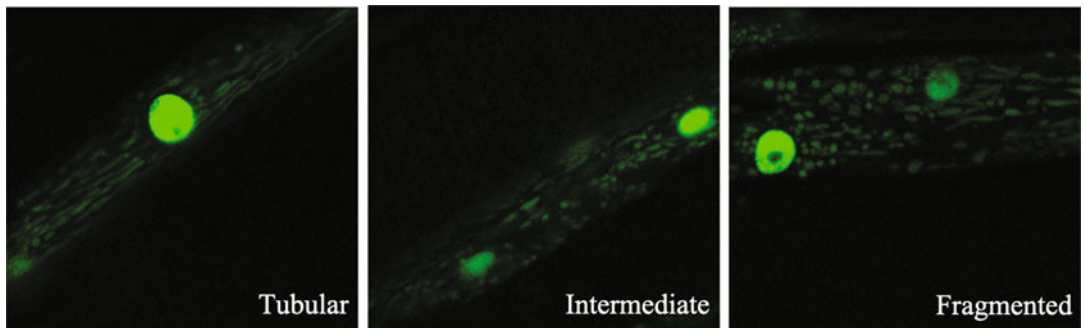


Fig. 1 Mitochondrial morphology category indices. Mitochondrial morphology was classified into three categories: tubular, intermediate, and fragmented (modified from [15])

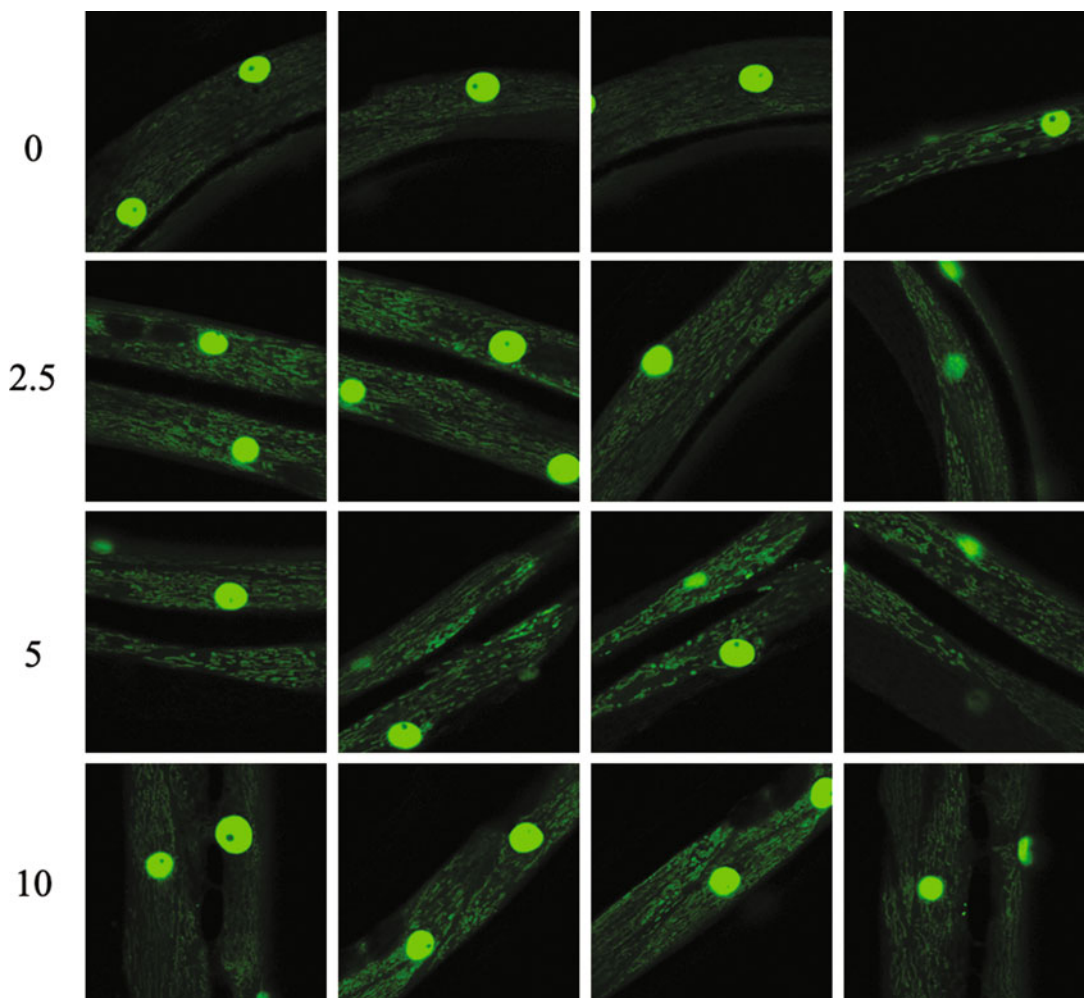


Fig. 2 CoCl_2 induces mitochondrial fission. SD1347 nematodes were exposed to CoCl_2 at various doses for 2 h, then examined by fluorescent microscopy ($N > 30$). Mitochondrial morphology of each exposure was demonstrated with the four representative images. Individual experiments were independently repeated for three times

3.4 Mitochondrial Function Evaluation

3.4.1 ATP Production Assessment

- Dilute ATP standards by serial dilutions in the range of 10 to 1×10^{-4} μM. Prepare serial dilutions of one ATP standard solution using ddH₂O to generate the ATP standard curve (*see Note 14*).
- After exposure, collect L4 nematodes (500 μL) by centrifugation and wash three times with 85 mM NaCl.
- Resuspend the nematodes with 500 μL MYOB and mix well.
- Prepare ATP reaction buffer according to manufacturer's protocol.
- Add 100 μL of nematode mixture to one well of opaques 96-well plate in triplicates.
- In another three wells, add 100 μL MYOB as negative control (*see Note 15*).
- Add 100 μL ATP reaction buffer to each of the above wells and mix for 5 min in a horizontal rotator.
- Measure luminescence in the 96-well plate and normalize with negative control.
- Calculate ATP content (nM) of each sample using ATP standard curve generated by ATP standards. For example, if the ATP curve equation generated is $y = 46.404x + 1638.1$ ($R^2 = 0.9998$), (y is the RLU, while x is the ATP content), then the ATP content for a sample with RLU of 37281.559 is 768.1118 nM.
- Measure protein concentrations of each sample (25 μL out of 500 μL) using BCA protein assay.
- Normalize ATP levels to protein concentration (nM/mg).
- Analyze ATP contents to reveal the role of environmental toxicant in mitochondrial function (*see Note 16*).

3.4.2 Oxygen Consumption Measurement

- Hydrate Seahorse cartridge probes: Open a new flux package and remove the sensor cartridge.
- Add 200 μL of the Seahorse Bioscience XF96 calibrant solution to each well of the utility plate. Multichannel pipette is preferred.
- Place the sensor cartridge back on the utility place and immerse the probes into calibrant solution. Place the lid on top and incubate it overnight at 37 °C without CO₂ (*see Note 17*).
- On the second day, set up XF96 respirometer using the standard software package.
- Turn off the heater and temperature control.
- Set the wells A1, A12, H1, and H12 as the background correction wells, and make sure background correction is on.

7. Create an XF assay and generate protocol in the XF96 respirometer software. Record the compounds to be injected, their concentrations and ports to be loaded. Protocol: (1) calibrate, (2) equilibrate, (3) loop five times, (3a) mix for 2 min, (3b) wait for 0.5 min, (3c) measure for 2 min, and (4) end loop. (Optional) (5) inject port A with FCCP, (6) loop nine times, (6a) mix for 2 min, (6b) wait for 0.5 min, (6c) measure for 2 min, (7) end loop, (8) inject port B with sodium azide, (9) loop four times, (9a) mix for 2 min, (9b) wait for 0.5 min, (9c) measure for 2 min, (10) end loop, and (11) end program.
8. Slowly add 22 μ L of 100 μ M FCCP into each port A on the cartridge as well as the background correction wells (*see Note 18*).
9. Slowly add 24 μ L of 400 μ M sodium azide into each port B on the cartridge in the same manner as described in **step 8** above (*see Note 19*).
10. Place the sensor cartridge back to the 37 °C incubator (non-CO₂) for at least 10 min until calibration start.
11. After exposure (*see Subheading 3.1* for details), record the developmental stages and anomalies (infections, starvation, etc.) of the nematodes (*see Note 20*).
12. Wash the nematodes three times with M9 to remove bacteria and resuspend with 1.5–3 mL M9.
13. Count the nematodes in each group.
14. Start the actual XF assay on the software.
15. Load 20–30 nematodes to each well in an unused cell culture microplate. Make the total volume of each well 200 μ L with M9.
16. Inspect the plate under a dissection microscope to make sure all experimental wells contain 20–35 worms except for A1, A12, H1, and H12.
17. Wait for at least 2 min for the nematodes to settle to the bottom of the wells.
18. Remove the calibration plate (utility plate) once the calibration is complete and replace with the nematode plate.
19. Press “continue” on the software interface to finish the run. Once complete, follow the instructions and remove the cartridge from the XF96 respirometer.
20. Count the numbers of nematodes in each well and record any anomalies observed.
21. Postexperimental analysis: Calculate oxygen consumption rates (OCR) values: basal OCR, FCCP-induced OCR, non-mitochondrial respiration (sodium azide-induced), etc. Transfer OCR per well to OCR per worm.

3.5 Mitochondrial Gene Expression and Modifications Assessment

3.5.1 RT-PCR

- Conduct three freeze and thaw cycles to the nematodes with liquid nitrogen to breakdown cuticles and release RNA (see Note 21).
- Isolate mRNA with TRIzol following manufacturer's protocol (Life Technologies, USA).
- Determine the concentration and purity (A_{260}/A_{280} and the A_{260}/A_{230} ratio) of the isolated RNA by a NanoDrop 2000 spectrophotometer.
- Reverse-transcribe cDNA from RNA using High Capacity cDNA Reverse Transcription kit following manufacturer's protocol. Briefly, prepare $2 \times$ reaction mix using the kit's components according to the protocol. Dilute 1 μ g RNA to 10 μ L solution with RNase-free water. Then mix the 10 μ L of $2 \times$ reaction mix with 10 μ L RNA. This would result in 0.5 μ g of cDNA per 10 μ L. The recommended cDNA transcription protocol is: 25 °C 10 min, 37 °C 2 h, 85 °C 5 min, and stop at 4 °C.
- Prepare PCR mix according to Taqman gene-expression assay probes protocol. 3 μ L of cDNA generated above is added to 5 μ L of the Taqman probes, followed by 1.5 μ L water to makeup 10 μ L system. The 10 μ L system could be scaled up to 50 μ L per tube.
- Run qPCR on the BioRad Real-time system. The recommended qPCR protocol is TaqMan standard protocol (1 h 30 min).
- Normalize the target gene expression to the relatively stable expression gene *tba-1* [17].
- Determine the relative mRNA levels of gene of interests with the $2^{-\Delta\Delta CT}$ method [18] (Fig. 3).

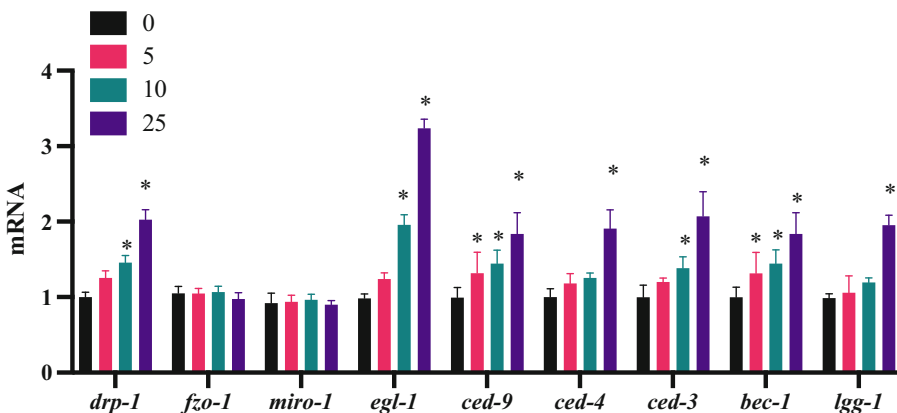


Fig. 3 Mitochondrial morphologic, autophagic, and apoptotic regulators are activated upon CoCl_2 exposure. mRNAs were isolated from L4 animals exposed to CoCl_2 (0, 2.5, 5, and 10 mM) for 2 h. Mitochondrial morphology, autophagy, and apoptosis-associated genes were examined by qRT-PCR. mRNA levels were normalized to *tba-1* ($N = 3$, 2500 animals per sample). Individual experiments were independently repeated for four times. * $P < 0.05$ compared with 0 mM CoCl_2 .

3.5.2 Functional Assessment Using Genetic-Modified Strains

1. Utilize CU6372, the *drp-1* null mutant, to confirm the causal relationship between *drp-1* and toxicant-induced mitochondrial damages.
2. Run similar assays such as survival, mitochondrial ROS generation, mitochondrial morphology, ATP production, and oxygen consumption.
3. Compare the results with wild-type strain to unveil the role of *drp-1* upon environmental toxicant exposure. A recent published paper can be used as an example [15].

4 Notes

1. If the metal(s) in the pollutant of interest interact(s) with M9 buffer, use 85 mM NaCl instead. For example, since cobalt ion reacts with phosphate groups in M9 buffer and forms insoluble $\text{Co}_3(\text{PO}_4)_2$, 85 mM NaCl was used instead for CoCl_2 exposure.
2. Pilot experiments with survival assays are encouraged to generate exposure doses.
3. FCCP can be acutely toxic even at low doses. Personal protective equipment should be worn at all times while handling this reagent.
4. Sodium azide, the electron transport chain inhibitor, can be acutely toxic even at low doses. Moreover, sodium azide changes rapidly into a toxic gas when mixed with water or acids. Personal protective equipment should be worn at all times while handling this reagent.
5. Synchronous L4 nematodes could be generated by L1 bleach synchronization, followed by seeding the L1 nematodes to NGM plates containing OP50 in the late afternoon of Day 1, which will result in synchronous L4 in the morning of Day 3 (40–44 h after plating). L4 nematodes are characterized with the iconic half circle in the ventral side representing the developing vulva.
6. Due to the difference in sensitivity and size, 5000 L1 nematodes are roughly equal to 2500 L4 nematodes in 500 μL reaction system containing 25 μL of 20 \times exposure solutions.
7. If solid exposure is preferred, i.e., the toxicant is mixed in plates for prolonged exposure, the doses should be 10 folds less than liquid exposure.
8. All fluorescent studies are suggested to perform at 20 °C in dim light.
9. This step is also important for the clearance of residual dye in their guts.

10. Nematode can be anesthetized by 1 mM levamisole.
11. Otherwise, genetic-modified *C. elegans* strains could be used directly, without fluorescent staining. These include nematodes which harbor mitochondrial-targeted roGFP, HyPer, and mt-cpYFP for monitoring redox state changes, peroxide, and superoxide contents, respectively. Those nematodes give instantaneous readouts and fluctuate based on mitochondrial redox levels [19–21]. Furthermore, MitoTimer reporter strain changes fluorescence from green to red under mitochondrial stress, therefore could demonstrate mitochondrial damage under physiological and pathological conditions in vivo [22].
12. Previously, we discovered that MitoTracker staining of the mitochondria and toxicant CoCl₂ exposure cannot be performed at the same time. When exposed to 10 mM of CoCl₂, only half of the nematodes had their mitochondria labeled. As the dose of CoCl₂ increased, the dye either failed to enter the nematodes or to target to the mitochondria (data not shown). Therefore, we dyed nematodes before toxicant exposure.
13. To identificate and characterize mitochondrial bioenergetics, individually analyze mitochondrial membrane potential by flow cytometry in combination with the ratiometric fluorescent probe JC-9 is encouraged [23].
14. Diluted ATP standards solutions are stable for 8 h at 4 °C. Store them at –20 °C for longer periods of time.
15. Unexposed group with the addition of CCCP (a mitochondrial oxidative phosphorylation uncoupler) could serve as a positive control.
16. Besides ATP luminescence assay, *C.elegans* reporter strains PE254 or PE255 can be used for direct determination of ATP levels and thus, an aspect of mitochondrial damage [24, 25].
17. Since cartridges cannot be used for multiple runs, hydrate enough cartridges to avoid shortness. Hydration can last 4–72 h. If longer than 24 h of hydration is needed, seal the plate with parafilm and store at 4 °C instead.
18. Be very gentle to avoid bubbles and adhere residues to the sides of the ports.
19. Inspect the injection ports A and B with eyes for even loading and to make sure all liquid is on the bottom of the ports.
20. OCRs change significantly during development and aging. Normally, adult nematodes show higher respiration than L4 nematodes, when adult Day 4 reaches the peak and slowly goes down afterwards [26]. Moreover, the size of nematodes, FUdR treatment, or RNAi could also influence OCR [27, 28].
21. 2500 L4 nematodes per exposure are adequate for qRT-PCR to generate reproducible results.

Acknowledgments

This work was supported by NSFC grant (81903352 and 81973083), the Joint Funds for the Innovation of Science and Technology, Fujian province (2019Y91010015 and 2017Y9105) and National Institutes of Health (R01ES07331, R01ES10563).

References

1. Zheng F, Gonçalves FM, Abiko Y, Li H, Kumagai Y, Aschner M (2020) Redox toxicology of environmental chemicals causing oxidative stress. *Redox Biol* 34:101475. <https://doi.org/10.1016/j.redox.2020.101475>
2. Diaz F, Moraes CT (2008) Mitochondrial biogenesis and turnover. *Cell Calcium* 44 (1):24–35. <https://doi.org/10.1016/j.ceca.2007.12.004>
3. Yoo SM, Jung YK (2018) A molecular approach to Mitophagy and mitochondrial dynamics. *Mol Cells* 41(1):18–26. <https://doi.org/10.14348/molcells.2018.2277>
4. Meyer JN, Leuthner TC, Luz AL (2017) Mitochondrial fusion, fission, and mitochondrial toxicity. *Toxicology* 391:42–53. <https://doi.org/10.1016/j.tox.2017.07.019>
5. Leung MCK, Williams PL, Benedetto A, Au C, Helmcke KJ, Aschner M, Meyer JN (2008) *Caenorhabditis elegans*: an emerging model in biomedical and environmental toxicology. *Toxicol Sci* 106(1):5–28. <https://doi.org/10.1093/toxsci/kfn121>
6. Heise T, Schmidt F, Knebel C, Rieke S, Haider W, Geburek I, Niemann L, Marx-Stoelting P (2018) Hepatotoxic combination effects of three azole fungicides in a broad dose range. *Arch Toxicol* 92(2):859–872. <https://doi.org/10.1007/s00204-017-2087-6>
7. Schmidt F, Marx-Stoelting P, Haider W, Heise T, Kneuer C, Ladwig M, Banneke S, Rieke S, Niemann L (2016) Combination effects of azole fungicides in male rats in a broad dose range. *Toxicology* 355–356:54–63. <https://doi.org/10.1016/j.tox.2016.05.018>
8. Brenner S (1974) The genetics of *Caenorhabditis elegans*. *Genetics* 77(1):71–94
9. Apfeld J, Alper S (2018) What can we learn about human disease from the Nematode *C. elegans*? *Methods Mol Biol* 1706:53–75. https://doi.org/10.1007/978-1-4939-7471-9_4
10. Hunt PR (2017) The *C. elegans* model in toxicity testing. *J Appl Toxicol* 37(1):50–59. <https://doi.org/10.1002/jat.3357>
11. Byrne JJ, Soh MS, Chandhok G, Vijayaraghavan T, Teoh JS, Crawford S, Cobham AE, Yapa NMB, Mirth CK, Neumann B (2019) Disruption of mitochondrial dynamics affects behaviour and lifespan in *Caenorhabditis elegans*. *Cell Mol Life Sci* 76 (10):1967–1985. <https://doi.org/10.1007/s00018-019-03024-5>
12. Tsang WY, Lemire BD (2003) The role of mitochondria in the life of the nematode, *Caenorhabditis elegans*. *Biochim Biophys Acta* 1638(2):91–105. [https://doi.org/10.1016/s0925-4439\(03\)00079-6](https://doi.org/10.1016/s0925-4439(03)00079-6)
13. Maglioni S, Ventura N (2016) *C. elegans* as a model organism for human mitochondrial associated disorders. *Mitochondrion* 30:117–125. <https://doi.org/10.1016/j.mito.2016.02.003>
14. McBride HM, Neuspiel M, Wasiak S (2006) Mitochondria: more than just a powerhouse. *Curr Biol* 16(14):R551–R560. <https://doi.org/10.1016/j.cub.2006.06.054>
15. Zheng F, Chen P, Li H, Aschner M (2020) Drp-1 dependent mitochondrial fragmentation contributes to cobalt chloride induced toxicity in *Caenorhabditis elegans*. *Toxicol Sci* 177 (1):158–167. <https://doi.org/10.1093/toxsci/kfaa105>
16. Rolland SG (2014) How to analyze mitochondrial morphology in healthy cells and apoptotic cells in *Caenorhabditis elegans*. *Methods Enzymol* 544:75–98. <https://doi.org/10.1016/B978-0-12-417158-9.00004-2>
17. Zhang Y, Chen D, Smith MA, Zhang B, Pan X (2012) Selection of reliable reference genes in *Caenorhabditis elegans* for analysis of nanotoxicity. *PLoS One* 7(3):e31849
18. Livak KJ, Schmittgen TD (2001) Analysis of relative gene expression data using real-time quantitative PCR and the 2(-Delta Delta C (T)) method. *Methods* 25(4):402–408. <https://doi.org/10.1006/meth.2001.1262>
19. Liu Z, Celotto AM, Romero G, Wipf P, Palladino MJ (2012) Genetically encoded redox sensor identifies the role of ROS in degenerative and mitochondrial disease pathogenesis.

- Neurobiol Dis 45(1):362–368. <https://doi.org/10.1016/j.nbd.2011.08.022>
20. Roma LP, Duprez J, Takahashi HK, Gilon P, Wiederkehr A, Jonas J-C (2012) Dynamic measurements of mitochondrial hydrogen peroxide concentration and glutathione redox state in rat pancreatic β -cells using ratiometric fluorescent proteins: confounding effects of pH with HyPer but not roGFP1. Biochem J 441(3):971–978. <https://doi.org/10.1042/BJ20111770>
21. Wang W, Fang H, Groom L, Cheng A, Zhang W, Liu J, Wang X, Li K, Han P, Zheng M, Yin J, Wang W, Mattson MP, Kao JPY, Lakatta EG, Sheu S-S, Ouyang K, Chen J, Dirksen RT, Cheng H (2008) Superoxide flashes in single mitochondria. Cell 134 (2):279–290. <https://doi.org/10.1016/j.cell.2008.06.017>
22. Laker RC, Xu P, Ryall KA, Sujkowski A, Kenwood BM, Chain KH, Zhang M, Royal MA, Hoehn KL, Driscoll M, Adler PN, Wessells RJ, Saucerman JJ, Yan Z (2014) A novel MitoTimer reporter gene for mitochondrial content, structure, stress, and damage in vivo. J Biol Chem 289(17):12005–12015. <https://doi.org/10.1074/jbc.M113.530527>
23. Daniele JR, Heydari K, Arriaga EA, Dillin A (2016) Identification and characterization of mitochondrial subtypes in *Caenorhabditis elegans* via analysis of individual mitochondria by flow cytometry. Anal Chem 88 (12):6309–6316. <https://doi.org/10.1021/acs.analchem.6b00542>
24. Lagido C, McLaggan D, Glover LA (2015) A screenable in vivo assay for mitochondrial modulators using transgenic bioluminescent *Caenorhabditis elegans*. J Vis Exp 105: e53083. <https://doi.org/10.3791/53083>
25. Luz AL, Lagido C, Hirshey MD, Meyer JN (2016) In vivo determination of mitochondrial function using luciferase-expressing *Caenorhabditis elegans*: contribution of oxidative phosphorylation, glycolysis, and fatty acid oxidation to toxicant-induced dysfunction. Curr Protoc Toxicol 69:25.8.1–25.8.22. <https://doi.org/10.1002/cptx.10>
26. Koopman M, Michels H, Dancy BM, Kamble R, Mouchiroud L, Auwerx J, Nollen EAA, Houtkooper RH (2016) A screening-based platform for the assessment of cellular respiration in *Caenorhabditis elegans*. Nat Protoc 11(10):1798–1816. <https://doi.org/10.1038/nprot.2016.106>
27. Davies SK, Leroi AM, Bundy JG (2012) Fluorodeoxyuridine affects the identification of metabolic responses to daf-2 status in *Caenorhabditis elegans*. Mech Ageing Dev 133(1):46–49. <https://doi.org/10.1016/j.mad.2011.11.002>
28. Rooney JP, Luz AL, González-Hunt CP, Bodhicharla R, Ryde IT, Anbalagan C, Meyer JN (2014) Effects of 5'-fluoro-2-deoxyuridine on mitochondrial biology in *Caenorhabditis elegans*. Exp Gerontol 56:69–76. <https://doi.org/10.1016/j.exger.2014.03.021>



Chapter 4

Methods to Assay the Behavior of *Drosophila melanogaster* for Toxicity Study

Guiran Xiao

Abstract

Drosophila melanogaster, the fruit fly, has been widely used in biological investigation as an invertebrate alternative to mammals for its various advantages compared to other model organisms, which include short life cycle, easy handling, high prolificacy, and great availability of substantial genetic information. The behavior of *Drosophila melanogaster* is closely related to its growth, which can reflect the physiological conditions of *Drosophila*. We have optimized simple and robust behavioral assays for determining the larvae survival, adult climbing ability (mobility assay), reproductive behavior, and lifespan of *Drosophila*. In this chapter, we present the step-by-step detailed method for studying *Drosophila* behavior.

Key words *Drosophila melanogaster*, Survival, Climbing ability, Reproductive, Lifespan

1 Introduction

These behavioral assays are widely applicable for studying the role of genetic and environmental factors on fly behavior [1, 2]. The larvae survival can be reliably used for determining early-stage changes in the development of *Drosophila* and also for examining effects of drugs or human disease genes (in transgenic flies) on their development [3–5]. The survival assay becomes more applicable if expression or abolition of a gene causes lethality in pupal or adult stages [6–11], as these flies do not survive to adulthood where they otherwise could be assessed. The adult climbing ability has been widely used to investigate the activity and coordination [9–13]. Reproductive behavior is a behavior related any activity directed toward perpetuation of a species. A lot of toxic substances would lead to suppression of reproductive behaviors [13–15]. The lifespan assay can be used to investigate the survival status or death process of a population [6, 9–11, 16, 17].

2 Materials

The solvent used in this experiment is ultrapure water unless indicated otherwise. Waste materials are disposed following all the disposal regulations.

2.1 Equipment

1. Stereomicroscope.
2. Microwave oven.
3. Constant temperature and humidity incubator.

2.2 Chemicals and Solution

1. Culture medium of corn powder for *Drosophila*: 25 g yeast powder, 100 g corn meal, 10 g soybean meal, 8 g agar, 14.5 g refined cane sugar, 40 g brown sugar, and 1 L water. Bring to a boil, cook and stir for 10 min or until thickened, cool, and then add 2% preservatives.
2. Preservative formulations: 50 g methyl 4-hydroxybenzoate, 500 mL ethanol, and 125 mL propionic acid.
3. Juice-agar plates: 100–150 mL grape juice, 25 g brown sugar, 10 g agar powder, and 400 mL distilled water. Bring to a boil, cool, and then add 2% preservatives, poured on the glass. Sprinkle with yeast and spread evenly by hand.
4. CO₂.

2.3 Lab Suppliers

1. 10 × 10 pallet.
2. 5 × 5 pallet.
3. Gauze.
4. Marker pen.
5. *Drosophila* bottle.
6. *Drosophila* vial.
7. Cotton stopper.
8. Measuring cylinder.
9. Beaker.

3 Methods

In addition to the special needs, the general experimental fruit flies are placed in constant temperature and humidity incubator, and the feeding conditions are 25 °C, 60% humidity, 12 h light/12 h dark, so as to achieve the effect of high survival rate, more eggs, and rapid passage. The behavior assay of each group of *Drosophila melanogaster* needs to be repeated three times independently, and the behavior assay of wild-type *Drosophila melanogaster* should be used as the control.

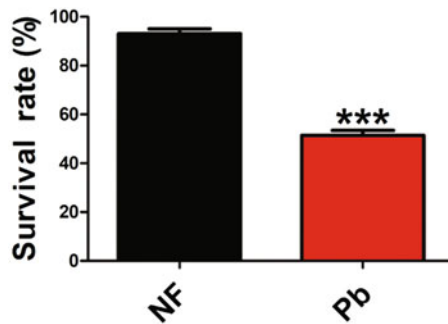


Fig. 1 Pb exposure resulted in reduced eclosion rate in *Drosophila* [13]. NF: normal food. Pb: 2 mM Pb acetate trihydrate

3.1 Survival Assay

1. 100 male and 300 virgin fruit flies are collected, isolated fed, and reared for 3–5 days (*see Notes 1 and 2*).
2. Male and female flies are mated for 3 days in the bottles, then 50 males and 150 females are transferred to a cage with juice-agar plate and let them lay eggs for 24 h (*see Note 3*).
3. Change the juice-agar plates every day and put the replaced plates in an incubator at 25 °C, 60% humidity, 12 h light/12 h dark (*see Note 4*).
4. Newly hatched first-instar larvae are transferred to normal food or food supplemented with toxicant, to a density of 100 larvae/vial (*see Note 5*).
5. Adults begin to emerge in about 10 days. Total numbers of emerging adults of each vial are counted (*see Notes 6 and 7*).
6. Record data.
7. The data are input into the software Prism 6 for statistical analysis (Fig. 1).

3.2 Climbing Ability (Mobility Assay)

1. 30 males and 60 virgin fruit flies are collected, isolated fed, and reared for 3–5 days (*see Notes 1 and 2*).
2. Put 5–7 male and 15–20 female *Drosophila* in each bottle where they will cross each other (*see Note 8*).
3. After 2–3 days, observe the situation of larva crawling out to avoid excessive oviposition. If necessary, transfer old *Drosophila* to another bottle.
4. Adults began to emerge in about 10 days. Collect flies emerging within 1 day (*see Note 9*).
5. According to the movement state of *Drosophila*, culture the collected flies for 1 week or longer and then test the mobility (*see Note 10*).

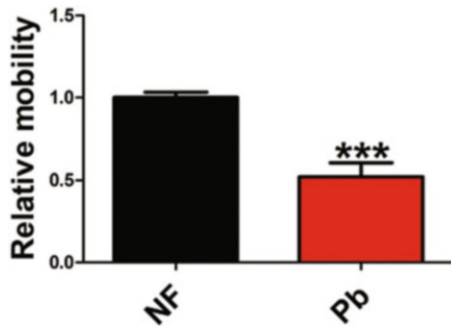


Fig. 2 Pb exposure resulted in defects in mobility of *Drosophila* [13]. NF: normal food. Pb: 2 mM Pb acetate trihydrate

6. Anesthetize the flies with CO₂, separate the female and male flies, put them in fresh medium, 20 flies per vial (*see Note 11*).
7. The anesthetized flies are allowed to recover for more than 24 h (*see Note 12*).
8. Place 20 flies in an empty plastic vial. Gently tap the recovered flies to the bottom. They will climb up against gravity (*see Note 13*).
9. According to the movement state of *Drosophila*, set a height to test the mobility (*see Note 14*).
10. The number of flies that reach the height is counted after 10 s (*see Note 14*).
11. The recorded data are input into the software Prism 6 for statistical analysis (Fig. 2).

3.3 Reproductive Behavior Assay

1. Repeat steps 1–3 in Subheading 3.2 to make cross.
2. Adults begin to emerge in about 10 days. Collect virgin flies emerging within 2 days (*see Note 15*).
3. Females are placed individually in a vial with 10 vials per group (*see Note 16*).
4. Change food every 12 h and eggs are counted for five successive days (*see Notes 17 and 18*).
5. The recorded data are input into the software Prism 6 for statistical analysis (Fig. 3).

3.4 Lifespan Assay

1. One of the principles of lifespan assay with *Drosophila* is to ensure that the genetic background of the mutant strain you are interested in is consistent with that of the wild-type control. Before the lifespan assay, the mutant *Drosophila* should be backcrossed with the wild-type control for at least 6 generations.

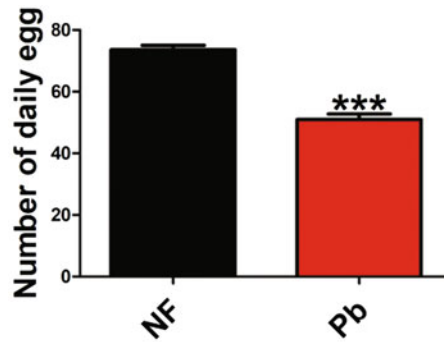


Fig. 3 *Drosophila* raised on Pb showed defects in reproduction [13]. NF: normal food. Pb: 2 mM Pb acetate trihydrate

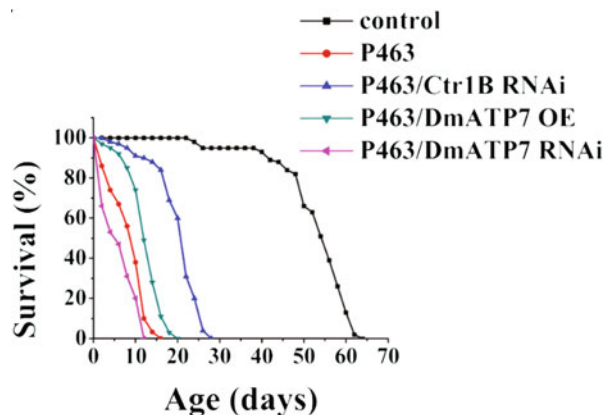


Fig. 4 Effect of copper transporters on the lifespan of a *Drosophila* model of Huntington disease [9]. P463 is the *Drosophila* model of Huntington disease. Ctr1B and DmATP7 are copper transporters

2. Repeat steps 1–3 in the Subheading 3.2 to make cross.
3. Adults begin to emerge in about 10 days. Select *Drosophila* at a fixed time point every day, separate the female and male flies, and put 20 flies in a vial with 10 vials per group, indicating the name of the flies and the selecting time (see Note 19).
4. Food is changed every 2 days.
5. The survival of the flies is recorded every time until all the flies die (see Notes 17 and 18).
6. The recorded data are input into the software Prism 6 for statistical analysis (Fig. 4).

4 Notes

1. 5–20 flies can be placed in the tube, and 10–50 flies can be placed in the bottle. Too many or too few flies are not conducive to the growth of fruit flies. The *Drosophila* parents should be poured out before the emergence of the offspring to avoid confusion between the offspring and the parents.
2. The selected virgin flies are usually stored in fresh medium for 2–3 days before cross. One is that the ovaries of the flies will develop and mature after 2 days of emergence, and the amount of eggs laid gradually increases; the other is to further determine whether the female is a virgin fly by observing whether there are larvae crawling out of the medium during the preservation period.
3. Before transferring flies to the plate, preheat the plate to 25 °C, and ensure that there is no moisture. Spread some yeast powder on the plate.
4. Seal the plate with a sealing film to prevent fruit flies from entering.
5. When transferring the larvae, be careful not to hurt them. 70–100 larvae are suitable to be placed in one vial.
6. Collect 70–100 larvae in one vial within 1 day.
7. Pay attention to observe the growth of *Drosophila* at any time. If there is a crack in the culture medium, appropriate amount of sterilized water can be added. If there are too many larvae, resulting in too thin medium, a small amount of sterile toilet paper can be put in.
8. The best time for cross is 3–15 days after eclosion, because the reproductive system of newly emerged male flies is not mature, and the mating ability of over aged male flies will decrease.
9. Ensure the same age of *Drosophila melanogaster*, similar growth status. This can reduce the variance and increase the reliability of the results.
10. Observe the crawling ability of *Drosophila* at any time. A good time to measure the mobility is important, and the fruit flies cannot climb too fast or too slowly. If the flies move too fast, it is difficult to measure; on the contrary, if the flies move too slowly, it is difficult to distinguish the control group from the treatment groups.
11. The operation of *Drosophila* should be carried out in small amount and in batches, and each operation should be as fast as possible to shorten the anesthesia time of *Drosophila* and reduce the damage to *Drosophila*.

12. The *Drosophila* with behavioral experiment should not be anesthetized within 24 h before the experiment.
13. Avoid shaking the fruit flies violently.
14. The test height and time should be adjusted according to the actual situation. The principle of setting the height and the time is that ~80% of the control group flies could reach the height within the test time.
15. Because most *Drosophila* eclose in the morning, it is better to start the selection of virgin flies at 8:00 a.m.
16. Do not pick flies with growth defects.
17. When changing food, be careful to avoid flies flying away or being crushed by cotton balls.
18. Before changing food, preheat the food to 25 °C, and ensure that there is no moisture.
19. Male and female *Drosophila melanogaster* have different life-span and must be detected separately.

Acknowledgments

This project was funded by the National Natural Science Foundation of China (31671284), the Fundamental Research Funds for the Central Universities (JZ2020HGPA0115), and the Youth Science and Technology Talents Support Program (2020) by Anhui Association for Science and Technology.

References

1. Simon AF et al (2012) A simple assay to study social behavior in *Drosophila*: measurement of social space within a group. *Genes Brain Behav* 11:243–252. <https://doi.org/10.1111/j.1601-183X.2011.00740.x>
2. Nichols CD, Becnel J, Pandey UB (2012) Methods to assay *Drosophila* behavior. *J Vis Exp* 61:3795. <https://doi.org/10.3791/3795>
3. Tennesen JM, Thummel CS (2011) Coordinating growth and maturation - insights from *drosophila*. *Current Biol* 21:R750–R757. <https://doi.org/10.1016/j.cub.2011.06.033>
4. Barrett M et al (2020) Larval mannitol diets increase mortality, prolong development and decrease adult body sizes in fruit flies (*Drosophila melanogaster*). *Biology Open* 8:bio047084. <https://doi.org/10.1242/bio.047084>
5. Wu M, Pastor-Pareja JC, Xu T (2010) Interaction between Ras(V12) and scribbled clones induces tumour growth and invasion. *Nature* 463:545–U165. <https://doi.org/10.1038/nature08702>
6. Xiao GR, Wan ZH, Fan QW, Tang XN, Zhou B (2014) The metal transporter ZIP13 supplies iron into the secretory pathway in *Drosophila melanogaster*. *Elife* 3:e03191. <https://doi.org/10.7554/elife.03191>
7. Sharma V, Swaminathan A, Bao RY, Pile LA (2008) *Drosophila SIN3* is required at multiple stages of development. *Dev Dynam* 237:3040–3050. <https://doi.org/10.1002/dvdy.21706>
8. Rodrigues APC, Camargo AF, Andjelkovic A, Jacobs HT, Oliveira MT (2018) Developmental arrest in *Drosophila melanogaster* caused by mitochondrial DNA replication defects cannot be rescued by the alternative oxidase. *Sci Rep* 8:10882. <https://doi.org/10.1038/S41598-018-29150-X>

9. Xiao G, Fan Q, Wang X, Zhou B (2013) Huntington disease arises from a combinatory toxicity of polyglutamine and copper binding. *Proc Natl Acad Sci U S A* 110:14995–15000. <https://doi.org/10.1073/pnas.1308535110>
10. Lang M et al (2012) Genetic inhibition of solute-linked carrier 39 family transporter 1 ameliorates abeta pathology in a *Drosophila* model of Alzheimer's disease. *PLoS Genet* 8: e1002683. <https://doi.org/10.1371/journal.pgen.1002683>
11. Wu Z, Li C, Lv S, Zhou B (2009) Pantothenate kinase-associated neurodegeneration: insights from a *drosophila* model. *Hum Mol Genet* 18:3659–3672. <https://doi.org/10.1093/hmg/ddp314>
12. Xue J, Wang HL, Xiao G (2020) Transferrin1 modulates rotenone-induced Parkinson's disease through affecting iron homeostasis in *Drosophila melanogaster*. *Biochem Biophys Res Commun* 531(3):305–311. <https://doi.org/10.1016/j.bbrc.2020.07.025>
13. Liu ZH et al (2020) Oxidative stress caused by lead (Pb) induces iron deficiency in *Drosophila melanogaster*. *Chemosphere* 243:125428. <https://doi.org/10.1016/j.chemosphere.2019.125428>
14. Wirth JJ, Mijal RS (2010) Adverse effects of low level heavy metal exposure on male reproductive function. *Syst Biol Reprod Med* 56:147–167. <https://doi.org/10.3109/19396360903582216>
15. Boyle D et al (2008) Natural arsenic contaminated diets perturb reproduction in fish. *Environ Sci Technol* 42:5354–5360. <https://doi.org/10.1021/es800230w>
16. Xiao GR, Liu ZH, Zhao MR, Wang HL, Zhou B (2019) Transferrin 1 Functions in Iron Trafficking and Genetically Interacts with Ferritin in *Drosophila melanogaster*. *Cell Rep* 26:748. <https://doi.org/10.1016/j.celrep.2018.12.053>
17. Bauer JH, Goupil S, Garber GB, Helfand SL (2004) An accelerated assay for the identification of lifespan-extending interventions in *Drosophila melanogaster*. *Proc Natl Acad Sci U S A* 101:12980–12985. <https://doi.org/10.1073/pnas.0403493101>



Chapter 5

Investigating the Joint Effects of Pesticides and Ultraviolet B Radiation in *Xenopus laevis* and Other Amphibians

Shuangying Yu and Mike Wages

Abstract

Exposure to multiple stressors often results in higher toxicity than one stressor alone. Examining joint effects of multiple stressors could provide more realistic exposure scenarios and a better understanding of the combined effects. In amphibian toxicology, simultaneous exposure to some pesticides and ultraviolet B (UVB) radiation has been suggested to be detrimental and more harmful in amphibian early-life stages than either stressor alone. Therefore, it is important to investigate the joint effects of these two stressors and provide data that could lead to more informed risk assessment. Here we describe how to set up a co-exposure to pesticides and ultraviolet B radiation to examine their joint toxicity in amphibian embryos and larvae, focusing on *Xenopus laevis* with notes on other amphibian species. With modifications, the methods may be applied to other types of chemicals or other aquatic organisms of interest.

Key words Multiple stressors, Environmental contaminants, Toxicity testing, FETAX, *Xenopus laevis* husbandry

1 Introduction

Most amphibian toxicological studies performed in the laboratory focus on chemical stressors. However, organisms are likely to be exposed to multiple stressors in the field that may increase or decrease chemical toxicity. Incorporating other common stressors in the experiment could provide more realistic exposure scenarios and produce data that may be more useful for risk assessment. Both environmental contaminants and ultraviolet B (UVB; 280–320 nm) radiation have been implicated in causing the worldwide amphibian declines [1]. Pesticides are a large group of chemicals that are ubiquitous in the environment. Studies have documented synergistic effects when amphibians are exposed to pesticides and UVB simultaneously, which is often attributed to the higher toxicity of photodegradation products than parent compounds (e.g., [2, 3]).

Many studies have examined the effects of ambient UV radiation on amphibians *in situ* (e.g., [4]). Although exposure to ambient UV radiation is more realistic, it is often difficult to apply chemical exposure in the field and achieve accurate target concentrations. Additionally, other unpredictable factors, such as temperature and cloud cover, could influence chemical toxicity and UV irradiance, respectively. Therefore, using artificial UV radiation in the laboratory is rather common (e.g., [3, 5]). Natural levels of UV radiation can be measured *in situ* or obtained from literature, and similar intensity and dose can be applied in the laboratory. Common materials used in aquatic research to manipulate UV transmission to achieve desired levels and spectrum include cellulose acetate as transmitting filters (e.g., [6, 7]), and Mylar-D film for blocking UV (e.g., [6]).

The most commonly used toxicity testing for amphibians is The Frog Embryo Teratogenesis Assay—*Xenopus* (FETAX), the first standard toxicity test assay that uses *X. laevis* to determine developmental toxicity of chemicals [8]. However, FETAX focuses on the embryonic development whereas there is often a need to test the larval stage. Our research has shown that *X. laevis* larvae can be used in toxicity testing using methods commonly developed for other non-laboratory amphibian species [9].

Here we describe methods used in our research to examine combined effects of pesticides and UVB in amphibian embryos and larvae with details on animal husbandry and breeding, preparation of chemical and UVB exposures, exposure conditions, and experimental procedures. Artificial UVB radiation is provided inside an enclosed chamber atop a flowing stream allowing precise control of factors such light:dark cycle, UVB dose, and temperature.

2 Materials

1. Chemical stock solution.

High purity (>99%) pesticides can be purchased from various vendors. Most pesticides are in a solid or highly viscous liquid form. Dissolve pesticides in a carrier solvent (ideally pesticide grade) to make a stock solution. As many pesticides are hydrophobic, dissolving the chemical in an organic solvent miscible with water will also facilitate the dispersion of chemical molecules in water-based test media (*see Note 1*). Vortex the pesticide and solvent mixture to facilitate dissolving and mixing, and store the stock solution in the freezer (*see Note 2*). Common solvents used in organic chemical toxicity testing are acetone, acetonitrile, dimethyl sulfoxide, dimethyl formamide, ethanol, methanol, tertiary-butyl alcohol, and triethylene glycol [10]. The solvent used in the stock solution will most likely

be the solvent in the solvent vehicle control. As such, an organic solvent that is of low toxicity to the test organism is recommended.

2. Reconstituted laboratory water for *X. laevis* and other amphibians.

FETAX solution for *X. laevis*: 0.016 g/L CaCl₂, 0.0616 g/L CaSO₄, 0.074 g/L MgSO₄, 0.030 g/L KCl, 0.621 g/L NaCl, and 0.096 g/L NaHCO₃ ([11]; see Note 3). Calculate the weight of each chemical needed by multiplying the concentration by the volume of solution needed. Dissolve all salts in 2 L deionized (DI) or milli-Q (MQ) 18.2 Ω water first until all salts dissolve before final dilution (see Note 4).

Laboratory water for other amphibians: 0.096 g/L NaHCO₃, 0.060 g/L CaSO₄·2H₂O, 0.060 g/L MgSO₄, and 0.004 g/L KCl [12]. Calculate the weight of each chemical needed by multiplying the concentration by the volume of solution needed. Dissolve all salts in 2 L DI or MQ 18.2 Ω water first until all salts dissolve before final dilution. This moderately hard reconstituted laboratory water is appropriate for most amphibians.

3. Human chorionic gonadotropin.

Human chorionic gonadotropin (hCG) is injected into adult frogs to induce reproduction. Lyophilized powder of hCG (1 vial of approximately 10,000 IU) can be purchased from Sigma-Aldrich or other vendors. Prepare 10% amphibian Ringers solution as a carrier for hCG in sterilized MQ water: 0.660 g/L NaCl, 0.015 g/L CaCl₂, 0.015 g/L KCl, and 0.015 g/L NaHCO₃. Inject the appropriate amount of 10% Ringer's into the hCG vial to create a concentration of 250 IU/mL. Each pair of frogs requires a total of 1000 IU hCG (male 250 IU [1 mL] and female 750 IU [3 mL]; see Note 5). Ringer's solution is useable for up to 90 days if stored at 4 °C.

4. A 10 g/L buffered MS-222 (tricaine methanesulfonate) with sodium bicarbonate added to adjust pH to 7.0–7.5 is needed for euthanasia of larvae [13].
5. A UVB exposure chamber should be equipped with both UVB light bulbs and light bulbs that offer blue light spectrum (360–460 nm) needed for enzymatic repair of DNA photo-adducts by photolyase. We have used chambers built upon an artificial flowing stream system where the exposure containers that hold the test organisms were placed in the circulating water produced by water pumps for temperature control. The system allows for easy temperature control using heaters (temperature can be adjusted with different numbers of heaters).

6. A UV meter is needed to measure UVB intensity and should be calibrated periodically following the manufacturer's recommendations. Check with the manufacturer about the calibration service. If such service is not available, companies that provide such calibration service can be found online.

3 Methods

3.1 Adult *X. laevis* Husbandry

1. Adult housing: *Xenopus* should be housed in flow-through or recirculating systems for best results. Static renewal systems require intense labor and continual stress on the frogs but can be successfully utilized. Both commercial frog systems and traditional fish aquaria with 10-gallon (approximately 38 L) tanks can be used for *Xenopus*. However, the tank must always have a cover to prevent escapes. Males and females should be housed separately. Mature females are larger than males (10 cm or larger) and have a more rounded pear-shaped body and have a distinct cloaca [14]. Mature males are smaller than the females (7–10 cm) and have a slender body without a cloaca.
2. Stocking density: Recommended stocking density for adult frogs varies considerably in the literature [15]. We had success with our colony by maintaining 1 adult female per 4 L of media (enough floor space for each frog to rest on the bottom without touching each other) and 1 adult male per 2 L media.
3. Water for colony: Aged and filtered tap water, well water, and FETAX have all been used for *Xenopus* husbandry. X-Mod water, a type of reconstituted DI water similar to FETAX, has also been developed for *Xenopus* husbandry by the addition of marine or cichlid salts [16]. For tap water, all chlorine and chloramines must be removed before use. Well water is usually safe to use but should be tested for metals (see Note 6).
4. Temperature: *X. laevis* is a very hardy species and the literature lists a wide range of temperatures (16–24 °C). Oocyte quality, however, seems best when frogs are housed at the lower end of the temperature range. In our lab we maintained the frogs at 18 °C. Before breeding, acclimate the frogs over several days to room temperature (22–23 °C).
5. Light cycle: Most labs have used a 12:12 light:dark cycle but others have done well using a 14:10 light:dark cycle. Provide shading so that *Xenopus* can retreat from direct lights.
6. Food: Several commercial sources are available for *X. laevis*, such as Xenopus Express and NASCO adult pellets. Feed females 6 pellets and males 3 pellets every other day.

3.2 Obtain *X. laevis* Eggs and Larvae

1. Five to seven days before the injections begin, acclimate breeding frogs to room temperature and to the media the eggs will be in. Select healthy adults that are plump, alert, and active for breeding.
2. Transfer selected adults to separate holding tanks for males and females. Capture the frogs with a deep (15 cm) fish net. *Xenopus* can easily jump out of smaller nets. Hold the body with one hand on top, covering the frog's head with the heel of the hand. Grasp the abdomen from underneath with the other hand, with two fingers between the hind legs. Never transport a large frog in a net without supporting the body with one hand from underneath. Some researchers wrap the frogs in paper towels, but it may stress the frogs more than using a net.
3. If the females have not ovulated in several (4–6) months or have never ovulated before, a priming dose will be necessary. Five days before breeding, inject 50 IU of hCG into the dorsal lymph sac 0.5 to 1 cm above the cloaca and 1 cm to either side of the midline (Fig. 1) [17, 18]. Do not isolate the female until the breeding event as she may ovulate due to the priming dose. Do not feed the frogs the last 2 days before breeding.
4. Prior to breeding, set up breeding tanks using 5-gallon (approximately 19 L) aquaria. Provide a false floor of plastic or epoxy-coated wire mesh 2.5 cm above the tank floor to keep the frogs from damaging or eating the eggs. The floor must have 0.5 cm or larger holes to ensure the egg masses can fall through (Fig. 2). A secure tight-fitting lid is required to prevent escape. The breeding tanks must be situated away from high traffic areas and bright lights.
5. Injections are usually given in late afternoon or early evening (250 IU for males and 750 IU for females). This allows the frogs to mate overnight in the dark. Lay several wet paper towels on the bench. Capture the frogs in a net as above. Carry to the bench, supporting the body with one hand. This will calm the frog. Set the net on the paper towels with the frog's head pointed away from the net handle. Gently pin the frog down with the heel of your hand on the frog's head and your fingers on the body. With your other hand carefully insert the syringe into the dorsal lymph sac (Fig. 1). Insert the needle just under the skin at a slightly downward angle and push slowly but not too slow. Use 26 or smaller gauge syringes.
6. Place the male and female together in each breeding tank. Provide gentle aeration which is important for the eggs. Amplexus will usually begin 2–6 h after injection and egg laying around 7–10 h later [11]. Several hundred to several thousand eggs may be obtained the next morning.

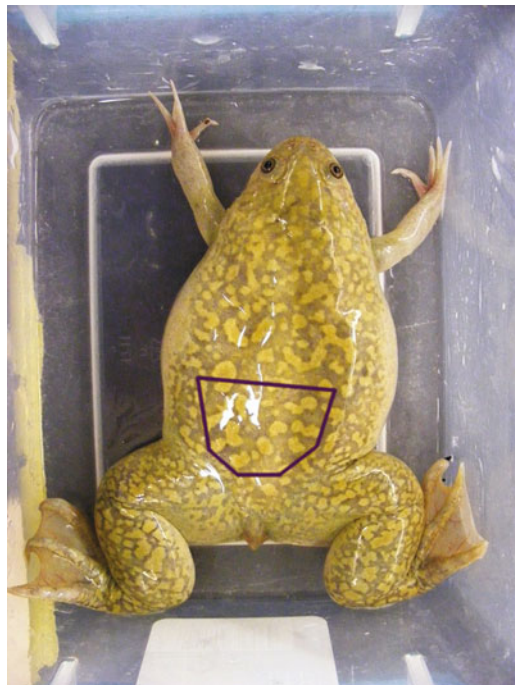


Fig. 1 A female *Xenopus laevis* frog with the dorsal lymph sac indicated for human chorionic gonadotropin injection to induce ovulation



Fig. 2 An amplexing pair of *Xenopus laevis* on a false floor of epoxy-coated wire mesh above the bottom of the tank with holes 0.5 cm or larger to prevent adult frogs from damaging or eating the eggs. Note that the white plastic mesh that also seems to be at the bottom of the tank is part of the platform that holds the tank in the flowing stream and is not inside the breeding tank

7. Removing the jelly coat may be problematic because the jelly coat may serve as a physical barrier that slows down the uptake of chemicals by ova [19]. Additionally, the jelly envelop may protect the ova by absorbing UVB and thus reducing UVB

transmission [20]. Due to the sticky nature of the *X. laevis* jelly coat, tools such as scalpels may be needed to sort the eggs for experiments.

8. To collect free swimming larvae, leave embryos in the breeding tank with aeration. As embryos develop, check daily for any unfertilized or dead eggs and remove them immediately as the decomposition fouls water quickly. Water change may be necessary. For larval testing, raise *X. laevis* embryos to NF stage 47/48 larvae [21]. Mix larvae from multiple clutches for genetic diversity and subsequently differential responses in the population (*see Note 7*).

3.3 Obtain Eggs and Larvae of Other Amphibians

If breeding in captivity is not possible, floating egg masses can be collected for some species from the field with no known history of contamination. Alternatively, our lab had success collecting amplexing pairs of the Mexican spadefoot toad (*Spea multiplicata*) at night in the field. Left in separate container undisturbed overnight, eggs from most pairs were obtained the next morning. Larval toxicity tests usually begin when larvae reach Gosner stage 25 [22].

3.4 Experimental Design

The 96-h test can be renewal or nonrenewal depending on the objective of the study. A renewal static test offers consistent daily chemical concentrations whereas a nonrenewal static test allows photodegradation of chemicals and exposure of organisms to degradation products. A full factorial design (e.g., 3×2) can be used incorporating various concentrations of a pesticide (e.g., acetone control, low, and high concentrations) and levels of UVB (e.g., low or high). Each treatment should have at least three jars (i.e., replicates) with multiple larvae per jar (*see Note 8*). All experimental procedures should be approved by the appropriate regulatory body for the country where the research occurs. For example, studies that take place in the U.S. should be approved by the Institutional Animal Care and Use Committee.

Each experiment should include a blank control (i.e., no solvent or test substance) and a solvent vehicle control. If the toxicity of the solvent is known and a small amount is determined to have negligible effect on the test organism, a solvent control may be sufficient without a blank control. The solvent control should be spiked with the highest amount of solvent used in the treatments, i.e., the amount of pesticide stock solution used to create the highest test concentration. The U.S. EPA guidelines for the fish acute toxicity test recommend the vehicle concentration be 0.1 mL/L or lower and may be as low as 0.02 mL/L [23].

3.5 Prepare UVB Exposure

In our study [24], we used eight total bulbs for the UVB exposure chamber, a set of two bulbs at each corner inside the exposure chamber: a UVB light bulb and a fluorescent white bulb. All four

sets of light bulbs were hung from the top and controlled by a timer. An adjacent chamber separated from the UVB chamber by Styrofoam sheets was used for UVB-absent treatments. Filters to attenuate UVB and provide desired spectrum can be used and may be placed on top of exposure containers. Wear eye protection when checking the animals in the UV exposure chamber.

3.6 Prepare Exposure Solutions

Add the predetermined volume of FETAX or other laboratory reconstituted water to glass jars (plastic containers should never be used in testing organic contaminants). The volume of the media is dependent on factors such as the size of exposure containers, the number of larvae per container, and the appropriate density for the test species. Spike the pesticide stock solution to FETAX or other media to achieve nominal test concentrations (*see Note 9*). Chemical analysis to verify nominal concentrations is often necessary.

3.7 Assign Animals to Treatments and Daily Observation

Larvae can be assigned in a haphazard fashion to each jar. Use a 1-mL disposable plastic pipette to transfer larvae. Cut the tip of the pipette to create a large opening to draw a larva into the pipette. The opening should be large enough so that going through the opening would not damage the larva. Gently release the larva into the jar without the pipette touching the solution to avoid contamination of the transfer pipette. Avoid dropping larvae from too high above the solution as this may cause damage and stress to larvae. Minimize the amount of water added to the test solution when releasing the larva as it may disrupt the exposure concentration. Larvae are not fed during the 96-h exposure. Check larvae multiple times a day during the exposure and remove dead larvae immediately.

3.8 Experimental Conditions

It is important to maintain a relatively constant temperature, for example, 22–25 °C, as temperature affects animal development and toxicity of some pesticides. Normally a light:dark cycle of 12:12 or 14:10 is provided. The UVB light bulbs can be set to turn on during certain hours to mimic natural conditions. The duration can be calculated based on the intended dose of UVB radiation. Water quality should be measured at the beginning and the end of the experiment. Common parameters reported include temperature, pH, dissolved oxygen, conductivity, and sometimes ammonia.

3.9 Experimental Endpoints

Mortality, malformation, and growth are three common endpoints measured. A common indicator of death used by ecotoxicologists studying amphibians is a lack of response to prodding. Many pesticides and UVB are teratogens resulting in malformations that can be easily identified using a stereomicroscope (Fig. 3) following previous published guides on *X. laevis* abnormalities (e.g., [25]). Delayed growth is another indicator of adverse effect. Euthanize alive larvae in MS-222 at the end of the exposure. Rinse and

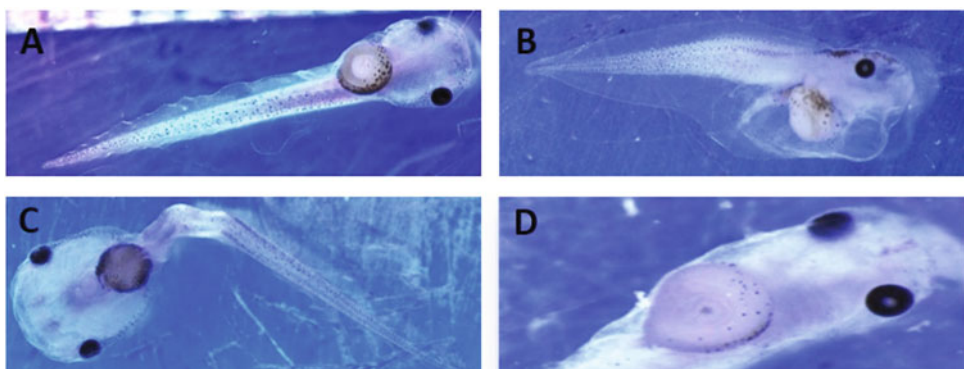


Fig. 3 Examples of *Xenopus laevis* malformations commonly observed in exposure to pesticides and ultraviolet B radiation: (a) control; (b) edema, axial deformity in the tail, and gut deformity; (c) severe axial deformity in the tail; (d) irregularly shaped gut

preserve larvae in 70% ethanol or isopropyl alcohol for further examination of sublethal effects, such as deformity, developmental stage, body length (snout-to-vent length [SVL] or total length [head to tail]), and body mass. It is often helpful to take digital images of each larva from dorsal and ventral views. These images can be used to examine abnormalities and measure larval size using freely available software such as Image J (National Institutes of Health, USA; <https://imagej.nih.gov/ij/>).

4 Notes

1. The concentration of the stock solution is calculated as the weight of the chemical divided by the volume of the solvent. Use a microbalance that can accurately weigh in the microgram range to measure a desired amount of the chemical and dissolve the chemical in the solvent. If such microbalance is not available and only a large amount of chemical can be measured accurately, a more concentrated stock solution can be made first upon which a second stock solution of a lower concentration is made by serial dilution. After weight is measured, calculate the volume of solvent needed to achieve the target stock concentration. If test concentrations and the volume of test solution have been determined, back calculate the appropriate stock concentration before preparing the stock solution. Factors to take into consideration when determining the stock concentration include (1) minimize the number of necessary serial dilution to make another stock solution of a lower concentration; (2) avoid spiking too little (e.g., 1–2 µL) or too much of stock solution to achieve testing concentrations. Accuracy of micropipettes drops when it is near the minimal amount. On the other hand, spiking too much stock solution

introduces a great amount of solvent which may cause undesired effects and confound results. The U.S. EPA recommends solvent concentrations be 0.1 mL/L or lower for fish toxicity testing [23]. Sometimes it may be necessary to make a second stock solution to achieve the nominal test concentrations.

2. Prepare and store the stock solution in an amber glass vial to minimize photodegradation. Wrap parafilm around the lid for a better seal. Store the stock solution in the freezer unless the manufacturer indicates otherwise. Organic pesticides dissolved in solvent and stored in the freezer generally have a long shelf life with minimal loss over a few years.
3. If using hydrated salts, adjust the concentration of salt accordingly to the water content. Use the increased concentrations for the following hydrated salts: 0.021 g/L $\text{CaCl}_2 \cdot 2\text{H}_2\text{O}$, 0.074 g/L $\text{CaSO}_4 \cdot 2\text{H}_2\text{O}$, and 0.152 g/L $\text{MgSO}_4 \cdot 7\text{H}_2\text{O}$.
4. Most salts, except for CaSO_4 , dissolve in water quickly with a magnetic stirring bar. Therefore, mix CaSO_4 in water first and wait until it is mostly dissolved to add other salts. This takes approximately 2 h. Note that if more than 50 L of FETAX is made which requires more CaSO_4 , dissolving CaSO_4 in two batches may be necessary. After the final dilution, it is important to provide aeration to the FETAX reservoir which facilitates dissolving and mixing of salts and ensures an appropriate oxygen level for test organisms.
5. If multiple clutches (e.g., 2–3 clutches) are desired, calculate how much hCG is needed for at least four pairs in order to obtain two or more clutches of eggs. It is not unusual for a pair to produce low-quality eggs.
6. *Xenopus* in the wild tend to favor ponds with moderately to very hard water (general hardness = 130–374 ppm). Most commercial vendors also favor hard water. If using aged tap water or well water, it may be necessary to increase the hardness. Research has shown that oocyte quality improves with increasing hardness [16].
7. Once most embryos hatch and develop, gently transfer larvae from all clutches in one tank to have a “mixed” pool of larvae for the experiment. However, such transfer may introduce stress to young larvae. Alternatively, the mixing can be done during the embryonic stage where viable embryos from all clutches are placed in one tank with a fish net to create the mix.
8. The number of larvae per jar depends on the specific requirement of a species and the volume of test solution in each jar. There should be enough larvae per jar to get an accurate estimate of effects such as percentages of mortality and malformation. On the other hand, a jar too crowded may introduce stress in the larvae. We have used five NF stage 47/48 *X. laevis*

larvae or Gosner stage 25 *S. multiplicata* per 400 mL of solution (1 larva per 80 mL solution) with success. A lower density may be needed for some amphibian species.

9. Use a micropipette to add the appropriate amount to each jar. You can use a clean pipette tip to mix the solution to facilitate a homogenous distribution of the pesticide solution. It is important to verify the calculations of serial dilution before the experiment. This can be done by simply asking another person to confirm the calculations.

References

1. Collins J, Storfer A (2003) Global amphibian declines: sorting the hypotheses. *Divers Distrib* 9:89–98
2. La Clair J, Bantle J, Dumont J (1998) Photo-products and metabolites of a common insect growth regulator produce developmental deformities in *Xenopus*. *Environ Sci Technol* 32:1453–1461
3. Zaga A, Little E, Rabeni C et al (1998) Photo-enhanced toxicity of a carbamate insecticide to early life stage anuran amphibians. *Environ Toxicol Chem* 17:2543–2553
4. Blaustein AR, Edmond B, Kiesecker JM et al (1995) Ambient ultraviolet radiation causes mortality in salamander eggs. *Ecol Appl* 5:740–743
5. Koponen PS, Kukkonen JVK (2011) Effects of bisphenol a and artificial UVB radiation on the early development of *Rana Temporaria*. *J Toxicol Environ Health A* 65:947–959
6. Bancroft BA, Baker NJ, Searle CL et al (2008) Larval amphibians seek warm temperatures and do not avoid harmful UVB radiation. *Behav Ecol* 19:879–886
7. Sampath-Wiley P, Jahnke LS (2011) A new filter that accurately mimics the solar UV-B spectrum using standard UV lamps: the photochemical properties, stabilization and use of the urate anion liquid filter. *Plant Cell Environ* 34:261–269
8. Dumont J, Schultz T, Buchanan M et al (1983) Frog embryo teratogenesis assay-*Xenopus* (FETAX)-a short-term assay application to complex environmental mixtures. In: Waters M, Sandhu S, Lewtas J, Claxton L, Chernoff N, Nesnow S (eds) Short-term bioassays in the analysis of complex environmental mixtures III. Springer, Boston, pp 393–405
9. Yu S, Wages M, Cai Q et al (2013) Lethal and sublethal effects of three insecticides on two developmental stages of *Xenopus laevis* and comparison with other amphibians. *Environ Toxicol Chem* 32:2056–2064
10. OECD (Organisation for Economic Co-operation and Development). (2019). Guidance document on aqueous-phase aquatic toxicity testing of difficult test chemicals. ENV /JM/MONO(2000)6/REV1
11. ASTM (American Society for Testing and Materials) (2004) Annual book of ASTM standards. Standard guide for conducting the frog embryo Teratogenesis assay-*Xenopus* (FETAX). ASTM E1439-98 (reapproved 2004). American Society for Testing and Materials, Philadelphia, PA, USA
12. U.S. EPA (2002) Methods for measuring the acute toxicity of effluents and receiving waters to freshwater and marine organisms (5th ed) EPA-821-R-02-021
13. AVMA (American Veterinary Medical Association) (2020) AVMA guidelines for the euthanasia of animals: 2020 edition. Version 2020. 0.1
14. Wlizla M, McNamara S, Horb ME (2018) Generation and care of *Xenopus laevis* and *Xenopus tropicalis* embryos. *Methods Mol Biol* 1865:19–32. https://doi.org/10.1007/978-1-4939-8784-9_2
15. Reed BT (2005) Guidance on the housing and care of the African Clawed frog *Xenopus laevis*. Research Animals Department of Royal Society for the Prevention of Cruelty to Animals (RSPCA)
16. Godfrey EW, Sanders GE (2004) Effect of water hardness on oocyte quality and embryo development in the African clawed frog (*Xenopus laevis*). *Comp Med* 54:170–175
17. Green SL (2009) The laboratory *Xenopus* sp. CRC Press, Boca Raton, FL
18. Sive HL, Grainger RM, Harland RM (2000) Early development of *Xenopus laevis*: a laboratory manual. Cold Spring Harbor Laboratory Press, Cold Spring Harbor NY

19. Edginton AN, Rouleau C, Stephenson GR et al (2007) 2,4-D Butoxyethyl ester kinetics in embryos of *Xenopus laevis*: the role of the embryo jelly coat in reducing chemical absorption. *Arch Environ Contam Toxicol* 52:113–120
20. Grant KP, Licht LE (1995) Effects of ultraviolet radiation on life-history stages of anurans from Ontario, Canada. *Can J Zool* 73:2292–2301. <https://doi.org/10.1139/z95-271>
21. Nieuwkoop PD, Faber J (eds) (1975) Normal table of *Xenopus laevis* development (Daudin): a systematical and chronological survey of the development from the fertilized egg until the end of metamorphosis, 2nd edn. North-Holland Publishing Company, Amsterdam, Netherland
22. Gosner KL (1960) A simplified table for staging anuran embryos and larvae with notes on identification. *Herpetologica* 16:183–190
23. U.S. EPA (2016) Ecological effects test guidelines: OCSPP 850.1075: Freshwater and saltwater fish acute toxicity test. EPA 712-C-16-007
24. Yu S, Wages M, Willming M et al (2015) Joint effects of pesticides and ultraviolet-B radiation on amphibian larvae. *Environ Pollut* 207:248–255
25. Bantle JA, Dumont JN, Finch RA et al (1998) Atlas of abnormalities: a guide for the performance of FETAX, 2nd edn. Oklahoma State University Press, Stillwater, OK, USA



Chapter 6

Identification of Stable Reference Genes for Toxicogenomic and Gene Expression Analysis

Xiaoping Pan and Baohong Zhang

Abstract

Gene expression analysis has been becoming a popular method for studying gene function and response to different environmental stresses, including toxin/pollution exposure. Selection of a suitable reference gene is critically important for gene expression analysis due to that wrong reference genes will cause misleading and even wrong conclusion. A good reference gene should be a more stable reference gene, particularly during the toxicant exposure treatment and/or other investigation condition. In this chapter, a step-by-step protocol is present for primer design, reverse transcription PCR, primer efficiency and specificity test, qRT-PCR, and the strategy for identifying most stable reference genes for toxicogenomic and gene expression analysis. The detailed method for determining the primer gene specificity and primer efficiency are also presented in this chapter. Low primer efficiency will affect the fold changes during gene expression analysis; however, it does not affect the conclusion, up- or downregulation. Choosing a wrong reference gene may result in wrong conclusion.

Key words Reference gene, Gene expression, Toxicogenomics, Housekeeping gene

1 Introduction

Gene expression analysis has been becoming one of the most important topics for gene function study and investigating organism response to different toxicant exposure. As time going, more and more researches are involved in analyzing gene expression. At RNA levels, there are many strategies and methods to study gene expression, which include the traditional Northern blotting and *in situ* hybridization as well as the most advanced deep sequencing (e.g., RNA-seq and small RNA-seq). Among all methods for studying gene expression at the RNA levels, quantitative real-time PCR (qRT-PCR) is the most sensitive and convenient method for studying gene expression. qRT-PCR can directly show the data with a short run time and do not require electrophoresis, that is generally

exposure to some chemicals, such as ethidium bromide (EBr); these chemicals are generally toxic and may cause carcinogenesis. Thus, qRT-PCR has become the most popular method for analyzing gene expression.

No matter what methods are employed for analyzing gene expression levels, a reference gene is required for serving as a standard for normalizing gene expression. This is because there are many factors affecting the raw data of gene expression, such as the sample RNA concentrations, RNA quality and even pipetting can induce errors. To avoid these errors, one or more reference genes are also run during the experimental stage. Additionally, most quantitative RNA data is not absolute, but relative [1]. Thus, it is critical to use one or more references as a standard for standardization of the gene expression in almost all gene expression analysis.

Many housekeeping genes, such as *actin* gene and *GADPH* gene, can be served as reference genes because of their relative stability on gene expression in different tissue, different developmental stage at different environmental conditions. However, there is no gene with consistent expression at any condition [2]. The expression of all genes varied at certain conditions, and different genes show different stability at certain conditions [3, 4]. Thus, to achieve the reliable data for gene expression analysis, it is better to analyze the expression of potential references for seeking the most stable genes as reference genes. In this chapter, we present a detailed step-by-step method for identifying most stable reference genes using qRT-PCR for gene expression analysis and toxicogenomics.

2 Materials

2.1 Cell Lines

1. The human breast adenocarcinoma cell line MCF-7 (see Note 1).

2.2 Chemicals and Regents

1. Roswell Park Memorial Institute Medium (RPMI) 1640 containing L-glutamine and 25 mM HEPES.
2. Double distilled H₂O (ddH₂O).
3. Deionized H₂O (diH₂O).
4. Insulin.
5. Gentamicin.
6. 10% FBS.
7. DMSO.
8. Liquid nitrogen.
9. Ice.

10. PBS buffer.
11. miRNA Isolation Kit.
12. Acid-phenol: chloroform.
13. Ethanol (100%).
14. Nuclease-free water.
15. RT-PCR kits.
16. SYBR Green mixture.

2.3 Instruments

1. Real-time PCR machine (*see Note 2*).
2. Regular PCR machine.
3. Water bath.
4. Clean hood.
5. Incubator with temperature and CO₂ controlling.
6. Centrifuges (for 15 mL and 2 mL centrifuge tubes).
7. Vortex.

2.4 Other Lab Suppliers

1. Centrifuge tubes (15, 2.0, 1.5, and 0.2 mL).
2. Sterile Disposable Filter Units with PES Membrane.
3. Cell culture flask (50 mL or 75 mL).
4. 6-well cell culture plate.
5. 0.22µm polyethersulfone filter.

3 Methods

3.1 Cell Culture and Treatment

1. Medium preparation. RPMI 1640 Medium containing L-glutamine and 25 mM HEPES is first sterilized by passing through a Sterile Disposable Filter Units with PES Membrane, followed by adding sterilized 10% fetal bovine serum (FBS), 10 mg/mL gentamicin, and 4 mg/mL insulin.
2. Add 5-Fluorouracil, melamine, and nicotine into the medium at appropriated concentrations as treatments (*see Notes 3–5*).
3. Add 2 mL prepared medium into each well of a 6-well cell culture plate.
4. Cells are seeded at 50,000 cell/cm² in a 6-well cell culture plate with RPMI medium without any tested chemicals (controlled medium).
5. After 24 h of culture, media are replaced with fresh media or with different concentrations of 5-Fluorouracil, melamine, and nicotine.
6. The cells are cultured under dark at 37 °C in a humidified incubator with 5% CO₂ and 95% air.

7. After 48 h of treatment, the cells are trypsinized for detaching the cells from the plate wall, washed using cold PBS buffer (pH 7.4) and collected into a 15 mL centrifuge tubes.
8. Centrifuge and collect cells from both treatments and the controls.
9. Put the collected cell sample in a 2.0 mL centrifuge tube. Clearly label the sample names, treatment types, and date.
10. Cells are immediately frozen in the liquid nitrogen (*see Note 6*).
11. Store the cell samples in -80 °C.

3.2 RNA Extraction

There are lots of kits used to extract RNAs. In this method, we employ the mirVana miRNA Isolation Kit (*see Note 7*) to extract the total RNAs according to the manufacturer's instructions and our previous reports [3, 5, 6].

1. Take off the cell samples from the -80 °C freezer.
2. Put the cell samples on ice.
3. Add 500µL of lysis/binding solution.
4. Vortex the cell samples with lysis buffer.
5. Add 50µL of miRNA homogenate additive.
6. Mix well by vortexing.
7. Incubate on ice for 10 min.
8. Add 500µL of acid-phenol: chloroform (*see Note 8*).
9. Vortex for 60 s.
10. Centrifuge for 5 min at 10,000 × g to separate the aqueous and organic phases.
11. Transfer (400µL) upper (aqueous) phase to a new 2 mL centrifuge tube (*see Note 9*).
12. Add 1.25 × (500µL) of 100% ethanol at room temperature to precipitate the RNAs.
13. Mix very well by gently vortexing or up-down for several times.
14. At the same time, prepare the filter cartridge, put a filter cartridge into a 2 mL labeled centrifuge tube.
15. Transfer the mixture of aqueous phase and ethanol into the cartridge (*see Note 10*).
16. Centrifuge at 10,000 × g for about 15 s to pass the mixture through the cartridge.
17. Discard the flow-through, and repeat until all of the lysate/ethanol mixture is through the cartridge.
18. Add 700µL miRNA Wash Solution 1 (working solution mixed with ethanol) to the filter cartridge.

19. Centrifuge at $10,000 \times g$ for ~5–10 s or use a vacuum to pull the solution through the filter. Discard the flow-through, and replace the filter cartridge into the same centrifuge tube.
20. Add 500 μ L Wash Solution 2/3 (working solution mixed with ethanol) and draw it through the filter cartridge as in the previous step.
21. Repeat with a second 500 μ L aliquot of Wash Solution 2/3 (*see Note 11*).
22. Transfer the filter cartridge into a fresh collection tube with clear label.
23. Add 50 μ L of pre-heated (95 °C) nuclease-free water to the center of the filter (*see Note 12*).
24. Spin for ~20–30 s at maximum speed to collect the RNAs from the filter cartridge.
25. Gently mix the collected RNA sample. If it is necessary, centrifuge for 5 s at low speed (5000 $\times g$) to make sure all collected sample sit on the bottom.
26. Measure the RNA concentration and quality using a NanoDrop.
27. Write down the concentrations, 260/280 and 260/230 ratio for each sample.
28. Clearly label each sample, including sample name and concentration as well as the date.
29. Store in –80 °C freezer.

3.3 Housekeeping Gene Selection, Primer Design and Preparation

3.3.1 Housekeeping Gene Selection

Generally speaking, any housekeeping gene has potential to serve as a reference gene for gene expression analysis. However, due to the factors that even housekeeping genes, their expression is not consistently expressed and their expression may change as developmental process and/or exposure to a specific condition, such as exposure to environmental pollution. If an instable housekeeping gene is served as a reference gene, it may cause the false conclusion. Thus, to better present the expression data, it is better to identify the most stable genes under the experimental condition. To find a better reference gene, you may search the literatures to see whether other studies have identified a better reference gene or not for the similar research, if so you may try to use that gene as reference gene. If not, it strongly suggests testing potential reference genes and identify one for your research. Normally, 8 to 16 commonly used reference genes are selected to test their stability under different experiment conditions that you will use in your research. Here, we select 12 commonly used housekeeping genes as examples to present the method and protocol for identifying most stable reference gene for toxicogenomic and gene expression analysis.

Table 1
12 housekeeping genes, as examples, for identifying the most stable reference genes in this method

Gene symbol	Gene name	Gene ID	Gene type	Function
βAct	β-Actin	NM_001101	Protein coding	Cytoskeletal structural protein
GADPH	Glyceraldehyde-3-phosphate dehydrogenase	NM_002046	Protein coding	Oxidoreductase in glycolysis and gluconeogenesis
SDHA	Succinate dehydrogenase complex, subunit A, flavoprotein (Fp)	NM_004168	Protein coding	Involved in the oxidation of succinate
TBCA	Tubulin folding cofactor A	NM_004607	Protein coding	Capturing and stabilizing beta-tubulin intermediates
TUBA1A	Tubulin, alpha 1a	NM_006009	Protein coding	Cytoskeletal structural protein
RNU44	Small nucleolar RNA, C/D box 44	NR_002750	snoRNA	RNA biogenesis
U6	RNA, U6 small nuclear 1	NR_004394	snRNA	Splicing of pre-mRNA
RNU48	Small nucleolar RNA, C/D box 48	NR_002745	snoRNA	RNA biogenesis
RNU47	Small nucleolar RNA, C/D box 47	NR_002746	snoRNA	RNA biogenesis
18 s	RNA, 18S ribosomal 1	NR_003286	rRNA	A component of small ribosomal subunit
TBP	TATA-binding protein	NM_003194	Protein coding	Involved in the activation of basal transcription from class II promoter
GNB2L1	Guanine nucleotide binding protein, β-peptide 2-like 1	NM_006098	Protein coding	Involved in binding and anchorage of protein kinase C

When the candidate genes are identified, the related information will be identified from the NCBI GenBank database [7] and listed in a table, which displays the gene symbol, gene name, gene ID, gene type, and gene function (Table 1).

3.3.2 Primer Design

Primer design is one of the most important steps for gene expression analysis using PCR and qRT-PCR. A good primer should meet the following features: (1) Primer length can be 18–30 nt, but majorly about 20–22 nt. Specificity is usually dependent on the primer length and annealing temperature; generally speaking, the longer the primer, the more the specificity; however the less the efficiency. (2) 3' primer end needs to be completely complementary with the DNA template. (3) It is better to have G or C or GC or CG

at the 3' end of the primer, which is known as a GC Clamp to help the primer tightly bind to their template for increasing primer efficiency and specificity due to the factor that G and C bases have three hydrogen bonds than two for A and T bases for the stability of the primer. (4) The GC content is about 40–60%. (5) The melting temperature (T_m) is between 60 and 70 °C and the difference between forward primer and reverse primer is less than 2 °C. If the T_m is too low, you may need to find a sequence with high GC content or extend the length of the primer. (6) Try to avoid 4 or more same continuous base or dinucleotide repeats (for example, CCCC or GCGCGCGC). (7) Try to avoid stem-loop structure of a primer, which usually displays more than 3 bases that complement within the primer, in which the primer will bind to themselves when running a PCR and significantly lower the primer efficiency. (7) Try to avoid primer-dimer, in which forward and reverse primer will bind to each other and significantly lower the primer efficiency (*see Note 13*).

Primer design can be performed manually or by computational software. Currently, many computational software, including both on-site and web-based programs, can be used for designing primers. Here, we suggest using Primer-BLAST to design primer. Primer-BLAST is a web-based computational program for designing primer with many advantages, including direct and easy input of Gene ID or nucleotide sequence, automatically checking the reference genome for primer gene specificity.

1. Open the Primer-BLAST website (<https://www.ncbi.nlm.nih.gov/tools/primer-blast/index.cgi>) (Fig. 1). If you cannot remember the website, you may direct search “Primer-BLAST” online, it will come out.
2. In the PCR Template window, input the gene ID or nucleotide sequence. If you use gene ID or give each DNA sequence with a name, you can input multiple sequence at a same time. Here, you also can choose the location where you want the forward and reverse primers sit. If not, you can leave there with blank.
3. For primer parameters, we can input the forward or reverse primer you already had, otherwise just leave them blank. For PCR product size, the default is 70–1000 nt; however, for most qRT-PCR run, the PCR products are about 70–200 nt in length; it is better to adjust to these number. Here, you also can adjust the primer melting temperatures according to your experiment design; however, in most times, you can just leave them as the defaults.
4. For exon/intron selection, you may leave as the defaults. You may also adjust it to selection your preference to design primer span on the exon-intron junction.

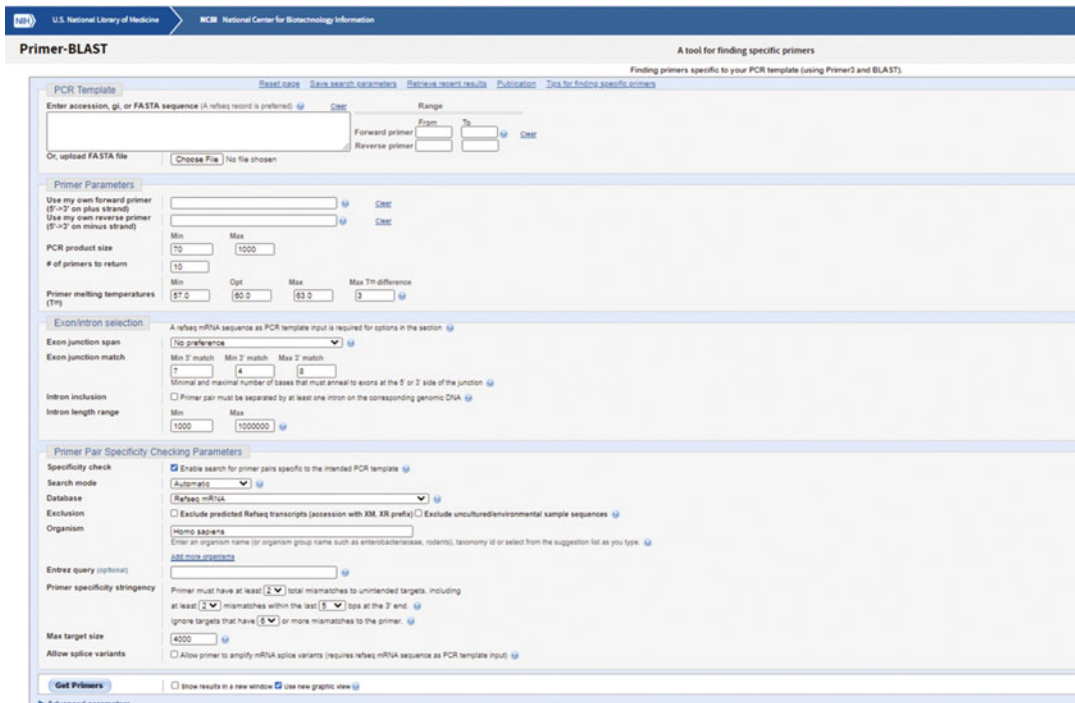


Fig. 1 Primer-BLAST window and input for designing primers

- For primer specificity checking parameters, you can input the specific species, such as human, to check whether the primer is gene specific or not.
 - After you input everything you need, click the Get Primers button. After a couple of seconds, depending on how many people using this website, it may take up to a couple of mins, the program will give you the designed primers on the next screen.
 - Compare and select the primers you want. Table 2 is an example for the designed primers of the candidate reference genes listed in Table 1.
 - Synthesize the designed primers by in house or by a commercial company.
- 3.3.3 Primer Preparation**
- Centrifuge the tubes with primers (*see Note 14*).
 - Add RNase and DNase free H₂O to make the final concentration of 100μM (*see Note 15*).
 - Vertebrate or up and down for several times to allow the primers completely dissolved. This primer solution will serve as stock solution for long-term usage, which should be stored in -80 °C or -20 °C freezer.

Table 2

Primers designed for 12 human candidate reference genes for toxicogenomic and gene expression analysis study

Gene name	Forward primer	Reverse primer	PCR amplicon size (bp)	Primer efficiency (%)
B-actin	CTCACCGAGCGCGGCTACAG	GGAGCTGGAAGCAGCCGTGG	126	92
GADPH	CCCGCTTCGCTCTCTGCTCC	GAGCGATGTGGCTCGGCTGG	77	101
SDHA	CGACACCGTGAAAGGGCTCCG	TCTAGCTCGACCACGGCGGC	90	103
TBCA	GCGTCGCCCTCCACGGTTAC	ACCAACCGCTTCACCACGCC	120	95
TUBA1A	CGCGAAGCAGCAACCATGCG	GGCATCTGGCCATCGGGCTG	125	99
RNU44	CCTGGATGATGATAAGCAAATG	GTCAGTTAGAGCTAACTTAAGACC	60	99
U6	CTGCGCAAGGATGACACGCA	AAAA58ATATGGAACGCTTACAG	45	102
RNU48	TGATGACCCCAGGTAACCTCTGAGTGTG	GGT102CAGAGCGCTCGGGT	58	98
RNU47	ACCAATGATGTAATGATTCTGCCA	ACCTCAGAACATCAAAA	75	93
18 s	TTGTACACACCGCCCCGTCGC	CTTCTCAGCGCTCCGCCAGG	102	65
TBP	GAAGAGTGTGCTGGAGATGC	AGGGATTCCGGGAGTCATGG	172	
GNB2L1	GAGTGTGGCCTCTCCTCTG	GGACACAAGACACCCACTCTG	137	

4. Prepare working solution. Prepare a new centrifuge tube clearly labeled with the primer name and date. Add 80µL RNase and DNase free H₂O into the tube; then add 10µL forward primer and 10µL forward primer, respectively, to the final volume of 100µL. Mix very well. The concentration of the working solution is 10µM for each primer (*see Note 16*).
5. Store the working solution of each primer pair in –20 °C freezer or 4 °C refrigerator if they will be used soon.

3.4 Reverse Transcription PCR (RT-PCR)

A total of 1µg of total RNAs is used to synthesize single-stranded cDNA with reverse transcription PCR (RT-PCR).

1. Calculate how much total RNAs needed for RT-PCR. Add the volume as mentioned in Table 3.
2. After calculating RNA sample, calculate how much water need to be added for making up the total volume of 15µL RT reaction. Then, add the water volume in Table 3.

Table 3
Each component in a RT-PCR reaction

Component	Volume/15- μ L reaction
Nuclease-free water	??
RNase inhibitor, 20 U/ μ L	0.19
100 mM dNTPs (with dTTP)	0.15
10 \times reverse Transcription buffer	1.50
Primer	1.00
Reverse transcriptase, 50 U/ μ L	1.00
RNA sample	??
Total	15

Table 4
Temperature program for RT-PCR

Temperature ($^{\circ}$ C)	Time (min)
16	30
42	30
85	5
4	Hold

3. Clearly label each 0.2 mL PCR tube with the sample and reaction names.
4. Add each component into the labeled PCR tube (*see Note 17*).
5. Mix gently.
6. Briefly centrifuge to bring solution to the bottom of the tube (2000 $\times g$ for 10 s).
7. Incubate the tube on ice for 5 min and keep on ice until you are ready to load the thermal cycler.
8. Load the thermal cycler and perform RT-PCR using the following temperature program (Table 4).
9. Add 80 μ L DNase free water into each RT-PCR product, mix thoroughly (*see Note 18*).
10. Perform qRT-PCR or store at -20° C or below.

3.5 Primer Efficiency Test

Primer efficiency, also called PCR efficiency, is the ratio of each PCR cycle run; it also refers the amplification efficiency of PCR. Based on the principle, after each cycle run, the copy number of DNA should be double. However, in the real world, it is not always this case.

Thus, primer efficiency is an important factor for performing PCR. Low primer efficiency will result in significant reduced number of PCR products after certain cycle running. Thus, for each designed primer pair, before performing PCR, the primer efficiency should be determined, particularly for reference genes. Primer efficiency test is also a straightforward method to be performed. Generally speaking, just diluting a cDNA or gRNA sample into a series of concentrations, and then using the series of concentrations to run PCR. Based on the Ct value for each DNA concentration, prime efficiency can be calculated. Most commonly used dilution is 10 \times or 2 \times dilution for at least five times. Following we present the primer efficiency test using 10 \times of PCR products generated in the section of RT-PCR.

1. Prepare 5 PCR tubes and clearly label the 10 \times , 100 \times , 1000 \times , 10,000 \times , and 100,000 \times .
2. Add 90 μ L DNase free water into each tube and cover the tube.
3. Dilute the cDNA from the RT-PCR section through a series of 1:10 covering 6 dilution points, e.g., 1:1; 1:10, 1:100, 1:1000, 1:10000, and 1:100000, by adding 10 μ L the 10 \times higher cDNA sample (*see Note 19*).
4. Prepare qRT-PCR plate.

qRT-PCR reaction majorly contains DNase free water, SYBR Green PCR Mixture, Forward and Reverse Primers, and DNA template (Table 5).

- (a) Prepare a 96-well plate (*see Note 20*).
- (b) Add 8 μ L DNase free water into each well for 20 μ L reaction.
- (c) Add 10 μ L 2 \times SYBR Green PCR Mixture into each well for 20 μ L reaction.
- (d) Add 1 μ L forward and reverse primer mixture into each well for 20 μ L reaction.
- (e) Add 1 μ L DNA template (*see Note 21*).

Table 5
Reaction mixture of qRT-PCR

Reagents	Volume (μ L) per a single 20 μ L reaction	Volume (μ L) per a single 50 μ L reaction
DNase free H ₂ O	8	22
2 \times SYBR green PCR mixture	10	25
Forward and reverse primer mixture	1	2
DNA template	1	1

Table 6
Temperature program for qRT-PCR primer efficiency test

		PCR cycle (45 cycles)	
Enzyme activation		denature	Anneal/extend
Time	10 min	15 s	60 s
Temp (°C)	95	95	60

- (f) Each concentration is repeated for three times for three technical replicates.
- (g) Run qRT-PCR using the following temperature program (Table 6, Note 22).
- (h) After qRT-PCR run, export the Ct value into an excel file.
- (i) Average the Ct value for three technical replicates if the difference between three technical replicates is less than one. If the difference among all the Ct is larger than 1, remove the one with large difference and keep the two with consistence for calculation.
- (j) Make figure using log (DNA copy #) as the x-axis and Ct on the y-axis.
- (k) Make a liner model between the DNA concentrations and the Ct values.
- (l) Calculate the slope of the standard curve.
- (m) Calculate the primer efficiency using the following equation (*see Notes 23 and 24*):

$$E = 10^{(-1/\text{slope})} - 1$$

3.6 Primer Specificity Test

For gene expression analysis using PCR or qRT-PCR, it is required to make sure the primers only bind to one specific DNA location and generate the unique PCR product. When designing a primer, it is best to do a primer blast against the reference genome or currently known genome sequence to make sure the designed primers only match to the gene targeted. However, even so, it is also required to do a primer specificity test when running a PCR or qRT-PCR. For regular PCR, it requires to run a gel electrophoresis to make sure there are only one corrected band with correct size. For qRT-PCR, the primer specificity test is very simple and just need to run a dissociation curve analysis as following (*see Note 25*). If there is only one peak show, it means the primer is gene specific primer (Fig. 2a). If there are two or more peaks (Fig. 2b), it needs to figure out what happened to the primer and/or PCR reaction,

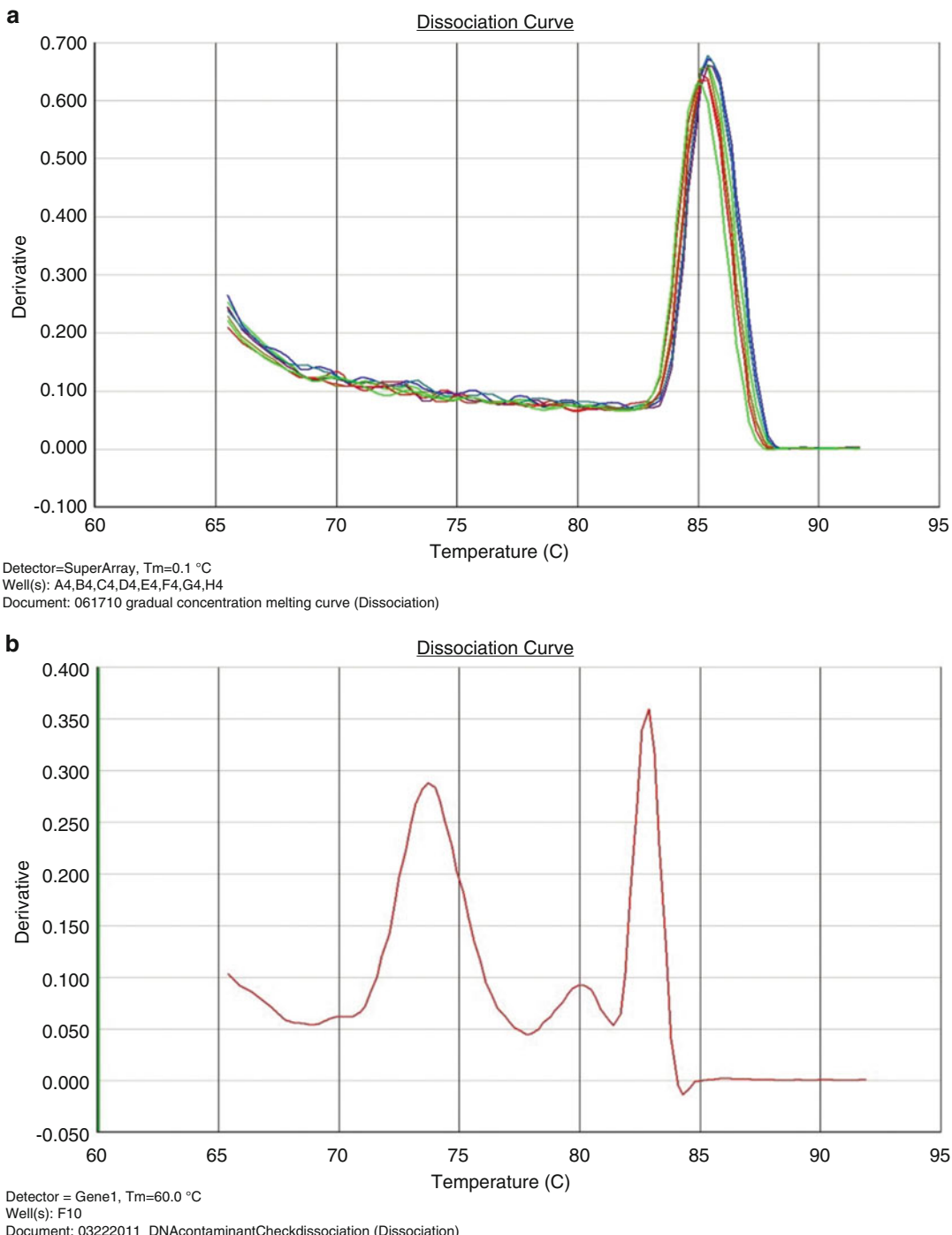


Fig. 2 Dissociation curve assay for testing primer gene specificity. **(a)** Primers with gene specificity; **(b)** primer without gene specificity

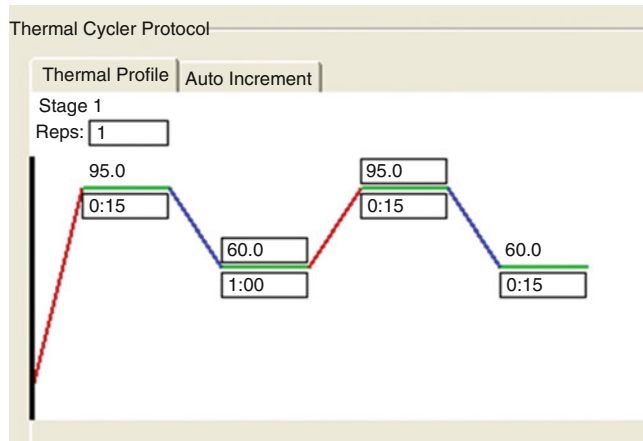


Fig. 3 Temperature program for melting point curve analysis for determining primer specificity

more likely it is not a gene specific primer if it were not genomic DNA contamination.

1. Leave the plate for primer efficiency test in the real-time PCR machine (*see Note 26*).
2. Set up melting point curve assay temperature program as following (Fig. 3).
3. Re-run the plate.
4. Observe the results and calculate whether or not the primer is gene specific or not.

3.7 qRT-PCR

1. Design the plate. When running an qRT-PCR, it is better to design the plate first to make sure which location which gene/sample will be loaded, and put all information in an excel file as following.
2. Prepare six 200µL PCR tubes.
3. Label clearly with the information in **Notes 1** and **2** of Table 7, such as S1TR1 that means technical replicate 1 for sample 1 (*see Note 27*).
4. Prepare PCR mixture as following in Table 8 (*see Note 28*).
5. Mix each reaction very well.
6. Centrifuge down the PCR mixtures.
7. Put the tubes with PCR mixture in a PCR plate holder at the same order as listed in Table 7. This way allows you to use a multiple-channel pipette to transfer the PCR mixture into each individual well.

Table 7
Plate design^a

		1	2	3	4	5	6	7	8	9	10	11	12	Note 1	Note 2
A															
B	Bact	GADPH	SDHA	TBCA	TUB	RNU44	U6	RNU48	RNU47	18s	TBP	GNB	TR1	S1	
C	Bact	GADPH	SDHA	TBCA	TUB	RNU44	U6	RNU48	RNU47	18s	TBP	GNB	TR2	S1	
D	Bact	GADPH	SDHA	TBCA	TUB	RNU44	U6	RNU48	RNU47	18s	TBP	GNB	TR3	S1	
E	Bact	GADPH	SDHA	TBCA	TUB	RNU44	U6	RNU48	RNU47	18s	TBP	GNB	TR1	S2	
F	Bact	GADPH	SDHA	TBCA	TUB	RNU44	U6	RNU48	RNU47	18s	TBP	GNB	TR2	S2	
G	Bact	GADPH	SDHA	TBCA	TUB	RNU44	U6	RNU48	RNU47	18s	TBP	GNB	TR3	S2	
H															

^aTR technical replicate, S sample

Table 8
Preparation of PCR mixture

Component	Volume/single 20- μ L reaction	Volume/13 20- μ L reaction
Nuclease-free water	6	78
2× SyberGreen PCR master mix	10	130
Product from RT-PCR reaction (after dilution)	2	26
Primer	—	—
Total	18	234

Table 9
Temperature program for qRT-PCR

PCR cycle (40 cycles)			
	Enzyme activation	Denature	Anneal/extend
Time	10 min	15 s	60 s
Temp (°C)	95	95	60

8. Prepare a 6- or 8-channel pipette with adjusting the volume to 18 μ L. At the same time, you also need to prepare a 96-well qRT-PCR plate by putting it on a 96-well PCR plate holder.
9. Transfer the prepared PCR mixture (18 μ L) into each well of the 96-well plate (*see Note 29*).
10. Add 2 μ L primers (forward and reverse primers) into each individual well.
11. Cover the 96-well plate with an optical adhesive film (*see Note 30*).
12. Centrifuge down the solution to avoid any air bubble by using a plate centrifuge. If there is no a centrifuge for plate, you may manually spin the plate for several times to remove the air bubble.
13. Load the plate on real-time PCR machine.
14. Perform the qRT-PCR using the following temperature program (Table 9).
15. After real-time PCR run, manually set the threshold value at the exponential phase to generate Ct value for individual gene for individual sample (*see Note 31*).
16. Export the Ct value in an excel file.

3.8 Identifying the Most Stable Reference Gene

A good reference gene is a gene with relative consistent expression level that does not change among different treatment and/or development stage. To test the expression stability of different genes, different computational programs have been developed. Currently, the most commonly used programs include geNorm [8], NormFinder [9], BestKeeper [10], and the comparative ΔCt method [11].

GeNorm [8] is an Excel-based computational program that can be used for the analysis of gene expression stability and eventually providing two most stable reference genes. The values of transformed C_t (relative expression values) were transferred into the geNorm applet as input data. The expression stability value (M value) was calculated by the geNorm program for each candidate gene, which is described as the average pairwise variation of a single candidate reference gene to all other tested genes. A low M value indicates high stability in gene expression, thereby maybe ideal reference genes. Furthermore, geNorm can also provide the minimal number of reference genes required for reliable normalization. According to the pairwise variation calculation, 0.15 is commonly accepted as the cutoff, below which an additional reference gene is not required for accuracy normalization.

NormFinder [9] uses the model-based strategy to identify suitable reference genes to normalize qRT-PCR data. Unlike geNorm, NormFinder assesses the expression stability of each candidate independently. This approach has the advantage of ranking the candidate reference genes both inter-group and intra-group according to their different expression stability.

BestKeeper [10] is also an Excel-based software, which is employed to evaluate the expression stability of candidate reference genes. This program creates an index using the geometric mean of each candidate gene's raw C_t values. Gene expression variation can be determined by the calculated standard deviation (SD) and coefficient of variance (CV) for all candidate reference genes based on their C_t values. Candidate genes with SD values greater than 1 were considered as inconsistent and were excluded. Then the BestKeeper program estimated the relationship between the index and the contributing reference gene by the Pearson correlation coefficient, the coefficient of determination (r^2), and the P value.

The comparative ΔCt method [11] assesses the most stable reference genes by comparing relative expression of “pairs of genes” within each tissue sample or each treatment. By comparing the relative expression of “pairs of genes” within each treatment, this method indicates the mean of standard deviation of each candidate reference genes. The candidate with lowest SD value is proposed to be the most stable gene and the highest SD value indicated the least stable gene.

Each of the four programs has its own advantages and disadvantages. In most cases, they give a consistent conclusion. However, in certain case, certain rank may be slightly different from each other. In 2012, we integrated the four computational programs and designed a web-based program, called RefFinder to directly analyze the reference genes based on the raw qRT-PCR C_t data [12]. This program is very easy to use and quickly generate the rank for each computational program. Additionally, this newly developed RefFinder also comprehensively analyzes each candidate reference gene and give a new rank based on the four computational programs.

When you get the C_t value, you can directly use the four mentioned programs to rank the potential reference genes, you may also directly input your data into RefFinder to rank your gene. In this method, we use RefFinder to identify the most reliable reference genes.

1. Export C_t values from each reference genes under specific conditions and samples to an Excel file.
2. List the C_t values in the following order, as seen in Table 10.
3. Copy and paste (input) the data into the RefFinder.

RefFinder

Evaluating Reference Genes Expression>

RefFinder is a user-friendly web-based comprehensive tool developed for evaluating and screening reference genes from extensive experimental datasets. It integrates the currently available major computational programs (**geNorm**, **NormFinder**, **BestKeeper**, and the **comparative Delta-Ct method**) to compare and rank the tested candidate reference genes. Based on the rankings from each program, it assigns an appropriate weight to an individual gene and calculated the geometric mean of their weights for the overall final ranking. Please cite F Xie, P Xiao, D Chen, L Xu, B Zhang. 2012. miRDeepFinder: a miRNA analysis tool for deep sequencing of plant small RNAs. Plant molecular biology 80 (1), 75-84.

Input your data:

References

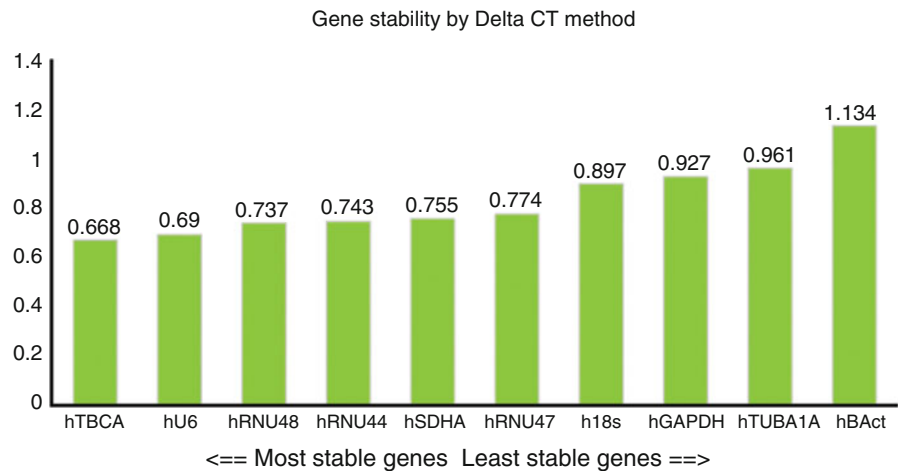
1. **BestKeeper**: Pfaffl MW, Tichopad A, Prgomet C, Neuvians TP. 2004. Determination of stable housekeeping genes, differentially regulated target genes and sample integrity: BestKeeper--Excel-based tool using pair-wise correlations. Biotechnology letters 26:509-515.
2. **NormFinder**: Andersen CL, Jensen JL, Orntoft TF. 2004. Normalization of real-time quantitative reverse transcription-PCR data: a model-based variance estimation approach to identify genes suited for normalization, applied to bladder and colon cancer data sets. Cancer research 64:5245-5250.
3. **geNorm**: Vandesompele J, De Preter K, Pattyn F, Poppe B, Van Roy N, De Paepe A, Speleman F. 2002. Accurate normalization of real-time quantitative RT-PCR data by geometric averaging of multiple internal control genes. Genome biology 3:RESEARCH0034.
4. **The comparative delta-Ct method**: Silver N, Best S, Jiang J, Thein SL. 2006. Selection of housekeeping genes for gene expression studies in human reticulocytes using real-time PCR. BMC molecular biology 7:33.

4. Click the button “Analyze.”

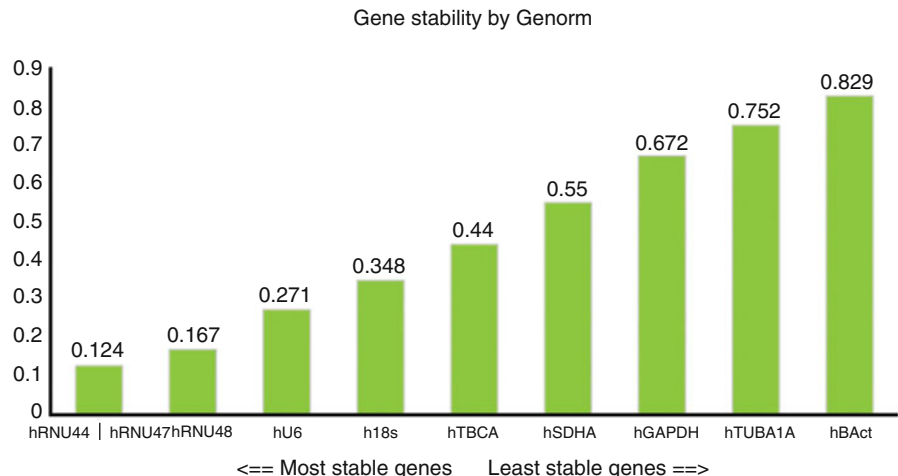
Table 10
Raw Ct values, directly exported from qRT-PCR, for ranking candidate reference genes

	hBAct	hGAPDH	hSDHA	hTBCA	hTUBA1A	hRNU44	hU6	hRNU48	hRNU47	h18 s
Sample 1	19.3112	22.28325	24.8479	22.9217	24.7194	17.5574	14.46205	19.4794	16.4062	18.99305
Sample 2	19.16265	22.63935	24.93535	22.8954	24.7734	17.58445	14.4329	19.5376	16.4733	19.33055
Sample 3	19.14815	22.3895	24.56275	22.51135	24.4619	17.93015	14.4635	19.73925	16.5504	19.5449
Sample 4	21.81065	24.6102	26.5362	23.36915	27.01725	18.1465	14.4691	20.0296	17.003	19.4468
Sample 5	21.1704	24.0964	26.02375	23.5005	26.0287	17.7986	15.0001	19.6619	16.43175	19.5778
Sample 6	23.4701	25.95015	27.0499	24.54845	28.30655	18.60915	16.04265	20.5171	17.3307	20.03305
Sample 7	19.27045	23.49115	25.0835	22.84805	24.67245	17.7206	14.336	19.8189	16.5204	19.30995
Sample 8	19.0253	22.8714	24.69045	22.7619	24.47635	17.8875	14.47215	19.87185	16.61655	20.05875
Sample 9	19.16015	22.9632	24.68925	22.5935	24.49845	18.026	14.72145	19.98605	16.76375	20.56225
Sample 10	20.23935	24.2292	25.4872	23.1425	25.45795	17.62315	14.73475	19.68395	16.3622	20.12155
Sample 11	20.6476	23.9726	25.84975	23.4667	25.92005	17.91115	15.0755	19.7871	16.47465	20.0937
Sample 12	22.8857	26.0722	27.2926	24.5212	27.9778	17.6749	15.2755	19.76915	16.386	20.35435
Sample 13	19.96615	22.7419	25.27745	22.9304	25.04025	18.04825	14.99655	20.29905	16.9748	20.3836
Sample 14	20.0786	22.61245	25.4461	22.79935	24.9942	17.74855	14.5316	20.155	16.67935	20.22445
Sample 15	20.7771	23.82425	25.7362	22.70535	25.11675	16.88815	13.50115	19.1055	15.6059	18.39635
Sample 16	21.58675	23.7839	26.3449	23.28645	26.0738	18.09565	15.0952	20.4421	17.02225	20.12955
Sample 17	22.15435	24.16015	26.665	23.533	26.52845	17.21855	14.51215	19.70135	16.02825	18.68725
Sample 18	24.07285	26.44245	27.4036	24.6452	29.01625	18.28	15.592	20.3794	16.7971	20.24645

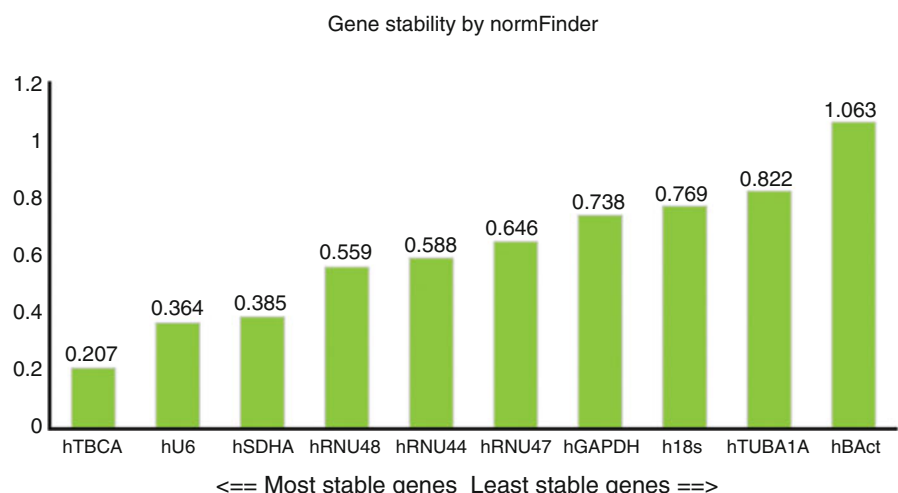
5. Run ΔC_t method.



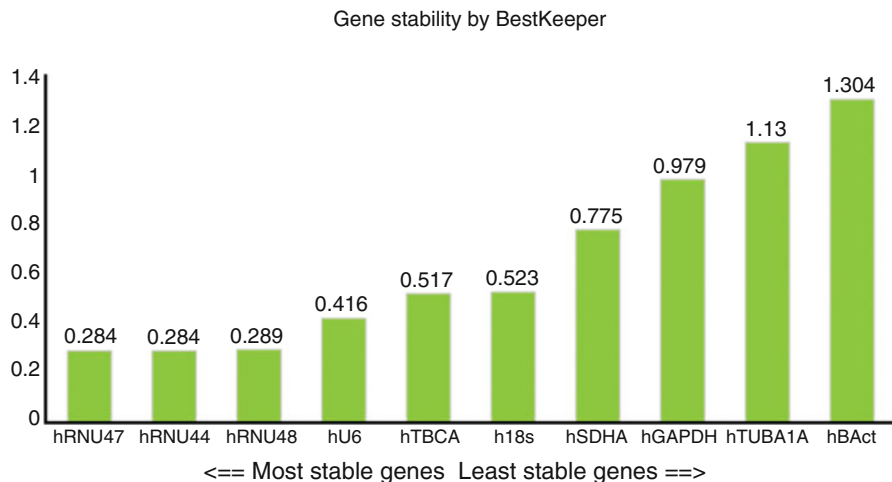
6. Run geNorm method.



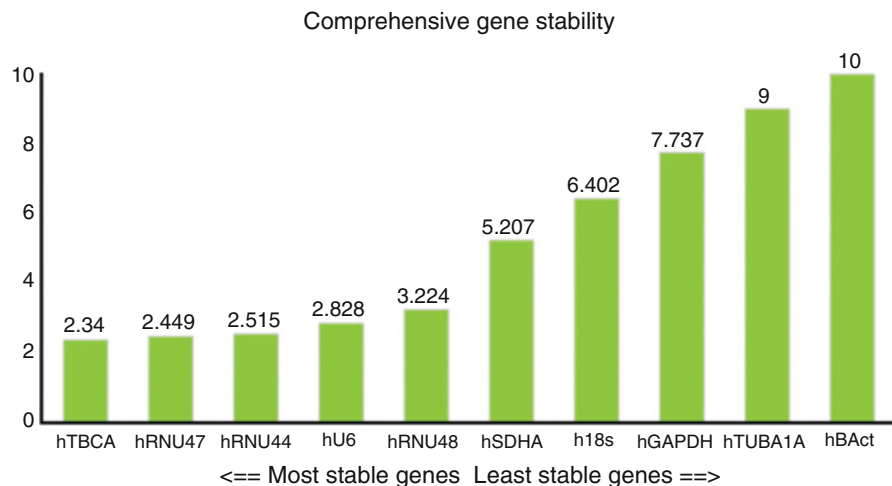
7. Run NormFinder method.



8. Run BestKeeper method.



9. Comprehensively rank the reference gene as follows:



10. Export and summarize the results on reference gene analysis (*see Note 32*). See Table 11 for the ranking of candidate reference genes based on the different computational programs.

4 Notes

1. Here, we use the breast cancer cell line as an example. Any other cell lines and even animal tissues can be used to test the housekeeping genes as reference genes.
2. There are many brands of real-time PCR. Any brands can be used in this experiment. In this method, we used Applied Biosystem ABI 7300 as an example.

Table 11
Ranking of candidate reference genes based on different computational programs

<i>Ranking order (Better--Good--Average)</i>										
Method	1	2	3	4	5	6	7	8	9	10
Delta CT	hTBCA	hU6	hRNU48	hRNU44	hSDHA	hRNU47	h18s	hGAPDH	hTUBA1A	hBAct
BestKeeper	hRNU47	hRNU44	hRNU48	hU6	hTB _{CA}	h18 s	hSDHA	hGAPDH	hTUBA1A	hBAct
NormFinder	hTBCA	hU6	hSDHA	hRNU48	hRNU44	hRNU47	hGAPDH	h18s	hTUBA1A	hBAct
Genorm	hRNU44/ hRNU47	hRNU48	hU6	h18s	hTB _{CA}	hSDHA	hGAPDH	hTUBA1A	hBAct	
Recommended comprehensive ranking	hTBCA	hRNU47	hRNU44	hU6	hRNU48	hSDHA	h18 s	hGAPDH	hTUBA1A	hBAct

3. Here, we use 5-Fluorouracil, melamine, and nicotine as examples for studying reference genes. 5-Fluorouracil is a pharmaceutical drug and also is an emerging environmental pollution because it was released into the environment by patients and other resources, melamine is also an emerging pollutant, and nicotine is a common abuse drug which is widely existed in tobacco.
4. Selecting the right concentration for each chemical is very important, it is better to use the concentrations environmentally related and do not cause too much cell death. This is because cell death may also change the gene expression and inference the results. If using some chemicals such as DMSO as solvent to make the solution, the same amount of solution needs to be added into each treatment and the controls to avoid the solvent effect.
5. Before adding each chemical for treatment, it is better to make stock and work solution of each tested chemical and sterilized. For short period, the stock and work solution can be stored in the refrigerator. In this method, because nicotine is hard to be dissolved in water, all chemicals are dissolved into DMSO and added into the medium. For final concentrations, all medium, including controls, contain the same amount of DMSO that should be less than 0.1% of final concentrations to avoid DMSO effect on cultured cells.
6. Liquid nitrogen is really cold liquid and handle with care. It may burn your skin if the skin is touched the liquid nitrogen for a long period. The liquid nitrogen cannot be dumped into the drain system. Just leave it on floor and let it evaporate, where people cannot reach.
7. Many kits can be used to extract RNAs from cell and/or tissue samples. Here, we just use the mirVana miRNA Isolation Kit as an example. One of the advantages of using this kit is that this kits can extract total RNAs, including both mRNA transcribed from protein-coding genes and small RNAs, such as microRNAs (miRNAs), an extensive class of small regulatory RNAs, that play versatile role in almost all biological and metabolic processes, including cancer development [13]. When you choose one RNA kit, you need to make sure you want all RNAs or just the mRNAs. If you also need to analyze the expression of small RNAs, you need to select some kits for total RNA extraction not only for mRNAs.
8. During RNA extraction, acid-phenol: chloroform aids in the removal of DNA (DNA partitions into the organic phase), helps to stabilize the interface and prevent foaming when mixing. This chemical is toxic and corrosive and should be handled carefully.

9. After centrifuge, the mix will separate into two layers, upper (aqueous) phase and lower (organic) phase. RNAs are in the aqueous phase, just gently remove the aqueous phase into a new centrifuge tube without interruption of the interface. If you have a very small amount of sample, you may need to transfer all aqueous phase into a new tube. For some cases, particularly when you need to transfer all aqueous phase, it may be a good idea to re-centrifuge the aqueous phase to remove potential organic phase residues. Contamination of organic phase will affect the RNA yield and quality.
10. You may transfer all 900 mL at one time; you may transfer it in two times, each with 450 mL.
11. It is important to make sure the filter cartridge is dried enough. After discarding the flow-through from the third wash, it may be better to replace the filter cartridge in the same collection tube and spin the assembly for 1 min to remove residual fluid from the filter.
12. You may adjust the volume of water. The less the volume of water, the higher the RNA concentration collected; however, the total RNAs is less. To obtain high yield, it is better to sit there for 1 min to allow RNA to dissolve in water.
13. A good forward primer and a good reverse primer do not mean that they are a good primer pair. When designing primers, after you design both forward and reverse primers, you also need to check whether they are good pair or not. This includes: (1) the Tm difference of two primers should be close to each other and better less than 2 °C; (2) more importantly, no primer-dimer between the forward and reverse primers.
14. Synthesized primers are usually shipped in particles in centrifuge tubes. During the handling and shipping, the particle can be anywhere including the wall and caps. Thus, when preparing the stock solution, the primers must be centrifuged down to avoid any contamination.
15. For commercial synthesis of PCR primers, the total amounts of PCR primers are usually listed in the paper sheet and also the amount (μ L) of water need to be added to make the primer stock solution with 100 μ M.
16. For most application of PCR and qRT-PCR, the concentration of each primer should be between 0.1 and 0.5 μ M. Usually, 1 μ L of forward and reverse primer mixture is added into a 20 μ L reaction volume. Thus, the working solution for primers is about 10 μ M. When making the working solution, the ratio of forward primer: reverse primer: H₂O is equal to 1:1:8 with the primer concentration 10 μ M. Too high concentrations of primers increase the chance of mispriming, resulting in nonspecific PCR products. Too low concentrations of primers result in extremely inefficient PCR reactions.

17. To avoid contamination, RNA sample is always the last one and water is the first one to be added into the reaction. Always change tips when you add different component or sample to the reaction. Always keep all reactions on ice before running. Before adding any component, please thaw the tubes on ice.
18. There are a couple of reasons for diluting the RT-PCR products. After RT-PCR, qRT-PCR will be run with multiple reactions; to run multiple reactiona, it requires lots of RT-PCR products; it is also a good idea to have some RT-PCR product leftover after running qRT-PCR in case something wrong and you need to re-run the qRT-PCR.
19. The original cDNA from the PCR products will serve as 1:1 dilution point. To get great results, it is better to do the series of dilution by diluting each previous solution by 10 times. For example add 10 μ L 1 \times cDNA into 90 μ L DNase free water, mix it very well. Then, take 10 μ L 10 \times cDNA dilution into 90 μ L DNase free water for 1:100 dilution, and so on to 1:100,000 dilution.
20. qRT-PCR needs special optical plates and covers to make sure light consistence. You can not label the top and bottom of the plates.
21. Always add DNA template for the last one to avoid DNA contamination.
22. Normally, 40 cycles should be enough for qRT-PCR. However, during primer efficiency test, to test the potential of low primer efficiency, it is suggested to run 45 cycles.
23. Primer efficiency should be about 90–100%. If it is too low, it will affect the fold change of expression during gene expression analysis. If the primer efficiency is less than 70%, it is better to design another primer or optimize the PCR condition.
24. There are a number of effectors affecting the primer efficiency, which include poor design, such as too short of PCR amplicon products, PCR primer secondary structures, primer-dimer, and stem-loop structure as well as the 3' end of primer is not G or C or GC or CG, not complementary with the DNA template. PCR condition, including annealing and extension temperature and Mg²⁺ concentrations, may also cause low primer efficiency. Table 12 shows the fold of PCR amplification and the corresponding primer efficiency for various values of the slope.
25. Dissociation curve analysis is also known as melting curve analysis, which is used to determine the melting temperature (T_m) of a PCR product. When there is one unique PCR product, the Tm is consistent and there is only one peak in the computer screen. Otherwise, there will be two or more peaks showing that the primer is not gene specific.

Table 12
Primer efficiency and the slope of the standard curve

Slope of the standard curve	Fold of PCR amplification	Primer/PCR efficiency
-5.68	1.500	0.500
-4.34	1.700	0.700
-4.11	1.751	0.751
-3.91	1.802	0.802
-3.85	1.819	0.819
-3.80	1.833	0.833
-3.75	1.848	0.848
-3.70	1.863	0.863
-3.65	1.879	0.879
-3.60	1.896	0.896
-3.55	1.913	0.913
-3.50	1.931	0.931
-3.45	1.949	0.949
-3.40	1.968	0.968
-3.35	1.988	0.988
-3.30	2.009	1.009
-3.25	2.031	1.031

26. For dissociation curve analysis, you do not need to prepare new plate, you can just use the plate for primer efficiency test or any plate for gene expression analysis. After the plate finished running, you can immediately run the melting point curve for determining the primer specificity. For many qRT-PCR machines, you can input the temperature with the regular RT-PCR temperature program so the dissociation curve analysis can be done just after the PCR.
27. The purpose of running three technical replicates is to avoid the pipetting-related issues. The three technical replicates need to be performed by adding each PCR agent independently, you cannot make the master mixture and then divide into three tubes.
28. It allows your qRT-PCR running simple, saving time, and receiving better reliable data to make a PCR mixture. Due to the fact that the components in each reaction are the same except the primer for each technical replicate of the same sample, thus we can make the PCR mixtures except the

primers. When you make the PCR mixtures, you cannot make the expected amount of the PCR solution, you must make about 10% extra. This will allow you have enough mixture for each reaction. For example, here there are 12 reactions for 12 genes, you make PCR mixture enough for 13 reactions. During this step, you also need to keep in mind to add the DNA template last to avoid the potential DNA contamination.

29. During this step, you need to be careful not to change the direction of the multiple-channel pipette, otherwise you will make a big mistake to add the sample into a wrong well and also cause the DNA contamination for your qRT-PCR.
30. You also can use an optical cap to cover each well, but the film will be better. Just like the plate, an optical film needs to be used to make sure the wavelength goes through the film evenly for reliable data. The adhesive film is easy to use by simply peeling the backing away from the adhesive film and apply firmly across the top of the prepared 96-well plate.
31. Setting a threshold value is very important for gene expression analysis using qRT-PCR. It is a line in the qRT-PCR graph that represents a level above background fluorescence; when your gene signal crosses the threshold line, the number will be called C_t volume that is what you need for analyzing gene expression. This line must sit at the exponential phase (Fig. 4). Threshold

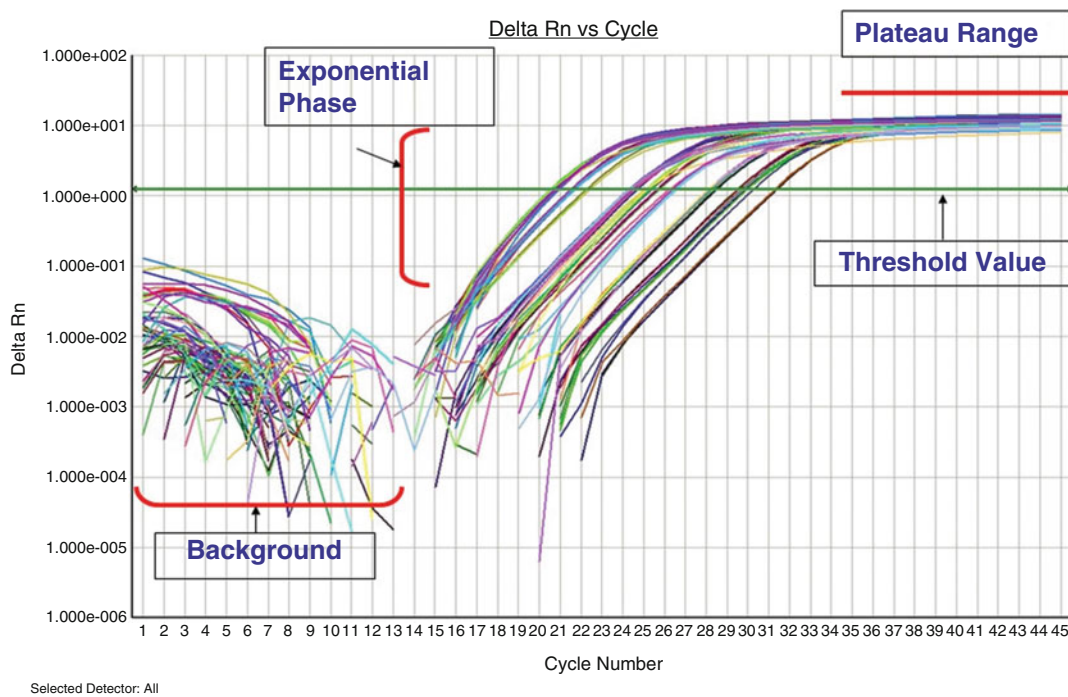


Fig. 4 Amplification plot for gene expression analysis

value can be set automatically by the computer program or manually. However, if you run multiple plates, you need to set the threshold value manually to make sure each plate has the same threshold value.

32. Based on previous studies [3, 4], two or more housekeeping genes as reference genes is better than one reference gene, in that case you may combine the two most stable references as one reference by averaging their C_t value. Using a reliable reference gene will enhance many molecular and toxicogenomic studies, including gene expression and transgenics as well as genome editing [14].

References

1. Bustin SA et al (2009) The MIQE guidelines: minimum information for publication of quantitative real-time PCR experiments. *Clin Chem* 55(4):611–622
2. Eisenberg E, Levanon EY (2013) Human housekeeping genes, revisited. *Trends Genet* 29(10):569–574
3. Chen D et al (2011) Evaluation and identification of reliable reference genes for pharmacogenomics, toxicogenomics, and small RNA expression analysis. *J Cell Physiol* 226 (10):2469–2477
4. Taki FA, Zhang B (2013) Determination of reliable reference genes for multi-generational gene expression analysis on *C. elegans* exposed to abused drug nicotine. *Psychopharmacology* 230(1):77–88
5. Fix LN et al (2010) MicroRNA expression profile of MCF-7 human breast cancer cells and the effect of green tea polyphenon-60. *Cancer Genomics Proteomics* 7(5):261–277
6. Shah MY et al (2011) 5-fluorouracil drug alters the microRNA expression profiles in MCF-7 breast cancer cells. *J Cell Physiol* 226 (7):1868–1878
7. Benson DA et al (2013) GenBank. *Nucleic Acids Res* 41(Database issue):D36–D42
8. Vandesompele J et al (2002) Accurate normalization of real-time quantitative RT-PCR data by geometric averaging of multiple internal control genes. *Genome Biol* 3(7):research0034.1
9. Andersen CL et al (2004) Normalization of real-time quantitative reverse transcription-PCR data: a model-based variance estimation approach to identify genes suited for normalization, applied to bladder and colon cancer data sets. *Cancer Res* 64(15):5245–5250
10. Pfaffl MW et al (2004) Determination of stable housekeeping genes, differentially regulated target genes and sample integrity: Best-Keeper—excel-based tool using pair-wise correlations. *Biotechnol Lett* 26(6):509–515
11. Silver N et al (2006) Selection of housekeeping genes for gene expression studies in human reticulocytes using real-time PCR. *BMC Mol Biol* 7(1):33
12. Xie F et al (2012) miRDeepFinder: a miRNA analysis tool for deep sequencing of plant small RNAs. *Plant Mol Biol* 80(1):75–84
13. Zhang B et al (2007) microRNAs as oncogenes and tumor suppressors. *Dev Biol* 302(1):1–12
14. Li C, Brant E, Budak H, Zhang BH (2021) CRISPR/Cas: a Nobel Prize award-winning precise genome editing technology for gene therapy and crop improvement. *Journal of Zhejiang University SCIENCE B*, 22 (4):253–284. <https://doi.org/10.1631/jzus.B2100009>



Chapter 7

Semi-Quantitative RT-PCR: An Effective Method to Explore the Regulation of Gene Transcription Level Affected by Environmental Pollutants

Fan Wang

Abstract

Semi-quantitative reverse transcription and polymerase chain reaction (sqRT-PCR) is a simple and specific method for quantitative RNA in recent years. The relative quantity of a specific mRNA in the samples can be inferred by reverse transcription of mRNA into cDNA, and PCR amplification and determination of the quantity of PCR products. The semi-quantitative analysis is carried out under a fixed number of PCR cycles, and the total RNA concentration is kept in the exponential phase of the PCR. The method is to use a housekeeping gene (usually actin, GAPDH, and EF1 α) as a reference standard in treated and control organisms to observe the expression of the interested genes (upregulated or downregulated) in toxicology. In this chapter, we describe a step-by-step method for determining the differential regulation of target genes in organisms exposed to environmental pollutants.

Key words sqRT-PCR, Gene expression, Differential regulation, Target gene, Toxicology

1 Introduction

Semi-quantitative reverse transcription polymerase chain reaction (sqRT-PCR) is an effective method to explore gene transcription level in recent years [1–3]. Total RNAs, isolated from tissues or cells, were reversely transcribed into cDNAs. The target genes and internal reference gene (usually actin, GAPDH, or EF1 α) are amplified simultaneously using cDNA as template with TaqDNA polymerase in the same or different tubes. The amplification product analysis steps are as follows: roughly judge whether the extraction efficiency, quality and amplification efficiency of each sample are consistent according to whether the amplification band density of internal reference gene is consistent among samples. Subsequently, the ratio of the amplified band density of the target genes to that of

internal reference gene was calculated by using the band density of the internal reference gene as the standard, and the relative expression changes of the target genes are obtained [4–7].

Compared with the traditional detection methods, such as Northern blot and RNase protection analysis, sqRT-PCR has been widely used for its high sensitivity (1000–10,000 times higher than hybridization), better specificity, rapidity and simplicity, and less strict requirements on the initial total RNA quantity, and no need for the standard substance with known concentrations [8–13]. So far, many researchers have applied this technique in the field of environmental toxicology [8, 14–16]. We also have used this method to study the effect of triclosan on gene expression in zebrafish gills in our laboratory [4, 17].

2 Materials

All solutions are prepared by using deionized water and analytical grade reagents. All reagents are prepared and stored at room temperature (unless specified otherwise). All waste disposal regulations should be strictly observed when handling waste materials.

2.1 RNA Extraction

1. Diethyl pyrophosphate (DEPC): store in dark at 4 °C.
2. RNase-free water: Add DEPC into double distilled water (ddH₂O) in a glass bottle without RNase to make 0.1% (V/V-DEPC/ddH₂O) of DEPC, stir evenly, place overnight, autoclave, and then store at 4 °C.
3. Chloroform: Store at 4 °C; treat at –20 °C for 30 min before usage to ensure cold.
4. Isopropanol: Store at 4 °C; treat at –20 °C for 30 min before usage to ensure cold.
5. 75% ethanol: Prepared using absolute ethanol and sterilized deionized water treated with 0.1% DEPC, store at 4 °C; treat at –20 °C for 30 min before usage to ensure cold.
6. Trizol: Store at 4 °C; treat at –20 °C for 30 min before usage to ensure cold.

2.2 Reverse Transcription

1. dNTP mix: Include dATP, dCTP, dGTP, and dTTP of 10 mM, respectively.
2. RNase inhibitor: 40 U/μL.
3. polyOligo(dT)12–18: 2.5 μ mol/L.
4. AMV reverse transcriptase: 5 U/μL.
5. 10 × RT buffer: Include 250 mmol/L Tris–HCl (pH 8.3), 375 mmol/L KCl, and 15 mmol/L MgCl₂, respectively.

2.3 PCR Amplification

1. Taq DNA polymerase: 5 U/ μ L.
2. Gene specific forward and reverse primers: 20 μ mol/L.
3. 10 \times PCR buffer: Consist of 100 mmol/L Tris-Cl (pH 9.0), 500 mmol/L KCl, 1.0% Triton X-100, and 15 mmol/L MgCl₂; the solution is sterilized before usage.
4. Acid Dyestuff: GoldView Ior II.
5. Agarose.
6. 50 \times TAE buffer: Weigh and add Tris 242 g and Na₂ EDTA·2H₂O 37.2 g into a beaker, add about 600 mL deionized water, and fully stir and dissolve, and then add 57.1 mL glacial acetic acid and stir well. Finally, add deionized water to make up the total volume of solution to 1 L.
7. 6 \times DNA loading buffer: Consist of 30 mM EDTA, 36%(v/v) Glycerol, 0.05%(w/v) Xylene Cyanol FF, and 0.05%(w/v) Bromophenol Blue.
8. 1% agarose gel: Weigh and add 0.5 g agarose powder into a conical flask, add 50 mL 1 \times TAE buffer solution, and mix well. Heat the conical flask in the microwave oven for 3 min to dissolve the agarose completely. After cooling slightly, add Goldview Ior II 2.5 μ L, mix well, pull the gel solution in the module with comb, and use it after the glue is solidified.

3 Methods

All experiments are performed at the condition of room temperature unless otherwise specified.

3.1 Treatment of Experimental Apparatus

1. Plastic containers: All plastic containers (Tips, EP tube, homogenizer tube, etc.) are treated by DEPC-treated water for overnight and then dried.
2. Glassware: Soaked in acid overnight, rinse thoroughly, and then soak in DEPC-treated water overnight, and finally dried.
3. Metalware: After washing, disinfect under ultrasound.

3.2 RNA Extraction and Detection (see Note 4)

1. For tissue samples, weight 50–100 mg tissues from each sample, including the controls and treatments. Put the weighted sample into a centrifuge tube; add 1 mL Trizol solution to lyse the tissue (see Note 2). For cell samples, the cells are centrifuged and precipitated, and then add 1 mL Trizol to every 5–10 \times 10⁶ cells; cells are broken by repeatedly blowing with a pipette or shaking violently (see Note 1).
2. The lysate of tissue or cell is transferred into an EP tube and placed at room temperature for 5 min.

3. In the abovementioned EP tube, add chloroform according to 0.2 mL chloroform per mL Trizol, cover the EP tube, vibrate in hands for 15 s, place at room temperature for 2–3 min, and centrifuge with $12,000 \times g$ (2–8 °C) for 15 min (see Note 3).
4. Transfer the upper water phase into a new EP tube, add isopropanol according to 0.5 mL isopropanol per mL Trizol, place at room temperature for 10 min, and centrifuge with $12,000 \times g$ (2–8 °C) for 10 min.
5. Discard the supernatant, wash using ethanol according to 1 mL 75% ethanol per mL Trizol, vortex mix, and centrifuge with $7500 \times g$ (2–8 °C) for 5 min.
6. Discard the supernatant, let the precipitated RNA to dry naturally at room temperature.
7. Dissolve precipitated RNA using RNase-free water.
8. Determine OD_{260/280} value and the concentrations of RNAs using ultramicro spectrophotometer. The OD_{260/280} value between 1.8 and 2.0 is considered as high purity.
9. Detection of RNA integrity: Put 1% agarose gel into the electrophoresis tank equipped with 1 × TAE buffer. Mix 1–2 μL RNA with the appropriate amount of loading buffer, and add them to the agarose gel combing hole. Electrophoresis for 10–20 min at 100 V, observe the results in the gel imaging system. The brightness and width of the 28S band should be twice as large as those of the 18S band, indicating that RNAs are not degraded (Fig. 1).
10. RNAs are stored at –80 °C till further usage.

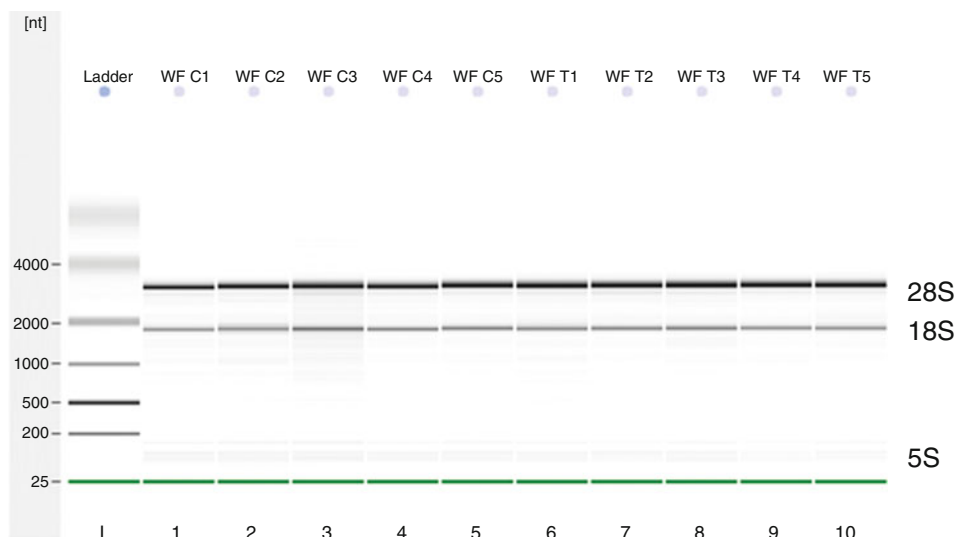


Fig. 1 Gel electrophoresis of RNA extracted from brain tissue of zebrafish (*Danio rerio*)

Table 1
Reverse transcription reaction system

Reagent	Volume
RNA	0.5–1 µg
dNTP mix	2 µL
Oligo(dT)12–18	1 µL
10 × RT buffer	2 µL
AMV reverse transcriptase	1 µL
RNase inhibitor	0.5 µL
Add DEPC water to make the solution	20 µL
Total volume	20 µL

3.3 Reverse Transcription (see Note 4)

1. A reverse transcription reaction contains the following reagents listed in Table 1 (*see Note 5–8, 11, 13*).
2. Mix the reaction well by vortex.
3. Let the reverse transcription going at 42 °C for 1 h, heat at 95 °C for 5 min, and then place on ice or store at –4 °C.

3.4 PCR Amplification and Electrophoresis Detection

1. Set up a PCR reaction system (Table 2) (*see Note 9, 11–14*).
2. Mix the reaction well by vortex.
3. Perform PCR according to the following temperature program (Table 3) (*see Note 10*).
4. Prepare 1% agarose gel by adding the 1% agarose gel into the electrophoresis tank with 1 × TAE buffer. Mix 1–2 µL PCR amplified product with the appropriate amount of loading buffer, and add them to the agarose gel combing hole. Electrophorese for 20 min at 120 V, observe the results in the gel imaging system, and finally take photos.
5. Quantification of amplified PCR products is carried out by lab software. The intensities of the target gene mRNA bands are normalized relative to that of housekeeping gene bands by dividing the former by the housekeeping gene specific PCR product densities (Fig. 1).
6. The relative expression changes of target genes are obtained by comparing the above specific value between the control groups and the treatment groups (Fig. 2).

Table 2
PCR reaction system

Reagent	Volume
cDNA obtained from reverse transcription	10 µL
dNTP mixture	1 µL
Forward and reverse primers	1 µL, respectively
10× PCR buffer	5 µL
Taq DNA polymerase	0.5 µL
DEPC-treated water	31.5 µL
Total volume	50 µL

Table 3
Temperature program for PCR reaction

Temperature	Time	Number of cycles
95 °C	5 min	
95 °C	1 min	
55 °C	90 s	
72 °C	90 s	
72 °C	10 min	
4 °C	1 h	

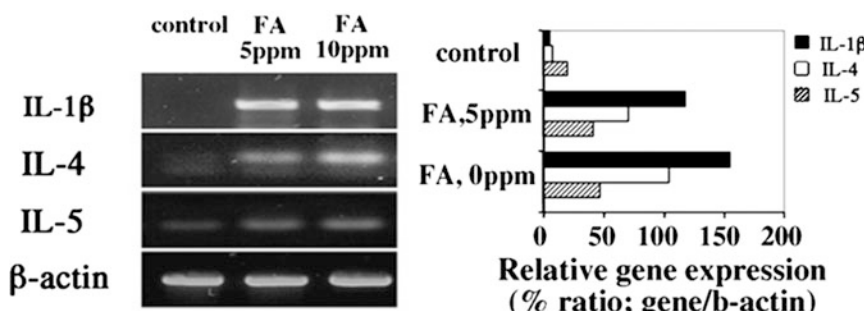


Fig. 2 Expression of inflammatory cytokines from the liver in FA-exposed mice. After quantitative normalization for each gene by densitometry using β -actin gene expression, semi-quantitative RT-PCR was performed for the indicated genes. PCR were run for 28 or 30 cycles (The figure is adopted from Ref. 8)

4 Notes

1. Always change new gloves in the process of RNA extraction. Because the skin often carries bacteria, it may cause RNase contamination. Use RNase-free plastic products and pipette tips to avoid cross contamination. RNAs are not degraded by RNase in Trizol reagent. However, RNase-free plastic and glassware used in the process should be disposed continuously after extraction. In addition, RNAs should be always kept on ice.
2. If the amount of tissue or cell is too small, the amount of Trizol buffer should be reduced; if the amount of tissue or cell is too large, DNA may contaminate the extracted RNA samples. If tissue samples are too large, cut the tissues with a tissue shear, and then fully homogenized.
3. If the tissue contains more protein, fat, polysaccharide, and extracellular substances (muscle, plant nodule, etc.) in the process of RNA extraction, centrifugation can be carried out by using $10,000 \times g$ for 10 min at 2–8 °C, and the supernatant is collected. The precipitate obtained by centrifugation includes extracellular model, polysaccharide, and high molecular weight DNA, and the supernatant contains RNA. In the treatment of adipose tissue, a large amount of grease in the upper layer should be removed, and clear homogenate should be collected for the next operation.
4. In the process of RNA extraction and reverse transcription, RNase-free environment should be established to avoid RNA degradation.
5. Successful semi-quantitative PCR depends on high quality of RNAs. High quality RNAs should be at least full length and free of reverse transcriptase inhibitors.
6. In reverse transcription, RNase inhibitor protein is often added to increase the yield of cDNA synthesis. RNase inhibitor protein should be added in the first chain synthesis reaction, and in the presence of buffer and reducing agent.
7. When PCR reaction is carried out, a non-reverse transcription control reaction should be carried out for each RNA template to ensure whether the amplified fragments are from genomic DNA or cDNA. The PCR products obtained without reverse transcription are from genome.
8. For most RNA templates, most of the secondary structures can be eliminated by keeping RNA and primer at 65 °C without buffer or salt, and then rapidly cooling down on ice.

9. When the PCR reaction system is established, template DNA and Taq DNA polymerase are added after adding other reactants, and then all reactants should be mixed well by vortex.
10. Generally, the number of PCR reaction cycles is 25–30. Too many cycles will cause non-specific amplification and waste of time; more important, high number of PCR cycle will eliminate the difference among different samples [18, 19].
11. Whether it is a reverse transcription reaction or a PCR amplification reaction, all kinds of reaction solutions should be prepared first, and then packed into each reaction tube. In this way, the volume of reagents taken can be more accurate, the loss of reagents can be reduced, and the error caused by experimental operation can also be reduced.
12. The calculation of the renaturation temperature of PCR amplification is generally approximate to T_m value of the primer, $T_m = 2(A + T) + 4(G + C)$. The proper renaturation temperature can improve the specificity of PCR amplification.
13. AMV reverse transcriptase, RNase inhibitor, Taq DNA polymerase, and other enzymes should be gently mixed to avoid foaming. Before separation, they should be centrifuged and collected to the bottom of the reaction tube. Because of their high viscosity, they should be separated gently. The enzymes must be taken out from -20°C freezer before the experiment and put back to -20°C freezer refrigerator immediately after usage.
14. The best PCR amplification conditions vary with different PCR amplification instruments, so it is better to explore the PCR amplification conditions before using sample PCR amplification.

References

1. Cottrez F, Auriault C, Apron A, Groux H (1994) Quantitative PCR: validation of the use of multispecific internal control. *Nucleic Acids Res* 22:2712–2713
2. Carding SR, Lu D, Bottomly KA (1992) A polymerase chain reaction assay for the detection and quantification of cytokine gene expression in small number of cells. *J Immunol Methods* 151:277–287
3. Marone M, Mozzetti S, De Ritis D, Pierelli L, Scambia G (2001) Semiquantitative RT-PCR analysis to assess the expression levels of multiple transcripts from the same sample. *Biol Proced* 3:19–25
4. Liu X, Zu E, Wang F (2020) Effect of Triclosan on expression of apoptosis-related genes in female zebrafish Hepatopancreas. *J Guangdong Ocean Univ* 40:15–18
5. Galbraith SM, Lodge MA, Taylor NJ, Rustin GJS, Bentzen S, Stirling JJ, Padhani AR (2002) Reproducibility of dynamic contrast-enhanced MRI in human muscle and tumours: comparison of quantitative and semi-quantitative analysis. *NMR Biomed* 15:132–142
6. Mathias C, Martine B, Anne VC (2004) A semi-quantitative RT-PCR method to readily compare expression levels within *Botrytis cinerea* multigenic families *in vitro* and *in planta*. *Curr Genet* 43:303–309
7. Rolland VG (2004) Semi-quantitative analysis of gene expression in cultured chondrocytes by RT -PCR. *Methods Mol Med* 100:69–78

8. Jung WW, Kim EM, Lee EH, Yun HJ, Ju HR, Jeong MJ, Hwang KW, Sul D, Kang HS (2007) Formaldehyde exposure induces airway inflammation by increasing eosinophil infiltrations through the regulation of reactive oxygen species production. Environ Toxicol Phar 24:174–182
9. Nassenstein C, Braun A, Erpenbeck VJ, Lommatsch M, Schmidt S, Krug N, Luttmann W, Renz H, Virchow JC Jr (2003) The Neurotrophins nerve growth factor, brain-derived neurotrophic factor, Neurotrophin-3, and Neurotrophin-4 are survival and activation factors for eosinophils in patients with allergic bronchial asthma. J Exp Med 198:455–467
10. Valiellahi E, Niazi A, Farsi M (2009) Semi-quantitative RT-PCR analysis to assess the expression levels of Wcor14 transcripts in winter-type wheat. Biotechnology 8:323–328
11. Wang R, Li H (2008) Application of semi-quantitative RT-PCR in analysis gene expression level. J Fuyang Teachers College (Natural Science) 24:49–52
12. Romero MM, Grasa MM, Esteve M, Fernández-López JA, Marià Alemany M (2007) Semi-quantitative RT-PCR measurement of gene expression in rat tissues including a correction for varying cell size and number. Nutr Metab 4:26
13. Veronesi E, Henstock M, Gubbins S, Batten C, Manley R, Barber J, Hoffmann B, Beer M, Attoui H, Mertens PPC, Carpenter S (2013) Implicating Culicoides biting midges as vectors of Schmallenberg virus using semi-quantitative RT-PCR. PLoS One 8:e57747
14. Xu B, Aoyama K, Takeuchi M, Matsushita T, Takeuchi T (2002) Expression of cytokine mRNAs in mice cutaneously exposed to formaldehyde. Immunol Lett 84:49–55
15. Liu L, Jin Y, Wang L, Yu H, Liu W, Yu Q, Wang K, Liu B, Wang J (2009) Effects of perfluorooctane sulfonate on learning and memory of rat pups. Chinese Prevent Med 43:622–627
16. Tian H (2010) Effects of monocrotaphos on reproductive axis of goldfish (*Carassius auratus*). Comp Biochem Physiol C Toxicol Pharmacol 152(1):107–113
17. Liu H, Wang F, Yao W (2019) Effect of tricosan on expression of apoptosis-related genes in male zebrafish gill tissue. Freshwater Fisheries 49:14–18
18. Fellner MD, Durand K, Correa M, Bes D, Alonso LV, Teyssie AR, Picconi MAA (2003) A semiquantitative PCR method (SQ-PCR) to measure Epstein-Barr virus (EBV) load: its application in transplant patients. J Clin Virol 28:323–330
19. Kuddus RH, Lee YH, Valdivia LA (2004) A semi-quantitative PCR technique for detecting chimerism in hamster-to-rat bone marrow xenotransplantation. J Immunol Methods 285:245–251



Chapter 8

Employing Multiple New Neurobiological Methods to Investigate Environmental Neurotoxicology in Mice

Ping Cai and Huangyuan Li

Abstract

The emergence of advanced and powerful neuroscientific technologies has greatly pushed forward the development of neurobiology in the last decade. Although neurotoxicology is an interdisciplinary subject sharing a mass of technologies with neurobiology, the implementation of these advanced technologies in neurotoxicology is merely seen. Here we describe the detailed methods and materials of some emerging neuroscientific technologies, including optogenetics, fiber photometry, *in vivo* two-photon Imaging, *in vivo* calcium imaging, and *in vivo* electrophysiological recording, hoping that the integration of technologies from neurotoxicology and neuroscience can lend weight to the development of neurotoxicology.

Key words Environmental neurotoxicology, Chemogenetics, Optogenetics, Fiber Photometry, *In vivo* Two-photon Imaging, *In vivo* Calcium Imaging, *In vivo* Electrophysiological Recording

1 Introduction

Environmental pollutants exposures, which cause millions of diseases and deaths every year, are inevitable in our life [1]. Environmental pollutants have been confirmed to be toxic for diverse organs and tissues [2], especially the brain. It has been well established that the brain is susceptible to environmental pollutants [3], possibly because of abundant blood supply in the head. Although a great deal of contaminants have already been identified as neurotoxic substances, potential neurotoxic properties of other chemicals need to be further examined [4]. Preclinical studies with experimental animals advance recognizing potential chemical risk and identifying subclinical brain dysfunction, which promotes evidence-based precaution.

To uncover the underlying neurotoxicological mechanism of certain pollutants, scientists concentrate mostly on the molecular signals than others. Thus, PCR, western blot, and histochemistries

are widely used. In the last decade, the emergence of advanced and powerful neuroscientific technologies greatly promoted the development of neurobiology [5]. Although in some neurotoxicological cases, new neuroscientific technologies are also used to explore the underlying neurotoxic mechanism of certain chemicals [6], the implementation of these advanced technologies in neurotoxicology is not common.

In this chapter, the methods of several advanced neurobiological technologies, including chemogenetics, optogenetics, fiber photometry, *in vivo* two-photon imaging, *in vivo* miniscope calcium imaging, and *in vivo* electrophysiological recording are introduced. By using these technologies, we are able to investigate the neurotoxic effect of environmental agents in high temporal and spatial resolution.

We expect that these advanced neurobiological technologies can help expand the scope of neurotoxicology research and carry forward the development of neurotoxicology.

2 Materials

2.1 Animals

Wild-type or transgenic mice with Cre knock-in gene are available. All animals are housed in a 12 h light/12 h dark cycle, and the temperature of the raising room is kept at 23–25 °C. All experiments are carried out in accordance with the guidelines of National Institutes of Health Guide for the Care and Use of Laboratory.

2.2 Equipment and Instruments

2.2.1 Equipments and Instruments of Chemogenetics

1. Compact small animal anesthesia device (*see Note 1*).
2. Automated stereotaxic instrument.
3. Temperature controller (*see Note 2*).
4. Rectal temperature probe.
5. Surgical microscope.
6. Cotton-tipped applicators.
7. Rectal temperature probe.
8. Electric hair trimmer (*see Note 3*).
9. Carbide drill burrs.
10. Cold light source.
11. Syringe pump.
12. Glass capillary.
13. Dental drill (*see Note 4*).
14. Pipette puller.
15. Surgical tools (scissor, forceps, needle drivers, needle, sutures).

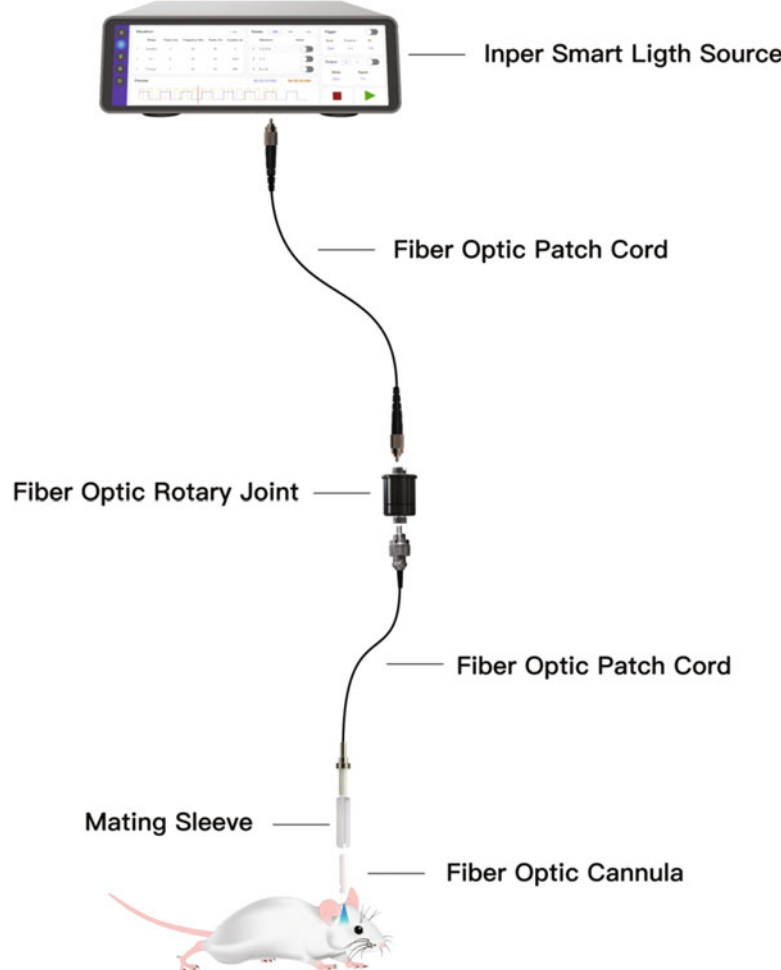


Fig. 1 Schematic diagram of laser light source. The laser light source system comprises fiber optic patch cord, fiber optic rotary joint, mating sleeve, and fiber optic cannula

2.2.2 Equipments and Instruments of Optogenetics

1. Compact small animal anesthesia device (*see Note 1*).
2. Automated stereotaxic instrument.
3. Laser light source (Inper Ltd.) (Fig. 1).
4. Optical power measuring instrument (measuring range: 0–100 mW, wavelength range: 400–1100 nm).
5. Fiber optic rotary joint (Interface: FC-FC).
6. Fiber optic patch cord (Fiber: 200/0.37, 200/0.50).
7. Mating sleeve (internal diameter: 1.25 mm, 2.5 mm).
8. Fiber optic cannula (outside diameter: 1.25 mm, 2.5 mm).
9. Temperature controller (*see Note 2*).
10. Surgical microscope.

- 11. Cotton-tipped applicators.
 - 12. Rectal temperature probe.
 - 13. Carbide drill burrs.
 - 14. Cold light source.
 - 15. Hair trimmer (*see Note 3*).
 - 16. Dental drill (*see Note 4*).
 - 17. Syringe pump.
 - 18. Glass capillary.
 - 19. Pipette puller.
 - 20. Surgical tools (scissor, forceps, needle drivers, needle, sutures).
- 2.2.3 Equipments and Instruments of Fiber Photometry**
- 1. Compact small animal anesthesia device (*see Note 1*).
 - 2. Automated stereotaxic instrument.
 - 3. Optical power measuring instrument (measuring range: 0–200 μ W, wavelength range: 400–1100 nm).
 - 4. Fiber optic patch cord (Fiber: 200/0.37, 200/0.50, 400/0.37, 400/0.50).
 - 5. Mating sleeve (internal diameter: 1.25 mm, 2.5 mm).
 - 6. Fiber optic cannula (outside diameter: 1.25 mm, 2.5 mm).
 - 7. Fiber optic rotary joint (Interface: FC-FC).
 - 8. Fiber photometry instrument (Inper Ltd.) (Fig. 2).
 - 9. Temperature controller (*see Note 2*).
 - 10. Cotton-tipped applicators.
 - 11. Rectal temperature probe.
 - 12. Surgical microscope.
 - 13. Cold light source.
 - 14. Carbide drill burrs.
 - 15. Glass capillary.
 - 16. Syringe pump.
 - 17. Hair trimmer (*see Note 3*).
 - 18. Surgical tools (scissor, forceps, needle drivers, needle, sutures).
- 2.2.4 Equipments and Instruments of In Vivo Two-Photon Imaging**
- 1. Compact small animal anesthesia device (*see Note 1*).
 - 2. High-speed two-photon microscope system (Olympus).
 - 3. Water-immersion high-power objective (Olympus).
 - 4. Optical filters (Chroma Technology).
 - 5. Temperature controller (*see Note 2*).
 - 6. Electric-heated thermostatic water bath.
 - 7. Custom-made head fixation plate.

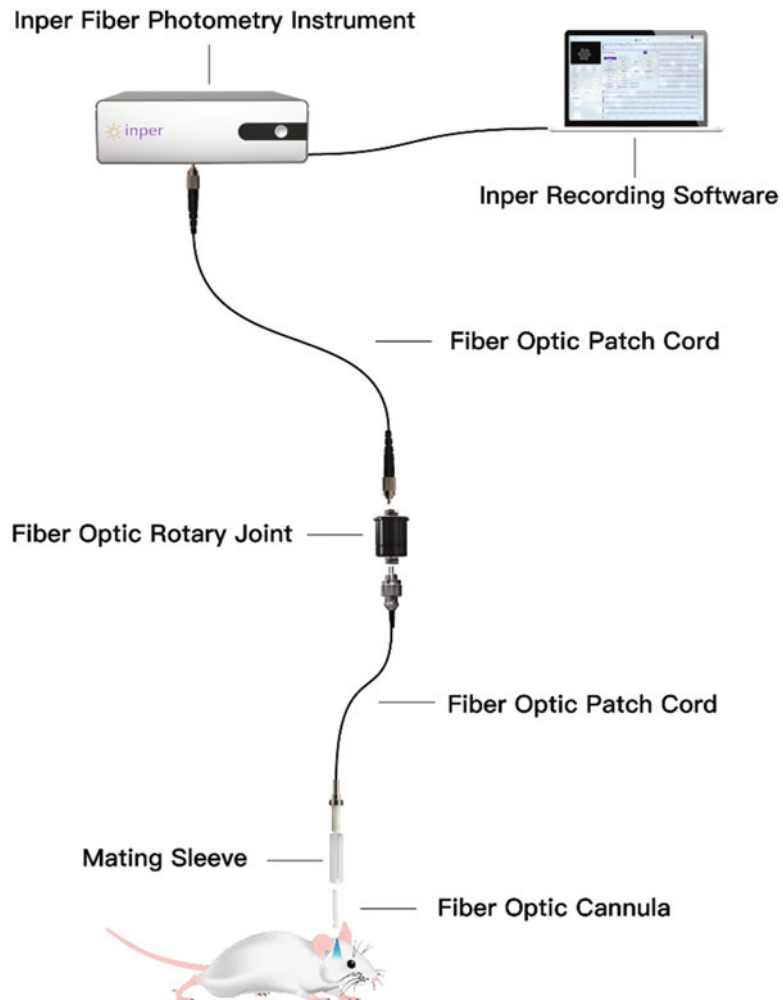


Fig. 2 Schematic diagram of fiber photometry instrument. The fiber photometry system comprises fiber photometry instrument, recording software, fiber optic patch cord, fiber optic rotary joint, mating sleeve, and fiber optic cannula

8. Cotton-tipped applicators.
9. Rectal temperature probe.
10. Stereotaxic apparatus.
11. Surgical microscope.
12. Carbide drill burrs.
13. Cold light source.
14. Glass capillary.
15. Cover glass.
16. Syringe pump.

17. Hair trimmer (*see Note 3*).
18. Dental drill (*see Note 4*).
19. Video camera.
20. Air pump.
21. Surgical tools (scissor, forceps, needle drivers, needle, sutures).

2.2.5 Equipments and Instruments of In Vivo Electrophysiological Recording

1. Multi-channel neural recording system (Bio-Signal Technologies) (Fig. 3).
2. Compact small animal anesthesia device (*see Note 1*).
3. Absorbent triangles (Sugi Saugtupfer, Kettenbach GmbH & Co. KG).
4. Stereotaxic apparatus (RWD Life Science).
5. Micro-Wire Array (Kedou BrainTech).
6. Mounting frame with micromanipulator.
7. Temperature controller (*see Note 2*).



Fig. 3 Schematic diagram of multi-channel recording system. A multi-electrode recording system consists of the following components: (1) Micro-electrode array, from 16 channels up to more than one thousand channels, implanted in the brain or peripheral nerve, picking up the neural active as electrical change. (2) Multi-channel amplifier to magnify the small neural signal few hundreds times larger. (3) Analog-to-digital converter, to convert the neural signal digitally for further process. (4) Neural signal processor to process the digital signal, (5) Software on PC for data visualizing and storage

8. Surgical microscope.
9. Cotton-tipped applicators.
10. Rectal temperature probe.
11. Carbide drill burrs.
12. Glass capillary.
13. Syringe pump.
14. Hair trimmer (*see Note 3*).
15. Needle.
16. Cold light.
17. Dental drill (*see Note 4*).
18. Surgical tools (scissor, forceps, needle drivers, needle, sutures).

**2.2.6 Equipments
and Instruments of In Vivo
Miniscope Calcium
Imaging**

1. Compact small animal anesthesia device (*see Note 1*).
2. Absorbent triangles (Sugi Saugtupfer, Kettenbach GmbH & Co. KG).
3. Stereotaxic apparatus (RWD Life Science).
4. Temperature controller (*see Note 2*).
5. Mounting frame with micromanipulator.
6. Surgical microscope.
7. Cotton-tipped applicators.
8. Rectal temperature probe.
9. Carbide drill burrs.
10. Syringe pump.
11. Vacuum pump.
12. Imaging systems.
13. Glass capillary.
14. Hair trimmer (*see Note 3*).
15. Dental drill (*see Note 4*).
16. GRIN lens.
17. Cold light.
18. Surgical tools (scissor, forceps, needle drivers, needle, sutures).

2.3 Viruses

1. Viruses expressing Channelrhodopsins (ChR2) or Halorhodopsins (NpHR) (HanbioBiotechnology, China) (*see Notes 5 and 6*).
2. Viruses expressing human Gq-coupled M3 muscarinic receptors (hM3Dq) or human Gi-coupled M4 muscarinic receptors (hM4Di) (HanbioBiotechnology, China) (*see Notes 5 and 6*).

3. Viruses that can express GCaMP or RCaMP (HanbioBiotechnology, China) (*see Notes 5 and 6*).

2.4 Chemicals

1. Agarose solution (1%): Dissolve agarose in sterile ACSF.
2. Clozapine-N-oxide (LKT Laboratories).
3. Artificial cerebrospinal fluid.
4. Isoflurane (*see Note 7*).
5. Eye ointment (*see Note 8*).
6. Cyanoacrylate glue.
7. Compressed air source.
8. Dental acrylic.
9. C&B Metabond.
10. 0.9% NaCl.
11. Cortex buffer.
12. Kwik-Cast.
13. Carbon.
14. ddH₂O₂.

3 Methods

3.1 Methods of Chemogenetics

1. To induce anesthesia, the mice are firstly placed in an anesthesia induction chamber prefilled with isoflurane 4%. Toe pinch is done to confirm the depth of anesthesia. Failing to response to toe pinch indicates reaching adequate anesthesia depth.
2. Mice under anesthesia are shaved off the hair with an electric trimmer or blade, and then transferred to and fixed on a stereotaxic apparatus. The isoflurane is maintained on 1–2% for inhalation throughout mask during the whole surgery (*see Note 10*).
3. After fixation, the eyes of experimental animals are gently covered with eye ointment to protect them from light stimulation.
4. The scalp is disinfected with tincture iodine solution or 75% ethyl alcohol, then make an incision along the midline of the scalp to expose the skull. Clean the skull with saline, remove the blood, and allow the skull to dry.
5. Mark the bregma and lambda and use a needle to locate the position of the accurate coordinate, mark this place with a marker pen.
6. The skulls of the mice are drilled with dental drill. Drill circularly over the center of the marked signal to avoid oversize skull hole.

7. About 100 nL virus is aspirated into the glass capillary.
8. Virus is injected into the interesting brain region with a micro-syringe pump at speed of 50 nL/min.
9. The needle is left in the injection place for 10 min to prevent virus reflux, the glass capillary is retracted slowly after completion of injection.
10. The skull hole is sealed by bone wax. Then the skin is sutured with needle and surgical suture. The wound would be disinfected with tincture iodine solution.
11. Following the surgery, the anesthetized mice are placed in a warmer to keep their core body temperature until they totally recover from anesthesia. Because animals are unable to regulate their temperature during anesthesia, insufficient heating may cause hypothermia and increase morality of recovering animals post operation.
12. After reviving, mice are put back to their home cage with food and water available ad libitum.
13. After about 4 weeks later, intraperitoneally administrate with 1 mg/kg CNO or equivalent volume saline to excite or inhibit target neurons expressing hM3D(Gq) or hM4D(Gi) neurons [7] 1 h before behavioral tests.
14. Behavioral tests.
15. Confirming the expression of viruses and their activated or inhibitory effect on the hM3D(Gq) or hM4D(Gi) expressing neurons with anti-fos immunofluorescence tests or patch clamp.

3.2 Methods of Optogenetics

1. Mice are anesthetized for the whole surgery with 1–2% isoflurane through mask accessory attached to the stereotaxic apparatus (*see Note 9*).
2. After head fixation on a stereotaxic apparatus, shave the heads of the mice with electric hair trimmer to explore the scalp.
3. Cut the scalp using sanitized scissors along the middle line of the head.
4. Use the H₂O₂ to completely remove periosteum, then dry the skull with a cotton swab (*see Note 10*).
5. Attach a needle to stereotaxic apparatus, find the target location according the coordinate related to bregma, and mark the location with a mark pen.
6. Small holes with about 0.3 mm diameter were drilled to make sure the glass capillary can pass through the hole.
7. Inject the virus into target region by micro-injection to ensure the expression of ChR2 or NpHR virus on the membrane of specific neurons [7].

8. After glass capillary was retracted 10 min after virus injection, the optical fiber is implanted above the injection sites and fixed with dental acrylic.
9. The avulsed scalp is sutured with suture needle and surgical suture.
10. Mice are put in a warming blanket to keep their body temperature at 37 °C.
11. After reviving, mice are placed back to their home cage with food and water available ad libitum.
12. After 2–3 weeks of virus injection, the effect of virus expression and their effect on the target neurons are determined by fluorescence microscope and patch clamp, and the function of ChR2 or NpHR was verified by in vitro light stimulation.
13. Deliver the light to the target region through optical fiber and carry out behavioral tests.

3.3 Methods of Fiber Photometry

1. Mice are anesthetized with 1–2% isoflurane and mounted on a stereotaxic apparatus (*see Note 10*).
2. Shave the scalp and cut the scalp along the middle line of the head.
3. Completely remove periosteum with H₂O₂.
4. Small craniotomy is performed to drill three holes (one for glass capillary and two for screws).
5. Inject the virus into target region by micro-injection to ensure the expression of GCaMP or RCaMP on the membrane of specific neurons.
6. Immediately after viral injection, two screws are fixed on the skull through the pre-prepared holes. After that, fiber optic is inserted above the expression site of the virus and fixed to the screws with dental acrylic.
7. The anesthetized animals need to transfer to a warmer or a heating blanket to maintain the core body temperature before fully recover.
8. About 4 weeks later, bleach the brand-new optical patch cables with a high intensity (e.g., 5 mW) light for at least 1 h before use.
9. Adjust the light intensity to about 40 μW at the tip of optical patch cables with an optical power measuring instrument.
10. Then link the optic fiber patch cable to the implanted optic fiber through black optic fiber cannula.
11. Then acclimate the animals to this appliance before behavioral test for at least 1 day.

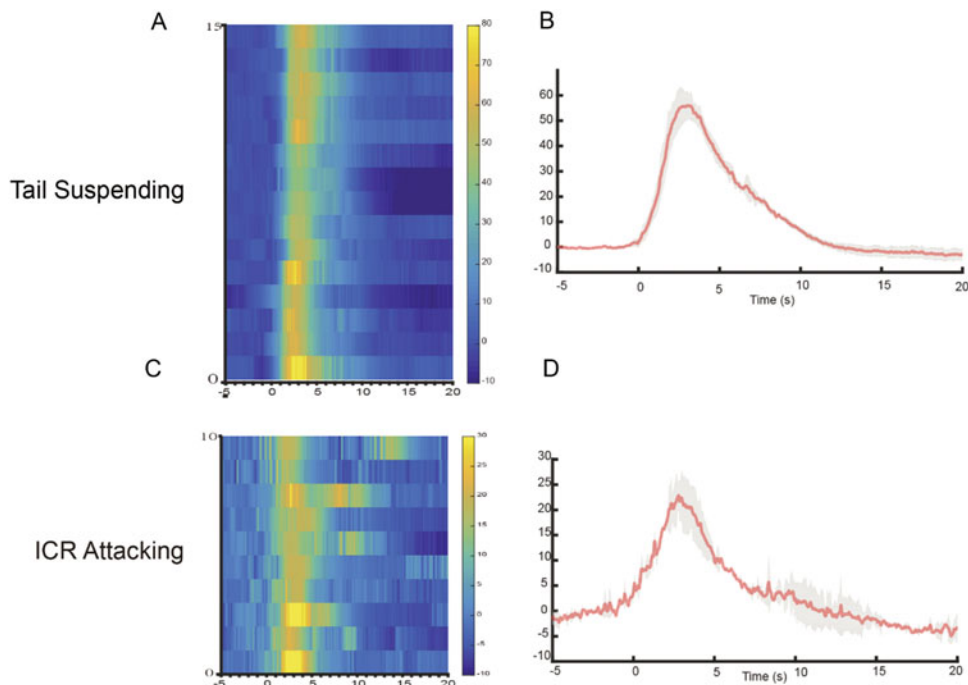


Fig. 4 Calcium fluorescence of astrocytes in lateral habenula during different stressor exposure. **(a)** Heat map of calcium fluorescence during tail suspending. **(b)** Peri-event plot of calcium fluorescence during tail suspending. **(c)** Heat map of calcium fluorescence during ICR attacking. **(d)** Peri-event plot of calcium fluorescence during ICR attacking. $n = 2$ or 3 , 5 trials for each mouse

12. Mice are habituated to the test apparatus at least 30 min to minimize the influence of anxiety caused by unfamiliar surroundings.
13. Real-time calcium signal is recorded synchronously with behavior video in different behavioral experiments through the fiber photometry instrument [8], sign the events manually based on experimental design.
14. The calcium fluorescence raw data is analyzed and processed by Inper Data Process and MATLAB, and the results are calculated as $(F - F_0)/F_0$. The value of F_0 is calculated from 10 s average fluorescence signal before each trial. At the end, heatmaps or peri-event plots are used to display dF/F values (Fig. 4).

3.4 Methods of *In Vivo Two-Photon Imaging*

1. The mice are anesthetized with 1–2% isoflurane and placed on a stereotactic apparatus (*see Note 10*).
2. Smear the eye ointment on the eyes of anesthetized animals to protect eyes from light illumination.
3. Shave the scalp and cut the scalp along the middle line of the head.

4. Following washing the cranium with saline, H₂O₂ is used to remove periosteum and adjacent connective tissues.
5. A diameter burr hole (~1 mm) is drilled in skull overlying target region and remove any fragments of skull from the hole.
6. Puncture the dura using a 30 G needle carefully without damaging the underlying brain tissue.
7. Thaw viral sample and centrifuge it at slow-speed revolution before loading desired volume virus into the glass capillary.
8. Advance the glass capillary into the target region and GCaMP or RCaMP-containing viruses are microinjected into the interest nucleus (mainly refer to cortex) with a syringe pump at 50 nL/s.
9. After each injection, the capillaries are left in the injection place for about 10 min to prevent virus reflux and ensure virus diffusion sufficiently.
10. After finishing injections, pad the hole with a drop of agarose at ~38 °C.
11. Close the lacerated scalp with absorbable suture.
12. Kept the recovering animals in a warmer until full revival, and give liquid diet post operation.
13. After virus expression (about 2 or 3 weeks), anesthetize animals and place mice in stereotaxic apparatus again.
14. Re-exposure of cranium and scrape skull with a scalpel blade, then dry the skull with cotton-tipped applicators, cement a headplate to the skull using tissue acrylic and C&B Metabond.
15. Remove skull flap by drilling along interior edges of headplate and then insert coverslip [9].
16. Put animal under two-photon microscope, record and analyze the signals according to manufacturer's introduction.

3.5 Methods of *In Vivo* Electrophysiological Recording

1. Place anesthetized animals under anesthesia on a stereotaxic apparatus, and 1.0–2% isoflurane in O₂ is used in the all surgery procedure (*see Note 10*).
2. Shave the mice using an electric hair trimmer, sterilized scalp with 75% ethyl alcohol.
3. Insert a rectal temperature probe, and use a temperature controller to maintain internal body temperature at 37 °C.
4. Make an incision along the midline of the scalp, clean blood, and dry the skull with cotton-tipped applicators (*see Note 11*).
5. Use the measured coordinates to calculate the ML and AP coordinates for the four corners of the “skull window” relative to bregma.

6. Perform a craniotomy, remove bone to expose the skull window (*see Note 12*).
7. Drill holes for the 4–5 skull screws and secure the screws in place.
8. Attach the array (Kedou BrainTech, China) to the stereotaxic arm through an adaptor.
9. Lower the array slowly until it reaches its final DV coordinate.
10. Use dental acrylic to cement the microwires in place.
11. Place the animal in a heating blanket until thermoregulation and locomotion have recovered.
12. A miniature head stage is plugged into the implanted array on animal's head. This head stage amplified, filtered and digitized the neural signal, and sent it to the DAQ box through a flex cable.
13. A rotary joint is used to avoid twisting of signal cable.
14. Recorded signals are digitized at 30KHz sampling, then further band-pass filtered digitally and separate into local field potential (0.3 Hz to 200 Hz) or single-unit spike (300 Hz to 7500 Hz).
15. The waveforms of the spike candidates are abstracted from continuous signal trace with threshold detection method.
16. The change of firing rate or firing pattern is used for analysis and usually is correlated with external events such as behavioral action or optical and electrical stimulation. The timestamps of those events are recorded with digital input on the recording system (Fig. 5).
17. Recorded neural activity is initially sorted using online sorting algorithm. At the end of the recording, potential single units should be resorted offline based on waveform, amplitude, and inter-spike interval histogram offline. Only units in which all the spikes have amplitudes well above the voltage threshold should be considered (to ensure that no spikes are lost). The sorted units together with continuous local field potential (LFP) are then imported into NeuroExplorer for analysis, such as rate histogram, peri-events histogram, spectrum, etc.

3.6 Methods of In Vivo Miniscope Calcium Imaging

1. Repeat the procedures (**steps 1–12**) mentioned in Subheading 3.5.
2. Two or three weeks later, repeat the procedures (**step 13**) mentioned in Subheading 3.5.
3. Cover the eyes gently with eye ointment to keep off light stimulation.

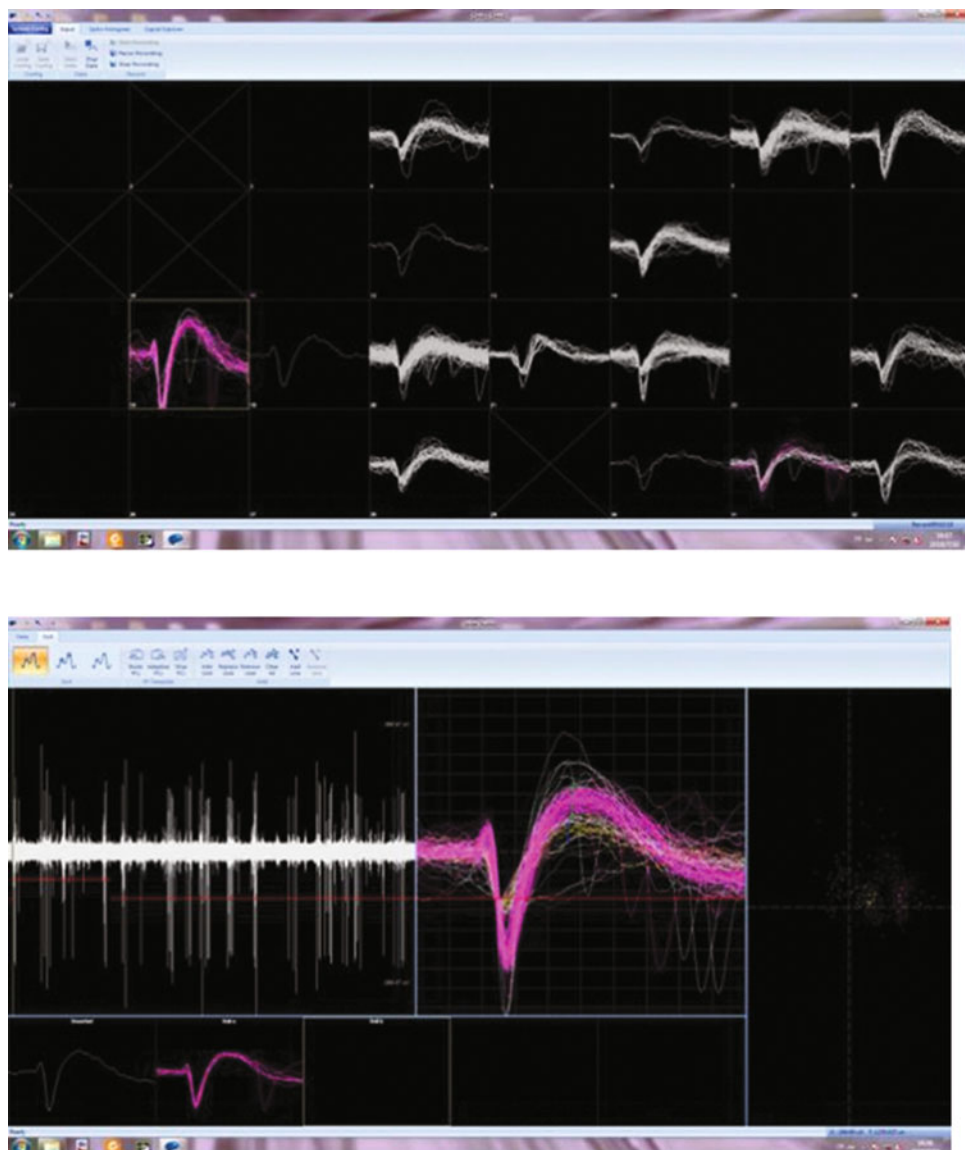


Fig. 5 Single-unit spike from multiple neurons. This figure shows a typical recording for multiple units from freely moving animal. The top figure showed signal from a 32-channel array implanted in rat's motor coortex. The bottom one showed a waveform of a sorted neuron from one of the electrodes

4. Remove the hair from the surgical area with an electric hair trimmer and perform aseptic procedures with tincture iodine solution.
5. After scissoring scalp, process the skull with saline and H_2O_2 successively or scrap the skull with blade to remove periosteum and other connective tissue.

6. Perform craniotomy and three screws are implanted into the skull in an equal triangle shape with lens landing point in the center.
7. Then drill the bone at the coordinate for future placement of lens implantation without destroying underlying brain (*see Note 13*).
8. Remove the bone debris with aurilave or cotton-tip applicator to prevent drop of debris into the craniotomy. And cool the skull with sterile saline during drilling prior to craniotomy to prevent overheating of brain.
9. Prior to lens implantation, a durotomy is performed to peel the dura from brain using a bent 30 G needle (*see Note 14*).
10. Following the durotomy, drop sterile saline into the craniotomy hole immediately to humidify exposed brain tissue (*see Note 15*).
11. Then, aspirate tissue above your region of interest with a blunt needle attached to a vacuum pump very slowly. Irrigate the tissue with sterile CSF continuously during the whole procedure.
12. After tissue aspiration, fix a lens holder to the stereotaxic apparatus, and grip the microendoscope using a lens holder with heat shrink covered forceps.
13. Next, microendoscope lens is loaded through the skull window and inserted into the interested region (about 0.1 mm above the viral injection area) alone the track very slowly (~100–200 μ m/min) (*see Note 16*).
14. Dry the surface of skull with a sterile paper towel, and fill the craniotomy around lens with melted agarose (1%, 40 degree, kept in an attemperator until use) to seal the gap and protect exposed tissue.
15. Apply Metabond to envelop the exposed skull and all sides of the microendoscope.
16. After that, pave a thin layer of dental acrylic around the lens. Once cement harden, a second layer of dental acrylic containing carbon powder is added to the first layer [10, 11].
17. Apply a head cap to cover the lens top, and stabilize the cap to the dental cement.
18. Microendoscope is removed from the bulldog serrefine when the acrylic has completely dried.
19. Enclose the microendoscope using black dental cement and cover the top of the head cap with Kwik-Cast.
20. Following the surgery, the mice are removed from the stereotaxic apparatus and then were placed to a warmer to recover from anesthesia.

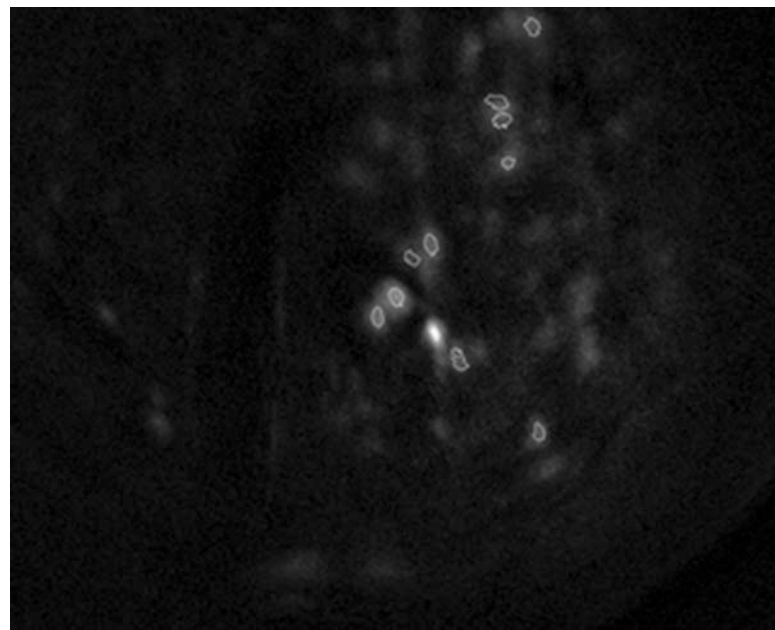


Fig. 6 Representative picture of GCaMP fluorescence imaging from hippocampus during sleeping. The lightspot represents GCaMP fluorescence

21. To relieve postoperative pain, mice are administered analgesic, such as buprenorphine (0.1 mg/kg sc) or carprofen (4 mg/kg sc), for 2 days.
22. After sufficient expression of GCaMP virus, fix the mice with a head restraint after anesthesia, then attach an imaging baseplate to microendoscope and adjust the focus before endoscopic imaging (*see Note 17*).
23. The GCaMP fluorescence imaging is acquired at 30 Hz (Fig. 6).
24. We interpret and analyze the collected data using Matlab software with a customer written script according to the experiment requirement.

4 Notes

1. Air and oxygen gas are both available for the anesthesia device.
2. During the surgery, temperature control is important to decrease the mortality of surgery.
3. Use an electric hair trimmer for small animals.
4. Dental drill with appropriate revolution and carbide drill burrs is benefit for surgery.

5. Most of current studies are based on Cre transgenic background experimental animals, while the strategy of wild-type animals combined with virus carrying cell-specific promoter is available. All animal experimental procedures were performed in accordance with the Guide for the Care and Use of Laboratory Animals.
6. The titer of virus will affect the results as well as expression time.
7. Other volatile anesthetics are also adopted in the anesthesia.
8. During the surgery, eye ointment is smeared on the eyes of experimental animals to prevent eye damage.
9. Before surgery, the tail pinch test is done to verify that the anesthesia has worked effectively.
10. It is imperative to remove the periosteum to completion in and around the area to be drilled. Failure to do so may result in the membrane becoming entangled in the drill bit.
11. If any remaining bleeding occurs, terminate the residual bleeding with a minor electro-surgical instrument.
12. Keep the window moist with saline for the whole remainder surgery. Use micro-forceps to carefully remove any remaining bone chips, debris, or dura mater inside the skull window. This step is extremely important, as these bits of material can compromise the integrity of the array during lowering.
13. The size of the windows is based on the type of lens.
14. Make sure that the dura is fully removed at the site of craniotomy to avoid impending penetration of microendoscope.
15. Sterile saline must be added to the craniotomy immediately after craniotomy to prevent the adhesion of dura and cortex.
16. Bleeding during lens implant procedure may induce inferior image.
17. Make sure that the focus remains the same across different testing days.

Acknowledgements

We would like to thank Cihang Yang for providing us the pictures of optogenetic and fiber photometry in Figs. 1 and 2, Meifang Ma for providing us the pictures of in vivo electrophysiological recording in Figs. 3 and 5.

This work was supported by NSFC grant (81973083 and 81601144), the Joint Funds for the Innovation of Science and Technology, Fujian province (2018Y9091 and 2017Y9105).

References

1. Hou L, Zhang X, Wang D, Baccarelli A (2012) Environmental chemical exposures and human epigenetics. *Int J Epidemiol* 41(1):79–105. <https://doi.org/10.1093/ije/dyr154>
2. Landrigan PJ, Sly JL, Ruchirawat M, Silva ER, Huo X, Diaz-Barrera F, Zar HJ, King M, Ha EH, Asante KA, Ahanchian H, Sly PD (2016) Health consequences of environmental exposures: changing global patterns of exposure and disease. *Ann Glob Health* 82(1):10–19. <https://doi.org/10.1016/j.agoh.2016.01.005>
3. Heyer DB, Meredith RM (2017) Environmental toxicology: sensitive periods of development and neurodevelopmental disorders. *Neurotoxicology* 58:23–41. <https://doi.org/10.1016/j.neuro.2016.10.017>
4. Grandjean P, Landrigan PJ (2006) Developmental neurotoxicity of industrial chemicals. *Lancet* 368(9553):2167–2178. [https://doi.org/10.1016/S0140-6736\(06\)69665-7](https://doi.org/10.1016/S0140-6736(06)69665-7)
5. Jorgenson LA, Newsome WT, Anderson DJ, Bargmann CI, Brown EN, Deisseroth K, Donoghue JP, Hudson KL, Ling GS, MacLeish PR, Marder E, Normann RA, Sanes JR, Schnitzer MJ, Sejnowski TJ, Tank DW, Tsien RY, Ugurbil K, Wingfield JC (2015) The BRAIN initiative: developing technology to catalyse neuroscience discovery. *Philos Trans R Soc Lond Ser B Biol Sci* 370 (1668):20140164. <https://doi.org/10.1098/rstb.2014.0164>
6. Serduc R, Verant P, Vial JC, Farion R, Rocas L, Remy C, Fadlallah T, Brauer E, Bravin A, Laissie J, Blattmann H, van der Sanden B (2006) In vivo two-photon microscopy study of short-term effects of microbeam irradiation on normal mouse brain microvasculature. *Int J Radiat Oncol Biol Phys* 64(5):1519–1527. <https://doi.org/10.1016/j.ijrobp.2005.11.047>
7. Chen L, Yin D, Wang TX, Guo W, Dong H, Xu Q, Luo YJ, Cherasse Y, Lazarus M, Qiu ZL, Lu J, Qu WM, Huang ZL (2016) Basal forebrain cholinergic neurons primarily contribute to inhibition of Electroencephalogram Delta activity, rather than inducing behavioral wakefulness in mice. *Neuropsychopharmacology* 41 (8):2133–2146. <https://doi.org/10.1038/npp.2016.13>
8. Cai P, Chen L, Guo YR, Yao J, Chen HY, Lu YP, Huang SN, He P, Zheng ZH, Liu JY, Chen J, Hu LH, Chen SY, Huang LT, Chen GQ, Tang WT, Su WK, Li HY, Wang WX, Yu CX (2020) Basal forebrain GABAergic neurons promote arousal and predatory hunting. *Neuropharmacology* 180:108299. <https://doi.org/10.1016/j.neuropharm.2020.108299>
9. Smith GB, Fitzpatrick D (2016) Viral injection and cranial window implantation for in vivo two-photon imaging. *Methods Mol Biol* 1474:171–185. https://doi.org/10.1007/978-1-4939-6352-2_10
10. Harrison TC, Pinto L, Brock JR, Dan Y (2016) Calcium imaging of basal forebrain activity during innate and learned behaviors. *Front Neural Circuits* 10:36. <https://doi.org/10.3389/fncir.2016.00036>
11. Zhang L, Liang B, Barbera G, Hawes S, Zhang Y, Stump K, Baum I, Yang Y, Li Y, Lin DT (2019) Miniscope GRIN lens system for calcium imaging of neuronal activity from deep brain structures in behaving animals. *Curr Protoc Neurosci* 86(1):e56. <https://doi.org/10.1002/cpns.56>



Chapter 9

Analyses of Epigenetic Modification in Environmental Pollutants-Induced Neurotoxicity

Guangxia Yu, Zhenkun Guo, and Huangyuan Li

Abstract

Epigenetics is one of the most rapidly expanding fields in biology, which plays important roles in environmental pollutant-induced neurotoxicity. Analyses of epigenetic modification is of great significance in providing more accurate information for the risk assessment and management of harmful factors. However, few studies have systematically summarized the analysis and detection methods for epigenetic modification. In this chapter, we summarized several popular methods for analyses of epigenetic modifications, including Methylated DNA Immunoprecipitation Sequencing (MeDIP-Seq) for genome-wide DNA methylation analyses, Quantitative Methylation Specific PCR (qMSP) for genome-specific DNA methylation analyses, methylated RNA immunoprecipitation sequencing (MeRIP-seq) for genome-wide RNA methylation analyses, MeRIP-qPCR for genome-specific RNA methylation analyses, qRT-PCR for the non-coding RNA, and western blot for the histone modification analyses. It could be helpful to the research about environmental epigenetic toxicology.

Key words Epigenetics, Neurotoxicology, DNA methylation, Histone modifications, Non-coding RNA, Chromatin structure, RNA methylation

1 Introduction

Epigenetics is generally defined as a change in gene function without alterations in the DNA sequences. Firstly, it does not involve changes in DNA sequences. Secondly, the expression and function of genes is changed. Thirdly, such changes in gene function may be heritable. On the other side, such changes may be inherited cross generations of cells and/or individuals through mitosis and/or meiosis. Recent years, epigenetics is one of the most rapidly expanding fields in biology, which is a bridge between genotype

Guangxia Yu and Zhenkun Guo contributed equally to this work.

and phenotype [1]. The epigenetic molecular factors include DNA methylation [2], histone modifications [3], non-coding RNAs (e.g., microRNAs) [4], chromatin structure [5], and RNA methylation [6]. Abundant studies demonstrated that epigenetic alterations play important roles in environmental pollutant-induced neurotoxicity [7]. Chemicals regulated gene expression by influencing gene transcription, mRNA degradation and translation, etc. Abnormal changes in DNA methylation, RNA methylation, non-coding RNAs, and histone modification can serve as biomarkers for environmental pollutant-induced neurotoxicity [8–11]. Zhan's work displayed paraquat could induce nerve cell damage via DNA methylation [12]. Li group observed multiple of m⁶A modification in neurodegenerative disease-associated genes changed upon CoCl₂ exposure [13]. Several studies have shown that miRNAs may contribute to neurodegeneration process (including neuroplasticity, stress responses, cellular signaling) in response to environmental risks [14–16]. It has also been reported that abnormal histone acetylation homeostasis may participate in neurodegenerative damage induced by neurotoxic chemicals (e.g., pesticide dieldrin, paraquat, manganese chloride) [17–20]. Therefore, analyses of epigenetic modification is of great significance in providing more accurate information for the risk assessment and management of harmful factors [21]. However, few studies have systematically summarized the analysis and detection methods for epigenetic modification.

In this chapter several popular methods have been summarized, including Methylated DNA Immunoprecipitation Sequencing (MeDIP-Seq) for analyses of genome-wide DNA methylation, Quantitative Methylation Specific PCR (qMSP) for analyses of genome-specific DNA methylation, methylated RNA immunoprecipitation sequencing (MeRIP-seq) for analyses of genome-wide RNA methylation, MeRIP-qPCR for analyses of genome-specific RNA methylation, qRT-PCR for the analyses of non-coding RNAs, and western blot for the analyses of histone modification. This work could be helpful to the research about environmental epigenetic neurotoxicology.

2 Materials

Prepare all solutions using ultrapure water (prepared by purifying deionized water to attain a resistivity of 18 MΩ cm at 25 °C) and analytical grade reagents. Prepare and store all stock solutions at room temperature, unless otherwise indicated, up to a month. When handling irritant or volatile compounds (such as TEMED), work under fume hood.

**2.1 Analyses
of Genome-Wide DNA
Methylation**

1. DNase, RNase-free water.
2. EZ-96 DNA Methylation Kit.
3. Ethanol.
4. Genomic DNA.
5. PCR reagents: PCR buffer, dNTPs, Taq, primers.
6. Infinium Human Methylation450 BeadChip Kit.

**2.2 Analyses
of Genome-Specific
DNA Methylation**

1. TE buffer.
2. DEPC water.
3. EZ-96 DNA Methylation Kit.
4. Ethanol.
5. AmpliTaq Gold 360 Master Mix.
6. Power SYBR Green PCR Master Mix.
7. DNA loading buffer.
8. The methylation-specific primer.

**2.3 Analyses
of Genome-Wide RNA
Methylation**

1. Antibody: Anti-m⁶A (*see Note 1*).
2. RNase-free water.
3. Ultrapure water.
4. Chloroform.
5. Absolute Ethanol.
6. Dynabeads Antibody Coupling Kit (*see Note 2*).
7. Acid-phenol: chloroform pH 4.5 (with IAA, 25:24:1).
8. RNase inhibitor.
9. Ambion Dynabeads mRNA Purification Kit.

**2.4 Analyses
of Gene-Specific RNA
Methylation**

1. Dynabeads® mRNA Purification Kit.
2. RNase-free water.
3. Anti-m⁶A antibody.
4. RNase Inhibitor.
5. qPCR SYBR Green master mix.

2.5 Non-coding RNA

1. Total RNA extract.
2. DNase I (RNase-free).
3. Reverse Transcriptase Mix from miRNA first-strand cDNA synthesis kit.
4. Bulge-LoopTM miRNA QRT-PCR Primer kit.
5. Primer sets for target genes listed in Table 6.

6. Thermal cycler.
7. Light Cycler instrument.
8. RNase-free water.

2.6 Histone Modification

2.6.1 Stock Solutions, Working Solutions, and Buffers

1. Resolving gel buffer: 1.5 M Tris–HCl, pH 8.8. Add 200 mL water into a 1 L glass beaker. Weigh 181.7 g Tris base and transfer to the glass beaker. Add water to a volume of 900 mL. Stir with a magnetic stir bar and adjust pH with concentrated HCl. Make the solution up to a final volume of 1 L with water. Store at 4 °C.
2. Stacking gel buffer: 0.5 M Tris–HCl, pH 6.8. Dissolve 60.6 g of Tris base in water to a final volume of 1 L as the above item 3. Keep at 4 °C.
3. 30% acrylamide-0.8% Bis-acrylamide (29.2:0.8).
4. 10% SDS: Dissolve 1 g of SDS in distilled water to a final volume of 10 mL (*see Note 3*).
5. 10% ammonium persulfate: Dissolve 0.1 g of ammonium persulfate with water to a final volume of 1 mL. Prepare this fresh each time.
6. Running buffer: 0.025 M Tris, pH 8.3, 0.192 M glycine, 0.1% SDS. Prepare 10× native buffer (0.25 M Tris, 1.92 M glycine): Dissolve 30.3 g Tris base and 144 g glycine in 800 mL water. Mix well and make it up to 1 L with water. To make 1000 mL working running buffer, dilute 100 mL of 10× native buffer to 890 mL with water and add 10 mL of 10% SDS (*see Note 4*).
7. Sample buffer (5×): 0.325 M Tris–HCl (pH 6.8), 10% SDS, 25% β-mercaptoethanol, 0.1% bromophenol blue, 45% glycerol. Right before use, 10% BME or 10–20 mM DTT should be added to the 5× sample buffer.
8. Bromophenol blue (BPB) solution: Dissolve 0.1 g BPB in 100 mL water. Store at –20 °C.
9. Transfer buffer (5×): Dissolve 30.3 g Tris base and 144 g glycine in 1 L water (pH 8.3). Make sure that all powders are completely dissolved and mixed fully before use. Store at room temperature.
10. Transfer buffer (1×): Mix 200 mL of 100% methanol, 100 mL of Transfer buffer (5×), and 700 mL water together to make 1000 mL working transfer buffer. Methanol should be added just before use.
11. Tris-buffered saline (TBS 10×): 1.5 M NaCl, 0.1 M Tris–HCl, pH 7.4. Dissolve 12 g Tris base and 80 g NaCl in 800 mL water and mix well. Adjust pH to 7.4 with concentrated HCl. Add water to a final volume of 1 L. TBS 1×: Mix 100 mL of 10× TBS and 900 mL of water together to make 1000 mL TBST solution.

12. TBST: 1× TBS with 0.1% Tween 20. Mix well and store at room temperature.
 13. Blocking Buffer: 5% nonfat dry milk powder. Dissolve 1 g of nonfat dry milk powder in TBST 1× to a final volume 20 mL.
- 2.6.2 Other Reagents, Materials, and Equipment**
1. Nuclear and cytoplasmic extraction reagents kit (Pierce).
 2. BCA protein assay kit (Beyotime).
 3. TEMED: *N,N,N,N'*-Tetramethyl-ethylenediamine. Store at 4 °C.
 4. Mini-PROTEAN® Tetra Cell system from Bio-Rad or equivalent.
 5. Tetra Blotting Module system from Bio-Rad or equivalent.
 6. Electrophoresis power supply.
 7. Polyvinylidene fluoride (PVDF) membranes.
 8. Methanol.
 9. Prestained protein ladder (e.g., Spectra™ Multicolor Low Range Protein Ladder, 1.7–40 kDa).
 10. Shaker and plastic containers.
 11. Histone modification antibodies, e.g., anti-histone 3, anti-acetyl-histone 3, anti-acetyl-histone 4 (Rabbit polyclonal).
 12. Secondary antibodies: Horseradish peroxidase (HRP)-conjugated anti-rabbit IgG.
 13. ECL developing kit.
 14. Luminescence detection machine.

3 Methods

3.1 Analyses of Genome-Wide DNA Methylation

1. Extract DNA from tissue.
2. Detect genomic DNA concentration with NanoDrop and determine $A_{260/280}$ ratio > 1.80.
3. Take out 1–2 µg DNA sample for bisulfite treatment using EpiTect Whole Bisulfite Kit (*see Note 5*).
4. Add 500 ng DNA sample into M-Dilution buffer, incubate samples at 37 °C for 15 min.
5. Add 100 µL CT Conversion Reagent to each sample and mix it.
6. Incubate samples on thermal cycler at 95 °C for 30 s and at 50 °C for 1 h. Repeat the previous two steps for more than 15 cycles, and then at 4 °C for 10 min.
7. Pipette 400 µL of M-Binding Buffer to Zymo-Spin IC Column.

8. Load the DNA samples from ice into the **step 4** prepared M-Binding Buffer and mix by pipetting up and down.
9. Centrifuge at room temperature at $\geq 10,000 \times g$ for 30 s and discard the flow-through.
10. Add 500 μ L of M-Wash buffer and centrifuge at $\geq 10,000 \times g$ for 30 s. Discard the flow-through.
11. Add 200 μ L of M-Desulfonation buffer and let it stand at room temperature for 15–20 min. After incubation centrifuge at $\geq 10,000 \times g$ for 30 s. Discard the flow-through.
12. Add 500 μ L of M-Wash buffer to each well and centrifuge at $\geq 10,000 \times g$ for 30 s. Discard the flow-through.
13. Repeat **step 9**.
14. Place Silicon A Binding Plate onto an elution plate.
15. Add 30 μ L of M-Elution buffer directly to the binding matrix in each well of Silicon A Binding Plate. Incubate for 1–2 min at room temperature and centrifuge for 30 s at $\geq 10,000 \times g$ to elute the DNA (*see Note 6*).
16. Keep aside 4 μ L of each (bisulfite converted) DNA sample for quality control.
17. Assess the quality of bisulfite converted DNA by using for instance methylation-specific PCR for gene of interest.
18. Determine concentration of bisulfite-treated DNA using NanoDrop.
19. Adjust DNA concentration of each sample to 50 ng/ μ L with M-Elution buffer or water.
20. DNA methylation detection according to Infinium HD Assay Methylation protocol guide. Include the procedures of genome-wide DNA denatured, fragmented, precipitated, resuspended, hybridized to the BeadChip, and then fluorescently stained, scanned and measured the intensities of beads.
21. Extract DNA methylation signals from scanned arrays.
22. Data analysis with Genome studio software. Carried out the GO analysis, pathway analysis, and cluster analysis of the methylated abnormal genes in the chip results and determine candidate genes for further studies.

3.2 Analyses of Genome-Specific DNA Methylation

1. Obtain the objective gene sequence from NCBI database, <http://www.ncbi.nlm.nih.gov/>.
2. Design primers using software: PyroMark Assay Design, meth-primer, methprimer DB, or others (*see Note 7*).
3. Extract DNA from tissues or cells (*see Note 8*).
4. Convert 1 μ g DNA by sodium bisulfite according to the EZ DNA Methylation kit protocol guide.

Table 1
Reagent and volume of qMSP reaction system

Reagent	Volume (μ L)
Power SYBR green PCR master mix	10
Forward primer	0.5
Reverse primer	0.5
Bisulfite-treated DNA	1
DEPC water	8
Total volume	Up to 10

- Carry out Quantitative Methylation Specific PCR(qMSP) reactions in the flowing reaction system as shown in Table 1 (see Note 9).
- The reactions are performed in triplicate on a Light Cycler 480 real-time cycler under the following thermal profile: 95 °C for 10 min activation step followed by 40 cycles: denaturation at 95 °C for 15 s, annealing and extension at 58–65 °C for 1 min.
- Cycle threshold (C_t) values for each target are normalized for DNA input. The values for all samples are transformed to relative quantity (RQ) compare to the calibrator (0.5% standard methylated DNA dilution) as the following formula: (see Note 10).

$$RQ_{\text{sample}} = 2^{[(Ct(\text{Target}) - Ct(\text{ACTB}))_{(\text{calibrator})} - Ct(\text{Target}) - Ct(\text{ACTB}))_{(\text{sample})}]}$$

3.3 Analyses of Genome-Wide RNA Methylation

3.3.1 RNA Isolation and Fragmentation

- Extract RNA from cell or tissue (see Note 11).
- Isolate mRNAs from total RNA according to the Dynabeads® mRNA Purification Kit protocol guide (see Note 12).
- Determine the concentration of purified mRNAs with Nano-Drop (see Note 13).
- Take 10 μ g purified mRNA in 50 μ L ultrapure water.
- Add 250 μ L of fragmentation buffer to the 50 μ L mRNA to a final volume of 300 μ L. Proceed to the fragmentation of the 300 μ L mRNA solution at 94 °C for exactly 5 min using a thermocycler (see Note 14).
- Stop the fragmentation reaction by adding 50 μ L of stop buffer to a final volume of 350 μ L and immediately put on ice (see Notes 15 and 16).

3.3.2 RNA Immunoprecipitation Reaction

1. Add 150 μ L of pre-equilibrated m⁶A-Dynabeads to the 350 μ L of fragmented RNA to a final volume of 500 μ L.
2. Rotate (tail-over-head) at 7 rotations per minute for 1 h to allow the fragmented RNA binding to the m⁶A-Dynabeads at room temperature.
3. Place the tubes on a magnet until the solution becomes clear, discard the 500 μ L liquid (*see Note 17*).
4. Resuspend m⁶A-Dynabeads-RNA complexes in 500 μ L of m⁶A Binding Buffer, incubate for 3 min at room temperature, and remove clear supernatant after placing the beads in the magnet.
5. Repeat **step 4** with 500 μ L of low salt buffer.
6. Repeat **step 4** with 500 μ L of high salt buffer. Do not exceed 3-min incubation time for this step to prevent release of the RNA from the beads.
7. Repeat **step 4** twice with 500 μ L of TET buffer (*see Note 18*).

3.3.3 Elution of m⁶A-Positive RNA

1. Add 125 μ L of 42 °C preheated Elution Buffer to the m⁶A-Dynabead complexes from Subheading **3.3.2, step 4** and incubate at 42 °C for 5 min.
2. Place the beads on the magnet.
3. Collect the liquid phase and transfer to a fresh tube, kept on ice, as it represents the eluate fraction containing the m⁶A “enriched RNA.”
4. Repeat **steps 1–3**.
5. Collect all of the liquid phase including m⁶A positive RNA fraction 500 μ L obtained from **steps 1 to 4** into one tube. Keep the tube on ice for next steps.

3.3.4 Extraction and Cleanup Step of the RIP

1. Extract the 500 μ L of m⁶A positive RNA collected in the previous step by adding 500 μ L of acid phenol-chloroform.
2. Centrifuge at 4 °C at 10,000 $\times \text{g}$ for 7.5 min.
3. Carefully collect the upper phase making sure not to touch the inter-phase and transfer to a fresh 1.5 mL tube.
4. Wash the pellet twice in 70% ethanol by centrifuging for 10 min at 4 °C at 16,000 $\times \text{g}$.
5. Dry the pellet at room temperature for 10 min, then resuspend it in the desired volume (typically 5–6 μ L) ultrapure water.

3.3.5 Library Construction and Sequencing

1. 100 ng of input and 100 ng of post m⁶A-IP positive fraction for library construction according to the Illumina TrueSeq Stranded mRNA Sample Preparation Guide.
2. Quantify the library by qRT-PCR.

3. Analysis of the methylated abnormal genes in the MeRIP-seq results and determine candidate genes for further studies (Fig. 1).

3.4 Analyses of Gene-Specific RNA Methylation

3.4.1 Site Prediction

1. Design primers directly targeting methylation sites or regions of sequencing target genes.
2. Primers are designed by predicting the methylation site information of target genes.
Prediction software:
 - (a) SRAMP:A sequence-based N6-methyladenosine (m^6A) modification site predictor (*see Note 19*).
 - (b) Online prediction tool address: <http://www.cuilab.cn/sramp>

3.4.2 mRNA Isolation and Fragmentation

1. Isolate mRNAs from total RNAs according to the Dynabeads® mRNA Purification Kit *protocol guide* (*see Note 20*).
2. Determine the concentration of purified mRNAs with Nano-Drop (*see Note 21*).
3. Fragment mRNAs with fragmented buffer (*see Note 14*).
4. Retain an appropriate amount of fragmented RNA samples and labeled as input, the rest is used for immunoprecipitation reaction.

3.4.3 Immunoprecipitation Reaction

1. Prepare immunoprecipitation reaction system as shown in Table 2.
2. Incubate the m^6A antibody conjugated Dynabead in immunoprecipitation buffer in 1.5 mL Eppendorf tube at 4 °C for 2 h.
3. Put the Eppendorf tube on magnetic rack, when the liquid becomes clear, discard the supernatant.
4. Add 500 μL IP buffer into the Eppendorf tube, repeat step 3 twice.
5. Add 100 μL eluting buffer into the Eppendorf tube, blow it gently to make the bead completely suspended, then incubate at 4 °C for 1 h.
6. Put the Eppendorf tube on magnetic rack, when the liquid becomes clear move the supernatant included mRNA fragment into a new 1.5 mL Eppendorf tube.
7. Repeat steps 5 and 6, get 200 μL eluted mRNA supernatant at last.
8. Purify the eluted mRNA samples according to the RNase Mini-Elute Kit protocol guide, got mRNA after immunoprecipitation reaction.

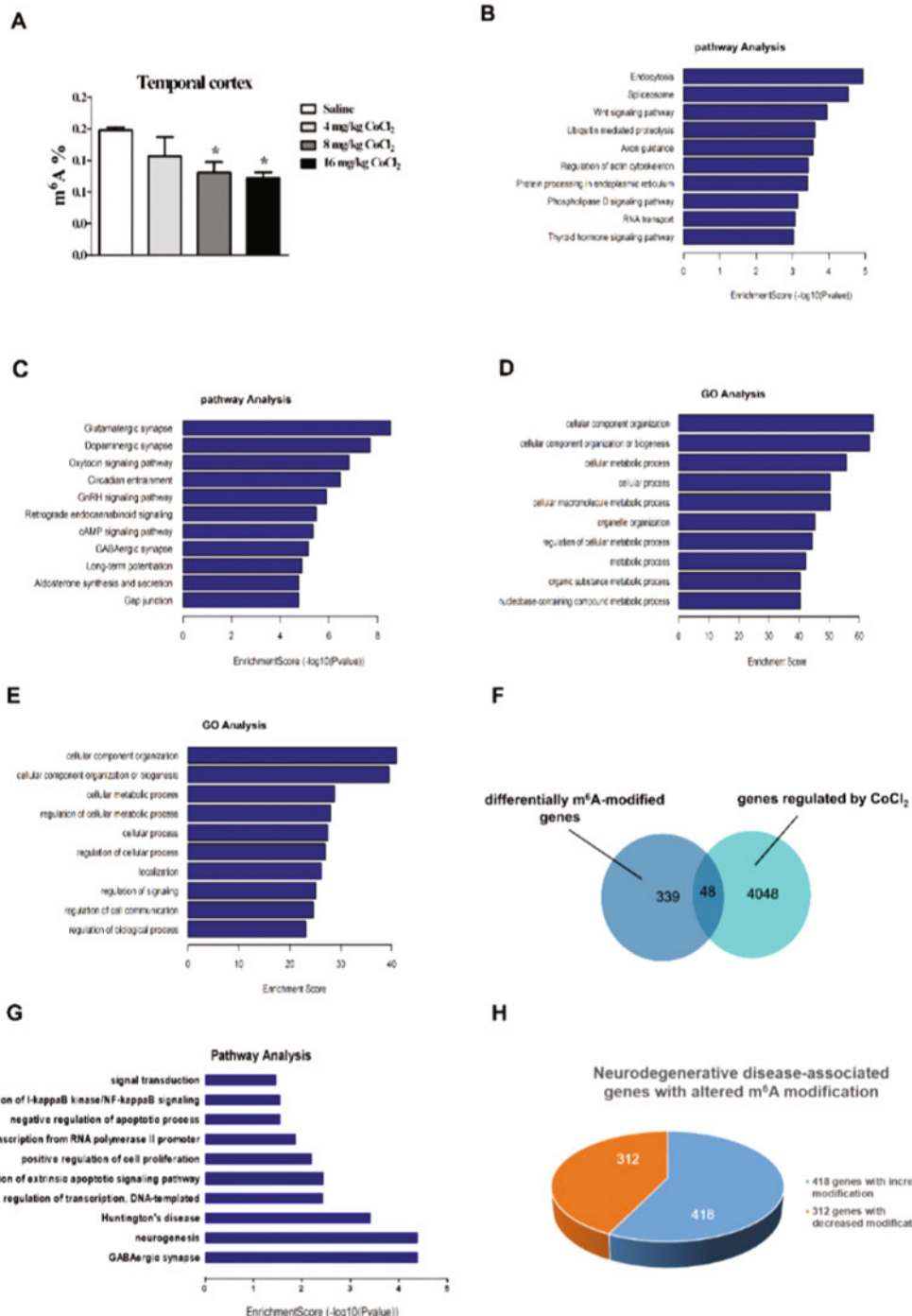


Fig. 1 Analysis of m⁶A methylation modification in C57BL/6 mice brain after CoCl₂ exposure. The level of total m⁶A methylation modification effect by CoCl₂ exposure and the GO analysis, pathway analysis, and cluster analysis of the methylated abnormal genes in the MeRIP-seq results [13]

Table 2
Reagent and volume of immunoprecipitation reaction system

Reagent	Volume (μ L)
Fragmented mRNA	790
RNase inhibitor	10
IP buffer, 5x	200
Total volume	Up to 1000

Table 3
Reagent and volume of anneal reaction mixture

Reagent	Volume (μ L)
mRNA	1 μ g (calculate the volume based on the concentrations)
Primer 0.5 μ g/ μ L	1
dNTPs mix (2.5 mM)	1.5
RNase-free water	calculate the volume based on miRNA volume
Total volume	15

3.4.4 RT-PCR

1. Prepare anneal reaction mixture during cDNA synthesis as shown in Table 3.
2. Anneal reaction condition: water bath at 65 °C for 5 min, ice bath for 2 min.
3. Prepare RT reaction mixture during cDNA synthesis as shown in Table 4.
4. RT reaction condition: water bath at 37 °C for 1 min, at 50 °C for 60 min, 70 °C for 15 min, then ice bath for real-time PCR.
5. Prepare PCR reaction system as shown in Table 5.
6. The reactions are performed in triplicate on a Light Cycler 480 real-time cycler under the following thermal profile: 95 °C for 10 min activation step followed by 40 cycles: denaturation at 95 °C for 15 s, annealing and extension at 60 °C for 1 min.

3.4.5 Data Analysis

The C_t values of each gene and reference gene are exported. The expression of each gene is calculated by using ΔC_t method. Calculation formula: % Input = $2^{\frac{Ct(\text{Input}) - Ct(\text{MeRIP})}{\text{Fd}}} \times 100\%$, Fd is the input dilution factor.

Table 4
Reagent and volume of RT reaction mixture

Reagent	Volume (μL)
mRNA	1
Primer 0.5 $\mu\text{g}/\mu\text{L}$	1
dNTPs mix(2.5 mM)	1.5
RNase-free water	11.5
Total volume	Up to 15

Table 5
Reagent and volume of PCR reaction system

Reagent	Volume (μL)
qPCR SYBR green master mix (2 \times)	5
Forward primer	0.5
Reverse primer	0.5
cDNA	2
RNase-free water	2
Total volume	10

3.5

Non-coding RNAs

1. Extract total RNAs using TRIzol or other phenol-based methods and pre-treat RNAs with DNase I (RNase-free) (TAKARA).
2. The quantitation of RNAs is determined by measuring the absorbance at 230 nm, 260 nm, and 280 nm using a Nano-Drop 2000. Determine the A_{260}/A_{280} 1.8–2.2 and the A_{260}/A_{230} ratio 2.0–2.2.
3. Prepare stem-loop primer for target genes (take miR-17-5p for example) listed in Table 6 (see Note 22).
4. Prepare one RT Mix for all reactions according to Table 7 (typically one reaction per sample). Mix well by gently pipetting up and down and distribute the RT Mix in separate reaction tubes.
5. Mix the RNA sample by gently pipetting up and down to homogenize the RNA solution and add the RNA sample (1 μg) to each RT tube. Mix gently and centrifuge samples at $1200 \times g$ for 3–5 s.
6. Run the RT reactions on the thermal cycler with temperature cycling conditions as follows: incubation at 16 °C for 30 min, at 37 °C for 30 min, at 85 °C for 5 min, followed by maintenance at –4 °C.

Table 6
Primer sequences used for amplification

miRNA	Primer	Primer Sequence (5'-3')
Mmu-miR-17-5p	Stem-loop	GTCGTATCCAGTGCAGGGTCCGAGGTA TTCGCACTGGATACGACCTACCT
	Forward	GCGGCAGCAAAGTGCTTACAGTG
	Reverse	ATCCAGTGCAGGGTCCGAGG

Table 7
Reverse Transcription (RT) Reaction

Reagent	Volume (μ L)
2 \times miRNA L-RT solution mix	10
miRNA L-RT enzyme mix	1.5
Total RNA/micro RNA	1 μ g/200 ng
Stem-loop primer (10 μ M)	1
RNase-free water	Up to 20

Table 8
Sample qPCR Reaction

Reagent	Volume (μ L)
2 \times miRNA qPCR master mix	10
Forward primer, 10 μ M	0.5
Reverse primer, 10 μ M	0.5
cDNA	2.0
ROX reference dye(L)/(H)	1
RNase-free water	6
Total	20

7. Prepare PCR reaction mixture for all samples and reference gene U6 (*see Note 23*) to be measured as shown in Tables 8 and 9 (*see Note 24*). A negative control without template should be included.
8. The PCR is conducted at 95 °C for 10 min, followed by 40 cycles of 95 °C for 5 s and 60 °C for 30 s in the Light cycler 480 Real-Time PCR System.

Table 9
U6 qPCR Reaction

Reagent	Volume (μ L)
2 \times miRNA qPCR master mix	10
U6 forward Primer (10 μ M)	0.5
U6 reverse Primer (10 μ M)	0.5
cDNA	2.0
ROX reference dye(L)/(H)	1
RNase-free water	6
Total	20

3.6 Histone Modification

9. Export raw C_t data according to the standard curves constructed by the Light Cycler software.
10. The delta C_t (ΔC_t) values in each sample are represented the relative expression amount of miRNA: $\Delta C_t = C_t(\text{miRNA}) - C_t(\text{U6})$. The fold expression changes between groups are determined using the $\Delta\Delta C_t$ method ($2^{-\Delta\Delta C_t}$).
1. Extract nuclear and cytoplasmic proteins with nuclear and cytoplasmic extraction reagents kits (Pierce) according to the manufacturer's protocol (*see Note 25*).
2. Protein concentrations are determined using BCA protein assay kit on a SpectraMax M3 plate-reader.
3. Dilute equal amounts of proteins in 5 \times SDS loading buffer and heat the samples at 100 °C for 5 min (*see Note 26*).
4. Separate nuclear extract or histones using 15% of sodium dodecyl sulfate-polyacrylamide gel electrophoresis (SDS-PAGE) according to standard procedure.
5. Transfer proteins onto PVDF membranes at 100 V for 0.5 h using 1 \times transfer buffer (*see Note 27*).
6. Block the nonspecific protein on the membrane in TBST with 5% nonfat dry milk for 1 h at room temperature.
7. Add the primary antibodies in TBST with 5% nonfat dry milk (*see Note 28*) and incubate the membrane overnight at 4 °C and rotation.
8. Wash the membrane with TBST on a shaker with at 40–50 rpm for 3 \times 10 min.
9. Incubate the membrane with secondary antibody conjugated to HRP at a concentration of 1:10000 in TBST and rotation at room temperature for 1 h.

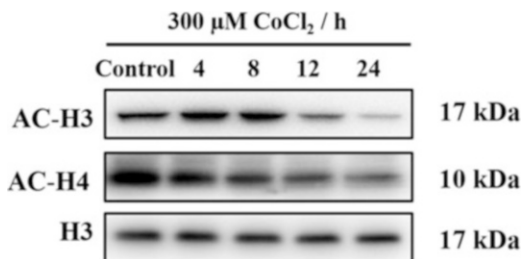


Fig. 2 CoCl₂ exposure reduced the acetylation of histone H3 and H4 in SHSY5Y cells. SHSY5Y cells were cultured with 300 μM CoCl₂ for 4, 8, 12, and 24 h. The Western Blot shows a decrease in acetylation following treatment with CoCl₂. H3 served as the loading control

10. Wash the membrane in TBST on a shaker for three times, 10 min each time, and once for 10 min in 1 × TBS.
11. The acetyl-histone 3 protein bands are visualized by enhanced chemiluminescence detection reagents with an instrument that detects luminescence (*see Notes 29 and 30*).
12. Analyze the optical density of bands using Image J software (Fig. 2).

4 Notes

1. All solutions, consumables, and glassware should be RNase and DNase free. All pipetting should be performed using sterile RNase/DNase-free low retention filtered tips.
2. The anti-m⁶A antibody is coupled to the Dynabeads at a ratio of 5–10 μg of anti-m⁶A antibody per 1 mg of Dynabeads as suggested by the manufacturer. In the experiment, the amount of Dynabeads and antibody to be coupled should be adjusted accordingly following the manufacturer's recommendations.
3. Dissolve in a water bath at 50 °C, filter with 0.22 μm membrane. If precipitation occurs, it can be used after melted (water bath).
4. Care should be taken to add SDS solution last, since it makes bubbles.
5. Disulfate conversion is of great importance in this step. The conversion rate directly affects the test results. Therefore, the requirement tester should constantly explore the appropriate test conditions in the test process to ensure a high conversion rate.
6. DNA should be used immediately for subsequent testing or storage at –20 °C.

7. Primer/probe design is of major importance for the specificity of the reaction. The designed primers not only require theoretical analysis verification (software), but also require experimental verification and selection. Therefore, an intention gene sometimes needs to plan several pairs of different primers for selection.
8. The number of cells should be $\geq 10^5$, and the tissues should be ≥ 50 mg.
9. The primer concentration is an important determinant of analytical sensitivity/specificity and has to be ascertained experimentally. In other words, the analytical sensitivity threshold is set to the dilution that has an overlapping 95% confidence.
10. Sample DNA modified with hydrogen sulfite, EpiTect Control DNA, and methylated positive reference was used as template, human ACTB gene was used as internal reference gene to standardize the amount of target DNA.
11. Cells 10^8 or 50–100 mg tissue is needed.
12. A minimum of 300 μg of total RNAs is required for profiling.
13. 400 μg total RNAs yield approximately 10 μg mRNA.
14. Fragmentation buffer: 10 mM ZnCl₂, 10 mM Tris-HCl pH 7.0.
15. Stop Buffer: 0.5 M EDTA.
16. Individual users might need to optimize the fragmentation conditions based on their samples.
17. The m⁶A negative fragments not captured by the anti-m⁶A antibody are discarded.
18. TET buffer: 10 mM Tris-HCl pH 8.0, 1 mM EDTA pH 8.0, 0.05% Tween-20; add RNA inhibitor at the manufacturer's recommended concentration.
19. According to the official SRMAP description, "High Confidence" is the most reliable prediction result in the prediction site.
20. For one dot blot assay, we recommend purifying at least 20 μg of total RNAs.
21. Make a serial dilution of mRNA to 50 ng/ μL , 10 ng/ μL , and 2 ng/ μL using RNase-free water.
22. There are two methods to measure expression of mature miRNA expression levels using qRT-PCR. The first method (TaqMan) utilizes stem-loop reverse transcription primers to produce cDNA of specific miRNAs. The second method (SYBR) uses a modified oligo (dT) primer to reverse transcribe all transcripts within an RNA sample, then using a PCR primer specific to the miRNA of interest and a primer specific to the tag. It can be difficult to quantitate the small miRNA fragments

by qRT-PCR due to their small length and sequence similarity. Therefore, it is important to design specific primers to distinguish each type of miRNA and its isoforms. Since the stem-loop primer system are better than the oligo(dT) method in terms of RT efficiency and specificity, the protocol described here will focus on the stem-loop qRT-PCR method.

23. Using the U6 small nuclear RNA for normalization (U6 small nuclear RNA was the most common internal control for the quantification of miRNAs expression).
24. Firstly, mix gently by pipetting up and down and distribute the qPCR mix in a 96-well qPCR plate. Then mix the diluted RT sample by gently pipetting up and down and add 2 µL of the product to the qPCR mix. For each qRT-PCR, reactions are usually done in triplicate to reduce effects from technical variability.
25. The samples are always kept cold (<4 °C). The samples were always kept cold (<4 °C). It is essential to add protease inhibitor cocktail to the lysis buffer to increase the protein concentration.
26. Briefly spin down the samples by centrifugation. Maintain the tubes at room temperature until loading the gel.
27. Activate the PVDF membrane with 100% methanol for 15 s before immersing in 1× transfer buffer for at least 10 min. Ensure that bubbles are completely eliminated by rolling over the membrane with a roller. Make sure that the blotting sandwich is always immersed in the transfer buffer.
28. Mark the membrane with a triangle notch (or other shapes) at one corner for identification of the membrane if you have two or more membranes.
29. Perform all the subsequent steps in the dark room.
30. As the detection of histone modification often uses histone H3 (molecular weight similar to the target protein) as an internal control, the Restore™ Western Blot Stripping Buffer can be used after the target protein is exposed. Then repeat **steps 5 to 11** for the detection of histone H3.

Acknowledgements

This work was supported by NSFC grant (81973083 and 22006019), the Joint Funds for the Innovation of Science and Technology, Fujian province (2019Y91010015 and 2017Y9105), and Fujian provincial health technology (2017-1-63). Guangxia Yu and Zhenkun Guo contributed equally to this work.

References

1. Goldberg AD, Allis CD, Bernstein E (2007) Epigenetics: a landscape takes shape. *Cell* 128 (4):635–638. <https://doi.org/10.1016/j.cell.2007.02.006>
2. Holliday R, Pugh JE (1975) DNA modification mechanisms and gene activity during development. *Science* 187(4173):226–232
3. Turner BM (1998) Histone acetylation as an epigenetic determinant of long-term transcriptional competence. *Cell Mol Life Sci* 54 (1):21–31. <https://doi.org/10.1007/s00180050122>
4. Zhang BH, Wang QL, Pan XP (2007) MicroRNAs and their regulatory roles in animals and plants. *J Cell Physiol* 210(2):279–289. <https://doi.org/10.1002/jcp.20869>
5. Yaniv M (2014) Chromatin remodeling: from transcription to cancer. *Cancer Genet* 207 (9):352–357. <https://doi.org/10.1016/j.cancergen.2014.03.006>
6. Schaefer M, Pollex T, Hanna K, Tuorto F, Meusburger M, Helm M, Lyko F (2010) RNA methylation by Dnmt2 protects transfer RNAs against stress-induced cleavage. *Genes Dev* 24(15):1590–1595. <https://doi.org/10.1101/gad.586710>
7. Feil R, Fraga MF (2012) Epigenetics and the environment: emerging patterns and implications. *Nat Rev Genet* 13(2):97–109. <https://doi.org/10.1038/nrg3142>
8. Forster VJ, McDonnell A, Theobald R, McKay JA (2017) Effect of methotrexate/vitamin B (12) on DNA methylation as a potential factor in leukemia treatment-related neurotoxicity. *Epigenomics* 9(9):1205–1218. <https://doi.org/10.2217/epi-2016-0165>
9. Neal M, Richardson JR (2018) Epigenetic regulation of astrocyte function in neuroinflammation and neurodegeneration. *BBA-Mol Basis Dis* 1864(2):432–443. <https://doi.org/10.1016/j.bbadi.2017.11.004>
10. Yang H, Lin Q, Chen N, Luo Z, Zheng C, Li J, Zheng F, Guo Z, Cai P, Wu S, Wang YL, Li H (2020) LncRNA NR_030777 alleviates Paraquat-induced neurotoxicity by regulating Zfp326 and Cpne5. *Toxicol Sci* 178 (1):173–188. <https://doi.org/10.1093/toxsci/kfaa121>
11. Gu C, Wen Y, Wu L, Wang Y, Wu Q, Wang D, Wang Y, Liu Q, Zhang J (2020) Arsenite-induced transgenerational glycometabolism is associated with up-regulation of H3K4me2 via inhibiting spr-5 in *Caenorhabditis elegans*. *Toxicol Lett* 326:11–17. <https://doi.org/10.1016/j.toxlet.2020.03.002>
12. Zhan Y, Guo Z, Zheng F, Zhang Z, Li K, Wang Q, Wang L, Cai Z, Chen N, Wu S, Li H (2020) Reactive oxygen species regulate miR-17-5p expression via DNA methylation in paraquat-induced nerve cell damage. *Environ Toxicol* 35(12):1364–1373. <https://doi.org/10.1002/tox.23001>
13. Tang J, Zheng C, Zheng F, Li Y, Wang YL, Aschner M, Guo Z, Yu G, Wu S, Li H (2020) Global N6-methyladenosine profiling of cobalt-exposed cortex and human neuroblastoma H4 cells presents epitranscriptomics alterations in neurodegenerative disease-associated genes. *Environ Pollut* 266 (Pt 2):115326. <https://doi.org/10.1016/j.envpol.2020.115326>
14. Zhang BH, Pan XP (2009) RDX induces aberrant expression of microRNAs in mouse brain and liver. *Environ Health Perspect* 117 (2):231–240. <https://doi.org/10.1289/ehp.11841>
15. Cai Z, Zheng F, Ding Y, Zhan Y, Gong R, Li J, Aschner M, Zhang Q, Wu S, Li H (2019) Nrf2-regulated miR-380-3p blocks the translation of Sp3 protein and its mediation of paraquat-induced toxicity in mouse neuroblastoma N2a cells. *Toxicol Sci* 171(2):515–529. <https://doi.org/10.1093/toxsci/kfz162>
16. Wang Q, Zhan Y, Ren N, Wang Z, Zhang Q, Wu S, Li H (2018) Paraquat and MPTP alter microRNA expression profiles, and downregulated expression of miR-17-5p contributes to PQ-induced dopaminergic neurodegeneration. *J Appl Toxicol* 38(5):665–677. <https://doi.org/10.1002/jat.3571>
17. Song C, Kanthasamy A, Anantharam V, Sun F, Kanthasamy AG (2010) Environmental neurotoxic pesticide increases histone acetylation to promote apoptosis in dopaminergic neuronal cells: relevance to epigenetic mechanisms of neurodegeneration. *Mol Pharmacol* 77 (4):621–632. <https://doi.org/10.1124/mol.109.062174>
18. Zhang Z, Guo Z, Zhan Y, Li H, Wu S (2017) Role of histone acetylation in activation of nuclear factor erythroid 2-related factor 2/heme oxygenase 1 pathway by manganese chloride. *Toxicol Appl Pharm* 336:94–100. <https://doi.org/10.1016/j.taap.2017.10.011>
19. Guo Z, Zhang Z, Wang Q, Zhang J, Wang L, Zhang Q, Li H, Wu S (2018) Manganese chloride induces histone acetylation changes in neuronal cells: its role in manganese-induced damage. *Neurotoxicology* 65:255–263. <https://doi.org/10.1016/j.neuro.2017.11.003>

20. Liu Z, Mahmood T, Yang P (2014) Western blot: technique, theory and trouble shooting. *N Am J Med Sci* 6(3):160. <https://doi.org/10.4103/1947-2714.128482>
21. Ray PD, Yosim A, Fry RC (2014) Incorporating epigenetic data into the risk assessment process for the toxic metals arsenic, cadmium, chromium, lead, and mercury: strategies and challenges. *Front Genet* 5:201. <https://doi.org/10.3389/fgene.2014.00201>



Chapter 10

The Application of Omics Technologies in the Research of Neurotoxicology

Wenya Shao and Huangyuan Li

Abstract

Omics technologies offer unprecedented perspectives for the systematic research of complex organisms. Especially, the comprehensive omics provide powerful tools for exploring extensive perception of the biochemical and/or physiological effects of the cells perturbed by poisons through systemic investigation on the different spatiotemporal expression profiles of transcriptomic expression profiling, expressed proteins and metabolites simultaneously by high-throughput and high-sensitivity technology. Therefore, it has been attracted extensive attention in neurotoxicology. During the recent years, the domain of neurotoxicology has progressively assimilated various emerging omics applications, which mainly include transcriptomics, proteomics, and metabolomics, to investigate the molecular mechanisms and potential molecular biomarkers of phenotypic modifications of organisms subjected to poisons or stress factors.

Key words Neurotoxicology, Omics technologies, Transcriptomics, Proteomics, Metabolomics, Sample pretreatment

1 Introduction

Transcriptome is the complete set and quantity of transcripts in a cell, tissue, or species for a specific developmental stage or physiological condition which include mRNAs and non-coding RNAs [1]. In neurotoxicology, it aims to elucidate the mechanism of action of exogenous factors (biotic, environmental, etc.) and look for biomarkers through analysis of the effect of exogenous factors on gene expression. Various technologies have been developed to identify the transcriptome, among which RNA sequencing (RNA-Seq) has clear advantages [2]. RNA-Seq can be used to obtain gene expression profiles rapidly and accurately analyze SNP, alternative splicing, epitranscriptome (modification of RNA), etc. at the sequence and structure information. For example, Li et al. [3] reported variation of N⁶-methyladenosine modification of RNAs

in neurodegenerative disease-associated genes upon CoCl₂ exposure by global N⁶-methyladenosine profiling using RNA-seq.

In principle, it is possible to determine the absolute quantity of RNA, and directly compare results between experiments [4] and capture transcriptome dynamics across different tissues or conditions without sophisticated normalization of data sets. Therefore, RNA-Seq will undoubtedly be valuable for study of transcriptome dynamics during physiological changes, and in the analysis of biomedical samples due to that it allows robust comparison between diseased and normal tissues in neurotoxicology study [5, 6].

As the direct performer of vital movement, protein is an important component of all cells in human body. Proteomics, determination of genes and cellular function directly at the protein level in large scale [7], is powerful strategy to efficiently discover and characterize specific disease-related proteins as biomarkers and elucidate the pathogenesis of many diseases [8]. Therefore, it is certainly of great significance to characterize the neuroproteome to recognize the target proteins and the possible mechanisms of action for toxicology and physiology. Previous studies have shown that proteomics could make it possible to probe the pathogenesis of many diseases that affect neural function, such as Alzheimer's disease (AD), Parkinson's disease (PD), and Huntington's disease [9, 10].

Metabolomics is an integral part of systems biology, which aims to the analysis of endogenous metabolite profiles in biological specimens [11], e.g., cells, tissues, and organisms. The metabolome is the set of all small molecules, such as amino acids, sugars, and lipids, in a biological system, which is considered to be an endpoint of biological processes [12]. Therefore, it has also been referred to as the “link between genotype and phenotype” [13]. Minimal changes in gene and protein expression will be amplified on metabolites, which makes detection much easier [14]. As a consequence, metabolites as ideal biomarkers to visible the majority of biological and medical perturbations, are of great interest. At present, metabolomics has been particularly successful in the field of neurotoxicology [15]. Additionally, it mainly focuses on the change of body and the pathophysiologic conditions and the biochemical mechanism result from exogenous factors.

In this chapter, the major process of research methods of RNA-Seq, proteomics, and metabolomics is described, includes sample pretreatment, sample identification or/and quantification and bioinformatics analysis, and highlights the sample preservation and extraction.

2 Materials

The water used in experiments is ultrapure water (prepared by purifying deionized water to attain a resistivity of 18 MΩ cm at 25 °C). All of the reagents are analytical grade and stored at the suitable temperature.

2.1 Transcriptomics

Prepare all solutions using sterilized distilled water and analytical grade reagents that are RNase-free. Use RNase-free consumables and glassware. All pipetting is performed using sterilized RNase-free low retention filtered tips.

The materials used in the following described methods contain (*see Note 1*):

1. PBS solution: NaCl (8.0 g), KCl (0.2 g), $\text{Na}_2\text{HPO}_4 \cdot 12\text{H}_2\text{O}$ (3.14 g), and KH_2PO_4 (0.2 g) dissolved in 1000 mL H_2O (RNase-free) and adjusted pH to 7.18 by H_3PO_4 .
2. 70% (v/v) and 100% ice-cold ethanol, 3 M sodium acetate, 10 mg/mL glycogen, 98% formic acid (e.g., Fluka, Germany), HPLC-grade ammonium acetate (e.g., Tedia, USA), MCE SYBR Green qPCR Master Mix, etc.

2.2 Proteomics

The materials used in the following described methods contain (*see Note 2*):

1. PBS solution: NaCl (8.0 g), KCl (0.2 g), $\text{Na}_2\text{HPO}_4 \cdot 12\text{H}_2\text{O}$ (3.14 g), and KH_2PO_4 (0.2 g) dissolved in 1000 mL H_2O and adjusted pH to 7.18 by H_3PO_4 .
2. UA: 8 M urea (e.g., Sigma-Aldrich) in 50 mM NH_4HCO_3 buffer (pH 8.0).
3. BCA assay kit (e.g., Shang-hai, China).
4. DTT solution: 1 M dithiothreitol (e.g., Sigma-Aldrich) in 50 mM NH_4HCO_3 buffer.
5. IAA solution: 2 M iodoacetamide (e.g., Sigma-Aldrich) in 50 mM NH_4HCO_3 buffer.
6. Trypsin solution: 1 mg trypsin (bovine pancreas, TPCK treated, e.g., Sigma-Aldrich) in 50 mM NH_4HCO_3 buffer.

2.3 Metabolomics

The materials used in the following described methods contain:

1. PBS solution: NaCl (8.0 g), KCl (0.2 g), $\text{Na}_2\text{HPO}_4 \cdot 12\text{H}_2\text{O}$ (3.14 g), and KH_2PO_4 (0.2 g) dissolved in 1000 mL H_2O and adjusted pH to 7.18 by H_3PO_4 .
2. HPLC-grade methanol (e.g., Merck, Germany), 98% formic acid (e.g., Fluka, Germany), HPLC-grade ammonium acetate (e.g., Tedia, USA).

3. Isotope internal standards: e.g., L-alanine-3,3,3-d₃ (Aldrich, USA), succinic acid-¹³C₄ (Aldrich, USA), and cholic acid-2,2,4,4-d₄, (Aldrich, USA).

3 Methods

3.1 Transcriptomics

3.1.1 Sample Pretreatment

Tissue samples:

1. Prior to be used, RNase-free tube is pre-cooled in -80 °C freezer (*see Note 3*).
2. Tissue piece is taken from living body rapidly and cut into small pieces (bean-size).
3. Washed by ice-cold PBS to get rid of residual blood and pollution, and dip in dry.
4. Collected by the pre-cooled tube and quick-freeze by liquid nitrogen (*see Note 4*).
5. Store at -80 °C before usage.

Cells:

- (a) Cells with nearly 90% confluence are harvested and washed with cold PBS for three times.
- (b) Add TRIzol and dispersed to lyse sufficiently.
- (c) Transfer the sample into tube stored at -80 °C before usage.

Exosomes:

Suspend in 100 µL PBS and store at -80 °C before usage.

3.1.2 Total RNA Extraction and Quality Control

1. RNA extraction.

- (a) Add 200 µL of chloroform to each sample and mix well by vortexing for 60 s.
- (b) Centrifuge the mixture for 15 min at 12,000 × g at 4 °C.
- (c) Remove the aqueous phase, and transfer the sample to a separate tube containing 500 µL of isopropanol, gently mix and centrifuge for 10 min at 12,000 × g at 4 °C.
- (d) Collect the RNA pellets to resuspend in 1 mL of 75% ethanol, mix well by vortexing and centrifuge for 5 min at 7500 × g at 4 °C.
- (e) Discard all the supernatants, RNAs are transferred to a miRNeasy mini kit column, and further purification steps are conducted according to the manufacturer's instructions.
- (f) Remove DNA residues by on-column DNase treatment step.

- (g) Assess RNA quantity and quality (e.g., using a Nano-Drop™ 1000 spectrophotometer and on an Agilent 2100 Bioanalyzer using an RNA 6000 Nano LabChip kit). All samples display a OD260/OD280 ratio greater than 2.0 and RNA integrity numbers (RIN) greater than 7.5.

2. Library Construction.

- (a) Remove rRNAs from total RNAs using Ribo-Zero rRNA Removal Kits (Illumina, USA) following the manufacturer's manual instruction.
- (b) Construct RNA libraries by using rRNA-depleted RNAs by TruSeq Stranded Total RNA Library Prep Kit (Illumina, USA) by following the manufacturer's protocol.
- (c) Libraries are assessed in quality and quantify on an BioAnalyzer 2100 system.

3.1.3 Illumina HiSeq Sequencing and Bioinformatics Analysis

1. According to the manufacturer's protocol, single-stranded DNA molecules are synthesized from libraries.
2. Capture on Illumina flowcells and amplify as clusters *in situ*.
3. Sequence the library with an Illumina HiSeq sequencer.
4. Analyze the results with relative bioinformatics methods according to your purpose.

3.2 Proteomics

3.2.1 Protein Extraction (See Note 5)

1. Tissue sample, e.g., rat brain tissue, is cut into small pieces, and try your best to get rid of blood vessel.
2. Then wash by ice-cold PBS for three times.
3. Finally ground to powder in liquid nitrogen.
4. The powder is suspended in the extraction buffer (4–20 mL per gram) composed of UA and 1% (v/v) protease inhibitor cocktail.
5. For cells sample, directly suspend with UV containing 1% cocktail (v/v), e.g., bv2 cells (10^7) are suspended with 1–2 mL UA containing 1% cocktail (v/v).
6. Sonicate in an ice ultrasonic bath for 150 s in total (10 s intervals every 5 s) to extract proteins.
7. The solution is then centrifuged at $25,000 \times g$ for 20–40 min at 20 °C. The resulting supernatants containing the total proteins are collected.
8. Take 50 µL of the obtained supernatants to determine the protein concentration by BCA assay, and the rest is stored at –80 °C before usage.

3.2.2 Sample Pretreatment

“Top down” and “bottom up” approaches are main methods for proteomic analysis, among which “bottom up” is widely used as its technology is developed and data analysis is simple. In “bottom up” strategy, the digestion of protein into peptide is necessary.

1. The obtained protein extracts are reduced by DTT at 56 °C for 1.5 h. The ratio of DTT-to-protein is 8 µL DTT (1 mol/L) to 1 mg protein.
2. Then alkylated by IAA for 40 min at room temperature in the dark. The ratio of IAA-to-protein is 8 µL IAA (2 mol/L) to 1 mg protein.
3. The solution is diluted ten-fold with 50 mM NH₄HCO₃ buffer (pH 8.0) and digest with trypsin (enzyme/protein ratio of 1:30, w/w) at 37 °C for 18–24 h.
4. The obtained tryptic digested peptides are desalted by C18 precolumn, then lyophilize and store at –20 °C before usage.

Usually, quantitative analysis of proteins is necessary for finding biomarker or elucidating the pathogenesis of diseases. Proteome quantification methods based on LC-MS/MS mainly are labeling quantitation and label-free quantitative technique. For labeling quantitation technique, you can label in proteins or peptides.

If you focused on protein post-translational modifications, e.g., protein glycosylation, the selective enrichment of glycopeptides is indispensable for MS identification. A variety of enrichment methods have been developed, among which boronic acid [16], hydrophilic interaction chromatography (HILIC) [17], lectin affinity, and hydrazide chemistry [18] are widely used.

3.2.3 Protein Identification and Data Analysis

1. A nano-RPLC-ESI-MS/MS system, e.g., integrated with Ultimate™ 3000 RSLCnano HPLC and Orbitrap Fusion™ Lumos™ MS (Thermo Fisher Scientific, USA) is used to profile the proteome.
2. The lyophilized sample is dissolved in 0.1% formic acid (FA) solution, and 0.1–1 mg peptide is loaded onto C18 capillary separation column.
3. C18 capillary separation (e.g., 150 µm i.d., 13 cm length), C18-AQ particle (e.g., 1.9 µm, Dr.Maisch, Ammerbuch-Entringen, Germany).
4. Mobile phase A: 2% (v/v) ACN containing 0.1% (v/v) FA, mobile phase B: 80% (v/v) ACN containing 0.1% (v/v) FA.
5. Flow rate: 600 nL/min.
6. Separation gradient: 9% B (0 min)–25% B (30 min)–50% B (71 min)–95% B (72 min)–95% B (87 min).

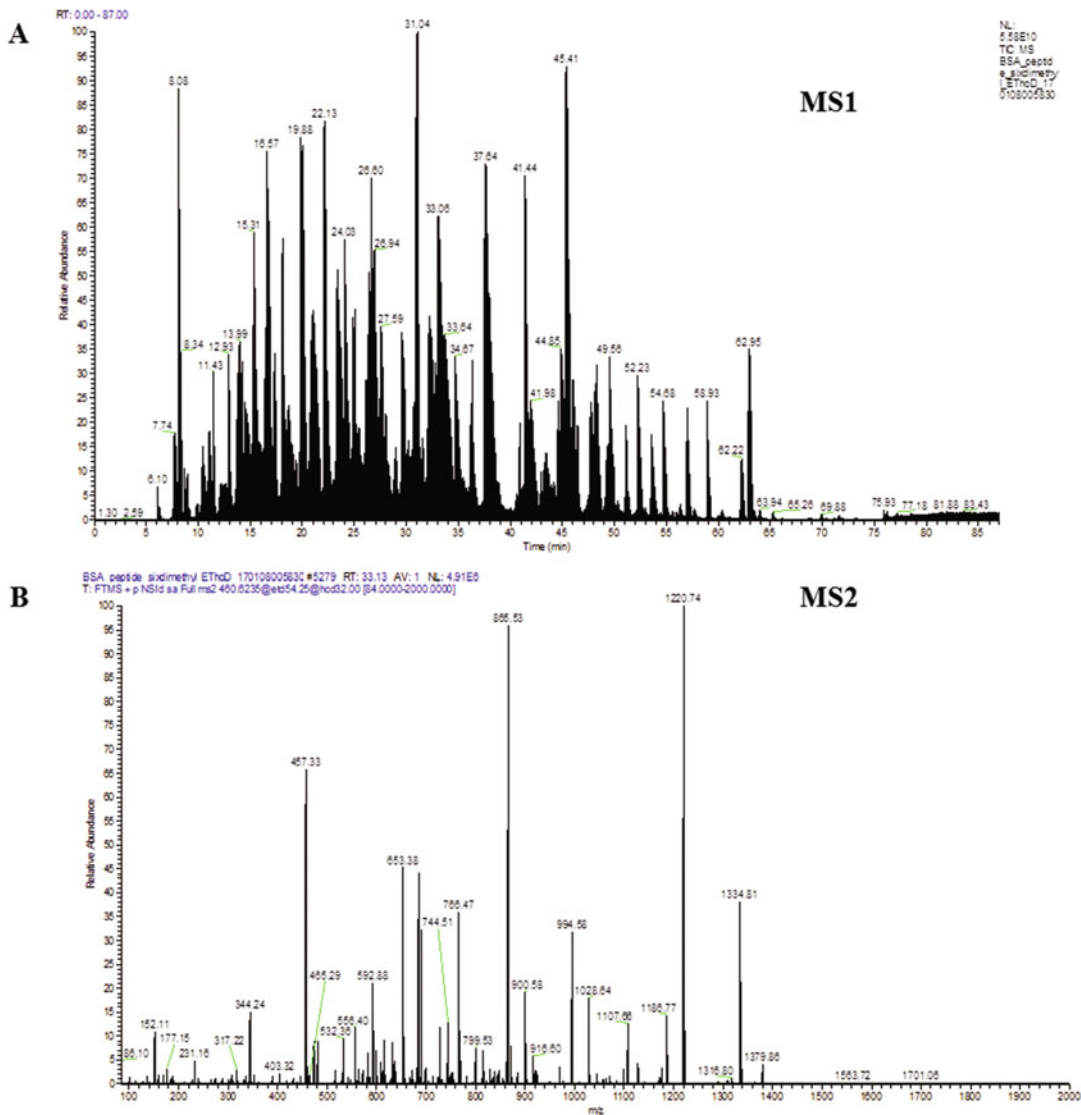


Fig. 1 Spectrogram of MS. (a) MS1. (b) MS2. Orbitrap Fusion™ Lumos™ mass spectra of bovine serum albumin digests labeled by pseudo-isobaric dimethyl in peptides

7. For MS1 orbitrap analysis, detector type: orbitrap, orbitrap resolution: 60000, scan range: 400–2000 m/z , RF lens: 30%, AGC target: 4.0 e^5 , Maximum injection time: 50 ms, exclusion duration: 20 s, mass tolerance: ppm, low: 10, intensity threshold: 2.0 e^4 . For MS2, isolation mode: quadrupole, window: 1.6, activation type: HCD, detector type: orbitrap, scan range: 50–2000.

8. The *.raw files which contain information of MS1 and MS2 (Fig. 1) produced on MS are searched against the proteome sequence database. The parameters are as follows: enzyme,

trypsin; missed cleavages, two; fixed modifications, carboxymidomethylation (C); variable modifications, oxidation (M) and deamidation (N); peptide tolerance, 7 ppm; MS/MS tolerance, 20 mmu; target FDR (Stric), 0.01; target FDR (Relaxed), 0.05.

9. At last, you can analyze them with relative bioinformatics methods, find the interested proteins or something else according to your requirement.

3.3 Metabolomics

3.3.1 Sample Pretreatment

Sample pretreatment is a crucial part of metabolomics study as it has a major effect on the metabolite coverage and the quality of the results obtained. Samples used in metabolomics mainly contain cells, tissues, biofluids (urine, blood plasma, and cerebrospinal fluid), feces, and so on.

1. Minimum amount of samples: cells (10^7), microorganism (10^8), tissues (20 mg), blood plasma (100 μ L), urine (1 mL), cerebrospinal fluid (200 μ L), and saliva (200 μ L).
2. Biological duplication (minimum number of samples): microorganism (8), model animal (10), and clinical sample (30).
3. Sample collection and preparation:

Tissue samples:

- (a) Tissue sample is washed by ice-cold PBS for three times to get rid of residual blood and pollution.
- (b) Remove fat and connective tissue rapidly.
- (c) Cut into small pieces, and store in labeled tubes.
- (d) Quench with liquid nitrogen rapidly for 1 min.
- (e) Store at -80°C before usage.

Cells:

- (a) Cells with nearly 90% confluence are harvested and wash with cold PBS for three times.
- (b) Add 500 μ L cold methanol/water (4/1, v/v) to petri dish and transfer cells into tube.
- (c) Then rinse the petri dish by 500 μ L cold methanol/water (4/1, v/v) and transfer into a new tube.
- (d) Cell pellet is collected by centrifugation ($1000 \times g$, 10 min).
- (e) Quench with liquid nitrogen and store at -80°C before usage.

Biofluids:

- (a) Blood plasma is centrifuged at $2000 \times g$ for 10 min at 4°C . The resulting supernatants are collected and package into 100 μ L in each tube. Store at -80°C before usage.
- (b) Urine, cerebrospinal fluid, and saliva are centrifuged at $10,000 \times g$ for 10 min at 4°C . The resulting supernatants are collected and stored at -80°C before usage.

4. Metabolites extraction: For cell and tissue samples, the first step is homogenization without degradation of metabolites. Several approaches can be used for sample homogenization, such as the manual disaggregation of cold tissue with scissors or a manual homogenizer, disruption using a bead homogenizer and a cryogenicall cooled pestle and mortar on frozen tissue and sonicated in an ice ultrasonic bath for cells. The most commonly used solvents for sample extraction are areacetonitrile (ACN), methanol (MeOH), isopropanol (IPA), chloroform (CHCl_3), methanol (MeOH), or a mixed solution of them. According to the polarity of metabolites, the right solution should be chosen.
5. Protein removal: The commonly used methods for protein removal is organic solvent-based protein precipitation (PPT) followed by centrifugation and/or membrane-based techniques, such as ultrafiltration in metabolomics.
 - (a) For tissue sample, e.g., hepatic tissue (20 mg), add 1 mL CHCl_3 , and sonicate in an ice ultrasonic bath for 4 min.
 - (b) Add 250 μL water and mix at $600 \times g$ in a thermo-mixer for 1 min, then incubate without mixing for 10 min.
 - (c) Transfer the supernatants to 5-kDa millipore (e.g., Millipore, USA), centrifuge the filter units at $13,000 \times g$ for 3 min at 4°C .
 - (d) Collect the precipitation and store at -80°C before usage.

For sample pretreatment, the analytical requirements for untargeted and targeted metabolomics studies are quite different. For untargeted metabolomics studies, the biological sample should preferably be analyzed with minimal pretreatment to prevent the potential loss of metabolites. For targeted metabolomics studies, sample pretreatment includes protein removal, often followed by liquid-liquid extraction (LLE) and/or off-line/online solid phase extraction (SPE) for the selective isolation and enrichment of the target compounds, and removal of interfering matrix components.

3.3.2 Metabolites Separation and Analysis

Main technologies used for metabolites separation and analysis are gas chromatography-mass spectrometry (GC-MS), liquid chromatography-mass spectrometry (LC-MS), capillary electrophoresis (CE-MS), nuclear magnetic resonance (NMR), and LC-NMR-MS in metabolomics.

1. GC-MS is very developed which had many standard database, and often used for qualitative analysis of volatile metabolites after derivatization.

2. LC-MS is the most widely used approach now. It has high sensitivity, wide dynamic range and does not need derivatization and can be used for polar and nonpolar metabolites. According to the analytes, RPLC-MS (reverse chromatography, RP), HILIC-MS (hydrophilic interaction chromatography, HILIC), and so on can be used.

3.3.3 Data Analysis and Study of Regulated/Diagnostic Functions

1. The data pre-processing mainly contains signal filter, peak extraction, peak matching, and data correction. Then qualitative and quantitative information (accurate mass, migration time, and peak area) of samples are obtained. In this process, Prognosis QI (Waters), Compound Discover (Thermo), MassHunter (Agilent), and Profile Analysis (Bruker) are often used.
2. Principal component analysis (PCA) model (Fig. 2), partial least squares discriminant analysis (PLS-DA) model, and hierarchical cluster analysis (HCA) model are often used for differential metabolites screens.
3. Online metabolomics databases for differential metabolites screens and identification: HMDB (human metabolites), Metlin (general), MassBank (general), LIPID MAPS (lipid classes), and so on.
4. Metabolic pathways and enrichment of functions can be conducted by some online resource, e.g., KEGG, HMDB, SMPDB, PMN, Metaboanalyst.

4 Notes

1. All solutions are prepared by RNase-free water and it is better to freshly prepare and use the solution within a day.
2. UA, DTT, and IAA solutions must be freshly prepared and used within a day.
3. Please add enough RNA later and keep the tube at 4 °C overnight if liquid nitrogen could not be obtained, then store at –80 °C before usage.
4. Dry ice or cryogenic refrigerator cooling down is slower, which cannot inhibit RNase. So quick-freeze in liquid nitrogen as far as you can is necessary.
5. Carry out all procedures on ice or 4 °C temperature unless otherwise specified and as quickly as possible.

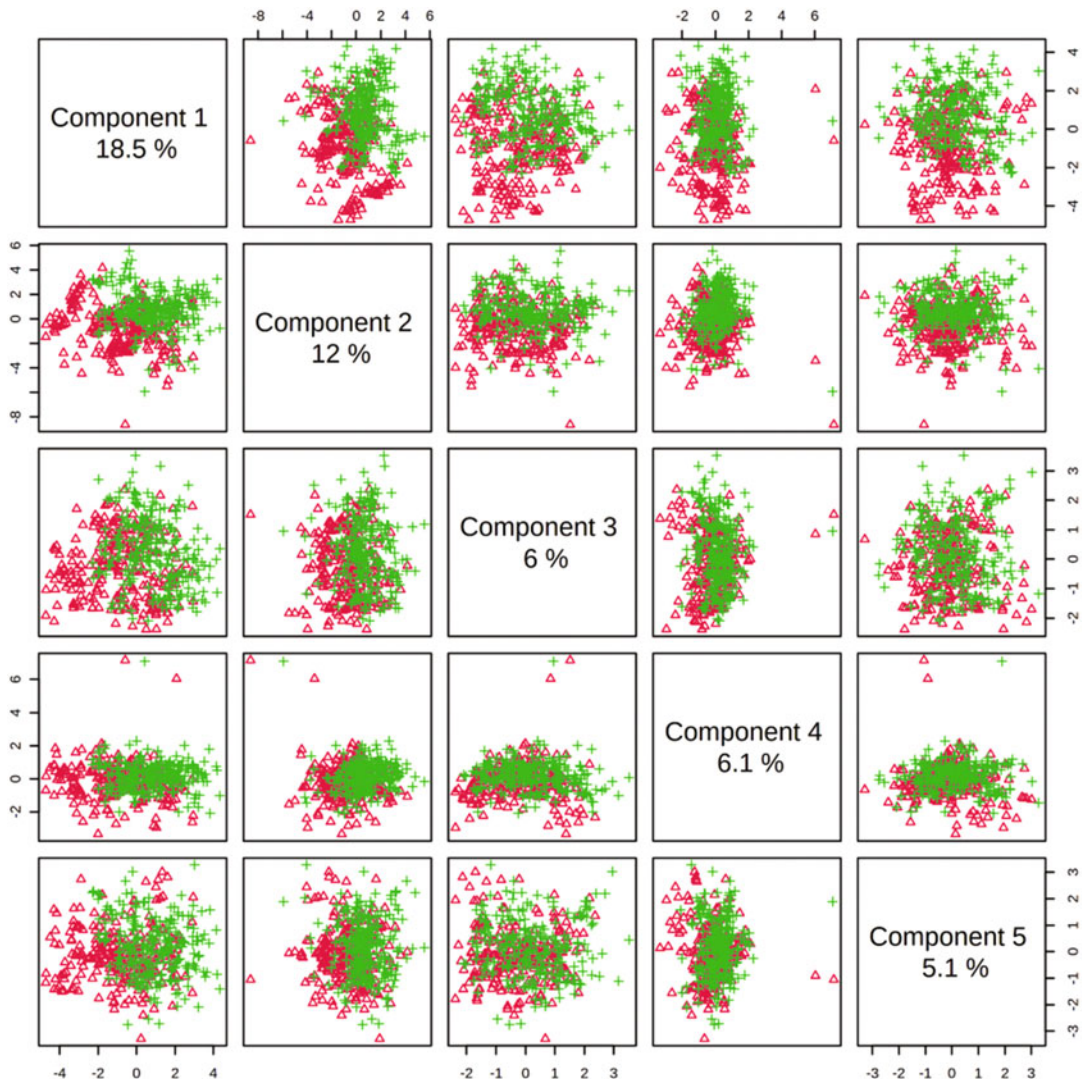


Fig. 2 Pairwise score plots between the selected PCs. The explained variance of each PC is shown in the corresponding diagonal cell (modified from [19])

References

1. Wang Z, Gerstein M, Snyder M (2009) RNA-Seq: a revolutionary tool for transcriptomics. *Nat Rev Genet* 10(1):57–63. <https://doi.org/10.1038/nrg2484>
2. Curtis C, Shah SP, Chin SF, Turashvili G, Rueda OM, Dunning MJ et al (2012) The genomic and transcriptomic architecture of 2,000 breast tumours reveals novel subgroups. *Nature* 486(7403):346–352. <https://doi.org/10.1038/nature10983>
3. Tang J, Zheng C, Zheng F, Li Y, Wang YL, Aschner M, Guo Z, Yu G, Wu S, Li H (2020) Global N6-methyladenosine profiling of cobalt-exposed cortex and human neuroblastoma H4 cells presents epitranscriptomics alterations in neurodegenerative disease-associated genes. *Environ Pollut* 266 (Pt 2):115326. <https://doi.org/10.1016/j.envpol.2020.115326>
4. Wang Q, Zhan Y, Ren N, Wang Z, Zhang Q, Wu S, Li H (2018) Paraquat and MPTP alter microRNA expression profiles, and downregulated expression of miR-17-5p contributes to PQ-induced dopaminergic

- neurodegeneration. *J Appl Toxicol* 38(5):665–677. <https://doi.org/10.1002/jat.3571>
5. Tang J, Zheng C, Zheng F, Li Y, Wang Y, Aschner M et al (2020) Global N6-methyladenosine profiling of cobalt-exposed cortex and human neuroblastoma H4 cells presents epitranscriptomics alterations in neurodegenerative disease-associated genes. *Environ Pollut* 266:115326. <https://doi.org/10.1016/j.envpol.2020.115326>
 6. Michalovicz LT, Kelly KA, Vashishtha S, Ben-Hamo R, Efroni S, Miller JV et al (2019) Astrocyte-specific transcriptome analysis using the ALDH1L1 bacTRAP mouse reveals novel biomarkers of astrogliosis in response to neurotoxicity. *J Neurochem* 150(4):420–440. <https://doi.org/10.1111/jnc.14800>
 7. Hasin Y, Seldin M, Lusis A (2017) Multi-omics approaches to disease. *Genome Biol* 18:83. <https://doi.org/10.1186/s13059-017-1215-1>
 8. Srivastava A, Creek DJ (2019) Discovery and validation of clinical biomarkers of cancer: a review combining metabolomics and proteomics. *Proteomics* 19(10):e1700448. <https://doi.org/10.1002/pmic.201700448>
 9. Keren-Shaul H, Spinrad A, Weiner A, Matcovitch-Natan O, Dvir-Szternfeld R, Ulland TK et al (2017) A unique microglia type associated with restricting development of Alzheimer's disease. *Cell* 169(7):1276. <https://doi.org/10.1016/j.cell.2017.05.018>
 10. Selkoe DJ, Hardy J (2016) The amyloid hypothesis of Alzheimer's disease at 25 years. *EMBO Mol Med* 8(6):595–608. <https://doi.org/10.15252/emmm.201606210>
 11. Johnson CH, Ivanisevic J, Siuzdak G (2016) Metabolomics: beyond biomarkers and towards mechanisms. *Nat Rev Mol Cell Biol* 17(7):451–459. <https://doi.org/10.1038/nrm.2016.25>
 12. Schmidt C (2004) Metabolomics takes its place as latest up-and-coming "omic" science. *J Natl Cancer Inst* 96(10):732–734. <https://doi.org/10.1093/jnci/96.10.732>
 13. Franceschi C, Garagnani P, Parini P, Giuliani C, Santoro A (2018) Inflammaging: a new immune-metabolic viewpoint for age-related diseases. *Nat Rev Endocrinol* 14(10):576–590. <https://doi.org/10.1038/s41574-018-0059-4>
 14. Cryan JF, O'Riordan KJ, Sandhu K, Peterson V, Dinan TG (2020) The gut microbiome in neurological disorders. *Lancet Neurol* 19(2):179–194. [https://doi.org/10.1016/s1474-4422\(19\)30356-4](https://doi.org/10.1016/s1474-4422(19)30356-4)
 15. Ulland TK, Song WM, Huang SCC, Ulrich JD, Sergushichev A, Beatty WL et al (2017) TREM2 maintains microglial metabolic fitness in Alzheimer's disease. *Cell* 170(4):649. <https://doi.org/10.1016/j.cell.2017.07.023>
 16. Liu J, Yang K, Shao W, Li S, Wu Q, Zhang S et al (2016) Synthesis of Zwitterionic Polymer Particles via Combined Distillation Precipitation Polymerization and Click Chemistry for Highly Efficient Enrichment of Glycopeptide. *ACS Appl Mater Interf* 8(34):22018–22024. <https://doi.org/10.1021/acsami.6b06343>
 17. Shao W, Liu J, Yang K, Liang Y, Weng Y, Li S et al (2016) Hydrogen-bond interaction assisted branched copolymer HILIC material for separation and N-glycopeptides enrichment. *Talanta* 158:361–367. <https://doi.org/10.1016/j.talanta.2016.05.034>
 18. Liu J, Yang K, Shao W, Qu Y, Li S, Wu Q et al (2016) Boronic acid-functionalized particles with flexible three-dimensional polymer branch for highly specific recognition of glycoproteins. *ACS Appl Mater Interf* 8(15):9552–9556. <https://doi.org/10.1021/acsami.6b01829>
 19. Yang S, Lv Y, Wu C, Liu B, Shu Z, Lin Y (2020) Pickled vegetables intake impacts the metabolites for gastric cancer. *Cancer Manag Res* 2020(12):8263–8273. <https://doi.org/10.2147/CMAR.S271277>



Chapter 11

Flow Cytofluorometric Analysis of Molecular Mechanisms of Premature Red Blood Cell Death

Mohammad A. Alfhili and Myon Hee Lee

Abstract

This chapter describes, in detail, the operational principles and experimental design to analyze the premature death of human red blood cells (RBCs; erythrocytes). Necrosis (i.e., hemolysis), eryptosis, and necroptosis are the three types of cell death thus far known to exist in RBCs, and distinctive markers of each are well established. Here, methods based on flow cytometry are presented in an easily reproducible form. Moreover, manipulation of incubation medium to promote or inhibit certain physiological phenomena, along with a step-by-step approach to examine membrane scrambling, cell volume, surface complexity, calcium activity, oxidative stress, and signal transduction pathways are also discussed.

Key words Hemolysis, Eryptosis, Necroptosis, Calcium, Signaling, Flow cytometry

1 Introduction

Red blood cells (RBCs; erythrocytes) are the most common cell type in the human body. The main function of RBCs is the transport of oxygen to various tissues. Although devoid of the central apoptotic machinery; mitochondria and nucleus, recent efforts have identified two forms of programmed cell death in RBCs, namely eryptosis and necroptosis [1]. Eryptosis either contributes to, or is a result of, a wide array of pathological conditions, ranging from diabetes mellitus to malignancy [2]. Necroptosis has also been shown to be elicited by toxins of certain microorganisms [3].

Premature RBC death results in augmented disposal of damaged RBCs from the circulation, predisposing individuals to anemia and associated disease [4]. Of interest, a number of environmental toxicants have been identified as modulators of RBC longevity, including triclosan [5], bisphenols [6], and flame retardants [7] (Fig. 1a).

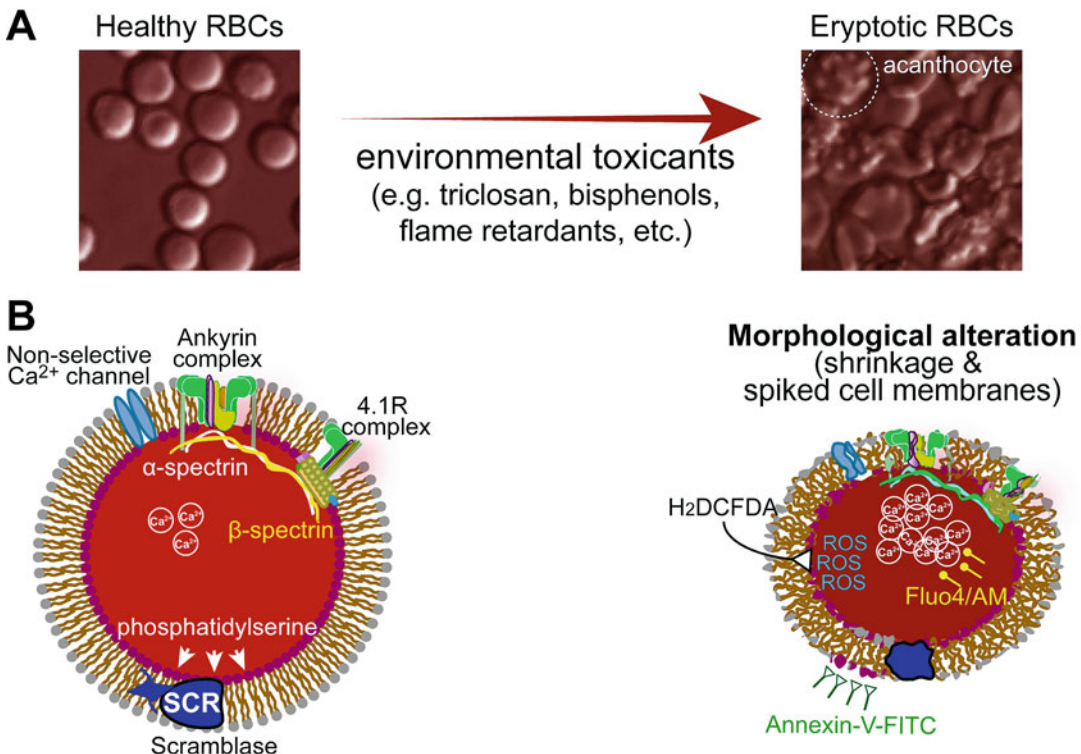


Fig. 1 Red blood cell (RBC) death. **(a)** Schematic of healthy and dying RBCs. **(b)** Hallmarks of premature RBC death

Identification of RBC death relies on the assessment of canonical biomarkers either shared or unique to a specific mode of cell death. Phosphatidylserine (PS) externalization serves as a binding site for engulfing macrophages to eliminate damaged RBCs and is detected by Annexin-V-FITC labeling (Fig. 1b). Dead cells commonly display dysregulated ion homeostasis resulting in elevated intracellular calcium (Ca²⁺) that is measured by Fluo4/AM staining (Fig. 1b). Increased Ca²⁺ opens Ca²⁺-responsive potassium (K⁺) channels, leading to KCl and water loss, and cell dehydration [4]. Cell shrinkage, thus, is also a sign of dead cells and is assessed by forward scatter (FSC) of light (Fig. 1b). Chemicals also cause morphological alterations on the cell surface (e.g., acanthocytes) resulting in increased side scatter (SSC) values (Fig. 1b). Furthermore, oxidative stress and accumulation of toxic reactive oxygen species (ROS) are a distinctive feature of a failed antioxidant system. Quantification of ROS levels is accomplished by 2',7'-dichlorodihydrofluorescein diacetate (H₂DCFDA) (Fig. 1b). The role of signaling mediators, such as caspases and p38 MAPK, can also be examined using small molecule inhibitors [5].

As it operates on a per-cell basis, flow cytometry offers superior sensitivity, specificity, and overall ruggedness to conventional fluorescence microscopy or spectroscopy. This chapter presents a detailed protocol for the cytofluorometric evaluation of the molecular mechanisms governing RBC physiology and survival in response to environmental toxicants.

2 Materials

Prepare all solutions using ultrapure water. Prepare and store all reagents at room temperature (unless indicated otherwise). Diligently follow all waste disposal regulations when disposing waste materials.

2.1 RBC Samples

Fresh blood specimens must be collected and processed as quickly as possible to avoid spontaneous cell death [1, 8]. Lithium heparin, EDTA, or citrated blood is acceptable [9–11]. Alternatively, fresh, leukoreduced erythrocyte suspensions may be obtained from a blood bank [12].

2.2 Blood/RBC Wash Buffer

Phosphate-buffered saline (PBS; 154 mM NaCl, 1 mM potassium phosphate monobasic, 5.6 mM sodium phosphate dibasic; pH 7.4). Add 800 ml of ultrapure water to a clean, glass bottle. Weigh 9.0 g NaCl, 136.09 mg KH₂PO₄, and 794.97 mg Na₂HPO₄, and dissolve in water. Make up the volume to 1000 ml by adding 200 ml ultrapure water. Autoclave or filter-sterilize and store at 2–8 °C. Physiological saline may suffice and is prepared essentially as PBS but without the sodium and potassium salts.

2.3 Alsever's Solution

0.42% NaCl, 0.8% sodium citrate, 0.05% citric acid, and 2.0% glucose. Add 400 ml of ultrapure water to a clean, glass bottle. Weigh 2.1 g of NaCl, 4 g of trisodium citrate dehydrate (C₆H₉Na₃O₉), 0.275 g of citric acid monohydrate (C₆H₁₀O₈), and 10.25 g of D-glucose, and add to the glass bottle. Dissolve the salts by manually shaking the bottle and make up the volume to 500 ml by adding 100 ml of ultrapure water. Filter-sterilize and store at 2–8 °C (*see Note 1*).

2.4 Ringer Buffer

125 mM NaCl, 5 mM KCl, 1 mM MgSO₄, 32 mM N-2-hydroxyethylpiperazine-N-2-ethanesulfonic acid (HEPES), 5 mM glucose, 1 mM CaCl₂ (pH 7.4). To 800 ml ultrapure water, weigh and add 7.3 g NaCl, 327.75 mg KCl, 120.36 mg MgSO₄, 7.62 g HEPES, 900 mg glucose, 110.98 g CaCl₂, to a clean, glass bottle. Shake until salts are fully dissolved, then make up the total volume to 1000 ml by adding 200 ml ultrapure water. Adjust pH to 7.4 by NaOH, filter-sterilize, and store at 2–8 °C.

- 2.5 *Ca²⁺-Free Ringer Buffer*** Prepare essentially as in Subheading 2.4 but without CaCl₂ or substitute it with 1 mM (380.35 mg/L) ethylene glycol-bis(-β-aminoethyl ether)-N,N,N',N'-tetraacetic acid (EGTA).
- 2.6 *Hyperosmotic Ringer Buffer*** Prepare essentially as in Subheading 2.4 in addition to 550 mM (188.26 g/L) sucrose.
- 2.7 *High-KCl Ringer Buffer*** Prepare essentially as in Subheading 2.4 but replace 125 mM NaCl and 5 mM KCl with 125 mM KCl (9.31 g/L).
- 2.8 *Chloride-Free Ringer Buffer*** Prepare essentially as in Subheading 2.4 but replace NaCl, KCl, and CaCl₂ with 125 mM sodium-gluconate, 5 mM potassium-gluconate, and 1 mM Ca-gluconate.
- 2.9 *High-Ca²⁺ Ringer Buffer*** Prepare essentially as in Subheading 2.4 but add 5 mM instead of 1 mM CaCl₂ (554.9 g/L). Annexin-V-FITC and Fluo4/AM are Ca²⁺-dependent stains, and require relatively higher (≥ 2.5 mM) CaCl₂ concentrations to bind to their targets.
- 2.10 *Energy-Depleted Ringer Buffer*** Prepare essentially as in Subheading 2.4 but without glucose with added 2.5 mM NaCl (127.5 mM NaCl in total).
- 2.11 *Hank's Balanced Salt Solution (HBSS)*** 138 mM NaCl, 5.33 mM KCl, 0.5 mM MgCl₂·6H₂O, 0.41 mM MgSO₄·7H₂O, 4 mM sodium bicarbonate (NaHCO₃), 5.60 mM glucose, 1.26 mM CaCl₂, 0.44 mM KH₂PO₄, 0.3 mM Na₂HPO₄ (pH 7.4). To 800 ml ultrapure water, weigh and add 8.0 g NaCl, 400 mg KCl, 100 mg MgCl₂·6H₂O, 100 mg MgSO₄·7H₂O, 350 mg NaHCO₃, 1.0 g glucose, 140 mg CaCl₂, 60 mg KH₂PO₄, 48 mg Na₂HPO₄ to the glass bottle. Shake until salts are fully dissolved, then make up the total volume to 1000 ml by adding 200 ml ultrapure water. Filter-sterilize, and store at 2–8 °C.
- 2.12 *Inhibitors***

Inhibitor	Target	References
Z-VAD-FMK	Caspases	[13]
SB203580	p38 MAPK	[14]
D4476	Casein kinase 1	[15]
Staurosporin	Protein kinase C	[12]
JANEX-1	JAK3	[16]
Necrostatin-2	RIP1	[5]
HS-1371	RIP3	[17]
Necrosulfonamide	MLKL	[5]
N-acetylcysteine	Antioxidant	[18]
Aspirin	COX-1/2	[19]

(continued)

Inhibitor	Target	References
BAPTA-AM	Intracellular Ca^{2+}	[20]
Senicapoc	Ca^{2+} channels	[21]
Amiloride	Cation channels	[22]

2.13 Annexin-V-FITC Commercially available and used to label PS-exposing cells.

2.14 Fluo4/AM Commercially available and used to measure intracellular Ca^{2+} levels.

2.15 H₂DCFDA Commercially available and used to quantify intracellular ROS.

2.16 A Confocal Microscope For visual examination of cells and assessment of fluorescence.

2.17 A Centrifuge To isolate RBCs and prepare supernatants.

2.18 A Spectrophotometer A plate reader capable of measuring light absorbance at 405 or 540 nm.

2.19 A Flow Cytometer To analyze RBC death parameters at different wavelengths.

3 Methods

All procedures are performed at room temperature ($\sim 23^\circ\text{C}$) unless otherwise specified.

3.1 RBC Isolation

1. Collect 3–5 ml blood in green-top (heparin), yellow-top (acid-citrate dextrose), or lavender-top (EDTA) vacutainer tube. Let stand for 20 min at room temperature.
2. Divide the blood into 1 ml aliquots in 15 ml conical tubes and add 14 ml PBS or saline. Invert gently to mix.
3. Centrifuge at $699 \times g$ for 15 min.
4. Discard the plasma, buffy coat, and upper 10% of RBCs using a Pasteur pipette.
5. Resuspend the RBC pellet in 2 ml PBS or saline and keep at 4°C .

3.2 Toxicant Treatment

1. Prepare as many microtubes as needed, each treatment group in triplicate.
2. To all tubes except the positive control, add 950 ml Ringer buffer or HBSS (*see Note 1*).

Table 1
Experimental setup of toxicant exposure

Treatment	Negative Control	Dose 1	Dose 2	Dose 3	Dose 4	Positive Control
Ringer/HBSS	950 ml	950 ml	950 ml	950 ml	950 ml	X
ddH ₂ O	X	X	X	X	X	950 ml
Toxicant	X	Variable	Variable	Variable	Variable	X
RBCs	50 µl	50 µl	50 µl	50 µl	50 µl	50 µl

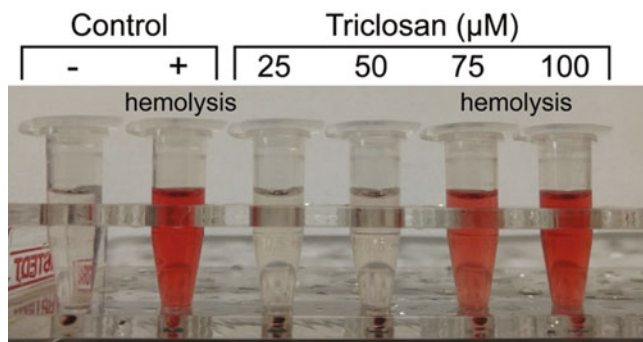


Fig. 2 RBC hemolysis. Supernatant appearance of control and triclosan-treated cells showing various red color intensities reflective of hemoglobin leakage. Cells at 5% hematocrit were treated with the vehicle (0.1% ethanol) or with indicated triclosan concentrations for 4 h at 37 °C and analyzed for hemolysis

3. For the positive control group, add 950 ml distilled water (Table 1).
4. To experimental tubes, add the required doses of the toxicant of interest (Table 1).
5. To all tubes, add 50 µl of RBCs for 5% hematocrit (Table 1) (*see Note 2*).
6. Invert the tubes once or twice for a homogeneous mixture.
7. Incubate at 37 °C for the desired amount of time (*see Note 3*).

3.3 Hemolysis (See Fig. 2)

1. Following incubation, centrifuge the tubes at 13,300 × g for 1 min.
2. Transfer 200 µl of the supernatant to a 96-well plate (*see Note 4*).
3. Reserve wells for plate and medium blanks.
4. Read the absorbance at 405 nm (*see Note 5*).
5. Subtract average plate blanks then the average medium blanks from all readings. Calculate the percentage of cell death by

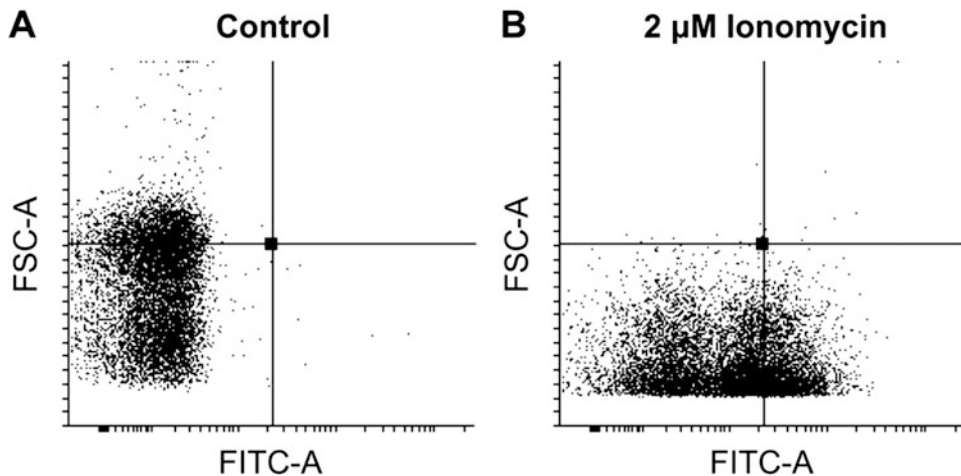


Fig. 3 Two-dimensional analysis of RBC distribution. Dot plots depicting RBC distribution of control (**a**) and ionomycin-treated cells (**b**) in terms of FITC and FSC properties. Cells at 5% hematocrit were treated with the vehicle (0.01% dimethylsulfoxide) or with 2 μ M of ionomycin for 24 h at 37 °C and analyzed for PS exposure (FITC) and cell size (FSC). Note the remarkable increase in FITC fluorescence upon ionomycin exposure along with diminished FSC values

dividing the average absorbance reading of control and experimental cells to that of the positive control.

3.4 Detection of PS Externalization, FSC, and SSC (Fig. 3)

1. Following treatment, spin down the cells and discard the supernatant.
2. Resuspend the cell pellet in 300 μ l of 5 mM CaCl₂ Ringer buffer.
3. Transfer 50 μ l of the cell suspension to a FACS tube.
4. Prepare Annexin-V-FITC staining solution as follows:
 - (a) Add enough 5 mM CaCl₂ buffer to a 15 ml conical tube.
 - (b) Add Annexin-V-FITC to a final concentration of 0.5–1.0% (v/v).
 - (c) Example for 12 tubes: $12 \times 150 = 2985 \mu\text{l}$ buffer + 15 μl Annexin (*see Note 6*).
5. Add 150 μl of the staining solution to the cells in FACS tubes.
6. Incubate for 10 min at room temperature away from light.
7. Analyze by flow cytometry at excitation and emission wavelengths of 488 and 530 nm, respectively (*see Note 7*).
8. Data for FSC and SSC are obtained simultaneously (*see Note 8*).

3.5 Intracellular Calcium

1. Following treatment, spin down the cells and discard the supernatant.

2. Resuspend the cell pellet in 300 μ l of 5 mM CaCl₂ buffer.
3. Transfer 50 μ l of the cell suspension to a FACS tube.
4. Prepare Fluo4/AM staining solution as follows:
 - (a) Add enough 5 mM CaCl₂ buffer to a 15 ml conical tube.
 - (b) Add Fluo4/AM to a final concentration of 2 μ M.
 - (c) Example for 12 tubes: $12 \times 150 = 2994 \mu\text{l}$ buffer +6 μl Fluo4 (from a 1 mM stock).
5. Add 150 μl of the staining solution to the cells in FACS tubes.
6. Incubate for 30 min at 37 °C.
7. Wash twice in PBS to remove excess dye.
8. Analyze by FACS at excitation and emission wavelengths of 488 and 530 nm, respectively.

3.6 Measurement of ROS

1. Following treatment, spin down the cells and discard the supernatant.
2. Resuspend the cell pellet in 300 μ l of 5 mM CaCl₂ buffer, PBS, or HBSS.
3. Transfer 50 μ l of the cell suspension to a FACS tube.
4. Prepare H₂DCFDA staining solution as follows:
 - (a) Add enough PBS to a 15 ml conical tube.
 - (b) Dilute H₂DCFDA to 5 μ M.
 - (c) Example for 12 tubes: $12 \times 150 = 2985 \mu\text{l}$ PBS + 15 μl (from 1 mM H₂DCFDA stock).
5. Add 150 μl of the staining solution to the cells in FACS tubes.
6. Incubate for 30 min at 37 °C.
7. Wash twice to remove unbound dye.
8. Analyze by FACS at excitation and emission wavelengths of 488 and 530 nm, respectively.

3.7 Signal Transduction Analysis

1. Treat cells as desired.
2. Set up tubes for inhibitor exposure (*see Note 9*).
3. Analyze cells for hemolysis or eryptosis markers as described earlier.

3.8 Confocal Microscopy

1. Treat cells as desired.
2. Stain as described earlier.
3. Spread up to 50 μl of cell suspension on a clean, glass slide.
4. Immediately observe under the microscope. Adjust fluorescence to suit the dye used.

4 Notes

1. Based on the overall aim of the experiment, the incubation medium may be changed to suit different purposes. For example, to test for the importance of extracellular Ca^{2+} to the toxic endpoint, cells may be incubated in both Ringer and Ca^{2+} -free Ringer buffers. Other approaches include subjecting the cells to osmotic stress (hyperosmotic Ringer buffer) and preventing K^+ efflux (high-KCl Ringer buffer). Also, adjust buffer volume to accommodate toxicant volume added.
2. Some authors prefer to use less concentrated RBC suspensions (e.g., 0.4% hematocrit) [23]. While the total number of cells does indeed influence their susceptibility to a given stressor, it is important to keep the cell suspensions consistent throughout the experimental procedures.
3. Appropriate incubation periods must be empirically determined based on the potency of the toxicant and the susceptibility of the cells. Generally, the longer the incubation time, the lesser concentrated the toxicant must be. A period of 24 and 48 h is most commonly used, although time-dependence starting from 5 min up to 72 h may be suitable.
4. The amount of supernatant in the wells is critical. We find that absorbance readings proportionately increase as the supernatant volume increases. As is with the hematocrit, the key is to keep the volume taken from each sample consistent as to allow for accurate analysis.
5. Some authors measure hemoglobin content at 540 nm instead [11]. Since significantly smaller values are obtained at 540 nm than at 405 nm, we suggest that it is best suited for highly concentrated RBC samples (i.e., high hematocrit).
6. The excess staining buffer is important to account for pipetting inaccuracies. We find that it is always best to prepare more than needed by accounting for two extra tubes ($\sim 300 \mu\text{l}$). This applies to staining live cells for FACS analysis regardless of the dye used.
7. We find that it is sometimes required to adjust the voltage of FITC, FSC, and SSC to obtain histograms within the reading frame. Adjustments are based on either the unstained control or the control groups. This is important to be able to distinguish control and experimental cells in terms of the toxic endpoint measured.
8. An arbitrary marker may be placed to discriminate cell populations based on fluorescence intensity. Such a marker reveals accurate proportions of cells exhibiting, for example, increased

Annexin-V-FITC, Fluo4, or DCF fluorescence, compared to the control group. Likewise, placing markers at the edges of FSC histograms counts the percentage of cells with increased and reduced volume.

9. Whether cells are pretreated or co-treated (along with toxicant) with inhibitors must be determined empirically. We and others have used both approaches [5, 24]. Interestingly, we also find that some toxicants exhibit complex drug–drug interactions with inhibitors that results in an additive toxic effect. In such cases, we suggest pretreating the cells with the inhibitor of interest, washing twice or thrice to remove the inhibitor, then proceeding with toxicant exposure. Alternatively, authors may opt to use very small concentrations of inhibitors as to limit their toxicity.

Acknowledgements

The authors are grateful to the Deanship of Scientific Research, King Saud University for funding this research project through Vice Deanship of Scientific Research Chairs (DSRVCH).

References

1. McCaig WD, Hodges AL, Deragon MA, Haluska RJ Jr, Bandyopadhyay S, Ratner AJ, Spitalnik SL, Hod EA, LaRocca TJ (2019) Storage primes erythrocytes for necroptosis and clearance. *Cell Physiol Biochem* 53:496–507. <https://doi.org/10.33594/000000153>
2. Qadri SM, Bissinger R, Solh Z, Oldenborg PA (2017) Eryptosis in health and disease: a paradigm shift towards understanding the (patho)-physiological implications of programmed cell death of erythrocytes. *Blood Rev* 31:349–361. <https://doi.org/10.1016/j.blre.2017.06.001>
3. LaRocca TJ, Stivison EA, Hod EA, Spitalnik SL, Cowan PJ, Randis TM, Ratner AJ (2014) Human-specific bacterial pore-forming toxins induce programmed necrosis in erythrocytes. *mBio* 5:e01251–e01214. <https://doi.org/10.1128/mBio.01251-14>
4. Foller M, Lang F (2020) Ion transport in eryptosis, the suicidal death of erythrocytes. *Front Cell Dev Biol* 8:597. <https://doi.org/10.3389/fcell.2020.00597>
5. Alfhili MA, Weidner DA, Lee MH (2019) Disruption of erythrocyte membrane asymmetry by triclosan is preceded by calcium dysregulation and p38 MAPK and RIP1 stimulation. *Chemosphere* 229:103–111. <https://doi.org/10.1016/j.chemosphere.2019.04.211>
6. Macczak A, Cyrlker M, Bukowska B, Michalowicz J (2016) Eryptosis-inducing activity of bisphenol a and its analogs in human red blood cells (in vitro study). *J Hazard Mater* 307:328–335. <https://doi.org/10.1016/j.jhazmat.2015.12.057>
7. Jarosiewicz M, Michalowicz J, Bukowska B (2019) In vitro assessment of eryptotic potential of tetrabromobisphenol A and other bromophenolic flame retardants. *Chemosphere* 215:404–412. <https://doi.org/10.1016/j.chemosphere.2018.09.161>
8. Lang E, Pozdeev VI, Xu HC, Shinde PV, Behnke K, Hamdam JM, Lehnert E, Scharf RE, Lang F, Haussinger D, Lang KS, Lang PA (2016) Storage of erythrocytes induces suicidal erythrocyte death. *Cell Physiol Biochem* 39:668–676. <https://doi.org/10.1159/000445657>
9. Jemaa M, Fezai M, Bissinger R, Lang F (2017) Methods employed in Cytofluorometric assessment of Eryptosis, the suicidal erythrocyte death. *Cell Physiol Biochem* 43:431–444. <https://doi.org/10.1159/000480469>
10. Ghashghaeinia M, Cluitmans JC, Akel A, Dreischer P, Toulany M, Koberle M,

- Skabytska Y, Saki M, Biedermann T, Duszenko M, Lang F, Wieder T, Bosman GJ (2012) The impact of erythrocyte age on eryptosis. *Br J Haematol* 157:606–614. <https://doi.org/10.1111/j.1365-2141.2012.09100.x>
11. Chakrabarty G, NaveenKumar SK, Kumar S, Mugesh G (2020) Modulation of redox signaling and thiol homeostasis in red blood cells by Peroxiredoxin mimetics. *ACS Chem Biol* 15:2673–2682. <https://doi.org/10.1021/acschembio.0c00309>
12. Ghashghaeinia M, Koralkova P, Giustarini D, Mojzikova R, Fehrenbacher B, Dreischer P, Schaller M, Mrowietz U, Martinez-Ruiz A, Wieder T, Divoky V, Rossi R, Lang F, Koberle M (2020) The specific PKC-alpha inhibitor chelerythrine blunts costunolide-induced eryptosis. *Apoptosis* 25:674–685. <https://doi.org/10.1007/s10495-020-01620-6>
13. Foller M, Mahmud H, Gu S, Wang K, Floride E, Kucherenko Y, Luik S, Laufer S, Lang F (2009) Participation of leukotriene C (4) in the regulation of suicidal erythrocyte death. *J Physiol Pharmacol* 60:135–143
14. Briglia M, Fazio A, Faggio C, Laufer S, Alzoubi K, Lang F (2015) Triggering of suicidal erythrocyte death by Ruxolitinib. *Cell Physiol Biochem* 37:768–778. <https://doi.org/10.1159/000430394>
15. Mischitelli M, Jemaa M, Almasry M, Faggio C, Lang F (2016) Stimulation of erythrocyte cell membrane scrambling by quinine. *Cell Physiol Biochem* 40:657–667. <https://doi.org/10.1159/000452578>
16. Bhavsar SK, Gu S, Bobbala D, Lang F (2011) Janus kinase 3 is expressed in erythrocytes, phosphorylated upon energy depletion and involved in the regulation of suicidal erythrocyte death. *Cell Physiol Biochem* 27:547–556. <https://doi.org/10.1159/000329956>
17. Park HH, Park SY, Mah S, Park JH, Hong SS, Hong S, Kim YS (2018) HS-1371, a novel kinase inhibitor of RIP3-mediated necroptosis. *Exp Mol Med* 50:125. <https://doi.org/10.1038/s12276-018-0152-8>
18. Alzoubi K, Egler J, Abed M, Lang F (2015) Enhanced eryptosis following auranofin exposure. *Cell Physiol Biochem* 37:1018–1028. <https://doi.org/10.1159/000430228>
19. Bentzen PJ, Lang F (2007) Effect of anandamide on erythrocyte survival. *Cell Physiol Biochem* 20:1033–1042. <https://doi.org/10.1159/000110714>
20. Ranzato E, Martinotti S, Magnelli V, Murer B, Biffi S, Mutti L, Burlando B (2012) Epigallocatechin-3-gallate induces mesothelioma cell death via H_2O_2 -dependent T-type Ca^{2+} channel opening. *J Cell Mol Med* 16:2667–2678. <https://doi.org/10.1111/j.1582-4934.2012.01584.x>
21. Stocker JW, De Franceschi L, McNaughton-Smith GA, Corrocher R, Beuzard Y, Brugnara C (2003) ICA-17043, a novel Gardos channel blocker, prevents sickled red blood cell dehydration in vitro and in vivo in SAD mice. *Blood* 101:2412–2418. <https://doi.org/10.1182/blood-2002-05-1433>
22. Lang KS, Myssina S, Tanneur V, Wieder T, Huber SM, Lang F, Duranton C (2003) Inhibition of erythrocyte cation channels and apoptosis by ethylisopropylamiloride. *Naunyn Schmiedeberg's Arch Pharmacol* 367:391–396. <https://doi.org/10.1007/s00210-003-0701-z>
23. Liu J, Bhuyan AAM, Ma K, Zhang S, Cheng A, Lang F (2020) Inhibition of suicidal erythrocyte death by pyrogallol. *Mol Biol Rep* 47:5025–5032. <https://doi.org/10.1007/s11033-020-05568-3>
24. Jemaa M, Mischitelli M, Fezai M, Almasry M, Faggio C, Lang F (2016) Stimulation of suicidal erythrocyte death by the CDC25 inhibitor NSC-95397. *Cell Physiol Biochem* 40:597–607. <https://doi.org/10.1159/000452573>



Chapter 12

Practical Methods and Technologies in Environmental Epidemiology

Chuancheng Wu, Donghong Wei, Huangyuan Li, and Siying Wu

Abstract

Environmental epidemiology is a science that applies traditional epidemiology methods and combines the characteristics of the relationship between environment and population health, and studies the relationship between external environmental factors and population health from a macro perspective. The following methods are usually used. (1) Descriptive research: including ecological research and current situation research. (2) Analytical research: including case-control research and group research. (3) Experimental epidemiological research. In this section, according to the short-term and long-term effects of studying environmental risk factors, it is divided into two parts. Short-term effect methods include time series study, case-crossover study, and panel study. Long-term effect methods include cross-sectional study, case-control study, and cohort study.

Key words Environmental epidemiology, Time series study, Case-crossover study, Panel study, Cross-sectional study, Case-control study, Cohort study

1 Introduction

Environmental epidemiology is the application of epidemiological theories and methods to study the prevalence of natural factors and pollution factors in the environment that harm the health of the population, especially the correlation and causality between environmental factors and human health. That is to clarify the exposure-response relationship in order to provide a basis for the formulation of environmental health (or quality) standards and preventive measures. Epidemiology studies the temporal and spatial distribution of diseases, health conditions and their influencing factors in the population. The research results of environmental epidemiology can provide the most direct scientific evidence for the prevention and treatment of environmental-related diseases.

Chuancheng Wu and Donghong Wei contributed equally to this work.

Environmental epidemiology emerged from the investigation and study of population health in major pollution incidents, common methods include the following:

Time series study is used to study the relationship between exposure and outcome variables within a certain period of time. Exposure and outcome variables are cumulative measurement values on the same time unit, and each variable constitutes a time series. Time series research is mainly used for short-term exposure research, to evaluate short-term changes in the series of health outcomes that change with exposure. The time period between the change in exposure and the change in outcome that it causes is called the lag. Therefore, the 0-day lag effect usually means the same-day effect. A 2-day lag effect means an effect after 2 days. In order to obtain long-term, high-quality daily measurement data, time series research is more inclined to use routine monitoring data rather than data obtained in a certain study (Advantages and disadvantages *see Note 1*).

Case-crossover study was first proposed by Macrone in 1991. It is an epidemiological method for studying the instantaneous effects of short-term exposure on rare acute diseases. Crossover A basic requirement is that at least some subjects must have crossed at least once from lower to higher exposure or vice versa. The minimum amount of crossover is exemplified by the death of a spouse. This is a one-time, irreversible, unidirectional change in exposure status (Advantages and disadvantages *see Note 2*). For the research objects, they must go through the process of Fig. 1.

Panel study is a prospective study, usually in a short period of time (usually a few days to several months), a group of individuals are followed up, and its purpose is to study the short-term effects of environmental exposures that change over time on health outcomes. During the entire study period, the researchers repeated observations on exposure and outcome variables and possible confounding factors, and the number of observations was more than two times. The goal of the panel study is to study the short-term effects of environmental exposure changes. However, there is a significant difference between panel research and time series/case-crossover research, which is mainly reflected in whether individual measurement data can be obtained, so the statistical analysis methods are also different. The panel study has been widely used to study the acute health effects of air pollutants. Similarly, panel studies can also be used to study the acute effects of air pollution on other sensitive groups such as the elderly and healthy adults. Because of the need to monitor the exposure and health of each individual researched, the workload is relatively large, and the sample of the panel study is generally small (Advantages and disadvantages *see Note 3*).



Fig. 1 The process of case-crossover study

Cross-sectional study, also called prevalence survey or prevalence study, is the most widely used method in descriptive studies, which is carried out census or sampling investigation in a designated time, region, and population so as to describe the distribution of diseases or health-related events and examine the relationships between the distribution and the factors of interest. Cross-sectional study has its characteristics different with others. It is a cross section in time series and does not set up control group in advance generally. Each subject's exposure and disease status are investigated at a given time-point, and comparison will be carried out between different exposure subpopulations or disease status only in analysis. Therefore, there is no causal conclusion that can be drawn in a cross-sectional study, it just provides clues to the etiologic study. In addition, it is not suitable for a disease with a short course. This survey is completed within a short space of time, many study objects would have recovered or died during the survey period if the course of disease is too short, and the associated factors found will be survival factors rather than risk factors (The advantages and disadvantage of the cross-sectional study *see Note 4*).

Case-control study is an observational analytic epidemiologic study, which subjects are selected based on whether they do (case) or do not (control) have a disease or other health outcome the study interest in. The groups are then compared in the proportions of exposure or other characteristics. As the causal factors have already had their effect in causing disease in the case group, and the acquired information pertains to the past, the case-control study is sometimes referred to as “retrospective study.” The design of the study is illustrated in Fig. 2, and for its advantages and disadvantages *see Note 5*.

Cohort study, known as a prospective study, evaluates the baseline exposure status of subjects who are without the study outcome like some disease or health condition, then takes a follow-up over a period of time to collect the exposure information and outcome data so as to compare the outcome rates associated with different exposures or risk factor levels and test for a possibly causal correlation and the intensity of correlation. Cohort studies can be classified as prospective (concurrent), retrospective (historical), and ambispective design, depending upon the temporal relationship between initiation of the study and occurrence of the outcome. Figure 3 illustrates the different types of cohort study design, and for its advantages and disadvantages *see Note 6*.

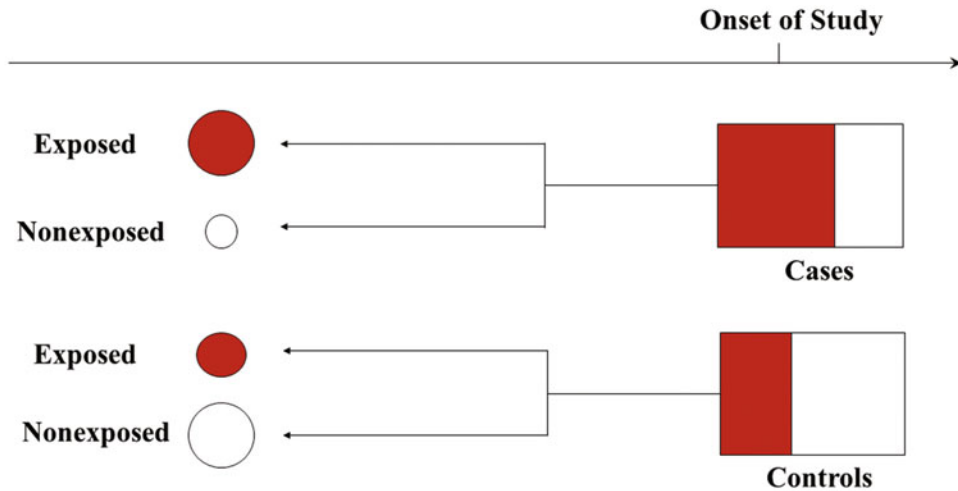


Fig. 2 Design principles of case-control studies. The red areas represent the population exposed and the white areas represent the population nonexposed

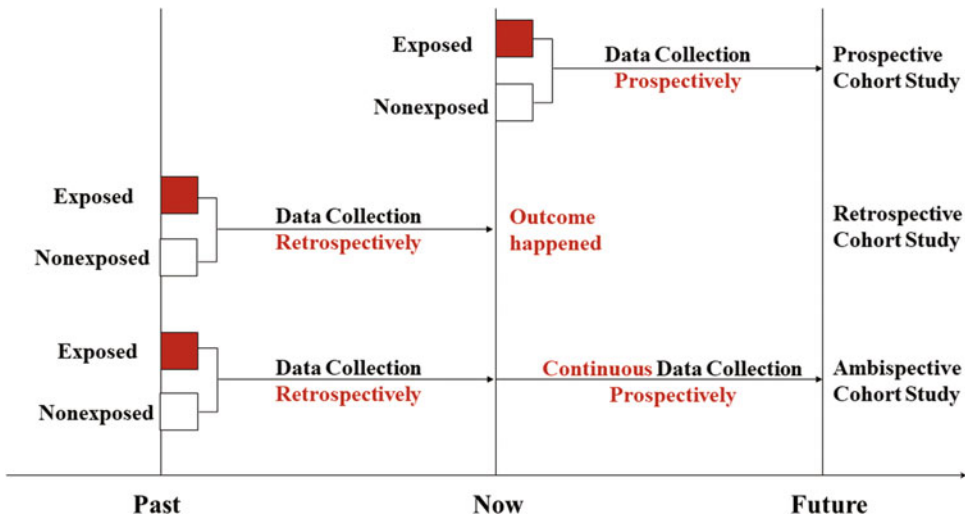


Fig. 3 Different types of cohort design

Environmental epidemiology covers a wide range of subjects. It could be summed up to environmental exposures, health effects and the relationship between them. Of the six methods mentioned above, time series study, case-crossover study, and panel study are mainly used to study the acute effects, and cross-sectional study, case-control study, and cohort study play key roles in the evaluation of environmental chronic health effects. But, the basic steps of them are similar as follows:

1. Make a research plan, including:
 - (a) **Establish the study purpose**, which can be obtained through literature review, work practices, expert consultation, and the studies of others.
 - (b) **Select the study population**. According to the purpose of the study, an appropriate population should be selected to make sure that generalizations from the findings are representative and reliable, and for more details *see* Subheading 3 and refer to professional books on epidemiology.
 - (c) **Determine the survey or design types**, which will be different among different methods. For cross-sectional study, census or sampling survey should be decided; for case-control study, matching methods of case and control groups should be considered; for cohort study, prospective or retrospective design should be confirmed.
 - (d) **Confirm the study variables and questionnaires**, which refers to Subheading 2.
 - (e) **Estimate the sample size**. Larger samples provide more precise estimations but cost more resources, and smaller samples are the opposite. For a statistical view, the best sample size would be the one that obtains all the data that our time, money, support facilities, and ethical concerns will permit. The calculation of sample size needs to integrate design types, variable types, and other factors, and the methods can be empirical methods, or table lookup methods, or formula methods.
 - (f) **Develop an implementation plan**, considering material preparation, staff training, quality control measures, and so on.
2. **Implement the plan**, which mainly involves questionnaire collection, exposure measurement and health effect evaluation. In epidemiological studies, especially large projects, need to establish management institutions before implementation, which could include a study steering committee, field center, and data coordinating center at least. At the same time, it is necessary to make sure preparations in the field, including standardized train, material preparations, pilot survey, and mobilization work. When it comes to investigation, the consistency of all variables' definition and measurement should be guaranteed, review and summary of the survey on the day should be taken to ensure quality control.
3. **Data sorting and analysis**, which will be detailed introduction in Subheading 3.

2 Materials

2.1 Questionnaires

Questionnaire data is an important material in epidemiological studies, which is the main form of variables collection that sufficient consideration should be given to. There is no fixed pattern for questionnaires, but they generally comprise the following parts, title, notes, questions, investigator information, and quality control. The questions can be open or closed questions, but usually cover sociodemographic characteristics, exposure data, outcome variables, and their content should be chosen based on one's own work practice and the experience of others, serving the study goals and suitable for sorting and analysis. For more specific details, please refer to professional books on social investigation or epidemiology.

2.2 Sociodemographic Data

Sociodemographic data include race, gender, birthplace, age, place of residence, educational level, occupation, marital status, income, and so on. It can be collected through a questionnaire survey, or it can be obtained by referring to relevant systems like household registration system.

2.3 Environmental Exposure

Environment mentioned in epidemiology usually refers to the environment in a broad sense, and it can be group exposure or individual exposure.

2.3.1 Population Exposure

It can be exposure to the social environment of a country or region, such as the number of doctors per thousand persons, GDP per capita, etc., which are available from local statistical yearbooks; it can be exposure to natural environment, like air quality, meteorological conditions, etc., which obtained from the local meteorological department or environmental protection department.

2.3.2 Individual Exposure

Individual exposure can be divided into internal exposure and external exposure.

1. Internal exposure in environmental epidemiology refers mainly to the exposure of substances in the body. For example, when assessing the exposure of lead, its concentration in the blood, urine, or hair can be measured to reflect the level of internal exposure.
2. External exposure in environmental epidemiology refers mainly to the individual exposure of substances in the environment. For example, a personal dust sampler can be carried to measure the individual exposure level of PM_{2.5}.

2.4 Health Effects

2.4.1 Population Health

Health effects can be divided into acute effects and chronic effects. In environmental epidemiology, it mainly refers to outcome variables, which can be specific diseases or subclinical changes, and it can be the health level of the group or the health status of the individual.

2.4.2 Individual Health

Population health effects are often described in terms of the incidence, prevalence, or mortality of a disease in a particular country or region, which can be obtained from the local Health Statistics Yearbook.

Individual's health can be a specific disease, a physical or psychological problem, or even changes in certain health indicators like weight, waist circumference, blood pressure, blood glucose, etc. It can be confirmed or tested by specialized medical institution, and it can also be self-reported.

3 Methods

As mentioned in the introduction, short-term effect methods include time series study, case-crossover study, and panel study; long-term effect methods include cross-sectional study, case-control study, and cohort study. The basic steps of these methods are generally similar (*see Subheading 1*), and we will highlight the differences between each method and the others here.

3.1 Time Series Study

3.1.1 Design and Implementation

Determination of the Study Purposes

When applying the principles of time series studies to practice, the following steps may serve as a guideline.

Data Collection

Understand the relationship between environmental exposure and health outcomes. For example, whether the two variables, PM_{2.5} (particulate matter <2.5 μm) concentration and the amount of outpatients in the respiratory department, are sequential in time and there is a correlation.

Data Analysis

Long-term monitoring of environmental pollutants is required, such as PM_{2.5} concentration, SO₂ concentration, meteorological factors, and health outcome. Usually daily data, data collection for more than 3 years is recommended.

There are three commonly used statistical models as follows:

1. Generalized Linear Model (GLM): It has been widely used in the early stage. It is a standard regression method, especially in Poisson regression using the parameter function of time covariate to control its periodic trend.

2. Autoregressive moving average (ARMA): It is an important method for studying time series, which is composed of autoregressive model (referred to as AR model) and moving average model (referred to as MA model).
3. Generalized Additive Model (GAM): Nonparametric smoothing function is used to simulate the nonlinear relationship of time co-variables, paying more attention to the local and more flexible. It is currently the most commonly used method. We introduce the process of the method as follows.

The model is as follows:

$$\log E(Y_t) = \beta K Z_t P_K + \text{ns}(\text{time}, df) + \text{ns}(X_t, df) + \text{DOW} \\ + \text{intercept}$$

Counting variables, such as the number of deaths or visits per day, are often assumed to obey the Poisson distribution and are connected using the Log function.

$E(Y_t)$ is the number of residents who died or visited a doctor on day t ;

Z_t is the air pollutant concentration level on day t , $\mu\text{g}/\text{m}^3$;

β is the exposure response coefficient, that is, the increase in daily deaths or doctor visits caused by the increase in the concentration of pollutants per unit;

ns is a natural smoothing spline function, and df is its degree of freedom;

Time is a date (calendar time) variable. Choosing an appropriate df value for the date can effectively control the long-term fluctuation and seasonal fluctuation trend of the pollution-death sequence data;

DOW is the indicator variable of “day of the week”;

X_t is the meteorological factor on day t , including average temperature and relative humidity.

Time Series Analysis Strategy

1. *Controlling factor.* Possible confounding factors such as daily average temperature, relative humidity, day of the week effect, and long-term trend of time. Set the day of the week as a dummy variable.
2. *Selection of model parameters.* Daily average temperature and relative humidity: As the relationship between weather and health is generally nonlinear, that is, too high or too low may produce harmful effects, so natural spline smoothing functions are used to control this nonlinear confounding effect. The degrees of freedom of temperature are all set to 3.
3. *Time trend degree of freedom.* In order to test the influence of the degree of control time trend on the effect estimation, the annual df of the time smoothing function of each city is changed from 5 to 9 successively, and the degree of freedom

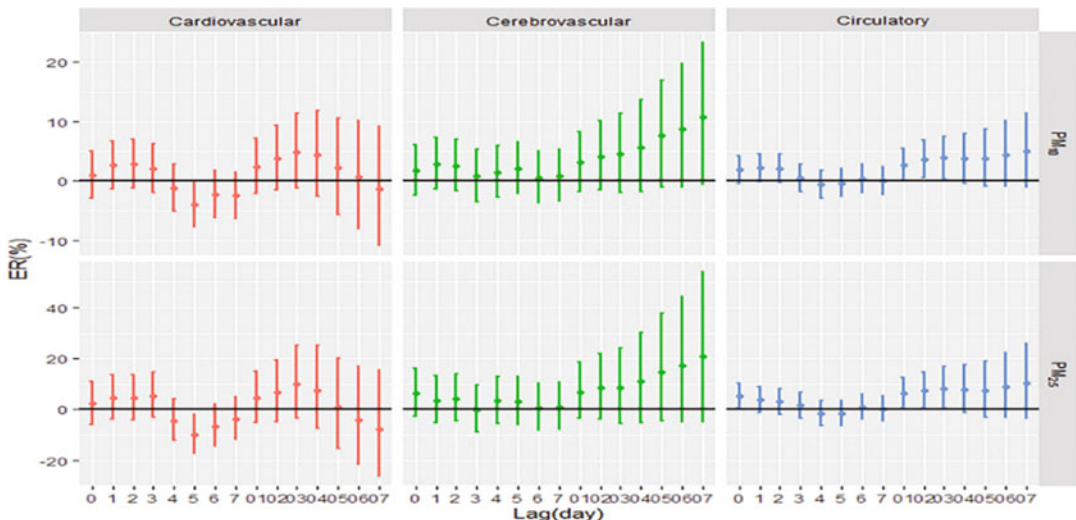


Fig. 4 Estimates of percent change in daily circulatory mortality associated with a $10 \mu\text{g}/\text{m}^3$ increase in particulate matter concentrations during days with heat waves [1]. PM₁₀: particulate matter less than $10 \mu\text{m}$ in aerodynamic diameter; PM_{2.5}: particulate matter less than $2.5 \mu\text{m}$ in aerodynamic diameter; ER: excessive risk. X-axis: lag0 to lag7 means a single-day lag. lag0-1 to lag0-7 means cumulative lag effect

value with the most stable RR value or the smallest AIC is selected. The degree of freedom of trend is 7/year (death) or 6/year (hospital and emergency).

4. *Analysis lag time.* The length is based on the result and ends when there is no significant effect.

Analysis Content

1. Analysis of the impact of air pollutants on health (Fig. 4).

Death Data: Total non-accidental death, death from circulatory and respiratory diseases, cardiovascular and cerebro-vascular diseases, lung cancer.

First aid: total number of first aid consultations.

Outpatient visits: Only the data with ICD(International Classification of Diseases) codes will analyze the impact on sub-system diseases, otherwise only the total amount of outpatients will be analyzed.

General hospitals: total number of outpatient clinics in hospitals, total number of medical outpatient clinics, outpatient visits for internal respiratory diseases and circulatory diseases.

Pediatrics in children's hospitals or general hospitals: total outpatient visits, outpatient visits for respiratory, skin, eye, and appendages.

Limitation: Need for years of stable quality data; the choice of model parameters will have a certain impact on the analysis results.

Statistical software: All data analyses were performed using “mgcv” package in statistical software R version 3.6.1.

3.2 Case-Crossover Studies

3.2.1 Determine the Study Purpose

3.2.2 Determine the Hazard Period

3.2.3 Choose an Appropriate Control Form

Case-crossover studies are mostly used to test a certain etiological hypothesis, but it can also be used for exploratory research of etiology.

The overestimation or underestimation of the hazard period will reduce the degree of association between exposure and disease, and no meaningful results can be obtained. The determination of the hazard period is generally based on the experience of the researcher or observer. For example, when studying the relationship between myocardial infarction and physical activity, the hazard period is 1 hour before the occurrence of myocardial infarction.

In fact, this is the type of crossover study that chooses different cases.

Type A (Fig. 5). It is a paired interval control, similar to the 1:1 ratio in a case-control study; compare the difference between A and E exposure factors.

Type B (Fig. 6). It is a multi-interval control, that is, the exposure during the risk period is compared with the exposure during multiple control periods within the day before the event. It is similar to the 1:M ratio study in the case-control study. The difference between the three models lies in the limitation of estimated parameters.

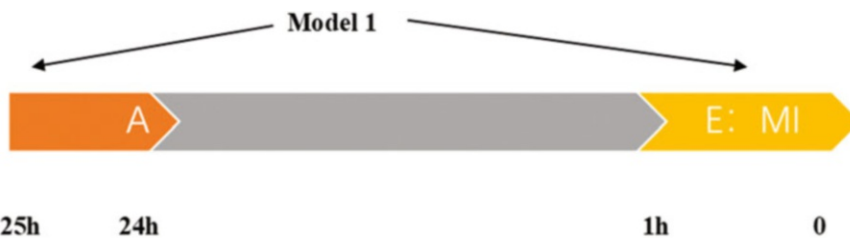


Fig. 5 Type A: Hours before the onset of myocardial infarction(MI)

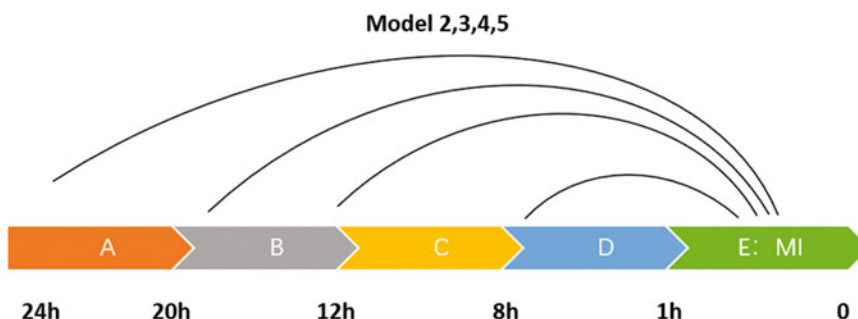


Fig. 6 Type B: Hours before the onset of myocardial infarction

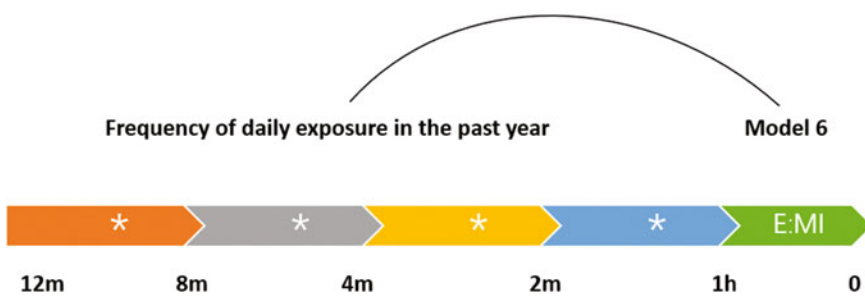


Fig. 7 Type C: Months before the onset of myocardial infarction

Type C (Fig. 7). It uses daily exposure frequency, which is the same as MacLure's second-type control data. Statistical methods can use M-H stratified analysis or conditional logistic regression.

First of all, it depends on whether to obtain the highest possible inspection efficiency with the smallest sample. If so, the 1:M pairing method can be used, or the usual frequency method can be used. Among all the methods, the frequency method usually has the highest relative efficiency. The relative efficiency of 1:1 pairing method is 14%, and as the control period increases, the relative efficiency gradually increases, but even if the most control period is selected, the relative efficiency is only half of the usual frequency method, but the usual frequency method can't control the bias within the individual, while the other two methods can well control the bias within the individual through conditional logistic regression.

In general, the frequency method is usually a recommended method, because its estimation is the most accurate, and its individual bias can be ignored. If possible, it is best to collect exposure information suitable for all research methods, so that various methods can be used to complement each other, but the specific situation depends on the research purpose and research conditions.

3.2.4 Selection of Cases

When selecting cases, try to use international or domestic uniform diagnostic standards. The source can be obtained from the medical records and discharge records of hospitals and outpatient clinics, and can also be obtained from the population data of disease surveillance, census, and spot checks in the community.

3.2.5 Selection of Research Factors

If it is a study to confirm the cause, the research variables should be broken down as much as possible. For example, in the study of physical activity and myocardial infarction, it is necessary to estimate the usual frequency of each level in the past year and the time, type and level of physical activity 26 h before the occurrence of myocardial infarction, and include all daily physical activities and the definition of exposure, etc. All these have a great influence on the research results.

3.2.6 Collection of Data	Collect the patient's general condition, exposure data, and possible covariate data by means of on-site inquiry and fill in the questionnaire. Especially when asking patients about long-term exposure in the past and exposure during the dangerous period before the acute event, different interview methods and techniques should be paid attention to.
3.2.7 Statistical Analysis of Data and Interpretation of Results	The data statistical analysis method of case-crossover design needs to be carried out by using paired tests. In univariate analysis, you can use paired chi-square test or paired t test, nonparametric test, and other methods for comparison; in multivariate analysis, conditional logistic regression is needed for analysis, and the calculation process can use SPSS, SAS or R Software, etc.
Data Analysis	
1:1 Paired Data Analysis	It is the same as the 1:1 matched case-control study analysis, except that the case and control are the risk period and the control period, respectively (Table 1).
Normal Frequency Analysis	<p>1. Calculate the concurrence observed odds. That is to calculate the observation ratio of exposure during the dangerous period ($a:b$), if a certain body is exposed in the dangerous period, the ratio is 1:0; if not, it is 0:1.</p> <p>2. Calculate the concurrence expected odds. Assuming that the occurrence and exposure of the event are purely accidental, that is to say, the disease is a random event, and the expected ratio is the ratio of the event that may occur during the exposure effect period. If in the past week, the individual has been exposed to physical activity for X h, then the remaining y h is the non-exposure time. Therefore, the ratio of events occurring during the exposure effect period is $x:y$, where the exposure time is estimated as the usual frequency of exposure multiplied by the length of the exposure effect period, and the nonexposed person time is the total person time minus the exposed person time. For example, if the length of the effect period of physical activity is 1 h, and its usual frequency is twice a week, the exposure time (x) in the past year is: $2 \times 52 \times 1 = 104$(h) instead of exposure time (y) is: $24 \times 365 - x = 8656$(h).</p>

Table 1
1:1 Matched case-crossover study

	Control period	Crossover	Hazard period	No
Case subject 1	Exposed	$OR = B/C$	Exposed	A
Case subject 2	Unexposed		Exposed	B
Case subject 3	Exposed		Unexposed	C
Case subject 4	Unexposed		Unexposed	D

3. Calculation of relative risk

$$RR = \left(\sum a_i y_i \right) / \left(\sum b_i x_i \right)$$

The numerator is the sum of individual y_i with an observation ratio of 1:0.

The denominator is the sum of individual x_i with an observation ratio of 0:1.

3.3 Panel Study

3.3.1 Basic Principles and Concepts

Exposure Measurement

Health Measurement

The essence of exposure measurement in panel research is the same as that of time series and case-crossover studies, that is, it measures short-term changes in air pollution. However, there are significant differences in measurement methods. Time series case-crossover research is an ecological research method. Exposure information generally comes from routine monitoring information at fixed environmental monitoring sites, while panel research specifically monitors the air pollution exposure of each research object, and exposure evaluation is possible. It will be very intensive, including individual monitoring of various environmental factors. Usually these studies involve individual sampling. Some studies also combine the use of diaries or GPS devices to track the activities and locations of researchers during the monitoring period to estimate the individual exposure of research subjects. The combination of environmental monitoring and time-activity tracking allows researchers to determine the sources of exposure factors, confounding factors, and effect modifiers. For example, outdoor activity time or living area may be an important effect modifier of individual air pollution exposure. However, at the same time, the cost of individual exposure monitoring will be more expensive, and it is not easy to strive for the active cooperation of the research subjects.

The panel study continuously measured the health outcomes of each subject during the study. Unlike time series and case-crossover studies, panel research is often not concerned with death and clinical diseases, but subclinical physiological indicators or certain symptoms. Most countries in the world routinely collect health data that are limited. Although some countries have better health information systems, the death and disease routine surveillance systems in most developing countries are not very complete. And these data are only limited to identifiable clinical events, such as outpatient, emergency, hospitalization, and death. However, air pollution can cause a wide range of health effects, from changes in a series of physiological indicators to disease and even death. Generally speaking, clinical morbidity and death only reflect the “iceberg model” of the health effect spectrum of air pollution. Compared with this, air pollution is more likely to produce mild clinical or subclinical, physiological indicators, and respiratory function indicators. These acute effect indicators are difficult to analyze through

time series/case-crossover studies, because apart from the routine monitoring system, it is difficult to achieve a long-term special health check for a large sample of people. These health indicators can be quantified and can be used to reflect the mechanism of health hazards caused by air pollution.

Confounding Factors

There are also a large number of confounding factors in panel research: on the one hand, because the nature of panel research is based on a repeated measurement design, there are some confounding factors that change over time, such as seasonality, day of the week effect, and weather conditions. If the research period is more than one season, seasonal factors need to be considered, and an indicator function of time (such as month or season) can be set to adjust the time trend. The day of the week effect is generally not obvious in panel studies. The inclusion of temperature and humidity in the model can better control the mixed effects of meteorology, and if necessary, consider controlling the nonlinear relationship with health. On the other hand, panel research can determine the age, gender, smoking, drinking, education, accompanying diseases and other individual information of each research subject, so as to control the confounding factors at the individual level. Since each research object is investigated separately in the panel study, the researcher can collect all possible confounding factor information through a carefully designed research plan.

Crowd Selection

In panel research, due to the need to conduct intensive exposure and health testing of the research subjects, it is difficult to carry out large-scale research. Therefore, researchers usually choose sensitive individuals to conduct research to maximize statistical power. At the same time, because panel research can expose the relationship with health at the individual level, the selected health indicators are generally sensitive physiological indicators, so the sample size required is relatively small. Panel studies mostly focus on children, the elderly, patients with asthma, and patients with chronic cardio-pulmonary diseases. When selecting sensitive populations as research subjects, researchers should be cautious when extrapolating research results based on sensitive populations to the general population. In recent years, several panel studies based on normal populations have also found the association between air pollution and health indicators.

In addition, in the panel research, the research subject may need to carry individual sampling equipment and require the completion of diary or time-activity records. When selecting the population, it is necessary to consider whether the research subject can actively cooperate. Therefore, the sample population who agrees to participate in the research may not be representative of the general population. The analysis of the pane study is based on the comparison of the same research object at different times. Therefore,

although the selection of the sample population may limit the extrapolation of the research results, it should not bias the research results. Researchers usually have to complete the recruitment. The research objects of the whole study put great effort.

Analysis Strategy and Basic Model

The data obtained from panel research generally requires individual-based analysis. Individual-based analysis must use more complex statistical models.

In a panel study, the researcher usually collects the individual exposure information of the research subjects and repeatedly measures the health outcomes of concern at multiple time-points. Therefore, the design of a panel study is similar to a cohort study, that is, both are prospective follow-up observations. The difference between the two research designs is that the cohort study usually evaluates the effect of exposure on a certain health event such as death or morbidity (usually a causal effect), and panel studies usually evaluate the short-term effects of exposure factors that change over time on health. The short-term effects are generally reflected in a series of short-term changes in physiological indicators and subclinical indicators, including reversible changes and irreversible changes. In addition, the study time usually has a big difference, although this is not necessary for the study design, the panel study usually lasts for several months or 1 year, and the cohort study may last for several years or even decades. Although cohort studies tend to adopt survival analysis methods (in the survival analysis, each research object is treated as an independent observation), due to the similar data structure, cohort studies and panel studies can use similar statistical analysis methods, and the analysis methods are also different. Cohort studies that repeatedly collect data on subjects during follow-up are similar.

In panel research, response variables are generally continuous variables, such as lung function and blood biochemical index values. At a certain point in time, the exposure measurement can be ecological, such as from a fixed monitoring point and the exposure measurement is completely consistent for all individuals; it can also be different for each research object, such as individual monitoring or other individual estimation time.

At present, in panel research, the linear mixed effect model (MEM) is generally used to analyze the acute health effects of air pollution. As the name suggests, MEM includes both fixed effects and random effects. The fixed effects, including the health effects of air pollution, are assumed to be unchanged during the study period, and the effects of confounding factors such as individual characteristics are also assumed to be unchanged during the study period. Random effects assume that exposure and health measurements between individuals are independent of each other, and the independence between measurements is caused by random effects within individuals. In MEM, in addition to the need to include

pollutants with different lags, it also needs control confounding factors such as individual characteristics, weather conditions, and time trends.

In panel research, it is very important to adjust the confounding factors that have a changing trend over time. In principle, the methods described in the time series analysis section are all suitable for panel research. Other fixed individual variables, such as demographic characteristics and basic health status, can be introduced into the model to improve research efficiency. Similar to longitudinal studies, the most challenging and difficult statistical problem in panel studies is the lack of outcome data due to the withdrawal of the research subjects. Whether or not the impact of missing data can be ignored on statistical inference depends on the underlying process of missing data, for example, whether the probability of a study subject's withdrawal depends on or to what extent depends on the incidence of health outcomes. Researchers need to be extra cautious about serious biases caused by missing data due to ignoring the withdrawal of research subjects. Under certain circumstances, certain methods can be used to fill in these missing data, but in practice there are very few applications.

Special software packages “me4” and “nhm4” have been developed in the R software to fit the mixed effect model, with corresponding operating instructions. Software such as SAS and SPSS can also be used to fit mixed effect models.

3.4 Cross- Sectional Study

3.4.1 Establish the Study Purposes

When applying the principles of cross-sectional studies to practice, the following steps may serve as a guideline. At the same time, an example from the China Pulmonary Health (CPH) study [2] is taken for illustration, and its workflow is served as a reference (*see Note 7*).

3.4.2 Select the Study Population and Determine the Survey Methods

The CPH researchers found the most recent Chinese national survey of chronic obstructive pulmonary disease (COPD) was done during 2002–2004, and no national data was available for COPD prevalence in age 40 or younger, so they aimed to estimate the prevalence and absolute burden of COPD in Chinese, and assessed risk factors for prevalent COPD.

3.4.3 Estimate the Sample Size

In the CPH study, a nationally representative sample of adults aged 20 years or older from communities was enrolled in ten provinces. In this situation, the sampling methods and the size of sample are very important issues.

Here, we take formula calculation for numerical variables as an example, estimation methods in other cases can be referred to professional books on epidemiology or health statistics, and statistical software can complete the above calculations.

To estimate a sample size for a single mean, such as comparison of blood pressure between noise-exposed subjects and normal adults, the formula for simple random sampling method is:

$$n = \left(\frac{z_{\alpha/2} s}{d} \right)^2$$

n : sample size S : standard deviation d : admissible error α : significant level.

S and d can be estimated from previous literature or from a professional perspective, and α is generally set as 0.05 or 0.01, so $Z_{\alpha/2}$ is equal to 1.96 or 2.58, respectively.

3.4.4 Confirm the Sampling Methods.

In the CPH study, a multistage stratified cluster sampling was used to select the participants, including province-city/county-district/township-community-household five stage (*see Note 8*). For more details, refer to professional books on epidemiology or health statistics.

3.4.5 Variables Selection

The selection of exposure and outcome variables is according to the objectives of the study, and the definition and measurement of them are extremely important, especially strict standards. For example, in the CPH study, current smoking was defined as having smoked 100 cigarettes at least in one's lifetime and currently smoking; COPD was defined as a post-bronchodilator FEV1: FVC ratio less than 0.70, according to 2017 Global Initiative for Chronic Obstructive Lung Disease (GOLD) guidelines.

3.4.6 Questionnaire Design

A standardized questionnaire was administered in CPH study, including information for demographic characteristics, medical history, parental history of respiratory disease, and risk factors like smoking habit. For more specific design details, please *see* Subheading 2.1 and refer to professional books on social investigation or epidemiology.

3.4.7 Establish the Study Purposes

Implementation of study project.

Taking the CPH study for instance, trained and certified technicians did pulmonary function tests on all participants with a MasterScreen Pneumo PC spirometer, and calibration with a 3 L syringe was done daily.

3.4.8 Data Analysis

In a cross-sectional study, there are at least three aspects of the analysis usually:

- (a) **The description of demographic characteristics**, including gender, age, educational level, occupation, marital status, social and economic status, and so on.
- (b) **The distribution of health conditions**, which can be grouped by various characteristics such as different population from urban or rural areas.

- (c) **The associations between exposures and diseases**, which can be supported by a measure of correlation that how strongly disease occurrence is related to some potentially predictive characteristics. In the CPH study, multivariable logistic regression analyses were done to investigate risk factors for COPD, and cigarette smoking ($OR = 1.95$, 95% CI 1.53–2.47) and heavy exposure to PM2.5 (50–74 $\mu\text{g}/\text{m}^3$, $OR = 1.85$, 1.23–2.77; $\geq 75 \mu\text{g}/\text{m}^3$, $OR = 2.00$, 1.36–2.92) were identified as major preventable risk factors.

There are different analysis methods; attention should be paid to the respective applied conditions when selecting descriptive indexes and analytical methods (see Note 9). Specific statistical methods can be referred to professional books on epidemiology and health statistics; statistical software can complete the above analysis.

3.5 Case-Control Study

When applying the principles of case-control studies to practice, the following steps may serve as a guideline; we take an example from a nationwide case-control study setting in Denmark [3] for illustration, and its workflow serves as a reference (see Note 10).

3.5.1 Determine the Study Purposes

More details can see Subheading 1.

3.5.2 Select the Study Population

Case group. The meaning of case is participants with a disease or some health state of interest, and they should represent as homogeneous an entity as possible, the basic principle is to establish strict and uniform diagnostic criteria.

- (a) Cases can be from hospitals, which will be easy to operate.
- (b) It can also come from the community, which selection bias will be smaller, but is not easy to operate.
- (c) It can also be new cases from a cohort study, but will be more susceptible to the cohort it belongs to.

Control group. There are several common sources of controls, including hospital patients, general population, and special controls such as cases' families or neighbors. Theoretically, controls should be an unbiased sample of the whole population, but in practice controls are often selected from the general population from which the case group is drawn. The key points of control's choice are representativeness and comparability; the distribution of control and case in any factors except exposure factors is as consistent as possible.

In the case-control study in Denmark, cases were drawn from the entire Danish population and comprised all children with a diagnosis of asthma or with a minimum of two prescriptions for asthma medicine from their 1st to 15th birthday. Controls were selected at random who had no asthma diagnosis, all children and their parents were born in Denmark.

3.5.3 Choice for Matching Methods

According to the different matching methods, there are three types of case-control study.

- Non-matched case-control studies.** There are no other restrictions except the number of control group is generally equal to or more than the number of case group.
- Frequency matched case-control studies.** Some factors or characteristics are required to be consistent in proportion between the case group and the control group when the study subjects are selected.
- Individual matched case-control studies.** Each control individual should be consistent with the corresponding case individual in some factors or characteristics. One case generally is matched with one control, and no more than four controls at most. In the case-control study in Denmark, case and control was individual matched by sex and birthday within 1 week.

3.5.4 Calculations of Sample Size

The calculation of sample size for a case-control study varies according to whether the design take the method of individual matching. We take formula calculation for frequency matched or non-matched case-control studies as an example, and here we assumed that the cases and the controls have the same size of sample. Estimation methods in other situations can be referred to professional books on epidemiology or health statistics, and statistical software can complete the above calculations.

$$n = \frac{\left[z_\alpha \sqrt{2\bar{p}(1-\bar{p})} + z_\beta \sqrt{p_0(1-p_0) + p_1(1-p_1)} \right]^2}{(p_1 - p_0)^2}$$

p : the proportion of exposure, 1 means cases, 0 means controls;

\bar{p} : the mean of p_1 and p_0 ;

z_α : the corresponding standard normal distribution threshold in α ;

z_β : the corresponding standard normal distribution threshold in β .

3.5.5 Ascertain the Exposure Variables

For more details, see Subheading 2.2 Environmental exposure. In the case-control study in Denmark, air pollution and family-related factors were identified for the onset of asthma in children.

3.5.6 Data Collection

Important thing is, the information collection of case and control groups should be synchronous and consistent. For other specific detailed rules of the implementation, please refer to Subheading 1 or professional books on social investigation or epidemiology.

3.5.7 Data Analysis

The basic analysis of a case-control study is a comparison between cases and controls with respect to the frequency of an exposure so as to evaluate potential etiologic role. This comparison entails an

Table 2
 2×2 table of data collected in a case-control study

Exposure	Case	Control	Total
Yes	a	b	$a + b$
No	c	d	$c + d$
Total	$a + c$	$b + d$	n

estimate of the relative risk, as computed by the odds ratio (*OR*). The most basic form of data for a case-control study is shown in a 2×2 table with four possible classifications of individual subjects, cases who were exposed (a), controls who were exposed (b), cases who were unexposed (c), and controls who were unexposed (d), which is illustrated in Table 2. The Chi-square test is the simplest method to examine the differences in proportion of exposure between cases and controls.

If the difference between groups is significant, then *OR* will be calculated with a confidence interval to evaluate the role of exposure, the basic calculation formula, and the formula and the evaluation criteria of *OR* (see Note 11). It should be emphasized that if there are confounding factors, a logistic regression model is needed to adjust the confounding effect to estimate the value of *OR*. In the case-control study in Denmark, having two parents with asthma was associated with a 2.40-fold (2.34, 2.47) increased risk of asthma and persistent wheezing. Specific statistical methods can be referred to professional books on epidemiology or health statistics; statistical software can complete the above analysis.

3.6 Cohort Study

3.6.1 Determine the Purposes, Exposure Factors, and Outcomes of the Study

3.6.2 Selection of the Fields of the Study and the Cohort

When applying the principles of cohort studies to practice, the following steps may serve as a guideline, we take an example from a prospective cohort study from the Prediction for Atherosclerotic Cardiovascular Disease Risk in China (China-PAR) project [4] for illustration, and its workflow is served as a reference in Note 12.

For more details, see Subheadings 1 and 2. It should be emphasized that cohort studies can simultaneously collect multiple outcomes related to exposure and analyze the relationship between one cause and many effects. In the China-PAR study, not only the association between PM_{2.5} and stroke incidence was focused on, but also the associations between PM_{2.5} and other cardiovascular diseases like coronary heart disease [5].

One of the major issues to be considered in a cohort study is the survey field and its cohort, the basic principle of choice are the following: small population mobility, easy to follow up, high incidence of expected outcomes, local government departments, and public support.

3.6.3 Calculations of Sample Size

In the cohort study, the type of outcome variable is the most important influencing factor in the estimation of sample size, and different types with different methods. We take outcome indicator as a categorical variable (like whether the outcome event happens or not) for example, and estimation methods in other situations can be referred to professional books on epidemiology or health statistics, and statistical software can complete the above calculations. Here we assume that the two groups have the same number of individuals, and the required sample size for each group is the following:

$$n = \frac{\left[z_\alpha \sqrt{2\bar{p}(1-\bar{p})} + z_\beta \sqrt{p_0(1-p_0) + p_1(1-p_1)} \right]^2}{(p_1 - p_0)^2}$$

p : the estimated incidence of outcome, 1 means exposed, 0 means nonexposed;

\bar{p} : the mean of p_1 and p_0 ;

z_α : the corresponding standard normal distribution threshold in α ;

z_β : the corresponding standard normal distribution threshold in β .

3.6.4 Data Collection

In the cohort study, continuous follow-up is needed after completion of the baseline survey, and the process has several key points.

- (a) A clear start and ending time of follow-up are required in order to calculate person time.
- (b) The incubation should be considered when ascertaining the follow-up interval.
- (c) The content of follow-up should be consistent with the baseline survey.
- (d) There are a variety of resources that can be used to complete the follow-up, including routine registration data, regular investigations or tests, or both. In the China-PAR study, the researchers used identical methods at baseline and follow-up surveys for all participants. Information on stroke incidence during the follow-up period was collected by interviewing participants or their proxies, and further checking hospital records or death certificates for verification.

3.6.5 Data Analysis

The basic data analysis of the cohort study includes the assessment of the baseline differences that outcome related among exposure groups, the measure of the incidence rates of outcome events, and the associations between exposures and outcome events.

Data from a cohort study can be conceptualized in the form of a 2×2 table as shown in Table 3. There are more available indicators in cohort studies compared to case-control studies,

Table 3
Data collected from a cohort study in a 2×2 table

Exposure	Outcome		Total
	Yes	No	
Yes	a	b	$a + b$
No	c	d	$c + d$
Total	$a + c$	$b + d$	n

involving relative risk (RR), attributable risk (AR), and so on, and can be used to evaluate the exposure effects. Relative risk, for example, also named hazard ratio (HR), is defined as the ratio of the incidence of disease in the exposed group (I_e) divided by that in the nonexposed group (I_0), which indicates the likelihood of developing the disease compared to the unexposed group. RR will be calculated with a confidence interval to evaluate the role of exposure, the calculation and the formula and the evaluation criteria of RR (see Note 13). Estimation of other indicators or analysis methods can be referred to professional books on epidemiology or health statistics.

4 Notes

1. Advantages and disadvantages of time series study.

Advantage: Based on the data collected routinely, the coverage is large and the duration is long.

Disadvantage: Often affected by disease codes: no coding or coding errors; often it is not possible to collect the health outcomes that researchers hope to study. The pollutants to be monitored are selected according to standards, usually without considering health factors, and it is impossible to estimate the differences in exposure between individuals.

2. Case-crossover studies have certain advantages and disadvantages.

The strengths are as follows:

- (a) Due to the self-control method, the influence of many individual factors on the outcome is well balanced (such as age, gender, genetic factor).
- (b) The research is suitable for research that can produce exposure effects in a short period of time, such as cardiovascular events, cerebrovascular events, and short-term treatment outcomes.

- (c) Because of the matching, the sample size can be saved to a certain extent.

But it also has some limitations:

- (a) Case cross-study requires that the time interval between exposure and event occurrence should not be too long, and the exposure should not have a legacy effect.
- (b) Information bias may occur during the collection of exposure data. In addition to the recollection bias of the research subjects, the bias may also be caused by the fact that the investigation of exposure in the case period is more stringent than the investigation of exposure in the control period.
- (c) It may be affected by certain characteristics that change over time. For example, in the same person, because the time period of the case and the control period do not occur at the same time, some characteristics of the individual may change over time.
- (d) Prospective controls may have cases where the individual deliberately reduces exposure due to the occurrence of cases.

3. The advantages and disadvantages of panel research.

The main advantages of panel research are as follows:

- (a) It is an individual-based research. Researchers can obtain information about the individual exposure, health and confounding factors of the research subjects, thereby avoiding exposure and health measurement bias and classification errors, so their ability to test etiological hypotheses is better than time series research.
- (b) Allow researchers to test hypotheses more accurately and effect modification effects, and identify sensitive populations. By detecting a series of physiological and subclinical indicators, it is possible to explore the mechanism of environmental exposure-induced health effects.

However, panel research also has some limitations, which are manifested in:

- (a) The participation of the research subjects is required, especially the direct environmental exposure sampling and health examination of the individual, which increases the burden on the research subjects and may also affect the compliance of the research subjects.
- (b) Intensive follow-up of each research object increases the research cost and limits the number of research objects.

(c) Because panel research focuses on subclinical health indicators, the research results have an impact on the environmental quality.

(d) The formulation and revision of standards, policy formulation, and health risk assessment have no direct significance.

4. Advantages and disadvantages of cross-sectional studies.

The advantages and disadvantages of cross-sectional studies should be considered comprehensively. Their advantages are that:

(a) They are a one-stop, collection of data, interview, examination, survey only once.

(b) They are less expensive and more expedient to conduct.

(c) They can illustrate the interrelatedness of diseases and exposure in a population. Cross-sectional studies can show the distribution of diseases in different characteristics, and investigate factors that are associated with causes of a disease.

(d) They can provide information that is useful for planning of health services and medical programs.

Disadvantages are following:

(a) Cross-sectional studies examine relationships as they exist in a population at a given time, so deaths are not included in the study, and recovered cases may be identified as non-diseased. Surveys thus measure prevalence rather than incidence, the occurrence of new events.

(b) Surveys are ill-suited for study of diseases and exposures that are rare or of short duration, because of the infrequency of these conditions in a population at any given time.

(c) Cross-sectional studies provide no information on the temporal sequence of cause and effect. In surveys, an exposure and an outcome are measured simultaneously and it is often hard to determine whether the exposure preceded the outcome or vice versa. They thus only provide early clues to etiology.

5. Advantages and disadvantages of case-control studies.

Case-control studies have some strengths compared to cohort studies, which include:

(a) Compared with cohort studies, case-control studies are relatively quick and inexpensive, especially in evaluating associations between exposures and diseases with very long latency periods.

- (b) Case-control studies are optimal for the evaluation of rare diseases because they select participants based on their disease status.
- (c) Case-control studies are especially useful in the early stages of the development of knowledge about a particular disease or outcome of interest, which allow for the evaluation of a wide range of potential etiologic exposures that might relate to a specific disease, as well as the interrelationships among these factors.

But their limitations also should be noted:

- (a) Case-control studies are inefficient for the evaluation of rare exposures, such as those related to a particular industry, unless the attributable risk is high.
- (b) Incidence rates of disease cannot be directly computed in exposed and unexposed individuals.
- (c) The temporal relationship between exposure and disease may be difficult to establish in some situations.
- (d) Compared with cohort studies, case-control studies are more prone to selection bias and recall bias.

6. Advantages and disadvantage of cohort studies.

Cohort studies have several advantages over other methods, that are:

- (a) The temporal sequence between exposure and outcome can be clearly indicated, because subjects are presumed to be disease-free at the beginning of a cohort study.
- (b) Incidence or mortality rates of disease in the exposed and unexposed groups can be calculated and relative and attributable risks can be estimated.
- (c) Cohort studies can be used to examine multiple outcomes associated with a single risk factor, such as risks of lung cancer and heart disease associated with smoking.
- (d) Cohort designs are particularly useful for evaluating the effects of rare or unusual exposures.

There are several disadvantages should be paid attention to in the practical application:

- (a) Cohort studies are inefficient for the evaluation of very rare diseases, unless there are distinct populations exposed to a risk factor for which the attributable risk percent is high.
- (b) Cohort studies may be more expensive and time-consuming compared to case-control studies.
- (c) The inevitable loss of follow-up may lead to bias.
- (d) Cohort studies usually require large sample sizes.

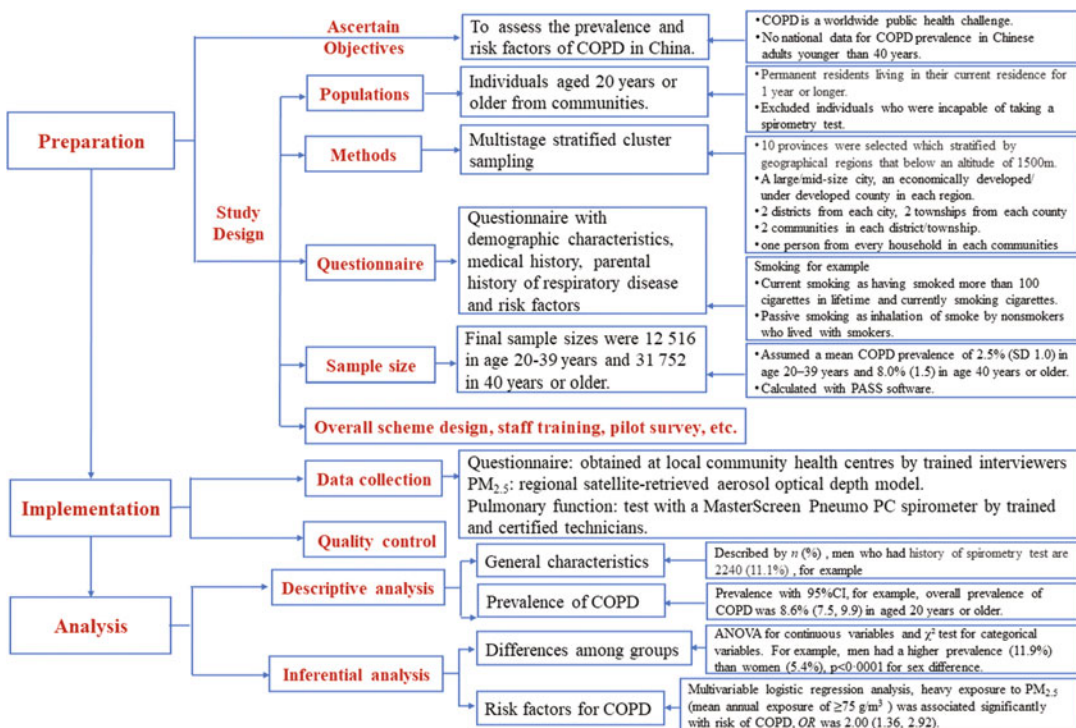


Fig. 8 The workflow of the cross-sectional study. Red words mean key steps or issues in the process, black words mean some details about what to do or how to do

7. See Fig. 8 for the workflow of the cross-sectional study.
8. Random sampling often uses a multistage sampling with a combination of different methods. For example, there is a five-stage stratified cluster sampling used in the CPH study:
 - Stage one, 10 provinces were selected by geographical regions that below an altitude of 1500 m were included;
 - Stage two, a large city, a mid-size city, an economically developed county, and an underdeveloped county were selected at random from each province.
 - Stage three, two urban districts from every city and two rural townships from every county were selected at random.
 - Stage four, two urban residential communities or rural village communities (about 1000–2000 households live) from the urban districts or rural townships were selected at random, respectively.
 - Stage five, individuals aged 20 years or older from the selected communities were selected at random. The final sampling was stratified by sex and age distribution based on 2010 China census data, and only one participant from every household was selected without replacement.

9. When selecting analysis methods, these key points should be noted as follows:

- (a) For quantitative data such as the concentration of blood mercury or NO_2 , mean, median, and other statistical indexes can be used to describe the distribution characteristics, t test, analysis of variance (ANOVA) and nonparametric test can be used to examine the differences between groups.
- (b) For qualitative data such as number of cases, incidence rate, mortality rate, and other frequency indexes can be used in description, and chi-square test, nonparametric test can be used to compare the differences between groups.
- (c) When exploring the relationship between diseases and exposures, Pearson correlation coefficient and Spearman correlation coefficient will be used respectively in quantitative data and qualitative data to describe the associations. However, confounding effects are present in general when associations are analyzed in a cross-sectional study, so multivariate analysis may be needed.

10. See Fig. 9 for the workflow of the case-control study.

11. The calculation formula of OR and confidence intervals are as follows:

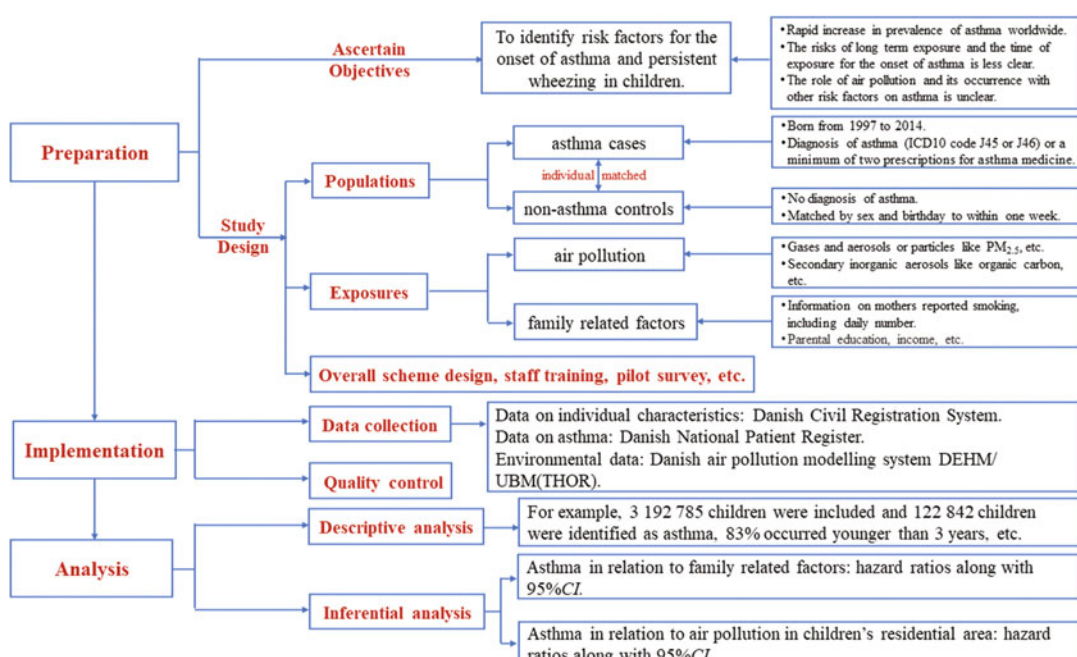


Fig. 9 The workflow of the case-control study. Red words mean key steps or issues in the process, black words mean some details about what to do or how to do

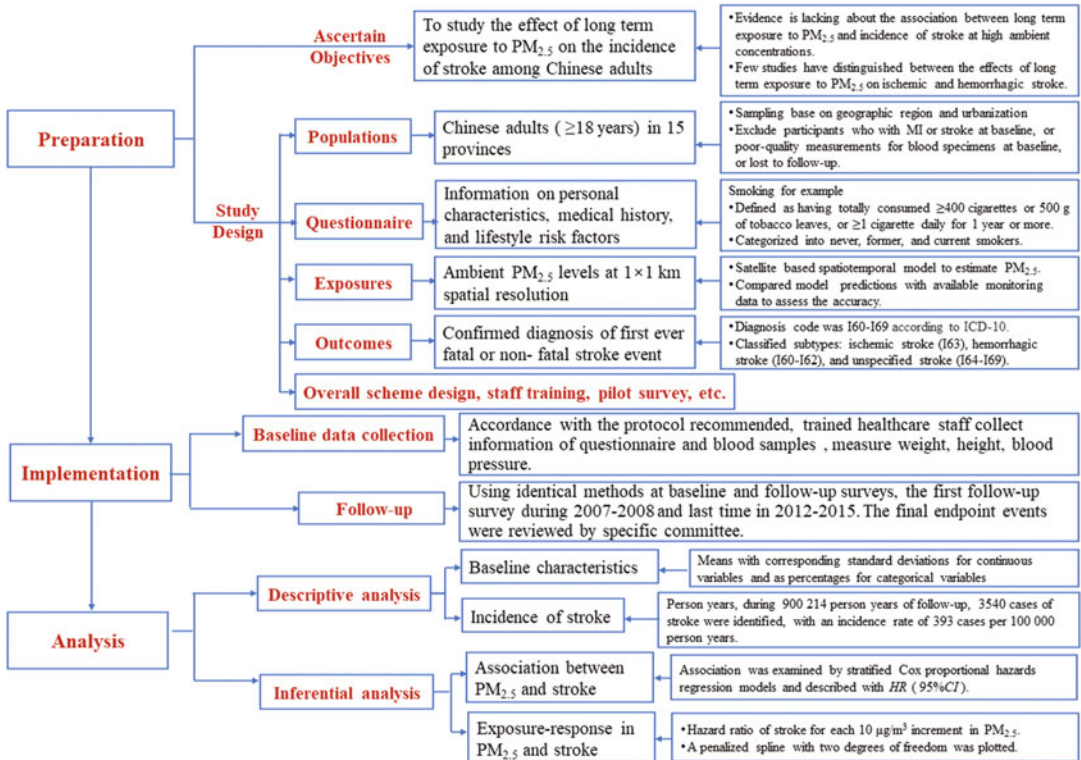


Fig. 10 The workflow of the cohort study. Red words mean key steps or issues in the process, black words mean some details about what to do or how to do

$$OR = \frac{a/c}{b/d}$$

$$\ln OR95\%CI = \ln OR \pm 1.96 \sqrt{Var(\ln OR)}$$

If the confidence interval does not include 1, then if $OR > 1$, suggests that exposure is a risk factor for disease; if $OR < 1$, suggests that exposure is a protective factor for disease.

12. See Fig. 10 for the workflow of the cohort study.

13. The calculation formula of RR and confidence intervals are as follows:

$$RR = \frac{I_e}{I_0}$$

$$RR95\%CI = (RR) \exp \left[\pm 1.96 \sqrt{Var(\ln RR)} \right]$$

If the confidence interval does not include 1, then if $RR > 1$ indicates a positive correction which means higher risk in the exposed group; $RR < 1$ indicates a negative correction which means lower risk in the exposed group.

Acknowledgements

This work was supported by NSFC grant (81973083), the Joint Funds for the Innovation of Science and Technology, Fujian Province (2018Y9089; 2017Y9105).

References

1. Ji S, Zhou Q, Jiang Y, He C, Wu C, Liu B (2020) The interactive effects between particulate matter and heat waves on circulatory mortality in Fuzhou, China. *Int J Environ Res Public Health* 17(16):5979. <https://doi.org/10.3390/ijerph17165979>
2. Wang C, Xu J, Yang L, Xu Y, Zhang X, Bai C et al (2018) Prevalence and risk factors of chronic obstructive pulmonary disease in China (the China pulmonary health [CPH] study): a national cross-sectional study. *Lancet* 391(10131):1706–1717. [https://doi.org/10.1016/S0140-6736\(18\)30841-9](https://doi.org/10.1016/S0140-6736(18)30841-9)
3. Holst GJ, Pedersen CB, Thygesen M, Brandt J, Geels C, Bønløkke JH et al (2020) Air pollution and family related determinants of asthma onset and persistent wheezing in children: nationwide case-control study. *Br Med J* 370:m2791. <https://doi.org/10.1136/bmj.m2791>
4. Huang K, Liang F, Yang X, Liu F, Li J, Xiao Q et al (2020) Long term exposure to ambient fine particulate matter and incidence of stroke: prospective cohort study from the China-PAR project. *Br Med J* 367:16720. <https://doi.org/10.1136/bmj.16720>
5. Liang F, Liu F, Huang K, Yang X, Li J, Xiao Q et al (2020) Long-term exposure to fine particulate matter and cardiovascular disease in China. *J Am Coll Cardiol* 75(7):707–717. <https://doi.org/10.1016/j.jacc.2019.12.031>



Chapter 13

In Ovo Early-in-Life Inhalation Exposure to Gas/Aerosol with a Chicken Embryo Model

Qixiao Jiang, Xiaohui Xu, Hao Ni, Yajie Guo, Junhua Yuan, and Yuxin Zheng

Abstract

To assess the toxicities of gas/aerosol, inhalation exposure model is necessary. Especially important is the inhalation exposure early in life. Traditional inhalation exposure method requires specific instruments and may have to imitate the exposure either days before or after birth. Here, a new inhalation exposure method is introduced, which may be performed without any specific instruments and effectively expose late stage chicken embryos to gas/aerosol very early-in-life by inhalation. This method may facilitate the risk assessment and mechanistic studies regarding the early-in-life effects of gas/aerosol exposure.

Key words *In ovo* exposure, Inhalation, Chicken embryo

1 Introduction

Many toxicants are in the physical form of gas/aerosol, such as particulate matter, diesel exhaust, and various nanomaterials [1–3]. The major route of exposure for these toxicants is inhalation, thus the assessment of inhalant toxicity is important. Currently, the inhalant toxicant assessments were performed either with intratracheal instillation [4] or inhalation chamber [5]. Intratracheal distillation allows accurate control of exposure doses, but the route of exposure is not identical with the real-world situation. Inhalation chamber provides much better relevancy, but would require a large amount of toxicant and specifically designed instruments, limiting the application.

Additionally, neonates are specifically sensitive to inhalant toxicities, making the neonate period one of the most sensitive periods to inhalant toxicants [6, 7]. To assess the potential effects of such early inhalation exposure (when the lungs open for the first time) is critical. Currently, most inhalation toxicity assessments performed in rodents initiated the exposure a few days post-delivery [8],

missing the first a few days. A few studies initiated the exposure prior to delivery [9], which offered better relevancy but also introduced varied maternal effects. To assess the effects of very-early-in-life inhalation exposure specific to the developing embryo/neonate, we established a novel *in ovo* inhalation exposure model with chicken embryo. Chicken embryos develop without maternal effects and allow relatively accurate exposure to each embryo. More importantly, chicken embryos undergo internal pipping in the late stage of development, during which their beaks penetrate the inner membrane and start to breath air from the air cell [10]. Chicken embryos of the identical strain usually start the internal pipping at relatively fixed time during development. For the chicken strain we used (barred Plymouth rock) [11], most chicken embryos internally pipped between the end of embryonic day 18 (ED18) and early embryonic day 19 (ED19). After internal pipping, the embryos would breathe from the air cell for approximately 18 hours, before they proceed to external pipping. During this period, the air cell serves as a naturally occurring inhalation chamber. By infusing the air cell with gas/aerosol-of-interest, we were able to fill up the lungs of chicken embryos when they were inflated for the first time during life, thus achieved very early-in-life inhalation exposure, which could offer valuable data regarding the effects of inhalant toxicants in infants.

2 Materials

This procedure requires minimal materials, we hereby provide a brief list, but anything with the same functionality may be used as well.

Sampling bag: The gas/aerosol needs to be collected prior to exposure. We used TedlarPVF sampling bags (Delin, Dalian, China) as they are durable and have the necessary valves for easy extraction of the gas/aerosol. Other airtight sampling bags should work as well.

Infusion needle: The infusion needle we used is a vein detained needle (Haifenghuang, Jiangxi, China), with the internal needle pulled out. The advantage is that the external plastic needle is elastic, a little pressure could easily push it against the egg shell, offering an airtight infusion airway.

Drill: We used an ordinary metal probe to drill holes on the egg shell. Any metal needle/drill that are capable of drilling holes of approximately 1 mm diameter should work.

Tape: We used ordinary tape to seal the small holes on the egg shell. Note that the area of tape should be as small as possible.

Syringe. We used 10 ml plastic syringes (Ganfa, Jiangxi, China). Candling light. We used the candling light that came with the egg incubator (KFX model, Dezhou, Shandong, China). Egg incubator: Egg incubator was purchased from Keyu (KFX model, Dezhou, Shandong, China) and used following manufacturer's instructions. Standard chicken incubation procedure was used.

3 Methods

3.1 Determine Air Cell Area

The air cell of chicken eggs enlarges throughout the incubation period, as the water evaporates, thus, the air cell area should not be marked until approximately 1 day prior to infusion. In our lab, this is performed by embryonic day 17 (ED17) (*see Note 1*). Remove the eggs from incubator, and candle them with candling light in a dark room (light from a cell phone usually works fine as well). Mark the air cell area with pencil and return the eggs to the incubator. Any dead/undeveloped embryos were removed at this step.

3.2 Air Cell Infusion

1. At desired time (internal pipetting may be visually confirmed by candling, by which the beak is directly visible) (*see Note 2*), take eggs out of the incubator, sanitize the air cell area with 75% ethanol, then drill two holes on two ends of the air cell area. Leave approximately 2 mm from the edge to minimize the risk of damaging the hatching chicks. One of the holes (infusion hole) should be made just large enough to insert the infusion needle, while the exhaust hole should be made a bit larger (1 mm in diameter) (Fig. 1).
2. Once the holes are ready, fill a 10 ml syringe with the gas/aerosol of interest, then switch its needle with a vein detention needle (internal needle removed), carefully insert the plastic needle into the infusion hole, gently press against egg shell to prevent gas/aerosol leakage, and then infuse the gas/aerosol with the syringe. To confirm the airtight condition, put a finger next to the exhaust hole, where the airflow coming out from there should be felt (*see Note 3*).
3. Once the infusion is finished (an additional infusion may be performed to make sure most of the original air inside the air cell has already been expelled), seal the holes with tape and return the egg to the incubator (*see Notes 4 and 5*). The whole process should be performed within a few minutes to avoid death of embryo due to low temperature.

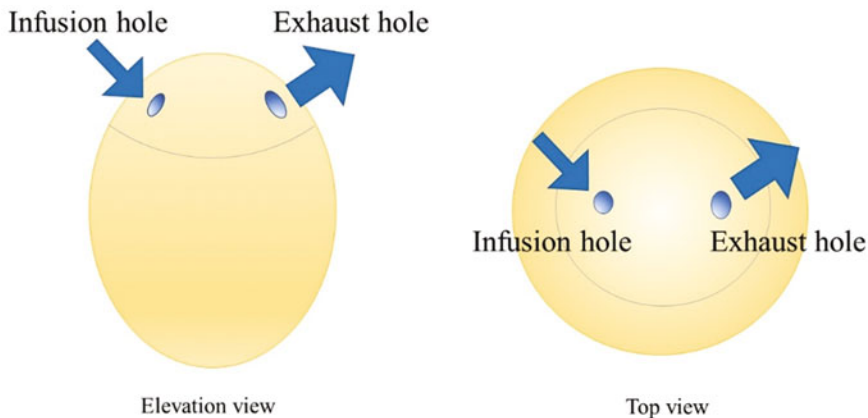


Fig. 1 Demonstration of the infusion/exhaust holes on the air cell area. Left picture is elevation view, and the right picture is top view. Note the different sizes of two holes

4 Notes

1. The air cell area may be marked at the day of infusion as well, but it may prolong the operation time during which the egg is removed from the incubator, increasing mortality. It is recommended to mark the air cell area 1 day before the infusion.
2. Determine the infusion time. For best results, the infusion should be performed prior to the internal piping. Only perform infusion after the internal piping if aerosol sedimentation or degradation is of concern. Different chicken strains internal pip at slightly different time points. For the chicken strain we used in the lab (barred Plymouth rock strain), they usually internal pip around the end of embryonic day 18 (ED18) or early embryonic day 19 (ED19). Thus, we usually infuse diesel exhaust in the middle of ED18. For higher exposure doses, infusion may be repeated once by the middle of ED19. This repeat had been demonstrated to induce more prominent effects comparing to a single infusion at ED18 [11].
3. Note that this procedure should be performed in fume hood to prevent potential health risk to the operators.
4. The exposure duration for this method can be quite accurately estimated by monitoring the time interval between internal piping and external piping, which varies by different strains of chicken. The strain we use (barred Plymouth rock strain) typically spent approximately 18 h between internal piping and external piping, and only 5–6 h from external piping to hatch, thus it is suitable for this procedure. Some chicken strains spend a relatively short time between internal piping and external piping, but a long time between external piping and hatch [12], thus they are not very suitable.

5. Whenever possible, use two identical, separated incubators for control and exposure groups, as once external pipetting occurred, the gas/aerosol may be released and affect the control animals.

Acknowledgements

This work was supported by National Natural Science Foundation of China (Grant No. 91643203, 91543208, 81872591).

References

1. Arias-Pérez RD, Taborda NA, Gómez DM, Narvaez JF, Porras J, Hernandez JC (2020) Inflammatory effects of particulate matter air pollution. *Environ Sci Pollut Res Int* 27:42390–42404
2. Weitekamp CA, Kerr LB, Dishaw L, Nichols J, Lein M, Stewart MJ (2020) A systematic review of the health effects associated with the inhalation of particle-filtered and whole diesel exhaust. *Inhal Toxicol* 32:1–13
3. You DJ, Bonner JC (2020) Susceptibility factors in chronic lung inflammatory responses to engineered nanomaterials. *Int J Mol Sci* 21 (19):7310
4. Lee W, Hahn D, Sim H, Choo S, Lee S, Lee T, Bae JS (2020) Inhibitory functions of cardamomin against particulate matter-induced lung injury through TLR2,4-mTOR-autophagy pathways. *Fitoterapia* 146:104724
5. Carrieri M, Guzzardo C, Farcas D, Cena LG (2020) Characterization of silica exposure during manufacturing of artificial stone countertops. *Int J Environ Res Public Health* 17 (12):4489
6. Goshen S, Novack L, Erez O, Yitshak-Sade M, Kloog I, Shtein A, Shany E (2020) The effect of exposure to particulate matter during pregnancy on lower respiratory tract infection hospitalizations during first year of life. *Environ Health* 19:90
7. Yang XY, Wen B, Han F, Wang C, Zhang SP, Wang J, Xu DQ, Wang Q (2020) Acute effects of individual exposure to fine particulate matter on pulmonary function in schoolchildren. *Biomed Environ Sci* 33:647–659
8. Tong H, Zavala J, McIntosh-Kastrinsky R, Sexton KG (2019) Cardiovascular effects of diesel exhaust inhalation: photochemically altered versus freshly emitted in mice. *J Toxicol Environ Health A* 82:944–955
9. To T, Zhu J, Stieb D, Gray N, Fong I, Pinault L, Jerrett M, Robichaud A, Ménard R, van Donkelaar A, Martin RV, Hystad P, Brook JR, Dell S (2020) Early life exposure to air pollution and incidence of childhood asthma, allergic rhinitis and eczema. *Eur Respir J* 55(2):1900913
10. Ide ST, Ide R, Mortola JP (2017) Aerobic scope in chicken embryos. *Comp Biochem Physiol A Mol Integr Physiol* 212:81–87
11. Jiang Q, Xu X, Zhang C, Luo J, Lv N, Shi L, Ji A, Gao M, Chen F, Cui L, Zheng Y (2020) *In ovo* very early-in-life exposure to diesel exhaust induced cardiopulmonary toxicity in a hatchling chick model. *Environ Pollut* 264:114718
12. Farzaneh M, Attari F, Khoshnam SE, Mozdziak PE (2018) The method of chicken whole embryo culture using the eggshell windowing, surrogate eggshell and ex ovo culture system. *Br Poult Sci* 59:240–244



Chapter 14

DNA Damage in Liver Cells of the Tilapia Fish *Oreochromis mossambicus* Larva Induced by the Insecticide Cyantraniliprole at Sublethal Doses During Chronic Exposure

Yongmei Fan, Chengbin Xu, and Weiguo Miao

Abstract

Cyantraniliprole can effectively control lepidopteran pests and has been used all over the world. In general, the risk of cyantraniliprole seems low for fish, but the toxicity selectivity among different fish species was not clear. Here, we present the methods for the acute toxicity and chronic effects of cyantraniliprole by using juvenile tilapia (*Oreochromis mossambicus*). Based on this test, 96 h LC₅₀ of cyantraniliprole to tilapia was 38.0 mg/L. After exposed for 28 days, specific growth rates of the blank control, solution control, and the treatments of 0.037, 0.37 and 3.7 mg/L of cyantraniliprole were 1.14, 0.95, 0.93, 0.82, and 0.70% per day, respectively. The results of micronucleus experiment and single cell gel electrophoresis showed that cyantraniliprole damaged DNA in liver cells of tilapia larvae. Quantitative PCR results showed that cyantraniliprole could induce the upregulation of *Rpa 3* that is responsible for the DNA repair. The significant downregulation of *Chk 2* gene was related to p53 pathway. It is therefore proposed that cyantraniliprole causes DNA damage in liver cells of tilapia and activates DNA damage and repair pathways.

Keywords Cyantraniliprole, *Oreochromis mossambicus*, Acute toxicity, Chronic toxicity, DNA damage

1 Introduction

The genotoxicity of pesticides to non-target organisms is well known, along with phenomenon of chromosome disorder, genic mutation [1, 2]. In many cases, such phenomena can be detected with in vitro and in vivo assays. For instance, genotoxicity of human lymphocytes and HepG2 cells could be induced by a-cypermethrin, chlorpyrifos, and imidacloprid as determined with in vitro assays, including the alkaline comet, cytokinesis-block micronucleus cytome, and cell viability assays [3]. The genotoxicity of human HELA and HEK293 cells could be induced by chlorpyrifos in vitro experiments, as gH2AX foci formation determined by the alkaline comet assay and DNA damage and apoptosis [4] determined by the

DNA laddering assay. Genotoxic effects of cyantraniliprole are evaluated by *Salmonella typhimurium* reverse mutation assay (i.e., Ames assay), in vitro chromosomal aberration assay, and in vivo micronucleus assay [5]. The results indicated that cyantraniliprole has no genotoxicity. Another report indicated that cyantraniliprole has no genotoxicity, according to in vitro bacterial mutagenicity, in vitro chromosomal aberration, in vitro mammalian cell mutagenicity, and in vivo micronucleus assay [6]. Here, the problem is whether in vitro experiments can fully represent in vivo experiments of organisms. Therefore, tilapia was used to investigate the genotoxicity of cyantraniliprole in vivo experiments in the present study.

The Mozambique tilapia *Oreochromis mossambicus* (Tilapia), a fish native to South Africa, is a species of non-crucian carp hatched orally in Mozambique. It is commonly known as several species of fish belonging to the genera of Cichlidae and non-crucian carp hatched orally [7]. Tilapia is an excellent aquaculture fish promoted by the Food and Agriculture Organization (FAO) of the United Nations to the world and has become one of the main cultured sources of food in the world [8]. Tilapia is still a leading species in fresh water aquaculture and will continue to be a main animal protein source in the future. Tilapia used to live in fresh water and characteristically demonstrates some degree of euryhalinity [9]. Tilapia could live in shallow waters of lakes, rivers, and ponds. Most tilapia is omnivorous, and feed on plants and debris in water [7].

Cyantraniliprole is an o-aminobenzylphthalide insecticide developed by the DuPont Company. It has been widely used because of its broad-spectrum insecticidal activity. It was reported that it had excellent control efficacies on *Citrus psyllid* [10], *Trialeurodes vaporariorum* [11], *Bactrocera dorsalis* [12], *Ostrinia furnacalis* [13], and so on. Cyantraniliprole products can be used in many ways, including spray, root irrigation, soil mixing, and seed treatment. Cyantraniliprole, as a seed dressing agent, can effectively control *Agrotis ipsilon* [14]. However, the degradation rate of cyantraniliprole in soil was slower than that in water [15]. It, therefore, has a high risk of runoff from soils into surface water, while it was overused.

The results of ecotoxicological studies on aquatic organisms indicated that the risk of cyantraniliprole was low for fish, including Rainbow trout, Bluegill sunfish, Static renewal, Channel catfish, Sheepshead minnow, *Lepomis macrochirus*, *Lepomis macrochirus*, and *Oncorhynchus mykiss*, whereas there was a high risk identified for invertebrates (both acute and chronic risk). The risk assessment of earthworms indicated a low toxicity by acute and chronic tests [16]. The chronic toxicity of cyantraniliprole (98.4%) to rainbow trout larvae was 10.7 mg/L (90 days) based on the no-observed effect concentration (NOEC) and growth and reproduction as the endpoint, while it was 9.9 mg/L (30 days) to sheepshead minnow

based on NOEC and growth by a flow through approach [16]. The results proposed that the toxicity varies among different fish species. To date, there has been no report on the chronic toxicity of cyantraniliprole to tilapia, and it needs to estimate the chronic toxicity based on growth as the endpoint.

The observation of relative organ weights and histopathological changes in rats and mice were increased by cyantraniliprole after oral administration, which suggests that the liver is the main target organ of toxicity in the long-term studies [6]. In the present study, the livers of tilapia were also the main target to evaluate the DNA damage and repair induced by cyantraniliprole.

The purpose of this method is to investigate the genotoxicity of cyantraniliprole to tilapia by chronic toxicity tests and further explore mechanism of action. DNA carries the genetic information in all cellular forms of life [17]. Micronucleus test [18] and comet assay [19] are the common methods to estimate the DNA damage in living cells in toxicological research. Hence, the micronucleus and comet assays were used to explore the effects of DNA damage in liver cells of tilapia induced by cyantraniliprole. It was reported DNA damage and the related repair in eukaryotic cells, including direct reversal, mismatch repair, nucleotide excision repair, non-homologous end joining, and homologous recombination pathway [20]. The *p53*, *Chk2*, *Ccne1*, *Cdk2*, *Orc1*, *Ccna1*, *Ccnb*, *Rpa3*, and *Fen1* genes were involved in the DNA damage and repair process [21]. DNA damage and repair in liver cells of treated tilapia after 28 days of exposure were determined with real-time quantitative PCR (RT-qPCR) method for the genes *p53*, *Chk2*, *Ccne1*, *Cdk2*, *Orc1*, *Ccna1*, *Ccnb*, *Rpa3*, and *Fen1*. This study provides useful data for consideration of how to minimize the effects of cyantraniliprole on fish.

2 Materials

2.1 Test Organism

The test organisms, *Oreochromis mossambicus*, can be purchased from Dingfa Fish Seedling Farm, Dingan County, Hainan Province, China, or other resources.

2.2 Chemicals

1. Cyantraniliprole (purity, 95% CAS 736994-63-1).
2. 3-bromo-1-(3-chloro-2-pyridyl)-40-cyano-20-methyl-6-'-(methylcarbamoyl) pyr-azole-5-carboxanilide.
3. Tween-80.
4. Dimethylformamide (DMF).
5. diH₂O.
6. TRIZOL reagent.

7. Agarose.
8. SYBR green PCR mixture.
9. Primers.

3 Methods

3.1 Fish Culture and Treatment

The fishes are raised in a 50-L aquarium for a week before experimentation. The test fish is fed twice a day with solid feed (1% of the body weight of the fish each feeding). An amount of about 40 L of water is used in the aquarium. The water is changed every other day and the feces are removed. Water temperature, dissolved oxygen, conductivity, and pH are $23 \pm 2^\circ\text{C}$, $7.5 \pm 0.5 \text{ mg/L}$, $0.20 \pm 0.01 \text{ mS/cm}$, and 6.8 ± 0.1 , respectively.

3.2 Acute Toxicity Test

1. The test fish is exposed to different concentrations of cyantraniliprole, which are 39, 46, 56, 67, and 80 mg/L based on pro-experiments, in the aquaria chambers (5 L) containing 3 L water [22].
2. DiH₂O is served as the controls, which is justified pH 7.2–7.8 with sodium bicarbonate solution and conductivity $500 \pm 50 \text{ mS cm}^{-1}$ with sodium chloride, exposed to air for 24 h. Filtered water containing DMF and Tween 80 less than 0.1% is used as the solvent control group.
3. Controls and treatments are in triplicates with 20 larvae per replication. The test fishes are not fed during the test period. Mortality is observed at 24, 48, 72, and 96 h. An LC₅₀ of tilapia to 24 h exposure of cyantraniliprole is 74 mg/L with 95% confidence interval (CI) between 70 and 82 mg/L, while a 96 h LC₅₀ is 38 mg/L with CI between 33 and 41 mg/L (Table 1). Therefore, according to the toxicity rating scale provided by the U.S. Fish and Wildlife Service (USFWS) [23], cyantraniliprole can be considered to be slightly toxic to tilapia.

Table 1
Acute toxicity data of cyantraniliprole to Tilapia

Compound	Time (hpf)	Regression equation	LC ₅₀ (mg/L)	95% confidence limits (mg/L)
Cyantraniliprole	24	$y = 0.2757x - 10.75$	74	70–82
	48	$y = 0.3347x - 8.012$	52	49–55
	72	$y = 0.3122x - 4.313$	45	42–48
	96	$y = 0.2003x + 4.794$	38	33–41

3.3 Chronic Toxicity Test

1. The testing period of chronic toxicity is 28 days based on the OECD Guideline (OECD, 2000. NO 215). The concentrations used in chronic toxicity tests, which are based on the results from the acute toxicity experiment, are 1/10, 1/100, 1/1000 of LC₅₀ (96 h) value.
2. The water in different treatments is changed every 3 days. The test fish are fed twice a day with solid feed (1% of the body weight of the fish per feeding) during the test period. The blank and solvent controls are also used. The controls and treatments are in triplicates with 30 larvae per replication.
3. The weight of each fish is measured prior to the start to 28-day during experiment and only fish of similar weight are used in the experiments.

3.4 Specific Growth Rate (%/Day)

1. The formula is as follows. $SGR = \frac{1}{4} \times 100 \times (\ln W_2 - \ln W_1) / (t_2 - t_1)$ where W_0 is the natural logarithm of the fish weight at the beginning of the experiment, and $\ln W_t$ is the natural logarithm of the fish weight at day t (W_0 and W_t are in gram).
2. Samples are taken every 4 days during the experiment. Five fishes from each treatment are weighed to observe the body weights randomly at each time point.
3. The growth rate of all experimental groups tend to decrease first and then increase over time, according to the chronic test of 28 days exposure (Table 2). The growth rate of the control group is the fastest among all groups with 1.14%/day after 28 days of exposure. The 3.7 mg/L-treated group is the slowest growing group at 0.70%/day growth rate after 28 days of exposure overall. The growth rates of 0.037 mg/L-treated and 0.37 mg/L-treated groups are 0.93%/day and 0.82%/day, respectively, after 28 days of exposure. The growth rate of tilapia are significantly decrease 28.07% and 39.47% in the dose of 0.37 and 3.7 mg/L, respectively, compared with the control group after 28 days of exposure (Table 2).

Table 2
Effects of cyantraniliprole on inhibition of Tilapia's specific growth rate

Compound	Specific growth rate (%/day)						
	4 days	8 days	12 days	16 days	20 days	24 days	28 days
Control	-1.47 ± 0.38	-0.68 ± 0.32	-0.21 ± 0.11	0.51 ± 0.16	0.71 ± 0.03	0.82 ± 0.11	1.14 ± 0.05
Solvent control	-1.18 ± 0.52	-1.14 ± 0.15	-0.62 ± 0.18	0.59 ± 0.22	0.66 ± 0.16	0.75 ± 0.16	0.95 ± 0.04
0.037	-2.31 ± 0.74	-1.48 ± 0.22	-0.38 ± 0.16	0.31 ± 0.09	0.58 ± 0.09	0.76 ± 0.12	0.93 ± 0.07
0.37	-0.95 ± 0.35	-0.92 ± 0.08	-0.92 ± 0.39	0.25 ± 0.17	0.46 ± 0.05	0.60 ± 0.19	0.82 ± 0.18*
3.7	-2.52 ± 0.85	-1.00 ± 0.08	-0.78 ± 0.04	0.08 ± 0.30	0.49 ± 0.05	0.75 ± 0.12	0.69 ± 0.01**

Note: Values are means of the standard deviation of means. Duncan test, * $p < 0.05$; ** $p < 0.01$

3.5 Preparation of Primary Liver Cells

- Four fishes are picked from each group every 4 days, at seven different time points, to dissect the fish livers from the chronic exposure test and observation.
- The livers are washed twice with iced PBS (pH 7.4) and then dissolved with trypsin at 37 °C for 15 min. After most tissues are digested into single cells, they are centrifuged at $1000 \times g$ for 7 min at 4 °C and the supernatant is discarded.
- The pellet is suspended with 1 mL of PBS and filtered through a 200-mesh sieve filter. The solution is centrifuged again at $1000 \times g$ for 7 min at 4 °C, and the supernatant is discarded. The pellet contained primary liver cells that are resuspended with 200 mL of PBS.

3.6 Micronucleus Test

- Slides are prepared with cytocentrifugation (20 mL), followed by fixation and staining of samples [24].
- Fixation is performed with cold methanol. The DAPI staining method was used to stain cells for 3–5 min, and then washed 3 times with PBS.
- Micronuclei are observed under a fluorescence microscopy and the number of micronucleus is recorded. The controls and treatments are in triplicates, respectively.
- The micronucleus rates of the blank control and solvent control groups are 7.00‰ and 8.00‰ and 11.7‰ and 12.0‰, respectively, and that of the treatments at 0.037, 0.37, and 3.7 mg/L of cyantraniliprole are 25.7‰ and 69‰, 36.7‰ and 84‰, and 54.7‰ and 92‰, respectively, at 4 day and 28 day of exposure. The other five time points are all among those data. The micronucleus rates significantly increased 2.3, 6.2, and 6.7-fold in the group of 0.037, 0.37, and 3.7 mg/L, respectively, in comparison with the control groups (Fig. 2) after 28 days exposure. The results suggest that DNA in liver cells of tilapia is damaged by low doses of cyantraniliprole (Fig. 1).

3.7 Single Cell Gel Electrophoresis

- For each comet assay, an aliquot of 20 mL cell suspension is obtained from cytocentrifugation of primary liver cells.
- Microscope slides are coated with 50 mL of 0.8% (v/v) agarose, 150 mL of 0.8% (v/v) agarose placed in lysis at 4 °C for 20 min.
- The slides are coated with 30 mL of the cell suspension and placed in lysis with 90 mL of 0.7% (v/v) low melting point agarose at 4 °C for 20 min.
- After lysis, the slides are incubated in 300 mM NaOH 1 mM EDTA buffer (pH > 13) for 20 min to denature the DNA and then submit to electrophoresis at 25 V and 300 mA for 20 min in the dark.

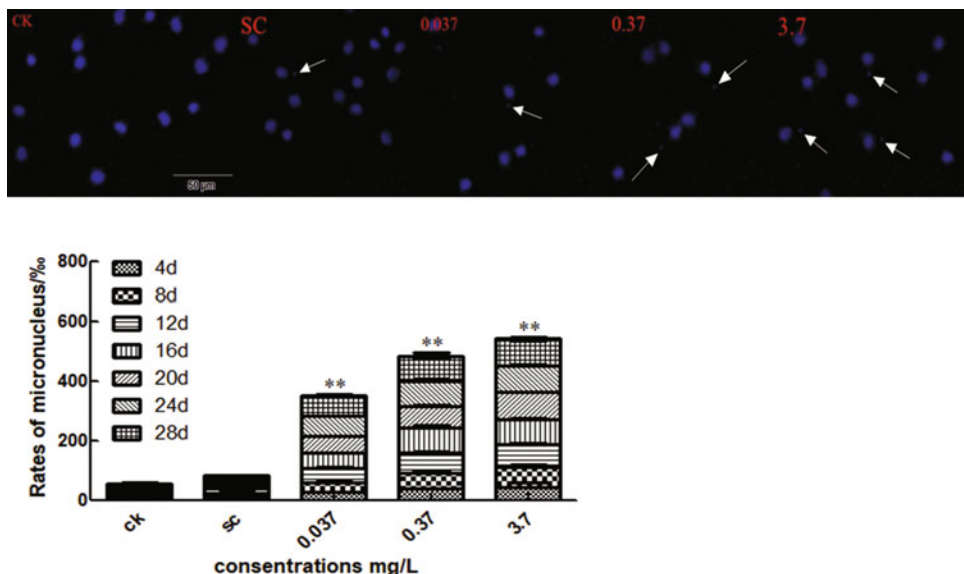


Fig. 1 Rats of micronucleus (DAPI staining) on tilapia liver cells induced by cyantraniliprole. ** mean significance level on Duncan test ($p < 0.01$); * mean significance level on Duncan test ($p < 0.05$). The pictures were picked from each treatment of 28 days exposure

5. After electrophoresis, the slides be neutralized with 0.4 M Tris (pH 7.4) for 5 min [25]. The slides are fixed sequentially in 50, 70, 95, and 100% ethanol for 5 min each.
6. Next, they are stained with Gelred 100× 40 mL and observed under an Olympus BX53F fluorescence microscope, use the 520 nm emission filter and a 40-objective lens. For each fish, 100 nuclei are analyzed per sample.
7. The tail length, olive tail moment, and tail DNA % are calculated as the sum of the number of nucleoids observed in each damage class by using the Comet Assay Software (CaspLab, USA) (Fig. 2).
8. The length of comet tails is increased by 2.5%, 8.0%, and 10.8% in the dose of 0.037, 0.37, and 3.7 mg/L of cyantraniliprole, respectively, compared with the blank control group at the time point of 4-day exposure. The length of comet tails is significantly increased 5.2, 9.0, and 11-fold in response to 0.037, 0.37, and 3.7 mg/L of cyantraniliprole, respectively, compared with the blank control group at time point of 28-day exposure. The length of comet tails of the black and solvent controls is 3.24 and 3.17 mm, respectively, at time point of 4-day exposure, and 3.04 and 3.24 mm at time point of 28 day after 28 days of exposure (Fig. 2).
9. The tail DNA% is significantly increased by 3.8, 6.6, and 4.4-fold in the dose of cyantraniliprole 0.037, 0.37, and 3.7 mg/L compared with blank control group, respectively. That of the

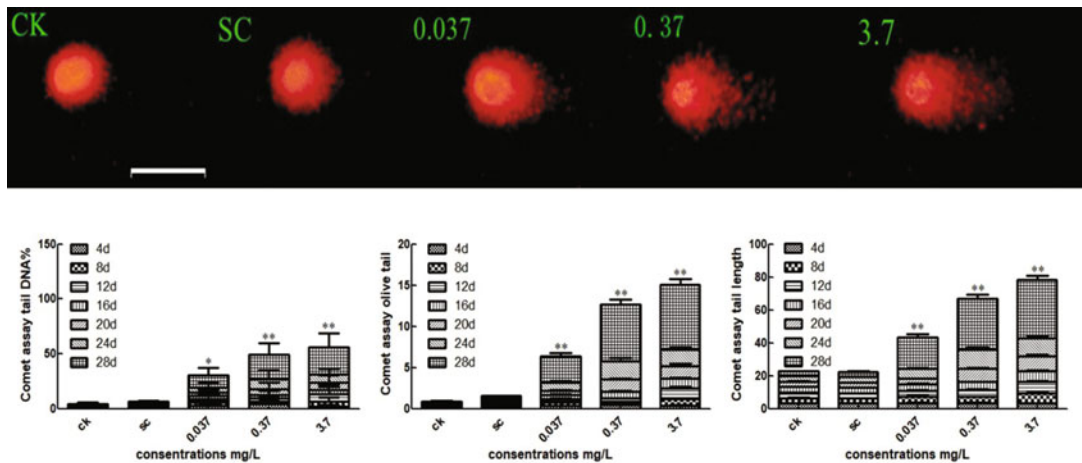


Fig. 2 Comet tails, tail DNA%, and olive tail moment of tilapia liver cells induced by cyantraniliprole. ** mean significance level on Duncan test ($p < 0.01$); * mean significance level on Duncan test ($p < 0.05$). The picture was picked from each treatment of 28 days exposure

respective blank and solvent controls are 0.53% and 0.88%, respectively, at the time point of 4-day exposure. The tail DNA% are significantly increased 18, 37, and 42-fold in the treatment groups of 0.037, 0.37, and 3.7 mg/L of cyantraniliprole compared with the blank control group, respectively, while those of the respective blank and solvent controls were 0.58% and 1.05% after 28 days of exposure (Fig. 2).

10. The olive tail moment was significantly increased 2.3, 3.3, and 2.8-fold in the dose of cyantraniliprole 0.037, 0.37, and 3.7 mg/L, respectively, compared with the blank control group. The olive tail moment of the respective blank and solvent controls was 0.099 and 0.190 mm, respectively, at the time point of 4-day exposure. The olive tail moment is significantly increased 27, 61, and 69-fold in the dose of 0.037, 0.37, and 3.7 mg/L-treated groups, respectively, compared with the blank control group. The olive tail moment of the blank and solvent controls were 0.11 and 0.27 mm after 28 days of exposure (Fig. 2).
- 3.8 Real-Time Fluorescence Quantitative PCR (qPCR)**
1. The liver RNA is extracted with TRIZOL reagent (see Notes 1 and 2) [26].
 2. The normal agarose gel electrophoresis and ultraviolet absorption method are used to detect the integrity and quality of RNA (Table 3), and Roche's transcriptor first strand cDNA synthesis kit is used to reverse transcribe RNA into cDNA after qualification according to the instructions.
 3. The detected genes and primers are all in Table 3. The reverse transcription of cDNA is diluted to the same concentration and

then pressed on the LightCycler 96® (Roche Diagnostics A/s) instrument by SYBR Green I Master (Roche Diagnostics A/s) kit method (*see Notes 3, 4 and 5*).

4. The data analysis of qPCR results is carried out according to the $2^{-\Delta\Delta C_q}$ method.
5. In this study, the effects of cyantraniliprole on the mRNA levels of liver cell cycle regulatory genes (indicated in parentheses) involved in p53 pathway (p53 and Chk2), G1/S phase (Cdk2, Orc1, Ccna1, Ccne1), G2/M phase (Ccnb), and DNA repair (Rpa3 and Fen1) are analyzed (Table 3). The expression of Rpa3 gene is significantly upregulated as compared with the blank control group induced by cyantraniliprole, mapping with GAPDH and b-actin as housekeeper genes. The expression of Chk2 gene, however, is significantly downregulated as compared with the blank control group induced by cyantraniliprole, mapping with GAPDH and b-actin as housekeeper genes, in a dose-response manner (Fig. 3, Table 3). The results

Table 3
Purity detection of RNA

Treatments	Concentration (mg/L)	RNA concentration (ng/ μ L)	OD260/OD280
Cyantraniliprole	0.037	746	1.96
	0.37	745	1.92
	3.7	748	1.88
Solvent control	48	745	1.95
Control	0	738	1.99

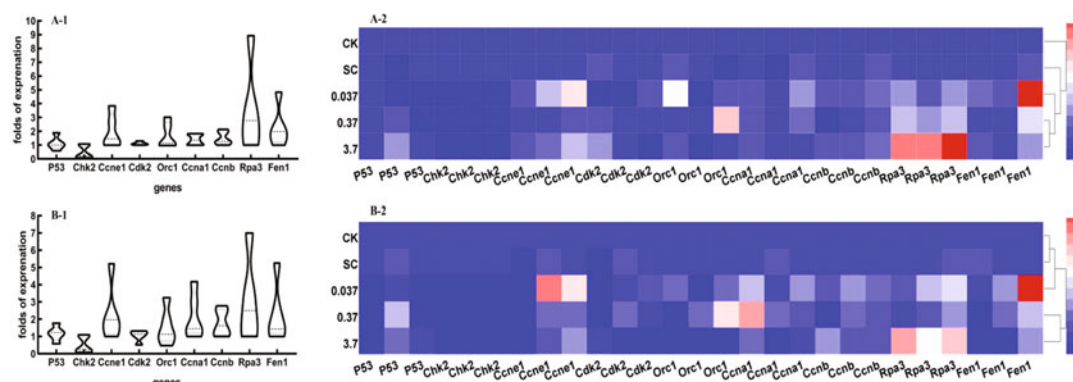


Fig. 3 Differential gene expression patterns in tilapia induced by cyantraniliprole. Note: Each row represents an experimental condition, every three columns represent a gene. Expression differences are shown in different colors. (a-1) Violin plots of the expression of genes by β -actin as housekeeper gene. (a-2) Heatmap of the expression of genes by β -actin as housekeeper gene. (b-1) Violin plots of the expression of genes by GAPDH as housekeeper gene. (b-2) heatmap of the expression of genes by GAPDH as housekeeper gene

suggest that DNA of liver cells of tilapia is damaged, which are related with the expression of Chk2 in p53 pathway and Rpa 3 genes in the repair pathway.

3.9 Data Analysis

1. The LC50 value is tested by probabilistic analysis. After performing Duncan Test, there is a significant difference in LC50 values ($*p < 0.05$; $**p < 0.01$; $***p < 0.001$). All data are analyzed with SPSS 17.0 (SPSS, Chicago, IL, USA). All values are represented by mean \pm standard deviation (SD).
2. The image analysis software of the Comet Assay Software Pect (CASP) is used to process comet image data and analyze the comet tail length, olive tail distance, and tail DNA content. The data of comet tail length, olive tail distance, and tail DNA % content are analyzed by SPSS statistics 17.0 software.
3. The quantification cycle (C_q) values of each gene are obtained and the obtained average C_q values are further analyzed. Multiple changes of the tested genes are calculated by the $2^{-\Delta\Delta C_q}$ method.

4 Notes

1. Isolation of RNA from small quantities of tissue or cell to samples: Add 800 μ L of TRIzol to the tissue or cells. Following sample lysis, add chloroform and proceed with the phase separation as described. Prior to precipitating the RNA with isopropyl alcohol, add 5–10 μ g RNase-free glycogen as carrier to the aqueous phase. To reduce viscosity, shear the genomic DNA with 2 passes through a 26 gauge needle prior to chloroform addition. The glycogen remains in the aqueous phase and is co-precipitated with the RNA. It does not inhibit first-strand synthesis at concentrations up to 4 mg/mL and does not inhibit PCR.
2. After homogenization and before addition of chloroform, samples can be stored at –60 to –70 °C for at least 1 month. The RNA precipitate can be stored in 75% ethanol at 2–8 °C for at least 1 week, or at least 1 year at –5 to –20 °C.
3. SYBR® GreenI is provided under licensing agreement with Molecular Probes Inc. for internal research use only.
4. LightCycler® is a trademark of Roche Diagnostics. This product is for research use only. It is not intended for use in therapeutic or diagnostic procedures for humans or animals. Also, do not use this product as food, cosmetic, or household item, etc.
5. TaKaRa products may not be resold or transferred, modified for resale or transfer, or used to manufacture commercial

products without written approval from TaKaRa Biotechnology (Dalian) Co., Ltd.

References

- Parolini M, Magni S, Castiglioni S, Binelli A (2016) Genotoxic effects induced by the exposure to an environmental mixture of illicit drugs to the zebra mussel. *Ecotoxicol Environ Saf* 132:26–30
- Alleva R, Manzella N, Gaetani S, Ciarapica V, Bracci M, Caboni MF, Pasini F, Monaco F, Amati M, Borghi B, Tomasetti M (2016) Organic honey supplementation reverses pesticide-induced genotoxicity by modulating DNA damage response. *Mol Nutr Food Res* 60:2243–2255
- Želježić D, Mladinić M, Žunec S, Lucić Vrdoljak A, Kašuba V, Tariba B, Živković T, Marjanović AM, Pavčić I, Milić M, Rozgaj R, Kopjar N (2016) Cytotoxic, genotoxic and biochemical markers of insecticide toxicity evaluated in human peripheral blood lymphocytes and an HepG2 cell line. *Food Chem Toxicol* 96:90–106
- Li D, Huang Q, Lu M, Zhang L, Yang Z, Zong M, Tao L (2015) The organophosphate insecticide chlorpyrifos confers its genotoxic effects by inducing DNA damage and cell apoptosis. *Chemosphere* 135:387–393
- Horibe A, Odashima S, Hamasuna N, Morita T, Hayashi M (2018) Weight of contribution of in vitro chromosomal aberration assay for evaluation of pesticides: experience of risk assessment at the food safety Commission of Japan. *Regul Toxicol Pharmacol* 95:133–141
- Yoshida M, McGregor D (2013) First draft prepared by Midori Yoshida¹ and Douglas McGregor² division of pathology. National Institute of Health Sciences, Tokyo, Japan
- Wang M, Lu M (2016) Tilapia polyculture: a global review. *Aquac Res* 47:2363–2374
- Chen L, Jiang X, Feng H, Shi H, Sun L, Tao W, Xi Q, Wang D (2016) Simultaneous exposure to estrogen and androgen resulted in feminization and endocrine disruption. *J Endocrinol* 228:205–218
- Stickney RR (1986) Tilapia tolerance of saline waters: a review. *Prog Fish-Cult* 48:161–167
- Tiwari S, Stelinski LL (2013) Effects of cyantraniliprole, a novel anthranilic diamide insecticide, against Asian citrus psyllid under laboratory and field conditions. *Pest Manag Sci* 69:1066–1072
- Moreno I, Belando A, Grávalos C, Bielza P (2018) Baseline susceptibility of Mediterranean strains of *Trialeurodes vaporariorum* (Westwood) to cyantraniliprole. *Pest Manag Sci* 74:1552–1557
- Zhang R, Jang EB, He S, Chen J (2015) Lethal and sublethal effects of cyantraniliprole on *Bactrocera dorsalis* (Hendel) (Diptera: Tephritidae). *Pest Manag Sci* 71:250–256
- Xu C, Ding J, Zhao Y, Luo J, Mu W, Zhang Z (2017) Cyantraniliprole at sublethal dosages negatively affects the Development, reproduction, and nutrient utilization of *Ostrinia furnacalis* (Lepidoptera: Crambidae). *J Econ Entomol* 110:230–238
- Zhang Z, Xu C, Ding J, Zhao Y, Lin J, Liu F, Mu W (2019) Cyantraniliprole seed treatment efficiency against *Agrotis ipsilon* (Lepidoptera: Noctuidae) and residue concentrations in corn plants and soil. *Pest Manag Sci* 75:1464–1472
- Sharma AK, Zimmerman WT, Singles SK, Malekani K, Swain S, Ryan D, McQuorcobale G, Wardrope L (2014) Photolysis of chlorantraniliprole and cyantraniliprole in water and soil: verification of degradation pathways via kinetics modeling. *J Agric Food Chem* 62:6577–6584
- Authority EFS (2014) Conclusion on the peer review of the pesticide risk assessment of the active substance cyantraniliprole. *EFSA Journal* 12:3814
- Lindahl T, Wood RD (1999) Quality control by. *DNA Repair* 286:1897–1905
- Hayashi M (2016) The micronucleus test—most widely used in vivo genotoxicity test. *Gene Environ* 38:18
- Glei M, Schneider T, Schlörmann W (2016) Comet assay: an essential tool in toxicological research. *Arch Toxicol* 90:2315–2336
- Pei DS, Strauss PR (2013) Zebrafish as a model system to study DNA damage and repair. *Mutat Res* 743–744:151–159
- Chen HY (2017) Hepatotoxicity of commonly used organophosphate flame retardants in Aebrafsh (*Danio rerio*) School of the Environment. Nanjing University, Nanjing, Jiangsu, China
- Development, O. f. E. C.-o. a. (1992) Test no. 203: fish, acute toxicity test. *OECD Guidel. Test. Chem.* 1, 1e10 (10)

23. El-Harbawi M (2014) Toxicity measurement of imidazolium ionic liquids using acute toxicity test. *Procedia Chem* 9:40–52
24. Thomas P, Holland N, Bolognesi C, Kirsch-Volders M, Bonassi S, Zeiger E, Knasmueller S, Fenech M (2009) Buccal micronucleus cytome assay. *Nat Protoc* 4:825–837
25. Lorenzo Y, Costa S, Collins AR, Azqueta A (2013) The comet assay, DNA damage, DNA repair and cytotoxicity: hedgehogs are not always dead. *Mutagenesis* 28:427–432
26. Jordon-Thaden IE, Chanderbali AS, Gitzen-danner MA, Soltis DE (2015) Modified CTAB and TRIzol protocols improve RNA extraction from chemically complex Embryo-phyta. *Appl Plant Sci* 3:apps.1400105

Part II

Plant Toxicity



Chapter 15

Impact of Nanoparticles on Plant Growth, Development, and Biomass

Ilya N. Boykov and Baohong Zhang

Abstract

Nanoparticles are an extensive class of naturally occurred or man-made objects; it has been widely using in our daily life. As increasing usage, nanoparticles are also released into the environment and are becoming an emerged environmental pollution. In the past decade, impact of nanoparticles on plant growth and development has been becoming a major research topic in the environmental toxicology. In this chapter, we introduce a step-by-step protocol for investigating the effects of nanoparticles on plant growth and development as well as biomass production. Additionally, this protocol also tests the water content and the rate of root and up-ground part to better explain the impact of nanoparticles on plant growth. This protocol adopts plant tissue culture technology to culture plants which makes test easier and can be tested anytime during the year.

Key words Nanoparticle, Plant, Seed germination, Plant biomass, Root development

1 Introduction

Nanoparticles are an extensive class of components. It can be naturally occurred and also can be man-made. A nanoparticle does not mean it is a tiny object; this is because, based on the commonly accepted definition, nanoparticles are any objects with size 1 to 100 nm in any one dimension. This means that there are three classes of nanoparticles based on their dimensions. Some nanoparticles only have one dimension with 1 to 100 nm, such as nanodiscs and nanoplates. Some nanoparticles may have two dimensions with 1 to 100 nm, such as nanofibers and nanotubes. There are also some nanoparticles with three dimensions with 1 to 100 nm. There are also other many classifications for nanoparticles. For example, according to their chemical composition, nanoparticle can be divided into metal nanoparticles, carbon nanoparticle, and others.

Nanoparticles have wide application in many fields, including biomedicine, agriculture, construction as well as daily life. In biomedicine, nanoparticles serve as a carrier for delivering drugs into specific cells for treating different diseases, including cancers [1–4]. In daily life, nanoparticles are an important component in many cosmetic products and also the food additives, for example titanium dioxide nanoparticle has strong ultraviolet light blocking properties and is widely added into sunscreen to protect people from sunlight burning. As increasing usage of nanoparticles, more and more nanoparticles are released into the environment and now nanoparticles have been becoming one of emerging environmental pollutions. Many studies show that nanoparticles have negative effects on plants, animals, and microbes although there are lots of application of nanoparticle on these organisms [5]. Many nanoparticles have phytotoxic effects on seed germination and root development and further affected plant growth and development [6–16]. Because of easy culture and no ethic-related issues, plants currently have been widely used to study the impact of nanoparticles at different levels, including individual, cellular, biochemical, physiological, and molecular levels. In this chapter, we present a step-by-step method for investigating the phytotoxic effects of nanoparticles on seed germination, seedling growth, and development. Here, we present a plant tissue culture method that allows to test nanoparticles in laboratory condition for obtaining constant results. In this chapter, we use metal oxide nanoparticle as an example. This method also can be employed to test other nanoparticles as well as other chemicals on their impact on plant seed germination as well as seedling growth and development.

2 Materials

2.1 Chemicals and Regents

1. Murashige and Skoog (MS) medium powder [17] (*see Note 1*).
2. Deionized water (diH₂O).
3. Agar.
4. Titanium dioxide (TiO₂) nanoparticle (*see Note 2*).
5. Isopropyl alcohol (70%).
6. Sucrose.
7. HCl (1 N).
8. NaOH (1 N).
9. Saturated CaSO₄ solution.

2.2 Plant Species

Any seeds can be used in this test. Here just using Alamo switchgrass seeds as an example.

2.3 Instruments

1. Autoclave.
2. Ultra-clean workbench.
3. Incubator with light control or plant tissue culture room.
4. Balance.
5. Pipette (10, 200, and 1000 µL).
6. pH meter.
7. Epson Perfection V800 Photo scanner.
8. Computer with software WinRHIZO 2007 (Regent Instruments Inc., Canada).
9. A polarographic O₂ electrode-Chlorolab 2 oxygen measurement system.
10. Oven for drying samples.

2.4 Other Lab**Suppliers**

1. Petri dishes (10 cm × 20 mm).
2. Pipette tips (10, 200, and 1000 µL).
3. Beaker (500 mL).
4. Flask (500 mL).
5. Weighting boat or weighting paper.
6. Aluminum paper.
7. Centrifuge tube (2 and 50 mL).
8. Bleach (8.25% sodium hypochlorite).
9. Filter paper.

3 Methods**3.1 Preparation
of Culture Medium**

1. Prepare five 500 mL beakers.
2. Add about 50 mL diH₂O into each beaker.
3. Weigh five 0.86 g MS medium powder.
4. Add 0.86 MS medium powder into each beaker.
5. Add 4 g sucrose into each beaker (*see Note 3*).
6. Weigh TiO₂ nanoparticle for making medium containing 0, 1.0, 2.0, and 5.0 g/L TiO₂.
7. Add the weighting nanoparticle into each prepared beaker with MS medium, no nanoparticle is added into the fifth one because it will serve as control.
8. Add diH₂O to the total volume to 200 mL.
9. Mix the medium very well.
10. Adjust pH volume to 5.8 by adding 1 N NaOH or HCl.
11. Add 8 g/L agar into each beaker.

12. Transfer the medium into a 500 mL flask.
13. Cover the flasks with aluminum paper.
14. Autoclave at 121 °C for 15 min.
15. Cool down the medium to about 50–60 °C.
16. Mix the medium very well and pour the medium into 5 Petri dishes and each dish contains 40 mL medium with/without nanoparticles (*see Note 4*).
17. Label each Petri dish with the nanoparticle concentration.
18. Cool down the medium to the room temperature.
19. Store at refrigerator if not used immediately.

3.2 Seed Sterilization

1. Select about 1000 mature and healthy seeds (*see Note 5*).
2. Add the seeds into a 50 mL centrifuge tube.
3. Add 15 mL 70% isopropyl alcohol into the tube (*see Note 6*).
4. Mix the alcohol with the seeds very well.
5. Sit there for 2 min sterilization. During this period, the tubes are inverted multiple times to make sure all seeds sterilized.
6. Discard the fluid. The floating seeds are also discarded because the floating seeds more likely are immature seeds and may also cause contamination.
7. Add 40 mL bleach into the tube with seeds.
8. Sit there and sterilize for 15 min. During this period, the tubes are inverted multiple times to make sure all seeds sterilized.
9. Discard the fluid.
10. Seeds are washed at least three times with sterilized diH₂O to remove the bleach residues (*see Note 7*).

3.3 Seed Plant and Culture

1. Transfer sterilized seeds onto a sterilized Petri dish containing sterilized filter paper (*see Note 8*).
2. Plant seeds on Petri dish. Each Petri dish will be planted 25 seeds with equally distributing on the plate.
3. Culture the seeds in a growth chamber, growth incubator, or a plant tissue growth room at 28 °C with 16/8 light/dark cycle (*see Note 9*).

3.4 Seed Germination, Observation, and the Study on Seedling Growth and Development

1. Observe the seed germination daily. Record the start day for seed germination, root and shot emergence, and the potential color change and the change between survival and death (*see Note 10*).
2. At day 14 after culture, the total number of seeds germinated in each plate is counted and recorded in an excel sheet.

3. The germination rate is calculated for each biological replicate and also for each treatment, including the control.
4. As per plate, for each seedling, the numbers of root and leaf are counted and recorded. The average is calculated, which will serve as a biological replicate.
5. As per plate, for each seedling, the length of root and the height of seedling is measured and recorded. The average is calculated for the plate, which will serve as a biological replicate.
6. An individual plant is scanned by using Epson Perfection V800 Photo scanner and pictures are taken.
7. Software WinRHIZO is employed to analyze the root length, root area, root volume, and the root diameter. The length of the main root and the length of root without branched roots are also measured.

3.5 Measurement of Root and Leaf Respiration

1. At day 14 of treatment, randomly pick six seedlings from each treatment groups or controls.
2. Roots and leaves are separated for each plant individually.
3. Root or leaves are weighted for each plant.
4. Samples are placed into the incubator chamber of the polarographic O₂ electrode-Chlorolab 2 oxygen measurement system.
5. Add 2 mL saturated CaSO₄ solution.
6. Close the chamber.
7. Measure the consumption of O₂ for 10 min.
8. The consumption rate of O₂ is calculated.

3.6 Measurement of Both Fresh and Dry Weight as Well as the Water Content

1. Fresh weight.
 - (a) At day 14 of treatment, all seedlings are collected and recorded from each plate of each treatment and the control.
 - (b) Roots and leaves are separated.
 - (c) The fresh weight of leaves and roots are weighted and recorded for each biological replicate.
 - (d) The average fresh weight of leaves and roots per seedling are calculated for each biological replicate.
 - (e) The average fresh weight of an entire seedling is calculated for each biological replicate.
 - (f) The rates of fresh roots and leaves are calculated for each biological replicate.

2. Dry weight

- (a) At day 14 of treatment, after weighing the fresh weight of leaves and roots for each biological replicate, the roots and leaves are placed on a weighting boat with clearly labeled in which what the samples belongs to.
- (b) Place the leaves and root samples in a dry oven.
- (c) Dry for 7 days at 70 °C.
- (d) When the samples are completely dried, weigh the dry weight for each sample.
- (e) The average dry weight of leaves and roots per seedling are calculated and recorded for each biological replicate.
- (f) The average dry weight of an entire seedling is calculated and recorded for each biological replicate.
- (g) The rates of dry roots and leaves are calculated for each biological replicate.
- (h) The water content (%) is calculated for each biological replicate by using the formula: water content (%) = (fresh weight – dry weight) ÷ fresh weight × 100.

3.7 Data Analysis

1. All data are recorded in an excel file.
2. All data were analyzed using the statistical software SPSS or other statistical software.
3. The means and standard derivations (or standard errors) are calculated for each trait.
4. An ANOVA test is employed to analyze the significance between treatments and the controls.

4 Notes

1. MS medium contains both macronutrient mixtures and vitamins mixtures [17]. It can be made in the lab by adding the individual components based on the original Ref. 17. However, a lot of company sell this pre-made products that make people easier to prepare the medium.
2. This chapter just use titanium dioxide (TiO_2) nanoparticle as an example; this method can be used to test any chemical or component.
3. Because seeds contain nutrient and carbohydrate for seed germination, it is not necessary to add the sugar. However, adding sugar has additional function in which it can be used to monitor bacteria contamination. If the seeds are not sterilized well, there will be bacteria colonies growing in about 3 days after planting the seeds on the medium. The sucrose can be replaced by other sugar and the concentration is also flexible.

4. This step need to be done in the ultra-clean workbench to avoid contamination. If the prepared media are not used immediately, it can be stored at refrigerator for a short time.
5. The method described in this chapter can be used to test any plant. Switchgrass is just an example to show this method. Selecting mature and healthy seeds is very important which will keep the experiment consistent and reproducible. Before sterilizing the seeds, it should calculate how many seeds needed for this experiment. In this method, there are 5 biological replicates for each of 5 treatment and controls, each biological replicate (plate) contains 25 seeds, there are a total $25 \times 5 = 125$ seeds for each treatment. For the total experiment, it will need a total of 575 seeds. However, to make sure there are enough good seeds for planting, in this chapter we suggest preparing about 1000 seeds.
6. From this step, all operation should be performed in clean hood or workbench to avoid contamination. The workspace is also cleaned by 70% alcohol.
7. It is very important to completely remove the bleach residue. This is because that bleach can damage or even kill the seeds if it is not washed off.
8. It is important to avoid any potential contamination during each step. Here, we suggest to take about 150–200 sterilized seeds for each time. After it is done, change a new sterilized Petri dish and transfer more seeds for continuously planting. During each step, it also needs to make sure the tools and your hands are sterilized by using 70% alcohol.
9. It is better to place the Petri dishes at some angle. In that way, root will grow down, and root will grow up, it is easy for observation and later seedling separation.
10. Nanoparticles significantly affect seed generation and seedling development with a dose-dependent manner. At low concentrations, nanoparticles did not inhibit seed germination and some case, if the concentration is suitable, it may enhance seed germination; however, high concentrations of nanoparticle do significantly inhibit seed generation [13, 14]. It is same for the seedling growth and development.

References

1. Nie SM, Xing Y, Kim GJ, Simons JW (2007) Nanotechnology applications in cancer. *Annu Rev Biomed Eng* 9:257–288
2. De Jong WH, Borm PJA (2008) Drug delivery and nanoparticles: applications and hazards. *Int J Nanomedicine* 3:133–149
3. Shipway AN, Katz E, Willner I (2000) Nanoparticle arrays on surfaces for electronic, optical, and sensor applications. *Chem Phys Chem* 1:18–52
4. Singh R, Lillard JW (2009) Nanoparticle-based targeted drug delivery. *Exp Mol Pathol* 86:215–223
5. Lopez-Serrano A, Olivas RM, Landaluze JS, Camara C (2014) Nanoparticles: a global vision. Characterization, separation, and

- quantification methods. Potential environmental and health impact. *Anal Methods* 6:38–56
6. Budhani S, Egbochue NP, Arslan Z, Yu H, Deng H (2019) Phytotoxic effect of silver nanoparticles on seed germination and growth of terrestrial plants. *J Environ Sci Health C Environ Carcinog Ecotoxicol Rev* 37:330–355
 7. Liu J, Wolfe K, Cobb GP (2019) Exposure to copper oxide nanoparticles and arsenic causes intergenerational effects on Rice (*Oryza sativa* japonica Koshihikari) seed germination and seedling growth. *Environ Toxicol Chem* 38:1978–1987
 8. López-Luna J, Cruz-Fernández S, Mills DS, Martínez-Enríquez AI, Solís-Domínguez FA, Del Carmen Ángeles González-Chávez M, Carrillo-González R, Martinez-Vargas S, Mijangos-Ricardez OF, Del Carmen Cuevas-Díaz M (2020) Phytotoxicity and upper localization of Ag@CoFe(2)O(4) nanoparticles in wheat plants. *Environ Sci Pollut Res Int* 27:1923–1940
 9. Pelegriño MT, Kohatsu MY, Seabra AB, Monteiro LR, Gomes DG, Oliveira HC, Rolim WR, de Jesus TA, Batista BL, Lange CN (2020) Effects of copper oxide nanoparticles on growth of lettuce (*Lactuca sativa* L.) seedlings and possible implications of nitric oxide in their antioxidative defense. *Environ Monit Assess* 192:232
 10. Singh D, Kumar A (2019) Assessment of toxic interaction of nano zinc oxide and nano copper oxide on germination of *Raphanus sativus* seeds. *Environ Monit Assess* 191:703
 11. Ullah H, Li X, Peng L, Cai Y, Mielke HW (2020) In vivo phytotoxicity, uptake, and translocation of PbS nanoparticles in maize (*Zea mays* L.) plants. *Sci Total Environ* 737:139558
 12. Wang W, Ren Y, He J, Zhang L, Wang X, Cui Z (2020) Impact of copper oxide nanoparticles on the germination, seedling growth, and physiological responses in *Brassica pekinensis* L. *Environ Sci Pollut Res Int* 27 (25):31505–31515
 13. Boykov IN, Shuford E, Zhang B (2019) Nano-particle titanium dioxide affects the growth and microRNA expression of switchgrass (*Panicum virgatum*). *Genomics* 111:450–456
 14. Burkew CE, Ashlock J, Winfrey WB, Zhang B (2012) Effects of aluminum oxide nanoparticles on the growth, development, and microRNA expression of tobacco (*Nicotiana tabacum*). *PLoS One* 7:e34783
 15. Frazier TP, Burkew CE, Zhang B (2014) Titanium dioxide nanoparticles affect the growth and microRNA expression of tobacco (*Nicotiana tabacum*). *Funct Integr Genomics* 14:75–83
 16. Khan MR, Adam V, Rizvi TF, Zhang B, Ahamad F, Joško I, Zhu Y, Yang M, Mao C (2019) Nanoparticle-Plant Interactions: Two-Way Traffic. *Small* 15:e1901794
 17. Murashige T, Skoog F (1962) A revised medium for rapid growth and bio assays with tobacco tissue cultures. *Physiol Plant* 15:473–497



Chapter 16

Biochemical and Physiological Toxicity of Nanoparticles in Plant

Zhiyong Zhang and Baohong Zhang

Abstract

As increasing application of nanoparticles, nanoparticles have been becoming a new emerging environmental pollution that attracts a lot of attention from the scientific community and also regulatory agents. In the past decade, studying the toxicity and environmental impacts of nanoparticles is becoming a hot research field and more and more researches have been published using both plant and animal system. In this chapter, using oxidized metal nanoparticles as an example, we introduce a detailed protocol for performing research on biochemical and physiological toxicity of nanoparticles in plant. We employ a hydroponics system to study phytotoxicity of nanoparticles, which makes it easier to study the impact of nanoparticles. In this chapter, we majorly focus on plant respiration and photosynthesis, root vigor as well as oxidative stress. Oxidative stress is one major physiological response to different environmental pollution, in which we present a detailed method for detecting free radical oxygen species as well as the major molecules and enzymes associating with oxidative stress, including SOD and POD. Although we introduce the methods using cotton as an example, the protocols presented in this chapter can be used almost any plant species to test the biochemical and physiological toxicity of an environmental pollution.

Key words Nanoparticle, Plant, Biochemical toxicity, Physiological toxicity, Photosynthesis

1 Introduction

Nanoparticles are one big family of components. Due to their special characteristics, nanoparticles are widely used in many fields, including construction, engineering, bioenergy, agriculture, and biomedicine [1]. Nanoparticles are also widely used in our daily life, such as in food and cosmetics. As increasing application of nanoparticles, more and more nanoparticle residues are also released into the environment and become a critical pollution. Although nanoparticles can be used in agriculture production in which nanoparticles can increase crop yield and increase pesticide efficiency [2–4], many studies also show that overuse of nanoparticles generates lots of negative impact on plant growth and development [5]. Several studies show that nanoparticles inhibited seed

germination, root elongation, and seedling development [5–11]. At molecular levels, nanoparticles induced aberrant expression of both protein coding genes [12–15] and small regulatory RNAs [6–8, 16–19], such as microRNAs (miRNAs), an important gene regulator controlling gene expression at the post-transcription levels [20]. Several studies also show that nanoparticles caused genetic mutants [21–23]. Nanoparticle exposure also caused plant response at the physiological and biochemical levels [13, 24–26].

Cotton is one of the most important economic crops and is also the leading crop for fiber; cotton is also an important resource for oil, protein, and vitamin E. Thus, cotton is widely cultivated in the world. Due to the long growth season and wide cultivation, cotton is more likely exposed to nanoparticle residues generated from our daily life, agriculture, and others. Thus, we use cotton as an example to present the step-by-step protocols for analyzing biochemical and physiological toxicity of nanoparticles in plants. These methods can be used to test other plant species with other nanoparticles with minor modification.

2 Materials

2.1 *Chemicals and Reagents*

1. Hoagland medium powder [27] (*see Note 1*).
2. Deionized water (diH₂O).
3. 10% hydrogen peroxide.
4. Titanium dioxide (TiO₂) nanoparticle (*see Note 2*).
5. Anhydrous sulfuric acid (H₂SO₄).
6. Saturated CaSO₄ solution.
7. Triphenyltetrazolium chloride (TTC).
8. Na₂HPO₄.
9. NaH₂PO₄.
10. NaCl.
11. KCl.
12. 3,3'-diaminobenzidine (DAB).
13. 95% ethanol.
14. 5% trichloroacetic acid solution.
15. Ice.
16. Quartz and 50 mM sodium phosphate buffer (pH 7.8).
17. 0.1 mM ethylenediaminetetraacetic acid (EDTA).
18. 0.3% guaiacol and hydrogen peroxide (H₂O₂).
19. 0.075 mM nitroblue tetrazolium (NBT).

20. 13 mM methionine.
21. 1.3 μ M riboflavin.
22. 10 mM hydroxylamine hydrochloride.
23. 17 mM sulfanilic acid.
24. 7 mM 1-naphthylamine solution.

2.2 Plant Species

Cotton (*Gossypium hirsutum* L.) cv. Texas Marker-1 (TM-1) (see Note 3).

2.3 Instruments

1. Autoclave.
2. A continuous excitation chlorophyll fluorimeter-Handy PEA (Hansatech).
3. Incubator with light control or plant culture room.
4. Balance.
5. Pipette (10, 200, 1000, and 5000 μ L).
6. pH meter.
7. Water bath.
8. A liquid-phase oxygen measurement system—Chlorolab 2.
9. Oven for drying samples.
10. Spectrophotometer.
11. Plate heater.
12. Centrifuge.

2.4 Other Lab Suppliers

1. Plastic box (internal length \times width \times depth = 23 cm \times 16 cm \times 15 cm)(the size is variable depending on the market supply).
2. Styrofoam board.
3. Aluminum paper.
4. Scissors.
5. Balance.
6. Weighting boat or weighting paper.
7. Beaker.
8. Graduated cylinder.
9. Seed germination paper (10 in. \times 15 in.).
10. Glass rod.
11. Centrifuge tube (15 mL).
12. Mortar and pestle.

3 Methods

3.1 Preparation of Culture Containers

1. Wrap the plastic box using aluminum paper (*see Note 4*).
2. Measure and cut the Styrofoam board (serve as cover) to a perfect size to cover the plastic boxes. The Styrofoam board is usually 2 cm thickness, and wedged to the plastic box, which makes the box solution depth 2 cm less. Alternatively, 0.5 cm thick board can be used to cover the box, which keeps the box solution depth same, but the board need to be fixed to avoid moving. The solution volume and sponge piece width were calculated according to 2 cm thickness Styrofoam.
3. Dig 8 holes evenly with 2 cm in diameter on the Styrofoam board cover (2×4). These holes will be used to hold the plants.
4. Cut sponge into pieces of about 2 cm in wide and 10 cm in length. These prepared pieces of sponge will be wrapped with the plants and provide support to the plants to hold on the Styrofoam board cover.

3.2 Preparation of Hoagland Medium

1. If using Hoagland medium powder purchased from Sigma-Aldrich, weight 1.6 g power (H2395) and then dissolve in 1 L diH₂O. If no pre-made medium, Hoagland solution can be made freshly in two steps: (a) making stock solution (1000×) for each macronutrient, micronutrients and ferric solution, separately; (b) dilute the stock solution into final concentration by diluting 1000×. The final concentration for individual component are as follows: Calcium nitrate·4H₂O (590.4 mg/L), Potassium dihydrogen phosphate (68.1 mg/L), Potassium chloride (186.4 mg/L), Sodium chloride (116.9 mg/L), Boric acid (1.2 mg/L), Cupric sulfate·5H₂O (0.05 mg/L), Ethylenediaminetetraacetic acid Ferric sodium (36.7 mg/L), Magnesium sulfate·5H₂O (246.5 mg/L), Manganese sulfate·1H₂O (0.2 mg/L), Hexaammonium heptamolybdate·4H₂O (0.006 mg/L), and Zinc sulfate·7H₂O (0.3 mg/L). Before preparing the solution, the total volume of solution is needed to calculate to make right amount solution for both treatments and control (taking 4 treatments and control as example). In this described study, we plan to plant a total of 24 plants for each treatment and control. For each plastic culture, box will hold 8 plants. Thus, 3 boxes are needed for each treatment or control. The box size containing solution is 23 cm × 16 cm × 15 cm, which will need a total of about $23 \text{ cm} \times 16 \text{ cm} \times 13 \text{ cm} = 4784 \text{ mL} = 4.784 \text{ L}$. Thus, a total solution need is $4.784 \text{ L} \times 3 \times 5 = 71.76 \text{ L}$. Thus, a total of 75 L Hoagland solution will be made for this presented method. If there is no so big container, this can be made for

multiple times, such as making each treatment per time. It may be good to make solution from low to high concentration, of nanoparticles in that way, the container do not need to be washed each time.

2. Mix it thoroughly.
3. Divide the medium into 5 big medium containers, in which each container has 15 L of Hoagland solution. Each container will be used to prepare the solution for 4 treatments and one control. Thus, label each container clearly.
4. Weight and add TiO_2 nanoparticle to the final concentrations of 0, 0.1, 1, 2, and 5%, respectively.
5. Mix the solution thoroughly and allow TiO_2 nanoparticles evenly distributed in the solution (*see Note 5*).
6. Divide the solution into the prepared plastic culture container box. Each treatment or control will have three containers.

3.3 Preparation of Seed Germination

1. Sterile medium and suppliers.
 - (a) Prepare 500 mL diH_2O for sterilization.
 - (b) Prepare 10 sheets of seed germination paper. The seed germination papers are submerged in the Hoagland solution or saturated CaSO_4 containing no TiO_2 nanoparticle prepared in Subheading 3.2.
 - (c) Place the wet seed germination papers in a plastic container.
 - (d) Prepare 2000 mL Hoagland solution containing no TiO_2 nanoparticle prepared in Subheading 3.2.
 - (e) Autoclave at 121 °C for 20 min.
 - (f) Leave at room temperature to cool down.
2. Prepare seeds for germination.
 - (a) Remove cotton fiber from cotton seeds. This can be done manually or by machine.
 - (b) Place about 1000 cotton seeds in a beaker.
 - (c) Add 50 mL anhydrous sulfuric acid (H_2SO_4) into the beaker (*see Note 6*).
 - (d) Continuously mix H_2SO_4 and cotton seeds using a glass rod till the fibers all gone.
 - (e) Washing the seeds through with tap water for at least six times (*see Note 7*).
 - (f) Dry cotton seeds by placing all seeds on a filter paper at room temperature.
 - (g) Select 250 mature and healthy seeds.
 - (h) Place seeds in a beaker.

- (i) Add 200 mL 10% hydrogen peroxide into the beaker.
- (j) Mix cotton seeds with 10% hydrogen peroxide.
- (k) Sterilize the seeds for 20 min. During the 20 min, mix them for several times. (for other crop seeds, references are as follows: 3% hydrogen peroxide for 5 min for peanut; 3% hydrogen peroxide for 20 min for wheat; 10% hydrogen peroxide for 5 min for corn).
- (l) Dump hydrogen peroxide out of the beaker.
- (m) Wash the seeds for five times using sterilized water.
- (n) Place the sterilized seed germination paper on desk.
- (o) Place 20 seeds evenly along about 2 cm from the tap of long side of the seed germination paper. The seed micropyle (tip) should point down.
- (p) Roll the seed germination paper with seeds into a cylinder.
- (q) Tight the cylinder at each side using two rubber bands.
- (r) Place the seed germination papers in a beaker containing about 200 mL sterilized Hoagland medium. The seed side is at the top.
- (s) Cover the seed germination paper using a plastic paper.
- (t) Puncture several holes on the plastic paper that will prevent water evaporation from the seed germination paper, keep the moisture and also allow the airflow.
- (u) Place the seeds in a dark room or an incubator at $26 \pm 2^\circ\text{C}$ for 4 days (*see Note 8*).

3.4 Seedling Treatment

1. Select the healthy and evenly grown cotton seedlings for nanoparticle treatments.
2. Pick up one selected seedling, wrap the seedling by using a prepared sponge at the location between cotyledons (first two leaves) and roots, usually the sponge close to the junction of root and stem.
3. Place the seedling into the hole of the Styrofoam board cover and then culture in the Hoagland solution with/without nanoparticles. Each Styrofoam board cover can hold 8 seedlings and each plastic box can be used to culture 8 cotton seedlings.
4. Place the seedlings in a culture room or an incubator.
5. Blow air into the Hoagland solution (*see Note 9*).
6. Culture the cotton seedling at 14/10-h light/dark cycle. The culture temperature is $30 \pm 2^\circ\text{C}$ for light stage and $25 \pm 2^\circ\text{C}$ for dark stage.

7. Observe the growth and development of cotton seedling daily.
8. At day 7, change the culture solution.

3.5 Measurement of Root and Leaf Respiration

1. At days 7 and 14 of the treatments, select six seedlings from each treatment group and the controls.
2. Roots and leaves are separated for each plant individually.
3. Two-centimeter roots (including both main root and the branch root) cut from the bottom of stem are used for measuring root respiration. The first fully opened true leaf is used for measuring leaf respiration.
4. Weight the selected root or leaf samples.
5. Samples are placed into the incubator chamber of the polarographic O₂ electrode-Chlorolab 2 oxygen measurement system.
6. Add 2 mL saturated CaSO₄ solution.
7. Close the chamber.
8. Measure the consumption of O₂ for 10 min.
9. The leaf/root respiration is calculated by calculating the consumption rate of O₂.(nmol O₂/min/g FW) as follows: computing downward sloping rate of O₂ concentration (nmol/mL/min) in CaSO₄ solution according to determining time and decreasing value of O₂ concentration, multiply 2 mL and then divide by sample fresh weight (FW).

3.6 Measurement of Plant Photosynthesis

Plant photosynthesis is a process to convert light energy to electro-nical energy and then chemical energy, to convert carbon dioxide to carbon hydrates, and split water to oxygen along with providing protons and electrons to the chloroplastic electron transferring chain. Light energy absorbed by chlorophyll molecule in a leaf is used not only to drive photosynthesis (photochemistry), but also to be dissipated as heat or be re-emitted as fluorescence. Therefore, photochemistry, heat, and fluorescence constitute a competing relationship for the light energy. Based on the above plant photosynthesis traits, there are plenty of methods available to measure photosynthesis, depending on oxygen release, carbon dioxide fixation, and chlorophyll fluorescence. Here we determine plant photosynthesis on the basis of oxygen release and chlorophyll fluorescence. Chlorophyll fluorescence is a non-invasive measurement of photosystem II (PSII) activity and is a commonly used technique in plant physiology. The sensitivity of PSII activity to abiotic and biotic stresses has made this a key technique not only for understanding the photosynthetic mechanisms but also as a broader indicator of how plants respond to environmental change.

*3.6.1 Chlorophyll
Fluorescence
Determination Using
Handy PEA*

1. At days 7 and 14 of treatment, turn off the light for at least 30 min before the measurement (*see Note 10*).
2. Attach the detector sensor on the second fully opened leaves.
3. Measure the photosynthesis-related parameters.
4. Repeat six times on six different plants.
5. Calculate the photosynthesis-related parameters.

*3.6.2 Oxygen Release
Determination Using
Chlorolab 2*

1. At days 7 and 14 of treatment, select six seedlings from each treatment group and the controls.
2. Leaves are separated for each plant individually.
3. The first fully opened true leaf is used for measuring leaf respiration.
4. Weight the selected leaf samples.
5. Samples are placed into the incubator chamber of the polarographic O₂ electrode-Chlorolab 2 oxygen measurement system.
6. Add 2 mL 0.4 mol/L NaHCO₃ solution.
7. Close the chamber.
8. Set the light intensity as 200 µmol/m²/s, 400 µmol/m²/s, 800 µmol/m²/s, respectively, and correspondingly measure the release of O₂ for 4, 3, and 3 min.
9. The leaf photosynthesis is calculated by calculating the release rate of O₂ (nmol O₂/min/g FW) as follows: computing upward sloping rate of O₂ concentration (nmol/mL/min) in CaSO₄ solution according to determining time and increasing value of O₂ concentration, multiply 2 mL and then divide by sample fresh weight (FW).

**3.7 Measurement
of Root Vigor (See Note
11)**

1. Make 0.1 M PBS (pH = 7.4) buffer with 0.6% triphenyltetrazolium chloride (TTC).
 - (a) Start with 800 mL diH₂O.
 - (b) Weight and add the following chemicals into the water: 29.01 g Na₂HPO₄·12H₂O, 2.96 g NaH₂PO₄·2H₂O.
 - (c) Mix them very well.
 - (d) Add 6 g TTC.
 - (e) Adjust the total volume to 1 L.
 - (f) Mix thoroughly.
2. Measure root vigor.
 - (a) Collect whole root or roots below five centimeters from the bottom of the stem down along the main root, including both main and lateral roots, from each plant (depending on root size and experimental aims).

- (b) Cut the roots into pieces with about 1 cm in length.
- (c) Weight the roots.
- (d) Place the root into a 15 mL centrifuge tube.
- (e) Add 10 mL 0.1 M PBS (pH = 7.4) with 0.6% TTC.
- (f) Mix very well.
- (g) Place in the dark for 24 h.
- (h) Dump the liquid.
- (i) Wash the root three times using diH₂O.
- (j) Add 5 mL 95% ethanol to extract triphenyltetrazolium formazan (TTF) from the roots.
- (k) Place at 85 °C water bath for 10 min.
- (l) Measure the light absorbance at wavelength of 485 nm.
- (m) Calculate root vigor using the following formula: root vigor = OD of 485 nm ÷ fresh weight (gram) of the samples.

3.8 Measurement of Oxidative Stress

Oxidative stress is an imbalance between antioxidants and free radicals in a cell. When plant-generated free radicals exceed the ability that plant can get rid of it, free radical will become harmful to plant cell and generate oxidative stress. Many environmental stresses, including nanoparticle exposure, caused oxidative stress in a variety of plant and animal species. Here, we present a step-by-step method for measuring H₂O₂ accumulation and the activities of enzyme associating oxidative stress.

1. Measure H₂O₂ accumulation in plant: 3,3'-diaminobenzidine (DAB) staining method is employed to analyze H₂O₂ accumulation in plant leaves.
 - (a) Make 1 mg/mL 3,3'-diaminobenzidine (DAB) solution with pH = 3.8.
 - (b) Pick the first fully open cotton leaves.
 - (c) Place the leaves in a 10 cm Petri dish, each Petri dish only hold one leaf.
 - (d) Add 15 mL DAB solution to completely immerse the leaves. If a leaf cannot fully be immersed, add more DAB solution.
 - (e) Place the Petri dishes with treated leaves in an incubator.
 - (f) Treat the leaves for 8 h under dark at 28 °C.
 - (g) Dump DAB solution.
 - (h) Add 95% ethanol for removing chlorophyll.
 - (i) Place at room temperature for 24 h.

- (j) Observe the leaves and take pictures. The brown spots are indicator of H₂O₂ accumulation. The spots with dark color and more density mean more H₂O₂ accumulation.
2. Malondialdehyde (MDA) analysis.
- Weight 1 g of fresh young leaves (FW).
 - Place leaves in a mortar.
 - Add 1 g of quartz sand.
 - Add 10 mL of 5% trichloroacetic acid buffer (V_1).
 - Mix and ground the leaves into pieces.
 - Transfer into a 15 mL centrifuge tube.
 - Centrifuge at $3000 \times g$ for 15 min.
 - Transfer the liquid homogenates into a new 15 mL centrifuge tube.
 - 2 mL 0.5% TBA is added to the 2 mL extract solution (V_2) and get 4 mL of reaction mixture solution (V_3).
 - Heat the mixture at 100 °C for 15 min.
 - Immediately place on ice to block the reaction.
 - Centrifuge the cooled mixture at $3000 \times g$ for 10 min.
 - Measure light absorbance of the supernatant at 532 and 600 nm with a UV spectrophotometer.
 - Calculate MDA contained in the reaction mixture solution as the following formula:

$$\text{Concentration of MDA (mM)} = (A_{532} - A_{600})/155(C)$$

(m) Calculate MDA contained in the leaves as the following formula: MDA content ($\mu\text{mol/g FW}$) = $C \times V_3 \div V_2 \times V_1 \div \text{FW}$.

3. Measure superoxide dismutase activity.

- Enzyme extraction.
 - Weight 1 g of fresh young leaves (1 g FW).
 - Place leaves in a mortar. The mortar is pre-treated on ice or refrigerator.
 - Ground and homogenize the leaves into small pieces with 5 mL of 50 mM sodium phosphate buffer with 0.1 mM ethylenediaminetetraacetic acid (EDTA) (pH 7.8).
 - Centrifuge the homogenate at $10,000 \times g$ for 20 min at 4 °C.
 - Transfer the liquid into a new centrifuge tube for analyzing superoxide dismutase (SOD) and peroxidase (POD) enzyme activity and the atomic oxide radical anion (O₂^{-·}) content.
 - Store the extract on ice.

- (b) Measure superoxide dismutase (SOD) activity.
- Prepare 3 mL reaction mixture that contains 50 mM sodium phosphate buffer (pH 7.8), 0.075 mM nitro-blue tetrazolium (NBT), 13 mM methionine, 1.3 μ M riboflavin, and 0.1 mM ethylenediaminetetraacetic acid (EDTA).
 - Add 1 mL enzyme extracts.
 - Mix thoroughly.
 - Measure optical density at 560 nm.
 - Record the time (min) for inhibiting 50% of NBT photochemical reduction. The enzyme unit is to inhibit 50% of NBT photochemical reduction.
 - Calculate SOD activity by the formula:

SOD activity = units of SOD activity per gram of fresh weight per min

4. Measure peroxidase (POD) activity.

- (a) Enzyme extraction.

The enzyme extraction is same as described in **step 3a**.

- (b) Measure peroxidase (POD) activity.

- Prepare 3 mL reaction mixture that contains 0.2 M sodium phosphate buffer (pH 6.0), 0.3% guaiacol and hydrogen peroxide (H_2O_2).
- Add 0.5 L enzyme extracts.
- Mix thoroughly.
- Measure optical density at 470 nm.
- The oxidation of guaiacol is monitored by the increase in absorbance at 470 nm for 1 min with a spectrophotometer.
- Calculate POD activity by the formula:

POD activity = units of POD activity per gram of fresh weight per min

5. The atomic dioxide radical anion ($O_2^{-\cdot}$) content assay.

- (a) $O_2^{-\cdot}$ extraction.

The $O_2^{-\cdot}$ extraction is same as described in **step 3(a)** enzyme extraction.

- (b) Measure atomic dioxide radical anion ($O_2^{-\cdot}$) content.

- Prepare 2 mL reaction mixture that contains 50 mM sodium phosphate buffer and 10 mM hydroxylamine hydrochloride.
- Add 1 mL extracts.
- Mix well.

- The reaction is performed at 25 °C for 30 min (Note: O_2^- reacts with hydroxylamine hydrochloride and produces same amount of nitrite).
- Add 1 mL of 17 mM sulfanilic acid.
- Add 1 mL of 7 mM 1-naphthylamine solution.
- Mix thoroughly.
- Continuously keep the reaction at 25 °C for another 20 min.
- The light absorbance is measured at 530 nm with a UV spectrophotometer.
- Respectively prepare 3 mL water solution containing 0, 1, 2, 4, 6, 8 μ mol sodium nitrite, repeat steps from v to ix, establish the standard curve between nitrite content and its corresponding absorbance.
- Calculate the sample O_2^- content in final OD determination solution (n) according to the standard curve of nitrite, and then calculate sample O_2^- content by the formula: Atomic dioxide radical anion (O_2^-) content (μ mol/g FW) = n (μ mol) ÷ 1 (1 mL extract solution in ii step) × 5 (total extract solution) ÷ 1 g FW.

3.9 Data Analysis

1. All data are recorded in an excel file.
2. All data are analyzed using the statistical software SPSS or other statistical software.
3. The means and standard derivations (or standard errors) are calculated for each experiment.
4. An ANOVA test is employed to analyze the significance between treatments and the controls.

4 Notes

1. Hoagland medium is a hydroponic nutrient solution. This solution is first developed by Hoagland and Snyder in 1933 [28]. This medium was modified in 1938 [27]. Currently, Hoagland medium is one of the major solutions used for growing plants in the laboratories. The Hoagland medium provides the nutrient necessary for growing plant and widely used for supporting plant growth and development for a large variety of plant species [29]. At present, pre-made Hoagland medium powder can be purchased from lots of chemical company, such as Sigma-Aldrich. However, it also can be made in laboratories by adding all nutrients together.

2. This method can be used to test any chemical. Here, we just use titanium dioxide (TiO_2) nanoparticle as an example to present the step-by-step method.
3. The protocol described in this method chapter can be used to test any plant. Here, we just use cotton as an example to present the detailed method. Cotton is an important crop and are widely cultivated around the world.
4. Almost all roots are grown in the dark. Exposing to light may inhibit root growth and development and further affect the experiment results. Thus, the plastic box needs to be covered using aluminum paper to block light get through into the box. At the same time, aluminum paper can avoid the box absorbing light and further avoid solution becoming hotter and hindering root growth.
5. TiO_2 nanoparticle is not soluble in water. When dividing the solution into each container, make sure the TiO_2 nanoparticle evenly distributed in the solution by continuously mixing. In another way, TiO_2 nanoparticle may be weighted separately and add into each plastic culture box and then add the solution.
6. Anhydrous sulfuric acid (H_2SO_4) is a chemical with strong corrosion, it may burn skin and damage our health. Thus, handling of anhydrous sulfuric acid (H_2SO_4) should be very careful.
7. After removing the cotton fiber, cotton seeds should be thoroughly washed using water to remove all sulfuric acid residues. Trace amount of sulfuric acid on the seed may affect seed germination and further affect the later experiments.
8. During the 4 days of culture, the seeds need to be checked daily to make sure no contamination. If there is a contaminated seed, the seeds need to be removed immediately.
9. Blowing air into the medium is very important with two major functions: (a) provide oxygen to the roots; (b) nanoparticle TiO_2 is not soluble in the water, flow air will mix the nanoparticle with the solution and allow roots to connect with the nanoparticles for treatment.
10. Keep on dark is very important. F_0 and F_m are two basic but necessary parameters when using chlorophylla fluorescence to reflect photosynthesis traits. F_0 is the minimum initial fluorescence, referring to fluorescence intensity of all PSII centers being fully open, which is only obtained by using “measuring light” upon leaf under darkness of usually 30 min. F_m is the maximum fluorescence induced by closing reaction centers with application of a saturating pulse to a fully dark-adapted leaf.

11. There are several ways to measure root vigor. In this chapter, we employ triphenyltetrazolium chloride (TTC) method to measure root vigor, in which dehydrogenase activity is an indicator for root vigor. In this reaction, dehydrogenase reduces TTC to triphenyltetrazolium formazan (TTF). TTF is a color dye and let the reaction change color to blue.

References

- Rai PK, Kumar V, Lee S, Raza N, Kim KH, Ok YS, Tsang DCW (2018) Nanoparticle-plant interaction: implications in energy, environment, and agriculture. *Environ Int* 119:1–19
- Abdelsalam NR, Kandil EE, Al-Msari MAF, Al-Jaddadi MAM, Ali HM, Salem MZM, Elshikh MS (2019) Effect of foliar application of NPK nanoparticle fertilization on yield and genotoxicity in wheat (*Triticum aestivum* L.). *Sci Total Environ* 653:1128–1139
- Yadav A, Yadav K (2018) Nanoparticle-based plant disease management: tools for sustainable agriculture. In: AbdElsalam KA, Prasad R (eds) *Nanobiotechnology applications in plant protection*. Springer, Berlin, pp 29–61
- Mosavikia AA, Mosavi SG, Seghatoleslami M, Baradaran R (2020) Chitosan nanoparticle and pyridoxine seed priming improves tolerance to salinity in milk thistle seedling *Silybum marianum* (L.) Gaertn. *Not Bot Horti Agrobo* 48:221–233
- Cox A, Venkatachalam P, Sahi S, Sharma N (2016) Silver and titanium dioxide nanoparticle toxicity in plants: a review of current research. *Plant Physiol Biochem* 107:147–163
- Boykov IN, Shuford E, Zhang B (2019) Nanoparticle titanium dioxide affects the growth and microRNA expression of switchgrass (*Panicum virgatum*). *Genomics* 111:450–456
- Burkew CE, Ashlock J, Winfrey WB, Zhang B (2012) Effects of aluminum oxide nanoparticles on the growth, development, and micro-RNA expression of tobacco (*Nicotiana tabacum*). *PLoS One* 7:e34783
- Frazier TP, Burkew CE, Zhang BH (2014) Titanium dioxide nanoparticles affect the growth and microRNA expression of tobacco (*Nicotiana tabacum*). *Funct Integr Genomics* 14:75–83
- Gong CC, Wang LH, Li XL, Wang HS, Jiang YX, Wang WX (2019) Responses of seed germination and shoot metabolic profiles of maize (*Zea mays* L.) to Y_2O_3 nanoparticle stress. *RSC Adv* 9:27720–27731
- Lu WY, Xu L, Zhang YY, Huang XL, Chen G, Xiong F, Wu YF (2020) Study on the effect of sodium-nanoparticle in rice root development. *Plant Signal Behav* 15(6):1759954
- Wu YF, Peng WMH, Dong ZD, Jiang QQ, Yu XR, Chen G, Xiong F (2020) Exogenous application of NaBiF4 nanoparticle affects wheat root development. *BMC Plant Biol* 20:140
- Chen GC, Ma CX, Mukherjee A, Musante C, Zhang JF, White JC, Dhankher OP, Xing BS (2016) Tannic acid alleviates bulk and nanoparticle Nd_2O_3 toxicity in pumpkin: a physiological and molecular response. *Nanotoxicology* 10:1243–1253
- Ma CX, Chhikara S, Xing BS, Musante C, White JC, Dhankher OP (2013) Physiological and molecular response of *Arabidopsis thaliana* (L.) to nanoparticle cerium and indium oxide exposure. *ACS Sustain Chem Eng* 1:768–778
- Xun HW, Ma XT, Chen J, Yang ZZ, Liu B, Gao X, Li G, Yu JM, Wang L, Pang JS (2017) Zinc oxide nanoparticle exposure triggers different gene expression patterns in maize shoots and roots. *Environ Pollut* 229:479–488
- Yadu B, Chandrakar V, Korram J, Satnami ML, Kumar M, Keshavkant S (2018) Silver nanoparticle modulates gene expressions, glyoxalase system and oxidative stress markers in fluoride stressed *Cajanus cajan* L. *J Hazard Mater* 353:44–52
- Adhikari S, Adhikari A, Ghosh S, Roy D, Azahar I, Basuli D, Hossain Z (2020) Assessment of ZnO-NPs toxicity in maize: an integrative microRNAomic approach. *Chemosphere* 249:126197
- Deng Y, Ai J, Guan X, Wang Z, Yan B, Zhang D, Liu C, Wilbanks MS, Escalon BL, Meyers SA, Yang MQ, Perkins EJ (2014) MicroRNA and messenger RNA profiling reveals new biomarkers and mechanisms for RDX induced neurotoxicity. *BMC Genomics* 15(Suppl 11):S1
- Srivastava AK, Yadav SS, Mishra S, Yadav SK, Parmar D, Yadav S (2020) A combined micro-RNA and proteome profiling to investigate the effect of ZnO nanoparticles on neuronal cells. *Nanotoxicology* 14(6):757–773

19. Zhang B, Pan X (2009) RDX induces aberrant expression of microRNAs in mouse brain and liver. *Environ Health Perspect* 117:231–240
20. Li C, Zhang BH (2016) MicroRNAs in control of plant development. *J Cell Physiol* 231:303–313
21. Das D, Datta AK, Kumbhakar DV, Ghosh B, Pramanik A, Gupta S (2018) Nanoparticle (CdS) interaction with host (*Sesamum indicum* L.)—its localization, transportation, stress induction and genotoxicity. *J Plant Interact* 13:182–194
22. Halder S, Mandal A, Das D, Gupta S, Chatto-padhyay AP, Datta AK (2015) Copper nanoparticle induced macromutation in *Macrotyloma uniflorum* (lam.) Verdc. (Leguminosae): a pioneer report. *Genet Resour Crop Evol* 62:165–175
23. Pan X, Redding JE, Wiley PA, Wen L, McConnell JS, Zhang B (2010) Mutagenicity evaluation of metal oxide nanoparticles by the bacterial reverse mutation assay. *Chemosphere* 79:113–116
24. Da Costa MVJ, Kevat N, Sharma PK (2020) Copper oxide nanoparticle and copper (II) ion exposure in *Oryza sativa* reveals two different mechanisms of toxicity. *Water Air Soil Pollution* 231
25. Iftikhar A, Ali S, Yasmeen T, Arif MS, Zubair M, Rizwan M, Alhaithloul HAS, Alayafi AAM, Soliman MH (2019) Effect of gibberellic acid on growth, photosynthesis and antioxidant defense system of wheat under zinc oxide nanoparticle stress. *Environ Pollut* 254:113109
26. Prakash S, Deswal R (2020) Analysis of temporally evolved nanoparticle-protein corona highlighted the potential ability of gold nanoparticles to stably interact with proteins and influence the major biochemical pathways in *Brassica juncea*. *Plant Physiol Biochem* 146:143–156
27. Hoagland DR, Arnon D (1938) The water-culture method for growing plants without soil. University of California, Berkeley, CA
28. Hoagland DR, Snyder WC (1933) Nutrition of strawberry plant under controlled conditions (a) Effects of deficiencies of boron and certain other elements, (b) susceptibility to injury from sodium salts. *Proc Am Soc Hort Sci* 30:288–294
29. Smith GS, Johnston CM, Cornforth IS (1983) Comparison of nutrient solutions for growth of plant in sand. *Culture* 94:537–548



Chapter 17

Determination of Oxidative Stress and Antioxidant Enzyme Activity for Physiological Phenotyping During Heavy Metal Exposure

Samrana Zahir, Fan Zhang, Jinhong Chen, and Shuijin Zhu

Abstract

The overproduction of reactive oxygen species during abiotic stress in plants causes oxidative stress that damage the cell normal functions. For reactive oxygen species (ROS) scavenging, plants developed a defense system with antioxidant enzymes. To measure the oxidative stress and antioxidant enzymes activity spectral enzymatic analysis was used, that is material-intensive, time-consuming, and inefficient. In the present study, the four more studied and main antioxidant enzymatic assays are miniaturized in a 96-well plate system and monitored the activity of enzymes by spectrophotometry. This method has obvious advantages over the standard cuvette analysis method because the miniaturization of the 96-well microplate system decreases the amount of reaction mixture and enzymes extract, thrifits working time, and consumable costs as well.

Key words Oxidative stress, Enzymatic activity, Spectrophotometry, 96-well microplate

1 Introduction

Anthropogenic activities, such as industrialization and expanding urbanization, are accompanied by the release of pollutants in the environment, i.e., heavy metals and nanomaterials. It causes phytotoxicity by affecting various biochemical and physiological processes in plants [1], such as including antioxidant enzymes activities, protein mobilization, and photosynthesis. One of the initial effects of exposure to a toxic concentration of heavy metals on plant cells is the production of reactive oxygen species (ROS), i.e., superoxide (O_2^-) and hydroxyl radicals ($\cdot OH$), hydrogen peroxide (H_2O_2) and singlet oxygen (1O_2) [2, 3]. ROS in plant cells plays an important role in plant biology as signaling molecules, affecting cell cycle regulation, seed germination, root development, etc. [4–7]. When ROS concentrations exceed the cell capacity, through detoxification, the cells enter a state of oxidative stress

which can be measured by the increase of the oxidation of proteins lipids and carbohydrates molecules. A cellular system based on enzymatic antioxidants is able to scavenge ROS produced in plants [8]. The first mechanism is based on the existence of enzymes **superoxide dismutase** (SOD), ascorbate peroxidase (APX), peroxidase (POD), and **catalase** (CAT). In the present study, we explained the method of measuring lipid peroxidation in terms of thiobarbituric acid reactive substance (TBARS) and antioxidant enzymes activity in cotton root under Cr stress, the part of previously published work [9].

Currently, the use of spectral enzymatic analysis for revealing the patterns of antioxidant enzymes that scavenging ROS is material-intensive, time-consuming, and inefficient. The four more studied and main antioxidant enzymatic assays are miniaturized in a 96-well plate system and the activity of enzymes was monitored by spectrophotometry. This method has obvious advantages over the standard cuvette analysis method as the miniaturization of the 96-well microplate system decreases the amount of reaction mixture and enzymes extract and eases working time and consumable costs. Another advantage of this method is that we can run all the samples at once in the same conditions, i.e., time and temperature that reduces the reaction error among samples.

2 Materials

As a plant material, the Cr treated roots and untreated seedlings of cotton are used [9]. All solutions are prepared by using distilled water and analytical grade reagents (Table 1). Sterilized apparatus are used throughout the experiments. The disposing of the waste should strictly follow all regulations about waste disposal.

2.1 Enzymes Extraction Buffer

Prepare a 50 mM phosphate buffer with pH 7.0 for enzyme extraction: Put 16.385 g Na₂HPO·12H₂O and 0.663 g NaH₂PO₄·2H₂O into a 1000 mL volumetric flask, add 950 mL distilled water, stir until dissolve and adjust pH with HCl and make the final volume 1000 mL (*see Note 1*). Store at 4 °C for further use.

2.2 Solutions for SOD Assay

Prepare reaction mixture containing 75 µM nitro blue tetrazolium (NBT), 20 µM riboflavin, 100 µM EDTA-Na₂, and 130 mM methionine: Weigh 0.0307 g NBT, 0.00038 g riboflavin, 0.0019 g EDTA-Na₂, and 0.9699 g methionine, and transfer into 500 mL solution (*see Note 2*).

2.3 Solution for POD Assay

1. 1.5% Guaiacol: Take 1.5 mL Guaiacol in a glass beaker (dissolve in ethanol) and make the final volume 100 mL with distilled water.

Table 1
Chemicals used for measurement of oxidative stress and antioxidant enzymes activities

Names	Chemical formula	Molecular weight
1 di-Sodium hydrogen phosphate dodecahydrate	Na ₂ HPO ₄ ·12H ₂ O	358.1422
2 Sodium dihydrogen phosphate dihydrated	NaH ₂ PO ₄ ·2H ₂ O	156.01
3 Nitro blue tetrazolium (NBT)	C ₄₀ H ₃₀ Cl ₂ N ₁₀ O ₆	817.60
4 Riboflavin	C ₁₇ H ₂₀ N ₄ O ₆	376.36
5 EDTA- Na ₂	C ₁₀ H ₁₄ N ₂ Na ₂ O ₈ ·2H ₂ O	372.24
6 Methionine	C ₅ H ₁₁ NO ₂ S	149.21
7 Guaiacol	C ₇ H ₈ O ₂	124.14
8 Hydrogen peroxide	H ₂ O ₂	34.01
9 Thiobarbituric acid (TBA)	C ₄ H ₄ N ₂ O ₂ S	144.15
10 Trichloroacetic acid (TCA)	C ₂ HCl ₃ O ₂	163.39
11 di-potassium hydrogen phosphate anhydrous	K ₂ HPO ₄	174.18
12 Potassium dihydrogen phosphate	KH ₂ PO ₄	136.09
13 Potassium iodide	KI	166.00
14 Butylated hydroxyl toluene (BHT)	C ₁₅ H ₂₄ O	220.35
15 Ascorbic acid (ASA)	C ₆ H ₈ O ₆	176.12

2. 300 mM H₂O₂: Take 1.53 mL of 30% H₂O₂ in a glass beaker and make the final volume 50 mL with distilled water.

2.4 Solution for CAT Assay Prepare 300 mM H₂O₂ as mentioned above for POD assay, and 50 mM phosphate buffer (same as extraction buffer).

2.5 Solution for APX Assay 1. Prepare 7.5 mM ascorbic acid (ASA): Take 66 mg ASA and make the final volume 50 mL with distilled water.
 2. 300 mM H₂O₂ and 50 mM phosphate buffer as mentioned above for CAT assay.

2.6 Solution for TBARS Prepare the solution containing 0.25% (w/v) thiobarbituric acid (TBA) in 10% (v/v) trichloroacetic acid (TCA): Weigh 10 g TCA and dissolve in 100 mL distilled water. Weigh 2.5 g TBA and add in 100 mL sol of 10% TCA.

2.7 Solution for H₂O₂ 1. Extraction solution contains 0.1% (w/v) TCA.
 2. Assay solution contains 10 mM potassium phosphate buffer (pH 7.0): weigh 0.467 g K₂HPO₄ and 0.3155 g KH₂PO₄ and dissolve in 500 mL distilled water.

3. 1 M (potassium iodide) KI: Weigh 33 g KI and dissolve in 200 mL distilled water.

3 Methods

3.1 Enzymes Extraction

Cut plant tissues and rinse it in distilled water. Weigh about 0.5 g sample and place in the pre-cooled mortar on ice. Add 2–3 mL pre-cooled phosphate buffer solution with pH 7.8. Homogenize the sample on ice and add the buffer solution up to 5 mL. Centrifuge the sample at 10000–15000 $\times \text{g}$ for 20 min at 4 °C. Preserve the supernatant at –80 °C in another small tube for further use in various antioxidant enzymes activity assay.

3.2 Superoxide Dismutase Activity (SOD)

The method of Giannopolitis and Ries [10] is used with slight modifications to assay the activity of superoxide dismutase (SOD). The method is based on NBT photoreduction to purple formazone formation (*see Note 3, Fig. 1*). For SOD activity assay, take 2.5 μL enzyme extract per well (where required) of a microplate, 250.5 μL of the reaction solution (as mentioned above in materials), 25 μL H₂O (*see Note 4*). For light control, take 253 μL reaction solution and 25 μL H₂O. For dark control, take 253 μL reaction solution and 25 μL H₂O in a separate tube and use it as a blank for reading.

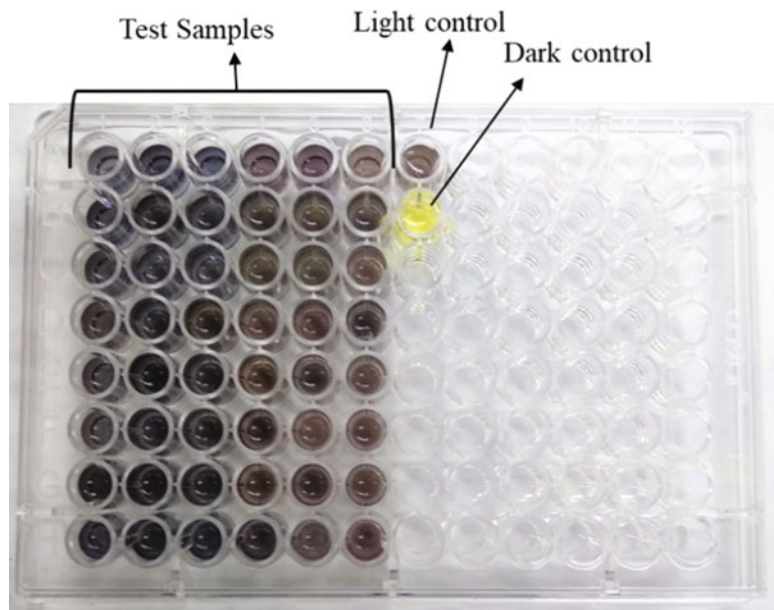


Fig. 1 Microplate-based superoxide dismutase (SOD) assay showing the NBT photoreduction to purple formazone formation. Out of 96 wells, 48 wells are filled with samples rows 1–6, and 2 wells (**a**, **b**) of row 7 contain light and dark control, respectively

Place the microplate contains light control and all other samples under light condition at 4000 lux for 20 min while control dark samples place in 100% dark condition. Read all samples spectrophotometrically at 560 nm.

Formula for SOD determination:

$$\text{SOD activity (U/g FW)} : \{(A_{\text{ck}} - A_e) \times V\} \div \{0.5 \times A_{\text{ck}} \times W \times V_t\}$$

A_e = OD value on the spectrophotometer.

A_{ck} = OD value for the control tube under light conditions (at 4000 lux for 20 min).

V = Total volume of the buffer solution used to extract the enzyme.

W = Fresh weight of the sample.

V_t = Amount of enzyme extract used in reaction solution to test SOD.

3.3 Dynamic Study of Peroxidase Activity (POD)

Peroxidase (POD) activity is estimated by the method of Zhang [11] with modification from cuvette to microplate. In each well, 10 μL enzyme extract, 10 μL guaiacol (1.5%), and 250 μL phosphate buffer (same in case of grinding) are added. In the end, add 10 μL of H_2O_2 to start the reaction and immediately take the absorbance 470 nm (see Note 5, Fig. 2). For blank, add 260 μL phosphate buffer (replace 10 μL enzyme extract). One unit of POD activity is the amount of enzyme oxidizing 1 nmol guaiacol min^{-1} .

Formula for POD determination:

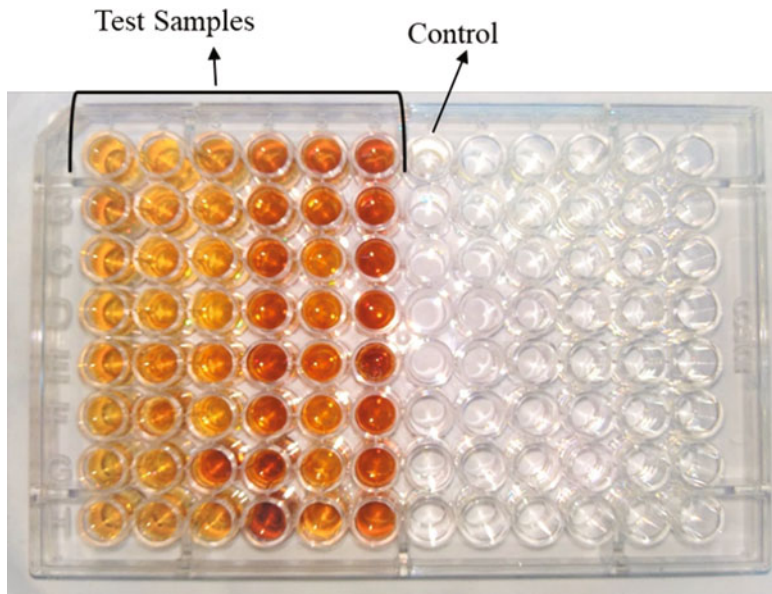


Fig. 2 Microplate-based peroxidase (POD) assay showing the formation of brown color after H_2O_2 addition. Out of 96 wells, 48 wells are filled with samples rows 1–6, and 1 well of row 7 contains the control with no reaction

POD (mM/gFW) activity = $(\text{activity} \times A \times V/\alpha)/(E \times W)$

Activity = OD value.

A = Total assay volume.

W = Fresh weight of the sample.

V = Total volume of the buffer solution used to extract the enzyme.

α = Amount of enzyme extract used in reaction solution to test.

E = activity constant, i.e., 25.5 mM/cm.

3.4 Catalase Activity (CAT)

Catalase (CAT) activity is examined by the modified method of Aebi [12]. Add 10 μ L enzymes extract and 250 μ L phosphate buffer in each well of microplate. In the end, add 10 μ L of H_2O_2 and give a gentle shake, then take the reading at 240 nm (*see Notes 6 and 7*). For blank, add 10 μ L H_2O instead of enzyme extract. One unit of enzyme activity is defined as 1 nmol H_2O_2 dissociated min^{-1} .

Formula for CAT determination:

CAT (mM/g FW) activity = $(\text{activity} \times A \times V/\alpha)/(E \times W)$

Activity = OD value.

A = Total assay volume.

W = Fresh weight of the sample.

V = Total volume of the buffer solution used to extract the enzyme.

α = Amount of enzyme extract used in reaction solution to test.

E = Extinction coefficient, i.e., 39.4 mM/cm.

3.5 Determination of APX Activity

The activity of ascorbate peroxidase (APX) is determined by modified method of Nakano and Asada [13]. Take 10 μ L of enzyme extract and 250 μ L phosphate buffer, 10 μ L ASA solution. Finally, add 10 μ L of H_2O_2 and monitor the oxidation rate of ascorbate at 290 nm at 30 °C (*see Note 8*). For blank reading, take distilled water instead of the enzyme extract. APX activity was expressed as nmol of ascorbate $\text{min}^{-1}/\text{mg}$.

Formula for APX determination:

APX (mM/g FW) activity = $(\text{activity} \times A \times V/\alpha)/(E \times W)$

Activity = OD value.

A = Total assay volume.

W = Fresh weight of the sample.

V = Total volume of the buffer solution used to extract the enzyme.

α = Amount of enzyme extract used in reaction solution to test.

E = Means activity constant, i.e., 2.8 mM/cm.

3.6 Lipid Peroxidation

Lipid peroxidation is measured by determining the content of reactive substances to thiobarbituric acid (TBARS), according to Chappell and Cohn [14] with slight modification. Take 0.2 g tissues then put in pre-chilled mortar, ground it to powder. Transfer the powder sample to 2 mL pre-cold TCA (1%, w/v) in Eppendorf tube. Vortex to homogenate and centrifuged for 15 min at 12,000 rpm. Add 0.5 mL of supernatant and 1 mL of TBA and TCA (add. 0.01% butylated hydroxytoluene, *see Note 9*) solution in 4 mL Eppendorf tube. Heat the samples at 95 °C for 15 min and then give an immediate ice bath. Centrifuge at 4800 rpm for 10 min. Add 250 µL of supernatant in each well of a microplate, and take the absorbance at 532 and 600 nm. Nonspecific turbidity correction was made by subtracting the absorbance at 600 nm. Use three technical replicates for each sample and for blank use distilled water.

Formulas:

$$\text{TBARS (nmol/g FW)} = [(OD_{532} - OD_{600}) \times A \times V] \div (\alpha \times E \times W)$$

A = Total assay volume.

V = Total volume of phosphate buffer used for enzyme extraction.

α = Volume of supernatant used.

W = Fresh weight of the sample.

E = Extinction coefficient (1.55×10^2) $155 \text{ mM}^{-1} \text{ cm}^{-1}$.

3.7 Determination of H₂O₂

To determine the concentration of hydrogen peroxide (H₂O₂), take 0.2 g tissues put in pre-chilled mortar, ground it to powder. Transfer the powder sample to 2 mL pre-cold TCA (0.1%, w/v) in Eppendorf tube. Vortex to homogenate and centrifuged for 15 min at $12,000 \times g$ [15]. Add in each well the reaction mixture, 50 µL supernatant, 50 µL of 10 mM potassium phosphate buffer (pH 7.0), and 100 µL of 1 M KI. Read the absorbance at 390 nm and calculate the H₂O₂ concentration using a standard curve with known concentrations of H₂O₂. Plot standard curve, with known concentrations of H₂O₂ against its O.D. and put use equation, $y = mx + c$, where $m = y_2 - y_1/x_2 - x_1$, to calculate samples concentration. The amount of H₂O₂ was expressed as µmol/g FW.

Formula for H₂O₂ determination:

$$\text{H}_2\text{O}_2 (\mu\text{M/g FW}) = C \times V_t / V_r \times W$$

C = Contents of H₂O₂ calculated from standard curve.

V_t = Volume of extraction solution to grind sample.

V_r = Volume of supernatant used for reaction.

W = Weight of leaf sample.

4 Notes

1. Various factors have influence on pH, it is intensely recommended that measure the pH of the prepared buffer before using and adjusting if needed.
2. Reagents NBT and riboflavin to be dissolved in distilled water separately in dark.
3. A unit of SOD activity is the amount of enzyme required to cause 50% inhibition in NBT reduction.
4. Add the reaction solution of SOD assay to microplate in dark.
5. Add H₂O₂ by using a multichannel pipette. Set time 30–60 s. Give gentle shake before testing spectrophotometrically at 470 nm.
6. Remember that set the time range 0–30 s and take the reading at 240 nm.
7. Use the quartz microplates for the wavelength below 300.
8. Remember that set the time range 0–60 s and take a reading at 290 nm.
9. Butylated hydroxyl toluene (BHT) is an antioxidant and inhibits malondialdehyde production.

References

1. Khan A, Khan S, Khan MA et al (2015) The uptake and bioaccumulation of heavy metals by food plants, their effects on plants nutrients, and associated health risk: a review. Environ Sci Pollut Res 22(18):13772–13799
2. Smeets K, Cuypers A, Lambrechts A et al (2005) Induction of oxidative stress and anti-oxidative mechanisms in *Phaseolus vulgaris* after Cd application. Plant Physiol Biochem 43(5):437–444
3. Tamas L, Mistrik I, Zelinova V (2017) Heavy metal-induced reactive oxygen species and cell death in barley root tip. Environ Exp Bot 140:34–40
4. Mullineaux PM, Exposito-Rodriguez M, Laisue PP et al (2018) ROS-dependent signalling pathways in plants and algae exposed to high light: comparisons with other eukaryotes. Free Radic Biol Med 122:52–64
5. Liu Y, He C (2016) Regulation of plant reactive oxygen species (ROS) in stress responses: learning from AtRBOHD. Plant Cell Rep 35 (5):995–1007
6. El-Maarouf-Bouteau H, Bailly C (2008) Oxidative signaling in seed germination and dormancy. Plant Signal Behav 3(3):175–182
7. Tsukagoshi H (2016) Control of root growth and development by reactive oxygen species. Curr Opin Plant Biol 29:57–63
8. Gill SS, Tuteja N (2010) Reactive oxygen species and antioxidant machinery in abiotic stress tolerance in crop plants. Plant Physiol Biochem 48(12):909–930
9. Samrana S, Ali A, Muhammad U et al (2020) Physiological, ultrastructural, biochemical, and molecular responses of glandless cotton to hexavalent chromium (Cr⁶⁺) exposure. Environ Pollut 266:115394
10. Giannopolitis CN, Ries SK (1977) Superoxide dismutases: I. occurrence in higher plants. Plant Physiol 59(2):309–314
11. Zhang X (1992) The measurement and mechanism of lipid peroxidation and SOD, POD and CAT activities in biological system. In: Research methodology of crop physiology. Agriculture Press, Beijing, pp 208–211

12. Aebi H (1984) Catalase in vitro. Methods Enzymol 105:121–126
13. Nakano Y, Asada K (1981) Hydrogen peroxide is scavenged by ascorbate-specific peroxidase in spinach chloroplasts. Plant Cell Physiol 22 (5):867–880
14. Chappell JH, Cohn MA (2011) Corrections for interferences and extraction conditions make a difference: use of the TBARS assay for lipid peroxidation of orthodox *Spartina pectinata* and recalcitrant *Spartina alterniflora* seeds during desiccation. Seed Sci Res 21 (2):153–158
15. Velikova V, Yordanov I, Edreva A (2000) Oxidative stress and some antioxidant systems in acid rain-treated bean plants: protective role of exogenous polyamines. Plant Sci 151 (1):59–66



Chapter 18

Comprehensive Phytotoxicity Assessment Protocol for Engineered Nanomaterials

Lok R. Pokhrel, Chukwudi S. Ubah, and Sina Fallah

Abstract

In order for nanotechnology to be sustainably applied in agriculture, emphasis should be on comprehensive assessment of multiple endpoints, including biouptake and localization of engineered nanomaterials (ENMs), potential effects on food nutrient quality, oxidative stress responses, and crop yield, before ENMs are routinely applied in consumer and agronomic products. This chapter succinctly outlines a protocol for conducting nanophytotoxicity studies focusing on nanoparticle purification and characterization, arbuscular mycorrhizal fungi (AMF)/symbiont inoculation, biouptake and translocation/localization, varied endpoints of oxidative stress responses, and crop yield.

Key words Sustainable nanotechnology, Agriculture, Nanophytotoxicity, Oxidative stress, Arbuscular mycorrhizal fungi, Tangential flow filtration

1 Introduction

Identifying putative mechanism(s) and methods to mitigate nanophytotoxicity are areas that are crucial to prioritize for sustainable agriculture, environmental health, and public safety [1]. The greater surface reactivity vis-à-vis smaller particle size may influence engineered nanomaterial (ENM) bioavailability compared to the bulk or ionic counterparts [2–4]. Such contrasting and other unique properties (high surface energy, more surface defects and reactive sites) of ENMs have raised concerns about their potential interactions with the abiotic and biotic components in the environment influencing toxicity [2, 4–10]. Among the biotic components, soil microorganisms such as arbuscular mycorrhizal fungi (AMF) and symbiont bacteria, in particular, play a crucial role in transforming or degrading a variety of pollutants, thereby sustaining plant productivity and ecological services and functions [11–15]. Particularly, AMF are known for metal tolerance and seque-

tration via secretion of metal-chelating glomalin or glomalin-related proteins [16–21], potentially suppressing metal toxicity in host plants [19–21].

Nanophytotoxicity studies have mostly addressed acute toxicity (short-term) at a single plant species level and in a controlled laboratory setting, providing valuable information on individual species responses to, and mechanistic understanding of, ENM stress [5]. However, studies investigating plant responses to ENMs in the field environment and chronic long-term exposures have not been fully realized and need to be prioritized [21–24]. Further, for nanotechnology to be sustainably used in agriculture, focus should be on comprehensive assessment of endpoints, including biouptake and translocation/localization of ENMs, effects on food nutrient quality, oxidative stress responses, and crop yield, before ENMs find routine applications in consumer and agronomic products (e.g., nanofertilizers, nanopesticides, nanoadditives) [21, 23, 24].

This chapter outlines methods for conducting nanophytotoxicity studies focusing on nanoparticle purification and characterization, AMF/symbiont inoculation, biouptake and translocation/localization, varied endpoints of oxidative stress responses, and crop yield.

2 Materials

Prepare all solutions using Type I Milli-Q/ultra-pure water (18 MΩ-cm at 25 °C, and TOC less than 10 ppb) and high-purity analytical grade reagents. Prepare and store all reagents at 4 °C (unless otherwise indicated). Follow all waste disposal regulations per the state and/or national standards when disposing waste materials generated from the experiments.

2.1 Nanoparticle Characterization

1. Dynamic light scattering (DLS): Cuvette (4 mL), syringe (5 mL), Malvern Zetasizer or Nicomp Particle Size Analyzer.
2. Electron microscopy: appropriate stub (scanning electron microscopy), appropriate support grid (transmission electron microscopy), and appropriate software for image analysis.

2.2 Nanoparticle Purification Via Tangential Flow Filtration

All equipment and supplies related to TFF can be procured from the supplier at: <http://www.spectrumlabs.com/>.

1. Balance, top-loading balance, weighing to nearest 0.01 g with maximum weight of 200 g (e.g., OHAUS Scout Pro Portable Balance).
2. KrosFlo® Research II Pump Drive & Pump Head, and KrosFlo® Research II Pressure Monitor.

3. Flow-path Kit.
4. KF Comm, a software program, and lab computer for software program.
5. pH and Conductivity meters.
6. Large beaker (e.g., 1000 mL for holding permeate), and 500 mL flask (for holding sample).

2.3 Soil Preparation

1. Sieve of different pore size.
2. Soil characteristics: pH, electrical conductivity, and ORP meters.
3. Total metal concentration: Inductively coupled plasma-optical emission spectroscopy (ICP-OES), mass spectroscopy (ICP-MS), or atomic absorption spectroscopy (AAS).
4. Soil amendment: appropriate ENMs and bulk or ionic counterparts.
5. Nanopure water: Milli-Q Direct Q3 UV water purification system (Millipore) or similar system.
6. Ultrasonicator (e.g., 100 W, 40 kHz).
7. A mechanical or hand mixer.

2.4 Plantation

1. High quality seeds of desired plants (e.g., soybean, fenugreek, corn, etc.).
2. Polyethylene pots (frequency depends on sample size).
3. Irrigation water supply.

2.5 Symbiont/AMF Preparation and Inoculation

1. N₂-fixing bacterium (e.g., *Rhizobium meliloti* strain PTTC 1684) inoculation: Tryptic Soy Agar (TSA), transfer loop, Petri dish, carboxy methyl cellulose, transplant trays, soil/sand, perlite or peat:cocopeat (1:1 w/w), incubator shaker, and centrifuge.
2. AMF (e.g., *Glomus intraradices*) inoculation: roots, spores (50–150 spores/g) and hyphae, soil/sand, or perlite.

2.6 Measurement of Malondialdehyde Concentration

1. 0.5% Thiobarbituric acid (TBA).
2. 0.1% and 20% trichloroacetic acid (TCA).
3. Water bath (95 °C) and ice bath.
4. Centrifuge.
5. UV-Vis spectrophotometer.

2.7 Measurement of Hydrogen Peroxide

1. Liquid nitrogen, cold acetone, and mortar pestle.
2. Whatman filter paper, reagent of titanium (16%), sulfuric acid, and ammonium hydroxide (28%).
3. UV-Vis spectrophotometer.

- 2.8 Measurement of Superoxide Dismutase**
1. Liquid nitrogen, 0.1 M potassium phosphate buffer (pH 7.5), and nitroblue tetrazolium (NBT).
 2. Centrifuge, -20 °C Freezer, and UV-Vis spectrophotometer.
- 2.9 Measurement of Catalase Activity**
1. Hydrogen peroxide, and UV-Vis spectrophotometer.
- 2.10 Measurement of Guaiacol Peroxidase Activity**
1. Potassium phosphate buffer (0.1 M, pH 6.0), guaiacol (45 mM), hydrogen peroxide (44 mM), and UV-Vis spectrophotometer.
- 2.11 Measurement of Ascorbate Peroxidase Activity**
1. Hydrogen peroxide, ascorbic acid, and UV-Vis spectrophotometer.
- 2.12 Measurement of Scavenging of Hydrogen Peroxide**
1. Hydrogen peroxide (2 mM), and phosphate buffer saline, and UV-Vis spectrophotometer.
- 2.13 Measurement of Root Parameters**
1. Distilled or Milli-Q water, ruler, 1000 mL graduated cylinder, and analytical balance.
- 2.14 Measurement of Biouptake**
1. Analytical balance, oven, mortar and pestle, and liquid nitrogen.
 2. Nitric acid (concentrated), metal standards, and ICP-MS, ICP-OES or AAS.
- 2.15 Localization of ENMs in Seed**
1. Glutaraldehyde (2.5%), 0.1 M phosphate buffer, 1% Osmium tetroxide, acetone, epoxy resin.
 2. Electron microscopy (TEM and/or SEM).
 3. Image analysis software (e.g., ImageJ, Digimizer).
- 2.16 Measurement of Crop Yield or Seed Biomass**
1. Plastic bag, oven, and analytical balance.

3 Methods

- 3.1 Nanoparticle Synthesis and Characterization**
1. Synthesize engineered nanoparticles (ENPs) using an established method. For example, ZnONPs or CuONPs of different sizes and/or shapes can be synthesized using the soil-gel method as previously described [22, 23, 25].
 2. Use X-ray diffraction (XRD) to determine crystal structure, and electron microscopy (TEM or SEM) for (core) particle size, size distribution, and shape of nanoparticles.

3. Measure the hydrodynamic diameter (HDD) and zeta (ζ) potential of the ENPs using the dynamic light scattering (DLS) method.

4. Image ENP samples using an electron microscopy (TEM or SEM) and analyze images using an appropriate software (e.g., ImageJ).

3.2 Nanoparticle Purification Via Tangential Flow Filtration

1. Place 500 mL ENP suspension in the feed flask as shown in Fig. 1.
2. Align the tubing on the peristaltic pump head and lock it.
3. Open the feed flow path toward the filter module. Also ensure that the permeate (waste) line is open and the weighing balance is powered on and is recognized by the tangential flow filtration (TFF) control software (KF COMM).
4. Make sure the feed flow path is aligned appropriately based on the placement of the filter module.
5. Slowly maintain the transmembrane pressure (TMP) between 15 and 20 psi for optimal retentate (filtrate) output.
6. Once the TMP pressure reaches optimal, maintain the feed flow at the rate of 50–70 mL/min.
7. Repeat the filtration until the retentate volume decreases to 150–50 mL from the original 500 mL of ENP.
8. Then add Milli-Q water to bring the retentate volume up to 500 mL.

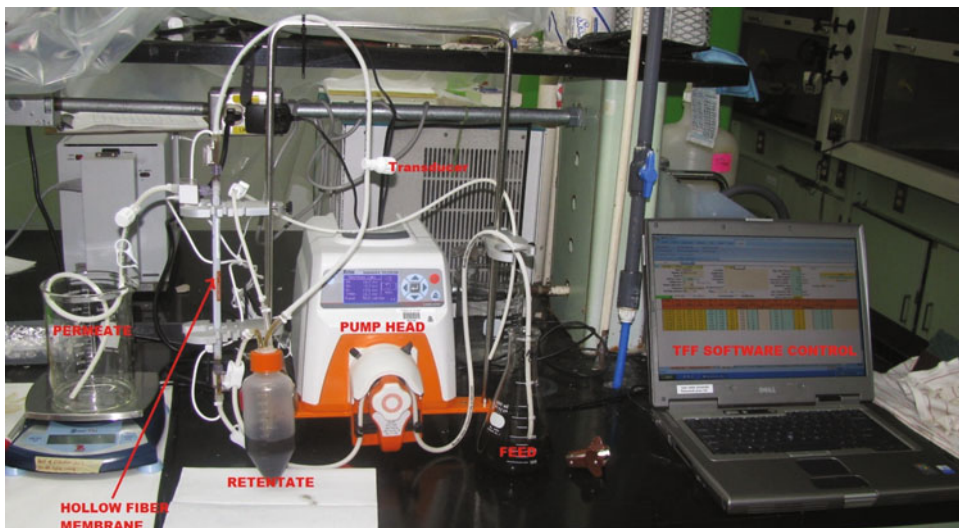


Fig. 1 Tangential flow filtration (TFF) instrumentation setup for nanoparticle purification. (Reproduced with permission from Ref. 34)

Table 1

Sample cleaning protocol for the purification of silver nanoparticles (AgNPs) using the Tangential Flow Filtration (TFF) system. (Reproduced with permission from Refs. 33, 34)

Purification of lab-synthesized AgNPs	Electrical conductivity ($\mu\text{S cm}^{-1}$)
Start volume = 500 mL	1095
End volume = 70 mL	1162
Increase volume to 500 mL adding nanopure water	185
End volume = 100 mL	283
Increase volume to 500 mL adding nanopure water	36
End volume = 75 mL	68
Increase volume to 500 mL adding nanopure water	11
End volume = 150 mL	20
Increase volume to 500 mL adding nanopure water	5

9. Repeat filtration until the retentate volume decreases to 150–50 mL.
10. Continue repeating the process until the final retentate demonstrates low conductivity ($10 \mu\text{S cm}^{-1}$ or below).
11. Typically, the process is completed in 9–10 iterations as shown in Table 1 below.
12. Upon completion of the process, clean the filter module, tubing, and glassware using dilute nitric acid.

3.3 Experimental Setup, Soil Preparation, and Exposure Conditions

1. Conduct experiment using randomized design with a minimum of three replicates per treatment.
2. Collect soil from a 0 to 30 cm depth, air-dry for 7 days, and sieve to separate any larger soil, wood chips or rocks that might be present in soil.
3. Determine the physical composition of soil in the form of sand, silt, and clay. Also, measure background metal concentration (e.g., Cu, Zn, Ag, etc.) in the soil. This can be achieved using an inductively coupled plasma-optical emission spectroscopy (ICP-OES), mass spectroscopy (ICP-MS), or atomic absorption spectroscopy (AAS).
4. Measure other soil characteristics (pH, conductivity, ORP, etc.) before planting.
5. Measure soil pH and electrical conductivity until harvest (at 15–30 days interval).
6. For soil amendment, suspend the test chemical in 100 mL of distilled water or nanopure water to achieve the desired (nominal/analytical) concentrations.

7. Use untreated soil to represent negative control, and appropriate compounds (e.g., dissolved Cu²⁺ ions, Zn²⁺ ions, Ag⁺ ions) as positive controls.
8. Disperse desired ENPs and respective bulk/ionic compounds using ultrasonication (e.g., 100 W, 40 kHz) for 30 min at 25 °C.
9. Stir the suspension with a magnetic bar to further minimize aggregation, especially for the ENPs with potential for aggregation.
10. Add the ENPs to the soil and mix using a mechanical or hand mixer before sowing.

3.4 Planting and Crop Management

1. Conduct study under outdoor micro/mesocosm condition mimicking the natural field environment.
2. Obtain seeds of desired plants (e.g., soybean, fenugreek, corn) and sow in polyethylene pots. Ensure each pot contains 4 kg soil.
3. Before sowing, immerse seed in a suspension of nitrogen fixing symbiotic bacteria (e.g., *Bradyrhizobium japonicum*) for 30 min.
4. Plant two inoculated seeds per pot at a soil depth of 2.5 cm following soil amendment with NPs (e.g., CuONPs, ZnONPs), corresponding metal ions (Cu²⁺, Zn²⁺) and/or bulk counterparts (micronized Cu/CuO or Zn/ZnO).
5. Evaluate sub-sample of irrigation water for total metal concentration using an ICP-OES, ICP-MS, or AAS.
6. Harvest plants (or their parts) upon maturity, oven-dry at 70 °C, weigh different parts separately in paper bags, and store in plastic bags until analysis.

3.5 Symbiont/AMF Preparation and Inoculation

1. Reconstitute freeze-dried N₂-fixing bacteria, *Rhizobium meliloti* strain PTTC 1684, in sterile Tryptic Soy Agar (TSA) and incubate for 3 days in dark at 25 °C.
2. Using loop, transfer the pure culture into sterile Tryptic Soy Broth (TSB) and incubate for 5 days in dark at 25 °C with constant shaking (180 rpm).
3. Centrifuge the culture at 6000 × g for 10 min and discard the supernatant.
4. Resuspend the cell pellets in distilled water containing 1% carboxy methyl cellulose to an optical density of 1 ($\lambda = 600$ nm).
5. Then, soak the desired plant seeds in the resuspended *R. meliloti* cells for 1 h before inserting into transplant tray filled with peat:cocopeat (1:1 w/w).

6. Also, deposit 100 μ L of resuspended *R. meliloti* culture into the planting holes to facilitate and establish AMF colonization.
7. Place the transplant trays in greenhouse for seedling growth and water daily for appropriate moisture before transferring to the field micro/mesocosm.
8. For AMF infection, mix fine sterilized sand (<2 mm diameter) and perlite (1:1 w/w) together.
9. Apply 20 g inoculum comprising of AMF (e.g., *Glomus intraradices*) roots, spores (50–150 spores/g), and hyphae into the sand and perlite mixture [21].
10. Transfer 400 g of the mixture into a 500 mL plastic pot.
11. Transplant two-three seedlings per pot and grow in field micro/mesocosm for full lifecycle.

3.6 Determination of Endpoints of Oxidative Stress Responses

3.6.1 Measurement of Malondialdehyde Concentration

1. Determine the level of lipid peroxidation by measuring the formation of malondialdehyde (MDA) content with thiobarbituric acid (TBA) using the method described by Heath and Packer [26].
2. With 1.5 mL of 0.1% trichloroacetic acid (TCA), homogenize fresh leaf tissue samples.
3. Centrifuge the resultant homogenate at 10,000 $\times \text{g}$ for 10 min.
4. Add 1 mL of the supernatant to 2 mL of 20% TCA containing 0.5% TBA.
5. Heat the extract in a water bath at 95 °C for 30 min, and then cool in an ice bath.
6. Centrifuge again at 10,000 $\times \text{g}$ for 10 min.
7. Read the absorbance of the supernatant at 532 nm and 600 nm using an UV-Vis spectrophotometer.
8. Express MDA concentration as nmol/g FW (using extinction coefficient of 155 mM⁻¹ cm⁻¹) [27].

3.6.2 Measurement of Hydrogen Peroxide

1. Measure the hydrogen peroxide produced in leaf following the established method (e.g., Ref. 28).
2. Add liquid nitrogen to fresh leaves and homogenize in 12 mL cold acetone.
3. Filter the homogenate using Whatman filter paper, then dilute using 4 mL reagent of titanium (16%) and 0.2 mL ammonium hydroxide (28%).

4. Centrifuge the tissue extract at 8500 rpm or about $8000 \times g$ for 5 min at 4 °C.
5. Isolate the supernatant and then wash the precipitate with 5 mL acetone.
6. Add 2 mL of sulfuric acid. Measure absorption at 410 nm using an UV-Vis spectrophotometer.
7. Finally, calculate hydrogen peroxide level using the standard curve prepared in similar way and express as nmol/g FW.

3.6.3 Measurement of Superoxide Dismutase

1. Freeze tissue samples (1 g of fresh leaf tissue) in liquid nitrogen and homogenize in 10 mL of 0.1 M potassium phosphate buffer at pH 7.5.
2. Centrifuge the tissue extract at $20,000 \times g$ for 30 min at 4 °C.
3. Then, collect the supernatant, and separate into several aliquots and store at –20 °C.
4. Determine the superoxide dismutase (SOD) level by measuring inhibition of the photochemical reduction of nitroblue tetrazolium (NBT) at 560 nm using an UV-Vis spectrophotometer [27].

3.6.4 Measurement of Catalase Activity

1. Determine the CAT activity by measuring decrease in absorbance at 240 nm following the decomposition of hydrogen peroxide [27].
2. Detect the decrease in absorbance for a period of 100 s at 5 s interval at room temperature (25 °C).

3.6.5 Measurement of Guaiacol Peroxidase Activity

1. Estimate leaf guaiacol peroxidase (POX) activity following the established method as previously developed by MacAdam et al. [29].
2. Add 50 µL of plant extract to 1.35 mL potassium phosphate buffer (0.1 M, pH 6.0), 100 µL guaiacol (45 mM), and 500 µL hydrogen peroxide (44 mM).
3. Then, measure changes in absorbance at 470 nm using an UV-Vis spectrophotometer at 10 s interval for 300 s at 25 °C.

3.6.6 Measurement of Ascorbate Peroxidase Activity

1. Measure leaf ascorbate peroxidase (APX) activity by monitoring the rate of ascorbate oxidation with hydrogen peroxide using the established method as previously developed by Narwal et al. [27].
2. Measure the decrease in ascorbic acid using UV-Vis spectrophotometer over a period of 500 s at 10 s interval at room temperature (25 °C).
3. Calculate APX activity using an extinction coefficient of $2.8 \text{ mM}^{-1} \text{ cm}^{-1}$.

3.6.7 Measurement of Scavenging of Hydrogen Peroxide

1. Measure the scavenging of hydrogen peroxide according to the method previously described by Benkebila [30].
2. Add 600 µL of freshly prepared 2 mM hydrogen peroxide in phosphate buffer saline into 1 mL of the plant extract.
3. Prepare the control sample by adding 1 mL of PBS and 600 µL of freshly prepared 2 mM hydrogen peroxide in PBS.
4. Leave the mixture for 10–15 min at room temperature.
5. Measure absorbance at 230 nm using the UV-Vis spectrophotometer.

3.7 Measurement of Root Parameters

1. To characterize the root system, measure the root length (RL; cm), root volume (RV; cm³), root area (RA; cm²), and root density (RD; g/cm³) as follows.
2. Wash the roots several times with distilled or Milli-Q water.
3. Using a 1000 mL graduated cylinder with water, measure the root volume via water displacement method.
4. Measure the root length using a ruler.
5. Measure the root dry weight using an analytical balance and express in gram per plant.
6. Determine root density (RD) as a ratio of mean root dry weight (RDW; g) to root volume (RV; cm³) [31]:

$$RD = \frac{RDW}{RV} \quad (1)$$

7. Determine root area (RA; cm²) using the following equation [31]:

$$RA = 2(RL \times \pi \times RV)^{0.5} \quad (2)$$

3.8 Measurement of Biouptake

1. Upon maturity or completion of lifecycle, harvest different plant parts as desired (root, shoot, seeds).
2. Measure the fresh weight (FW) of each part separately. Alternately, they can be oven-dried at 70 °C overnight and report the biomass as dry weight (DW).
3. Grind the tissue using mortar and pestle in liquid nitrogen.
4. Acid digest the tissue for metal uptake following the USEPA Method 3050B (SW-846).
5. Determine total metal concentration in each plant part using an ICP-MS, ICP-OES, or AAS.

3.9 Localization of ENPs in Seed

1. Prefix seed samples in 2.5% glutaraldehyde for 1.5 h.
2. Wash three times in 0.1 M phosphate buffer.
3. Postfix in 1% Osmium tetroxide for 1 h, dehydrate in acetone, and infiltrate and embed in epoxy resin.

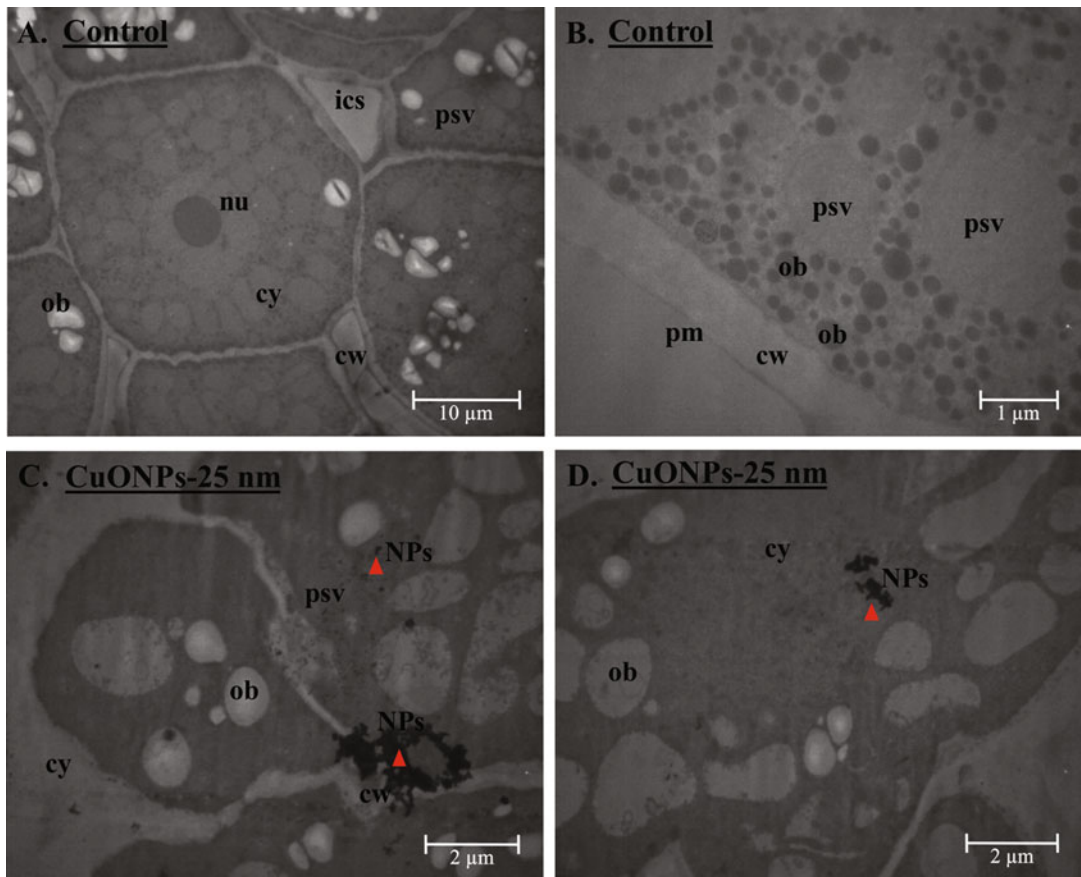


Fig. 2 TEM analysis of ultrastructure of soybean (*Glycine max* cv. Kowsar) seed embryo with 25 nm CuONPs treatment at 500 µg/g-soil (**c, d**) and compared with control seeds (without nanoparticles) (**a, b**). Electron dense metal aggregates are clearly visible within cell wall (cw)/plasma membrane (pm) including within the cytoplasm (cy) and/or protein storage vacuoles (psv) for the seeds with 25 nm CuONPs treatment at 500 µg/g-soil (**c, d**). nu = nucleus, ics = intracellular space, ob = oil bodies, NPs = nanoparticles (red triangle). (Reproduced with permission from Ref. 23)

4. Image samples using electron microscopy (TEM and/or SEM) and locate singular ENPs and/or aggregates as shown in Figs. 2 and 3.
5. The morphological parameters of ENPs such as size, shape, and state of aggregation within the tissue can be analyzed using software such as ImageJ or Digimizer.

3.10 Measurement of Crop Yield or Seed Biomass

1. Upon maturity or completion of lifecycle, harvest the seeds.
2. Air-dry the seeds, or alternately, oven-dry at 70 °C overnight, and record the biomass using an analytical balance.

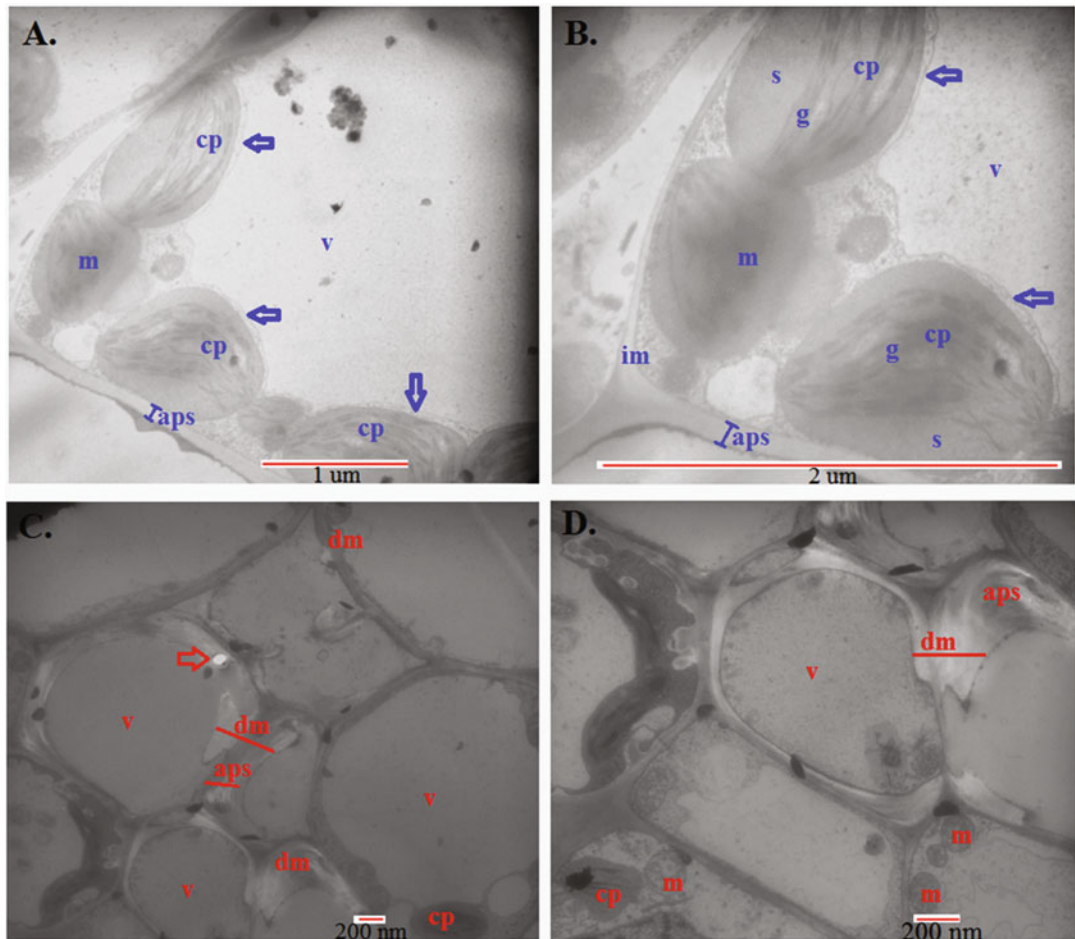


Fig. 3 TEM analysis of ultramicroscopic structure of fenugreek (*Trigonella foenum-graecum*) leaf mesophyll cells showing: **(a, b)** typical subcellular organelles including chloroplast (cp), mitochondria (m), central vacuole (v), apoplastic space (aps), intact plasma membrane (im), grana (g), and stroma (s) in non-AMF inoculated control leaves; **(c, d)** whereas plants (non-AMF inoculated) exposed to 18.4 nm ZnONPs ($1000 \mu\text{g g}^{-1}$) showed anomalies, including disintegrated plasma membrane (dm), wider apoplastic spacing, and lower chloroplast number. Blue arrow points to intact chloroplast membrane **(a, b)**. Electron dense spot (red arrow; **c**) is suggestive of particle transport into the mesophyll cell leading to membrane damage. (Reproduced with permission from Ref. 21)

4 Notes

1. Designated personal protective equipment (PPE) must be worn at all times when dealing with ENPs and other harsh chemicals.
2. Harsh chemicals such as nitric acid or sodium hydroxide must be prepared or diluted under a working chemical fume hood.
3. It is recommended to grow plants for the entire lifecycle to determine comprehensive understanding of nanophytotoxicity.

4. Phytotoxicity investigation using high-purity ENPs is critically important, and to this end, application of ultrapurification techniques such as TFF coupled with suitable pore size hollow fiber membranes have enabled separation of toxic dissolved ions and impurities from the ENP suspensions [7, 8, 32–34]. Use of commercially procured ENPs without further purification (as has been routinely reported in the literature) could complicate the mechanistic understanding of ENP toxicity to plants, due to potential confounding effects of toxic impurities (e.g., heavy metal ions in carbon nanotubes samples, and dissolved Cd/Se ions in commercial quantum dots samples) that might be present in the nanosuspensions [7, 8, 32–34].
5. Electrical conductivity (EC) is used as a surrogate measure for ENP purity as zero valent nanoparticles do not significantly contribute to the suspension's EC [33]. The purified nanosuspension obtained following TFF should be analyzed for basic characteristics using methods such as dynamic light scattering (DLS) and electron microscopy (EM) [33, 34].
6. Further, a minor pH adjustment might be necessary prior to any toxicity studies, which can be achieved using dilute nitric acid or sodium hydroxide.
7. Higher feed flow rate can also be maintained for fast filtration (should the need be) during TFF, but it may come with a cost of increased TMP, which can automatically shut down the system for safety. In addition, excessive TMPs (above 20 psi) may lead to the rupture of the tubing and/or filter membranes, including leakage at various connection points [34].
8. When the final retentate demonstrates conductivity of $10 \mu\text{S cm}^{-1}$ or less, the TFF purified nanosuspension is deemed of highest purity, and thus the process is considered successful in removing the impurities. However, one must characterize the nanosuspension using DLS before and after TFF to understand potential changes that might have occurred in the HDD and zeta potential of the suspensions (this should be a part of routine nanosuspension characterization, and is not unique to TFF). The zeta potential may change in magnitude following TFF, if not in polarity (e.g., negative to positive, or vice-versa). If the ENPs are plasmonic (e.g., AuNPs, AgNPs, CuNPs), UV-Vis spectroscopy can be used alongside the DLS to corroborate any changes in HDD and zeta potential. In some cases, the removal of contaminants and/or larger biomolecules is difficult to document. Since the range of sizes is dependent on material type, vendor, and other factors, there is no uniform set of data quality objectives (DQOs) that can be established for use with TFF [34].

9. Data from the TFF software can be stored electronically, but in general are not very meaningful and typically are not reported in research publications. They do, however, provide information on operational history of the instrument for any given sample. Since the operator attends the instrument during TFF, the data can be observed on the pump head's screen in real time and operation parameters can be adjusted as necessary without the use of the software and computer [34].
10. Ensure irrigation water does not contain significant amount of pollutants.
11. Make sure to express one unit of APX as 1 mM of ascorbate oxidized per min per mg of protein.
12. Make sure to express one unit of SOD activity as the amount of enzyme which causes 50% inhibition of oxidation reactions per mg of protein in extract.
13. Make sure to express one unit of CAT activity as 1 mM of hydrogen peroxide consumed per mg of protein using an extinction coefficient of $40 \text{ mM}^{-1} \text{ cm}^{-1}$.
14. Make sure to express one unit of POX activity as 1 mMol tetrاغuaicacol consumed per min per mg of protein using an extinction coefficient of $26.6 \text{ mM}^{-1} \text{ cm}^{-1}$.
15. For easier plant removal from the pot at harvest, it is recommended to place an inner liner of polyethylene (PE) mesh in each pot. The PE mesh can have holes of 5 mm diameter to allow for drainage of any excess irrigation water [23].

Acknowledgements

LRP gratefully acknowledges funding support from East Carolina University (grant #111101 to LRP). CSU thanks ECU Graduate School and Department of Public Health for the graduate assistantship. SF would also like to thank Shahrekord University for the financial support (grant #96-GRN1M731 to SF).

References

1. White JC, Gardea-Torresdey JL (2018) Achieving food security through the very small. *Nat Nanotechnol* 13:627–629. <https://doi.org/10.1038/s41565-018-0223-y>
2. National Nanotechnology Initiative (NNI) (2006). Environmental, health and safety research needs for engineered nanoscale materials. September nanoscale science, engineering, and technology subcommittee, Committee on technology, National Science and Technology Council. http://www.nano.gov/sites/default/files/pub_resource/nni_ehs_research_needs.pdf?q=NNI_EHS_research_needs.pdf
3. Milani N, McLaughlin MJ, Stacey SP, Kirby JK, Hettiarachchi GM, Beak DG, Cornelis G (2012) Dissolution kinetics of macronutrient fertilizers coated with manufactured zinc oxide nanoparticles. *J Agric Food Chem* 60:3991–3998
4. Wiesner MR, Lowry GV, Alvarez P, Dionysiou D, Biswas P (2006) Assessing the

- risks of manufactured nanomaterials. Environ Sci Technol 40:4336–4345
5. Pokhrel LR, Dubey B (2013) Evaluation of developmental responses of two crop plants exposed to silver and zinc oxide nanoparticles. Sci Total Environ 452–453:321–332
 6. Andersen CP, King G, Plocher M, Storm M, Pokhrel LR, Johnson MG, Rygiewicz PT (2016) Germination and early plant development of 10 plant species exposed to TiO₂ and CeO₂ nanoparticles. Environ Toxicol Chem 35 (9):2223–2229
 7. Pokhrel LR, Dubey B, Scheuerman PR (2013) Impacts of select organic ligands on the colloidal stability, dissolution dynamics, and toxicity of silver nanoparticles. Environ Sci Technol 47:12877–12885
 8. Pokhrel LR, Andersen CP, Rygiewicz PT, Johnson MG (2014) Preferential interaction of Na⁺ over K⁺ with carboxylate-functionalized silver nanoparticles. Sci Total Environ 490:11–18
 9. Pokhrel LR, Dubey B, Scheuerman PR (2014) Natural water chemistry (dissolved organic carbon, pH, and hardness) modulates colloidal stability, dissolution, and antimicrobial activity of silver nanoparticles. Environ Sci Nano 1:45–54
 10. Maynard AD, Aitken RJ, Butz T, Colvin V, Donaldson K, Ober dorster G (2006) Safe handling of nanotechnology. Nature 444:267–269
 11. Ahmed B, Zaidi A, Khan MS, Rizvi A, Saif S, Shahid M (2017) Perspectives of plant growth promoting rhizobacteria in growth enhancement and sustainable production of tomato. Microb Strat Veg Prod:125–149. https://doi.org/10.1007/978-3-319-54401-4_6
 12. Smith SE, Read DJ (2008) Mycorrhizal Symbiosis. Academic Press, London
 13. Miller RM, Jastrow JD (2000) Mycorrhizal fungi influence soil structure. In: Kapulnik Y, Douds DD (eds) Arbuscular mycorrhizas: molecular biology and physiology. Kluwer Academic, Dordrecht, pp 3–18
 14. Miransari M (2011a) Arbuscular mycorrhizal fungi and nitrogen uptake. Arch Microbiol 193:77–81
 15. Miransari M (2011b) Hyperaccumulators, arbuscular mycorrhizal fungi and stress of heavy metals. Biotechnol Adv 29:645–653
 16. Gaur A, Adholeya A (2004) Prospects of arbuscular mycorrhizal fungi in phytoremediation of heavy metal contaminated soils. Curr Sci 86:528–534
 17. Wright SF, Upadhyaya A (1996) Extraction of an abundant and unusual protein from soil and comparison with hyphal protein of arbuscular mycorrhizal fungi. Soil Sci 161:575–586
 18. Gonzalez-Chavez MC, Carrillo-Gonzalez R, Wright SF, Nichols KA (2004) The role of glomalin, a protein produced by arbuscular mycorrhizal fungi, in sequestering potentially toxic elements. Environ Pollut 130:317–323
 19. Xu ZY, Tang M, Chen H, Ban YH, Zhang HH (2012) Microbial community structure in the rhizosphere of *Sophora viciifolia* grown at a lead and zinc mine of northwest China. Sci Total Environ 435–436:453–464
 20. Chen BD, Shen H, Li XL, Feng G, Christie P (2004) Effects of EDTA application and arbuscular mycorrhizal colonization on growth and zinc uptake by maize (*Zea mays* L.) in soil experimentally contaminated with zinc. Plant Soil 261:219–229
 21. Ghasemi Siani N, Fallah S, Pokhrel LR, Rostamnejadi A (2017) Natural amelioration of zinc oxide nanoparticles toxicity in fenugreek (*Trigonella foenum-gracum*) by arbuscular mycorrhizal (*Glomus intraradices*) secretion of glomalin. Plant Physiol Biochem 112:227–238. <https://doi.org/10.1016/j.plaphy.2017.01.001>
 22. Yusefi-Tanha E, Fallah S, Rostamnejadi A, Pokhrel LR (2020) Particle size and concentration dependent toxicity of copper oxide nanoparticles (CuONPs) on seed yield and antioxidant defense system in soil grown soybean (*Glycine max* cv. Kowsar). Sci. Total Environ 715:136994. <https://doi.org/10.1016/j.scitotenv.2020.136994>
 23. Yusefi-Tanha E, Fallah S, Rostamnejadi A, Pokhrel LR (2020) Root system architecture, copper uptake and tissue distribution in soybean (*Glycine max* (L.) Merr.) grown in copper oxide nanoparticle (CuONP) amended soil and implications for human nutrition. Plan Theory 9(10):1326. <https://doi.org/10.3390/plants9101326>
 24. Yusefi-Tanha E, Fallah S, Rostamnejadi A, Pokhrel LR (2020) Zinc oxide nanoparticles (ZnONPs) as a novel Nanofertilizer: influence on seed yield and antioxidant defense system in soil grown soybean (*Glycine max* cv. Kowsar). Sci Total Environ 738:140240. <https://doi.org/10.1016/j.scitotenv.2020.140240>
 25. Zandi S, Kameli P, Salamat H, Ahmadvand H, Hakimi M (2011) Microstructure and optical properties of ZnO nanoparticles prepared by a simple method. Phys B 406:3215–3218
 26. Heath RL, Packer L (1968) Photoperoxidation in isolated chloroplast: i. kinetics and stoichiometry of fatty acid peroxidation. Arch Biochem Biophys 125(1):189–198. [https://doi.org/10.1016/0003-9861\(68\)90654-1](https://doi.org/10.1016/0003-9861(68)90654-1)

27. Narwal SS, Bogatek R, Zagdanska BM, Sam Pietro DA, Vattuone MA (2009) Plant biochemistry. Studium Press LLC, Texas
28. Nag S, Saha K, Choudhuri MA (2000) A rapid and sensitive assay method for measuring amine oxidase based on hydrogen peroxide–titanium complex formation. *Plant Sci* 157 (2):157–163. [https://doi.org/10.1016/S0168-9452\(00\)00281-8](https://doi.org/10.1016/S0168-9452(00)00281-8)
29. MacAdam JW, Nelson CJ, Sharp RE (1992) Peroxidase activity in the leaf elongation zone of tall fescue. *Plant Physiol* 99:872–878. <https://doi.org/10.1104/pp.99.3.872>
30. Benkeblia N (2005) Free-radical scavenging capacity and antioxidant properties of some selected onions (*Allium cepa* L.) and garlic (*Allium sativum* L.) extracts. *Braz Arch Biol Technol* 48(5):753–759. <https://doi.org/10.1590/S1516-89132005000600011>
31. De Baets S, Poesen J, Knapen A, Barbera GG, Navarro JA (2007) Root characteristics of representative Mediterranean plant species and their erosion-reducing potential during concentrated runoff. *Plant Soil* 294:169–183. <https://doi.org/10.1007/s11104-007-9244-2>
32. Dorney KM, Baker JD, Edwards ML, Kanel SR, O’Malley M, Pavel Sizemore IE (2014) Tangential flow filtration of colloidal silver nanoparticles: a “green” laboratory experiment for chemistry and engineering students. *J Chem Educ* 91(7):1044–1049
33. Pokhrel LR, Silva T, Dubey B, El Badawy AM, Tolaymat TM, Scheuerman PR (2012) Rapid screening of aquatic toxicity of several metal-based nanoparticles using the MetPLATE™ bioassay. *Sci Total Environ* 426:414–422
34. Pokhrel LR, Andersen CP. SOP for Purification of Engineered Nanoparticles Using the Tangential Flow Filtration (TFF) System. National Health and Environmental Effects Research Laboratory, Western Ecology Division, USEPA, OR. January 2015, Pages 1-12. DCN: EEB/CA/2015-01-r0



Chapter 19

Detection of Cadmium Toxicity in Plant

Xiaoxiao Liu, Lina Yin, Shiwen Wang, and Zhiyong Zhang

Abstract

Cadmium (Cd) is widespread in the soil, water, and atmosphere, so Cd toxicity to human can happen by breathing in air, drinking water, and eating food from plant grown in Cd-contaminated soil. Cd pollution draws a lot of attention from the scientific community and also regulatory agents and is researched widely by using both plant and animal system. In this protocol, the detection of cadmium (Cd) is described in soil and mature maize (*Zea mays*) plant with the atomic absorption spectrometer. The Cd uptake, translocation factor, and Cd health risk index are also introduced. The protocol can be modified slightly to measure Cd in different types of plants.

Key words Cadmium, Toxicity, Plant, Atomic absorption spectrometer

1 Introduction

Environment pollution by metals is a major environmental challenge. Cadmium (Cd) is of worldwide concerned toxic metal, being detrimental to humans, animals, and plants [1]. Cd has the nature of high mobility and hydrophilic in the plant-soil system, so plants can take up Cd even when only low levels of Cd [2]. High Cd concentrations in plants not only negatively affect plant growth, crop production and quality but also threaten human food security by transmitting via the food chain [3]. Cd is considered a human carcinogen as it can cause organ lesions and other diseases such as cancer, heart disease, and diabetes [4].

Rapid industrialization has increased the amount of environmental Cd pollution. Anthropogenic sources such as mining, plastic manufacturing, Cd-containing fertilizers, and sewage sludge account for nearly 90% of released Cd [5]. The large quantities of Cd that have been released into the environment have led to high concentrations of Cd in soil [6]. Cd concentrations in soil solutions from 0.32 to 1 $\mu\text{mol/L}$ are considered moderately polluted [7]. The excessive presence of Cd in soil is of great concern considering that the material is transported very efficiently from soil into

plants by root uptake [1]. Compared with other heavy metals, Cd is readily soluble and transferable, and thus is more easily absorbed by plants and accumulated in different plant tissues. Humans can ingest Cd in food from any part of the food chain and can easily accumulate Cd levels above the safety limit [8, 9]. Therefore, efforts to understand plant Cd uptake or Cd transfer from soil to plant are crucial for food security and human health.

2 Materials

2.1 Reagents

1. Concentrated hydrochloric acid (HCl).
2. Concentrated nitric acid (HNO₃).
3. Aqua regia (HCl:HNO₃ = 3:1) (*see Note 1*).
4. Perchloric acid (HClO₄).

2.2 Equipment

1. Magnetic stirrer and stirring bar.
2. Pipette grinding.
3. Hot-plate.
4. Pipettor.
5. Sieve with pores of 2 mm diameter, here abbreviated as 2 mm sieve.
6. Shaker.
7. Volumetric flask.
8. Filter paper.
9. Atomic absorption spectrometer.

2.3 Plant Species (See Note 2)

Maize (*Zea mays* L.) cultivar.

2.4 Soil Type (See Note 3)

Loessial soil.

3 Methods

3.1 Detection of Cd in Soil

1. Soil samples are ground to small particles with homogenizer and then sieved with a 2 mm sieve.
2. 0.3 g soil is placed in a digestion tube, 10 mL aqua regia (HCl: HNO₃ = 3:1) is added to each tube with simultaneous gentle shaking, and then stood overnight.
3. The tubes are placed on a hot-plate set to 160 °C for 1 h and cooled.

4. 4 mL HClO₄ is added to tubes and digestion was performed at 230 °C until the digested solution samples have turned colorless (*see Note 4*)
5. The cooled digestion liquid is transferred into a 25 mL volumetric flask with filter paper and diluted to a constant volume with deionized water.
6. The supernatant is assessed with an atomic absorption spectrometer. (*see Note 5*).

3.2 Detection of Cd in Plant Tissue

1. Plant tissue samples are added with 5 mL HNO₃ in tubes and then kept overnight.
2. The tubes are placed on a hot-plate set to 100 °C.
3. When the samples change to yellow color, the boiling liquid samples are cooled and then added to 2 mL HClO₄.
4. The samples are digested at 180 °C until the digested samples turn colorless.
5. The digested samples are diluted to a constant volume of 25 mL.
6. The digested samples are assessed with an atomic absorption spectrometer to measure Cd content in plant tissues.

3.3 The Cd Uptake in Plant Tissues

The total uptake of Cd is calculated by multiplying the measured Cd content by the sample biomass.

3.4 Calculation of Cd Translocation from Soil to Plant

1. *Cd bioaccumulation factor* is calculated at mature stage of maize according to the method of Kalcikova et al. [10] as follows:

$$\text{Cd bioaccumulation factor} = \text{Cd in plant tissue}/\text{Cd in soil}$$

Cd in plant tissues (root, shoot, and grain) is given in mg/kg dry weight while that in soil is given in mg/kg soil dry weight.

2. *Cd translocation factors* of different plant tissues at mature stage of maize are determined as described by Rezvani and Zaefarian [11] according to the following calculations:

$$\text{Translocation factor (grain to shoot)} = \text{Cd (grain)}/\text{Cd (shoot)}$$

$$\text{Translocation factor (shoot to root)} = \text{Cd (shoot)}/\text{Cd (root)}$$

$$\text{Translocation factor (root to soil)} = \text{Cd (root)}/\text{Cd (soil)}$$

where grain, shoot, root, and soil Cd contents are given as mg/kg dry weight.

3. *Human Cd Health Risk Index (HRI)* of maize is calculated according to Rizwan et al. [12] as follows:

$$\text{HRI} = \frac{\text{C(Cd)} \times \text{C(factor)} \times \text{DFI(daily food intake)}}{\text{ABW(average body weight)} \times \text{RDC(oral reference dose of Cd)}}$$

where $C(\text{Cd})$ is the Cd content in grains (mg/kg), $C(\text{factor})$ is a correction factor, the value is 0.085, and DFI is set at 0.4 kg/person/day according to the FAO/WHO-proposed Provisional Tolerable Daily Intake (PTDI). ABW is set at 70 kg assuming an average human adult body weight. ORDC is 0.001 mg/kg/day according to the U.S. EPA [13].

4 Notes

1. Aqua regia ($\text{HCl}:\text{HNO}_3 = 3:1$) is highly corrosive, please pay attention to safety.
2. The protocol described in this method chapter can be used to test any plant. Here, we just use maize as an example to present the detailed method. Corn is one of the major cereal crops cultivated worldwide.
3. The protocol described in this method chapter can be used to test any type of soil. Here, we just use loessial soil as an example to present the detailed method.
4. Digestion could be stopped until the liquid is completely colorless.
5. Atomic absorption spectrometer could be used to detect more than 70 elements.

References

1. Ismael MA, Elyamine AM, Moussa MG, Cai M, Zhao X, Hu C (2019) Cadmium in plants: uptake, toxicity, and its interactions with selenium fertilizers. *Metalomics* 11:255–277
2. Zia-ur-Rehman M, Khalid H, Akmal F, Ali S, Rizwan M, Qayyum MF, Iqbal M, Khalid MU, Azhar M (2017) Effect of limestone, lignite and biochar applied alone and combined on cadmium uptake in wheat and rice under rotation in an effluent irrigated field. *Environ Pollut* 227:560–568
3. Clemens S, Aarts MG, Thomine S, Verbruggen N (2013) Plant science: the key to preventing slow cadmium poisoning. *Trends Plant Sci* 18:92–99
4. Chaney RL (2015) How does contamination of rice soils with Cd and Zn cause high incidence of human Cd disease in subsistence rice farmers. *Curr Pollut Rep* 1:13–22
5. Jarup L, Akesson A (2009) Current status of cadmium as an environmental health problem. *Toxicol Appl Pharm* 238:201–208
6. Khan MA, Khan S, Khan A, Alam M (2017) Soil contamination with cadmium, consequences and remediation using organic amendments. *Sci Total Environ* 601–602:1591–1605
7. Sanita di Toppi L, Gabbielli R (1999) Response to cadmium in higher plants. *Environ Exp Bot* 41:105–130
8. Gallego SM, Pena LB, Barcia RA, Azpilicueta CE, Iannone MF, Rosales EP, Zawoznik MS, Groppa MD, Benavides MP (2012) Unraveling cadmium toxicity and tolerance in plants: insight into regulatory mechanisms. *Environ Exp Bot* 83:33–46
9. Du Y, Hu XF, Wu XH, Shu Y, Jiang Y, Yan XJ (2013) Affects of mining activities on Cd pollution to the paddy soils and rice grain in Hunan province, central South China. *Environ Monit Assess* 185:9843–9856
10. Kalcikova G, Zupancic M, Jemec A, Gotvajn AZ (2016) The impact of humic acid on chromium phytoextraction by aquatic macrophyte *Lemna minor*. *Chemosphere* 147:311–317

11. Rezvani M, Zaefarian F (2011) Bioaccumulation and translocation factors of cadmium and lead in *Aeluropus littoralis*. Austr J Agric Eng 2: P114
12. Rizwan M, Ali S, Hussain A, Ali Q, Shakoor MB, Zia-Ur-Rehman M, Farid M, Asma M (2017) Effect of zinc-lysine on growth, yield and cadmium uptake in wheat (*Triticum aestivum* L.) and health risk assessment. Chemosphere 187:35–42
13. U.S. EPA (1985) Updated mutagenicity and carcinogenicity Assement of cadmium. Addendum to the health assessment document for cadmium (EPA 600/b-B1-023). EPA 600/B-83-025F

Part III

Microbe Toxicity



Chapter 20

Mutagenicity Evaluation of Nanoparticles by the Ames Assay

Xiaoping Pan

Abstract

The Ames assay is a classic and robust method for identifying and evaluating chemical mutagens that reverse the mutations of *Salmonella typhimurium* and/or *Escherichia coli* bacteria strains with amino acid synthesis defects. It is also called the bacterial reverse mutation assay. Ames assay has been widely used for detecting genetic toxicity of many chemicals and gained increased applications in risk assessment of emerging environmental pollutants such as nanomaterials. In this chapter, we presented a detailed step-by-step method using the Ames assay to detect potential mutagenicity of metal oxide nanoparticles. The strategy to use the liver S9 fraction for bioactivation and a preincubation procedure is recommended. This method is easy to use to test genetic toxicity of other environmental contaminants and new chemicals.

Key words Mutagenicity, Genetic toxicity, The Ames assay, Nanomaterials, Metal oxide nanoparticles

1 Introduction

Nanoparticles are an extensive class of man-made or naturally occurred chemicals with less than 100 nm in at least one dimension. Nanoparticles have been widely used in basic and applied fields, such as in the electronics industry, as catalysts in chemical engineering, as new aerospace materials, as drug delivery vehicle in biomedicine, and as components in personal care products such as toothpaste and sunscreen [1]. Given the rapid development of nanotechnology and the increasing application of nanomaterials, more and more industrial wastes containing nanomaterials are being released into the environments, which has been detected in soil and water resources [2]. This represents an important group of emerging environmental pollution and has raised the public's concern regarding their environmental and human health impacts.

Since two individual groups published the toxicity study on polyalkylcyanoacrylate nanoparticle in *Journal of Pharmaceutical Sciences* in 1982 [3, 4], researches on nanoparticle toxicity have

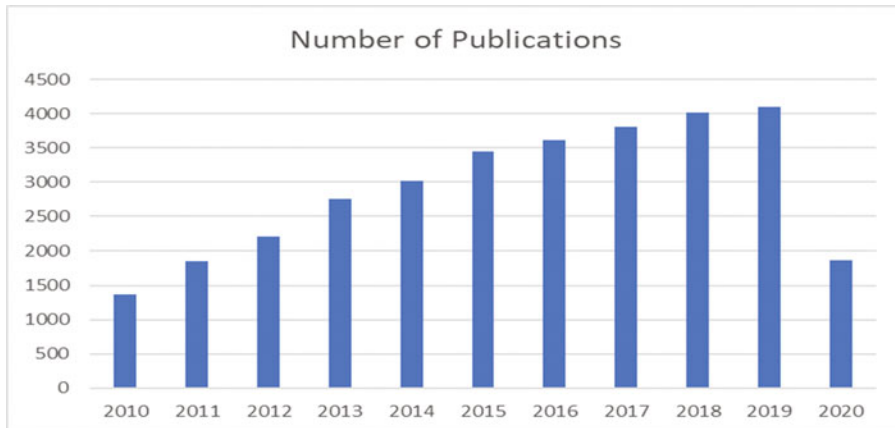


Fig. 1 The number of publications on nanoparticle toxicity based on PubMed literature search on June 9th, 2020

been significantly increased. Up to June 9th, 2020, a total of 29,766 papers were shown by simply using the key words “nanoparticle” and “toxicity” in literature search on PubMed. Most of these papers were published after 2010 (Fig. 1). Before 2000, there were only 77 publications on this topic.

Many studies show that nanoparticles affect organisms at different levels, including individual, cellular, biochemical and physiological levels [5–8]. Nanoparticles also induced abnormal expression of protein-coding and noncoding RNA genes [9–15]. A few experiments also show that nanoparticles induced genetic toxicity resulting in gene mutations implicated in various plant and animal diseases. [16–20]. Thus, the investigation of potential nanoparticle-induced mutagenesis is necessary and important. In this chapter, we described the utilization of the Ames reverse mutation assay for detecting the mutagenesis of metal oxide nanoparticles.

The Ames assay, also called the bacterial reverse mutation assay, is a classic and robust bioassay widely employed for testing whether a chemical or a chemical mixture is mutagenic by testing on bacterial strains of *Salmonella typhimurium* or *Escherichia coli* that contain different types of mutations for amino acid synthesis (*His*⁻ for *S. typhimurium* and *Trp*⁻ for *E. coli*) [21]. Given the mutation, the *Salmonella typhimurium* or *Escherichia coli* tester strains cannot grow in the absence of histidine or tryptophan unless the mutation is reversed by a mutagen or by a spontaneous process that restore the gene function for the amino acid synthesis [21]. Thereby chemicals/materials that induce significant more reversed mutants/colonies than spontaneous reverse mutants (revertant) of negative control are mutagenic. In Ames assay, this is displayed as significantly more bacterial colonies growing on the minimal amino acid medium in mutagen containing plates than on vehicle control

plates. Since its first introduction, the Ames assay has been evolved and modified for a better performance, focusing on adding new tester strains for detection of different types of DNA damages [22, 23]. Currently, there are about 10 different *Salmonella typhimurium* and *Escherichia coli* strains commonly used in the Ames test. For example, the *S. typhimurium* strain TA98 is suitable to detect frameshift mutation whereas the *S. typhimurium* strain TA100 is sensitive to detect the base pair substitution DNA damage [22]. To increase the sensitivity of tester strains, some other mutations were added. The *rfa* mutation has defective lipopolysaccharide (LPS) on the bacterial membrane so the membrane permeability to mutagens is increased. The DNA excision repair mechanism is eliminated on *uvrA* (for *E. coli*) and *uvrB* (*S. typhimurium*) strains. In addition, the pKM101 R-Factor Plasmid enhance the sensitivity to detect chemical and UV-induced mutagenesis. Given some mutagens need metabolic activation by liver enzymes to manifest the mutagenicity, rat or mice livers were used for preparation of the S9 fraction (supernatant collected from drug induced-liver homogenate by centrifuging at $9000 \times g$ for 20 min) which contains general liver enzymes to be used for bioactivation of tested chemicals/materials [22]. In the past couples of decades, Ames assay have been employed to test many chemicals for genetic toxicity [20, 24–30].

Since significant physical and chemical properties alter as the particle size is reduced to the nano range, impacts of manufactured nanomaterials to biological systems are likely different from their bulky-sized counterparts. Toxicological testing is needed to provide dataset necessary for the risk assessment of nanomaterials. This study uses several metal oxide nanoparticles as an example to demonstrate the use of the Ames assay to test potential mutagenicity of nanoparticles. We describe in this method to use S9 activation and a preincubation procedure to enhance the possibility to detect mutagenicity of nanoparticles.

2 Materials, Medium, and Nanoparticle Preparations

2.1 Tested Metal Oxide Nanoparticles

1. Aluminum oxide (Al_2O_3) nanopowder.
2. Cobalt oxide (Co_3O_4) nanopowder.
3. Copper oxide (CuO) nanopowder.
4. Titanium dioxide (TiO_2) nanopowder.
5. Zinc oxide (ZnO) nanopowder.

2.2 Bacterial Strains

1. *Salmonella typhimurium* TA97a (hisD3052/rfa/ ΔuvrB /pKM101).
2. *Salmonella typhimurium* TA98 (hisD3052/rfa/ ΔuvrB /pKM101).

3. *Salmonella typhimurium* TA100 (hisG46/rfa/ Δ uvrB/pKM101).
4. *Salmonella typhimurium* TA1535 (hisG46/rfa/ Δ uvrB).
5. *Escherichia coli* WP2 uvrA (trpE/uvrA).

2.3 Control Reagents

1. Positive control: 2-aminoanthracene dissolved in DMSO at 2 μ g/plate for *S. typhimurium* TA97a, 98, 100, and 1535, and at 10 μ g/plate for *E. coli* WP2 uvrA.
2. Negative control: autoclaved distilled water.

2.4 Working S9 Mix

Treatment of rat or mice with chemical mutagens such as Aroclor-1254 results in general activation of liver enzymes [22]. The original S9 solution should be obtained from a commercial resource since the rodent dosing experiment to produce S9 is not the focus of this study. After obtaining the S9 from a commercial resource, the working S9 mix to be used in this assay can be prepared: S9 fraction at 9% (v/v) from original S9, $\text{Na}_2\text{HPO}_4/\text{NaH}_2\text{PO}_4$ 100 mM, MgCl_2 8 mM, KCl 8 mM, NADP 4 mM, NAD 4 mM, and glucose-6-phosphate 5 mM.

2.5 Preparation of Medium

Reagent	For 500 mL
Bacto-tryptone	5 g
Yeast extract	2.5 g
NaCl	5 g
DI water	Add to 500 mL

Autoclave at 121 °C for 20 min. Aliquot LB broth to 100 mL Erlenmeyer flasks. Each flask contains about 20 mL LB medium. Wait until LB broth to cool down to the room temperature and then inoculate a pure colony of each tester bacterial strain to each flask. Each strain will be cultured separately. Culture the bacteria for ~10–12 h at 37 °C in a shaker incubator at 120 rpm. The cell densities of each culture will then be verified to be $>1 \times 10^9$ cells/mL by measuring the measuring optical density at 600 nm (OD_{600}).

2. Minimal VBE-glucose agar (bottom agar) plate for mutagenicity assay.
 - (a) Firstly, the Vogel-Bonner Medium E, 50× (50× VBE) needs to be made.

Reagent	For 500 mL
Distilled water (45 ° C)	335 mL
Magnesium sulfate MgSO ₄ (7H ₂ O)	5 g
Citric acid monohydrate	50 g
Potassium phosphate, dibasic (anhydrous) K ₂ HPO ₄	250 g
Sodium ammonium phosphate NaNH ₄ PO ₄	87.5 g

Add reagents to warm water in a flask on stirring hotplate in order as listed above. Wait for each to dissolved completely before adding the next, then autoclave at 121 °C for 20 min.

- (b) The minimal VBE-glucose agar plate recipe.

Reagent	Quantity for 1 L
Agar	15 g
Distilled water	930 mL
50× VBE	20 mL
40% glucose	50 mL

Add agar and stir bar to distilled water in a flask, autoclave at 121 °C for 20 min. Sterile filter 40% glucose and 50× VBE and add to the agar solution using sterile technique. Mix well and pour 20 mL minimal agar into each 10 cm petri dish as the bottom agar.

3. Tested mutagens (nanoparticles and positive controls).

Weight 100 mg of each nanoparticle, suspended in 10 mL of water, sonicated overnight and vortex mixed before use. Serial dilutions will be performed to generate the treated concentrations of 10, 100, and 1000 µg/plate of each tested nanoparticles. Each treatment plate contains 0.1 mL of a nanoparticle solution.

4. Top agar.

- (a) D-Biotin solution (5 mM) for top agar.

Reagent	Quantity for 100 mL
D-Biotin	122 mg
Distilled water	Add to 100 mL

(b) L-Histidine solution (5 mM) for top agar.

Reagent	Quantity for 100 mL
L-Histidine	72.5 mg
Distilled water	Add to 100 mL

(c) Top agar for *S. Typhimurium* tester strain.

Reagent	Quantity for 200 mL
Agar	1.2 g
NaCl	1 g
D-Biotin solution (5 mM)	2 mL
L-Histidine solution (5 mM)	2 mL
Distilled water	Add to 200 mL

(d) Top agar for *E. coli* tester strain.

Reagent	Quantity for 200 mL
Agar	1.2 g
NaCl	1 g
L-Histidine solution (5 mM)	2 mL
Distilled water	Add to 200 mL

Autoclave the top agar at 121 °C for 20 min.

2.6 Other Supplies

1. Petri dishes 10 cm in diameter.
2. 5 mL tubes.
3. Flasks.
4. Tips (10, 200, 1000, and 5000 µL).
5. L-shaped spreader.

3 Methods

1. Prepare 5 mL tubes, add the followings in order and label each tube properly:
 - (a) 0.1 mL fresh culture of tester bacterial strains
 - (b) 0.5 mL of S9 working mix prepared as in Subheading 2.4.
 - (c) 0.1 mL nanoparticles, negative control (autoclaved distilled water), or positive control (2-aminoanthracene) solutions.

2. Preincubation for adequate S9 activation: Incubate the 5 mL tube at 37 °C in a shaken water bath at 90 rpm for 60 min.
3. After 60 min incubation, 2 mL of top agar (kept in 45 °C water bath) were added into the 5 mL tube, vortex mixing for 3 s and then pour on top of each bottom agar plate, spread well with a sterile L-shape spreader. Label the plates properly.
4. Incubate at 37 °C for 72 h.
5. After 72 h incubation, plates are taken out of incubator and his⁺ (*S. typhimurium*) and trp⁺ (*E. coli*) revertant colonies are counted within 24 h and recorded in an Excel spreadsheet. Assays should be performed in triplicate/three independent experiments.

4 Data Analysis

Data analysis is performed using the standard statistical software SPSS. Analysis of variance (ANOVA) is used for comparing means of different treatment groups. If there is a significant difference among groups, least significant difference (LSD) multiple comparisons will be conducted to compare means of each group. The *p* value of less than 0.05 is the significant level.

The mutagenicity ratio (MI) should also be calculated [22]:

MI = the total number of revertant colonies in a tested chemical plate
 (spontaneous revertant colonies + induced revertant colonies)/
 the number of revertant colonies in negative control plate (spontaneous revertant colonies)

If the average MI of three biological replicates is equal to or larger than 2 (≥ 2) and the mean difference between the chemical treated group is significantly higher than the control group ($p < 0.05$) determined by the ANOVA analysis, the tested chemical is mutagenic. If the average MI value falls between 1 and 2 and the difference is significant ($p < 0.05$), the tested chemical is still considered mutagenic but of relatively weak mutagenicity. If the average MI is equal to or lower than 1 (≤ 1) and the difference is significant ($p < 0.05$), the chemical should be considered as cytotoxic at the tested concentration. In this case it is necessary to lower the tested concentration and test mutagenicity again using the Ames assay.

5 Notes

1. It is recommended to test the potential mutagenicity of nanoparticles on 5 different bacterial strains in the Ames assay. This is because that different bacterial strain detects a certain type of DNA damage and using multiple strains increase the opportunity to identify mutagens with different action mechanisms.

The *S. typhimurium* TA98 and TA1537 detect frameshift mutations, the *S. typhimurium* TA100 and TA1535 detect base pair substitution mutations, and the TA 97a detects both base-pair substitution mutation and frameshift mutations [22]. The *E. coli* WP2 trp uvrA is used specifically to detect mutations caused by oxidative stress [31].

2. Phenotypic characterization of tester strains is recommended before using, please refer to literature for tester strain phenotyping methods [22]. These include to confirm histidine deficiency (His^-) for *S. typhimurium* strains, tryptophan deficiency (Trp^-) for *E. coli* strains, sensitivity to crystal violet (rfa), sensitivity to ultraviolet light (ΔuvrA for *E. coli* strains and ΔuvrB for *S. typhimurium* strains), and ampicillin resistance (pKM101).
3. Working medium and S9 mix should be freshly made. If leftover medium is intended to be used, they should be stored in refrigerator and use within 1 week.
4. Nanoparticles are unsolvable in the water, when aliquoting the medium into petri dishes, the medium should be mixed thoroughly by vortex mixing to make sure the nanoparticles are evenly distributed in the medium.
5. Autoclaved distilled H_2O which is also the solvent for nanoparticles will be used as the negative control, other solution background should be the same as nanoparticle containing groups. For the positive control, many known mutagens can be used. A different positive control chemical can be selected according to the research purpose and/or the tester strain producer's recommendations.
6. Liver S9 bioactivation: Some chemicals become mutagenic *in vivo* due to bioactivation by liver enzymes such as cytochrome-P450s. To mimic mammalian *in vivo* conditions, the S9 fraction of liver extracts from drug-induced rodent livers are used [21].
7. Three biological replicates should be performed for each treatment and controls.
8. The petri dishes should be placed upside down and cultured in the dark or covered by sterilized aluminum foil to avoid potential photodegeneration.
9. The reverse mutant colonies can be counted by unaided eyes. Please refer to the literature regarding the range of spontaneous revertant counts among different tester bacteria strains [22, 32]. The number of spontaneous revertant is also affected by experimental conditions: preincubation time, concentration of S9 fraction, culturing time, etc. Each lab should maintain a record of spontaneous revertant ranges of their negative and positive controls and check if the spontaneous revertant count is within historical values when conducting a new experiment.

10. Culture plates should be taken out for observation after incubation for 48 h since a 48-h incubation time may be sufficient. The 72 h incubation is recommended in this study which allows the detection of weak mutagens.
11. Some nanoparticles have cytotoxic effects that displays as decreased spontaneous revertant counts compared with the negative control. In this case, it is necessary to lower the tested concentrations of the nanoparticle. Preliminary dose range finding experiment is recommended.
12. Ames assay can be used to test any chemical for potential mutagenicity. This chapter only chooses metal oxide nanoparticles as an example.
13. *Salmonella typhimurium* is a pathogenic bacterium. Cautions should be taken when handling the bacteria. Standard biosafety guideline should be followed, including the use of personal protection equipment, practicing aseptic techniques, operation in biosafety cabinet, autoclave and proper disposal of contaminated biohazards.
14. Figure 2 is an example that CuO nanoparticles induced significant more reverse mutants than control in *S. typhimurium* TA100 [20]. The results suggest CuO naoparticles is mutagenic and may cause base pair substitution mutations. Also, CuO nanoparticles is cytotoxic to *E. coli* WP2 as indicated by decreased number of revertant counts as compared to the negative control.

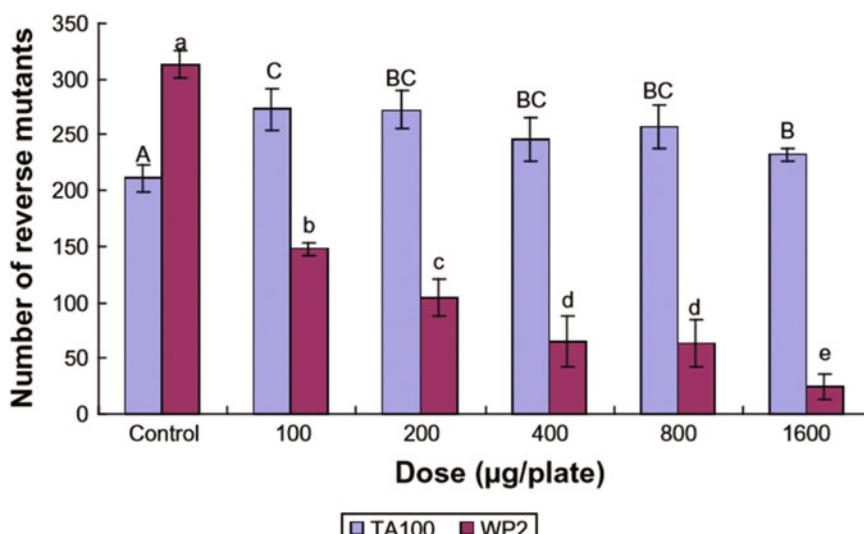


Fig. 2 The nanoparticle CuO induced reverse mutants in *S. typhimurium* TA100 and *E. coli* WP2 at different doses with S9 activation [20]. Error bars represent the standard deviation. Different letters show the significant difference at $p < 0.05$

References

1. Gupta R, Xie H (2018) Nanoparticles in daily life: applications, toxicity and regulations. *J Environ Pathol Toxicol Oncol* 37:209–230
2. Bundschuh M, Filser J, Lüderwald S, McKee MS, Metreveli G, Schaumann GE, Schulz R, Wagner S (2018) Nanoparticles in the environment: where do we come from, where do we go to? *Environ Sci Eur* 30:6
3. Couvreur P, Kante B, Grislain L, Roland M, Speiser P (1982) Toxicity of polyalkylcyanoacrylate nanoparticles II: doxorubicin-loaded nanoparticles. *J Pharm Sci* 71:790–792
4. Kante B, Couvreur P, Dubois-Krack G, De Meester C, Guiot P, Roland M, Mercier M, Speiser P (1982) Toxicity of polyalkylcyanoacrylate nanoparticles I: free nanoparticles. *J Pharm Sci* 71:786–790
5. Alqahtani S, Kobos LM, Xia L, Ferreira C, Franco J, Du X, Shannahan JH (2020) Exacerbation of nanoparticle-induced acute pulmonary inflammation in a mouse model of metabolic syndrome. *Front Immunol* 11:818
6. Batista D, Pascoal C, Cássio F (2020) The increase in temperature overwhelms silver nanoparticles effects on the aquatic invertebrate Limnephilus sp. *Environ Toxicol Chem* 39:1429–1437
7. Körich JS, Nogueira DJ, Vaz VP, Simioni C, Silva M, Ouriques LC, Vicentini DS, Matias WG (2020) Toxicity of binary mixtures of Al(2)O(3) and ZnO nanoparticles toward fibroblast and bronchial epithelium cells. *J Toxicol Environ Health A* 83:363–377
8. Li K, Qian J, Wang P, Wang C, Lu B, Jin W, He X, Tang S, Zhang C, Gao P (2020) Effects of aging and transformation of anatase and rutile TiO(2) nanoparticles on biological phosphorus removal in sequencing batch reactors and related toxic mechanisms. *J Hazard Mater* 398:123030
9. Gao X, Li R, Sprando RL, Yourick JJ (2020) Concentration-dependent toxicogenomic changes of silver nanoparticles in hepatocyte-like cells derived from human induced pluripotent stem cells. *Cell Biol Toxicol*. <https://doi.org/10.1007/s10565-020-09529-1>
10. Katiyar P, Yadu B, Korram J, Satnami ML, Kumar M, Keshavkant S (2020) Titanium nanoparticles attenuates arsenic toxicity by up-regulating expressions of defensive genes in *Vigna radiata* L. *J Environ Sci (China)* 92:18–27
11. Zakaria BS, Dhar BR (2020) Changes in syntrophic microbial communities, EPS matrix, and gene-expression patterns in biofilm anode in response to silver nanoparticles exposure. *Sci Total Environ* 734:139395
12. Adhikari S, Adhikari A, Ghosh S, Roy D, Azahar I, Basuli D, Hossain Z (2020) Assessment of ZnO-NPs toxicity in maize: an integrative microRNAomic approach. *Chemosphere* 249:126197
13. Srivastava AK, Yadav SS, Mishra S, Yadav SK, Parmar D, Yadav S (2020) A combined microRNA and proteome profiling to investigate the effect of ZnO nanoparticles on neuronal cells. *Nanotoxicology* 14:1–17
14. Boykov IN, Shuford E, Zhang B (2019) Nanoparticle titanium dioxide affects the growth and microRNA expression of switchgrass (*Panicum virgatum*). *Genomics* 111:450–456
15. Frazier TP, Burkley CE, Zhang B (2014) Titanium dioxide nanoparticles affect the growth and microRNA expression of tobacco (*Nicotiana tabacum*). *Funct Integr Genomics* 14:75–83
16. Ansari MO, Parveen N, Ahmad MF, Wani AL, Afrin S, Rahman Y, Jameel S, Khan YA, Siddique HR, Tabish M, Shadab G (2019) Evaluation of DNA interaction, genotoxicity and oxidative stress induced by iron oxide nanoparticles both in vitro and in vivo: attenuation by thymoquinone. *Sci Rep* 9:6912
17. Cardozo TR, De Carli RF, Seeber A, Flores WH, da Rosa JAN, Kotzal QSG, Lehmann M, da Silva FR, Dihl RR (2019) Genotoxicity of zinc oxide nanoparticles: an in vivo and in silico study. *Toxicol Res* 8:277–286
18. Wang X, Li T, Su X, Li J, Li W, Gan J, Wu T, Kong L, Zhang T, Tang M, Xue Y (2019) Genotoxic effects of silver nanoparticles with/without coating in human liver HepG2 cells and in mice. *J Appl Toxicol* 39:908–918
19. Wills JW, Hondow N, Thomas AD, Chapman KE, Fish D, Maffeis TG, Penny MW, Brown RA, Jenkins GJ, Brown AP, White PA, Doak SH (2016) Genetic toxicity assessment of engineered nanoparticles using a 3D in vitro skin model (EpiDerm™). *Part Fibre Toxicol* 13:50
20. Pan X, Redding JE, Wiley PA, Wen L, McConnell JS, Zhang B (2010) Mutagenicity evaluation of metal oxide nanoparticles by the bacterial reverse mutation assay. *Chemosphere* 79:113–116
21. Ames BN, Lee FD, Durston WE (1973) An improved bacterial test system for the detection and classification of mutagens and carcinogens. *Proc Natl Acad Sci U S A* 70:782–786

22. Maron DM, Ames BN (1983) Revised methods for the SALMONELLA mutagenicity test. *Mutat Res* 113:173–215
23. Levin DE, Mullins MC, Ames BN (1985) The development of SALMONELLA tester strains for classifying mutagens as to their base-substitution specificity. *Environ Mutagen* 7:46–46
24. Demir E, Qin T, Li Y, Zhang Y, Guo X, Ingle T, Yan J, Orza AI, Biris AS, Ghorai S, Zhou T, Chen T (2020) Cytotoxicity and genotoxicity of cadmium oxide nanoparticles evaluated using *in vitro* assays. *Mutat Res* 850-851:503149
25. Rainer B, Mayrhofer E, Redl M, Dolak I, Mislivecek D, Czerny T, Kirchnawy C, Marin-Kuan M, Schilter B, Tacker M (2019) Mutagenicity assessment of food contact material migrates with the Ames MPF assay. *Food Addit Contam Part A Chem Anal Control Expo Risk Assess* 36:1419–1432
26. Pan X, San Francisco MJ, Lee C, Ochoa KM, Xu X, Liu J, Zhang B, Cox SB, Cobb GP (2007) Examination of the mutagenicity of RDX and its N-nitroso metabolites using the Salmonella reverse mutation assay. *Mutat Res* 629:64–69
27. Akhtar MF, Ashraf M, Javeed A, Anjum AA, Sharif A, Saleem M, Mustafa G, Ashraf M, Saleem A, Akhtar B (2018) Association of textile industry effluent with mutagenicity and its toxic health implications upon acute and sub-chronic exposure. *Environ Monit Assess* 190:179
28. Bolsunovsky AY, Sinityna OI, Frolova TS, Vasyunina EA, Dementev DV (2016) Genotoxicity assessment of low-level doses of gamma radiation with the SOS chromotest and the Ames test. *Dokl Biochem Biophys* 469:309–312
29. Khan S, Anas M, Malik A (2019) Mutagenicity and genotoxicity evaluation of textile industry wastewater using bacterial and plant bioassays. *Toxicol Rep* 6:193–201
30. Maisuls I, Cabrerizo FM, David-Gara PM, Epe B, Ruiz GT (2018) DNA oxidation Photoinduced by Norharmane rhenium (I) Polypyridyl complexes: effect of the bidentate N,N'-ligands on the damage profile. *Chemistry* 24:12902–12911
31. Blanco M, Urios A, Martinez A (1998) New Escherichia coli WP2 tester strains highly sensitive to reversion by oxidative mutagens. *Mutat Res* 413(2):95–101
32. Kato M, Sugiyama K, Fukushima T, Miura Y, Awogi T, Hikosaka S, Kawakami K, Nakajima M, Nakamura M, Sui H, Watanabe K, Hakura A (2018) Negative and positive control ranges in the bacterial reverse mutation test: JEMS/BMS collaborative study. *Gene Environ* 40:7

Part IV

Extraction and Detection Analytical Methods



Chapter 21

Dispersive Solid-Phase Extraction of Multiresidue Pesticides in Food and Water Samples

Hongxia Guan

Abstract

Pesticides have become an essential part of our life and have entered and bioaccumulated in water, air, soil ecosystem, and food. However, the majority of the pesticides are not biodegradable and eco-friendly, and the accumulation of them in food and the ecosystem could constitute a serious risk to human and environmental health. It is critical to understand pesticides' identities and level of residues present in environment and food. Robust analytical techniques that offer easy, fast, and reliable extraction of multi-residue pesticides in water, soil and food with matrix interference-free quantification are necessary for proper risk assessment. Although various methods have been reported for pesticides extraction in food and environment samples, dispersive solid-phase extraction (d-SPE) has become the most popular sample preparation method for pesticides analysis today. Multiresidue pesticides extraction in food and environmental sample using a novel d-SPE method, dispersive pipette extraction (DPX), is described step-by-step in this chapter.

Key words Pesticides, Human and environmental health, Robust analytical techniques, Dispersive solid phase extraction, QuEChERS, DPX

1 Introduction

The extensive use of pesticides worldwide to help increase food production has made them an essential part of our life. Even with the tremendous benefits of pesticide use, most of them are not biodegradable and eco-friendly, and they have entered and bioaccumulated in water, air, soil ecosystem, and food [1–5]. There has been increasing concern over the undesirable impact of pesticides in environment shortly after the publication of Dr. Rachel Carson's book "Silent Spring" in 1963 [6]. It has been estimated that only small amount of pesticides (0.1%) applied to crops reaches the target pest; the majority enters the environment systems through various routes such as surface runoff, leaching, and improper disposal and contaminates soil, water and air [5]. Water is considered one of the prevalent mediums by which pesticides enter the

environment [7]. Generally, pesticides reach the aquatic ecosystems through surface runoff of agricultural pesticides used for pest control, rainfall, accidental spraying and spills of industrial waste, as well as the pesticides used to eliminate unwanted aquatic animals or plants [8].

The soil ecosystem may be contaminated by pesticides through four major ways: direct application to protect crops and plants, accidental spill of industrial waste, run-off from plant surfaces, and use of pesticide-contaminated plant materials [9, 10]. Similarly, the presence of pesticides in air can be caused by spray drift during application of pesticides around homes, buildings, and farms, accidental release from manufacturer of pesticides, and volatilization from the treated surfaces [11].

Continuous research about environmental and human health hazards associated with the unrestrained usage of pesticides and adverse effect on nontarget organisms has clearly shown severe consequences. It has been reported that pesticides caused the decease of bio diversity of aquatic insects and other fresh water invertebrates [12]. In addition, repeated exposure to toxic pesticides has been found to be responsible for physiological and behavioral changes in fish such as reduction in populations and immunity [13]. The toxicity of exposure to pesticides in soil ecosystems has also been addressed and the adverse effects of pesticides on soil function, diversity, and fertility have been observed [14–18].

Consequently, general population have been exposed to pesticides through contaminated water, air, and food supplies. Evidence of both acute and chronic human cancer and other disorders associated with pesticides have been reported. For instance, pesticides have shown to be involved in breast cancer [19], Parkinson's disease [20] as well as the respiratory and reproductive disorders [21, 22].

It is clear that the presence of pesticides in the ecosystem could constitute a serious risk to human and environmental health; therefore, it is critical to understand pesticides' identities and level of residues present in environment and food. Robust analytical techniques that offer complete extraction of multiresidue pesticides in water, soil and food with matrix interference-free quantification are necessary for proper risk assessment. Although various methods have been reported for pesticides extraction in food and environment samples, dispersive solid phase extraction (d-SPE) has become the most popular sample preparation method for multi-residue pesticides analysis today. The mechanism employed in d-SPE is that the sorbent is loosely filled in the tube and mixed with sample solution subsequently to either trap matrix interferences or retain the target analytes. According to the nature of the sorbent and the sample solution, either the solution or eluent will be analyzed for the target. Whereas, the sorbent for traditional SPE is tightly packed in the cartridge and the sample solution needs to

pass through the sorbent and the target analytes are usually retained by the sorbent and then eluted using appropriate solvent for analysis.

One specific d-SPE method that has recently attracted attention for pesticide analysis is the QuEChERS (Quick, Easy, Cheap, Effective, Rugged, and Safe) method [10, 23–27]. The QuEChERS approach is a cleanup method based on mixed mode sorbent using primary–secondary amine (PSA), MgSO₄, C18 or graphitized carbon black (GCB) to remove fatty acid components, pigments, and water residue from sample matrix rather than extracting and isolating the pesticides. The QuEChERS cleanup method is comprehensive and provides very high recoveries for almost all pesticides. However, the disadvantage of QuEChERS is that the resultant sample solutions are relatively “dirty” due to low selectivity of the sorbent. There have been different modifications and variations of the original method, for example, some QuEChERS methods include the use of dispersive tubes or cartridges, and some use graphite or other additives (such as C18-bonded silica) to remove sample matrix interferences.

Recently, there has been growing interest in using dispersive pipette extraction (DPX), a novel d-SPE method that is based on retaining of target analyte or matrix interferences using a small amount of sorbent filled in disposable pipette tips. DPX combines the features of both traditional solid phase extraction and dispersive solid phase extraction. DPX mixes solutions with the sorbent in a dynamic dispersive manner to provide rapid equilibration by increasing contact between analytes and the solid-phase sorbent. The matrix interferences are retained on the sorbent and a clean extract of analytes can be dispensed using small amount of solvent (less than 1000 µL), solvent evaporation is usually unnecessary [10, 28–31]. There are several advantages of the DPX method: first, it is fast and takes less than 1 min to mix sample solution with the sorbent; second, the screen of the DPX tip acts as a filter removing the sorbent and salt particulate matter from the solution without centrifugation; third, DPX is flexible and offers two different modes of sample loading, sample solution can be loaded from the top of the pipette tip or drawn in from the bottom.

Below, we will focus on multiresidue pesticides analysis in food and environmental samples using DPX for sample preparation.

2 Materials

1. Produce samples. Fruits and vegetable samples from local grocery stores or farmer’s market.
2. Grain product samples (cornmeal) from local grocery stores.
3. Environmental samples (drinking water and surface water).

4. Pesticides analytical standards. Prepare working solutions by diluting the stock solution into desired concentration using acetonitrile. Store all standards at -20°C prior to use.
5. Solvents and chemical reagents: GC grade acetonitrile, hexane, ethyl acetate, and acetone, HPLC grade water, and ACS reagent sodium chloride.
6. Heat resistant blender.
7. Glass microfiber (grade 691, size 9.0 cm), VWR West Chester, PA.
8. DPX-RP 5 and DPX-WAX 5 tips (Fig. 1) are purchased from DPX Laboratories, LLC (Columbia, SC). DPX- RP 5 tip contains 60 mg of poly styrene-divinylbenzene (PSDVB) sorbent, DPX-WAX 5 tip is filled with 60 mg of weak anion exchange sorbent.
9. 10 mL plastic syringes.
10. Test tubes and rack.
11. Autosampler vials.
12. Solvent evaporation system.
13. Ultrasonic bath.

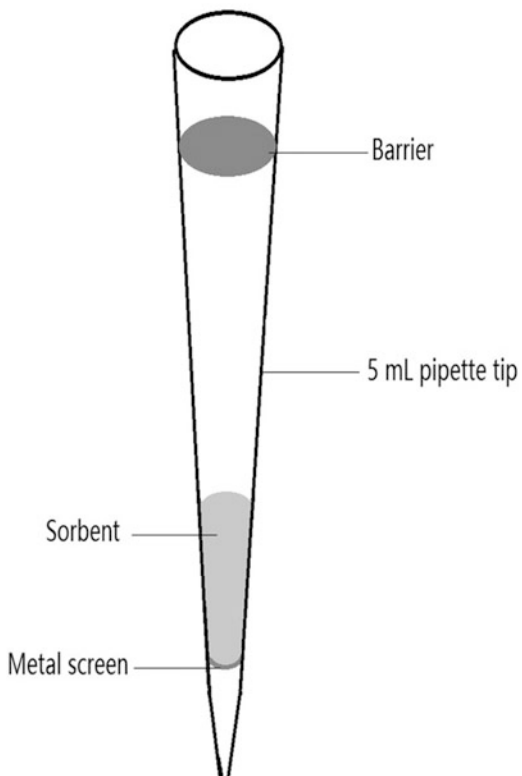


Fig. 1 Diagram of a 5 mL DPX tip

3 Method

3.1 Determination of Pesticides in Fruit and Vegetables

1. Remove stalks, caps, and stems from fresh fruits and vegetables.
2. Chop the sample and weigh out 100 g into a blender (*see Note 1*), blend the sample in 200 mL of acetone for 2 min followed by filtration using a Glass microfiber (grade 691, size 9.0 cm).
3. Wet the DPX-RP 5 tip using 1.0 mL of methanol.
4. 2.5 mL of the initial acetone extract is transferred into a test tube for DPX extraction, 6.0 mL of deionized (DI) water is added to decrease the strength of the organic solvent (acetone) in the sample system, then 2.0 mL of saturated sodium chloride is added and the goal is to increase the ionic strength of the solution or “salt out” pesticides.
5. Aspirate about 1/3 of the total solution into a DPX-RP 5 tip (*see Note 2*). A 10 mL syringe is used as a pipettor by attaching it to the top of the DPX-RP 5 tip.
6. Small air bubbles are also drawn into the DPX tip to create a perturbation of the solution and provide thorough mixing of the DPX sorbent with the sample solution (*see Note 3*). This step is to increase the interaction between the sorbent and the sample solution.
7. Let the solution and sorbent mixture to stand for 30 s to 1 min to allow the retention of analytes onto the PSDVB sorbent. The solution is dispensed to waste, and steps 5–7 are repeated twice till the entire sample solution (approximately 10.5 mL) is extracted.
8. 1.0 mL DI water is added to the top of the DPX-RP 5 tip to remove salt residue and any water soluble interferences in the matrix.
9. Finally, pesticides can be eluted from the PSDVB sorbent by adding 0.7 mL of hexane/ethyl acetate (50:50, v/v) to the top of the DPX-RP 5 tip or draw in from the bottom of the tip (*see Note 4*). Pesticide analytes are collected into an autosampler vial and ready for GC or GC/MS analysis (*see Note 5*).
10. A diagram of pesticides extraction using DPX-RP 5 is shown in Fig. 2.

3.2 Determination of Pesticides in Food with High Fat Content (Cornmeal) (Fig. 3)

1. Weight out 50 g of cornmeal sample and blend with 100 mL of 85% acetonitrile in deionized (DI) water.
2. Filtrate the sample solution through a glass microfiber filter 691.
3. Wet the DPX-WAX 5 tip using 1.0 mL of methanol.
4. 0.5 mL of the resulting acetonitrile extract is added to the top of DPX-WAX 5 tip for cleanup (*see Note 6*).

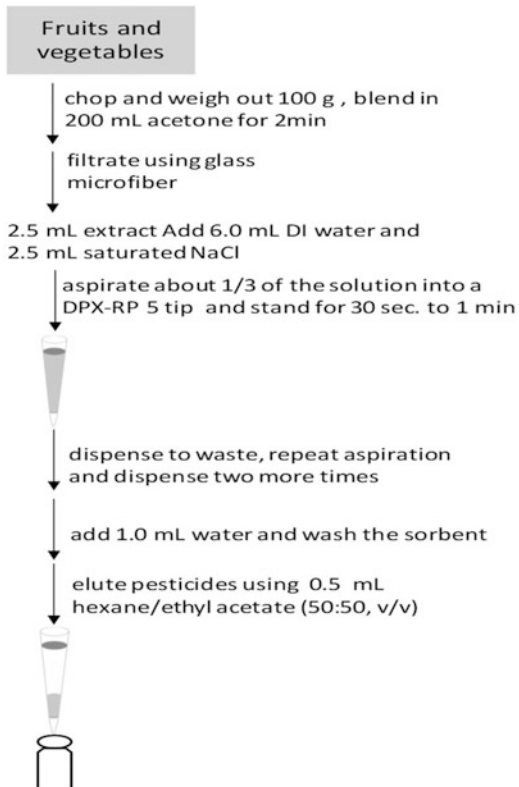


Fig. 2 Pesticide extraction in fruits and vegetables using DPX-RP 5

5. Attach a 10 mL syringe to the top of the DPX-WAX 5 tip and use it as a pipettor to push the sample solution through the WAX sorbent. Collect the eluate in an autosample vial.
6. To recover residual analytes from the WAX sorbent, additional elution using 0.2 mL of acetonitrile is employed and combined. The resulting eluate is injected into the GC-MS without further processing.

3.3 Ground and Surface Water Sample (Fig. 4)

1. 50 mL of the water sample is centrifuged at $1006 \times g$ for 10 min under room temperature to remove the suspended solid particles from natural water (i.e., soil, sand, and organic plant matter)
2. Wet the DPX-RP 5 tip using 1.0 mL of methanol.
3. 5 mL of the water sample (after centrifugation) is then aspirated into a dispersive DPX-RP 5 tip to be mixed with PSDVB sorbent, a 10 mL syringe is used as a pipettor.
4. Draw in about 5 mL of air bubbles into the tip to ensure thorough mixing of water sample and the sorbent.
5. Allow the solution and sorbent mixture to stand for 30 s to 1 min to allow the retention of analytes onto the PSDVB

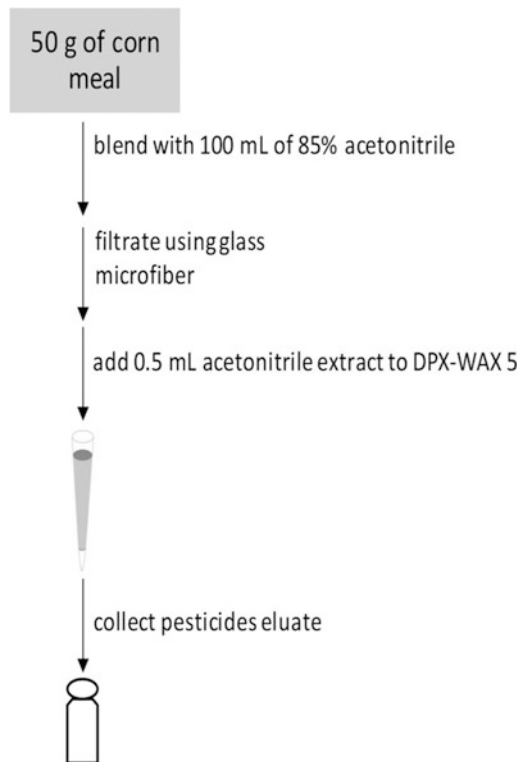


Fig. 3 Pesticide extraction in cornmeal using DPX-WAX 5

sorbent. The solution is dispensed to waste to remove water soluble components in the surface/ground water.

6. PSDVB sorbent is then cleaned by adding 0.5 mL of HPLC water to further remove water soluble matrix interferences.
7. The pesticides are finally eluted using 0.5 mL of acetonitrile and collected into an autosampler vial for instrumental analysis (*see Note 7*).

3.4 Determination of Pesticides in Soil Using DPX (Fig. 5)

1. Weight out 5 g of soil sample into a 50 mL centrifuge tube and add 10 mL of acetonitrile and 3 mL of water.
2. The soil sample is vortexed for 1 min followed by the addition of 6 g anhydrous magnesium sulfate, 1.5 g sodium chloride, 1.5 g trisodium citrate dihydrate, and 0.75 g disodium hydrogenocitrate sesquihydrate. Vortex the sample in the centrifuge tube for 1 min.
3. The centrifuge tube is then sonicated for 5 min in an ultrasonic bath followed by 5 min centrifugation at $1006 \times g$ at room temperature.

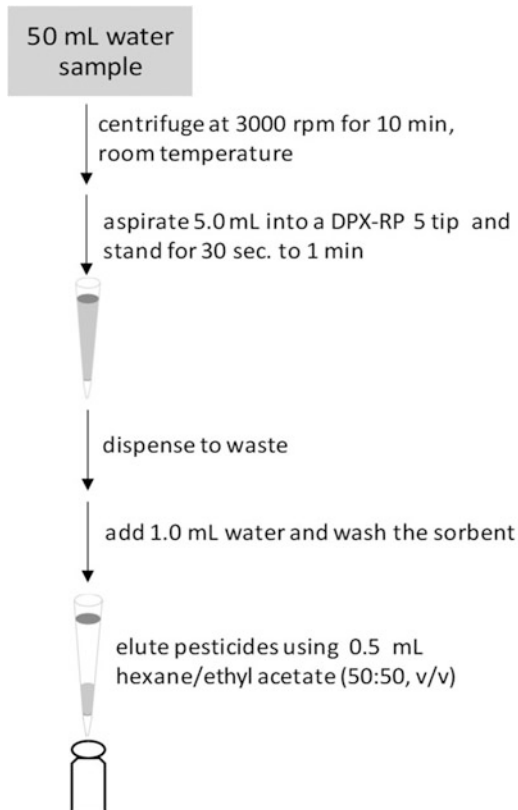


Fig. 4 Pesticide extraction in water using DPX-RP 5

4. Transfer 1.0 mL of the soil extract upper layer in **step 3** into a test tube and draw into DPX-Q (150 mg of QuEChERS dispersive sorbent containing anhydrous MgSO₄, PSA and GCB 1/1/1, g/g/g) for cleanup by attaching a 10 mL syringe to the top of the DPX-Q tip (*see Note 8*).
5. Dispense the extract into an autosampler vial for GC analysis.

4 Notes

1. Pesticides will be blended in acetone that is extremely flammable and potentially explosive, therefore, a heavy duty blender with heat resistant glass jar must be used.
2. The total volume of acetone extract, water, and saturated sodium chloride is 10.5 mL. The maximum solution volume allowed in DPX-RP 5 is about 4.0 mL since the sorbent occupied about 1.0 mL in the tip. 1/3 of the sample solution will be aspirated into the tip every time to make sure the tip is not too full. It is not necessary to draw in sample solution very slow; however, researchers need to monitor the tip while drawing

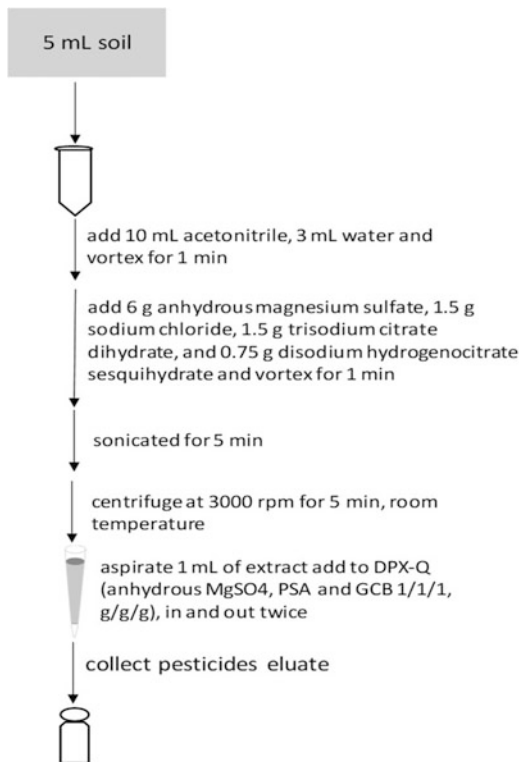


Fig. 5 Pesticide extraction in water using DPX-Q

solution into the tip to ensure no solution is accidentally drawn into the syringe and cause cross contamination for the next sample. The syringe should not be detached from the DPX tip to avoid dripping and sample loss.

3. Small air bubbles help to provide thorough mixing of the DPX sorbent and the sample solution, about 5 mL of air bubbles should be drawn into the DPX tip right after the sample solution.
4. Hexane/ethyl acetate is an excellent “keeper” solvent that minimizes sample degradation, and is ideally suited for GC analysis. The final eluate volume is about 0.5 mL due to retention of small amount of solvent exchange between hexane-ethyl acetate and water residue on the PSDVB sorbent.
5. There may be some water residue at the bottom of the auto-sampler vial that can be easily removed using a Pasteur pipette to avoid injecting water into GC or GC/MS and interfere with the GC column. If HPLC or LC/MS are to be used for analysis, the hexane-ethyl acetate eluate needs to be taken to dryness and then reconstitute in acetonitrile or methanol before injection.

6. This is a one-step cleanup method using WAX (weak anion exchange) sorbent, matrix interferences are retained by the sorbent and pesticide analytes pass through the sorbent directly, no washing step is needed. Another option for sample loading is to have the acetonitrile solution aspirated into the DPX-WAX 5 tip from the bottom, however, the extract will be relatively “dirty” if the sample only goes in and out of the tip once. The sample aspiration needs to be repeated one more time to obtain clean extract, which will increase the total sample preparation time.
7. If GC/MS is going to be used for pesticides analysis, the pesticides eluate should be taken to dryness using a solvent evaporation system (e.g., Thermo Scientific Reacti-Vap™ under nitrogen) due to small amount of water residue in the acetonitrile eluate. Reconstitute the sample in 0.5 mL of acetonitrile or less before injection. The volume of the reconstitution solvent should depend on the sensitivity desired. If LC/MS is employed for pesticides analysis, the eluate from DPX-RP 5 tip can be injected directly without solvent exchange.
8. This multiresidue pesticides analysis in soils using DPX was published by Valentina F, Domingues V, Mateus N et al. [10]. This is a cleanup method using the QuEChERS concept. The DPX tip has loosely contained anhydrous magnesium sulfate ($MgSO_4$), primary and secondary amines (PSA), and graphitized carbon black (GCB) inside a pipette tip (150 mg of sorbent mixture, 1/1/1, g/g/g). The matrix interferences are retained on the sorbent and the pesticides analytes are dispensed for analysis. Although acetonitrile extract of soil is aspirated in and out of the tip twice for cleanup in the current method, adding soil extract to the top of the DPX tip and push through for cleanup is another option, which has been demonstrated in the study of pesticides analysis in cornmeal sample above.

References

1. Younes M, Galal-Gorchev H (2000) Pesticides in drinking water a case study. *Food Chem Toxicol* 38(1):87–90
2. Rao P, Mansell R, Baldwin LB (1983) Pesticides and their behavior in soil and water. In: Soil Science Fact Sheet. Florida Cooperative Extension Service, Institute of Food and Agricultural Sciences, University of Florida, Gainesville, Florida
3. Aktar M, Sengupta D, Chowdhury A (2009) Impact of pesticides use in agriculture: their benefits and hazards. *Interdiscip Toxicol* 2:1–12
4. Sullivan J, Krieger G (2001) Clinical environmental health and toxic exposures, 2nd edn. Lippincott Williams & Wilkins, Philadelphia
5. ManuelArias-Estévez EL-P et al (2008) The mobility and degradation of pesticides in soils and the pollution of groundwater resources. *Agric Ecosyst Environ* 123:247–260
6. Carson R, Wilson E (2002) Silent spring, 40th anniversary edition. Houghton Mifflin Harcourt, Boston, Massachusetts
7. Lakhani L (2015) How to reduce impact of pesticides in aquatic environment. *Int J Res* 3 (9):1–5

8. Tardiff R (1992) Methods to assess adverse effects of pesticides on non-target organisms, 1st edn. Wiley, Hoboken
9. National Pesticides Information Center (2016) <http://npic.orst.edu/envir/soil.html>. Accessed 19 Sep 2020
10. Valentina F, Domingues V, Mateus N et al (2013) Multiresidue pesticides analysis in soils using modified QuEChERS with disposable pipette extraction and dispersive solid-phase extraction. *J Sep Sci* 36:376–382
11. National Pesticides Information Center (2016) <http://npic.orst.edu/envir/air.html>. Accessed 19 Sep 2020
12. Mikhail B, Kefford B, Schäfer R et al (2013) Pesticides reduce regional biodiversity of stream invertebrates. *Proc Natl Acad Sci U S A* 110(27):11039–11043
13. Helfrich L, Hipkins P et al (2009) Pesticides and aquatic animals: a guide to reducing impact on aquatic systems. Virginia Cooperative Extension, Virginia Polytechnic Institute and State University, Blacksburg, Blacksburg, Virginia
14. Bunemann E, Schwenke G, Zwieten L (2006) Impact of agricultural inputs on soil organisms—a review. *Aust J Soil Res* 44:379–406
15. Johnsen K, Jacobsen C, Torsvik V et al (2001) Pesticide effects on bacterial diversity in agricultural soils - a review. *Biol Fert Soils* 33:443–453
16. Kalam A, Tah J, Mukherjee A (2004) Pesticide effects on microbial population and soil enzyme activities during vermicomposting of agricultural waste. *J Environ Biol* 25:201–208
17. Bromilow R, Evans A, Nicholls P et al (1996) The effect on soil fertility of repeated applications of pesticides over 20 years. *Pest Sci* 48:63–72
18. Crouzet O, Batisson I, Besse-Hoggan P et al (2010) Response of soil microbial communities to the herbicide mesotrione: a dose-effect microcosm approach. *Soil Bio Biochem* 42:193–202
19. Pestana D, Teixeira D, Faria A et al (2015) Effects of environmental organochlorine pesticides on human breast cancer: putative involvement on invasive cell ability. *Environ Toxicol* 30(2):168–176
20. Brown T, Rumsby P, Capleton A et al (2006) Pesticides and Parkinson's disease—is there a link? *Environ Health Perspect* 114 (2):156–164
21. Salam M, Li Y, Langholz B et al (2004) Early-life environmental risk factors for asthma: findings from the Children's health study environ. *Health Perspect* 112(6):760–765
22. Greenlee A, Arbuckle T, Chyou P (2003) Risk factors for female infertility in an agricultural region. *Epidemiology* 14(4):429–436
23. Anastassiades M, Lehotay S, Stajnbaher D et al (2003) Fast and easy multiresidue method employing acetonitrile extraction/partitioning and "dispersive solid-phase extraction" for the determination of pesticide residues in produce. *J AOAC Int* 86:412–431
24. Payá P, Anastassiades M, Mack D (2007) Analysis of pesticide residues using the quick easy cheap effective rugged and safe (QuEChERS) pesticide multiresidue method in combination with gas and liquid chromatography and tandem mass spectrometric detection. *Anal Bioanal Chem* 389:1697–1714
25. Koesukwiwat U, Lehotay S, Miao S (2010) High throughput analysis of 150 pesticides in fruits and vegetables using QuEChERS and low-pressure gas chromatography-time-of-flight mass spectrometry. *J Chromatogr A* 1217(43):6692–6703
26. Lehotay S, Son K, Kwon H (2010) Comparison of QuEChERS sample preparation methods for the analysis of pesticide residues in fruits and vegetables. *J Chromatogr A* 1217 (16):2548–2560
27. Brondum S, Macedo A, Vicente G (2011) Evaluation of the QuEChERS method and gas chromatography-mass spectrometry for the analysis of pesticide residues in water and sediment. *Bull Environ Contam Toxicol* 86:18–22
28. Guan H, Brewer W, Morgan S (2009) New approach to multiresidue pesticide determination in foods with high fat content using disposable pipette extraction (DPX) and gas chromatography-mass spectrometry (GC-MS). *J Agric Food Chem* 57:10531–10538
29. Guan H, Brewer W, Garris S et al (2010) Disposable pipette extraction for the analysis of pesticides in fruit and vegetables using gas chromatography/mass spectrometry. *J Chromatogr A* 1217:1867–1874
30. Guan H, Brewer W, Garris S et al (2010) Multiresidue analysis of pesticides in fruits and vegetables using disposable pipette extraction (DPX) and micro-Luke method. *J Agric Food Chem* 58:5973–5981
31. Guan H, Huang W, Li X et al (2018) Determination of atrazine, simazine, alachlor, and metolachlor in surface water using dispersive pipette extraction and gas chromatography–mass spectrometry. *Anal Lett* 51(4):613–625



Chapter 22

Quantitative Analysis of Multiresidue Pesticides Using Gas Chromatography–Mass Spectrometry

Qingsong Cai and Hongxia Guan

Abstract

Despite the fact that pesticides help increase food production, widespread application of pesticides has resulted in negative impact in the environment and human health. Routine and comprehensive screening of pesticides in food and water is important for regulatory agencies to ensure that concentrations of toxic pesticides are below maximum allowable levels. Regardless of the pesticides that are not GC amenable, GC-MS still dominates the analysis of pesticides. The focus of the current chapter is a step-by-step method for GC-MS approaches in analysis of several classes of pesticides, including organochlorines, organophosphates, and triazines. GC-MS is superior or at least equivalent to LC-MS method and derivatization is not required prior to instrumental analysis.

Key words Pesticides, GC-MS, Method calibration, Qualitative identification, Quantification

1 Introduction

Pesticides have been excessively applied worldwide to control weeds, insect infestation, and diseases. Despite the fact that pesticides help farmers and businesses in the agriculture community increase food production and profits, broad application of pesticides has resulted in negative impact in environment and human health. Their toxic effects include but are not limited to disturbance of natural ecosystem, human cancer, endocrine disruption, cardiovascular disease, reproductive disorders, and respiratory diseases [1–5]. Regulatory and public concern over pesticides has led to more strict legislation to ensure that they do not pose unintended risks to humans, animals, and the environment. Under the Federal Food, Drug and Cosmetic Act (FFDCA), EPA is responsible for regulating the pesticides and establishing tolerances (maximum legally permissible levels) for pesticide residues in food and animal feed [6] in the USA.

Pesticides enter environment system through various routes such as spray drift, surface runoff, leaching, improper disposal, and accidental spill [7, 8]. Due to the persistency and slow degradation nature of pesticides, they have entered various ecosystem and food chain at high levels. Routine and comprehensive screening of pesticides in food and water is important for regulatory agencies to ensure that concentrations of toxic pesticides are below maximum allowable levels. Recent trend toward quantification of pesticides has been made possible by high quality confirmatory techniques using mass spectrometry (MS) platforms. Gas chromatography-mass spectrometry (GC-MS) [9–13] and liquid chromatography-mass spectrometry (LC-MS) [14–16] have been the most desired instruments. Determination of pesticides in food and water samples usually includes sample extraction, cleanup, concentration, followed by GS-MS or LC-MS analysis. Preliminary sample extraction using solvent extraction followed by cleaning up and concentration using solid-phase extraction (SPE) is the most commonly used sample preparation method for pesticides analysis [9–15].

Several factors need to be considered during the selection of instrumental method for pesticides analysis. These factors include polarity, stability, solubility of the target analytes, as well as matrix interferences. Moreover, limit of detection and quantification, regulatory requirements, and method linear range also need to be evaluated. Pesticides that are stable in GC liners and mass spectrometer ion source and those that do not require derivatization are suitable for GC-MS analysis. Pesticides that can be readily analyzed using GC-MS include organochlorines (OCs), organophosphates (OPs), pyrethroids, triazines, and chloroacetanilides. Additionally, some other pesticides that can be derivatized and transformed into OCs, OPs, pyrethroids, and triazines can also be analyzed using GC-MS. Unlike GC-MS, LC-MS column is usually operated at room temperature, and mobile phase can be adjusted to accommodate chromatographic behavior of various analytes. There has been growing interest in developing LC-MS methods focusing on analysis of thermolabile, polar, and nonvolatile pesticides.

GC-MS methods continue to be the essential method in pesticide residue analysis [9–13]. Despite the pesticides that are not GC amenable, GC-MS still dominates the analysis of pesticides in many regulatory labs [17–20]. The clear advantage of the GC-MS method is the availability of the commercially available electron ionization (EI) pesticide libraries in full scan mode made possible by National Institute for Standard and Testing (NIST), less skills requirement for analysts is often another important consideration in selecting GC-MS.

To meet the EPA regulation and achieve the necessary sensitivity required for environmental or food analysis, the majority of quantitative analysis of pesticides employs GC-MS with EI

(electron ionization) source in selected ion monitoring (SIM) mode. In general, the most abundant (intense) peak in the mass spectrum along with two other confirmation ions are selected with one of them being the molecular ion. Both retention time and relative peak intensity ratio are used for confirmation. Peak area of the most abundant ion is used in quantitative analysis to provide the highest sensitivity. GC-MS coupled with large volume injection (LVI) can further increase method sensitivity if needed.

The focus of the current chapter is GC-MS approaches in analysis of GC amenable pesticides (organochlorines, organophosphates, and triazines), where GC-MS is superior or at least equivalent to LC-MS method and derivatization is not required prior to analysis. The method does not include sample preparation (extraction, cleanup, and concentration) procedures and does not discriminate different fruit and vegetables, grain products, and water sample matrices.

2 Materials

1. Pesticide standards that include organochlorine standard solution (1000 µg/mL prepared in acetonitrile, aldrin, alpha-BHC, gamma-BHC, beta-BHC, delta-BHC, 4,4'-DDD, 4,4'-DDE, 4,4'-DDT, dieldrin, endosulfan I, endosulfan II, endosulfan SO₄, endrin, heptachlor, heptachlor epoxide, methoxychlor), organophosphate standard solution (1000 µg/mL prepared in acetonitrile, bolster, chlorpyrifos, coumaphos demeton-S, diazinon, dichlorvos, disulfoton, ethoprophos, fensulfothion, fenthion, merphos, methyl parathion, mevinphos, phorate, ronnel, stirofos, tokuthion, trichloronat), and triazine pure material (alachlor, atrazine, metolachlor, and simazine).
2. Deuterated pesticides parathion-diethyl-d10 and alachlor-d13 are used as internal standards (ITSD) (*see Note 1*).
3. Solvents: GC grade acetonitrile, methanol, acetone, and HPLC water.
4. Micro pipette and tips (20–200 µL and 100–1000 µL, respectively).
5. GC-MS benchtop system: GC coupled to mass spectrometer (MS) with EI (electron ionization) source.
6. GC-MS carrier gas: ultra-pure helium.
7. GC-MS analytical column: DB-17 MS column (50%-phenyl-methylpolysiloxane coated column, 30 m × 0.25 mm ID, 0.25 µm film thickness, Agilent Technologies) is used for simultaneous determination of organochlorines (OCs) and organophosphates (OPs) in fruit and vegetables. RTX-5 MS column (30 m × 0.25 mm ID, 0.25 µm of film thickness,

Restek) is used for analysis of OCs and OPs in sample with high fat content. HP-5 MS column (30 m × 0.25 mm ID, 0.25 µm film thickness, Agilent Technologies) is used organochlorines (OCs) in water. DB-5 column (5%-phenyl-methylpolysiloxane coated column, 30 m × 0.25 mm ID, 0.25 µm film thickness) is used for triazines in water (*see Note 2*).

3 Method

1. Preparation of internal standard (ITSD) solutions. Individual stock solutions of 1000 µg/mL parathion-diethyl-d10 and alachlor-d13 are prepared by accurately weighing, to the nearest 0.01 mg, 10 mg of the pure material into a 10-mL volumetric flask and dissolved in acetone (*see Note 3*).
2. Preparation of pesticides stock solutions. Individual stock solutions containing 20 µg/mL of organochlorines, organophosphates, and triazines are prepared by diluting individual 1000 µg/mL standard solutions (500 µL each) into acetonitrile in a 25-mL volumetric flask (*see Note 4*).
3. Internal standard stock (ISTD) solution. Individual stock solutions (*see Note 5*) containing 10 µg/mL of parathion-diethyl-d10 and alachlor-d13 are prepared by diluting 1.0 mL of each 1000 µg/mL ISTD standard solution into acetonitrile in a 100-mL volumetric flask.
4. GC-MS performance evaluation. Before sample analysis, a new GC liner and septa are installed on the GC. The MS is auto tuned daily to check potential air and water leaks (mass to charge ratio m/z of 28 and 32, and 18, respectively) prior to sample injection, and the tune file is compared with the previous result. Moreover, perfluorotributylamine (PFTBA) is used daily to optimize mass resolution and calibrate mass to charge of the MS. Additionally, a solvent blank (*see Note 6*) is injected to determine if there is carryover of target analytes between sample injections. Appearance of any analyte in the solvent blank is suspicious, therefore, the source of carryover (*see Note 7*) needs to be determined and verified, and the sample batch is reanalyzed. The performance of the GC-MS is also evaluated by injecting a method calibration standard sample before each batch. Retention times, peak areas, and product ion abundances and ratios are checked and compared with the results generated when the GC-MS is operated under optimized conditions. Table 1 shows an example of GC-MS sequence in determination of organochlorine pesticides in water.

Table 1
Example of GC-MS sequence in analysis of pesticides in water

Sample number	Vial position	Sample type
1	1	Acetonitrile solvent blank
2	2	Organochlorines calibration standard 1
3	3	Organochlorines calibration standard 2
4	4	Organochlorines calibration standard 3
5	5	Organochlorines calibration standard 4
6	6	Organochlorines calibration standard 5
7	1	Acetonitrile solvent blank
8	7	Unknown sample 1
9	1	Acetonitrile solvent blank
10	8	Unknown sample 2
11	1	Acetonitrile solvent blank
12	9	Unknown sample 3
13	1	Acetonitrile solvent blank
14	10	Unknown sample 4
15	4	Organochlorines calibration standard 3
16	1	Acetonitrile solvent blank
17	11	Unknown sample 5
18	1	Acetonitrile solvent blank
19	12	Unknown sample 6
20	1	Acetonitrile solvent blank
21	13	Unknown sample 7
22	1	Acetonitrile solvent blank
23	14	Unknown sample 8
24	4	Organochlorines calibration standard 3
25	1	Acetonitrile solvent blank

5. GC-MS parameters for OC and OP analysis in fruit and vegetables. The instrument is equipped with a DB-17 column (50%-phenyl-methylpolysiloxane coated column, 30 m × 0.25 mm ID, 0.25 µm film thickness, Agilent Technologies). The carrier gas is ultra-pure helium at constant flow rate of 1.0 mL/min. The inlet temperature is 250 °C. The oven is programmed to hold 1 min at 80 °C, then ramp at 20 °C/

min until final temperature 280 °C and hold 8 min. The total analysis time is 19 min. Injection volume is 2 µL in splitless mode.

The mass spectrometer (MS) is operated in electron ionization (EI) mode at 70 eV. The ion source temperature is 230 °C, and the transfer line from GC to MS is set at 290 °C. Data acquisition is accomplished in selected ion monitoring (SIM) mode. The identification of pesticide peak is confirmed by matching with retention time of the standard (within ± 0.02 min) and the presence of confirmation and quantification ions. Details of major MS ions, confirmation ions, and quantitation ions for the SIM method is summarized in Table 2.

6. GC-MS parameters for OCs and OPs analysis in food with high fat content. Analysis of OCs and OPs in corn meal by GC-MS is carried out on a RTX-5 MS column (30 m × 0.25 mm ID, 0.25 µm of film thickness, Restek) and a program temperature vaporization (PTV) inlet. Large volume injection (LVI) with 5 µL of sample extract in splitless mode is used (*see Note 8*). The initial temperature of PTV is programmed to 50 °C, ramp at 12 °C/s to 280 °C, and hold for 3 min. The carrier gas is ultra-pure helium at constant flow of 1.0 mL/min. The GC oven program is 60 °C for 1 min at, ramp at 40 °C/min to 200 °C, and then ramp at 20 °C/min until 300 °C and hold for 11 min.

The mass spectrometer (MS) was operated in electron ionization (EI) mode at 70 eV. The source temperature was 230 °C, and the MS transfer line temperature was set at 290 °C. The mass spectrometer scanned range of 50–500 *m/z*. The identification of pesticide peak is confirmed by matching with retention time of standard (within ± 0.02 min) and the presence of qualification and quantification ions. Details of major MS ions, confirmation ions, and quantitation ions for the SIM method can be found in Table 2.

7. GC-MS parameters for OCs analysis in water. The instrument is equipped with a HP-5 MS column (30 m × 0.25 mm ID, 0.25 µm film thickness, Agilent Technologies). The carrier gas is ultra-pure helium at constant flow rate of 1.0 mL/min. The oven is programmed to hold 1 min at 80 °C, then ramp at 20 °C/min until final temperature 280 °C and hold 8 min. The total GC analysis time is 19 min. Injections of 1 µL is made the inlet temperature at 250 °C.

The mass spectrometer (MS) is operated in electron ionization (EI) mode at 70 eV. The ion source temperature is 230 °C, and the transfer line from GC to MS is set at 290 °C. Data collection is accomplished in selected ion monitoring (SIM) mode. The identification of pesticide peaks is confirmed by matching retention times of standards (within ±0.02 min),

Table 2**Major ions, qualification ions, and quantification ion for OCs and OPs analysis using GC-MS (SIM)**

Pesticide	Major ions in full scan mode (<i>m/z</i>)	Confirmation ions (<i>m/z</i>)	Quantitation ion (<i>m/z</i>)
Aldrin	66, 79, 91, 101, 263, 293	66, 263, 293	293
Alpha-BHC	109, 111, 181, 183, 219	111, 181, 219	219
Beta-BHC	109, 111, 181, 183, 219	109, 181, 219	219
Delta-BHC	109, 111, 181, 183, 219	109, 181, 219	219
Gamma-BHC	109, 111, 181, 183, 219	109, 181, 219	219
Bolstar	125, 139, 140, 156, 322	139, 156, 322	139
Captan	79, 151	79, 151	151
Chlorpyrifos	97, 197, 199, 258, 286, 314	97, 197, 314	314
Chlorothalonil	268, 266, 264	266, 268, 264	268
Coumaphos	97, 109, 210, 226, 362	109, 226, 362	226
4,4'-DDD	75, 165, 235, 237	165, 235, 237	235
4,4'-DDE	176, 246, 248, 316, 318	176, 246, 318	246
4,4'-DDT	75, 165, 199, 235, 237	165, 199, 235	235
Demeton-S	60, 81, 88, 170	60, 88, 170	88
Diazinon	137, 152, 179, 199, 304	137, 152, 179	137
Dichlorvos	79, 109, 185	79, 109, 185	185
Dieldrin	79, 81, 263	79, 81, 263	263
Disulfoton	88, 89, 97, 125, 142, 274	88, 97, 274	88
Endosulfan I	195, 237, 241, 265, 339	195, 241, 339	195
Endosulfan II	109, 159, 170, 195, 237	170, 195, 237	195
Endosulfan SO ₄	170, 229, 237, 272, 387	237, 272, 387	237
Endrin	67, 79, 81, 263, 345	81, 263, 345	345
Endrin aldehyde	67, 250, 345	67, 250, 345	345
Ethoprophos	97, 126, 139, 158, 242	97, 139, 158	158
Fenthion	79, 109, 125, 153, 169, 278	109, 125, 278	278
Fensulfothion	97, 125, 141, 153, 293, 308	141, 293, 308	293
Heptachlor	100, 237, 272, 274, 270, 331, 374	100, 237, 272	100
Heptachlor epoxide	81, 237, 263, 351, 353, 355	81, 263, 353	81
Merphos	57, 113, 169, 202, 314	57, 169, 314	169
Methoxychlor	227, 288, 346	227, 288, 346	227
Methyl parathion	63, 79, 93, 109, 125, 263	109, 125, 263	263

(continued)

Table 2
(continued)

Pesticide	Major ions in full scan mode (<i>m/z</i>)	Confirmation ions (<i>m/z</i>)	Quantitation ion (<i>m/z</i>)
Mevinphos	67, 109, 127, 192	109, 127, 192	127
Phorate	75, 97, 121, 260	75, 121, 260	75
Ronnel	79, 109, 125, 285, 287	125, 285, 287	285
Stirofos	79, 109, 329, 331	109, 329, 331	329
Tokuthion	43, 113, 162, 267, 309	113, 162, 267	267
Trichloronat	109, 267, 297	109, 267, 297	297

and by the presence of confirmation and quantification ions. Details of major MS ions, qualification ions, and quantitation ions for the SIM method can be found in Table 2.

8. GC-MS parameters for triazine analysis. The instrument was equipped with a DB-5 column (5%-phenyl-methylpolysiloxane coated column, 30 m × 0.25 mm ID, 0.25 µm film thickness, Agilent Technologies). The carrier gas is ultrapure helium at constant flow rate of 1.0 mL/min. The oven is programmed to hold 1 min at 80 °C, then ramp at 20 °C/min until final temperature 280 °C and hold 8 min. The total GC analysis time is 19 min. Injections of 2 µL is made in the inlet at 250 °C.

The mass spectrometer (MS) is operated in electron ionization (EI) mode at 70 eV. The ion source temperature is 230 °C, and the transfer line from GC to MS is set at 290 °C. Data collection is accomplished in selected ion monitoring (SIM) mode. The identification of pesticide peaks is confirmed by matching retention times of standards (within ± 0.02 min), and by the presence of confirmation and quantification ions. Details of the major ions in full scan MS, quantitation ions and qualification ions for the SIM is summarized in Table 3.

9. Method calibration for analysis OCs and OPs in fruit and vegetables. One of the most important factors when considering calibration of pesticides analysis in complex sample matrices such as food and environmental samples is matrix interference. Therefore, matrix-matched calibration is necessary to minimize the potential matrix effects. OCs and OPs stock solutions (20 µg/mL) are spiked into preliminary extracts of organic fruit and vegetables (*see Note 9*) at five levels. The calibration range is 0.1 µg/mL to 2.0 µg/mL with multiple replicates at

Table 3
Major ions, confirmation ions, and quantification ion for triazine analysis using GC-MS (SIM)

Pesticide	Major ions in full scan mode (<i>m/z</i>)	Confirmation ions (<i>m/z</i>)	Quantitation ion (<i>m/z</i>)
Alachlor	160,188, 224, 237, 269	160, 188, 269	160
Atrazine	173, 200, 202, 215, 217	173, 200, 215	200
Metolachlor	146, 162, 211, 238, 240	146, 162, 238	162
Simazine	158, 173, 186, 188, 201, 203	173, 186, 201	201

each level. Calibration data are generated from 6 individual samples at 0.1 µg/mL, 2 individual samples at 0.2 µg/mL, 2 individual samples spiked at 0.5 µg/mL, 2 individual samples at 1.0 µg/mL, and 6 individual samples at 2.0 µg/mL. 25 µL of ISTD (10 µg/mL of parathion-diethyl-d10) is added to all final extracts before injection.

10. Method calibration for analysis of OCs and OPs in food with high fat content. As mentioned earlier, matrix interference has to be considered when calibrating GC-MS method for pesticides analysis in food with high fat content. Matrix-matched calibration is performed by spiking OCs and OPs stock solutions (20 µg/mL) into preliminary extracts of corn muffin (*see Note 10*) at five levels ranging from 0.02 µg/mL to 1.0 µg/mL. Calibration data are generated from responses of 5 individual samples at 0.02 µg/mL, 3 individual samples at 0.05 µg/mL, 5 individual samples at 0.1 µg/mL, 3 individual samples at 0.5 µg/mL, and 5 replicate individual samples at 1.0 µg/mL. 25 µL of ISTD (10 µg/mL of parathion-diethyl-d10) is added to all final extracts before injection.
11. Method calibration for analysis of OCs in water. OCs are spiked into 10 mL of water at 5 different concentrations ranging from 0.5 ng/mL to 50 ng/mL. Calibration plots are generated from six individual samples at 0.5 ng/mL, 2 individual samples at 1.5 ng/mL, 2 individual samples at 15 ng/mL, 2 individual samples at 15 ng/mL, and 6 individual samples at 50 ng/mL. 25 µL of ISTD (10 µg/mL of parathion-diethyl-d10) is added to all final extracts before injection.
12. Method calibration for analysis of triazines in water. Triazines are spiked into 5 mL of water at 5 different concentrations ranging from 0.1 ng/mL to 10 ng/mL. Calibration plots are generated from 5 individual samples at 0.1 ng/mL, 2 individual samples at 1.0 ng/mL, 2 individual samples at 2.0 ng/mL, 2 individual samples at 5.0 ng/mL, and 5 individual samples at 10 ng/mL. 25 µL of ISTD (10 µg/mL of alachlor-d13) is added to all final extracts before injection.

13. Method linearity, method detection limits (MDLs) and method quantification limits (MQLs). Microsoft Excel is used to generate linear calibration plots for pesticides response. The method detection limits (MDL) is calculated as 3.3 times the standard deviation of the lowest fortification level (*see Note 11*), divided by the slope of the calibration plot; the method quantification limits (MQL) is determined as 10 times the standard deviation of the lowest fortification level, divided by the slope of the calibration relationship [21]. MDL and MQL are calculated using Eqs. (1) and (2).

$$\text{MDL} = \frac{3.3s_{\text{bl}}}{m} \quad (1)$$

$$\text{MQL} = \frac{10s_{\text{bl}}}{m} \quad (2)$$

14. Where m is the slope of the calibration plot, and the standard deviation of the blank (s_{bl}) is estimated by calculating the standard deviation of the replicate results at the lowest calibration level.
15. Qualitative identification. Quantitative identification of each pesticide is performed before quantitative analysis. To meet qualitative criteria, retention time of a peak in the unknown sample has to be consistent (± 0.02) with that of the pesticide standard. The quantitative ion (the most abundant peak in the mass spectrum) along with two other per-selected confirmation ions must be identified, their relative peak intensity ratios are within $\pm 25\%$ of the average ratio obtained from the standard.
16. Quantification. Linear regression is used to generate calibration plot using at least five different calibration standards ranging from low to high concentration. Concentration of pesticides in the unknown sample extract is calculated using the linear calibration equation (*see Note 12*) of the calibration plot obtained from the best fit between the calibration standards. The correlation coefficient (R^2) for each standard plot indicates linearity of the method, and it has to be equal or above 0.99 to be accepted. An example of GC-MS (SIM) method calibration result for analysis of OCs in orange is shown in Table 4.

4 Notes

1. Deuterated pesticide meets the requirement of proper internal standard since they are chemically similar to the pesticides but is not expected to be present in the sample. Parathion-diethyl-d10 is used as internal standard for OCs and OPs analysis, and alachlor-d13 is used as internal standard for triazine analysis.

Table 4**Example of method calibration for analysis of OCs in carrot using GC-MS (SIM)**

OCs	linear correlation coefficient (R^2)	linear calibration equation ^a	MDL ($\mu\text{g/mL}$)	MQL ($\mu\text{g/mL}$)
Aldrin	0.9979	$y = 0.5961x - 0.0083$	0.0172	0.0521
Alpha-BHC	0.9988	$y = 4.8512x - 0.0710$	0.0072	0.0219
Beta-BHC	0.9991	$y = 4.1217x - 0.0722$	0.0069	0.0210
Delta-BHC	0.9990	$y = 1.2596x - 0.0077$	0.0329	0.0998
Gamma-BHC	0.9991	$y = 3.9332x - 0.0559$	0.0100	0.0303
4,4'-DDD	0.9986	$y = 5.6235x - 0.0175$	0.0039	0.0120
4,4'-DDE	0.9955	$y = 3.7513x - 0.0518$	0.0141	0.0426
4,4'-DDT	0.9974	$y = 3.1810x - 0.1945$	0.0220	0.0668
Dieldrin	0.9991	$y = 2.7855x - 0.0421$	0.0170	0.0516
Endosulfan I	0.9990	$y = 0.6641x - 0.0028$	0.0099	0.0299
Endosulfan II	0.9974	$y = 0.7430x + 0.0072$	0.0136	0.0411
Endosulfan sulfate	0.9990	$y = 0.3373x + 0.0293$	0.0182	0.0551
Endrin	0.9992	$y = 0.7507x - 0.0105$	0.0246	0.0745
Heptachlor	0.9984	$y = 3.0761x - 0.0702$	0.0116	0.0351
Heptachlor epoxide	0.9978	$y = 1.9612x - 0.0278$	0.0224	0.0680
Methoxychlor	0.9982	$y = 6.1146x - 0.3025$	0.0051	0.0154

^ax is the concentration of OC in sample extract; y is ratio of OC peak area/ITSD peak area

2. Selection of GC-MS column depends on the polarity of target analytes and column availability in the laboratory. OCs and OPs are nonpolar to slightly polar, therefore both nonpolar column (HP-5 MS, DB-5 MS, and RTX-5 MS, containing 5%-phenyl-methylpolysiloxane) and slightly polar column (DB-17 contains 50%-phenyl-methylpolysiloxane) can be used for multi residue analysis of OCs and OPs simultaneously.
3. Deuterated internal standard has the highest solubility in acetone compared with acetonitrile and methanol.
4. Stock solution can be diluted from the primary standard solution using any organic solvent that is compatible with the original solvent. Common organic solvents such as acetonitrile, acetone and methanol are miscible with each other and therefore can be used to dilute primary standard. OCs, OPs, and triazine stock solutions are prepared individually.

5. Internal standard is added to correct quantitative differences in extract volume as well as to compensate for differences in extract volume injected. Internal standard is also used to monitor instrument conditions, such as extract injection errors, retention time shifts, or instrument abnormalities or malfunctions.
6. Solvent blank is dependent on the solvent that is used is standards or sample extract.
7. Source of carry over may include but is not limited to solvent contamination, pipette contamination, auto sampler vial contamination, or GC-MS system contamination.
8. Only minimum amount of high fat content sample is used to minimize matrix effect; therefore, large volume injection (LVI) is employed to increase method sensitivity.
9. The preliminary extraction of OCs and OPs in fruit and vegetable is detailed in Guan H, Brewer W, Garris S et al. (2010) Disposable pipette extraction for the analysis of pesticides in fruit and vegetables using gas chromatography/mass spectrometry. *Journal of Chromatography A* 1217: 1867–1874.
10. The preliminary extraction of OCs and OPs in corn meal is detailed in Guan H, Brewer W, Morgan S (2009) New approach to multiresidue pesticide determination in foods with high fat content using disposable pipette extraction (DPX) and gas chromatography-mass spectrometry (GC-MS). *Journal of Agricultural and Food Chemistry* 57: 10531–10538.
11. The maximum allowable concentration may be used as reference in determining the lowest fortification level in a specific sample.
12. The linear calibration plot is generated where x -axis is the concentration of the calibration standard, and y -axis is peak area ratio of the calibration standard and the internal standard. The general format of the linear calibration equation is $y = mx + b$, where m is the slope of the linear calibration plot, x is concentration of an analyte in sample extract, y is peak area ratio between the analyte and the internal standard; b is the intercept on the y -axis. An example of linear calibration equation for analysis of OCs in carrot is shown in Table 4.

References

1. Alavanja M, Bonner M (2005) Pesticides and human cancers. *Cancer Investig* 23 (8):700–711
2. Cecchi A, Rovedatti M, Sabino G et al (2012) Environmental exposure to organophosphate pesticides: assessment of endocrine disruption and hepatotoxicity in pregnant women. *Eco-toxicol Environ Saf* 80:280–287
3. Kopf P, Walker M (2009) Overview of developmental heart defects by dioxins, PCBs, and Pesticides. *J Environ Sci Health* 29 (4):276–285

4. Frazier L (2007) Reproductive disorders associated with pesticide exposure. *J Agromedicine* 12(1):27–37
5. Salameh P, Waked M, Baldi I et al (2006) Respiratory diseases and pesticide exposure: a case-control study in Lebanon. *J Epidemiol Community Health* 60(3):256–261
6. United States Environmental Protection Agency (EPA) (2020). <https://www.epa.gov/regulatory-information-topic/regulatory-information-topic-pesticides>. Accessed 20 Sep 2020
7. Sun P, Backus S, Blanchard P et al (2006) Temporal and spatial trends of organochlorine pesticides in Great Lakes precipitation. *Environ Sci Technol* 40(7):2135–2141
8. Fogg P, Alistair B (2004) Leaching of pesticides from biobeds: effect of biobed depth and water loading. *J Agric Food Chem* 52 (20):6217–6227
9. Guan H, Brewer W, Morgan S (2009) New approach to multiresidue pesticide determination in foods with high fat content using disposable pipette extraction (DPX) and gas chromatography-mass spectrometry (GC-MS). *J Agric Food Chem* 57:10531–10538
10. Guan H, Brewer W, Garris S et al (2010) Disposable pipette extraction for the analysis of pesticides in fruit and vegetables using gas chromatography/mass spectrometry. *J Chromatogr A* 1217:1867–1874
11. Guan H, Brewer W, Garris S et al (2010) Multiresidue analysis of pesticides in fruits and vegetables using disposable pipette extraction (DPX) and micro-Luke method. *J Agric Food Chem* 58:5973–5981
12. Guan H, Huang W, Li X et al (2018) Determination of atrazine, simazine, alachlor, and metolachlor in surface water using dispersive pipette extraction and gas chromatography–mass spectrometry. *Anal Lett* 51(4):613–625
13. Nasiri A, Amirahmadi M, Mousavia Z et al (2016) A multi residue GC-MS method for determination of 12 pesticides in cucumber. *Iran J Pharm Res* 15(4):809–816
14. Choi S, Kim S, Shin J et al (2015) Development and verification for analysis of pesticides in eggs and egg products using QuEChERS and LC-MS/MS. *Food Chem* 173:1236–1242
15. Pareja L, Cesio V, Heinzen H et al (2011) Evaluation of various QuEChERS based methods for the analysis of herbicides and other commonly used pesticides in polished rice by LC-MS/MS. *Talanta* 83(5):1613–1622
16. Fernández-Alba A, García-Reyes J (2008) Large-scale multi-residue methods for pesticides and their degradation products in food by advanced LC-MS. *TrAC Trends Anal Chem* 27(11):973–990
17. U.S. Department of the Interior, U.S. Geological Survey Techniques (2012) Methods of Analysis—Determination of Pesticides in Sediment Using Gas Chromatography/Mass Spectrometry. <https://pubs.usgs.gov/tm/tm5c3/pdf/tm5-C3.pdf>. Accessed 15 Sep. 2020
18. EPA Method 614: The Determination of organophosphorus pesticides in municipal and industrial wastewater. https://www.epa.gov/sites/production/files/2015-10/documents/method_614_1992.pdf. Accessed 10 Sep. 2020
19. Pepich B, Prakash B, Domino M et al (2005) Development of U.S. EPA method 527 for the analysis of selected pesticides and flame retardants in the UCMR survey. *Environ Sci Technol* 39(13):4996–5004
20. USDA National Organic Program, USDA Science and Technology Programs (2012) 2010–2011 Pilot study pesticide residue testing of organic produce. https://www.ams.usda.gov/sites/default/files/media/Pesticide%20Residue%20Testing_Org%20Produce_2010-11PilotStudy.pdf. Accessed 10 Sep. 2020
21. US Food and Drug Administration (1997) Q2B Validation of Analytical Procedures: Methodology. <https://www.fda.gov/regulatory-information/search-fda-guidance-documents/q2b-validation-analytical-procedures-methodology>. Accessed 29 Sep 2020



Chapter 23

Determination of the N-Nitroso Compounds in Mouse Following RDX Exposure

Xiaoping Pan

Abstract

Hexahydro-1,3,5-trinitro-1,3,5-triazine, commonly called RDX, is an important explosive, which is widely used in military and civic activities. As it is used, RDX is widely found in many locations and caused soil and water contamination. Many studies show that RDX is toxic to many organisms, including plants, animals, and microbes. RDX causes genetic toxicity and neurotoxicity as well as potential carcinogenesis. Even it is worse that RDX can be biotransformed into other N-nitroso derivatives, such as MNX, DNX, and TNX; these derivatives can be found in both naturally in RDX-contaminated soil and also in the animal GI tracks. To study the potential effect of RDX and its N-nitroso derivatives, this chapter presents a step-by-step method for detect RDX and its N-nitroso derivatives in animal stomach and GI tracts followed RDX exposure by gas chromatography with electron capture detector (GC/ECD). This method can also be used to detect RDX and its N-nitroso derivatives in other tissues and in other animals and plants.

Key words Explosive, RDX, N-nitroso compound, Gas chromatography (GC), Electron capture detector (ECD)

1 Introduction

RDX is the common name for hexahydro-1,3,5-trinitro-1,3,5-triazine, an important explosive. Due to its wide usage during military and civic activities, many locations have been found to be contaminated by RDX. Many studies show that RDX is toxic to many organisms, including fishes [1–5], birds [6], lizard [7], worms [8–11], rats [12], mouse [13–15], cricket [16], tadpoles as well as microbes [17] and plants [18, 19]. RDX exposure not only inhibited organism growth and development as well as reproduction but also induced genetic mutation [20, 21]. The US Environmental Protection Agency (EPA) classifies RDX as a potential human carcinogen (Class C) [22]. Several studies also show that RDX caused neurotoxicity [6, 23, 24].

At nature condition, such as under anaerobic conditions in soil, RDX can be transformed into more toxic N-nitroso component, such as hexahydro-1-nitroso-3,5-dinitro-1,3,5-triazine (MNX), hexahydro-1,3-dinitroso-5-nitro-1,3,5-triazine (DNX), and hexahydro-1,3,5-trinitroso-1,3,5-triazine (TNX) [25]. After exposure to RDX, N-nitroso derivatives of RDX, MNX, DNX, and TNX, were also detected in the mouse stomach and GI track [13]. These N-nitroso components may be more toxic to organisms.

To better understand the effect of RDX and its N-nitroso derivatives in the environment, it is better to have a method for detecting RDX and its N-nitroso derivatives in different medium. In this chapter, we present a detailed step-by-step method for determining RDX and its transformed N-nitroso derivatives in mouse stomach and GI tracts,

2 Materials

2.1 Chemicals and Regents

1. RDX (CAS: 121-82-4) standard (*see Notes 1 and 2*).
2. MNX (CAS: 5755-27-1) standard (*see Note 2*).
3. DNX (CAS: 80251-29-2) standard (*see Note 2*).
4. TNX (CAS: 13980-04-6) standard (*see Note 2*).
5. HPLC-grade acetone.
6. HPLC-grade acetonitrile.
7. Ultrapure water.
8. Deionized water (diH₂O).

2.2 Animals and Foods

1. Female virgin deer mouse (*Peromyscus maniculatus*) (*see Note 3*).
2. Rodent chow.

2.3 Instruments

1. HP6890 gas chromatography with electron capture detector (GC/ECD).
2. A 30 m × 0.25 mm i.d. × 0.25 μm film thickness HP-5 column.
3. Fume hood.
4. Dionex Accelerated Solvent Extractor (Model 200).
5. Rotary evaporator.
6. A 24-port manifold.

2.4 Other Lab Suppliers

1. 250 mL flask.
2. Tips (10, 200, and 1000 μL).
3. Animal facility.

4. Animal cage with drinking bottle and food container.
5. Mortar.
6. Pestle.
7. Florisil cartridges.
8. Autosampler viral.
9. 0.45 µm membrane filters.
10. Helium gas with 99.999% purity.
11. Argon gas and methane gas.

3 Methods

3.1 Preparation of RDX-Spiked Food

1. Prepare 100 mL RDX work solution in an individual flask by solving RDX in acetone to final concentrations (0, 500, and 5000 mg/L) (*see Note 4*).
2. Measure three 1000 g rodent chow food.
3. Spray 20 mL RDX work solution to the 1000 g food individually to form the three groups of foods containing 0, 10, and 100 mg RDX per kg food. Here, 0 mg/kg serve as controls that containing the same amount of acetone solvent (*see Note 5*).
4. Mix the chow food with RDX thoroughly.
5. Spread the spiked chow food in a fume hood to allow acetone completely evaporated (*see Note 6*).
6. Sample the dried spiked food for GC/ECD conformation of RDX concentrations. Each concentration should be taken at least 3 biological replicates.
7. Collect the food and keep in a conditioner.
8. Store at 4 °C prior to feed animals.

3.2 Animal Treatments (See Note 7)

1. Select 18 female virgin dee mice with a same age, for example 45 days of age (*see Note 8*).
2. Acclimate the select mice for 7 days before the treatment.
3. Randomly assign the selected mice into three groups; each group contains six mice.
4. Each cage house three mice and each treatment or control has two cages. Thus, a total of 6 mice for each treatment group or the control group.
5. One drink bottle is supplied for each cage; food is added into a food container sit in the cage.

6. Animals are cultured in an animal root with temperature ranging from 18 to 25 °C, 25% to 75% relative humidity, and 16:8-h light-dark cycle.
7. Food and drinking water are checked and added twice per day.
8. The mice are treated for 9 days.
9. At day 10, mice are euthanized by CO₂ asphyxiation and heart puncture (*see Note 9*).
10. Dissect and remove the tissues from each mouse.
11. Collect stomach and intestinal tract from each individual mouse for each group, including two treatment group and one control (*see Note 10*).
12. Each sample is immediately put in a centrifuge tubes with clearly labeled.
13. Immediately store the sample (in the tubes) in liquid nitrogen or on dry ice (*see Note 11*).
14. Store the samples at -80 °C (*see Note 12*).

3.3 Extract RDX and its Derivatives

1. Extract RDX from the food samples.
 - (a) Weigh 1 g of food from each samples of each treated group or the control.
 - (b) Grind the food into fine prices in a mortar by using a pestle.
 - (c) Mix the grinded food with 10 g dried Na₂SO₄ thoroughly.
 - (d) Load the food- Na₂SO₄ mixture into a 22 mL steel cell.
 - (e) Load the steel cells into the Dionex Accelerated Solvent Extractor (Model 200).
 - (f) Run the solvent extraction. Each extraction cycle includes a 5 min preheat step, followed by a 5 min static extraction with 100% acetonitrile at constant temperature (100 °C) and pressure (1500 psi).
 - (g) Collect extraction into a glass collection vial for each sample.
 - (h) Reduced the collected extraction to 1–2 mL by using a rotary evaporation.
 - (i) Place Florisil cartridges on a 24-port manifold.
 - (j) Condition each cartridge by adding 5 mL acetonitrile.
 - (k) Repeat the **step (j)** and condition the cartridge again using 5 mL acetonitrile.
 - (l) Load the collected samples to individual cartridge.
 - (m) Collect the eluted sample from each cartridge (*see Note 13*).

- (n) Rinse the cartridge using 1 mL acetonitrile and collect the sample into the sample collection vial.
 - (o) Repeat **step (n)** twice, each time using 1 mL acetonitrile to rain the cartridge and collect the sample into the sample collection vial.
 - (p) The extract volume is reduced to about 1.0 mL by blowing the extract using nitrogen gas (*see Note 14*).
 - (q) Adjust the final volume to 1 mL by adding acetonitrile.
 - (r) Filter the final solution into an autosampler viral by using an 0.45 µm membrane filter.
 - (s) Store at 4 °C until GC/ECD analysis.
2. Extract RDX and its derivatives from mouse stomach and GI tracts.
 - (a) Weigh the stomach and GI tracts for each sample.
 - (b) 50 g of sample is used for extracting RDX and its derivatives.
 - (c) Sample is homogenized with dried 10 g dried Na₂SO₄ thoroughly.
 - (d) Load the sample- Na₂SO₄ mixture into a 22 mL steel cell.
 - (e) Load the steel cells into the Dionex Accelerated Solvent Extractor (Model 200).
 - (f) Run the solvent extraction. Each extraction cycle includes a 5 min preheat step, followed by a 5 min static extraction with 100% acetonitrile at constant temperature (100 °C) and pressure (1500 psi).
 - (g) Collect extraction into a glass collection vial for each sample.
 - (h) Reduced the collected extraction to 1–2 mL by using a rotary evaporation.
 - (i) Place Florisil cartridges on a 24-port manifold.
 - (j) Condition each cartridge by adding 5 mL acetonitrile.
 - (k) Repeat the **step (j)** and condition the cartridge again using 5 mL acetonitrile.
 - (l) Load the collected samples to individual cartridge.
 - (m) Collect the eluted sample from each cartridge (*see Note 13*).
 - (n) Rinse the cartridge using 1 mL acetonitrile and collect the sample into the sample collection vial.
 - (o) Repeat **step (n)** twice, each time using 1 mL acetonitrile to rain the cartridge and collect the sample into the sample collection vial.

- (p) The extract volume is reduced to about 1.0 mL by blowing the extract using nitrogen gas (*see Note 14*).
- (q) Adjust the final volume to 1 mL by adding acetonitrile.
- (r) Filter the final solution into an autosampler viral by using an 0.45 µm membrane filter.
- (s) Store at 4 °C until GC/ECD analysis.

3.4 Detect the Concentrations of RDX and its Derivatives

1. Run standard solution and construct standard calibration curve.
 - (a) For each analyte (RDX and its N-nitroso derivatives MNX, DNX, and TNX), 10 standard concentration levels are prepared in a glass tube. These concentrations include 1, 2, 5, 10, 20, 50, 100, 200, 500, and 1000 ng/mL.
 - (b) Filter each standard solution into an autosampler viral by using an 0.45 µm membrane filter (*see Note 15*).
 - (c) Load the standards on the autosampler of GC/ECD. The GC is equipped with an autosampler and an electron capture detector (ECD) and is controlled by ChemStation chromatography software (Agilent, Palo Alto, CA, USA). The chemical separation is performed on a capillary HP-5 column (30 m × 0.25 mm i.d. × 0.25 µm).
 - (d) Run standards in order of increasing concentrations (*see Note 16*).
 - (e) The GC/ECD program is settled up as following: the GC oven temperature is initially held at 90 °C for 3 min. Then, increasing the oven temperature to 200 °C at a rate of 10 °C/min, and then raise to 250 °C at 25 °C/min with finally holding temperature of 250 °C for 5 min. The injector temperature is 170 °C; the detector temperature is 270 °C. The injection volume is 2 µL. The carrier gas is helium with 99.999% purity at a constant flow rate of 9.2 mL/min. The makeup gas for the ECD detector is argon and methane (95:5) at a combined flow rate of 60.0 mL/min. The ECD is operated in the constant current mode.
 - (f) Construct the calibrations curves. Calibration curves are constructed by plotting concentration of the analyte versus response peak area. The relations between the analytes and the response peak area are best fitted to a polynomial regression. Thus, polynomial regression analysis is used to calculate the slope, intercept, and correlation coefficient for the calibration curves. It is also used for analyzing the real samples.

- (g) Calculate the method detection limit. The method detection limit (MDL) for each analyte is calculated by the following formula: $MDL = 3.14 \times S.D.$, where S.D. is the standard deviation of the measurements of seven spiked samples, and 3.14 is the student's *t*-value at the 99% confidence level (*t* = 3.14 for *n* – 1 degrees of freedom). In this method, the MDL is about 10 µg/kg for each detected compound [13] (see Note 17).

2. Sample analysis.

- (a) Load each sample on the autosampler of GC/ECD. The GC is equipped with an autosampler and an electron capture detector (ECD) and is controlled by ChemStation chromatography software (Agilent, Palo Alto, CA, USA).
- (b) Run each sample on a capillary HP-5 column (30 m × 0.25 mm i.d. × 0.25 µm).
- (c) The GC/ECD program is settled up as following: the GC oven temperature is initially held at 90 °C for 3 min. Then, increasing the oven temperature to 200 °C at a rate of 10 °C/min, and then raise to 250 °C at 25 °C/min with finally holding temperature of 250 °C for 5 min. The injector temperature is 170 °C; the detector temperature is 270 °C. The injection volume is 2 µL. The carrier gas is helium with 99.999% purity at a constant flow rate of 9.2 mL/min. The makeup gas for the ECD detector is argon and methane (95:5) at a combined flow rate of 60.0 mL/min. The ECD is operated in the constant current mode (see Note 18).
- (d) Calculate the response peak area of RDX and its N-nitroso derivatives for each sample.
- (e) Use the calibration curve to calculate the concentration of RDX and its N-nitroso derivatives (MNX, DNX, and TNX).

3.5 Date Analysis

The data on the concentrations of RDX and its N-nitroso derivatives are recorded in an excel sheet for each tissue and each sample. The means and standard errors are calculated, SPSS or other biostatistics software is employed to analyze the data. Analysis of variance (ANOVA) is used to compare the means of different treatment groups and controls. If there is a significant difference (*p* < 0.05), least significant difference (LSD) multiple comparisons are conducted to compare the means of each treatment groups and the controls.

Table 1 is a representative results showing the RDX and its N-nitroso derivatives in dee mouse stomach and GI tracts after 10 days of RDX dosage [13]. From here, it clearly shows that RDX can be transformed into its N-nitroso derivatives, MNX and

Table 1
RDX and its N-nitroso derivatives detected in deer mouse stomach and GI tracts after 10 days of RDX exposure^a

Dose (mg/kg)	Stomach ($\mu\text{g}/\text{kg}$)				GI tracts ($\mu\text{g}/\text{kg}$)			
	RDX	MNX	DNX	TNX	RDX	MNX	DNX	TNX
0	0	0	0	0	0	0	0	0
10	7324a	85a	217a	0	18a	14a	40a	0
100	48622b	1318b	498b	0	22a	43b	53a	0

^aDifferent letter in the same column represents a significant difference within the same compound at the $p = 0.05$

DNX in both mouse stomach and GI tracts. However, no TNX was detected in either mouse stomach or GI tracts potentially due to that the TNX concentration is below the detection limit or it is quickly degraded into other components in the mouse stomach or GI tracts. This data suggests that RDX can be transformed into its N-nitroso derivatives in both mouse stomach and GI tracts. This data also suggests that RDX and its N-nitroso derivatives can be quickly degraded in mouse stomach and GI tract.

Figure 1 is a representative GC/ECD figure for samples with/without 5 ng/g RDX and its N-nitroso derivatives, MNX, DNX, and TNX, respectively.

4 Notes

1. RDX is an explosive. It should take special attention and care to handle explosive.
2. Both RDX and its derivatives are toxic, and potentially cause neurotoxicity, genetic toxicity and carcinogenesis. Thus, personal protection should be taken when handling these components. People should wear goggles, face mask, and gloves.
3. Here, deer mouse is just used as an example. Any other mouse or rat, even other animals also can be used. The method should seminar with each other.
4. Many chemicals used in this method is toxic, including RDX, MNX, DNX, TNX, acetone, and acetonitrile. When handle these chemicals, more attention should be taken and avoid breathe these chemicals or any skin directly contacts these chemicals.
5. This should be done in a fume hood because acetone is volatile solvent and toxic with bad smelling.
6. This usually takes at least 3 days to allow the acetone completely evaporated.

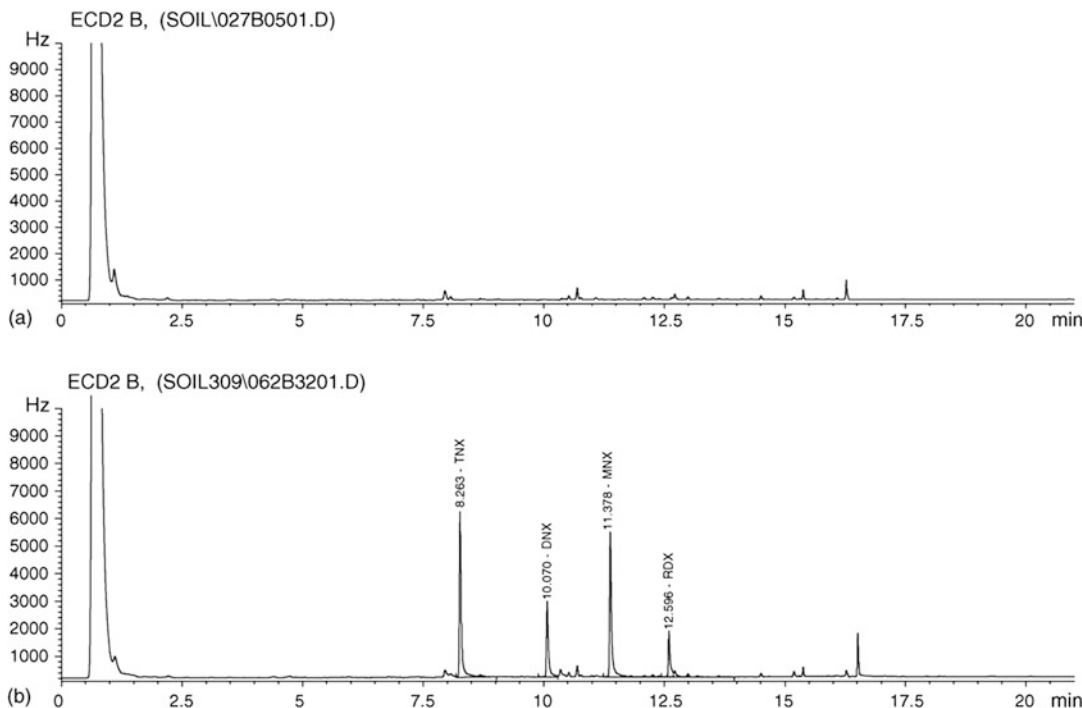


Fig. 1 A representative figure for GC/ECD detection of RDX and its N-nitroso derivatives. (a) blank sample without RDX and its N-nitroso derivatives. (b) Blank sample with spiked 5 ng/g RDX and its N-nitroso derivatives, MNX, DNX, and TNX, respectively

7. Mice are rodent animals. Before working on mice, the institution's approval should be taken based on the Animal Use and Care Guidelines.
8. The total number of mice is just for an example. The actual number mice should be adjusted according to the experimental design.
9. This should follow the approved Animal Use and Care Guidelines. Different method may be used based on the animal facility.
10. Other tissues may also be collected for chemical analysis and other studies, such as pathogenic study.
11. Samples should be quickly referred in liquid nitrogen or on dry ice to stop enzyme activities and keep sample as it is, particularly if you study the gene expression.
12. If the samples are analyzed in a short period, it can also be stored at -20°C .
13. If the solution elutes too slow, vacuum may be used to speed this process.
14. If there is no nitrogen gas, using air evaporation is also fine.

15. Standard solutions need to be prepared daily. It can be stored in the refrigerator is not used in several hours.
16. The standards need to run in the order of increasing concentrations. Otherwise, the column needs to be washed after each run by injecting a blanket acetonitrile solvent to get off the residues.
17. The method detection limit (MDL) varies among different detection method and among different samples, such as soil, animal tissue, or plant tissues. Thus, for each time, it is better to run the MDL detection for determining the MDL for your study. For example, the MDLs were 0.243, 0.095, 0.138, and 0.057 ng/g for RDX, MNX, DNX, and TNX, respectively, in soil samples [26].
18. To obtain the best performance of GC/ECD and good detection results, it is better to replace the septum and inlet liner of GC/ECD after every 50 injections.

References

1. Mukhi S, Pan X, Cobb GP, Patiño R (2005) Toxicity of hexahydro-1,3,5-trinitro-1,3,5-triazine to larval zebrafish (*Danio rerio*). Chemosphere 61:178–185
2. Mukhi S, Patiño R (2008) Effects of hexahydro-1,3,5-trinitro-1,3,5-triazine (RDX) in zebrafish: general and reproductive toxicity. Chemosphere 72:726–732
3. Williams LR, Wong K, Stewart A, Suciu C, Gaikwad S, Wu N, Dileo J, Grossman L, Cachat J, Hart P, Kalueff AV (2012) Behavioral and physiological effects of RDX on adult zebrafish. Comp Biochem Physiol C Toxicol Pharmacol 155:33–38
4. Belden JB, Lotufo GR, Lydy MJ (2005) Accumulation of hexahydro-1,3,5-trinitro-1,3,5-triazine in channel catfish (*Ictalurus punctatus*) and aquatic oligochaetes (*Lumbriculus variegatus*). Environ Toxicol Chem 24:1962–1967
5. Gust KA, Brasfield SM, Stanley JK, Wilbanks MS, Chappell P, Perkins EJ, Lotufo GR, Lance RF (2011) Genomic investigation of year-long and multigenerational exposures of fathead minnow to the munitions compound RDX. Environ Toxicol Chem 30:1852–1864
6. Gust KA, Pirooznia M, Quinn MJ Jr, Johnson MS, Escalon L, Indest KJ, Guan X, Clarke J, Deng Y, Gong P, Perkins EJ (2009) Neurotoxicogenomic investigations to assess mechanisms of action of the munitions constituents RDX and 2,6-DNT in northern bobwhite (*Colinus virginianus*). Toxicol Sci 110:168–180
7. McFarland CA, Quinn MJ Jr, Bazar MA, Talent LG, Johnson MS (2009) Toxic effects of oral hexahydro-1,3,5-trinitro-1,3,5-triazine in the western fence lizard (*Sceloporus occidentalis*). Environ Toxicol Chem 28:1043–1050
8. Zhang B, Cox SB, McMurry ST, Jackson WA, Cobb GP, Anderson TA (2008) Effect of two major N-nitroso hexahydro-1,3,5-trinitro-1,3,5-triazine (RDX) metabolites on earthworm reproductive success. Environ Pollut 153:658–667
9. Zhang B, Freitag CM, Cañas JE, Cheng Q, Anderson TA (2006) Effects of hexahydro-1,3,5-trinitro-1,3,5-triazine (RDX) metabolites on cricket (*Acheta domesticus*) survival and reproductive success. Environ Pollut 144:540–544
10. Zhang B, Kendall RJ, Anderson TA (2006) Toxicity of the explosive metabolites hexahydro-1,3,5-trinitroso-1,3,5-triazine (TNX) and hexahydro-1-nitroso-3,5-dinitro-1,3,5-triazine (MNX) to the earthworm *Eisenia fetida*. Chemosphere 64:86–95
11. Kuperman RG, Checkai RT, Simini M, Phillips CT, Kolakowski JE, Lanno R (2013) Soil properties affect the toxicities of 2,4,6-trinitrotoluene (TNT) and hexahydro-1,3,5-trinitro-1,3,5-triazine (RDX) to the enchytraeid worm *Enchytraeus crypticus*. Environ Toxicol Chem 32:2648–2659
12. Bannon DI, Dillman JF, Hable MA, Phillips CS, Perkins EJ (2009) Global gene expression in rat brain and liver after oral exposure to the

- explosive hexahydro-1,3,5-trinitro-1,3,5-triazine (RDX). *Chem Res Toxicol* 22:620–625
- 13. Pan X, Zhang B, Smith JN, Francisco MS, Anderson TA, Cobb GP (2007) N-Nitroso compounds produced in deer mouse (*Peromyscus maniculatus*) GI tracts following hexahydro-1,3,5-trinitro-1,3,5-triazine (RDX) exposure. *Chemosphere* 67:1164–1170
 - 14. Parker GA, Reddy G, Major MA (2006) Reevaluation of a twenty-four-month chronic toxicity/carcinogenicity study of hexahydro-1,3,5-trinitro-1,3,5-triazine (RDX) in the B6C3F1 hybrid mouse. *Int J Toxicol* 25:373–378
 - 15. Smith JN, Pan X, Gentles A, Smith EE, Cox SB, Cobb GP (2006) Reproductive effects of hexahydro-1,3,5-trinitroso-1,3,5-triazine in deer mice (*Peromyscus maniculatus*) during a controlled exposure study. *Environ Toxicol Chem* 25:446–451
 - 16. Karnjanapiboonwong A, Zhang B, Freitag CM, Dobrovolsky M, Salice CJ, Smith PN, Kendall RJ, Anderson TA (2009) Reproductive toxicity of nitroaromatics to the cricket, *Acheta domesticus*. *Sci. Total Environ* 407:5046–5049
 - 17. Anderson JA, Cañas JE, Long MK, Zak JC, Cox SB (2010) Bacterial community dynamics in high and low bioavailability soils following laboratory exposure to a range of hexahydro-1,3,5-trinitro-1,3,5-triazine concentrations. *Environ Toxicol Chem* 29:38–44
 - 18. Vila M, Mehier S, Lorber-Pascal S, Laurent F (2007) Phytotoxicity to and uptake of RDX by rice. *Environ Pollut* 145:813–817
 - 19. Ekman DR, Wolfe NL, Dean JF (2005) Gene expression changes in *Arabidopsis thaliana* seedling roots exposed to the munition hexahydro-1,3,5-trinitro-1,3,5-triazine. *Environ Sci Technol* 39:6313–6320
 - 20. Pan X, San Francisco MJ, Lee C, Ochoa KM, Xu X, Liu J, Zhang B, Cox SB, Cobb GP (2007) Examination of the mutagenicity of RDX and its N-nitroso metabolites using the salmonella reverse mutation assay. *Mutat Res* 629:64–69
 - 21. Reddy G, Erexon GL, Cifone MA, Major MA, Leach GJ (2005) Genotoxicity assessment of hexahydro-1,3,5-trinitro-1,3,5-triazine (RDX). *Int J Toxicol* 24:427–434
 - 22. US, E. P. A. (1988) Health advisory of RDX, EPA, Washington DC
 - 23. Zhang B, Pan X (2009) RDX induces aberrant expression of microRNAs in mouse brain and liver. *Environ Health Perspect* 117:231–240
 - 24. Deng Y, Ai J, Guan X, Wang Z, Yan B, Zhang D, Liu C, Wilbanks MS, Escalon BL, Meyers SA, Yang MQ, Perkins EJ (2014) MicroRNA and messenger RNA profiling reveals new biomarkers and mechanisms for RDX induced neurotoxicity. *BMC Genomics* 15(Suppl 11):S1
 - 25. McCormick NG, Cornell JH, Kaplan AM (1981) Biodegradation of hexahydro-1,3,5-trinitro-1,3,5-triazine. *Appl Environ Microbiol* 42:817–823
 - 26. Zhang B, Pan X, Cobb GP, Anderson TA (2005) Use of pressurized liquid extraction (PLE)/gas chromatography-electron capture detection (GC-ECD) for the determination of biodegradation intermediates of hexahydro-1,3,5-trinitro-1,3,5-triazine (RDX) in soils. *J Chromatogr B Anal Technol Biomed Life Sci* 824:277–282



Chapter 24

Determination of Metal Content in *Drosophila melanogaster* During Metal Exposure

Guiran Xiao

Abstract

Trace metal elements, such as zinc, iron, copper, and manganese, play catalytic or structural roles in many enzymes and numerous proteins, and accordingly, contribute to a variety of fundamental biological processes. During the past decade, the fruit fly (*Drosophila melanogaster*) has become an important model organism for elucidating metal homeostasis in metazoan. We have been using *Drosophila* as a model to study metal metabolism for many years and have optimized simple and robust assays for determining the metal content in *Drosophila*, such as inductively coupled plasma mass spectrometry (ICP-MS), the activity assay of enzymes dependent on metals, and staining metal ions in tissues of *Drosophila*. In this chapter, we present the step-by-step detailed methods for detecting the metal content in *Drosophila melanogaster* during metal toxicity study.

Key words *Drosophila*, Zinc, Iron, ICP-MS, ALP, Aconitase, Ferrozine, Iron staining

1 Introduction

Iron, copper, and zinc are transition metals essential for life because they are required in a multitude of biological processes [1]. The main components of metal homeostatic pathways are conserved, with many orthologs of the human metal-related genes having been identified and characterized in *Drosophila melanogaster* [2–9]. *Drosophila* is useful for studying potential toxic effects of different compounds, such as metals [10–13]. It is also simple to investigate toxicity-mediated mechanisms at the molecular level in *Drosophila* [2, 14–16].

The inductively coupled plasma mass spectrometry (ICP-MS) is mainly used for chemical element analysis, especially for metal element analysis. ICP-MS possesses extremely high sensitivity and its detection limit can reach the parts per trillion (PPT) level (10^{-12}) [17]. Approximately 25% of proteins require metals to perform their functions. For example, secretory enzyme alkaline

phosphatase (ALP) activity is dependent on zinc loading in the Golgi [18]. Activity of the ALP is very sensitive to zinc deficiency [19–21]. The activity of aconitase, a protein contains iron-sulfur (Fe-S) clusters, is sensitive to the level of bioavailable iron [17, 22]. The activity of these enzymes can be estimated by the spectrophotometric method of Racker. Iron exists in two valence states in solution, namely, ferrous ions and ferric ions. Divalent iron can react with ferrozine to form a violet complex, which has a maximum absorption peak at 562 nm. Using hydroxylamine hydrochloride as the reducing agent, ferric iron is reduced to divalent iron and the total iron content can be accurately determined. Perl's Prussian blue staining enables iron ions to be visualized in tissues [23]. Under acidic conditions, the ferric iron ions are stored in ferritin [24], react with ferrocyanide, and produce insoluble Prussian blue crystals, which are indicative of the iron amount in the tissues. Perl's Prussian blue staining is a method frequently used to detect ferric iron ions that are stored in ferritin. To detect the ferrous iron in tissues by the Perl's Prussian blue staining, Prussian blue staining solution should be replaced with freshly made Turnbull Blue staining solution. The midgut of *Drosophila melanogaster* expresses abundant ferritin and can be readily stained by Perl's Prussian blue solutions [3, 23]. Here, using this method, we monitored the iron status in the midgut directly and determined the iron contents in intact iron-loaded ferritin extracted from the midgut during metal exposure.

2 Materials

The solvent used in this experiment is ultrapure water, unless indicated otherwise. Waste materials are disposed following all the disposal regulations.

2.1 Equipment

1. Cryogenic centrifuge.
2. Pipette.
3. Multiskan Spectrum.

2.2 Chemicals and Solutions

1. Homogenization medium for ALP: 10 mM Tris-HCl (pH = 7.4), 0.5 mM MgCl₂, 0.1% Triton X-100, precool and add protease inhibitors before use.
2. PBST: 1× PBS, 1% Triton X-100, pH = 7.4.
3. ALP assay buffer A: 1.0 M diethanolamine, 0.5 mM MgCl₂, pH = 9.8.
4. ALP assay buffer B: 150 mM p-nitrophenyl phosphate (pNPP).

5. 20% K₄Fe(CN)₆ stock solution: Weigh 20 g K₄Fe(CN)₆ and add ultrapure water to 100 mL. Store at room temperature in the dark.
6. 20% hydrochloric acid (HCl): Add 80 mL water to a glass breaker. Add 20 mL concentrated HCl to the water slowly. Mix it well with a glass rod carefully.
7. 1.5 M NaOH.
8. Citrate reaction solution: 30 mM citrate, 50 mM K₂HPO₄, pH = 7.4.
9. [BCA Protein Assay Kit](#)
10. 11.6 M concentrated HCl.
11. 50 µM ammonium ferric citrate (FAC).
12. 75 mM ascorbate.
13. 10 mM ferrozine.
14. Saturated ammonium acetate.

2.3 Native Polyacrylamide Gel

1. Separating gel buffer: 1.5 M Tris–HCl, pH 8.8. Weigh 181.7 g Tris and add it to a glass breaker carefully. Add 900 mL ultrapure water and mix it well. Adjust pH with HCl carefully. Make up to 1 L with water. Store at 4 °C.
2. Stacking gel buffer: 0.5 M Tris–HCl, pH 6.8. Weigh 60.6 g Tris and add it to a glass breaker. Add 900 mL ultrapure water and mix it well. Adjust pH with HCl carefully. Make up to 1 L with water. Store at 4 °C.
3. Native-gel running buffer: Weigh Tris 3.02 g and glycine 18.8 g, then make up to 1 L with water. Store at 4 °C.
4. Protein-loading buffer (5×): 1 M Tris–HCl (pH 6.8) 12.5 mL. Add Bromophenol blue 250 mg and glycerol 25 mL. Mix well and store at 4 °C.
5. Protein lysis buffer: 1% PBST (Triton X-100). Before used, add protease inhibitors, including 21 mg/mL aprotinin, 0.5 mg/mL leupeptin, 4.9 mM MgCl₂, 1 mM sodium metavanadate, and 1 mM PMSF. Mix well and store at 4 °C.
6. Separating gel preparation: Add 2.60 mL water, 1.00 mL 30% acrylamide, 1.30 mL 1.5 M Tris–HCl (pH 8.8), 0.05 mL 10% ammonium persulfate and 0.004 mL TEMED. Mix well and cast gel within a 7.25 cm × 10 cm × 1.5 mm gel cassette. Isopropanol or 70% ethanol is used to make the gel smooth and flat.
7. Stacking gel preparation: Add 2.10 mL water, 0.50 mL 30% acrylamide, 0.38 mL 0.5 M Tris–HCl (pH 6.8), 0.03 mL 10% ammonium persulfate and 0.003 mL TEMED. Mix well and insert a 10-well gel comb immediately.

2.4 Lab Suppliers

1. 10×10 pallet.
2. 5×5 pallet.
3. Gauze.
4. Marker pen.
5. *Drosophila* bottle.
6. *Drosophila* vial.
7. Cotton stopper.
8. Dissecting tools, including scissors, razor blade, and forceps.

3 Methods

In addition to the special needs, the general experimental fruit flies are placed in constant temperature and humidity incubator, and the feeding conditions are 25°C , 60% humidity, 12 h light–12 h dark, so as to achieve the effect of high survival rate, more eggs, and rapid passage. To detect the ferrous iron in tissues by Perl's Prussian blue staining, Prussian blue staining solution should be replaced with freshly made Turnbull Blue staining solution (a mixture of 20% $\text{K}_3[\text{Fe}(\text{CN})_6]$ and 20% HCl in a ratio of 1:1 for in-gel staining. For tissue staining, the final concentration of $\text{K}_3[\text{Fe}(\text{CN})_6]$ and HCl is 2%).

3.1 ALP Activity Assay

1. Collect samples for experiments, such as *Drosophila* larvae, adults, or tissues (*see Note 1*).
2. Suspend samples in homogenization medium and grind thoroughly (*see Note 2*).
3. Transfer homogenate to a 1.5-mL microcentrifuge tube and centrifuge 10 min at $14,000 \times g$, 4°C , in a high-speed centrifuge (*see Note 3*). Repeat this operation to ensure that most of the tissue fragments and fat are removed.
4. Transfer suspension to a clean 1.5-mL tube and place it on ice.
5. Determine protein concentration with the BCA kit.
6. Add 90 μL ALP assay buffer A and 1 μg protein in 96-well plates, mix 10 μL ALP assay buffer B with the mixture above, shake the plate gently to mix these mixture (*see Note 4*).
7. Incubate the plates at 30°C for 30 min (*see Note 5*).
8. Add 50 μL 1.5 M NaOH to terminate the reaction.
9. Measure the absorption value of 405 nm.

3.2 Aconitase Activity Assay

1. Collect samples for experiments, such as *Drosophila* larvae, pupae, adults, or tissues (*see Note 6*).
2. Suspend samples in PBST and grind well (*see Note 7*).

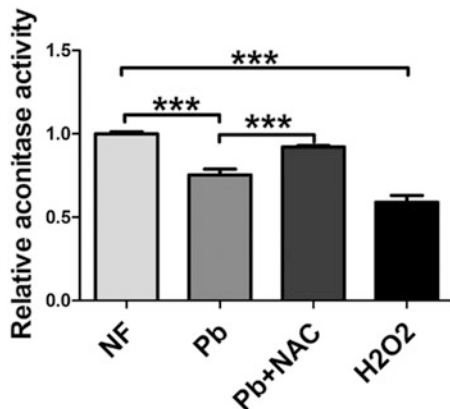


Fig. 1 Aconitase activity was decreased upon 2 mM Pb acetate trihydrate (Pb) and H₂O₂ treatment. Decreased aconitase activity caused by Pb could be reversed when 1 mg/ml N-Acetylcysteine (NAC) was added [4]

3. Transfer homogenate to a 1.5-mL microcentrifuge tube and centrifuge for 10 min at 14,000 × φ , 4 °C, in a high-speed centrifuge (*see Note 8*).
4. Discard the sediment, transfer the supernatant to a clean 1.5-mL tube, and place it on ice.
5. Measure protein concentration with the BCA kit (*see Note 9*).
6. Add 700 μL citrate reaction solution in quartz cuvette. Add this solution first, then add protein extract, mix well.
7. Measure the absorption value of 240 nm for 120 s (Fig. 1). Record the initial value and terminal value (usually the lowest and highest). The difference in $A_{240\text{nm}}$ can be regard as the value of aconitase activity (*see Note 10*).

3.3 Ferrozine-Based Colorimetric Assay

1. Collect samples for experiments, such as *Drosophila* larvae, pupae, adults, or tissues (*see Notes 11 and 12*).
2. Homogenize samples in 100 μL of PBST (*see Note 13*).
3. Samples are centrifuged to remove insoluble material. Set 100 μL lysis buffer as blank control, and set 100 μL 50 μM FAC as positive control.
4. Add 22 μL concentrated HCl to the samples and mix well (*see Note 14*).
5. Heat the mixture at 95 °C for 20 min (*see Note 15*).
6. Centrifuge for 20 min at 20,000 × φ at room temperature.
7. Place 70 μL supernatant in a fresh tube and recentrifuge at 20,000 × φ for 20 min (*see Note 16*).
8. Add 50 μL supernatant to 20 μL 75 mM ascorbate, and then vortex and spin down.

9. Keep away from light at room temperature for 2 min.
10. Add 20 μ L 10 mM ferrozine, and then vortex and spin down (*see Note 17*).
11. Keep away from light at room temperature for 2 min.
12. Add 40 μ L saturated ammonium acetate to each tube, and then vortex and spin down (*see Note 17*).
13. Keep away from light at room temperature for 2 min.
14. Measure the absorbance at 562 nm.
15. The following formula is used to calculate concentration of iron: $[Fe] \text{ (pmol}/\mu\text{L}) = [(OD_{562} \times 94/77 \times 130/50)/27,900] \times 10^6$.

3.4 ICP-MS Analysis

1. Collect samples for experiments, such as *Drosophila* larvae, pupae, adults or tissues (*see Note 18*).
2. Dry the samples, weigh, and record (*see Note 19*).
3. Dissolve the dried samples in 1 mL 65% HNO₃ and boil in 100 °C water bath for 10 min (*see Note 20*).
4. Dilute the samples to 10 mL for metal content analysis with ICP-MS XII (Thermo Electron Corp., Waltham, MA, USA) (Fig. 2).

3.5 Perl's Prussian Blue Staining for Iron Detection in Midgut

1. The wandering third-instar larvae are washed with PBS to remove the food on the body. The midguts of third-instar larvae are dissected in cold PBS solution (*see Note 21*).
2. To detect the iron in the midgut directly, the midguts dissected are fixed with 4% paraformaldehyde for 10 min (*see Note 22*).

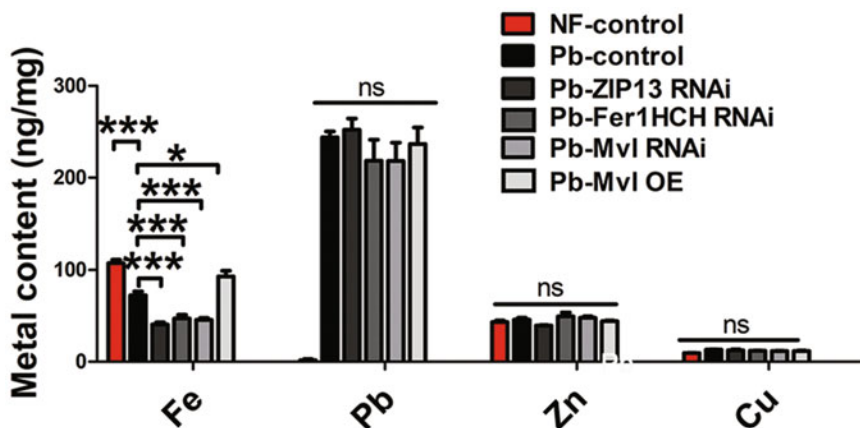


Fig. 2 Pb exposure resulted in increased Pb and decreased iron content in *Drosophila*. No significant changes of zinc and copper level were detected. Knocking down ZIP13, Ferritin or Mvl resulted in iron reduction, while Pb level stayed almost unchanged [4]

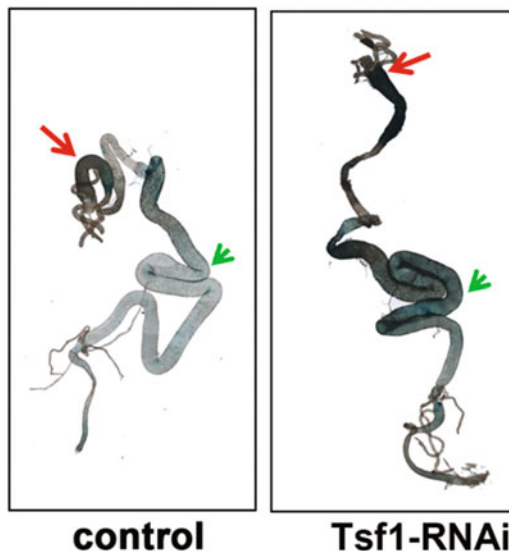


Fig. 3 Staining of ferric iron in the midgut. The ferric iron in the midgut is visualized by blue crystals [3]

3. Mix the Perl's Prussian blue solution. The solution is a mixture of 2% $K_3[Fe(CN)_6]$ stock solution and 2% HCl in a ratio of 1:1 (*see Note 23*).
4. Transfer the fixed midguts to the Perl's Prussian blue solution for 1 h (*see Notes 24 and 25*).
5. Make the seal and observe under a microscope (*see Note 26*) (Fig. 3).

3.6 Determining Iron Contents in Intact Iron-Loaded Ferritin Extracted from Tissues

1. The wandering third-instar larvae are washed with PBS to remove the food on the body. The midguts of third-instar larvae are dissected in cold PBS solution (*see Note 21*).
2. The midguts are homogenized using 200 μ L protein lysis buffer and centrifuged at 12,000 $\times g$ at 4 °C for 7 min. Supernatants are collected (*see Notes 27 and 28*).
3. Determine the concentration of the protein samples. About 120 μ g protein extract is needed. Protein preparation is conducted at 4 °C throughout (*see Note 29*).
4. Mix protein samples with protein-loading buffer (*see Notes 27 and 28*).
5. Add protein samples in the gel. Electrophoresis at 300 mA for about 1–2 h.
6. Pry the gel plates open with the use of a spatula. Immerse the gel into the Perl's Prussian blue solution. The solution is a mixture of 20% $K_3[Fe(CN)_6]$ stock solution and 20% HCl in a ratio of 1:1 (*see Notes 25 and 30*) (Fig. 4).

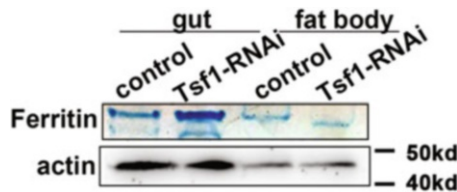


Fig. 4 Staining of ferric iron loaded in ferritin on native PAGE. The iron-loaded ferritin is visible as blue bands [3]

4 Notes

1. Wash the larvae with cold PBS for three times and dissect the tissues needed in cold PBS. 10 larvae/pupae/adults, 30 guts or brains are needed. In general, 6 µg protein is enough for ALP test.
2. The whole process of this experiment should be carried out on ice.
3. Repeat this operation to ensure that most of the tissue fragments and fat are removed.
4. The amount of protein can be changed appropriately, but 5 µg protein is saturated in this reaction system.
5. Shake the plate gently every 10 min.
6. Wash the larvae with cold PBS and dissect the tissues needed in cold PBS. 5 larvae/pupae/adults, 50 guts or brains are enough, the more the better. In general, each sample needs at least 10 µg protein.
7. The whole process of this experiment should be carried out on ice. PBST should be precooled and added Protease inhibitors before use.
8. Do not collect fat when transferring the supernatant.
9. It is better to ensure that the protein concentration is above 2 µg/µL, at least not less than 1 µg/µL.
10. A straight line in the reaction curve indicates that the enzyme activity is normal. Otherwise, the enzyme activity may be damaged.
11. 10 wandering larvae or female adults are good for this experiment. Heads were removed from adults to avoid potential interference from eye pigments.
12. Wash the larvae with PBS before homogenize.
13. Don't add protease inhibitors. The volume can be adjusted according to the actual situation.

14. Operate the reaction in a fume hood.
15. Shake the tubes every 5 min during the process.
16. When isolate the supernatant, be careful not to take the fat.
17. Try to avoid light during operation.
18. At least 50 wandering larvae or adults are needed for this experiment, the more the better. At least 100 guts or heads are needed for this experiment, less tissues are difficult to detect the metal content by ICP-MS.
19. Dry the sample fully.
20. Fully dissolve all tissues until the solution is clear.
21. Keep operating at low temperature.
22. Observe the gut at any time, avoid destroying the gut after too long fixation time.
23. The Perl's Prussian blue solution should be prepared fresh.
24. Observe the gut at any time, stop the reaction when the iron cell region becomes bright blue.
25. Iron-containing containers should be avoided in the process of staining.
26. Be careful not to destroy the guts.
27. To avoid protein denaturation, SDS should be excluded in protein-loading buffer, gel and running buffer in this experiment [25].
28. Protease inhibitors used in this study should be free of EDTA.
29. Protein preparation (tissue dissection and protein extraction) should be conducted in low temperature to avoid protein degradation.
30. For in-gel staining, the reaction takes about 1–3 days and should be carried out in the dark. Additionally, Perl's Prussian blue solutions should be frequently replaced to avoid strong background.

Acknowledgments

This project was funded by the National Natural Science Foundation of China (31671284), the Fundamental Research Funds for the Central Universities (JZ2020H GPA0115), and the Youth Science and Technology Talents Support Program (2020) by Anhui Association for Science and Technology.

References

1. Calap-Quintana P, Gonzalez-Fernandez J, Sebastia-Ortega N, Llorens JV, Molto MD (2017) *Drosophila melanogaster* models of metal-related human diseases and metal toxicity. *Int J Mol Sci* 18:1456. <https://doi.org/10.3390/ijms18071456>
2. Xiao G, Fan Q, Wang X, Zhou B (2013) Huntington disease arises from a combinatorial toxicity of polyglutamine and copper binding. *Proc Natl Acad Sci U S A* 110:14995–15000. <https://doi.org/10.1073/pnas.1308535110>
3. Xiao G, Liu ZH, Zhao M, Wang HL, Zhou B (2019) Transferrin 1 functions in iron trafficking and genetically interacts with ferritin in *Drosophila melanogaster*. *Cell Rep* 26:748–758 e745. <https://doi.org/10.1016/j.celrep.2018.12.053>
4. Liu ZH et al (2020) Oxidative stress caused by lead (Pb) induces iron deficiency in *Drosophila melanogaster*. *Chemosphere* 243:125428. <https://doi.org/10.1016/j.chemosphere.2019.125428>
5. Lang M et al (2013) Inhibition of human high-affinity copper importer Ctrl orthologous in the nervous system of *Drosophila* ameliorates Abeta42-induced Alzheimer's disease-like symptoms. *Neurobiol Aging* 34:2604–2612. <https://doi.org/10.1016/j.neurobiolaging.2013.05.029>
6. Richards CD, Warr CG, Burke R (2017) A role for the drosophila zinc transporter Zip88E in protecting against dietary zinc toxicity. *PLoS One* 12:e0181237. <https://doi.org/10.1371/journal.pone.0181237>
7. Marelja Z, Leimkuhler S, Missirlis F (2018) Iron sulfur and molybdenum cofactor enzymes regulate the drosophila life cycle by controlling cell metabolism. *Front Physiol* 9:50. <https://doi.org/10.3389/fphys.2018.00050>
8. Tejeda-Guzman C et al (2018) Biogenesis of zinc storage granules in *Drosophila melanogaster*. *J Exp Biol* 221:jeb168419. <https://doi.org/10.1242/jeb.168419>
9. Richards CD, Burke R (2016) A fly's eye view of zinc homeostasis: novel insights into the genetic control of zinc metabolism from drosophila. *Arch Biochem Biophys* 611:142–149. <https://doi.org/10.1016/j.abb.2016.07.015>
10. Xiao G, Zhou B (2016) What can flies tell us about zinc homeostasis? *Arch Biochem Biophys* 611:134–141. <https://doi.org/10.1016/j.abb.2016.04.016>
11. Tang X, Zhou B (2013) Iron homeostasis in insects: insights from drosophila studies. *IUBMB Life* 65:863–872. <https://doi.org/10.1002/iub.1211>
12. Poulsen DF, Bowen VT, Hilse RM, Rubinson AC (1952) The copper metabolism of drosophila. *Proc Natl Acad Sci U S A* 38:912–921. <https://doi.org/10.1073/pnas.38.10.912>
13. Hosamani R (2013) Acute exposure of *Drosophila melanogaster* to paraquat causes oxidative stress and mitochondrial dysfunction. *Arch Insect Biochem Physiol* 83:25–40. <https://doi.org/10.1002/arch.21094>
14. Bonilla-Ramirez L, Jimenez-Del-Rio M, Velez-Pardo C (2011) Acute and chronic metal exposure impairs locomotion activity in *Drosophila melanogaster*: a model to study parkinsonism. *Biometals* 24:1045–1057. <https://doi.org/10.1007/s10534-011-9463-0>
15. Paula MT et al (2014) Effects of Hg (II) exposure on MAPK phosphorylation and antioxidant system in *D. melanogaster*. *Environ Toxicol* 29:621–630. <https://doi.org/10.1002/tox.21788>
16. Xue J, Wang HL, Xiao G (2020) Transferrin 1 modulates rotenone-induced Parkinson's disease through affecting iron homeostasis in *Drosophila melanogaster*. *Biochem Biophys Res Commun* 531(3):305–311. <https://doi.org/10.1016/j.bbrc.2020.07.025>
17. Tang X, Zhou B (2013) Ferritin is the key to dietary iron absorption and tissue iron detoxification in *Drosophila melanogaster*. *FASEB J* 27:288–298. <https://doi.org/10.1096/fj.12-213595>
18. Vallee BL, Auld DS (1990) Zinc coordination, function, and structure of zinc enzymes and other proteins. *Biochemistry* 29:5647–5659. <https://doi.org/10.1021/bi00476a001>
19. Suzuki T et al (2005) Zinc transporters, ZnT5 and ZnT7, are required for the activation of alkaline phosphatases, zinc-requiring enzymes that are glycosylphosphatidylinositol-anchored to the cytoplasmic membrane. *J Biol Chem* 280:637–643. <https://doi.org/10.1074/jbc.M411247200>
20. Le Du MH, Stigbrand T, Taussig MJ, Menez A, Stura EA (2001) Crystal structure of alkaline phosphatase from human placenta at 1.8 Å resolution. Implication for a substrate specificity. *J Biol Chem* 276:9158–9165. <https://doi.org/10.1074/jbc.M009250200>
21. Qiao W, Ellis C, Steffen J, Wu CY, Eide DJ (2009) Zinc status and vacuolar zinc transporters control alkaline phosphatase accumulation and activity in *Saccharomyces cerevisiae*. *Mol*

- Microbiol 72:320–334. <https://doi.org/10.1111/j.1365-2958.2009.06644.x>
22. Xiao G, Wan Z, Fan Q, Tang X, Zhou B (2014) The metal transporter ZIP13 supplies iron into the secretory pathway in *Drosophila melanogaster*. eLife 3:e03191. <https://doi.org/10.7554/eLife.03191>
23. Perl DP, Good PF (1992) Comparative techniques for determining cellular iron distribution in brain tissues. Ann Neurol 32(Suppl): S76–S81. <https://doi.org/10.1002/ana.410320713>
24. Krijt M et al (2018) Detection and quantitation of iron in ferritin, transferrin and labile iron pool (LIP) in cardiomyocytes using (55)Fe and storage phosphorimaging. Biochim Biophys Acta Gen Subj 1862:2895–2901. <https://doi.org/10.1016/j.bbagen.2018.09.005>
25. Nowakowski AB, Wobig WJ, Petering DH (2014) Native SDS-PAGE: high resolution electrophoretic separation of proteins with retention of native properties including bound metal ions. Metallomics 6:1068–1078. <https://doi.org/10.1039/c4mt00033a>



Chapter 25

Microplastics: A Review of Methodology for Sampling and Characterizing Environmental and Biological Samples

Christiana H. Shoopman and Xiaoping Pan

Abstract

In response to apparent damaging effects of plastics, especially microplastics, exposure to life, scientists have begun the arduous task of standardizing methods for the sample collection, separation, detection, and identification of microplastic particles. The ability to detect plastics depends upon the type of sample, procedure, instrument, expertise of the examiner, and the exact research question. The wide variability of sample processing and analyses does not lend itself well for cross-comparison of studies. However, with a multitude of procedures, techniques may be used in combination to successfully identify microplastic particles. Our goal in this chapter is not to provide a complete guide on plastic analyses, but to present an overview of the different sample collection, pretreatment, detection, and identification methodologies used for microplastic samples located in environmental and biological samples and to review advantages and limitations of each strategy.

Key words Microplastics, Separation, Sampling

1 Introduction

Over 359 million metric tons of plastics were manufactured in 2018 [1]. Human beings have become reliant on plastic due to its flexible and durable properties. Accounting for 5–25% of the total weight in landfills [2], plastics are found as pollutants in the air, water, and soil [3]. Plastics are so ubiquitous that they have been found in places where human presence is nearly nonexistent, such as Point Nemo, the farthest oceanic point away from land [4], the French Pyrenees mountains [5], and Antarctica [6]. Ironically, even though human beings benefit from plastics in many ways, constant exposure of plastics to the human body can be damaging and have been linked to asthma, cardiovascular disease, endocrine disruption, infertility, and cancer [7, 8]. Additives, such as stabilizers and fire retardants, introduce additional chemicals to plastics during

manufacturing, which also present additional health risks that need to be further investigated [9, 10]. Modes of exposure range from ingestion to inhalation, and the possible accumulation of these toxins causes paramount concerns to human health [8]. Growth rates of seeds and earthworms subjected to soil contaminated by plastic debris have even found to be negatively affected, possibly due to the leaching of chemicals into the soil [11]. Plastics are so pervasive that organisms including zooplankton, seabirds, and humpback whales are known to ingest plastic [3, 12], indicating the ease of ability for chemicals to enter the food chain and cause inflammation, injury, and death in these unintended victims [3, 13].

According to the American Chemistry Council, plastics are synthetic or natural polymers of repeating units composed of carbon, hydrogen, oxygen, nitrogen, chlorine, and sulfur [14, 15]. Although plastics are known for their durability, they can become brittle, crack, and degrade into smaller fragments [16]. Microplastics were first described by Thompson et al. in 2004 and are defined as particles with less than 5 mm in diameter [17] and can further break down into nanoplastics ($\leq 1 \mu\text{m}$) [18]. Microplastics are classified as primary or secondary, the former describing plastics in their original form, manufactured for a commercial purpose, such as beads in personal care products. Secondary microplastics refer to the smaller pieces of plastic that are the result of plastics breaking down. These smaller pieces may have altered physical or chemical properties due to this degradation [19]. Degradation rates of microplastics vary based on exposure to UV light, temperature, moisture, wind, chemicals, microbes, and biofilms [20, 21]. In 2016, Lambert and Wagner examined the photodegradation effect on polystyrene by exposing 1 cm pieces of a disposable coffee cup lid to visible and UV light in demineralized water at 30 °C. After 56 days, 1.26×10^8 particles/mL were present in the sample with an average particle size of 224 nm, exemplifying the break down that can occur from plastics floating in water exposed to sunlight [17].

Although the variety of plastics is vast, the Society of Plastics Industry has developed schema by which they can be differentiated. They are each assigned a resin code and are classified into seven categories: [1] polyethylene terephthalate (PETE) (drink bottles, food jars), [2] high-density polyethylene (HDPE) (milk and detergent containers), [3] polyvinyl chloride (PVC) (pipes, flooring), [4] low-density polyethylene (LDPE) (grocery and sandwich bags), [5] polypropylene (PP) (to-go containers), [6] polystyrene (PS) (plastic cutlery, fast food trays), and [7] other, constituting plastics not designated as category 1–6 or consisting of a mix of resins, such as polylactide (PA/nylon), polycarbonate (PC), acrylonitrile butadiene styrene (ABS) and cellulose acetate (CA). This uniform numeric system allows consumers to properly identify the

resin code of a product and aids in the sorting process for recycling programs, which is a necessary step before a plastic item can be reprocessed for reuse [2, 22].

2 Sampling

The investigation of plastic contamination in the environment began in 1971 when Carpenter and Smith recorded observations of plastic particles in the Sargasso Sea, a remote area with no land boundaries within the North Atlantic Ocean [23, 24]. Plastics, mainly in the form of pellets, were collected in neuston nets, intended to catch organisms on the surface of the water [23]. Since that time, numerous researchers have used multiple methods to collect microplastic debris, mostly are similar to approaches used in the 1970s. Comparative quantitative analyses cannot be performed without the standardization of these techniques [25].

2.1 Trawl Sampling

The use of a manta trawl (Fig. 1), a winged floating apparatus with a trailing net composed of a mesh surface, is a strategy that was first used by Brown and Cheng (1981) to collect marine organisms and debris while trawling [26]. This collection tool, appropriately named for the manta ray's shape and feeding habits, was modified by Eriksen et al. (2013) for the purpose of capturing microplastic particles on the surface of the water [27]. This technique enables a broad range of water to be continuously surveyed over a short period of time [28]. Common manta trawls used for this type of collection are approximately three meters in length [29] with 300 µm nets [30]. Typically, trawling occurs by continuous movement for approximately 30–60 min at a speed of 2–4 knots [27, 29, 31]. The trawling device is towed alongside the boat to avoid the

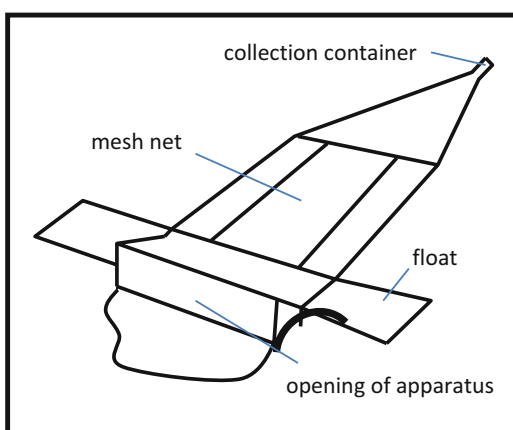


Fig. 1 Manta trawl used to collect microplastics on the surface of water

wake, as movement may push plastic pollutants away from the collection net [32, 33]. Material captured in the net is rinsed with distilled water and stored in clean glass bottles. However, the composition of the mesh net may introduce plastic contamination to the sample through the shedding of fibers and debris, resulting in the overestimation of the amount of plastic debris present [32]. Furthermore, care should be taken when storing the manta net, as loose paint and rust debris from the vessel have been identified as contaminants in samples [34].

The main limitation of this technique is the inability to collect samples smaller than 0.3 mm, as the size of the netting restrict the size of captured particles [32, 35], possibly underrepresenting the amount of plastics present [36]. Smaller mesh nets have been evaluated, but they are problematic as organisms and algae blooms may be trapped and obstruct the net [37]. Sampling is restricted to the surface of the water and is diminished in rough waters [38]. Additionally, more dense plastics may be underestimated as they are not as buoyant, while Styrofoam, polyethylene, and polypropylene may be in abundance. Degraded plastics are likely to sink and will not be detected utilizing this method [39]. Care should be taken to consider weather conditions, tides, and currents as factors that can affect collection volume, influence the concentration and dispersal of plastic litter [35].

2.2 Grab Sampling

Grab sampling is a method used to obtain microplastics from freshwater, ocean water, and sediment at a certain time, rather than by a lengthy continuous collection as used when trawling. This technique usually involves the manual collection of a sample using rudimentary tools. Utilizing this method allows for the recovery of plastic particles less than 0.3 mm in size [35].

Grab samples are commonly collected from freshwater and marine water utilizing an inexpensive collection container, such as a jar [28], pail, bottle, or steel sampler to manually retrieve the sample [40]. Nonplastic equipment, such as glass and stainless steel, should always be chosen over plastics [35]. Collection equipment should be cleaned in the laboratory and rinsed with distilled water prior to the collection of samples [41]. Since no net is involved, there is no limitation on the size of sample obtained or the depth of the water being tested [35]. This simple process is advantageous in areas where towing a manta net is not feasible [42].

Grab sampling of sediment samples has been evaluated as a collection method for retrieving microplastic specimens from shorelines and lake or ocean floors [30, 43]. This principle is based on the sampling technique first reported by Petersen and Jensen in 1911 to collect benthic organisms. A device attached to a pole was used to remove samples from the sea floor while preserving the natural layers of the sediment [44]. Equipment used for grab collection is based on the study location and desired depth of the

sediment. Beach samples are typically collected from the uppermost 5 cm of sediment along the high-tide mark using a metal ruler for depth accuracy. Simple tools made from metal or stainless steel, such as spoons [43], spatulas, scoops [45, 46], and cylindrical corers [47] are manually used to push into the sediment. However, if large quantities of algae are present at the high tide line, it is more advantageous to collect samples at the low tide mark [48]. Box and grab corers can be used at locations near shore or offshore, but they require divers and/or a boat capable of hauling and operating specialized equipment [47]. A box corer consists of a weighted container that is remotely lowered into the water and inserted into the floor bed to scoop a sample of sediment. After retrieval, samples are dried and weighed at the laboratory before performing additional treatment processes [43].

The grab sampling technique is not advantageous with respect to the time and effort required for collection. An increased number of sampling attempts are necessary over a smaller range for a reliable sample, and results will vary based on the depth of collection [14]. Besley et al. (2017) reported a minimum collection of 22 sediment samples is needed for each 100 meters of beach to reach a 99% confidence level [43]. The capacity and number of collection containers limits the volume that can be sampled, which can produce unreliable and inconsistent comparisons between samples [42]. The collection of sediment samples located from seabed surfaces are more difficult, expensive, and time-consuming. However, these samples will be less degraded than beach samples exposed to degradation due to sunlight, temperature, and wind [47]. Multiple filtration steps may be necessary to reduce the volume of the sample [42]. Obscure sources of plastic, such as the lids of containers, can introduce possible contaminants to the sample [35]. Collection tools need to be cleaned between samples [43]. Collection of sediment located under the water may require access to watercraft and equipment specifically designed to collect sediment samples in unique places [47]. Scuba divers have been involved in shallow waters to collect samples [20].

A sampling plan that implements more than one method may provide a more accurate representation of the microplastics collected at the study site [49, 50]. Samples may be rinsed with distilled water or be lightly wiped instead of subjected to harsh chemicals to avoid breakage [20]. Collected samples are placed in glass bottles and should be preserved in either 70% ethanol or isopropyl alcohol [49, 51, 52].

2.3 Sampling of Biota

Most studies examining the amount of microplastic debris ingested by biota have involved marine and terrestrial organisms [3, 53, 54]. Harper and Fowler (1987) were among the first to examine animals for ingested plastic. They discovered plastic pellets in the

gizzards of beached seabirds collected in New Zealand from 1958 to 1977, long before plastic pollution was a mainstream concern [55].

Corpses of beached turtles, birds, fish, or mammals may be easily found and require modest equipment for collection. Di Beneditto and Ramos (2014) examined the stomach contents of dolphins inadvertently caught in fishing nets [56]. Bravo Rebollo et al. (2013) examined the intestines of over 100 carcasses of harbor seals that died from Phocine Distemper Virus (PDV) and subsequently washed ashore in the Netherlands [57].

Live invertebrates and fish may be purposefully collected using manta trawls or grab sampling, as previously described, or using weighted nets that are drug along the seafloor [58, 59]. Mollusks, crustaceans, and earthworms can be collected by hand or with traps [60]. Birds can be captured utilizing lighting techniques that temporarily impair their vision to aid in their collection with nets [61]. Other live organisms, such as mussels, can be purchased directly from farms or food markets for analysis [62, 63].

Samples can be indirectly obtained from wildlife by collecting bolus or feces. This type of sampling is advantageous in comparison to examinations of deceased animals as it allows for recurring collections. Bond and Lavers (2013) performed catch and release methods to examine plastic ingestion of live storm petrels. These seabirds were injected with syrup of ipecacuanha to induce vomiting and the regurgitated sample was examined for microplastics [61].

2.4 Methods to Investigate Human Routes of Exposure to Microplastics

Several studies identifying microplastics in fish, oysters, mussels, and shrimp have increased concerns related to the probability of human's uptake levels of plastics in their systems by way of ingestion [62, 64, 65]. It has been found that for foods that are wholly ingested, such as anchovies and scallops, this effect may be heightened [66]. A study by Karbalaei et al. (2018), however, suggested the inhalation of plastic particles through dust and laundry may be more common routes of exposure compared to ingestion [67]. Additional studies are needed to investigate the ingestion, accumulation, translocation, retention, and elimination of microplastics by marine organisms before associating links between seafood consumption and human health [68].

Schwabl et al. (2019) were the first researchers to identify microplastics in adult stool samples. Eight participants from across the globe (Japan, Russia, the Netherlands, the UK, Italy, Poland, Finland, and Austria) were required to keep a log of their unrestricted diet 6–7 days prior to the collection of the specimen, along with nonconsumables such as toothpaste, gum, and cosmetic samples. Six of the eight volunteers ate seafood, and seven individuals drank from plastic water bottles. A kit containing instructions, a metal spoon, and a glass bottle were provided to each volunteer to

self-administer the collection of one stool sample. Microplastics (sized 50–500 µm), specifically polypropylene and polyethylene, were identified in all samples by Fourier Transform Infrared (FTIR) Microscopy, indicating unintentional plastic consumption. This study was limited due to the small sample size of the participants with no replicate samples, as well as a lack of tracing to the source of exposure [69].

Porras et al. (2020) tested urine samples of twenty workers exposed to phthalate, a plasticizer added to make plastic flexible [70], to monitor occupational inhalation exposure levels. Twenty participants from four different factories in Finland producing cables, PVC resins, textiles, and tarpaulin took part in the study. Urine samples were collected from each volunteer at five specific timepoints to monitor changes in metabolites over time: after a holiday, just after waking up, immediately after work, during the evening and following morning. A control group of volunteers not exposed to the contaminant were used for comparison. After collection, the urine samples were frozen at –20 °C for preservation. Isotype-labeled phthalate metabolites were added to each sample to serve as an internal standard to assist with determining the limit of quantitation. The separation and quantitation of different compounds in the urine was performed using a liquid chromatography system coupled with a quadrupole mass spectrometer (LC-MS/MS). This method detected phthalate metabolites, which allowed the researchers to estimate the level of the hazardous exposure. Detectable levels of phthalates were observed in samples of workers from each of the factories, indicating exposure. However, most of the exposure levels were below the daily limit for hazardous exposure. Further studies utilizing a larger sample size over a longer period may provide valuable insight into occupational exposures to phthalates and resulting health effects due to frequent exposure [71].

Christensen et al. (2018) performed a review to investigate occupational exposures to styrene. The cohort consisted of over 73,000 workers employed by 456 plastic companies in Denmark from 1968 to 2011. Information obtained from these records were compared to cancer registries to determine if exposure to styrene is associated with cancer. Positive associations were made linking exposure to styrene and occurrence of acute myeloid leukemia [72]. Advantages of this chart review include the ability to evaluate a large cohort of studies over a four-decade period to help determine trends in the correlation of human disease and microplastics, but it does not provide discriminative evidence. There exists, at the time of this printing, a lack of studies that investigate the effects on human health and microplastics.

3 Sample Preparation/Separation

Organic debris, such as algae and animal matter; nonorganic debris, such as nonplastic litter; and plastics larger than 5 mm need to be removed from the microplastic samples before further identification procedures are employed. This can be achieved by separating microplastic particles from other debris based on density and physical size. Once samples have been separated, they are rinsed with deionized water [31].

3.1 Separation by Density

Density separation is an efficient, simple, and inexpensive screening technique that aids in differentiating plastic materials from nonplastic components collected from water and sediment samples [32]. Thompson et al. (2004) was one of the first to use this technique to separate microplastic debris from sediment samples; however, the technique only permitted the detection of plastics that did not look like sediment or plankton [73]. This method has been optimized to obtain higher recovery rates of microplastics [74]. In this procedure, a salt solution is added to the sample, which is then typically vortexed and centrifuged or allowed to settle so components will sink, or float based on their density [75]. The floating materials in the supernatant are collected for further analysis while other materials and debris that are heavier or have settled are discarded [76]. Microplastics typically float when introduced to a salt solution, due to their low density [54], and separate according to their respective class [77]. For example, pure forms of polypropylene and low- and high-density polyethylene have densities ($<1\text{ g/cm}^3$) less than nylon, polycarbonate, and polyethylene terephthalate ($>1\text{ g/cm}^3$) [20, 77] and can be easily separated. Common salt solutions used for this process include sodium bromide (NaBr), sodium chlorine (NaCl), zinc bromide (ZnBr₂), zinc chloride (ZnCl₂), sodium iodide (NaI), and sodium lauryl sulfate (SLS) [40, 74, 77].

The matrix of the sample containing the microplastic pieces should be taken into consideration when choosing a particular salt solution for density separation [77]. For instance, sediment (2.7 g/cm³) has a considerably higher density than plastic ($<1.45\text{ g/cm}^3$); therefore, the separation of microplastics can be achieved in a salt solution with a lower density ($<1.3\text{ g/cm}^3$), such as NaCl [77]. Nuelle et al. (2014) reported a high recovery rate (91–99%) using NaI to separate higher density microplastics from marine sediments [78]. Conversely, compost and sludges (1.2–1.4 g/cm³) have densities similar to many polymers, which makes separation more difficult, but it may be resolved in a solution with a density greater than 1.2 g/cm³ [77]. After the salt solution is added to the specimens, the sample is shaken and allowed to settle before potential plastic particles are collected from the supernatant [19].

Reduced recovery rates may occur utilizing the density separation method which partition due to the size [74], purity, and level of degradation [14, 20, 33] of the microplastic pieces. Plastics within the same classification group may also have additives, which alter the density of the material [20]. For example, the composition of mixed polymers and concentration of additives may vary depending on the plastic, such as tires of different manufacturers [14]. Furthermore, shredded tire pieces may also contain asphalt and road debris, which alters the density of the sample [14]. Therefore, caution is advised when choosing the salt solution used for this technique as desired microplastic pieces may sink and be discarded [79]. Alternatively, if a conservative approach is taken, the separation may need to be repeated to obtain an improved recovery rate since particles other than plastic can float [77]. Debris attached to bubbles may falsely float and be collected in the supernatant [54], and microplastics attached to the side of the glass may be inadvertently missed [80].

3.2 Separation by Size

Sieving and filtration steps can be useful to reduce larger-sized samples while removing unwanted matter and liquid [35]. Sieving allows the sample to be concentrated utilizing a funnel, sieve, and glass container for collection [31]. Filters contain pores that allow the water to pass through while trapping particles of desired size on its surface. The recommended size for filters is around 300- μm [81] and a 300–500- μm sieve is typically used in microplastic examinations [78, 81]. After sieving, particles are weighed and dried. Rodrigues et al. (2019) reported that the optimal temperature to dry the plastic particles is overnight at 90 °C. Using a lower temperature significantly increased the time to process the samples, and a higher temperature (100 °C) caused degradation of the plastic samples [82].

3.3 Separation by Dissection

Dissection is the most common method used to retrieve microplastic particles from wildlife, with gills, tissues, and intestinal tracts being the primary areas examined [35]. Specimens captured from the collection site should be immediately frozen, stored on ice, or placed in ethanol or formaldehyde for preservation until processing can take place in a clean laboratory setting [83]. The examination should be performed utilizing a dissecting microscope, and clean scissors and tweezers for opening tissues and retrieving possible plastics. When examining the intestines, it is recommended to remove the entire GI tract for examination. The oral cavity should also be examined during this process [84].

Murphy et al. (2017) examined the intestines of fish collected from waters off the coast of Scotland for microplastic particles and reported that 47.7% of fish captured near the shoreline at a water depth of 8–78 m ingested a significantly higher percentage of plastics compared to 2.4% of the fish collected offshore in deeper

waters (290–1010 m). Due to limited space on the boat, the entire intestinal tract was removed while onboard, and stored frozen in bags at -20°C until dissection could be performed with a stereomicroscope in the lab. Materials not representative of the normal diet were removed, rinsed with distilled water, and stored on filter paper in a glass petri dish for further analysis [58].

Dissections should be performed as quickly as possible after collection. If this is not feasible, the carcass should be kept frozen until dissection is able to be performed [84]. After microplastics are located by dissection methods, they can be processed similarly to water and sediment samples [85].

3.4 Digestion

Samples collected from water, sediment, and organisms may also contain organic debris, such as mollusks, crustaceans, fish, other tissues and bones, feathers, algae, and wood that can conceal the presence of microplastic particles during microscopic examinations [65, 86]. Digestion treatments are used to remove organic and inorganic matter from microplastic samples. This technique is particularly important for microplastic pieces smaller than 300 μm , to avoid misidentifying debris as plastic in later processing steps [83]. Many different digestion methods have been validated based on the purification technique and chemical used, such as oxidative (H_2O_2) [87], acid (HNO_3) [88], alkaline (KOH) [89], and enzymatic digestion (SDS) [90]. For example, Fig. 2 shows the effective removal of debris in sediment sample by the hydrogen peroxide (H_2O_2) treatment [78]. Cole et al. first established a technique in 2014 to dissolve plankton from marine water samples without degrading microplastic debris [85]. Chemical digestive treatments using acids should never be used in digestion procedures with microplastic samples as they can alter the color of the plastics, and hinder identification [91]. The most commonly used

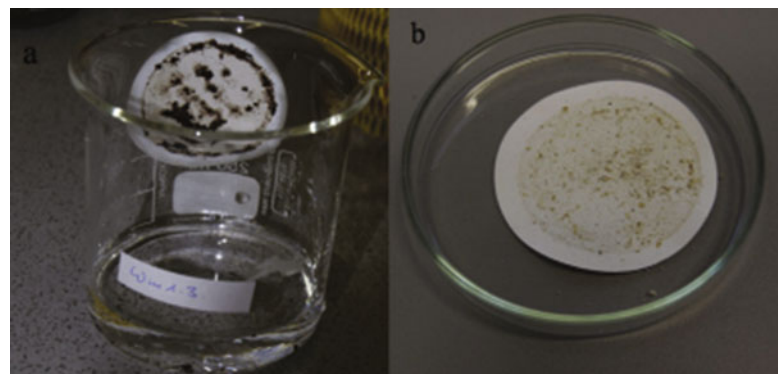


Fig. 2 Sediment sample on filter paper (a) before and (b) after oxidative digestion treatment of H_2O_2 to remove biota. (Reprinted from “A new analytical approach for monitoring microplastics in marine sediments,” by Nuelle, M.-T., 2014, *Environmental Pollution* 184, p. 165)

solution for alkaline digestion is potassium hydroxide (KOH) [83], although comparisons have been performed using other solutions, such as hydrogen peroxide (H_2O_2), sodium hydroxide (NaOH), proteinase K, and trypsin [63, 65, 91–93]. Potassium hydroxide is an inexpensive solution that successfully digests animal tissues with minimal damage to microplastic samples, requires a shorter incubation, is less hazardous compared to other digestion chemicals, and does not interfere with downstream identification processes such as spectroscopy [86, 91].

Dehaut et al. (2016) modified the digestion procedure reported by Fockema et al. [89] and concluded that specimens containing microplastics should be incubated with a 10% KOH solution at 60 °C for 24 h for the highest recovery rate without causing degradation to the plastic [65]. Prata et al. (2019) further reported the use of KOH at 50 °C for 1 h as an effective digestion for animal tissues, and hydrogen peroxide combined with an iron catalyst at 50 °C for 1 h to successfully digest plant material. After digestion, the sample is filtered, rinsed with distilled water, and weighed [86].

4 Microscopy Detection and Quantitation

Microscopy techniques are common, low-cost screening methods for the visual detection and sorting of plastics [54]. Samples can be placed in a glass petri dish and viewed with a stereomicroscope at 40× magnification [31, 43] to count, characterize the shape, color and type, and measure microplastic pieces [31]. Plastics are characterized by their shape as films, foams, fragments, fibers, and pellets, which are then sorted, weighed, and stored separately based on these physical properties [36]. Figure 3 shows the microscopy classification of microplastic pollutants found in estuarine waters [82]. According to Hidalgo-Ruz et al. [94], the evaluation and quantitation of plastic particles involves the following four rules: [1] plastic particles will not exhibit any organic or cellular structures; [2] plastics are typically uniform in colors; [3] plastic fibers must exhibit the same width along the entirety of the filament; [4] particles must display a clear and even color [94]. Additionally, all nonfiber particles are measured on the longest diagonal [31]. This visual detection method allows plastic particles to be quantitated and measured, while eliminating nonplastic particles from being processed further [54]. Large microplastic pieces should be examined thoroughly, yet carefully, with tweezers to ensure smaller particles are not hidden [31].

Microscopy works well when screening for larger plastic samples, but it is limited as its ability to detect smaller fragments is time consuming [79]. A stereomicroscope should not be used to characterize microplastic particles less than 500 µm in size [95]. Identification using a compound microscope is useful to rule out

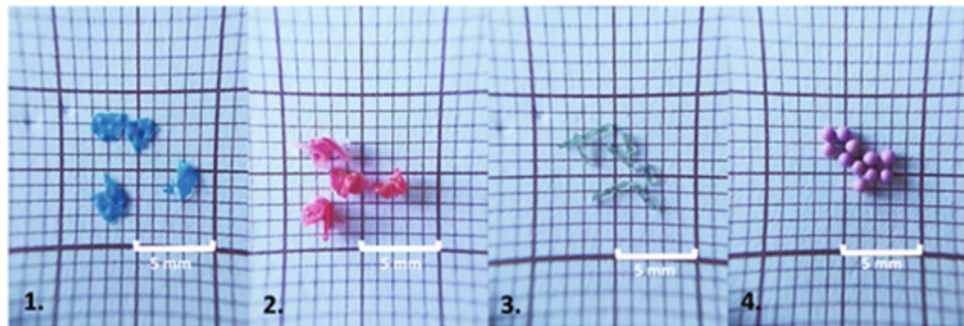


Fig. 3 Known microplastics sorted by shape and color. (1) film (plastic bags); (2) particles (bottle caps); (3) Fibers (fishing line); and (4) pellets (microspheres). (Reprinted from “Adaptation of a laboratory protocol to quantify microplastics contamination in estuarine waters,” by Rodrigues, S., 2019, *MethodsX* 6, p.742)

inconclusive results observed with the stereomicroscope; however, high error rates are expected as plastic particles degrade and exhibit various sizes, colors, and shapes in comparison with pristine samples [37]. If sediment is not properly removed during these prior separation steps, it may be problematic when differentiating between the sand pieces and microplastic particles, particularly when examining minute plastic debris [96]. Also, microplastic specimens may be inadvertently discarded or inaccurately identified as plastic due to the lack of expertise or bias of the examiner [95]. In order to help mitigate the subjective nature of this method, a review by multiple individuals may aid with confirmation; although, it has been reported that there is a high degree of variability depending on the examiner [14]. Chemical identification steps are necessary after performing visual inspections with microscopy, since microscopy often involves inaccurate assessments resulting in increased error rates [81].

Fluorescent microscopy methods can be used to identify, quantify, and characterize microplastics [97]. Andrade (2010) was the first to suggest the use of Nile Red (9-diethylamino-5H-benzo[α]phenoxazine-5-one) dye to stain polymers [98]. This method has been further optimized as an effective staining technique to aid in the detection of microplastic samples from beach sediment and sea surfaces. The lipophilic fluorescent dye adheres to the outside surface of plastics enabling identification [97]. Maes et al. (2017) determined that a 30-min incubation period with 10 $\mu\text{g}/\text{mL}$ of Nile Red is sufficient for detection [79]. Protocols involve capturing microplastic particles on a 25 mm polycarbonate filter to minimize unwanted background fluorescence [77].

Operationally, Nile Red is directly added to the sample on a polycarbonate filter, and the filter is transferred to the slide for examination utilizing a fluorescence microscope [77]. Plastic particles exposed to Nile Red dye will fluoresce [28, 99]. A count can be performed on the number of observed fluorescent structures.

Additionally, the morphological size, shape, and differences in intensity of the color of the objects are noted to aid in classifying the type of plastic observed [79].

Although not confirmatory, the use of Nile Red dye in tandem with fluorescent microscopy is a quick, low-cost, and relatively high-throughput screening method to determine the amount of microplastics present in a sample [46]. Nile Red does not have a specificity for microplastics [54], since organic matter not properly removed from prior digestion steps will fluoresce as well, resulting in erroneous identifications [77].

Maes et al. (2017) spiked sediment samples with six different polymer types: polyamide (nylon), polystyrene (PS), polyvinylchloride (PVC), polyethylene terephthalate (PET, polyester), polyethylene (PE), and polypropylene (PP) to evaluate and compare the sensitivity of Nile Red. False negative results were obtained with PVC, nylon, and PET, as well as for plastic debris smaller than 100 μm [79]. Ruggero et al. (2020) confirmed that the fluorescent signal was strong for PP, PE, PS, Nylon, and PUR, but the sensitivity for PET and PVC was weak [77]. The use of Nile Red may interfere with downstream identification processes [100].

5 Spectroscopy Identification

Spectroscopy methods such as Fourier Transform Infrared Spectroscopy (FTIR) and Raman used in tandem with microscopy allow for the visual identification and chemical composition of microplastic samples [101]. In these techniques a spectrum is produced, which displays a pattern of the vibration of the chemical bonds due to the absorption or transmittance of infrared light (FTIR) or scattering of visible light (Raman). The detected spectrum displays the molecular “fingerprint” of the substance, which represents the distinctive attributes of the functional groups. This spectrum of the unknown sample is then compared to a spectra of known polymers via a reference library to determine its identification. For example, the infrared spectrum of polystyrene displays bands around 3090 cm^{-1} , which corresponds to the vibration of aromatic groups. High- and low-density polyethylene both have bands present at 1377 cm^{-1} indicating symmetric bending of the CH_3 groups [102].

Identification by spectroscopy is only as robust as the quality of the reference library used for comparison, and reference libraries can be costly. It is advantageous to use a library containing spectra of common additives, such as diethylhexyl phthalate (DEHP), and possible contaminants from collection equipment, such as a manta net [35]. Alternatively, if access to a reference library is not feasible, known standards, such as reference materials from the National Institute of Standards and Technologies (NIST SRMs), can be analyzed and used for comparison and assessment [103].

5.1 Fourier Transform Infrared (FTIR) Microscopy

Fourier transform infrared microscopy is the most common method used for the identification of microplastics due to its capability to produce rapid and reliable results. The technique combines the use of a FTIR microscope with chemical imaging to aid in the identification and quantitation of plastic pieces [104]. It is recommended to first concentrate microplastic samples less than 500 µm in size on a filter before micro-FTIR analysis to avoid handling minute samples manually [105]. The filter is then placed on a microscope stage to locate, measure, and characterize particles based on their sizes. A spectrum is obtained by FTIR followed by a library search for comparison [33].

Vianello et al. (2013) and Fockema et al. [89] were the first to report the use of reflectance micro-FTIR techniques for environmental samples. Reflectance micro-FTIR measures the energy of light reflected from the particles to produce a chemical map. The spectrum displays a pattern of peaks, which provides the chemical structure of the material. This technique is advantageous when analyzing thick or nontransparent materials with reflective surfaces, as it measures refractive index instead of the absorption intensity of the sample. Conversely, performing this method is very time consuming as it lacks the capacity to rapidly scan the filter in its entirety [105].

Löder et al. (2015) were the first to apply an alternate method, focal plane array (FPA) micro-FTIR, for the identification of microplastics in sediment and marine plankton samples. FPA micro-FTIR rapidly scans the entire filter containing plastic particles and converts those scans to an image. FTIR has the capability to detect samples down to 5 µm, but it should only be used to identify and analyze plastic particles larger than 20 µm and works best with flat surface materials as uneven edges may create spectral errors [105].

5.2 Attenuated Total Reflection (ATR)-FTIR Spectroscopy

ATR-FTIR involves the use of a diamond, germanium, or zinc selenide crystal to interact with the sample during FTIR analysis [45]. To help prevent contamination, the crystal should be wiped with alcohol or acetone before processing the first sample and between samples [20]. A background spectra is conducted before testing samples and in between samples to ensure there is no contamination [47]. Pressure is applied to allow the sample to be in direct contact with the crystal [14].

The advantage of micro ATR-FTIR spectroscopy (attenuated total reflection) is the ability to analyze microplastic particles in their present state without destroying the sample, therefore reducing potential preprocessing steps required for other types of analysis. Other benefits of this application include that only a small sample size is needed (<0.1 g) and spectra can be produced rapidly, which allows many specimens to be processed in a relatively short amount of time [106]. Asymmetrical microplastics can be tested utilizing this method [81].

This identification technique does have some limitations. The spectra provide information for only the portion of the sample that is in direct contact with the crystal [95]. Degraded microplastic samples may be challenging to identify as they may produce a spectrum that differs from the same type of plastic in pristine condition [103]. Using proper separation and digestion techniques to purify the sample can help produce a more reliable spectrum [65].

5.3 Raman Spectroscopy

Raman spectroscopy is a technique developed in 1927 that has been further optimized for the detection and identification of microparticles [107]. This method is similar to FTIR as it is a nondestructive process which can analyze the sample in its natural state. A monochromatic laser interacts with the surface of the sample causing a scattering of photons and shift in energy, commonly referred to as a “Raman shift” (Zada, 2018). Confocal laser scanning microscopy improves the resolution of the sample. This method is more sensitive ($1 \mu\text{m}$) than FTIR ($10 \mu\text{m}$) and can better distinguish the vibrations of nonpolar functional groups (Lv, 2018). Certain digestion, extraction, and fluorescent processing methods performed prior to Raman spectroscopy may result in unintended consequences and interfere with analysis and proper identification of microplastics [95].

Käppler et al. (2016) were the first to provide an in-depth comparison of the FTIR and Raman spectroscopy methods for the identification of microplastics. After isolating the microplastics from the sediment, the same samples were detected by FTIR and Raman spectroscopy. Similar results were obtained from both techniques; however, FTIR allows for high throughput analysis as measurements are obtained more rapidly and Raman spectroscopy is preferable for analyzing microplastic particles smaller than $50 \mu\text{m}$. The ability to analyze one sample with both techniques can provides a comprehensive chemical assessment. This process is advantageous as it has the potential to reduce misidentifications, but duplicate work and expensive to perform [95].

Zada et al. (2018) were the first to use stimulated Raman scattering (SRS) for the identification of microplastics in environmental samples. This spectroscopy method also scans and detects microplastic particles on membrane filters, but it utilizes two laser beams to rapidly acquire data [108]. The entire filter can be analyzed simultaneously, just as noted in micro ATR-FTIR analysis, allowing it to potentially be a comparable method for identifying microplastics.

6 Conclusion

A variety of methods can be used for the evaluation of microplastic particles in biological and environmental samples. However, accurate and informative comparison studies cannot occur without standardized protocols that define sample collection, separation, and identification procedure and criteria. This work provides a review of common methods for microplastics sampling, separation, detection, and quantitation which provide comprehensive information related to revealing the route of exposure to microplastics and their adverse effects on the environmental and human health. Further research is needed to develop, optimize, and validate various methods and applications we have described. The successful implementation of best practices within the scientific community will help to reduce misidentifications attributed to bias and instrumental limitations, and to strengthen the reliability and robustness of methodologies used in microplastic analyses.

References

1. Garside M (2020) Global plastic production 1950–2018. <https://www.statista.com/statistics/282732>. Accessed 17 October 2020
2. Scalenghe R (2018) Resource or waste? A perspective of plastics degradation in soil with a focus on end-of-life options. *Helion* 4(12):e00941
3. Thompson RC, Moore CJ, vom Saal FS, Swan SH (2009) Plastics, the environment and human health: current consensus and future trends. *Phil Trans R Soc B* 364:2153–2166
4. Volvo Ocean Race 2017–2018. Science programme final report (2018) <https://11thhourracing.org>. Accessed 10 October 2020
5. Allen S, Allen D, Phoenix VR, Le Roux G, Jimenez PD, Simonneau A, Binet S, Galop D (2019) Atmospheric transport and deposition of microplastics in a remote mountain catchment. *Nat Geosci* 12:339–344
6. Waller CL, Griffiths HJ, Waluda CM, Thorpe SE, Loaiza I, Moreno B, Pacherres CO, Hughes KA (2017) Microplastics in the Antarctic marine system: an emerging area of research. *Sci Total Environ* 598:220–227
7. Benjamin S, Masai E, Kamimura N, Takahashi K, Anderson RC, Faisal PA (2017) Phthalates impact human health: epidemiological evidences and plausible mechanism of action. *J Hazard Mater* 340:360–383
8. Campantate C, Massarelli C, Savino I, Locaputo V, Uricchi VF (2020) A detailed review study on potential effects of microplastic and additives of concern on human health. *Int J Environ Res Public Health* 17:1212
9. Wright SL, Kelly FJ (2017) Plastic and human health: a micro issue? *Environ Sci Technol* 51:6634–6647
10. Shen M, Zhang Y, Zhu Y, Song B, Zeng G, Hu D, Wen X, Ren X (2019) Recent advances in toxicological research of nanoplastics in the environment: A review. *Environ Pollut* 252 (Pt A):511–521
11. Boot B, Russell CW, Green DS (2019) Effects of microplastics in soil ecosystems: above and below ground. *Environ Sci Technol* 53:11496–11506
12. Jâms IB, Windsor FM, Poudevigne-Durance-T, Ormerod SJ, Durance I (2020) Estimating the size distribution of plastics ingested by animals. *Nat Commun* 11:1594
13. Hermsen E, Pompe R, Besseling E, Koelmans A (2017) Detection of low numbers of microplastics in North Sea fish using strict quality assurance criteria. *Mar Pollut Bull* 122:253–258
14. Huppertsberg S, Knepper T (2018) Instrumental analysis of microplastics—benefits and challenges. *Anal Bioanal Chem* 410:6343–6352
15. American Chemistry Council, Inc (2020) Plastic – The basics: Polymer definition and properties <https://plastics.americanchemistry.com>. Accessed 25 Oct 2020

16. Andrade AA (2011) Microplastics in the marine environment. *Mar Pollut Bull* 62:1596–1605
17. Lambert S, Wagner M (2016) Characterisation of nanoplastics during the degradation of polystyrene. *Chemosphere* 145:265–268
18. Pinto de Costa J, Santos PSM, Duarte AC, Rocca-Santos T (2016) (Nano)plastics in the environment – sources, fate and effects. *Sci Total Environ* 556–567:15–26
19. Horton AA, Svendsen C, Williams RJ, Spurgeon DJ, Lahive E (2017) Large microplastic particles in sediments of tributaries of the river Thames, UK—abundance, sources and methods for effective quantitation. *Mar Pollut Bull* 114:218–226
20. Brignac KC, Jung MR, King C, Royer S-J, Blickley L, Lamson MR, Potemra JT, Lynch JM (2019) Marine debris polymers and man Hawaiian island beaches, sea surface, and seafloor. *Environ Sci Technol* 53 (21):12218–12226
21. Yuan J, Ma J, Sun Y, Zhou T, Zhao Y, Yu F (2020) Microbial degradation and other environmental aspects of microplastics/plastics. *Sci Total Environ* 715:136968
22. Clauson D (2013) Modernizing the Resin Identification Code (2013) ASTM Standardization News. ASTM International. <https://www.astm.org>. Accessed 16 October 2020
23. Carpenter EJ, Smith KL (1972) Plastics on the Sargasso Sea surface. *Science* 175:1240–1241
24. NOAA (2019) What is the Sargasso Sea? <http://www.noaa.gov>. Accessed 25 Oct 2020
25. Law KV (2017) Plastics in the marine environment. *Annu Rev Mar Sci* 9:205–229
26. Brown DM, Cheng L (1981) New net for sampling the ocean surface. *Mar Ecol Prog Ser* 5:225–227
27. Eriksen M, Maximenko N, Thiel M, Cummins A, Lattin G, Wilson S, Hafner J, Zellers A, Rifman S (2013) Plastic pollution in the South Pacific subtropical gyre. *Mar Pollut Bull* 68:71–76
28. Scircle A, Cizdziel JV, Missling K, Li L, Vianello A (2020) Single-pot method for water samples in microplastic analyses. *Environ Toxicol Chem* 39:986–995
29. Sutton R, Mason SA, Stanek SK, Willis-Norton E, Wren IF, Box C (2016) Microplastic contamination in the San Francisco Bay, California, USA. *Mar Pollut Bull* 109:230–235
30. Mai L, Bao L-J, Shi L, Wong CS, Zeng EY (2018) A review of methods for measuring microplastics in aquatic environments. *Environ Sci Pollut Res* 25:11319–11332
31. Kovac Viršek M, Palatinus A, Koren S, Peterlin M, Horvat P, Kržan A (2016) Protocol for microplastics sampling on the sea surface and sample analysis. *J Vis Exp* 118: e55161
32. Lv L, Yan X, Feng L, Jiang S, Lu Z, Xie H, Sun S, Chen J, Li C (2019) Challenge for the detection of microplastics in the environment. *Water Environ Res* 93(1):5–15. <https://doi.org/10.1002/wer.1281>
33. Lebreton L, Slat B, Ferrari F, Sainte-Rose B, Aitken J, Marthouse R, Hajbane S, Cunsolo S, Schwarz A, Levivier A, Noble K, Debeljak P, Maral H, Schoeneich-Argent R, Brambini R, Reisser J (2018) Evidence that the great Pacific garbage patch is rapidly accumulating plastic. *Sci Rep* 8:4666
34. Setälä O, Magnusson K, Lehtiniemi M, Norén F (2016) Distribution and abundance of surface water microlitter in the Baltic Sea: a comparison of two sampling methods. *Mar Pollut Bull* 110(1):117–188
35. Brander SM, Renick VC, Foley MM, Steele C, Woo M, Lusher A, Carr S, Helm P, Box C, Cherniak S, Andrews RC, Rochman CM (2020) Sampling and quality assurance and quality control: a guide for scientists investigating the occurrence of microplastics across matrices. *Appl Spectrosc* 74(9):1099–1125
36. Baldwin AK, Corsi SR, Mason SA (2016) Plastic debris in 29 Great Lakes tributaries: relations to watershed attributes and hydrology. *Environ Sci Technol* 50:10377–10385
37. Löder MGJ, Gerdts G (2015) Methodology used for the detection and identification of microplastics—a critical appraisal. In: Bergmann M, Gutow L, Klages M (eds) *Marine anthropogenic litter*. Springer, Cham
38. Karlsson TM, Kärrman A, Rotander A, Hassellöv M (2020) Comparison between manta trawl and in situ pump filtration methods, and guidance for visual identification of microplastics in surface waters. *Environ Sci Pollut Res* 27:5559–5571
39. Eriksen M, Lebreton LCM, Carson HS, Thiel M, Moore CJ, Borerro JC, Galgani F, Ryan PG, Reisser J (2014) Plastic pollution in the World's oceans: more than 5 trillion plastic pieces weighing over 250,000 tons afloat at sea. *PLoS One* 9(12):e111913
40. Cutroneo L, Reboa A, Besio G, Borgogno F, Canesi L, Canuto S, Dara M, Enrile F, Forioso I, Greco G, Lenoble V, Malatesta A, Mounier S, Petrillo M, Rovetta R, Stocchino A, Tesdan J, Vagge G, Capello M

- (2020) Microplastics in seawater: sampling strategies, laboratory methodologies, and identification techniques applied to port environment. *Environ Sci Pollut Res* 27:8938–8952
41. Koelmans AA, Mohamed Nor NH, Hermen E, Kooi M, Mintenig SM, De France J (2019) Microplastics in freshwaters and drinking water: critical review and assessment of data quality. *Water Res* 155:410–422
 42. Barrows A (2017) National Microplastics Field Methodology Review. <https://doi.org/10.13140/rg.2.2.19421.41446>. Accessed 17 October 2020
 43. Besley A, Vijver MG, Behrens P, Bosker T (2017) A standardized method for sampling and extraction methods for quantifying microplastics in beach sand. *Mar Pollut Bull* 114:77–83
 44. Adams CC (1913) Reviewed work(s): valuation of the sea. I. Animal life of the seabottom, its food and quantity. *Am Nat* 47 (558):378–384
 45. Song YK, Hong SH, Jang M, Han GM, Rani M, Lee J, Shim WJ (2015) A comparison of microscopic and spectroscopic identification methods for analysis of microplastics in environmental samples. *Mar Pollut Bull* 93:202–209
 46. Shim WJ, Song YK, Hong SH, Jang M (2016) Identification and quantification of microplastics using Nile red staining. *Mar Pollut Bull* 113:469–476
 47. Cheang CC, Ma Y, Fok L (2018) Occurrence and composition of microplastics in the seabed sediments of the coral communities in proximity of a metropolitan area. *Int J Environ Res Public Health* 15:2270
 48. Edo C, Tamayo-Belda M, Martínez-Campos S, Martín-Betancor K, González-Pleiter M, Pulido-Reyes G, García-Ruiz C, Zapata F, Leganés F, Fernández-Piñas F, Rosal R (2019) Occurrence and identification of microplastics along a beach in the biosphere reserve of Lanzarote. *Mar Pollut Bull* 143:220–227
 49. Sutton R, Franz A, Gilbreath A, Lin D, Miller L, Sedlak M, Wong A, Box C (2019) Understanding microplastic levels, pathways, and transport in the San Francisco Bay region. SFEI-ASC Publication #950, Richmond (CA)
 50. Hung C, Klasios N, Zhu X, Sedlak M, Sutton R, Rochman CM (2020) Methods matter: methods for sampling microplastic and other anthropogenic particles and their implications for monitoring and ecological risk assessment. *Integr Environ Assess Manag* 17:282–291. <https://doi.org/10.1002/ieam.4325>
 51. Hendrickson E, Minor EC, Schreiner K (2018) Microplastic abundance and composition in western Lake Superior as determined via microscopy, Pyr-GC/MS, and FTIR. *Environ Sci Technol* 52(4):1787–1796
 52. Lahens L, Strady E, Kieu-Le T-C, Dris R, Boukerma K, Rinnert E, Gasperi J, Tassin B (2018) Macroplastic and microplastic contamination assessment of a tropical river (Saigon River, Vietnam) transversed by a developing megacity. *Environ Pollut* 236:661–671
 53. Li J, Liu H, Paul Chen J (2018) Microplastics in freshwater systems: a review on occurrence, environmental effects, and methods for microplastics detection 137. In: Water research (Oxford), vol 137. Elsevier BV, England, pp 362–374. <https://doi.org/10.1016/j.watres.2017.12.056>
 54. Nguyen B, Claveau-Mallet D, Hernandez LM, Xu EG, Farner JM, Tufenkji N (2019) Separation and analysis of microplastics and nanoplastics in complex environmental samples. *Acc Chem Res* 52(4):858–866
 55. Harper PC, Fowler JA (1987) Plastic pellets in New Zealand storm-killed prions (*Pachyptila* spp.) 1958–1977. *J Ornithol New Zealand*
 56. Di Benedetto A, Ramos R (2014) Marine debris ingestion by coastal dolphins: what drives differences between sympatric species? *Mar Pollut Bull* 83:298–301
 57. Bravo Rebollo EL, Van Franeker JA, Jansen OE, Brasseur SMJM (2013) Plastic ingestion by harbour seals (*Phoca vitulina*) in the Netherlands. *Mar Pollut Bull* 67(1-2):200–202
 58. Murphy F, Russell M, Ewins C, Quinn B (2017) The uptake of macroplastic & microplastic by demersal & pelagic fish in the Northeast Atlantic around Scotland. *Mar Pollut Bull* 122:353–359
 59. Wieczorek AM, Morrison L, Croot PL, Allcock AL, MacLoughlin E, Savard O, Brownlow H, Doyle TK (2018) Frequency of microplastics in mesopelagic fishes from the Northwest Atlantic. *Front Mar Sci* 5:39
 60. Lusher AL, Welden NA, Sobral P, Cole M (2017) Sampling, isolating and identifying microplastics ingested by fish and invertebrates. *Anal Methods* 9:1346–1360
 61. Bond A, Lavers JL (2013) Effectiveness of emetics to study plastic ingestion by Leach's storm-petrels (*Oceanodroma leucorhoa*). *Mar Pollut Bull* 70:171–175

62. Cauwenberghe V, Janssen CR (2014) Microplastics in bivalves cultured for human consumption. *Environ Pollut* 193:65–70
63. Catarino A, Thompson R, Sanderson W, Henry TB (2017) Development and optimization of a standard method for extraction of microplastics in mussels by enzyme digestion of soft tissues. *Environ Toxicol Chem* 36 (4):947–951
64. Bouwmeester H, Hollman PCH, Peters RJB (2015) Potential health impact of environmentally released micro- and nanoplastics in the human food production chain: experiences from nanotoxicology. *Environ Sci Technol* 49:8932–8947
65. Dehaut A, Cassone A-L, Frère L, Hermabessiere L, Himber C, Rinnert E, Rivière G, Lambert C, Soudant P, Huvet A, Duflos G, Paul-Pont I (2016) Microplastics in seafood: benchmark protocol for their extraction and characterization. *Environ Pollut* 215:223–233
66. Baechler BR, Stienbarger CD, Horn DA, Joseph J, Taylor AR, Granek EF, Brander SM (2019) Microplastic occurrence and effects in commercially harvested north American finfish and shellfish: current knowledge and future directions. *Limnol Oceanogr Lett* 5:113–136
67. Karbalaei S, Hanachi P, Walker TR, Cole M (2018) Occurrence, sources, human health impacts and mitigation of microplastic pollution. *Environ Sci Pollut Res Int* 25:36046–36063
68. De Sales-Ribeiro C, Brito-Casillas Y, Fernandez A, Caballero MJ (2020) An end to the controversy over the microscopic detection and effects of pristine microplastics in fish organs. *Sci Rep* 10:12434
69. Schwabl P, Köppel S, Königshofer P, Bucsics T, Trauner M, Reiberger T, Liebmann B (2019) Detection of various microplastics in human stool: a prospective case series. *Ann Intern Med* 171(7):453–457
70. Woishnis WA, Ebnesajjad S (2012) Effect of chemicals on plastics and elastomers. In: *Plastics Design Library, Chemical Resistance of Thermoplastics*. William Andrew Publishing, Norwich, NY
71. Porras SP, Hartonen M, Koponen J, Ylinen K, Louhelainen K, Tornaeus J, Kiviranta H, Santonen T (2020) Occupational exposure of plastics workers to Diisononyl phthalate (DiNP) and Di(2-propylheptyl) phthalate (DPHP) in Finland. *Int J Environ Res Public Health* 17:2035
72. Christensen M, Vestergaard J, d'Amore F, Gørløv J, Toft G, Ramlau-Hansen C, Stockholm Z, Iversen I, Nissen M, Kolstad H (2018) Styrene exposure and risk of lymphohematopoietic malignancies in 73,036 reinforced plastics workers. *Epidemiology* 29 (3):342–351
73. Thompson RC, Olsen Y, Mitchell RP, Davis A, Rowland SJ, John AWG, McGonigle D, Russell AE (2004) Lost at sea: where is all the plastic? *Science* 304 (5672):838
74. Quinn B, Murphy F, Ewins C (2017) Validation of density separation for the rapid recovery of microplastics from sediment. *Anal Methods* 9(9):1491–1498
75. Kershaw P, Turra A, Galgani F, van Franeker JA (2019) Guidelines for the monitoring and assessment of plastic litter in the ocean. *GESAMP Reports and Studies* 99:123
76. Masura J, Baker JE, Foster GD, Arthur C, Herring C (2015) Laboratory methods for the analysis of microplastics in the marine environment: recommendations for quantifying synthetic particles in waters and sediments. *NOAA Technical Memorandum NOS-OR&R 48*, Silver Spring, MD
77. Ruggero F, Gori R, Lubello C (2020) Methodologies for microplastics recovery and identification in heterogeneous solid matrices: a review. *J Polym Environ* 28:739–748
78. Nuelle M-T, Dekif JH, Remy D, Fries E (2014) A new analytical approach for monitoring microplastics in marine sediments. *Environ Pollut* 184:161–169
79. Maes T, Jessop R, Wellner N, Haupt K, Mayes AG (2017) A rapid-screening approach to detect and quantify microplastics based on fluorescent tagging with Nile red. *Sci Rep* 7:44501
80. Lares M, Ncibi MC, Sillanpää M, Sillanpää M (2019) Intercomparison study on commonly used methods to determine microplastics in wastewater and sludge samples. *Environ Sci Pollut Res Int* 26(12):12109–12122
81. Prata JC, da Costa JP, Duarte AC, Rocha-Santos T (2019) Methods for sampling and detection of microplastics in water and sediment: a critical review. *Trends Anal Chem* 110:150–159
82. Rodrigues SM, Almeida CMR, Ramos S (2019) Adaptation of a laboratory protocol to quantify microplastics contamination in estuarine waters. *MethodsX* 6:740–749

83. Hermsen E, Mintenig SM, Besseling E, Koelmans AA (2018) Quality criteria for the analysis of microplastic in biota samples: a critical review. *Environ Sci Technol* 52:10230–10240
84. Tóth G, Jones A, Montanarella L (eds) (2013) Guidance on monitoring of marine litter in European seas European Commission. Joint Research Centre & Institute for Environment and Sustainability, Ispra, Italy
85. Cole M, Webb H, Lindeque PK, Fileman ES, Halsband C, Galloway TS (2014) Isolation of microplastics in biota-rich seawater samples and marine organisms. *Sci Rep* 4:4528
86. Prata JC, da Costa JP, Girão AV, Lopes I, Duarte AC, Rocha-Santos T (2019) Identifying a quick and efficient method of removing organic matter without damaging microplastic samples. *Sci Total Environ* 686:131–139
87. Liebezeit G, Dubaish F (2012) Microplastics in beaches of the East Frisian Islands Spiekeroog and Kachelotplate. *Bull Environ Contam Toxicol* 89:213–217
88. Claessens M, Van Cauwenbergh L, Vandegeuchte MB, Janssen CR (2013) New techniques for the detection of microplastics in sediments and field collected organisms. *Mar Pollut Bull* 70:227–233
89. Foekema EM, De Gruijter C, Mergia MT, van Franeker JA, Murk AJ, Koelmans AA (2013) Plastic in North Sea fish. *Environ Sci Technol* 47:8818–8824
90. Löder MGJ, Imhof HK, Ladehoff M, Löschel LA, Lorenz C, Mintenig S, Piehl S, Primpke S, Schrank I, Laforsch C, gerdts G (2017) Enzymatic purification of microplastics in environmental samples. *Environ Sci Technol* 51(24):14283–14292
91. Thiele CJ, Hudson MD, Russell AE (2019) Evaluation of existing methods to extract microplastics from bivalve tissue: adapted KOH digestion protocol improves filtration at single-digit pore size. *Mar Pollut Bull* 142:384–393
92. Monteleone A, Schary W, Fath A, Wenzel F (2019) Validation of an extraction method for microplastics from human materials. *Clin Hemorheol Micocirc* 73:203–217
93. Nakajima R, Lindsay DJ, Tsuchiya M, Matsui R, Kitahashi T, Fujikura K, Fukushima T (2019) A small, stainless-steel sieve optimized for laboratory beaker-based extraction of microplastics from environmental samples. *MethodsX* 20(6):1677–1682
94. Hidalgo-Ruz V, Gutow L, Thompson RC, Thiel M (2012) Microplastics in the marine environment: a review of the methods used for identification and quantification. *Environ Sci Technol* 46(6):3060–3075
95. Käppler A, Fischer D, Oberbeckmann S, Schernewski G, Labrenz M, Eichhorn K-J, Voit B (2016) Analysis of environmental microplastics by vibrational microspectroscopy: FTIR, Raman or both? *Anal Bioanal Chem* 408:8377–8391
96. Shim WJ, Hong SH, Eo SE (2017) Identification methods in microplastic analysis: a review. *Anal Methods* 9:1384
97. Erni-Cassola G, Gibson MI, Thompson RC, Christie-Oleza JA (2017) Lost, but found with Nile red: a novel method for detecting and quantifying small microplastics (1 mm to 20 µm) in environmental samples. *Environ Sci Technol* 51(23):13641–13648
98. Andrady AL (2010) Using flow cytometry to detect micro- and nano-scale polymer particles on Proceedings of the Second Research Workshop on Microplastic Marine Debris NOAA Tech Memo 54
99. Lv L, Qu J, Yu Z, Chen D, Zhou C, Hong P, Sun S, Li C (2019) A simple method for detecting and quantifying microplastics utilizing fluorescent dyes—Safranine T, fluorescein isophosphate, Nile red based on thermal expansion and contraction property. *Environ Pollut* 255(2):113283
100. Tamminga M, Stoewer S-C, Fischer EK (2019) On the representativeness of pump water samples versus manta sampling in microplastic analysis. *Environ Pollut* 254:112970
101. Barbosa F, Adeyemi JA, Bocato MZ, Comas A, Campiglia A (2020) A critical viewpoint on current issues, limitations, and future research needs on micro- and nanoplastic studies: from the detection to the toxicological assessment. *Environ Res* 182:109089
102. Blettler MCM, Ulla MA, Rabuffetti AP, Garcello N (2017) Plastic pollution in freshwater ecosystems: macro-, meso-, and microplastic debris in a floodplain lake. *Environ Monit Assess* 189:581
103. Jung MR, Horgen FD, Orski SV, Rodriguez CV, Beers KL, Balazs GH, Jones TT, Work TM, Brignace KC, Royerf S-J, Hyrenbacha KD, Jensen BA, Lynch JM (2018) Validation of ATR FT-IR to identify polymers of plastic marine debris, including those ingested by marine organisms. *Marine Pollution Bull* 127:704–716
104. Corami F, Rosso B, Bravo B, Gambara A, Barbante C (2020) A novel method for purification, quantitative analysis and

- characterization of microplastic fibers using micro-FTIR. *Chemosphere* 238:124564
105. Löder MGJ, Kuczera M, Mintenig S, Lorenz C, Gerdts G (2015) Focal plane array detector-based micro-Fourier-transform infrared imaging for the analysis of microplastics in environmental samples. *Environ Chem* 12:563
106. Melucci D, Zappi A, Poggioli F, Morozzi P, Giglio F, Tositti L (2019) ATR-FTIR spectroscopy, a new non-destructive approach for the quantitative determination of biogenic silica in marine sediments. *Molecules* 24:3927
107. Kneipp K, Kneipp H, Itzkan I, Dasari RR, Feld MS (1999) Ultrasensitive chemical analysis by Raman spectroscopy. *Chem Rev* 99:2957–2975
108. Zada L, Leslie HA, Vethaak AD, Tinnevelt GH, Jansen JJ, de Boer JF, Ariese F (2018) Fast microplastics identification with stimulated Raman scattering microscopy. *J Raman Spectrosc* 49(7):1136–1144

INDEX

0-9, and Symbols

- 2',7'-dichlorodihydrofluorescein diacetate (H₂DCFDA) 156
260/230 71
260/280 71
4,4'-DDD 303, 307, 311
4,4'-DDE 303, 307, 311
4,4'-DDT 303, 307, 311
5-fluorouracil 69, 89
- A**
- Acanthocytes 156
Acetonitrile 56, 292–295, 297, 298, 303–305, 311, 316, 318–320, 322, 324
Aconitase 328, 330, 331
Acute toxicity 60, 206, 207, 252
Agriculture 218, 225, 226, 252, 301
Alachlor 303, 309
Aldrin 303, 307, 311
Alkaline phosphatase (ALP) 327, 328, 330, 334
Alpha-BHC 303, 307, 311
Alternative splicing 143
Alzheimer's disease (AD) 144
Ames assay 204, 275–284
Amino acids 144, 276
Anemia 155
Anesthesia 52, 106–109, 111–113, 116, 118–121
Animals 25, 34, 42, 56, 60, 62, 87, 105–109, 111–118, 121, 149, 201, 204, 211, 218, 233, 267, 276, 290, 301, 316–318, 322–324, 343, 344, 346, 349
Annexin-V-FITC labeling 156
Antioxidant enzymes 241–248
Antioxidants 156, 158, 233, 242, 248
Apoptosis 3–15, 203
Apoptotic 4, 5, 9, 13–16, 42, 155
Arbuscular mycorrhizal fungi (AMF) 251–253, 257, 258
Ascorbate peroxidase (APX) 242, 243, 246, 254, 259, 264
Atomic absorption spectrometer 268–270
Atomic absorption spectroscopy (AAS) 253, 254, 256, 257, 260

- ATP 34, 36, 40, 43, 44
Atrazine 303, 309
Attenuated Total Reflection (ATR)-FTIR Spectroscopy 352, 353

B

- Bacterial reverse mutation assay 276
Behaviors 20, 27, 47–53, 115, 302
BestKeeper 83, 87, 88
Beta-BHC 303, 307, 311
Biochemical toxicity 225–238
Biomarkers 124, 143, 144, 148, 156
Biomass 217–223, 254, 260, 261, 269
Bisphenols 155
Bluegill sunfish 204
Bolster 303
Brain 98, 105, 110, 113, 116, 119, 132, 147, 334
Breast adenocarcinoma cell line MCF-7 68
Breast cancer 87, 290
Brood size 25–27

C

- Cadmium (Cd) 21, 267
Cancer 19, 89, 175, 191, 218, 267, 290, 301, 339, 345
Cardiovascular diseases 186, 339
Case-control study 169–171, 173, 176, 178, 184–186, 193
Case-crossover study 168–170, 173, 176–180, 189
Catalase (CAT) 242, 243, 246, 254, 259, 264
cDNAs 12, 37, 41, 75, 77, 91, 95, 100, 101, 125, 133–136, 138, 209
Cell culture 41, 69
Cell death 4, 89, 155–164
Cell dehydration 156
Cell surface 156
Cell viability assays 203
Channel catfish 204
Channelrhodopsins (ChR2) 111, 113, 114
Chemogenetics 106, 112
Chicken 197–201

- Chloroacetanilides 302
 Chlorpyrifos 203, 303, 307
 Chromatin structure 124
 Chromosomal aberration 204
 Chromosome disorder 203
 Chronic exposure 203–213
 Chronic toxicity 204, 205, 207
 Climbing ability 47
 Coefficient of variance (CV) 83
 Cohort studies 169–171, 173, 181, 184, 186–188, 190, 191, 194
 Comet assays 203, 205, 208, 209, 211
 Comparative ΔC_t method 83
 Confidence intervals (CI) 20, 27–29, 184, 206
 Copper 51, 277, 327, 332
 Corn 48, 230, 253, 257, 270, 291, 293–295, 298, 306, 309, 312
 Cosmetic 211, 218, 225, 301, 344
 Cotton 28, 48, 53, 113, 226, 227, 229–231, 233, 237, 242, 330
 Coumaphos demeton-S 303
 Cross-sectional study 169–171, 173, 182–184, 192, 193
 Cyantraniliprole 203–211
 Cycle threshold (C_t) values 77, 78, 82, 84, 85, 94, 133
 CYP450 4, 11, 13

D

- Deep sequencing 67
 Deepwater Horizon 3, 7
 Deer mice 316, 322
 Delta-BHC 303, 307, 311
 Diabetes 155, 267
 Diazinon 303, 307
 Dichlorvos 303, 307
 Dieldrin 124, 303, 307, 311
 Diesel exhaust 197, 200
 Diseases 19, 47, 51, 105, 144, 148, 155, 167–169, 173, 175–180, 182–184, 186, 188, 190, 191, 193, 194, 218, 267, 276, 301, 345
 Dispersive pipette extraction (DPX) 291–293, 295–298, 312
 Dispersive solid phase extraction (d-SPE) 290, 291
 Disulfoton 303, 307
 DNA damage 4, 5, 203, 205, 277, 281
 DNA damage and repair process 205
 DNA methylation 124, 125, 127–129
 Doses 27, 28, 39, 43, 44, 56, 59, 62, 160, 197, 200, 203–211, 283, 322
Drosophila melanogaster 47–53, 327–335

E

- Ecosystems 289, 290, 301, 302
 Electron capture detector (ECD) 316, 317, 319–324
 Electron ionization (EI) 302, 303, 306, 308
 Embryos 21, 23, 56, 61, 64, 197–201, 261
 Emerging environmental pollutant 89, 218, 275
 Endocrine disruption 301, 339
 Endosulfan I 303, 307, 311
 Endosulfan II 303, 307, 311
 Endosulfan SO₄ 303, 307
 Endrin 303, 307, 311
 Engineered nanoparticle (ENP) 255, 263
 Environmental epidemiology 167, 170, 172, 173
 Environmental factors 47, 167, 179
 Environmental pollution 71, 89, 218, 275, 348
 Environmental Protection Agency (EPA) 60, 64, 270, 301, 302, 315
 Environmental toxicity v
 Epigenetic modification 123–139
 Epitranscriptome 143
 Eryptosis 155, 162
Escherichia coli 6, 8, 9, 11, 15, 35, 276–278, 280–283
 Ethidium bromide (EBr) 68
 Ethoprophos 303, 307
 Explosive 296, 315, 322

F

- Feeding 20, 25–27, 48, 206, 207, 330, 341
 Fensulfothion 303, 307
 Fenthion 303, 307
 Ferrozine 329, 332
 Fertilizers 267
 Fiber photometry 106, 108, 109, 114, 115, 121
 Fish 58–60, 64, 203–211, 290, 344, 347, 348
 Flame retardants 155
 Flow cytometry 44, 157, 161
 Food additives 218
 Food and Agriculture Organization (FAO) 204, 270
 Foods 9, 21, 23, 25, 26, 49–51, 53, 58, 113, 114, 204, 211, 225, 252, 267, 268, 289–298, 301, 302, 306, 308, 309, 312, 316–318, 332, 333, 340, 344
 Fourier Transform Infrared (FTIR) Microscopy 345, 352
 Fruits 48, 49, 52, 53, 291, 293, 294, 303, 305, 308, 312, 330

G

- Gamma-BHC 303, 307, 311
 Gas chromatography (GC) 72, 73,
 91, 292, 293, 296–298, 301–312, 316, 317,
 319–324
 Gene expressions 5, 7, 37, 41,
 67–94, 96, 100, 124, 143, 211, 226, 323
 Genes 4, 8, 9, 11–13,
 34, 41, 42, 47, 67, 68, 71–75, 77, 79, 80, 82–84,
 89, 91, 93, 95–102, 106, 123–125, 128,
 131–134, 138, 144, 205, 209, 211, 212, 226,
 276, 327
 Genetic mutation 315
 Genetic toxicity 276, 277, 322
 geNorm 83, 86, 88
 Genotoxicity 203–205
 Germ cells 3–15
 GFP 5, 7, 13–15, 35, 38
 GI track 316
 Gi-coupled M4 muscarinic receptors
 (hM4Di) 111
 Gq-coupled M3 muscarinic receptors
 (hM3Dq) 111
 Grains 269, 270, 291, 303

H

- Halorhodopsins (NpHR) 111, 113, 114
 Health Risk Index (HRI) 269, 270
 Heavy metals 19, 241–248,
 263, 268
 HEK293 cell 203
 HEЛА cell 203
 Hemolysis 160, 162
 HepG2 cell 203
 Heptachlor 303, 307, 311
 Heptachlor epoxide 303, 307, 311
 Hexahydro-1,3,5-trinitro-1,3,5-triazine
 (RDX) 315–324
 Hexahydro-1,3,5-trinitroso-1,3,5-triazine
 (TNX) 316, 319, 321–324
 Hexahydro-1,3-dinitroso-5-nitro-1,3,5-triazine
 (DNX) 316, 319, 321–324
 Hexahydro-1-nitroso-3,5-dinitro-1,3,5-triazine
 (MNX) 316, 319, 321–324
 High-throughput platform analysis
 (COAPS Biosort) 20
 Histidine 276, 282
 Histochemistry 105
 Histone modifications 124, 126–127,
 135, 139
 Homeostasis 124, 156
 Homologous recombination pathway 205
 Housekeeping genes 68, 71–75, 87, 94, 99

- HPLC 148, 292, 295, 297, 303
 Human 47, 68, 74,
 75, 111, 125, 138, 144, 152, 155, 203, 267, 270,
 290, 301, 315, 327, 339, 344, 345
 Human chorionic gonadotropin (hCG) 57, 60
 Human health 20, 33, 167,
 268, 275, 290, 301, 340, 344, 345, 354
 Huntington's disease 144
 Hydrogen peroxide (H_2O_2) 226, 230,
 235, 241, 243, 247, 253, 254, 258–260, 264,
 348, 349
 Hydroxyl radicals (OH) 241

I

- Immunofluorescence 113
 In situ hybridization 67
In vivo calcium imaging 111, 117–118
In vivo electrophysiological recording 106, 109,
 116, 117, 121
In vivo micronucleus assay 204
In vivo two-photon imaging 106, 108, 115, 116
 Inductively coupled plasma-mass spectrometry
 (ICP-MS) 253, 254, 256,
 257, 260, 327, 332, 335
 Inductively coupled plasma-optical emission
 spectroscopy (ICP-OES) 253, 254,
 256, 257, 260
 Inhalation 112, 197–201, 340, 344, 345
 Insecticides 203–211
 Insects 290, 301
 Internal standards 146, 303, 304, 310–312, 345
 Intracellular 156, 159, 161, 261
 Invertebrates 204, 290, 344
 Iron 327, 328, 330, 332–335, 349
 Iron staining 328, 332–334

J

- Joint effects 55–65

K

- Knock in 106

L

- Larvae 21, 26, 31, 47,
 49, 52, 56, 57, 60–64, 204, 206, 207, 330–335
 LC/MS 297, 298
 LC₅₀ 206, 207, 212
 Lead 21, 34, 47, 172, 191, 263
Lepomis macrochirus 204
 Lifespan 34, 47, 50, 51, 53
 Light stimulation 112, 114, 117
 Lipids 144, 152, 242, 247, 258
 Liquid chromatography 302, 345

- Liver 100, 203–212, 277, 278, 282
 Longevity 155
 Lungs 175, 181, 183, 191, 197, 198
 Lymphocytes 203
- M**
- Macrophages 156
 Maize 268–270
 Malignancy 155
 Mammals 344
 Manganese 21, 124, 228
 MAPK 156, 158
 Mass spectrometry (MS) 148–150, 218, 219, 222, 293, 297, 298, 301–312, 345
 Mellitus 155
 Merphos 303, 307
 Metabolome 144
 Metabolomics 144, 145, 149–152
 Metal mixtures 19–31
 Metal oxide nanoparticles 218, 276, 277, 283
 Method calibration 304, 308–311
 Methoxychlor 303, 307, 311
 Methylated DNA immunoprecipitation sequencing (MeDIP-seq) 124
 Methylated RNA immunoprecipitation sequencing (MeRIP-seq) 124, 131, 132
 Methyl parathion 303, 307
 Metolachlor 303, 309
 Mevinphos 303, 308
 Mice 100, 105–121, 132, 205, 277, 278, 315–324
 Microbes 218, 315, 340
 Micronucleus 203, 205, 208, 209
 Microorganism 149
 Microplastics 340–354
 MicroRNA (miRNA) 7, 10, 11, 69, 70, 89, 125, 133, 135, 136, 138, 139
 Mitochondria 34, 38, 44, 155, 262
 Mitochondrial morphology 34, 38, 39, 42, 43
 Mitochondrial toxicity 33–45
 Model organism 20
 mRNA 13, 41, 42, 89, 99, 124, 125, 129–131, 133, 134, 138, 143, 211
 Murashige and Skoog (MS) medium 218, 219, 222
 Multiple stressors 55
 Mutagenicity 204, 277, 278, 281, 283
 Mutagens 276–279, 281–283
 Mutations 203, 276, 277, 282, 283
- N**
- N_2 -fixing bacterium 253
 Nanoadditives 252
 Nanodiscs 217
 Nanofertilizers 252
 Nanofibers 217
 Nanomaterials 197, 241, 251–264, 275, 277
 Nanoparticles 217–223, 225–238, 251–256, 261, 263, 275–283
 Nanopesticides 252
 Nanophytotoxicity 251, 252, 262
 Nanoplates 217
 Nanotubes 217, 263
 National Institute for Standard and Testing (NIST) 302, 351
 Necroptosis 155
 Negative controls 26, 40, 135, 160, 257, 276, 278, 280, 282, 283
 Nematode growth medium (NGM) 6, 8, 9, 11, 15, 20, 21, 25, 26, 35, 37, 38, 43
 Nematodes 6, 20, 21, 26, 27, 30, 31, 37–41, 43, 44
 Neurobiology 106
 Neurotoxicology 105–121, 124, 143–153
 Neurotoxic substances 105
 N-Nitroso Compound 315–324
 Non-coding 124, 125, 134, 143, 276
 No-observed effect concentration (NOEC) 204, 205
 NormFinder 83, 86
 Northern blotting 67
 Nucleus 116, 155, 261
- O**
- Oil spill 3
 Omics 143, 152
Oncorhynchus mykiss 204
 Optogenetics 106, 107, 113, 114, 121
Oreochromis mossambicus 203–211
 Organism 27, 57, 60, 67, 205, 315
 Organochlorines 302–305
 Organophosphates 302–304
 Oxidative stress 34, 156, 233–236, 241–248, 252, 258, 259, 282
 Oxygen consumption 34, 41, 43
- P**
- P38 156, 158
 PAH 4, 11, 12
 Panel studies 168, 170, 173, 179–182
 Parathion-diethyl-d10 303, 304, 309, 310
 Parkinson's disease 144, 290
 Pathogenesis 144, 148
 Peroxidase (POD) 127, 234, 235, 242, 243, 245, 246, 254, 259
 Pesticides 55–65, 124, 203, 225, 289–298, 301–312

- Phenotyping 241–248, 282
 Phorate 303, 308
 Photosynthesis 231–232, 237, 241
 Physiological toxicity 225–238
 Phytoxic 218
 Plant growth 217–223, 225, 234, 267
 Plants 101, 204, 218, 220, 221, 223, 225–238, 241, 242, 244, 251–253, 257–260, 262–264, 267–270, 276, 290, 294, 315, 324, 349
 Polymerase chain reaction (PCR) 7, 8, 10–12, 15, 41, 67, 69, 72, 73, 75–78, 80, 82, 87, 90–93, 95, 97, 99–102, 105, 125, 128, 129, 133–135, 138, 205, 209, 211
 Positive controls 44, 159–161, 257, 278–280, 282, 331
 Primer-BLAST 73, 74, 77
 Primer efficiency 73, 75–78, 80, 91, 92
 Primer specificity 77, 80, 92
 Primers 7, 8, 11, 12, 71–77, 79, 80, 82, 90–92, 97, 100–102, 125, 128, 129, 131, 133–136, 138, 139, 206, 209
 Protein expression 144
 Proteomics 144, 145, 147–149
 Public safety 251
 Pyrethroids 302

Q

- Quantitative Methylation Specific PCR(qMSP) 124, 129
 Quantitative real-time PCR (qRT-PCR) 5, 12, 42, 44, 67, 68, 72, 73, 76–78, 80, 82–85, 90–93, 124, 125, 130, 138, 139

R

- Radiation 55–65
 Raman spectroscopy 353
 Reactive oxygen species (ROS) 33, 34, 38, 43, 156, 159, 162, 241, 242
 Real time PCR 12, 135
 Red blood cell (RBC) 155–164
 Reference genes 12, 13, 67–96, 133, 135, 138
 RefFinder 84
 Reproductive disorders 290, 301
 Respiration 33, 41, 44, 221, 231, 232
 Respiratory diseases 175, 183, 301
 Reverse mutation assay 204, 276
 Reverse transcription 11, 37, 41, 76, 95, 96, 99–102, 135, 138, 209
 Reverse transcription-PCR 75
 Risk assessment 55, 124, 190, 204, 277, 290

- RNA 10, 11, 15, 41, 67, 68, 71, 72, 75, 76, 89–91, 96, 98, 99, 101, 125, 129–131, 134, 135, 138, 139, 143, 144, 146, 147, 152, 209, 211, 276
 RNA extraction 10, 15, 70, 71, 89, 96, 97, 101, 146
 RNA methylation 124, 125, 129–133
 RNA-seq 67, 143, 144
 Robust analytical techniques 290
 Ronnel 303, 308
 Roots 204, 218, 220–223, 226, 230–233, 237, 238, 241, 242, 253, 254, 258, 260, 268, 269, 318
- S**
- Salmonella typhimurium* 204, 276–278, 280–283
 Sampling 30, 117, 169, 171, 179, 180, 182, 183, 189, 192, 198, 339–354
 Seed germination 218, 220–223, 225, 227, 229, 230, 237, 241
 Selected ion monitoring (SIM) 303, 306–311
 Semi-quantitative RT-PCR 100
 Separation 102, 148, 151, 211, 223, 263, 319, 345–350, 353, 354
 Sheepshead minnow 204
 Signaling 124, 156, 241
 Simazine 303, 309
 Singlet oxygen (O_2) 241
 Small RNA-seq 67
 SNP 143
 Soils 204, 251, 253, 256, 257, 267–270, 275, 289, 290, 294–296, 298, 316, 324, 339, 340
 Solid-phase extraction (SPE) 151, 290, 302
 Spectrophotometry 242
 Spontaneous reverse mutants 276
 Standard deviation (SD) 83, 183, 207, 211, 283, 310, 321
 Static renewal 58, 204
 Stirofos 303, 308
 Stomach 316, 318, 319, 321, 322, 344
 Sublethal 63, 203–213
 Sugar 48, 144, 222
 Sunscreen 218
 Superoxide ($O\cdot_2^-$) 44, 241
 Superoxide dismutase (SOD) 234, 235, 242, 244, 245, 248, 254, 259, 264
 Sustainable agriculture 251
 Switchgrass 218, 223
 SYBR green PCR mixture 77, 206
 Symbiont bacteria 251
 Systems biology 144

T

- Tangential flow filtration 252, 253, 255, 256
The Frog Embryo Teratogenesis Assay-Xenopus (FETAX) 56–58, 62, 64
Thiobarbituric acid reactive substance (TBARS) 242, 243, 247
Tilapia 203–212
Time series studies 168, 170, 173, 188
Titanium dioxide 218, 222, 226, 237, 277
Tokuthion 303, 308
Toxicants 3–5, 20, 34, 35, 37, 38, 40, 43, 44, 49, 67, 155, 157, 159, 160, 163, 164, 197, 198
Toxicogenomics 67–94
Toxicology 96, 144
Toxins 155, 340
Transcriptomics 145–147
Triazines 302–304, 308–311
Trichloronat 303, 308
Triclosan 96, 155, 160
Trout 204
Tryptophan 276, 282

U

- Ultraviolet-B (UVB) 55–58, 60, 62
U.S. Fish and Wildlife Service (USFWS) 206

V

- Vegetables 291, 293, 294, 303, 305, 308, 312
Vehicle control 57, 60, 276
Virus 113, 114, 116, 120, 121, 344

W

- Western blot 105, 124, 137, 139

X

- Xenopus laevis* 55–65

Z

- Zinc 228, 277, 327, 328, 332, 346, 352